ANNUAL REVIEW OF NUCLEAR SCIENCE

JAMES G. BECKERLEY, *Editor*
United States Atomic Energy Commission

MARTIN D. KAMEN, *Associate Editor*
Washington University Medical School

LEONARD I. SCHIFF, *Associate Editor*
Stanford University

VOLUME 4

1954

PUBLISHED BY
ANNUAL REVIEWS, INC.
IN CO-OPERATION WITH THE
NATIONAL RESEARCH COUNCIL
OF THE NATIONAL ACADEMY OF SCIENCES

ON SALE BY
ANNUAL REVIEWS, INC.
STANFORD, CALIFORNIA, U.S.A.

Engin. Library
QC
770
.A65
v.4

ANNUAL REVIEWS, INC.
STANFORD, CALIFORNIA, U.S.A.

FOREIGN AGENCIES

H. K. Lewis & Company, Ltd.
136 Gower Street
London, W.C. 1

Maruzen Company, Ltd.
6 Tori-Nichome Nihonbashi
Tokyo

PRINTED AND BOUND IN THE UNITED STATES OF AMERICA BY
THE GEORGE BANTA PUBLISHING COMPANY

Engin Lib
Direct
1.755
S0022

PREFACE

This volume is the second to be planned and executed by the present Editors and Editorial Committee. Although the chapters of Volumes 3 and 4 review a substantial fraction of what we believe to constitute "nuclear science," it should be understood that some topics will be reviewed less frequently than in alternate years.

Although editors and editorial committees can plan the scope of a volume, offer guidance to authors, and dot an "i" now and then, still it is the individual author who creates the real substance of any publication. It is a pleasure to express our sincere thanks to the authors of the various chapters of this volume for their considerable contribution.

We note the increasing number of readers of the *Annual Review of Nuclear Science* and hope this indicates that the volumes are a useful addition to the literature of Nuclear Science.

J.G.B. M.D.K.
C.D.C. L.I.S.
L.F.C. E.S.
R.E.Z.

ENRICO FERMI
1901–1954

Just as this volume was going to press, nuclear science suffered a most grievous loss in the untimely death of Enrico Fermi.

Born in Rome, Italy on September 29, 1901, he studied at Rome and then at Pisa, where he obtained his doctor's degree in 1922. After some minor works, the series of his memorable achievements started with the establishment of the statistical mechanics appropriate for antisymmetric particles (fermions). In short succession there followed the theory of beta decay and, in 1934, the start of experiments on neutrons which, through the discovery of slow neutrons, by a logical continuation led to the first self-sustaining nuclear chain reaction in 1942.

In the postwar years he turned his attention to pion-nucleon interactions and was engaged in this work until a few weeks before his death.

There is no page of these volumes which does not reflect his activity, no article which will not bear the imprint of his mind.

The grievous loss to science is even more poignant to his many personal friends who have had the good fortune to experience his kindness.

Chicago, Illinois
November 28, 1954

TOPICS AND AUTHORS
ANNUAL REVIEW OF NUCLEAR SCIENCE
VOLUME 5 (1955)

GAMMA RADIATION FROM NUCLEI, *M. Goldhaber*
ELECTRIC CHARGE DISTRIBUTION IN NUCLEI, *D. Hill*
NUCLEAR RADIATION SHIELDING, *E. P. Blizard*
NUCLEAR REACTIONS OF INTERMEDIATE ENERGY HEAVY PARTICLES, *D. C. Peaslee*
NUCLEAR PARTICLE DETECTION (CLOUD CHAMBER), *W. B. Fretter*
DESIGN OF NUCLEAR REACTORS FOR RESEARCH, *L. B. Borst*
INDUSTRIAL APPLICATIONS (MASS SPECTROSCOPY), *H. W. Washburn*
RADIATION CHEMISTRY, *F. S. Dainton*
MASS SPECTROMETRIC ANALYSIS OF ELECTRON IMPACT PROCESSES, *H. Eyring*
RADIOCHEMICAL SEPARATION TECHNIQUES, *H. L. Finston and J. Miskel*
RADIO-AUTOGRAPHIC TECHNIQUES, *W. P. Norris and L. A. Woodruff*
CELLULAR RADIOBIOLOGY, *R. K. Mortimer*
VERTEBRATE RADIOBIOLOGY (PATHOLOGY AND METABOLISM OF RADIOISOTOPES), *H. Lisco and J. Schubert*
VERTEBRATE RADIOBIOLOGY (PHYSIOLOGY), *A. Edelmann*

CONTENTS

PAGE

RECENT DEVELOPMENTS IN PROTON SYNCHROTRONS, *J. P. Blewett* . . 1

THEORIES OF PHOTONUCLEAR REACTIONS, *J. S. Levinger* 13

RADIOFREQUENCY AND MICROWAVE SPECTROSCOPY OF NUCLEI, *G. E. Pake* 33

STANDARDIZATION OF RADIOACTIVE SOURCES, *G. G. Manov*. . . . 51

FISSION RADIOCHEMISTRY (LOW-ENERGY FISSION), *L. E. Glendenin and E. P. Steinberg* 69

STABLE ISOTOPE DILUTION AS AN ANALYTICAL TOOL, *M. G. Inghram* 81

NUCLEAR PARTICLE DETECTION (FAST ELECTRONICS), *R. E. Bell* . . 93

NUCLEAR PARTICLE DETECTION (CHARACTERISTICS OF SCINTILLATORS), *R. K. Swank* 111

NUCLEAR PARTICLE DETECTION (CHARACTERISTICS OF ČERENKOV COUNTERS), *J. Marshall* 141

ALPHA RADIOACTIVITY, *I. Perlman and F. Asaro* 157

POSITRONIUM, *S. DeBenedetti and H. C. Corben* 191

THE INTERACTIONS BETWEEN π-MESONS AND NUCLEONS, *M. Gell-Mann and K. M. Watson* 219

HEAVY MESONS, *C. Dilworth, G. P. S. Occhialini, and L. Scarsi* . . 271

PENETRATION OF HEAVY CHARGED PARTICLES IN MATTER, *E. A. Uehling* 315

BIOCHEMICAL EFFECTS OF RADIATION, *K. P. DuBois and D. F. Petersen* 351

VERTEBRATE RADIOBIOLOGY (LETHAL ACTIONS AND ASSOCIATED EFFECTS), *J. F. Thomson* 377

RADIOACTIVITY IN GEOLOGY AND COSMOLOGY, *T. P. Kohman and N. Saito* 401

Annual Reviews, Inc., the National Research Council, and the Editors of this publication assume no responsibility for the statements expressed by the contributors of this *Review*.

RECENT DEVELOPMENTS IN PROTON SYNCHROTRONS[1]

By John P. Blewett

Brookhaven National Laboratory, Upton, Long Island, New York

This chapter will present the important developments which have taken place in the proton synchrotron field during 1952, 1953, and the first three months of 1954, During that period, three proton synchrotrons have come into operation: the first was the 3-Bev "Cosmotron" at the Brookhaven National Laboratory in the United States; the second was the 1-Bev machine at the University of Birmingham in England; and the third, at the University of California Radiation Laboratory, reached the end of the construction phase and was operated successfully at 5 Bev in March of 1954. In the meantime, the new alternating-gradient method for focusing beams of charged particles has made possible the design of proton synchrotrons for energies several times higher than those attained at present. Design studies for machines using alternating-gradient focusing have been initiated in at least five centers. In the sections which follow, these developments will be summarized individually.

The Brookhaven Cosmotron

The Brookhaven Cosmotron is a proton synchrotron designed to accelerate protons to a maximum energy of 3 Bev. Its 2000-ton magnet is divided into four quadrants so that the proton orbit consists of four circular arcs of 30 ft. radius joined by straight sections each 10 ft. long. Protons are injected at 3.6 Mev from an electrostatic accelerator and are accelerated to their final energy in about one second. A very complete description of the Cosmotron and its components, written by members of the Cosmotron staff and edited by M. H. Blewett, was published in September, 1953 (1).

The first successful acceleration of protons to energies over 1 Bev took place in the Cosmotron in May, 1952. About a month later the final proton energy had been increased to 2.2 Bev. At this energy the magnetic field pattern begins to deteriorate as the magnet yoke saturates, and correction to the field pattern is made by passing current through windings on the magnet pole faces. Since the power supply for the pole-face windings was not yet completed, the Cosmotron was operated temporarily at 2.2 Bev.

The first operation showed that a shielding wall was essential for protection of personnel; operation revealed also several minor defects in machine components. During the second half of 1952 a concrete shielding wall 8 ft. thick was erected and the machine components were brought to final form, and by the end of 1952 the machine was available for experimental work.

After about a year of operation at 2.2 Bev, the pole-face windings were energized and the final proton energy was raised to about 3 Bev. In present

[1] The survey of literature pertaining to this review was concluded in April, 1954.

operation about 10^{10} protons are accelerated in each pulse, once every five seconds. The Cosmotron is in operation 16 hr. a day, five days a week. Once every five or six weeks the machine is shut down for a week for maintenance and for rearrangement of experimental equipment.

As yet the accelerated proton beam has not been extracted from the Cosmotron. Experimental studies are made at present in each of three types of emergent beams of secondary particles, emanating from targets located in the field-free straight sections. A well collimated exchange neutron beam emerges from the target along a tangential continuation of the path of the incident protons. This beam has a half width of about seven degrees and includes neutrons of all energies up to almost the incident proton energy. Beams of particles scattered from the targets are defined by apertures which, at present, limit the scattered beams to regions around 22 degrees and 30 degrees deflection from the direction of the incident proton beam. These so-called "direct beams" include all sorts of high-energy radiation: protons, mesons, neutrons, and γ-rays. The third emergent beam type consists of negative mesons produced in the target. As these mesons emerge through the stray field of the Cosmotron magnet, they are deflected outwards in such a way that mesons of a given energy are brought to a rough focus at distances of the order of 20 ft. from the proton orbit. It is possible by inclusion of channels in the shielding wall to define negative meson beams of a variety of energies from 0.3 to about 2 Bev. Unfortunately, positive mesons are not so easily extracted since they are deflected inwards toward the yoke of the C-shaped Cosmotron magnet. Positive meson studies must, accordingly, be made in the direct beams.

Efforts will probably be made during 1954 to extract the accelerated proton beam. After the protons reach full energy, the accelerating field will be removed and, as the magnetic field continues to rise, the orbit will shrink in diameter until it is intercepted by absorbers about one inch thick. These absorbers will slow the protons down so that on the following turn they will be displaced inward about four inches into the field of a pulsed electromagnet. This field will deflect the beam outward so that, one or two quadrants later, it can be completely extracted by another pulsed electromagnet.

The proton synchrotron is unique among accelerators in the long duration of the accelerating cycle. The one-second acceleration in the Cosmotron is slow enough that it is possible to wait until the initial oscillations in radial beam position have damped to small values, and then to insert targets to positions where they would have intercepted the beam during the injection period. This possibility has been exploited in the Cosmotron, and many of the experimental targets are inserted at the end of each accelerating cycle by hydraulic rams, then removed before the beginning of the next cycle.

As the energy and intensity of the Cosmotron has steadily increased, shielding has been a continuous problem. By mid-1953 the level of scattered background radiation was approaching dangerous values in the adjacent

control and experimental rooms. This scattered background makes experimentation difficult since it fills cloud chambers and photographic emulsions with spurious tracks and makes counter detection of particle direction impossible unless the coincidence counters that are used have resolving times less than about 10^{-7} sec. A detailed study of the distribution of radiation in the neighborhood of the Cosmotron has been continually in progress by the Cosmotron staff and by the Brookhaven Health Physics group (2). As a result of the findings of this study, the shielding around the target straight-section has been increased. This section of the machine is now completely enclosed by the original eight foot wall on the outside, a three foot wall inside the ring, and a roof of 30 in. thick reinforced-concrete beams. This enclosure extends for a distance of 12 ft. in each direction from the target. This improvement in shielding has decreased the radiation intensity in the control room and experimental area by a factor of about ten. With the increase in proton energy to 3 Bev and with the continual improvement in beam energy, however, even this shield is becoming marginal and further shielding may become necessary in the near future.

The Birmingham Proton Synchrotron

The proton synchrotron at the University of Birmingham (England) came into operation in June, 1953 and is now accelerating about 3×10^9 protons per pulse to an energy of about 1 Bev (3). A description of this machine was published by Hibbard in 1950 (4).

The magnet in the Birmingham machine is constructed for an orbit radius of 450 cm. The orbit is circular including no field-free straight sections. The magnet consists of half-inch laminations, eight feet square, and has separate pole pieces of one-eighth inch thick laminations. Power for the magnet is supplied by two dc generators in parallel; energy is stored in a 36-ton flywheel.

The magnet gap at the equilibrium orbit is 21 cm. In this gap is mounted a 60-section porcelain vacuum chamber which provides a useful aperture 10 cm. high by 35 cm. in the radial direction.

Protons are injected at 460 Kev through a μ-metal tube which provides shielding against the fringing fields of the magnet. Acceleration is provided by a radio-frequency signal applied to a drift tube which extends over 102 degrees in azimuth and is formed by metallic coatings on the inside of the vacuum chamber. Because of the low injection energy, the frequency of the accelerating signal varies over a 30:1 range during the cycle. The accelerating signal is generated by a mechanically controlled beat frequency oscillator which is maintained in synchronism with the magnetic field by mechanical links with the magnet power supply. The drift tube is maintained in resonance with an inductance coil whose inductance is varied by plunging it into a mercury pool.

The successful operation of the Birmingham machine is a remarkable

triumph over an extreme shortage of manpower and financial resources. These factors have, however, introduced several difficulties in the operation of the machine. For example, the magnet winding does not include a return around the outside of the magnet gap. Consequently, the leakage fields around the machine are very high, even at considerable distances. A secondary result of this flux distribution is the generation, in operation, of very high circulating currents in the welds which hold the magnet structure together. These currents continue to circulate after the end of the magnet cycle and introduce large perturbations in the remanent field. This trouble has been surmounted by careful control of the magnet cycle. Another difficulty which will be less easily removed is associated with the very limited space between the machine and the walls of the room in which it is built. Adequate radiation shielding cannot be included without major building changes; in the meantime, it is not possible to operate the machine for more than half an hour per day without exceeding radiation tolerances in the neighboring laboratories. A third source of trouble is the low injection energy which makes the beam very sensitive to gas scattering. Best operation occurs at pressures below 8×10^{-7} mm. Hg; if the pressure rises above 2×10^{-6} mm., the beam effectively disappears.

The Bevatron

The Bevatron is a proton synchrotron designed for acceleration to about 6 Bev and is located at the Radiation Laboratory of the University of California. As yet, the only descriptions of the Bevatron in the literature are the design report written by Brobeck in 1948 (5) and a report by Lofgren (6) on the operation of a quarter-scale model which preceded the construction of the Bevatron.

The basic design features of the Bevatron are similar to those found in the Brookhaven Cosmotron. The proton orbit consists of four circular quadrants about 50 ft. in radius separated by field-free straight sections 20 ft. long. The component designs in the Bevatron, however, differ from those in the Cosmotron in most cases. The Bevatron magnet, for example, is roughly symmetrical about the proton orbit, with two magnetic return yokes, one inside and one outside the orbit. This design is less susceptible to yoke saturation effects than is the C-shaped magnet of the Cosmotron, but it does not permit the easy access to the vacuum chamber that is possible with the C-shaped magnet. The radio-frequency accelerating unit is a short drift tube whose capacity is continuously tuned by saturation of a ferrite-cored inductor, whereas the accelerating unit in the Cosmotron is a ferrite-loaded cavity. Injection into the Bevatron is at 10 Mev from a linear accelerator instead of the 4-Mev electrostatic injection used in the Cosmotron.

Construction of the Bevatron is essentially complete and protons were injected in February, 1954. Acceleration tests were successful almost immediately and a proton energy of 5 Bev was achieved in March, 1954.

The Alternating-Gradient Focusing Principle

It is easy to show that it is impossible, using combinations of electrostatic or magnetostatic fields in free space, simultaneously to focus beams of charged particles in all planes through the beam axis. This difficulty can be circumvented if the beam travels in a curved path because of the additional terms introduced by the centrifugal force; a weak focusing in all directions can be achieved by field shaping and it is this technique which is used in conventional betatrons and synchrotrons. The focusing is weak, however, and the aperture required to contain the particle excursions from the stable orbit is so large that accelerators for energies above 10 Bev become prohibitively expensive.

A much stronger focusing method was discovered in 1949 by Christofilos (7) in Athens. His work was not published and the principle was rediscovered and published in 1952 by Courant, Livingston & Snyder in 1952 (8). Its applications to the linear accelerator were studied at the same time by Blewett (9). The principle is based on the observation that successive applications of strong focusing and defocusing forces to a particle beam can result in a strong net focusing. A good analogy exists with the optical system consisting of a focusing and a defocusing lens, of equal focal lengths, separated by a finite distance. This combination of lenses has a focusing effect no matter which lens comes first.

In the ion optical case the lenses consist of electric or magnetic fields normal to the ion beam direction and having high gradients in the direction normal to the field and to the beam. Such fields will focus the beam in one plane and will defocus it in the plane normal to the focusing plane. If, elsewhere on the beam path, similar fields but with reversed gradients are applied, the beam will be defocused in the original focusing plane and focused in the original defocusing plane. The combination of fields can now give focusing in both planes with net focusing forces much stronger than were achieved in conventional circular accelerators. A beam can be continually focused along a long path by successive application of fields whose gradients alternate along the beam path. For this reason the new technique, originally known as "strong focusing," is also described as "alternating-gradient focusing."

The stability limits for such focusing systems have been studied by Courant, Livingston, Snyder, and others. In the case where a particle beam is to be focused by successive applications, over distances of length L of the beam path, of an electric field E_1 having a gradient dE_1/dx, and a field E_2 having a gradient dE_2/dx, the condition for stability is

$$-1 < \cos\alpha_1 \cos\alpha_2 - \frac{\alpha_1^2 + \alpha_2^2}{2\alpha_1\alpha_2} \sin\alpha_1 \sin\alpha_2 < 1 \qquad 1.$$

where

$$\alpha_1 = \left(\frac{L^2}{\beta^2 W}\frac{dE_1}{dx}\right)^{1/2}$$

$$\alpha_2 = \left(\frac{L^2}{\beta^2 W}\,\frac{dE_2}{dx}\right)^{1/2}$$

$\beta = v/c$

W = total particle energy in electron volts.

All quantities are in mks units. If magnetic fields B are used for focusing, it is necessary only to substitute vB for E in the above relation.

Equation 1 indicates stable focusing over a generous range of parameters. For example, if dE_1/dx is kept equal to $-(dE_2/dx)$, the parameters α_1 and α_2 can range from zero to an absolute value of about two. The strongest focusing occurs for the highest stable values of the field gradient. In view of this fact, the first proton synchrotron design studies based on the new principle used magnetic field gradients as high as were physically realizable. In the paper of Courant, Livingston & Snyder, a proton synchrotron magnet was proposed in which, at fields of 10,000 gauss, the field gradient would be 10,000 gauss per inch. It was shown that the proton oscillations in a 30-Bev proton synchrotron using such a magnet would require an aperture only 0.5 by 0.5 in., instead of the 5 by 20 ft. aperture which would be required in a scaled-up version of the Cosmotron. These first designs were soon shown to be somewhat overoptimistic. In a study of the effects of small misalignments of components of an alternating-gradient synchrotron, Adams, Hine & Lawson (10) showed that with the highest gradients the proton orbits are extremely sensitive. Small misalignments in magnet sectors are magnified into very large orbit deviations. This is particularly so whenever the number of free oscillations about the equilibrium orbit in one complete revolution approaches integral values. In this case, a resonant build-up of oscillation amplitude takes place and the beam is lost.

Since the misalignment sensitivity decreases as the focusing gradients are decreased whereas the amplitudes of oscillations, resulting from errors in injection or to gas scattering, increase as the gradients are decreased, it follows that the aperture required to contain these oscillations will have a minimum for some intermediate value of gradient. This value, for practical tolerances in magnet construction, proves to be about one-tenth of the highest realizable. Aperture dimensions required are of the order of three inches which, although somewhat larger than those that, at first, seemed possible, are still smaller by a factor of almost 30 than those which would have been required in a machine of the Cosmotron type.

In an alternating-gradient synchrotron, particles whose energy is greater than or less than the equilibrium energy travel on orbits whose average radius is slightly larger or slightly smaller than the radius of the equilibrium orbit. The sign of this effect is the same as it is in the conventional synchrotron but its value is much less. In the conventional synchrotron it is this effect which results in stability of phase oscillations around an equilibrium phase on the falling side of the accelerating rf wave. In the low-energy range of operation of the alternating-gradient synchrotron, on the other hand, the

orbit radius varies so slowly with energy that the synchrotron phase-stability mechanism is overpowered by the mechanism which induces phase stability on the rising side of the rf wave in the linear accelerator. In this case, of course, phase corrections are induced by differences in particle and wave velocities. In the alternating-gradient synchrotron, as energy is increased and the particle velocity approaches the velocity of light, the linear acceleration mechanism grows weaker and weaker and finally is overpowered by the weak synchrotron mechanism. The energy at which this occurs is known as the "transition energy." In order that acceleration can continue above the transition energy, it is necessary to make a sudden shift in the phase of the accelerating wave so that the particle bunch, formerly distributed around a stable phase on the rising part of the rf wave, is grouped around a phase on the falling side of the accelerating wave. The phase oscillation behavior through the transition energy has been studied in detail by Johnsen and others (11), and it appears that no serious difficulties should be experienced in making the transition.

The theory of the alternating-gradient synchrotron has been developed in considerable detail both in the United States and in Europe. Analysis and numerical computations have given a reasonably clear picture of orbit behavior in the presence of nonlinearities in field and field gradient and under the influences of various sorts of misalignments and construction errors. For the most part, the results of these studies are, as yet, available only in the form of internal project reports. One rather complete compilation is available, however, in the published *Lectures on the Theory and Design of an Alternating-Gradient Proton Synchrotron* which were presented in October, 1953 by the proton synchrotron group of the European Council for Nuclear Research (11).

Structures for maintaining fields with high gradients can take the form of four-pole or four-electrode systems in which the pole or electrode contours are sections of rectangular hyperbolas. Many modifications of this design are in the process of evolution and magnet modeling programs are in progress in many institutions.

The alternating-gradient principle has had several preliminary tests. Theoretical predictions were verified in a conversion of the University of California 30-Mev proton linear accelerator to electrostatic alternating-gradient focusing. An alternating-gradient electron synchrotron has been constructed at Cornell University and electrons have been accelerated during several thousands of revolutions after injection. The success of this machine will not provide any information about passage through the transition energy because its 2-Mev injection energy is already above the transition which takes place at relatively low energies for electrons.

The sections which follow are brief descriptions of five design studies now in progress. In two of these cases, at Brookhaven and in Geneva, Switzerland, construction of a machine is definitely planned. In the other three cases the planning for construction is less definite.

The Brookhaven Project

Design studies at Brookhaven, under the direction of L. J. Haworth, have covered the range of accelerated proton energies up to 100 Bev. Costs of construction of machines have been estimated at several points in this range and have been considered in the light of the best available evaluation of the scientific desirability of protons in the various energy ranges. In the light of these studies, a final proton energy of 25 Bev has been chosen and work at present is aimed at component design for a 25-Bev alternating-gradient synchrotron.

The magnet will be enclosed in a ring-shaped building about 800 ft. in diameter. The present design indicates subdivision of the magnet into 240 sections each about 7 ft. long. Between the magnet sections will be field-free sections in which accelerating units, correcting lenses, and beam detection equipment will be situated. These field-free sections will vary in length from two to five feet. The peak magnetic field on the orbit will be 10,000 gauss, and the radius of curvature of the orbit in the magnet sections will be 280 ft. The total amount of iron in the magnet, and the power which it will require will be of the same order of magnitude as those in the Cosmotron. The field gradients at the orbit will be approximately 1000 gauss per inch at a field of 10,000 gauss (the field index $n = 300$ approximately). Erection tolerances for the magnet will be of the order of 0.01 inches. In this field configuration, the particles will make between eight and nine free betatron oscillations per revolution.

Injection into the machine is to be at 50 Mev or about one-third of the velocity of light. The injector will be a linear accelerator since this is the only accelerator capable of delivering a well focused beam at this energy.

For the proposed acceleration period of one second, the protons must gain about 70 Kev per revolution. This energy will be supplied at several points around the machine across gaps which form part of resonant cavities kept continually resonant by saturation of ferrite loading. The radio-frequency will probably be the twelfth harmonic of the revolution frequency since this gives a convenient working range of frequency (1.5 to 5 Mc.).

The frequency tolerance over the greater part of the range is so severe that it cannot be programmed. It will be necessary to control frequency from information derived from the proton beam itself. The proposed method involves derivation of the primary signal by inductive pickup from the proton beam. The radial beam location will then be derived from the signal from a pair of differential inductive pickup electrodes located one inside and one outside of the orbit. This signal will be amplified and used to control a phase-shifter in the line to the accelerating units, the polarity being chosen so that the beam is automatically restored to the equilibrium orbit. This method has been tested by G. K. Green and E. C. Raka on the Cosmotron where it proved to be entirely satisfactory.

Analysis of proton orbits indicates that the beam will be very sensitive to the changes in field gradient to be expected with the onset of magnetic

saturation. Further perturbations are expected if the gradient changes materially across the working aperture. To control these variations, extra magnetic lenses will be included in the spaces between magnet sections. Four-pole lenses will supply gradient corrections, and six-pole lenses can correct second-order field perturbations. The cycle for these lenses can be programmed from preliminary magnetic measurements.

To verify the conclusions which have been derived from analysis regarding free oscillations, resonance effects, and phenomena at the transition energy, the Brookhaven group has under construction a 10-Mev alternating-gradient electrostatic electron accelerator. Injection into this machine will be at 1 Mev, and the phase transition will be passed at 3 Mev. The orbit in this machine will be 45 ft. in diameter. The alternating electrostatic gradients will be set up by 80 pairs of shaped electrodes. Various multipole electrostatic lenses are included so that a thorough study can be made of all types of field perturbations.

The European Proton Synchrotron Project

The European Council for Nuclear Research (usually abbreviated to CERN), which is supported by twelve European nations, is designing in Geneva, Switzerland, a laboratory which will include a 25-Bev proton synchrotron (12). The proton synchrotron project is directed by O. Dahl of Norway. The plans of the CERN proton synchrotron group were presented at a conference in Geneva in October, 1953 (11, 13). At that time, the peak proton energy contemplated was 30 Bev; since that date the design energy has been reduced to 25 Bev.

Although the design studies at Brookhaven and CERN have been relatively independent, the two machine designs which have emerged are very similar. A very extensive theoretical program in Europe has yielded conclusions regarding the proton orbits which are substantially in agreement with the results derived in the United States.

Differences in choices of design parameters between CERN and Brookhaven include the choice of a peak magnetic field of 12,000 gauss for CERN rather than 10,000 gauss. The radio-frequency harmonic planned at CERN is about the fortieth rather than the twelfth. Magnet apertures, field gradients, and injection parameters are almost identical for the two projects.

The agreement establishing the European organization has not yet been ratified by all of the parliaments involved. Until a sufficient number of ratifications are obtained, the CERN group cannot place orders but will continue with analysis and model studies; ratification is expected during 1954, however, and machine construction is expected to extend over a six-year period from that date.

The Cambridge (Massachusetts) Design Study

A design study for a 15-Bev alternating-gradient proton synchrotron has been completed by a joint Harvard-Massachusetts Institute of Tech-

nology group under the direction of M. S. Livingston. The main emphasis in this design has been on simplicity and economy of time and money. The design details have been presented in a report issued in 1953 (14). The orbit diameter is 250 ft. corresponding, at the peak proton energy, to a peak magnetic field of 14,000 gauss.

Injection in this design is at 4 Mev, a choice governed by the availability of electrostatic accelerators for this energy. The low injection energy introduces difficulties in the rf system which must operate over an 11:1 frequency range instead of the 3:1 range in the Brookhaven and CERN designs. It is proposed to cut the operating frequency range by two shifts of the rf harmonic order during the accelerating cycle.

The conclusions of the Cambridge group are supported by a series of studies of rf components and of measurements, still in progress, on magnet models.

In spite of the emphasis in economy in this design, the Cambridge group feels that the cost of constructing and operating a 15-Bev machine is still rather high for a university group, and the present preference of the group is for a machine at a somewhat lower energy. Consequently, the Cambridge design is now in the process of redesign for an energy of about 6 Bev.*

The Princeton Design Study

A group at Princeton, New Jersey under the direction of M. G. White has concerned itself with general studies of orbit behavior and design concepts for alternating-gradient synchrotrons, rather than with the engineering details of design for a particular machine. Where a final proton energy has been necessary to clarify specific concepts, a value of 15 Bev has been chosen.

Attention at Princeton has been concentrated on the possible advantages of separating the functions of guiding and focusing which are combined in the magnets of all of the synchrotron designs discussed above. Separation of these functions would result in an alternation along the proton path of deflecting magnets with uniform fields and four-pole focusing magnets. The advantages claimed for this system are the achievement of higher guiding fields in parallel pole magnets and better linearity in the focusing system. These advantages are offset to some extent by a necessary increase in the total orbit circumference to accommodate the increased number of field components.

Theoretical studies have been made at Princeton of the ion optics of the separated-function machine with results essentially similar to those found for combined-function machines. A model study of a four-pole focusing lens indicates that no serious deviations from linearity are to be expected in the field pattern for gradients in the desired range.

* The Cambridge group now has under consideration a 5 Bev electron synchroton (July, 1954).

The Midwest Design Study

Early in 1953 representatives from a number of institutions in the Middle West of the United States met in Chicago to discuss possible studies of accelerator designs for a minimum energy of 20 Bev. A group under the direction of D. W. Kerst is now engaged in exploratory studies to this end. The members of the group, still located at their home institutions, are engaged in theoretical studies of orbits and in component design studies. This group is considering also possible alternative machines such as linear accelerators and electron synchrotrons for energies of about 10 Bev.

LITERATURE CITED

1. Blewett, M. H., *et al.*, *Rev. Sci. Instr.*, **24,** 723–870 (1953)
2. Cowan, F. P., and Handloser, J. S., "Health Physics Program for the Brookhaven Cosmotron," *Brookhaven National Laboratory Report 264* (T-43) (November, 1953)
3. "The Proton Synchrotron of the University of Birmingham," *Nature*, **172,** 704 (1953)
4. Hibbard, L. U., *Nucleonics*, **7**(4), 30–43 (1950)
5. Brobeck, W. M., *Rev. Sci. Instr.*, **19,** 545–51 (1948)
6. Lofgren, E. J., *Science*, **111,** 295–300 (1950)
7. Courant, E. D., Livingston, M. S., Snyder, H. S., and Blewett, J. P., *Phys. Rev.*, **91,** 202 (1953)
8. Courant, E. D., Livingston, M. S., and Snyder, H. S., *Phys. Rev.*, **88,** 1190–96 (1952)
9. Blewett, J. P., *Phys. Rev.*, **88,** 1197–99 (1952)
10. Adams, J. B., Hine, M. G. N., and Lawson, J. D., *Nature*, **171,** 926–27 (1953)
11. *Lectures on the Theory and Design of an Alternating-Gradient Proton Synchrotron* (Blewett, M. H., Ed., CERN Proton Synchrotron Group, Institut de Physique, Geneva, Switzerland, 180 pp., October, 1953)
12. Fry, D. W., *Nature*, **172,** 646 (1953)
13. Notes from the Conference on the Alternating-Gradient Proton Synchrotron (Blewett, M. H., Ed., CERN Proton Synchrotron Group, Institut de Physique, Geneva, Switzerland, 180 pp., October, 1953)
14. Livingston, M. S., "Design Study for a 15-Bev Accelerator," *Technical Report No. 60* (Laboratory for Nuclear Science, Massachusetts Institute of Technology, Cambridge, Mass., 212 pp., June, 1953)

THEORIES OF PHOTONUCLEAR REACTIONS[1]

By J. S. Levinger

Department of Physics, Louisiana State University, Baton Rouge, Louisiana

Introduction

In this review we shall discuss various theories of absorption of photons by nuclei. In this introduction we give a very brief review of experimental results for the interaction of moderate energy photons with medium to heavy nuclei. The next three sections compare briefly the theoretical and experimental results for the photodisintegration of the deuteron and other light nuclei. Following this, in the major section of this review, we shall discuss and compare various nuclear models for absorption of moderate energy photons by medium and heavy nuclei. Finally we shall consider briefly the products of photonuclear disintegration and the nuclear absorption of high-energy photons.

Experiments on photonuclear reactions were reviewed two years ago by Strauch (1), and by Chastel (2). More recently, Montalbetti, Katz & Goldemberg (3) and Nathans & Halpern (4) have summarized the systematics of measurement with 24 Mev *bremsstrahlung* interacting with medium and heavy nuclei. [Also see Titterton's (5) review article now being prepared.] The cross section $\sigma(W)$ for nuclear absorption of photons of energy W has the general appearance of a rather broad peak at about 20 Mev (E_m) with a peak cross section of the order of 0.1 barns. E_m decreases with mass number A about as $A^{-0.2}$. The full width of the peak at half-maximum, called Γ, is about 5 Mev. The area under the $\sigma(W)$ curve,

$$\sigma_{int} = \int \sigma(W)dW$$

is proportional to A, with proportionality constant about 0.02 Mev-barns. [σ_{int} falls below this value for light nuclei. See Nathans & Halpern (4).]

Other new results: (*a*) Measurements with higher energy *bremsstrahlung* by Jones & Terwilliger (6) indicate that for Ta the cross section is flat from 30 to 80 Mev, increasing by about 20 per cent the integrated cross section measured with 24 Mev *bremsstrahlung*. (*b*) Measurements by Stearns (7), Goldemberg & Katz (8), del Rio & Telegdi (9) and Fuller & Hayward (10) show that elastic and inelastic photon reactions contribute about 10 per cent of σ_{int}. (*c*) Recent measurements by Brown & Wilson (11) on electrodisintegration indicate that the photon absorption is mainly electric dipole.

The determination of σ_{int} and of the curve $\sigma(W)$ present two major problems which are not yet completely solved, though the solutions have been improved: measurements with a *bremsstrahlung* spectrum are much more difficult to interpret than those with monoenergetic photons; and any given

[1] The survey of literature pertaining to this review was concluded in February, 1954.

measurement measures partial cross sections for particular nuclear reactions, rather than the photon absorption cross section $\sigma(W)$. A method being developed by Koch (see 12) would measure $\sigma(W)$ directly.

Basic Theory

The basic theory of photonuclear reactions is an application of the quantum-mechanical theory of the interaction of charged particles with the electromagnetic field. The validity of this theory has been well demonstrated in calculations of the absorption or emission of photons by electrons bound in atoms. An initial step in this theory, performed and discussed by very many authors, involves separation of the electromagnetic field into the various electric multipoles and magnetic multipoles. [See Blatt & Weisskopf (13) and Sachs (14).] As in the case of interaction of photons with electrons, the allowed electric dipole transitions are strong, and the forbidden transitions are weak. The forbidden transitions have maximum cross sections of order of magnitude β^2 times the electric dipole transition. In a nucleus β^2, which is (nucleon velocity / velocity of light)^2, is about equal to 0.01, so forbidden transitions play only a minor role in the nuclear photoeffect. In this paper we shall consider the forbidden transitions only twice: for the magnetic dipole photodisintegration of the deuteron just above threshold, and for the effect of electric quadrupole interaction on the angular distribution of photoprotons.

In the interaction of bound electrons with photons the electric dipole transitions from state 0 to state n are calculated as proportional to the square of the dipole matrix element p_{0n} where

$$p_{0n} = im\omega_{0n}z_{0n} = im\omega_{0n}\int \psi_0^* \Sigma_i z_i \psi_n d\tau$$

Here p is the component of the momentum and z is the component of the displacement along the electric vector of the electromagnetic field. ω_{0n} is the difference of energies $E_n - E_0$ divided by $\hbar$. The initial and final state wave functions are functions of the coordinates of all the electrons in the atom, and the integral is taken over all these coordinates. $\Sigma_i z_i$ is the dipole moment of the atom, found by summing the component of displacement over all electrons in the atom.

In treating the interaction of photons with protons and neutrons (i.e., nucleons) in nuclei we have two major changes. First, we must use an effective charge of eN/A for protons, and $-eZ/A$ for neutrons, where A is the mass number, Z the atomic number, and $N = A - Z$ is the neutron number [Bethe (15)]. This effective charge is introduced since the displacements of the nucleons should be measured from the center of mass of the nucleus. We can see that a neutron has an effective charge by the following argument: a photoproton is ejected from the nucleus as a result of the electric force on the proton; but a photoneutron can be ejected because of the electric force on the remainder of the nucleus pushing the nucleus away and leaving the

neutron free. The charge to mass ratio for the residual nucleus introduces the value $-eZ/A$ for the neutron's effective charge.

The other major difference between the atomic and the nuclear photoeffect arises from the partly exchange (Majorana) character of the neutron-proton potential. An exchange potential (or any potential that does not commute with position, such as a velocity-dependent potential, or a spin-orbit potential) is essentially nonclassical. The classical correspondence $p = m\dot{z}$, written above as a quantum-mechanical equation between matrix elements ($p_{0n} = im\omega_{0n}z_{0n}$) no longer holds for such a potential. While the expression p_{0n} seems at first to be the correct expression to choose, Siegert (16) argued that for large photon wave lengths the expression $im\omega_{0n}z_{0n}$ was actually correct. Siegert's work has been generalized, and based on the principle of gauge invariance, by Sachs & Austern (17), and most recently by Foldy (18). The argument runs that exchange forces between neutrons and protons imply the existence of a current of charged particles (pions) between the nucleons. The complete calculation of the dipole matrix element should involve the sum of nucleon and pion currents. But the nucleons are the source of the pion current, which makes it possible to relate this total current to the nucleon position alone.

Sachs & Austern showed that this same argument applied to all electric multipole matrix elements in the long wave-length limit where the photon interacts with the total current, without separating it into nucleonic and mesonic components. However, exchange currents give small contributions to magnetic multipole matrix elements. Foldy has considered the possibility that the nucleon charge distribution should be regarded as spread out over a small volume, creating a modification of Siegert's theorem even in the long wave-length limit. We believe that until meson-theoretic calculations can be made correctly, we must use a phenomenological theory for nuclei. A phenomenological theory cannot be rigorously justified, so we shall for the present take the simplest available: i.e., Siegert's theorem, as generalized by Sachs to all electric multipoles.

Two methods have been used to calculate the photon absorption cross section for nuclei. First, the dipole matrix element can be calculated for absorption of photons of various energies if explicit assumptions are made as to both the ground state wave function and the excited state wave function (for various energies). Present work uses either an independent particle model (IPM), a subunit model, or a model of collective motion of the nucleus. The last model has been treated classically.

A second method makes use of sum-rules, and involves knowledge only of the nuclear wave function for the ground state. It may seem surprising that one wave function alone should be sufficient to determine very much about the photon absorption cross section. But we can argue as follows: the ground state wave function is a solution of Schrödinger's equation and thus, together with the energy eigenvalue, determines the potential. (Here we assume that the operational character of the potential is known: e.g., that the

potential merely multiplies the wave function.) Schrödinger's equation could then in principle be solved for this potential for the wave functions of the various excited states, and the first method used for calculations. Thus the sum-rule method involves no new physical assumptions. However, potentials that do not commute with position, such as the neutron-proton exchange potential, will in general be different for the excited states than for the ground state. Then the argument given above that the photon absorption cross section can be determined from the ground state wave function alone does not apply in the simple manner given above. We can still use the sum-rule method based only on the ground state wave function; but the results are changed by an amount proportional to the strength of the exchange force.

Photodisintegration of the Deuteron

The comparison between theory and experiment for the photodisintegration of the deuteron serves to test the basic theory of photonuclear reactions given above, since we have reasonably accurate wave functions for at least the ground state of the two-body system. We shall find agreement in the moderate energy region; but we shall see that the experimental cross section is much higher than that calculated by the theory given above for the high-energy region from 70 to 300 Mev. There is at present a gap in experimental knowledge in the extremely interesting region from 25 to 70 Mev.

The effective range calculations of Bethe & Longmire (19) and Austern (20) give the essential results in the moderate energy region. The cross section for photodisintegration of the deuteron shows a resonance peak near the threshold attributable to photomagnetic transitions from the ground ^3S state to the virtual ^1S state. This theory agrees within experimental error with measurements of photodisintegration near threshold; but more accurate measurements of the same matrix element by study of the inverse reaction of radiative neutron capture by protons [von Dardel & Waltner (21)] show a discrepancy with the effective range theory calculation. About 6 per cent of the measured (n, γ) cross section should be attributed to the interaction of the magnetic field with the mesonic exchange currents in the deuteron. This experimental value is in agreement with theoretical estimates of the exchange current affect by Austern & Sachs (17) and Gray (22).

Above the resonance peak of the photomagnetic reaction, the deuteron photodisintegration cross section exhibits a peak at energy E_m double the threshold energy. This peak is not a resonance peak. Instead it is a result on the photoelectric cross section of the peaked momentum distribution in the ground state of the deuteron. (It is still an open question whether the peaks observed in the photodisintegration cross sections of moderate weight and heavy nuclei have a bona fide resonance character, like the photomagnetic disintegration of the deuteron, or whether they are more like the photoelectric disintegration of the deuteron.)

The calculations of effective range theory [Bethe (19)] on the photoelec-

tric disintegration have been checked to an accuracy of about 10 per cent by the total cross section measurements of Carver & Wilkinson (23) and others up to an energy of 17.6 Mev. Schiff (24) and Marshall & Guth (25) have calculated an angular distribution of photoprotons of the form $\sin^2\theta\,(1+2\beta\cos\theta)$, where β equals the velocity of the emitted proton divided by the speed of light. This forward asymmetry in the laboratory system is caused both by the momentum of the γ-ray, and by the interference of the electric quadrupole with the dominant electric dipole photodisintegration. Austern (26) has calculated a small isotropic term in the angular distribution attributable to noncentral forces. Careful measurements by Halpern & Weinstock (27) have checked the calculated forward asymmetry, but show an isotropic term in the angular distribution appreciably larger than Austern's calculated value. At present, the interpretation of this discrepancy is not clear.

Recent measurements of the high energy photodisintegration of the deuteron by Keck *et al.* (28) at Cornell, and Schriever *et al.* (29) at Illinois are in reasonable agreement with each other concerning the total cross section, and the angular distribution of the photoprotons. The total cross section for 200 Mev photons is almost ten times larger than that given by the (extrapolated) calculations of Schiff (24) and Marshall & Guth (25). Even at 70 Mev the Illinois measurement of total cross section disagrees with the calculations, but in a less striking manner. The large isotropic term in the experimental angular distribution at 70 Mev is suggestive of the similar term found by Halpern & Weinstock at lower energies.

While the large high-energy cross sections appear to be the result of photon interaction with the meson cloud, meson-theoretic calculations have not been successful to date. In any event, the failure in the deuteron case of the high-energy calculations, using Siegert's theorem, sets 70 Mev as a rough upper limit for the moderate energy calculations discussed in this paper.

Photodisintegration of Light Nuclei

In this section we shall discuss briefly Guth & Mullin's (30) calculation of the low-energy nuclear photoeffect in Be^9; the special selection rules for isotopic spin for electric dipole transitions; and measurements of electric dipole matrix elements from inverse reactions in which photons are emitted.

The nucleus Be^9 is especially simple to treat theoretically since for low-energy photodisintegrations one might only consider the transitions resulting from the one loosely bound "valence neutron." Guth & Mullin (30) have been remarkably successful in treating this low-energy photoeffect by making the approximation that the valence neutron with effective charge $-eZ/A$ moves in a square well potential of radius 5×10^{-13} cm., and depth 12 Mev for the (ground) P state, but depth only 3 Mev for the (excited) S and D states; this is because of the partly exchange character of the nucleon force. This model gives the sharp peak in the total cross section just above threshold, the subsequent dip, and gradual rise at higher energies; it also predicts the angular distribution of the emitted neutron. The calculations are in

reasonable agreement with experiments by Hammermesh & Kimball (31) and earlier measurements. At still higher energies, Nathans & Halpern's (32) measurements show that photoelectric transitions of the other more tightly bound nucleons become of major importance. The low-energy peak resulting from the transition of the valence neutron is clearly resolved from the high-energy peak, for which $E_m = 22$ Mev. The high-energy peak has the same form as the Be^9 (γ, p) or C^{12} (γ, n) cross sections.

Photodisintegrations of other light nuclei, such as those summarized by Ajzenberg & Lauritsen (33), provide a large amount of information about energies, spins, and parities of different nuclear levels; but do not appear so far to give as complete a picture as has been achieved in the Be^9 case.

However, one very useful unifying principle, the selection rule of isotopic spin (designated here by T), has been applied recently with great success by Telegdi (34), Wilkinson (35), Radicatti (36), and others. Since Telegdi is preparing a review article on this subject, we shall only state the assumptions and conclusions. The assumption is that nuclear forces are charge-symmetric (neutron-neutron equals proton-proton force) in which case the isotopic spin T is conserved in nuclear reactions. But for a self-conjugate nucleus, with $N = Z$, there is the additional selection rule that electric dipole transitions are forbidden for $\Delta T = 0$ transitions. One might understand this by arguing that electric dipole transitions must treat neutrons and protons differently, since they experience a different force in an electric field. But for a self-conjugate nucleus undergoing a $\Delta T = 0$ transition, the initial and final states are each completely symmetric for neutrons and protons; thus there is no possibility for the asymmetric electric dipole transition to occur between these states. This selection rule sets a threshold for allowed photoelectric transitions, and also establishes selection rules for the possible disintegrations of the excited nucleus.

In the preceding section we discussed the inverse process to photomagnetic disintegration of the deuteron as a valuable source of information on the photomagnetic cross section. The study of inverse reactions (i.e., radiative capture of neutrons, protons, etc.) has proved very helpful in studies of other light nuclei. In the last several years measurements have shown the presence of quite strong, and therefore electric dipole transitions. Wilkinson (37) has summarized recent data, and compares the experimental results with approximate estimates made by Weisskopf (13). In seven well-established cases of electric dipole transitions, Wilkinson finds that the quantity $(2J+1)$ (experimental width)/(Weisskopf width) varies from 0.08 to 0.45 (J is the spin of the excited state). This is certainly a surprisingly good agreement between inaccurate experiments and an order of magnitude theory.

Similar agreement between experimental widths and the Weisskopf approximate widths has been found from γ-transitions following neutron capture in light elements by Wilkinson (38) and Critchfield (39). The former considers slow neutron capture by nuclei from Li to C, and the latter, capture of neutrons of about $\frac{1}{2}$ Mev by nuclei from Na to Cu. These results all em-

phasize the importance of electric dipole transitions in photonuclear reactions, and further support the applicability of the independent particle model (IPM) for at least some calculations of dipole transition probabilities. (Weisskopf's approximation is based on the IPM, making the additional rough approximation that the wave functions for the individual nucleon being considered are constant throughout the nucleus and zero outside the nucleus for both initial and final nucleon states. This gives a dipole matrix element of about the radius of the nucleus, which is usually an overestimate of the value based on a more careful calculation with the IPM for some assumed common potential well.)

Nuclear Models for the Photoeffect

In this section we shall discuss in some detail various models that have been proposed for the absorption of moderate energy photons by medium and heavy nuclei: independent particle models; sub-unit models; and collective models. We then discuss sum-rule calculations which use only the ground state wave function. First let us summarize the results of the preceding two sections on photodisintegration of the deuteron and other light nuclei.

Measurements on the photodisintegration of the deuteron show the dominance of electric dipole transitions, and justify the calculations at moderate energies using Siegert's theorem. The relatively large experimental cross section above 70 Mev shows the inadequacy of Siegert's theorem, and thus provides an upper limit of 70 Mev, or less, for the calculations made in this section for heavier nuclei. Experiments on light nuclei show the success of the IPM for Be^9. Two principles were used successfully in the application of the IPM: the transitions of the loosely bound nucleons may be clearly separated from the transitions of the core nucleons; and exchange potentials give different well-depths for initial and final states. Experiments on other light nuclei show the success of isotopic spin selection rules for electric dipole transitions. Further, electric dipole transitions are observed with matrix elements comparable to Weisskopf's rough approximation, based on the IPM.

Most of these principles discussed for light nuclei should apply in calculations of the photoeffect for medium and heavy nuclei, ($A \geqq 40$): electric dipole transitions are predominant at moderate energies, but other (mesonic) effects predominate at high energies; the IPM might have appreciable successes, even using Weisskopf's rough matrix elements; exchange effects on the wave functions should be included. However, isotopic spin is no longer a good quantum number, because of the importance of the electrostatic repulsion of the protons. Of course the separation between light and medium nuclei is not sharp; Critchfield's work on neutron capture includes both groups, as does some of the theoretical work in this section.

The Mayer-Jensen shell model has had great success in dealing with the ground and lower excited states of very many nuclei. Calculations using the shell model, here referred to as the IPM, have been made by Wu (40),

Reifman (41), and Burkhardt (42). All three workers use the wave functions for ground and excited states for the same assumed nuclear potential (since exchange forces are neglected); and then calculate the matrix elements and cross sections for electric dipole photonuclear transitions. They all use a nuclear size parameter $r_0=1.5$, which is 20 per cent larger than some recent values [Hofstadter (43) and Rainwater (44)] of $r_0=1.2$ or less. (The nuclear radius $R=r_0\times10^{-13}\,A^{1/3}$.) They differ in the assumed shape of the nuclear potential. Wu uses a simple harmonic oscillator potential; Reifman, an infinite square well; and Burkhardt, a finite square well, adjusted to give the observed binding energy.

Wu's simple harmonic oscillator potential clearly gives a single sharp resonance peak at the energy difference E_m between the evenly spaced nuclear quantum levels. Wu has made an estimate of this resonance energy for various light nuclei: using $r_0=1.37$, E_m has the value 36 Mev for He^4; 29 Mev for Be^9; 24 Mev for Ne^{20}; and 16 Mev for Ca^{40}. For larger A we can estimate

$$E_m = 2.3A^{1/3}\hbar^2/MR^2 = 70A^{-1/3}\text{ Mev},$$

where we have used $r_0=1.2$. Here we have extended Wu's calculations to heavier nuclei and used a different r_0. Our equation gives the general trend of E_m; actually E_m would show jumps at the closed shell values.

Neither Wu nor the present author takes this extreme model seriously. The model suffers from the neglect of spin-orbit coupling; the poor approximation that the oscillator potential continues upward indefinitely; and the probable failure of the IPM, particularly for the excited state. The actual transitions would be over a band of single particle transitions, perhaps centered at E_m. However, this model gives the right order of magnitude of E_m (that is, in approximate agreement with experiment, and with other calculations using the IPM) rather simply; and it shows a pronounced resonance resulting from transitions between individual nucleon energy levels as an alternative to resonance caused by collective motion of the entire nucleus.

Reifman (41) discusses in some detail the relation between the IPM and the collective model for the entire nucleus. He discusses the rather close relation between the transition energies for single nucleon levels in an infinite square well, and Jensen's result using a collective model. (See discussion below.) Reifman's numerical results are meant just as an illustration. Our oversimplified presentation of his calculation of the transition energies follows. Let us, for simplicity, work with a rectangular box instead of the more appropriate spherical one. The energy of a level is proportional to the square of the wave number of a particle in the box: i.e. proportional to n^2/R^2, for quantum number n and size R for the box. The difference between the energies of successive levels is then proportional to n/R^2. The predominant electric dipole transitions are between successive levels, so E_m is proportional to n/R^2, or to $A^{-1/3}$, since n and R are each proportional to $A^{1/3}$. (We have found the dependence of n on A from the argument that the volume in phase space, which is proportional to n^3, must be sufficient to provide room

for A particles.) This is the same A-dependence of photon energy for the peak absorption as found above for the simple harmonic oscillator potential. Reifman finds $E_m = 83\ A^{-1/3}$ Mev for $r_0 = 1.2$, as used in this paper. (Note that E_m is inversely proportional to r_0^2 in all these models, so the result is quite sensitive to the assumed nuclear radius.)

Burkhardt (42) has made a detailed calculation of electric dipole absorption for the neutrons in the Cu^{63} nucleus. He uses a square well, with $r_0 = 1.5$, adjusted to give the observed neutron binding energy of 10.9 Mev. Burkhardt also includes spin-orbit coupling. (The present author believes that his treatment is inconsistent, but the spin-orbit coupling should not have very large effects on the shape of the photon absorption curve.) Burkhardt finds that almost all photon absorptions are for photons of energy near 9 Mev. The transitions are almost all to bound levels of the compound nucleus, in sharp contrast to the observed peak at about 17 Mev, almost always followed by particle emission. Burkhardt concludes that the IPM is inconsistent with photonuclear experiments. As discussed below, we believe that the IPM is reasonably successful in calculations for moderately heavy nuclei such as Cu, since the calculated value of E_m would be doubled if we used a smaller radius, and included the effect of exchange forces.

Winslow and Morrison (45) use both a different method of calculation and a different model from the rather similar models above: they calculate in momentum space, using the momentum distribution for assumed nuclear subunits. A momentum space calculation was used earlier by Levinthal & Silverman (46) for the high-energy photoeffect. If in our expression for the dipole matrix element we use the IPM and take the final nucleon wave function as a plane wave for the emitted nucleon, the squared dipole matrix element is proportional to the square of the momentum space wave function evaluated for the momentum of the emitted nucleon. That is, the photon absorption cross section is proportional to the probability of the nucleon having in its initial state the momentum that it has in the final state. The physical explanation is that, in the nonrelativistic approximation used here, a photon has a negligible momentum. Then if a nucleon is to have a given momentum in the final state, it must have already possessed it in the initial bound state. The assumption of a free final state is necessary, because otherwise the forces between nucleon and remaining nucleus in the final state could effect a transfer of momentum after the photon absorption. (We note that exchange forces should help validate this assumption of a free final state, as discussed above for Guth's work on Be.)

The assumption of nucleon wave functions without correlations in both initial and final states is necessary for the entire calculation, as for the other calculations above. But the qualitative results may well not depend on this dubious assumption. Levinthal & Silverman take their momentum distribution as that determined empirically from the neutron pick-up reaction. This distribution applies to high momenta, but probably not to the values corresponding to E_m, so Levinthal & Silverman's work will not be discussed

further here. These individual nucleon wave functions can be taken either for the entire nucleus using the IPM; or for a nuclear subunit, as by Winslow and Morrison. The first treatment neglects correlations resulting from forces between individual nucleons; the second treatment neglects the effect of the nucleus as a whole, and thus will give an answer completely independent of A. The truth might well lie between the two extreme models.

Winslow and Morrison argue that the individual nucleon is in an S-state in a nuclear subunit, for which they assume a variety of different potentials. In all cases, the positive energy of the emitted nucleon for the maximum cross section is about equal to the binding energy of the nucleon in the subunit. (As seen above, the two energies are exactly equal for the Bethe-Peierls or effective range treatment of the photodisintegration of the deuteron.) Then the photon energy E_m is about twice the binding energy of the nucleon in the subunit. The remainder of the nucleus greatly influences the subunit binding energy, thus affecting E_m. The calculated E_m is in reasonable agreement with experimental results of 15 to 20 Mev.

Winslow and Morrison also use a model in which the momentum distribution is that for the relative momentum of two nucleons in a degenerate Fermi gas without interactions. We interpret this as a first approximation to a quasi-deuteron model, a nucleon forming a quasi-deuteron with its nearest neighbor. This simple model gives the excellent value $E_m = 17$ Mev.

Winslow & Morrison further obtain asymptotic expressions for the shape of the photon absorption curve, both for low photon energies and for high photon energies. These asymptotic expressions, together with the peak energy E_m, and the area under the curve, which is determined by sum-rules, determine the general features of the photon absorption curve. They show that these general features are quite insensitive to the details of the assumed subunit model, and are in general agreement with experiment.

We note that these general features persist in the IPM. Electric dipole transition of low-energy do not occur since, in the present shell model, the low-lying states have angular momentum either the same or quite different from that of the ground state.

We have seen that these different models give rather similar and rather reasonable values for the peak energy E_m particularly if the smaller nuclear radius is used. Models using the IPM for the entire nucleus give E_m proportional to $A^{-1/3}$; while the subunit model gives E_m independent of A. An IPM with some nucleon correlations would be expected to give an A-dependence less rapid than $A^{-1/3}$, and thus in better agreement with present experimental results of $A^{-0.2}$ [Katz (3) and Halpern (4)]. However, while there is good evidence for the IPM for the ground state, it is unlikely to apply to states 10 or 20 Mev above the nuclear ground state. On the other hand we show below, using sum-rules, that the main features of the photon absorption curve are determined by the properties of the ground state alone. We believe that this provides the justification for using the IPM for both ground and excited states: the general features found in the calculation will persist even if the IPM does not apply to the excited states considered.

In the IPM we made the extreme assumption of noninteracting nucleons. An opposite approximation is that of very strongly coupled nucleons. In the latter approximation, here called the collective model, we concern ourselves with the normal modes of oscillation of the entire nucleus. This collective model of the compound nucleus has had considerable success in treating the properties of heavy nuclei at moderate excitation energies. The particular normal modes reached by absorption of electric dipole radiation will be those in which there is mass motion of protons against neutrons. If this motion can be treated as a damped simple harmonic oscillator, the calculation of the resonance energy can be performed classically, because of the close correspondence between classical and quantum-mechanical treatments of the simple harmonic oscillator problem.

We shall see that the calculations of Goldhaber & Teller (47), Steinwedel, Jensen & Danos (48), and Ferentz, Gell-Mann & Pines (49) give results for the resonance energy E_m which are in reasonable agreement with experiment. The calculations are not complete since the damping force on the simple harmonic oscillator is not calculated.

Goldhaber & Teller's work was of great significance as they were the first to emphasize the dipole character of the large photonuclear cross sections found in the 1947 General Electric Research Laboratory experiments. (See 49a, 49b.) They discuss three different approximations for classical harmonic oscillation of neutrons with respect to protons: each proton and each neutron oscillates around its equilibrium position, like ions in a crystal; protons and neutrons oscillate against each other as two compressible fluids; protons and neutrons oscillate against each other as two incompressible fluids. The three models give the classical frequency, proportional to E_m, varying respectively as: independent of A; $A^{-1/3}$; and $A^{-1/6}$. Since the last A-dependence was in best agreement with contemporary experiments (and also with more recent work [Katz (3), Halpern (4)]), Goldhaber & Teller pursued the last model and found that with not unreasonable choices of parameters it gave the experimental values of E_m.

Despite its good agreement with experiment, there are two major objections to Goldhaber & Teller's third model: it is not clear why the neutrons and protons should behave as "incompressible" fluids, and the theory contains two arbitrary parameters. The second objection is discussed by Present (50), who shows that E_m is related to the surface term for the dependence of binding energy on $Z-Z_0$ (the distance from the most favorable atomic number) in the semi-empirical binding energy formula. However, this surface energy term is poorly determined experimentally: in fact Present uses the comparison between Goldhaber-Teller's third model and photonuclear experiments to determine this surface energy term.

The second Goldhaber-Teller model of compressible neutron and proton fluids has been pursued in some detail by Steinwedel, Jensen & Danos (48). They answer the second objection concerning arbitrary constants by use of the accurately known volume term in the semi-empirical binding energy formula for dependence of energy on $(Z-Z_0)$. This term gives them the en-

ergy density corresponding to motion of the neutron fluid against the proton fluid with the constraint that the total nuclear density remains constant. From this energy density they compute the phase-velocity of the waves for the two-fluid oscillation. This phase velocity of about one fifth the speed of light is, to a first approximation, independent of A. The wave length of the oscillation of neutron fluid against proton fluid is determined as 3.02 R by the boundary conditions of an anti-node of displacement at the spherical nuclear surface of radius R. The frequency of the photons equals that of the nuclear oscillation: i.e., ν equals the phase velocity divided by the wave length or ν is proportional to $1/R$, or $A^{-1/3}$.

This A-dependence was already given by Goldhaber & Teller. Steinwedel, Jensen & Danos calculate the proportionality constant, finding a value of 60 $A^{-1/3}$ Mev for E_m. This value, computed for $r_0=1.42$, is about 30 per cent less than the experimental values; but much of this discrepancy is removed by the use of the value $r_0=1.2$ adopted in this paper, since the proportionality constant is proportional to r_0^{-1}. Steinwedel, Jensen & Danos also find that transitions to other excited states for the nuclear oscillation are quite small. However, they have made an error of a factor of two in σ_{int} for the integral over energy of the electric dipole cross section. [See Reifman (41) and also Danos, private communication for which we are grateful.] Their corrected σ_{int} agrees with the sum-rule result (for pure ordinary forces), discussed below.

Quite recently Ferentz, Gell-Mann & Pines (49) have considered plasma oscillations for the neutron and proton fluids. Starting with a quantum-mechanical treatment of a many-body system with the partly exchange two-body neutron-proton forces, they argue that plasma oscillations of fluids should occur. They calculate the resonance frequency for excitation of the first plasma oscillation, giving $E_m=80\ A^{-1/3}$ Mev in reasonable agreement with the Steinwedel-Jensen-Danos classical calculation. But the later calculation would be more fundamental in that it uses the two-body potential, and attempts a quantum-mechanical justification of the two-fluid model. (We have not seen the complete calculation, and therefore cannot evaluate it.) Ferentz, Gell-Mann & Pines also calculate E_m for plasma oscillations using sum-rules for various moments of the $\sigma(W)$ curve, including the nucleon correlations of the two-fluid model, obtaining again the result given above. (Sum-rule calculations must agree with direct calculations of the $\sigma(W)$ curve if the same nuclear model is used.)

The electric dipole absorption of electromagnetic energy by a charged classical simple harmonic oscillator, integrated over the resonance absorption curve, gives a result that depends on the charge and mass of the oscillator, but is independent of the natural frequency of the oscillator, or of the amount of damping. This result for the integrated absorption of electromagnetic energy carries over exactly into quantum-mechanical calculations in atomic physics, giving the Thomas-Reiche-Kuhn sum-rule for electric dipole

absorption of photons by Z electrons in an atom:

$$\sigma_{int} = \int \sigma dW = (2\pi^2 e^2 \hbar/mc)Z.$$

Here e is the electron's charge, and m its mass. This result is derived by summing over all possible final states (hence the name "sum-rule"); the derivation needs only the quantum-mechanical expression for the commutator between the momentum and position operators.

The integrated cross section is modified for the nuclear photoeffect by the two effects discussed above (Basic Theory): the use of effective charges; and the significance of exchange forces. The first changes the factor Z to NZ/A, where Z is the atomic number, and $N=A-Z$ is the neutron number. Also, the proton mass should be used in the denominator in place of m. We then have the expression, known for about 20 years,

$$\sigma_{int} = 0.06\ (NZ/A) = 0.015A \text{ Mev-barns.}$$

The last expression makes the good approximation $NZ/A = A/4$. All detailed models that neglect exchange forces must give this result.

Feenberg (51) first showed that neutron-proton exchange forces modified sum-rule results; while Siegert (16) estimated that attractive exchange forces would roughly double σ_{int}. Levinger & Bethe (52) made a more detailed, but still rather approximate, calculation of the increase in σ_{int} attributable to exchange forces, and found that if the neutron-proton potential were entirely exchange in character, this would cause an 80 per cent increase in σ_{int}. If exchange forces are a fraction x of the two-body neutron-proton force we have:

$$\sigma_{int} = 0.015A(1 + 0.8x) \text{ Mev-barns.}$$

The number 0.8 was calculated using a nuclear model of a degenerate Fermi gas. Levinger & Bethe neglect effects of the nuclear surface which would give some A-dependence to the coefficient 0.8. Also, other potentials that do not commute with position (e.g. spin-orbit coupling) will change the integrated cross section [see Sachs & Austern (17)], but we believe that the change in σ_{int} should be considerably smaller than that caused by exchange forces. The value of σ_{int} is then independent of the nuclear model, except for the value of the coefficient 0.8 and possible small terms.

The first stage in the study of the nuclear photoeffect was to establish reasonably good agreement between experimental values of σ_{int} and the equation given above, since if this failed, any specific model would fail as well. The present stage is the examination of specific models. In the first stage of making the comparison for σ_{int} two difficult problems arise. The first mentioned in our introductory section, is that the cross section for photon absorption is usually not measured directly, but must be inferred from various partial cross sections. The second problem is the upper limit to be taken in the integral for the experimental determination of σ_{int}. The theoretical

value of infinity is worse than impractical: we now know that it is incorrect since at energies of above about 70 Mev mesonic processes greatly influence the nuclear photoeffect. [This is most clearly shown at present by measurements on the photodisintegration of the deuteron, as discussed above; but it is also demonstrated by Jones & Terwilliger's (6) neutron yield measurements.] These mesonic processes, in which the electromagnetic field acts on the mesonic charge, are not explicitly taken into account in the present theory. (While the present work does include exchange forces, ultimately based on meson currents, it includes them in a phenomenological manner. The large explicit mesonic effects occur at high photon energies, where the photon wave length is short enough for the photon to see the details of the mesonic exchange currents, and Siegert's theorem fails.) The rule-of-thumb of integrating the experimental cross section only to 80 Mev, as done by Jones & Terwilliger (6), seems the best solution for the present. We should then include little of the mesonic processes, and miss not too much of the nonmesonic σ_{int} since nonmesonic photonuclear cross sections decrease rapidly at higher energies.

Jones & Terwilliger find for Ta^{181} that $\sigma_{int}=5.1$ Mev-barns, with an uncertainty of 20 per cent. This is larger than the calculated value of 2.61 $(1+0.8x)$ Mev-barns, even using the extreme value $x=1$, for complete exchange force. Using the 20 per cent experimental uncertainty to find the lower limit for σ_{int}, we find that $x>0.85$, or rather larger than the values from 0.5 to 0.7 found from neutron-proton scattering. We regard this as a reasonable agreement between experiment and calculation for Ta^{181}, considering that both are still somewhat preliminary.

Katz (3) and Halpern (4) have made a similar comparison for many nuclei; they integrate only to 25 Mev and find deviations from the calculated σ_{int} at low A. We believe that use of 70 Mev as an upper limit would give reasonable agreement with the calculated σ_{int}. [See Nathans & Halpern (4).]

Sum-rule calculations can also be used in the second stage to give various moments of the photon absorption curve, thus making it possible to estimate the peak energy E_m, and even the width Γ. Levinger & Bethe (52) define two energies: the mean energy

$$\overline{W} = \int \sigma(W) W dW / \sigma_{int}$$

and the harmonic mean energy

$$W_H = \sigma_{int} / \int \sigma(W) W^{-1} dW.$$

Calculation of these energies demands knowledge of the nuclear ground state wave function, while calculation of σ_{int} did not need such knowledge, except for the calculation of the coefficient 0.8 for the effects of exchange forces. Levinger & Bethe assume no correlations between the nucleons. For ordinary forces this gives W_H proportional to $A^{-2/3}$ and $\overline{W}$ independent of A. They also calculate the effects of exchange force on W_H and $\overline{W}$. The

former calculation is quite simple: the denominator in the expression for W_H is unchanged by exchange forces; while the numerator σ_{int} is increased by about $0.8x$, as discussed above. Then exchange forces increase W_H by about 50 per cent above its value for ordinary forces. The numerator in the expression for $\overline{W}$ is greatly increased by exchange forces, becoming a quadratic function of x:e.g. for a Yukawa potential between neutrons and protons, and $r_0=1.37$, Levinger & Bethe find

$$\overline{W} = (19 + 36x + 48x^2)/(1 + 0.7x) \text{ Mev}$$

$\overline{W}$ would be increased by about 20 per cent if we used our present value $r_0=1.2$, but the number 19 in the numerator should be decreased, as discussed in the next paragraph.

The values of W_H and $\overline{W}$ given by Levinger & Bethe for pure ordinary forces do not apply even to the IPM, since they assumed no correlations among the nucleons, and correlations are always present because of the Pauli exclusion principle. We find a large discrepancy between Levinger & Bethe's calculations for the Cu^{63} nucleus (pure ordinary force) and Burkhardt's (42) recent calculations discussed above. Only part of this discrepancy can be explained by the somewhat different varieties of IPM used.

The present author and Kent are at present using sum-rules to find $\overline{W}$ and W_H for ordinary forces for the IPM. Calculations were made including Pauli-principle correlations for nucleon wave functions in a square-well of the nuclear radius, and depth adjusted to give the proper binding. The latter is Burkhardt's model, but without any spin-orbit coupling. While Levinger & Bethe gave $W_H=2.9$ Mev for Cu, in contrast to Burkhardt's 8.4 Mev, the present calculation (53) gives 8.3 Mev in excellent agreement with Burkhardt. We see that a calculation using sum-rules will agree, as indeed it must, with a direct calculation for cross sections for transitions to the various excited states. (We want to emphasize that a sum-role calculation is just another way of finding the moments of the $\sigma(W)$ curve.) A more interesting question is whether the two calculations, now in agreement with each other, are in agreement with experiment. Even the sum-rule calculation using the smaller radius $r_0=1.2$ gives $W_H=12.7$ Mev, which is still appreciably less than the experimental value of about 20 Mev. (The latter is found from Jones & Terwilliger's data.) Most of this discrepancy would be removed by the roughly 50 per cent increase in the harmonic mean energy W_H which arises from exchange forces.

We conclude that the IPM works reasonably well for calculations of the photoeffect in Cu since we modify Burkhardt's (42) results by using a smaller r_0 and by including the effects of exchange forces. Levinger & Kent (53) have calculated W_H for Ta^{181} finding $W_H=8.9$ Mev for $r_0=1.2$ and pure ordinary forces. Again, a 50 per cent increase for exchange forces would remove most of the discrepancy with the experimental value of W_H about 15 Mev.

We see that there are several apparently quite different nuclear models that give values of E_m in reasonable agreement with each other, and not in

disagreement with photonuclear experiments. The relationship between the IPM for noninteracting nucleons and the collective model for motion of the entire nucleus has recently been discussed by Bohr (54), Hill & Wheeler (55), and Reifman (41). These workers believe that the apparently contradictory models are each reasonable approximations; Reifman has discussed their applicability to photonuclear reactions. (The IPM should correspond to Goldhaber & Teller's second model, also used by Jensen, Steinwedel & Danos; while the subunit model of Winslow & Morrison should correspond to Goldhaber and Teller's first model.) More work is needed to clarify further the relations among the various nuclear models. Measurements of E_m alone will not decide between them. [See Morrison in (56).]

The sum-rules show that exchange forces have an appreciable effect on photonuclear reactions. Exchange forces should be taken into account in the various models; but this has proved quite difficult.

The Products of Photonuclear Reactions and the High-Energy Nuclear Photoeffect

In this section we discuss briefly the third stage of development of photonuclear theories: i.e., the explanation of the width of the $\sigma(W)$ curve, of the products of photonuclear reactions, and of the high-energy nuclear photoeffect. The various theories, while rather successful in explaining the energy E_m for the peak of the photon absorption curve, have not progressed far beyond this point. In this section we shall state the problems (with only a few references to the experiments); but we shall not be able to give any answers.

The width Γ shows interesting variations at the magic number nuclei, as shown by Nathans & Halpern (4).

While the main features of the competition among the possible products of photonuclear reactions are given by the statistical theory of the compound nucleus, experiments have shown the existence of photoprotons with total yield and energy distribution inconsistent with the statistical theory. [See, for example, Butler & Almy (57).] This indicates a direct photoeffect, as proposed by Courant (58). Courant's calculations for the IPM in a square well should be modified for a smaller nuclear radius, and to include effects of exchange forces: both these changes would increase the cross section so as to give better agreement with experiment. Experiments also indicate the existence of direct photoneutron emission. The angular distributions of the high-energy photoprotons vary markedly from one nucleus to another. Results on some nuclei can be interpreted as primarily electric dipole absorption, with a forward asymmetry attributable to interference with electric quadrupole absorption; but other nuclei do not fit this picture. The yield of photodeuterons is also higher than given by the statistical theory.

Measurements of elastic and inelastic γ-scattering [Stearns (7), Katz *et al.* (8), Telegdi *et al.* (9) and Fuller & Hayward (10)] are of importance both for determination of the complete photon absorption curve, and for evalua-

tion of the various theories of the photonuclear effect. Thus, the existence of appreciable inelastic scattering rules out a strict interpretation of the collective model, in which there is one excited state, and one ground state. But a first correction to this model shows that the excited state has a large energy spread, and the nuclear "ground state" is also split into different quantum states all of which have no mass motion of neutrons versus protons, but differ somewhat in energy because of various perturbations. On the other hand, the extreme IPM, as discussed by Levinger & Bethe (52) would give γ-scattering rather less than experimental values, though here the theoretical estimate is inaccurate. We should note that Telegdi (9) was able to use the IPM to obtain reasonable agreement with his experimental results on excitation of nuclear isomers by inelastic γ-scattering. Further experimental work in the difficult field of cross sections and angular distributions of γ-rays scattered by nuclei will be of great help in improving the various theories of the nuclear photoeffect.

The high-energy nuclear photoeffect lies outside the scope of this article, as it involves explicit mesonic effects; but it is of interest here as evidence for the applicability of a nuclear subunit model at least in the high-energy region. Wilson (59) reconciled the arguments supporting a nuclear subunit model with those supporting an interpretation in terms of meson production. He proposed photon interaction with "virtual mesons" in a small nuclear subunit (quasi-deuteron) thus obtaining the relatively large high-energy cross sections implied by mesonic interactions, and the strongly forward angular distribution attributable to the large center of mass motion for absorption of a high-energy γ-ray by a small nuclear subunit.

Yoshida (60) has calculated the effects of different assumed sizes for the subunit. Recent measurements by Weil & McDaniel (61) on high-energy protons ejected from carbon by monoenergetic γ-rays are in fortuitously good agreement with the two particle quasi-deuteron model of the present author (62), using experimental cross sections for the deuteron photodisintegration. (However, recent results of Feld *et al.* (63) disagree with other experiments, and with the quasi-deuteron model.) Since the quasi-deuteron model has worked unexpectedly well, we might mention two factors which would make it more trustworthy than anticipated for high-energy processes and perhaps even for moderate energy processes. First, the experiments which select high-energy protons (or neutrons) also select just those high-energy processes where the photon has interacted with a very small nuclear subunit; since interaction with a larger subunit would tend to distribute the photon's energy among more particles, thus making it unlikely for a high-energy nucleon to be produced. (Experiments on high-energy stars might well agree with a different model.) Second, the possible existence of repulsive three-body forces, combined with the Pauli principle correlations, would greatly inhibit the formation of subunits larger than the quasi-deuteron.

Thus theories and experiments on photonuclear reactions have passed the first stage of establishing the predominance of electric dipole absorption

in the moderate energy region, and of checking σ_{int} for the absorption curve. Theories and experiments have made considerable progress in the second stage of interpreting and measuring the peak energy E_m for the photon absorption curve for various nuclei. Here we have several successful approximate theories without a clear understanding of why they agree so well with each other. Experiments have made considerable progress on the third stage of the detailed shape of the absorption curve (such as the width Γ), and on the products of photonuclear disintegration. Some experimentalists hope to determine whether a collective model or an IPM many-level model is correct. Each model is incorrect if taken literally, and must be regarded only as a preliminary first approximation. The theorists face the problem of how to make the next approximation.

LITERATURE CITED

1. Strauch, K., *Ann. Rev. Nuclear Sci.*, **2**, 105–28 (1952)
2. Chastel, R., *J. phys., radium*, **14**, 50–61 (1953)
3. Montalbetti, R., Katz, L., and Goldemberg, J., *Phys. Rev.*, **91**, 659–73 (1953)
4. Nathans, R., and Halpern, J., *Phys. Rev.*, **93**, 437–42 (1954)
5. Titterton, E. W., (Review article being prepared for *Progr. Nuclear Phys.*)
6. Jones, L. W., and Terwilliger, K. M., *Phys. Rev.*, **91**, 699–707 (1953)
7. Stearns, M. B., *Phys. Rev.*, **87**, 706–15 (1952)
8. Goldemberg, J., and Katz, L., *Phys. Rev.*, **90**, 308–14 (1953)
9. del Rio, C. S., and Telegdi, V. L., *Phys. Rev.*, **90**, 439–42 (1953)
10. Fuller, E. G., and Hayward, E., *Natl. Bur. Standards* (*U.S.*), Report 3129 (1954) (Unpublished)
11. Brown, K. L., and Wilson, R., *Phys. Rev.*, **93**, 443–52 (1954)
12. Koch, H. W., and Foote, R. S., *Phys. Rev.*, **91**, 455 (A) (1953)
13. Blatt, J. M., and Weisskopf, V. F., *Theoretical Nuclear Physics*, Appen. B, Ch. XII (John Wiley & Sons, Inc., New York 16, N. Y., 846 pp., 1952)
14. Sachs, R. G., *Nuclear Theory*, Ch. 9 (Addison-Wesley, Cambridge, Mass., 383 pp., 1953)
15. Bethe, H. A., *Revs. Mod. Phys.*, **9**, Sect. 87–90, 71–229 (1937)
16. Siegert, A. J. F., *Phys. Rev.*, **52**, 787–89 (1937)
17. Sachs, R. G., and Austern, N., *Phys. Rev.*, **81**, 705–9 (1951); Austern, N., and Sachs, R. G., *Phys. Rev.*, **81**, 710–16 (1951)
18. Foldy, L. L., *Phys. Rev.*, **92**, 178–88 (1953)
19. Bethe, H. A., and Longmire, C., *Phys. Rev.*, **77**, 647–54 (1950)
20. Austern, N., *Phys. Rev.*, **92**, 670–74 (1953)
21. von Dardel, G., and Waltner, A. W., *Phys. Rev.*, **91**, 1284–85 (1953)
22. Gray, E. P. (Doctoral thesis, Cornell Univ., Ithaca, New York, 1952) (Unpublished)
23. Carver, J. H., and Wilkinson, D. H., *Nature*, **167**, 154–55 (1951)
24. Schiff, L. I., *Phys. Rev.*, **78**, 733–37 (1950)
25. Marshall, J. F., and Guth, E., *Phys. Rev.*, **78**, 738–44 (1950)
26. Austern, N., *Phys. Rev.*, **85**, 283–90 (1952)
27. Halpern, J., and Weinstock, E. V., *Phys. Rev.*, **91**, 934–39 (1953)
28. Keck, J., Littauer, R. M., O'Neill, G. K., Perry, A. M., and Woodward, W. M. (Submitted to *Phys. Rev.*)
29. Schriever, B. D., Whalin, E. A., and Hanson, A. O., *Bull. Am. Phys. Soc.*, **29**, No. 1, paper JA 4 (1954)
30. Guth, E., and Mullin, C. J., *Phys. Rev.*, **76**, 234–44 (1949); *Phys. Rev.*, **76**, 682 (1949)
31. Hammermesh, B., and Kimball, C., *Phys. Rev.*, **90**, 1063–65 (1953)
32. Nathans, R., and Halpern, J., *Phys. Rev.*, **92**, 940–41 (1953)
33. Ajzenberg, F., and Lauritsen, T., *Revs. Mod. Phys.*, **24**, 321–402 (1952)
34. Gell-Mann, M., and Telegdi, V. L., *Phys. Rev.*, **91**, 169–74 (1953); Telegdi, V. L. (Review article being prepared for *Revs. Mod. Phys.*)
35. Wilkinson, D. H., and Jones, G. A., *Phils. Mag.*, **44**, 542–47 (1953)
36. Radicatti, L. A., *Phys. Rev.*, **78**, 521 (1952); *Proc. Phys. Soc.* (*London*) [A]**67**, 39–43 (1954)
37. Wilkinson, D. H., *Phil. Mag.*, **44**, 450–51 (1953)
38. Wilkinson, D. H., *Phil. Mag.*, **44**, 1019–27 (1953)
39. Critchfield, C. L., *Calculation of Capture Cross Sections* (Unpublished, 1953)

40. Wu, S. S. (Doctoral thesis, University of Illinois, Urbana, Illinois, 1951) (Unpublished)
41. Reifman, A., *Z. Naturforsch.*, **8a,** 505–22 (1953)
42. Burkhardt, J. L., *Phys. Rev.*, **91,** 420 (1953)
43. Hofstadter, R., Fechter, H. R., and McIntyre, J. A., *Phys. Rev.*, **92,** 978–87 (1953)
44. Fitch, V. L., and Rainwater, J., *Phys. Rev.*, **92,** 789–800 (1953)
45. Winslow, A. (Doctoral thesis, Cornell Univ., Ithaca, New York, 1952) (Unpublished); Morrison, P., Report to Photonuclear Conference, Cambridge, Mass., May, 1953 (Unpublished)
46. Levinthal, C., and Silverman, A., *Phys. Rev.*, **82,** 822–26 (1951)
47. Goldhaber, M., and Teller, E., *Phys. Rev.*, **74,** 1046–49 (1948)
48. Steinwedel, H., and Jensen, J. H. D., *Z. Naturforsch.*, **5a,** 413–19 (1950); Danos, M., *Ann. phys.*, **10,** 265–81 (1952)
49. Ferentz, M., Gell-Mann, M., and Pines, D., *Phys. Rev.*, **92,** 836–37 (1953)
49a. Lawson, J. L., and Perlman, M. L., *Phys. Rev.*, **74,** 1190 (1948)
49b. Baldwin, G. C., and Kleiber, G. S., *Phys. Rev.*, **73,** 1156 (1948)
50. Present, R. D., *Phys. Rev.*, **77,** 355–56 (1950)
51. Feenberg, E., *Phys. Rev.*, **49,** 328–31 (1936)
52. Levinger, J. S., and Bethe, H. A., *Phys. Rev.*, **78,** 115–29 (1950)
53. Levinger, J. S., and Kent, D. C. (Paper in preparation for submission to *Phys. Rev.*)
54. Bohr, A., and Mottelson, B. R., *Phys. Rev.*, **89,** 316–17 (1953)
55. Hill, D. H., and Wheeler, J. A., *Phys. Rev.*, **89,** 1102–45 (1953)
56. Segrè, E., *Experimental Nuclear Physics*, **II,** 114–23 (John Wiley & Sons, Inc., New York 16, N. Y., 600 pp., 1953)
57. Butler, W. A., and Almy, G. M., *Phys. Rev.*, **91,** 58–65 (1953)
58. Courant, E. D., *Phys. Rev.*, **82,** 703–9 (1951)
59. Wilson, R. R., *Phys. Rev.*, **86,** 125–26 (1952)
60. Yoshida, S., *Progr. Theoret. Phys. (Japan)*, **6,** 1032–34 (1951)
61. Weil, J. W., and McDaniel, B. D., *Phys. Rev.*, **22,** 391–400 (1953)
62. Levinger, J. S., *Phys. Rev.*, **84,** 43–51 (1951)
63. Feld, B. T., Godbole, R. D., Odian, A., Scherb, F., Stein, P. C., and Wattenberg, A. (Submitted to *Phys. Rev.*)

RADIOFREQUENCY AND MICROWAVE SPECTROSCOPY OF NUCLEI[1]

By G. E. Pake[2]

Department of Physics, Washington University, St. Louis, Missouri

Introduction

Radiofrequency spectroscopy has grown rapidly following the successful application in 1945 of the magnetic resonance principle to nuclei in bulk matter. There have been, of course, immediate consequences for Nuclear Science, and the past year has seen a continued compilation of nuclear moment data, with unstable nuclei becoming less infrequently the subjects of study. But it is also a delightful feature of the accelerated activity in this field that it has operated to retard the seemingly inevitable march of modern science toward further compartmentalization. Whether one observes a nuclear magnetic dipole transition in the radiofrequency range or the influence of nuclei upon such electronic transitions in the microwave region of the spectrum, a resonance experiment is just as likely to bear upon questions concerning the structure and properties of molecules, of liquids, and of solids as it is upon nuclear structure. Results reported in 1953 continued to weave strong ties between the well-recognized and labeled areas of Nuclear Physics, the Physics of Solids, and Chemistry.

This report seeks to outline, with emphasis upon the implications for Nuclear Science, the year's progress in atomic and molecular beam radiofrequency spectroscopy, nuclear induction or nuclear magnetic resonance, and microwave spectroscopy as it reflected nuclear properties. Because of limitations in space and time, much of the report can be little more than a guide to the periodical literature.[3] However, two events considered to be of special significance will be treated in more detail: the development in Canada of a new detector for atomic beams (Wessel & Lew), and a proposal by Overhauser of a new method for polarizing nuclei, subsequently verified in a magnetic resonance experiment by Carver & Slichter.

New Measurements of Nuclear Spins and Moments

The number of stable nuclides with unknown spin or magnetic moment has further dwindled in 1953. The great body of unstable nuclides, on the

[1] The survey of literature pertaining to this review was concluded in February, 1954.

[2] The author wishes to thank Dr. H. Lew for permission to use Figures 1 and 2, Dr. C. P. Slichter for permission to use Figure 4, and Dr. H. S. Gutowsky for permission to use Figure 5.

[3] More detailed treatment of certain topics discussed in this chapter, as well as background material for the entire chapter, can be found in an excellent book by N. F. Ramsey entitled *Nuclear Moments* (John Wiley & Sons, New York, N.Y., 169 pp., 1953).

TABLE I

NUCLEAR SPIN AND MOMENT MEASUREMENTS REPORTED IN 1953

Z	Atom	A	I	μ (nuclear magnetons)	Q (10^{-24} cm.^{2})	References		
						I	μ	Q
1	D, H	2	(1)		0.002738[14]			5
5	B	10	(3)		0.0740[50]			6
5	B	11	(3/2)		0.0355[20]			7
11	Na	24*	4	1.688[5]		8	8	
13	Al	27	(5/2)		0.149[2]			9
14	Si	29	1/2	−0.55492[4]		10, 11	1	
16	S	33	(3/2)	0.64292[14]			1	
19	K	42*	2	−1.137[5]		8	8	
20	Ca	43	7/2	−1.3152[2]		12	12	
22	Ti	47	5/2	−0.78706[10]		13	13	
22	Ti	49	7/2	−1.1022[2]		13	13	
23	V	50	6			14		
24	Cr	53	(3/2)	−0.47351[60]			15, 16	
26	Fe	57		<0.05			17	
27	Co	57*	7/2	4.6[2]		18	18	
29	Cu	63	(3/2)		−0.16			19
29	Cu	65	(3/2)		−0.14			19
30	Zn	67	(5/2)	0.87378[13]			1	
32	Ge	73	(9/2)	−0.87675[12]			13	
33	As	75	(3/2)	1.4347[3]			1	
34	Se	77	(1/2)	0.53326[5]			1	
34	Se	79*	(7/2)	−1.015[15]	0.7[2]		20	20
37	Rb	86*	2	−1.69[1]		8	8	
38	Sr	87	(9/2)	−1.0892[1.5]			16	
47	Ag	107	(1/2)	−0.113024[13]			21†	
47	Ag	109	(1/2)	−0.129936[13]			21†	
52	Te	123	(1/2)	−0.73188[4]			1	
52	Te	125	(1/2)	−0.88235[4]			1	
53	I	131	7/2		−0.412[4]	22		22
55	Cs	131	5/2	3.48[4]		8	8	
55	Cs	134*	4	2.95[1]		8	8	
59	Pr	141	(5/2)	3.8[4]	−0.054[?]		23	23
79	Au	197	(3/2)	0.13[1]			21	
83	Bi	210	0			24		

* An asterisk following the mass number indicates a radioactive nuclide.

† Measurement by Jeffries & Sogo quoted from private communication. This has subsequently appeared in *Phys. Rev.*, *93*, 174 (1954).

Parentheses around the nuclear spin signify that it was known prior to 1953. Magnetic moments are given without diamagnetic correction, and the number in brackets following a nuclear magnetic or quadrupole moment is the estimated error in the last significant figure quoted.

other hand, has scarcely been touched by radiofrequency and microwave techniques. Table I tabulates those data representing new nuclear spin and/or moment measurements made during the year by these techniques. An asterisk after the mass number identifies an unstable nuclide. Parentheses about the spin indicate that it was previously known.

A number of the entries in Table I were contributed by Weaver, who describes in detail the improved nuclear induction spectrometer with which excellent sensitivity has been obtained (1). Several other descriptions of magnetic resonance apparatus appeared during the year (2, 3, 4).

Atomic and Molecular Beam Magnetic Resonance

By extending experiments to higher frequencies, Lew & Wessel (9) have measured the hyperfine structure interval for the $3p\ ^2P_{1/2}$ state of Al^{27} as 1506.14 ± 0.05 Mc./sec. This experiment has also afforded the new determination of the Al^{27} quadrupole moment given in Table I.

The Harvard molecular beam study of H_2 and D_2 has been extended (5) to intermediate and high magnetic fields, testing the validity of the theory of molecular H_2 in the intermediate field region for the first time. The D_2 measurements, taken at a stronger field than any used previously, provide more accurately determined molecular constants and the most recent value (Table I) of the quadrupole moment of the deuteron, $(2.738 \pm 0.014) \times 10^{-27}$ cm.^{2}. The uncertainty here is that of the theoretically calculated electric field gradient. In general, the validity of the interaction Hamiltonian seems to be confirmed in these new regions of magnetic field.

In Canada, Lew has begun a study of the rare earths by the atomic beam magnetic resonance method (23), the first to be investigated being Pr^{141}. Considerable information on the rare earth nuclear moments is lacking, and this program of experiments is thus a most welcome one. For Pr^{141}, it is found that $\mu = +(3.8 \pm 0.4)\ nm$ and $Q = -0.054 \times 10^{-24}$ cm.^{2}.

The development by Wessel & Lew (21) of a new detector for atomic beams, as mentioned in the introduction above, is of particular interest. The problem of detecting neutral atoms or molecules, after they have passed through the deflecting fields of the beam apparatus, has long been the bottleneck in wide application of this powerful and elegant experimental technique to all the elements. Essentially two methods have been used: one, the Pirani detector, is applicable only to gases; the second is the surface detector, which places a heated filament in the path of the beam. If the atom has an ionization potential smaller or at most nearly equal to the work function of the filament, there is a probability that the atom will give its electron up to the metal and thus become a positive ion. Special properties, such as radioactivity or the electron affinity of the halogens help somewhat to extend the use of beams, but most nongaseous elements with ionization potentials exceeding six volts have not been accessible.

In searching for a detector of general applicability, Wessel & Lew have sought to ionize atoms of the beam by means of electrons oscillating transversely across the beam. The ionizer probably is capable of ionizing any

atom or molecule, but it therefore may ionize atoms of the residual gases in the vacuum, and thus there is a severe background problem. Of course, a very strong source can in principle overcome such difficulties, but the ionizer efficiency for beam atoms is low enough to assure that background must almost always be reckoned with. Sensitivity is improved up to 100 fold by employing the so-called "lock-in" amplifier which has played such an important role in nuclear magnetic resonance and induction. In this case, the modulation is achieved by a rotating chopper which interrupts the beam near the source at 10 c.p.s. The reference signal is obtained from a photocell upon which falls a light beam modulated by a rotating disk. The same motor drives both this disk and the chopper.

The means of detecting ions produced by the electron bombardment ionizer is a mass spectrometer which focuses the ions on an electron multiplier. An indication of the seriousness of the background problem is that the spectrometer is not, in most cases, adequately selective without the use of the beam chopper and lock-in amplifier to distinguish the signal from the unmodulated background.

The apparatus is diagrammed in Figure 1, which also shows the amplification system. Figure 2 is an exploded view of the electron bombardment ionizer. Ionization occurs in a chamber (*a*) which has slits on either side exposing the beam to electrons from tungsten filaments, one of which (*b*) is shown stretched between clamps (*c*). The mounting is a piece of fired lava (*l*). The ions formed are accelerated out of the chamber by electrodes (*e*), (*g*), and (*h*). The potential difference between (*e*) and the chamber (*a*) is from 0 to 20 volts. The potential of (*a*) relative to (*h*), which is at ground, is determined by the mass of the ion and the mass spectrometer magnetic field.

As a first test for this detector, Wessel & Lew have studied stable isotopes of silver and gold, which have respectively ionization potentials of 7.57 and 9.22 volts. They have measured the hyperfine structure of the ground states, and have compared the gyromagnetic ratios of the free atoms with that of the free electron (using Cs^{133}). Although the obtained nuclear magnetic moments for the silver isotopes do not improve on previous data from optical spectroscopy, these measurements indicate that the best value for Au^{197} is $\mu = 0.13 \pm 0.01$ *nm*. (Subsequent to Wessel & Lew's work, Jeffries & Sogo have measured the moments of the stable silver isotopes; see footnote to Table I.) Another atom made accessible by the new detector is Cr^{52}, which has $I = O$ and a $^7S_3$ ground state (25).

The improved value of the B^{11} quadrupole moment (Table I) was obtained with this apparatus by Wessel (7). From it, and Dehmelt's (6) value of the ratio $Q(B^{10})/Q(B^{11})$, the improved value of the B^{10} quadrupole moment has also been obtained.

Polarization of Nuclear Spins by the Overhauser Method

One of the outstanding developments of 1953, in radiofrequency and microwave spectroscopy of nuclei, was the proposal by Overhauser of a new

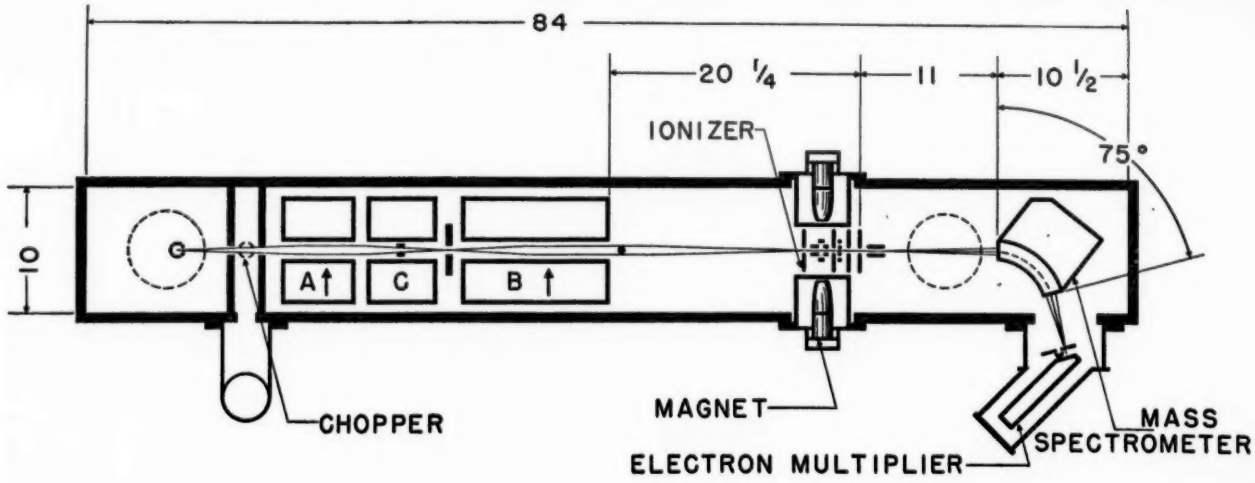

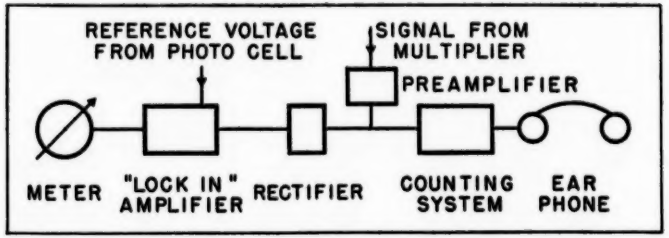

FIG 1. Atomic beam apparatus of Wessel & Lew, showing location of the electron bombardment ionizer and a block diagram of the amplification system.

method for polarizing nuclei (26, 27). Subsequently, Carver & Slichter (28) verified the principle experimentally, although it may be some time before experimental difficulties involved in applying the method at low temperatures will be overcome in order to obtain appreciable ($\geqq 10$ per cent) polarization.

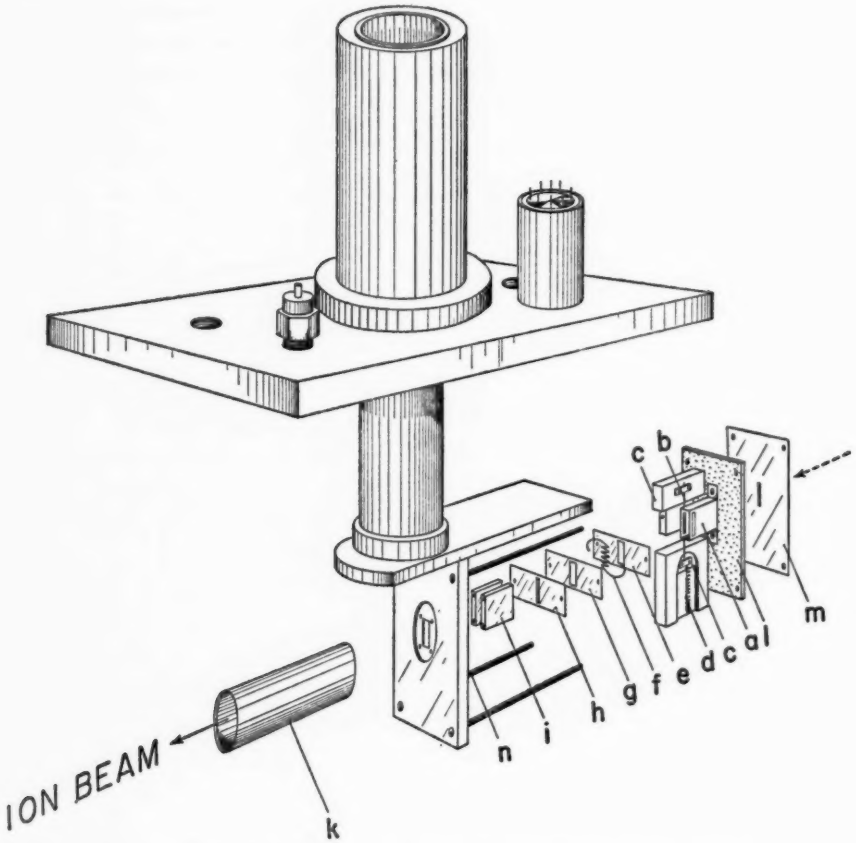

FIG. 2. Exploded view of the electron bombardment ionizer used by Wessel & Law.

The method has essentially two requirements: (*i*) the nuclear spins must "relax" through an interaction with electron spins of the form $a\mathbf{I}\cdot\mathbf{s}$; and (*ii*) the electron spins should be maintained as nearly as possible in a state of saturation, i.e., the $m_s=\frac{1}{2}$ and $m_s=-\frac{1}{2}$ states should be artificially kept equally populated even though the sample is in a magnetic field. The detection of electron spin resonance in metals (29), and the existence in metals of the hyperfine interaction between the nuclear spins and an electron spin,

$$\mathcal{H} = -\frac{8\pi}{3}\boldsymbol{\mu}_e \cdot \boldsymbol{\mu}_n \delta(r), \qquad 1.$$

help to qualify metallic substances for the effect. Note that one can write

$$\mathcal{H} = a\mathbf{I}\cdot\mathbf{s} = a[I_z s_z + \tfrac{1}{2}(I_+ s_- + I_- s_+)], \qquad 2.$$

where $I_\pm = I_x \pm iI_y$, etc. The $I_z s_z$ portion of the interaction provides effectively an additional local magnetic field which produces, depending upon the existing degree of polarization of either spin system, a shift in the resonance location for the other spins; for the nuclear resonance, this is often called the Knight shift (30).

The portion $(I_+ s_- + I_- s_+)$ of 2. is of primary interest for Overhauser's method. The only nonvanishing off-diagonal matrix elements give rise to transition probabilities which represent compensating flips of the nuclear spin and the electronic spin, so that the total angular momentum of the pair is conserved.

An interesting description of the effect has been presented by Bloch,[4] who pictures a collision of an electron and a nuclear spin as in diagrams B (before collision) and A (after collision) of Figure 3. The vertical arrows represent the static components of spin vectors, assumed to correspond to an external magnetic field H in the direction shown. Dashed arrows schematically represent the translational momentum of the electron. A metal with $I = \frac{1}{2}$ is assumed for simplicity, and both the nuclear spectroscopic splitting factor, g_n, and that for the electron g_e, are to be taken relative to the same magneton, μ_0. Thus $|g_e|$ is about three orders of magnitude larger than $|g_n|$.

Consider the time-rate-of-change in n_+, the population of the nuclear spin state $m_I = +\frac{1}{2}$. The probability that a given electron approaching a nucleus flips it to $m_I = +\frac{1}{2}$ is proportional to the number of nuclei n_- having $m_I = -\frac{1}{2}$, and to the probability p_+ that the approaching electron has $m_s = +\frac{1}{2}$. Thus there is a contribution to dn_+/dt given by

$$\left(\frac{dn_+}{dt}\right)_1 \propto n_- p_+. \qquad 3.$$

There is a second term $(dn_+/dt)_2$ which represents transitions out of $m_I = +\frac{1}{2}$ to $m_I = -\frac{1}{2}$, and which therefore subtracts from dn_+/dt. This term is proportional to n_+ and p_-:

$$\left(\frac{dn_+}{dt}\right)_2 \propto -n_+ p_+. \qquad 4.$$

Before combining these terms into a complete expression for dn_+/dt, note that the factor multiplying n_- or n_+ in the right member of equation 3 or equation 4 plays the role of a transition probability. Accordingly, that factor representing the emission probability must be supplied with the ap-

[4] American Physical Society meeting, Stanford University, California, December, 1953.

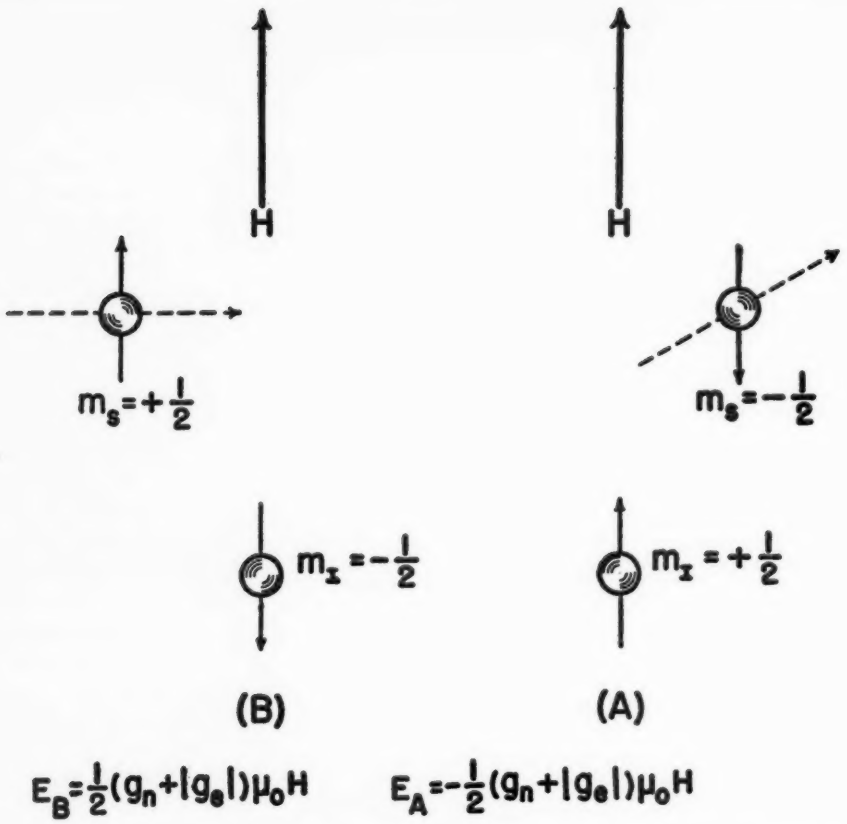

FIG. 3. Schematic representation of a collision between an electron spin and a nuclear spin of a metal in which the interaction of equation 2 effects nuclear magnetic relaxation.

propriate Boltzmann factor. Since the electron has a negative magnetic moment much larger than the nuclear moment, situation B of Figure 3 has the higher potential energy of spin orientation, and the emission transition from situation B to situation A is enhanced by a factor $\exp[(|g_e| + g_n)\mu_0 H/kT$ which thus allows for spontaneous emission. Therefore, the proper combination of equation 3 and equation 4 is

$$\frac{dn_+}{dt} \propto \{n_- p_+ \exp[(|g_e| + g_n)\mu_0 H/kT] - n_+ p_-\}. \qquad 5.$$

The condition for stationarity (not necessarily thermal equilibrium) is $dn_+/dt = 0$, or

$$\frac{n_+}{n_-} = \frac{p_+}{p_-} \exp[(|g_e| + g_n)\mu_0 H/kT] \qquad 6$$

which gives the population ratio of the two nuclear spin states. A quick check of equation 6 is provided by inserting $p_+/p_- = \exp[-|g_e|\mu_0 H/kT]$, which corresponds to thermal equilibrium, and noting that the equilibrium ratio n_+/n_- is obtained.

Overhauser's point is that if one excites the conduction electron resonance with a sufficiently intense radiation field to produce "saturation," i.e., to maintain $p_+ = p_-$, then the ratio of nuclear spin state populations in equation 6 becomes $\exp[(|g_e|+g_n)\mu_0 H/kT]$. Since the electronic magnetic moment is much larger than the nuclear moment, appreciably greater nuclear polarization occurs at a given temperature under conditions of electron spin resonance saturation. If the metal is at 2° K in $H = 10^4$ oersteds, then $n_+/n_- = 2.1$; the corresponding polarization is, for a spin $\frac{1}{2}$ metal, 37 per cent of the maximum theoretically attainable. If, on the other hand, the electron spins were in thermal equilibrium, a spin $\frac{1}{2}$ metal with one nuclear magneton would be but 0.02 per cent polarized for the same ratio of H/T.

There is evidently a third requirement to be added to (*i*) and (*ii*) above in order that a substance qualify for Overhauser polarization: (*iii*) the electronic orbital energy states must be sufficiently broad in energy to permit the orbital motion to absorb or give up the difference in energy $(|g_e|+g_n)\mu_0 H$ as transitions between situations A and B occur. A metal, with its unfilled energy states in a region of width ~kT at the top of the Fermi distribution possesses this property even at temperatures near 1° K.

In the experiment by Carver & Slichter, a suspension of Li in oil was used. A test is provided by the fact that the nuclear magnetic resonance signal is proportional to the degree of polarization of the nuclear spin system. The Li^7 resonance intensity was observed in 30.3 oersteds, and Figure 4 summarizes the results. The top trace "exhibits" the Li^7 nuclear resonance at 50 kc./sec. in the Li metal, the signal actually being lost in noise. The middle trace shows the Li^7 resonance observed while a 50 watt oscillator excited, at 84 Mc./sec. a coil perpendicular to both the 30.3 oersted field and the axis of the nuclear resonance coil, thus saturating the conduction electron resonance. The third trace is a feeble but observable proton resonance obtained under the conditions of the first trace, but with a sample containing eight times as many protons as the metal-oil sample contained Li^7 nuclei.

The estimated enhancement of about 100, obtained by Carver & Slichter, falls short of the theoretical maximum. This is probably caused by incomplete saturation of the electron resonance, or by the existence of competing nuclear relaxation processes which are not of the form $\boldsymbol{I}\cdot\boldsymbol{s}$. For a discussion of the effect of partial electron saturation, the reader is referred to Overhauser's paper (27).

A number of associated effects are worth noting. When the electron resonance is saturated, the Knight shift of the nuclear resonance will disappear. Concomitantly, if large nuclear polarization is effected, there will be a corresponding shift of the electron resonance location.

Overhauser polarization has intrinsic interest, among other reasons, be-

cause it is an example *par excellence* of an ingenious theoretical prediction of a new phenomenon, rather than the more usual theoretical explanation *post facto* of an experimental discovery. But it has also great potential implications for Nuclear Science. In the first place, if particle radius can be kept adequately near the skin-depth appropriate to the electron resonance frequency in several thousand oersteds, the enhanced sensitivity in detecting nuclear resonance would make many more radioactive nuclides accessible to moment and spin measurement.

• A second but more difficultly realizable potentiality is, of course, for the study of radiation patterns from polarized radioactive nuclides. The technical difficulties of maintaining a conductor at 2° K in the presence of the intense heating effect of the saturating microwave field appear to be considerable. Methods of reducing conductivity will need to be explored, and a search for relatively nonconducting substances (perhaps certain free radicals?) meeting conditions (*i*), (*ii*), and (*iii*) should be made. In this connection, C. P. Slichter (private communication) reports at this writing that enhancement of the proton nuclear resonance has been observed in metal-ammonia solutions when the electron resonance is saturated. The enhancement has a strong concentration dependence, full enhancement as predicted by the Overhauser factor of equation 6 occurring at high concentration.

An interesting proposal for detecting magnetic resonance of aligned radioactive nuclei may be discussed here. Bloembergen & Temmer (31) point out that the application of a sufficiently intense rf magnetic field at nuclear resonance for the radionuclide will, at the low lattice temperatures required for any kind of alignment, increase the entropy of the spins very quickly. Thus, at resonance, the anisotropy of the nuclear decay radiation will be reduced or lost, and the monitoring counters would detect the existence of nuclear resonance. The method can be applied to stable nuclides of a sample in which radionuclides are also imbedded. When spin resonance of the stable nuclide occurs, the energy absorbed by these spins will be passed to the lattice, which has a low heat capacity at low temperatures, and the rise in lattice temperature will in turn be felt by the radionuclide spins, whose radioactive anisotropy would decrease. The sensitivity of these methods depends upon the statistics of the counters, rather than upon the usually more troublesome signal-to-noise problems presented by radiofrequency detection equipment.

Theoretical Advances

Apart from Overhauser's work, theoretical advances in the year have tended to place previous work on firmer ground. Wangsness & Bloch (32) have begun from fundamental principles of quantum statistics and arrived at the very successful equations originally put forth by Bloch (33) on a phenomenological basis. Even so, the particular sets of conditions under which the rigorous theory yields these equations are thus far rather limited.

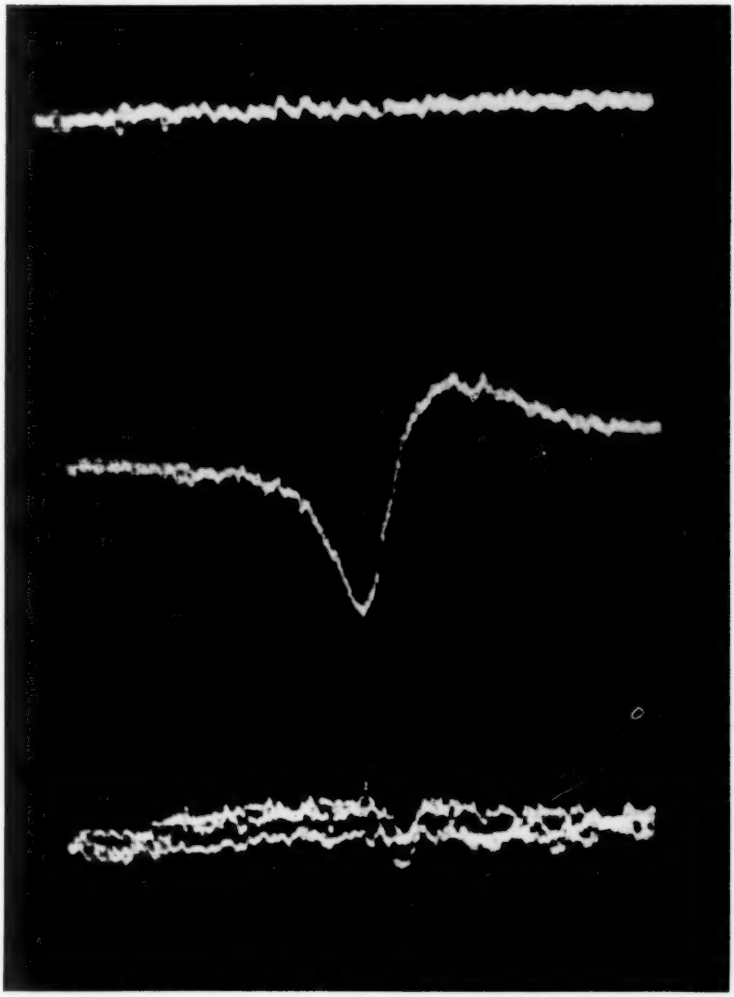

FIG. 4. Demonstration of Overhauser polarization of nuclei by Carver & Slichter. The top trace is the Li^7 resonance (lost in noise) at 50 kc./sec. The second trace is the Li^7 resonance from the same sample observed under conditions of electron resonance saturation. The third trace is a proton resonance observed under the conditions of the top trace, but with a sample containing eight times as many resonating nuclei.

Torrey (34) has developed a theory of nuclear spin relaxation by translational diffusion which clarifies the nature of the assumptions in the Bloembergen, Purcell & Pound (35) correlation spectrum theory.

Electric Quadrupole Splittings and Pure Quadrupole Resonance

The group at British Columbia has extended its work on the quadrupole splittings of Al^{27}, Li^{7}, and Li^{6} in spodumene (36 to 39), including treatment of nonaxially symmetric field gradients and improved measurement of the quadrupole moment ratio for the Li isotopes.

Effects of strains and lattice flaws have been found to influence nuclear resonances significantly through the spurious electric field gradients and associated quadrupole couplings. Watkins & Pound (40) discovered that the alkali halides, which should have no quadrupole couplings if the ideal simple cubic lattice is realized, can have much reduced resonance intensities because of lattice flaws or strains which produce random shifts of the quadrupole satellite lines. The remaining detectable central line of the quadrupole pattern (for half-integral spin) may even be less intense than expected because an appreciable number of lattice sites have large enough gradients to produce second order perturbations. Similarly, Bloembergen & Rowland (41) find

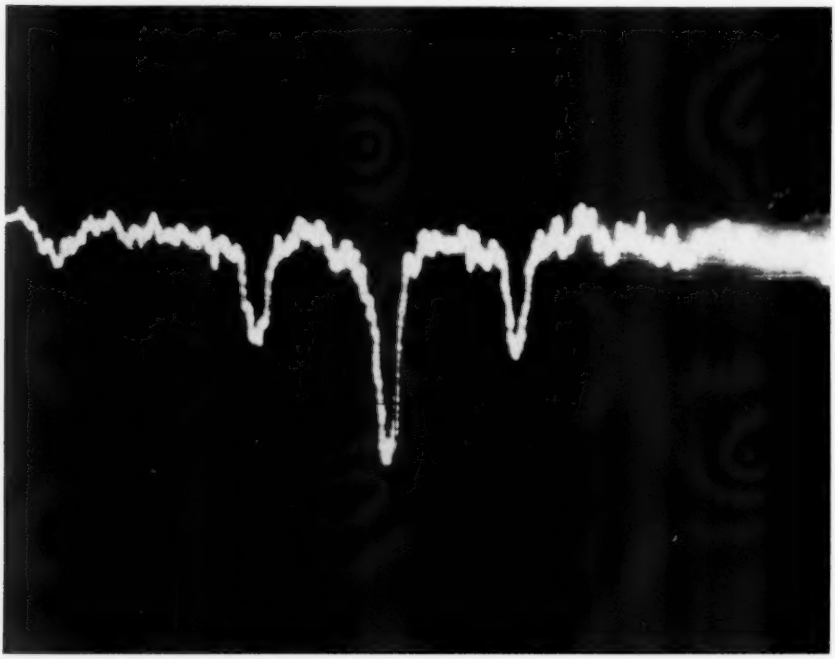

Fig. 5. Spectrum showing the F^{19} resonance multiplet structure in liquid SiF_4 from which Williams, McCall & Gutowsky have determined that the spin of Si^{29} is $\frac{1}{2}$. The center line is from $Si^{28}F_4$ and has no structure since Si^{28} has zero spin. The pair of satellite lines is from $Si^{29}F_4$, indicating that Si^{29} has two possible m_I values and therefore spin $\frac{1}{2}$. Separation of the satellites is 46 milligauss. The pip at the far left is produced by the return trace of the saw-tooth sweep employed.

effects of annealing on the intensity and width of resonances in metals containing quadrupole moments.

The effect noted by Watkins & Pound is presumably responsible, at least in part, for the anomalous result of Sands & Pake (42) for the spin of Si^{29}, since the I^{127} resonance in KI was used as an intensity standard. Recent work by Williams, McCall & Gutowsky seems to offer the best evidence that the spin of Si^{29} is $\frac{1}{2}$, based upon the splitting of the F^{19} resonance by the Si^{29} moment in SiF_4. See Figure 5.

There was much activity in pure quadrupole resonance, although this work has ramifications primarily for theories of chemical binding. Nuclear Science profits, of course, from occasionally measured ratios of the quadrupole moments of isotopic pairs (6, 43 to 53).

Applications to the Physics of Solids and to Chemical Physics

Because the second moment of the nuclear resonance line shape is extremely important in applications to structural problems, attention is called to Andrew's calculation (54) of the correction for finite modulation amplitude h_m. The result is

$$\langle H^2 \rangle_{av}^{\text{true}} = \langle H^2 \rangle_{av}^{\text{apparent}} - \tfrac{1}{2} h_m^2.$$

Andrew & Eades (55), have also discussed a method for separating inter- and intramolecular contributions to the second moment in molecular solids.

Studies of metals, in addition to the Overhauser effect, include the discovery of anisotropy in the Knight shift by Bloembergen & Rowland (41), investigation of temperature dependence of the Knight shift by McGarvey & Gutowsky (56), and observation of line width transitions in Al by Seymour (57).

The Leiden investigations of antiferromagnetism, by nuclear resonance methods, have included measurement of the temperature dependence of the spontaneous magnetization in an antiferromagnetic single crystal by Poulis & Hardeman (58).

A most interesting experiment on solid hydrogen was performed by Reif & Purcell (59), who find the proton line shape depends upon the nature of the electric potential to which the H_2 molecule is subject. They also describe an ingenious measurement of the zero field resonance in solid hydrogen.

The multiplet structure in liquids, which has considerable potentiality for nuclear spin measurements (Figure 5), has been discussed in a very informative paper by Gutowsky, McCall & Slichter (60). A stringent test of the theoretical prediction that the multiplet splittings, measured in units of magnetic field, should be independent of external field, was provided by Quinn & Brown (61), who verify that the splittings for a number of substances in fields of a few 100 gauss are identical with the results for 6385 gauss.

A detailed discussion of applications to essentially chemical problems

would carry this review too far afield from Nuclear Science. It may, however, emphasize the contention of the Introduction if one lists an array of additional problems to which nuclear magnetic resonance was applied throughout the year: rotational states in solid methane (62); liquid crystals (63, 64); sorbed water (65); complex ion formation (66); dissociation and chemical exchange (67); electronegativity of substituents (68); structure of crystalline hydrates (69 to 72); molecular motions in solid cetyl alcohol (73); the structure and behavior of rubber (74); and indication of a planar structure for the urea molecule (75).

Hyperfine Structure in Microwave Electronic Resonance

The hyperfine splitting of the V^{50} paramagnetic resonance in a magnettically dilute crystal of vanadium tutton salt has provided direct measurement (14) of the spin of V^{50} as six.

During the year, more and more complicated hyperfine patterns in free radical resonances have been resolved. Simple patterns contributed by one or two nuclei received further attention (76, 77), but in addition, a splitting into 16 resolvable lines was observed by Owen & Stevens (78) for $(NH_4)_2$ Ir Cl_6. It is necessary to consider effects of the Cl nuclear moments as well as those of the Ir isotopes in order to explain the observed spectrum. Meanwhile, Weissman *et al.* (79), have resolved 39 lines in the paramagnetic resonance of Wurster's blue ion, $[(CH_3)_2N\ C_6H_4\ N(CH_3)_2]^+$, exhibited in Figure 6. Evidently hydrogen nuclei must be invoked in the explanation of this spectrum. There are similar indications for many other free radicals observed in sufficiently dilute solutions (80); H. S. Jarrett (private communication) has resolved over 100 lines in the triphenyl methyl spectrum.

Portis *et al.* (81, 82) proposed that the shape and saturation behavior of the F-center resonance in an alkali halide crystal can be explained upon the assumption of hyperfine coupling of the six alkali nuclear moments surrounding an anion vacancy to the trapped electron at that site. Schneider (83) reports experiments which resolve the 19 such hyperfine components predicted by this proposal for LiCl, but the intensities of these components are, astonishingly, essentially equal, whereas the proposal of Kip predicts an approximately Gaussian envelope for the 19 lines. The problem remains unsettled at this writing.

No account of hyperfine structure would be complete without reference to the fifth and sixth papers by Lamb and his co-workers (84, 85) in the outstanding sequence on the hydrogen atoms. These papers present improved measurements of the Lamb shift and other energy separations for hydrogen and deuterium. Analysis by Salpeter (86) shows the experimental Lamb shifts of 1057.77 ± 0.01 Mc./sec. (hydrogen) and 1059.00 ± 0.10 Mc./sec. (deuterium) to be about 0.5 Mc./sec. larger than expected from present theory.

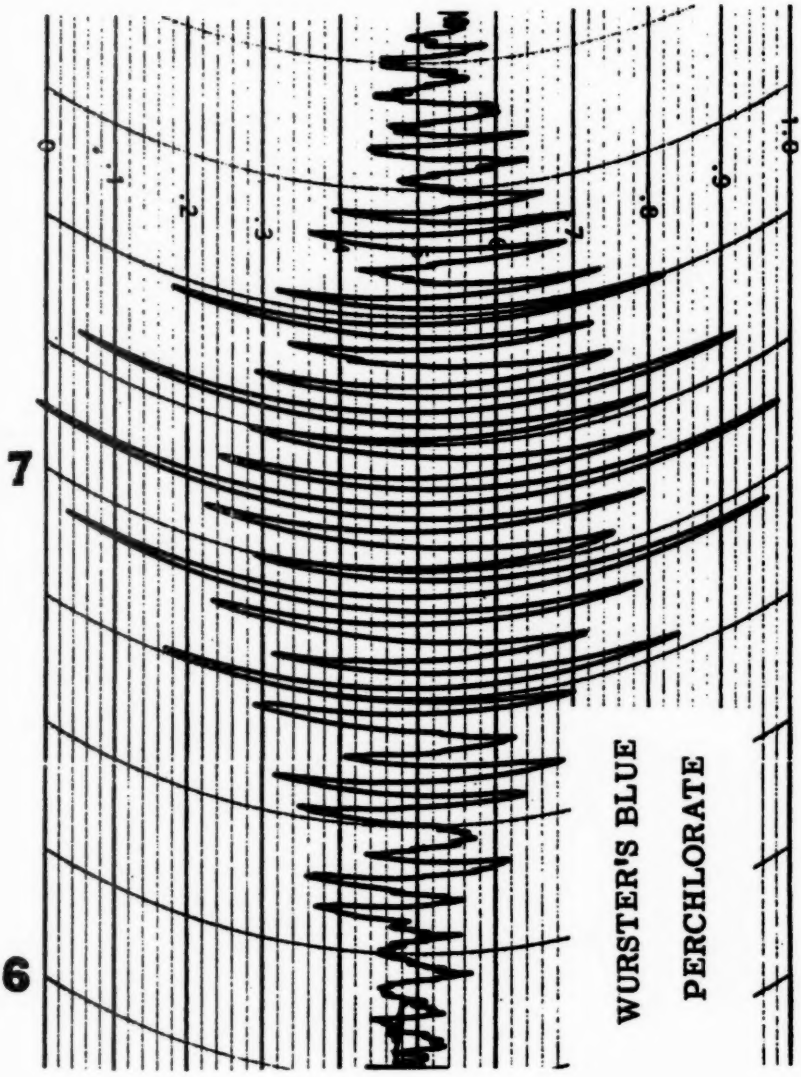

FIG. 6. Hyperfine structure of the paramagnetic resonance of the unpaired electron in Wurster's blue ion, $[(CH_3)_2NC_6H_4N(CH_3)_2]^+$. Since the absorption curve derivative was recorded, two additional weak triplets have been observed at the extremes of the spectrum, making 39 lines in all. The pattern extends over about 100 oersteds and is observed at 9000 Mc./sec.

LITERATURE CITED

1. Weaver, H. E., *Phys. Rev.*, **89,** 923 (1953)
2. Malling, L., *Electronics*, **26,** 184 (1953)
3. Suryan, G., *J. Indian Inst. Sci.*, [A]**35,** 25 (1953)
4. Gutowsky, H. S., Meyer, L. H., and McClure, R. E., *Rev. Sci. Instr.*, **24,** 644 (1953)
5. Harrick, N. J., Barnes, R. G., Bray, P. J., and Ramsey, N. F., *Phys. Rev.*, **90,** 260 (1953)
6. Dehmelt, H. G., *Z. Physik*, **134,** 642 (1953)
7. Wessel, G., *Phys. Rev.*, **92,** 1581 (1953)
8. Bellamy, E. H., and Smith, K. F., *Phil. Mag.*, **44,** 33 (1953)
9. Lew, H., and Wessel, G., *Phys. Rev.*, **90,** 1 (1953)
10. White, R. L., and Townes, C. H., *Phys. Rev.*, **92,** 1256 (1953)
11. Williams, G. A., McCall, D. W., and Gutowsky, H. S., *Phys. Rev.*, **93,** 1428 (1954)
12. Jeffries, C. D., *Phys. Rev.*, **90,** 1130 (1953)
13. Jeffries, C. D., *Phys. Rev.*, **92,** 1262 (1953)
14. Kikuchi, C., Sirvetz, M. H., and Cohen, V. W., *Phys. Rev.*, **92,** 109 (1953)
15. Alder, F., and Halbach, K., *Helv. Phys. Acta*, **26,** 426 (1953)
16. Jeffries, C. D., and Sogo, P. B., *Phys. Rev.*, **91,** 1286 (1953)
17. Trenam, R. S., *Proc. Phys. Soc.* (*London*), [A]**66,** 414 (1953)
18. Baker, J. M., Bleaney, B., Bowers, K. D., Shaw, P. F. D., and Trenam, R. S., *Proc. Phys. Soc.* (*London*), [A]**66,** 305 (1953)
19. Bleaney, B., Bowers, K. D., and Trenam, R. S., *Proc. Phys. Soc.* (*London*), [A]**66,** 410 (1953)
20. Hardy, W. A., Silvey, G., Townes, C. M., Burke, B. F., Strandberg, M. W. P., Parker, G. W., and Cohen, V. W., *Phys. Rev.*, **92,** 1532 (1953)
21. Wessel, G., and Lew, H., *Phys. Rev.*, **92,** 641 (1953)
22. Livingston, R., Benjamin, B. M., Cox, J. T., and Gordy, W., *Phys. Rev.*, **92,** 1271 (1953)
23. Lew, H., *Phys. Rev.*, **91,** 619 (1953)
24. Fred, M., Tomkins, F. S., and Barnes, R. F., *Phys. Rev.*, **92,** 1324 (1953)
25. Brix, P., Eisinger, J. T., Lew, H., and Wessel, G., *Phys. Rev.*, **92,** 647 (1953)
26. Overhauser, A. W., *Phys. Rev.*, **91,** 476 (1953)
27. Overhauser, A. W., *Phys. Rev.*, **92,** 411 (1953)
28. Carver, T. R., and Slichter, C. P., *Phys. Rev.*, **92,** 212 (1953)
29. Griswold, T. W., Kip, A. F., and Kittel, C., *Phys. Rev.*, **88,** 951 (1952)
30. Knight, W. D., *Phys. Rev.*, **76,** 1259 (1949)
31. Bloembergen, N., and Temmer, G. M., *Phys. Rev.*, **89,** 883 (1953)
32. Wangsness, R. K., and Bloch, F., *Phys. Rev.*, **89,** 728 (1953)
33. Bloch, F., *Phys. Rev.*, **70,** 460 (1946)
34. Torrey, H. C., *Phys. Rev.*, **92,** 962 (1953)
35. Bloembergen, N., Purcell, E. M., and Pound, R. V., *Phys. Rev.*, **73,** 679 (1948)
36. Volkoff, G. M., *Can. J. Phys.*, **31,** 820 (1953)
37. Petch, H. E., Cranna, N. G., and Volkoff, G. M., *Can. J. Phys.*, **31,** 837 (1953)
38. Lamarche, G., and Volkoff, G. M., *Can. J. Phys.*, **31,** 1010 (1953)
39. Cranna, G., *Can. J. Phys.*, **31,** 1185 (1953)
40. Watkins, G. D., and Pound, R. V., *Phys. Rev.*, **89,** 658 (1953)
41. Bloembergen, N., and Rowland, T. J., *Acta Metal.*, **1,** 731 (1953)

42. Sands, R. H., and Pake, G. E., *Phys. Rev.*, **89,** 896 (1953)
43. Livingston, R., and Zeldes, H., *Phys. Rev.*, **90,** 609 (1953)
44. Dehmelt, H. G., *Phys. Rev.*, **91,** 313 (1953)
45. Dehmelt, H. G., *Phys. Rev.*, **92,** 1240 (1953)
46. Ting, Y., Manring, E., and Williams, D., *Phys. Rev.*, **92,** 1581 (1953)
47. Dehmelt, H. G., *J. Chem. Phys.*, **21,** 380 (1953)
48. McCall, D. W., and Gutowski, H. G., *J. Chem. Phys.*, **21,** 1300 (1953)
49. Kojima, S., Tsukada, K., Ogawa, S., and Shimauchi, A., *J. Chem. Phys.*, **21,** 1415 (1953)
50. Zeldes, H., and Livingston, R., *J. Chem. Phys.*, **21,** 1418 (1953)
51. Bray, P. J., and Ring, P. J., *J. Chem. Phys.*, **21,** 2226 (1953)
52. Kojima, S., Tsukada, K., and Ogawa, S., *J. Chem. Phys.*, **21,** 2237 (1953)
53. Bassompierre, A., *Compt. rend.*, **237,** 39 (1953)
54. Andrew, E. R., *Phys. Rev.*, **91,** 425 (1953)
55. Andrew, E. R., and Eades, R. G., *Proc. Phys. Soc.* (*London*), [A]**66,** 415 (1953)
56. McGarvey, B. R., and Gutowsky, H. G., *J. Chem. Phys.*, **21,** 2114 (1953)
57. Seymour, E. F. W., *Proc. Phys. Soc.* (*London*), [A]**66,** 85 (1953)
58. Poulis, N. J., and Hardeman, G. E. G., *Physica*, **19,** 391 (1953)
59. Reif, F., and Purcell, E. M., *Phys. Rev.*, **91,** 631 (1953)
60. Gutowsky, H. G., McCall, D. W., and Slichter, C. P., *J. Chem. Phys.*, **21,** 279 (1953)
61. Quinn, W. E., and Brown, R. M., *J. Chem. Phys.*, **21,** 1605 (1953)
62. Tomita, K., *Phys. Rev.*, **89,** 429 (1953)
63. Spence, R. D., Moses, H. A., and Jain, P. L., *J. Chem. Phys.*, **21,** 380 (1953)
64. Spence, R. D., Gutowsky, H. S., and Holm, C. H., *J. Chem. Phys.*, **21,** 1891 (1953)
65. Shaw, T. M., and Elsken, R. H., *J. Chem. Phys.*, **21,** 565 (1953)
66. Zimmerman, J. R., *J. Chem. Phys.*, **21,** 1605 (1953)
67. Gutowsky, H. S., and Saika, A., *J. Chem. Phys.*, **21,** 1688 (1953)
68. Shoolery, J. N., *J. Chem. Phys.*, **21,** 1899 (1953)
69. Itoh, J., Kusaka, R., Kiriyama, R., and Mabumoto, S., *J. Chem. Phys.*, **21,** 1895 (1953)
70. Itoh, J., Kusaka, R., Yamagata, Y., Kiriyama, R., and Ibamoto, H., *Physica*, **19,** 415 (1953)
71. Itoh, J., Kusaka, R., Yamagata, Y., Kiriyama, R., Ibamoto, H., Kanda, T., and Masuda, Y., *J. Phys. Soc. Japan*, **8,** 287 (1953)
72. Itoh, J., Kusaka, R., Yamagata, Y., Kiriyama, R., and Ibamoto, H., *J. Phys. Soc. Japan*, **8,** 293 (1953)
73. Kojima, S., and Ogawa, S., *J. Phys. Soc. Japan*, **8,** 283 (1953)
74. Gutowsky, H. S., and Meyer, L. H., *J. Chem. Phys.*, **21,** 2122 (1953)
75. Andrew, E. R., and Hyndman, D., *Proc. Phys. Soc.* (*London*), [A]**66,** 1187 (1953)
76. Townsend, J., Weissman, S. I., and Pake, G. E., *Phys. Rev.*, **89,** 606 (1953)
77. Jarrett, H. S., *J. Chem. Phys.*, **21,** 761 (1953)
78. Owen, J., and Stevens, K. W. H., *Nature*, **171,** 836 (1953)
79. Weissman, S. I., Townsend, J., Paul, D. E., and Pake, G. E., *J. Chem. Phys.*, **21,** 2227 (1953)
80. Chu, T. L., Pake, G. E., Paul, D. E., Townsend, J., and Weissman, S. I., *J. Phys. Chem.*, **57,** 504 (1953)

81. Kip, A. F., Kittel, C., Levy, R. A., Portis, A. M., *Phys. Rev.*, **91**, 1066 (1953)
82. Portis, A. M., *Phys. Rev.*, **91**, 1071 (1953)
83. Schneider, E. E., *Bull. Am. Phys. Soc.*, **28**(6), 15 (1953)
84. Triebwasser, S., Dayhoff, E. S., and Lamb, W. E., *Phys. Rev.*, **89**, 98 (1953)
85. Dayhoff, E. S., Triebwasser, S., and Lamb, W. E., *Phys. Rev.*, **89**, 106 (1953)
86. Salpeter, E. E., *Phys. Rev.*, **89**, 92 (1953)

STANDARDIZATION OF RADIOACTIVE SOURCES[1,2]

By George G. Manov
Atomic Energy Commission, Washington, D. C.

INTRODUCTION

Primary standards of radioactivity are in some ways, analogous to fixed points in the temperature scale in that each can be used for comparison with "unknowns" not too far removed from the standard. Over a thousand radioactive species are known to exist, but only a comparatively few satisfy such basic requirements for primary standards as: known decay scheme; appropriate half life and disintegration energy; radiochemical and radioisotopic purity; and ease of preparation and availability.

Whereas it had originally been considered that a relatively few standards covering the range of β- and γ-energies of interest would suffice, the thought has been recently expressed that standards may be required for many additional radionuclides. For example, discrepancies in measurements using end-window counters may arise in extrapolating to "zero total absorber" because of the difference in the energy distribution of the β-ray spectra of two isotopes that have approximately the same maximum β-energy. Similarly, although a given β-γ-standard may be suitable for determining quantitatively the activity of a second radionuclide by comparison of respective beta activities, it may be totally inapplicable, for example, for use in corresponding measurements involving comparative γ-ray counting.

Where chemical methods are involved in the assay, interference has been found to occur from analogous compounds of the same element (e.g., $Na_2HP^{32}O_4$ and $Na_2HP^{32}O_3$), as well as from different radio-species of the same element in a given compound (e.g., $Na_2HP^{32}O_4$ and $Na_2HP^{33}O_4$).

Radium was formerly unique in being the only radionuclide for which the establishment of radiochemical purity was equivalent to primary standardization. The curie was officially redefined, however, as reported by Evans (1b) and Paneth (2) at the July, 1950, meeting of the Joint Commission on Standards, Units, and Constants of Radioactivity as "the quantity of any radioactive nuclide in which the number of disintegrations per second is 3.700×10^{10}." This new definition divorces the curie unit from a special association with radon and radium. The use of the term "rutherford" to denote 10^6 disintegrations per second was abandoned in 1950.

The progress in the acceptance of definitions for radioactivity units and standards has been reported by Evans (1a, 1b). The present survey of the problems involved in the preparation and certification of primary standards

[1] The survey of the literature pertaining to this review was concluded on March 1, 1954.

[2] The following abbreviations are used: MIT for Massachusetts Institute of Technology; NBS for National Bureau of Standards; ORNL for Oak Ridge National Laboratory; AECL for Atomic Energy of Canada, Limited.

of radioactivity indicates major progress in the determination of the absolute disintegration rates of β- and of β-γ-emitters. The situation is much improved over the period 1947–49, and the availability of standards within the United States such as C^{14}, Co^{60}, I^{131}, P^{32}, Ra^{226}, Pb^{210} (Radium D-E), Sr^{90} and Tl^{204} is one measure of the advances made.

Assembly by the National Bureau of Standards (3a) of published information on the decay scheme, half life and energy distribution of many radionuclides has served as a spur for additional research in these fields. Prompt publication of such summaries is now a routine matter (3b), and some of the information is available on punched cards (4).

ADVANCE IN TECHNIQUES OF MEASUREMENTS

Determination of the Half Life of Radionuclides

The determination of the half life of a nuclide by any method at constant, but unknown, efficiency is essentially a straightforward procedure. If R_1 and R_2 are the observed counting rates obtained with a given detector during a time interval, t, the half life, $T_{\frac{1}{2}}$ can be calculated:

$$T_{\frac{1}{2}} = 0.693t/[2.3 \log_{10} (R_1/R_2)] \qquad 1.$$

The method is best adapted to those nuclides for which the initial and final measurements can be obtained in a reasonable length of time.

Half lives have been measured to four significant figures by use of a differential ionization chamber and a vibrating reed amplifier with feedback (5, 6). With this device, it has been possible to obtain significant measurements over a period of 12 half lives with some short-lived radionuclides. An automatic recording electroscope has been constructed (7) to determine half lives of the order of a few minutes with an accuracy of ± 0.02 min. If a nuclide has a long life (such as C^{14}), the half lives can be calulated from the expression

$$T_{\frac{1}{2}} = 0.693N/(-dN/dt), \qquad 2.$$

where N is the total number of radioactive atoms present (determined by mass-spectrographic analysis and the weight of the sample present) and $-dN/dt$ is the measured rate of disintegration. Calorimetric methods have been used to determine directly the half life of radionuclides such as P^{32} (8).

Determination of the Rate of Disintegration

Measurements of the rate of disintegration can be made by: (*a*) coincidence counting (either β-γ or γ-γ); (*b*) Geiger-Mueller (G-M) or other type counters[3] under conditions of known geometry; and (*c*) calorimetry. Coincidence counting (11 to 15) involves the use of two counters: one for detecting

[3] The development of scintillation counters and the advantages thereto have been reported in several symposia (9) as well as in the present volume, page 111. Halogen-quenched G-M counters have been developed (10) which are said to have a very long operating life and which use a visibly transparent, nonmetallic electrically conducting film as a cathode.

the β- (or γ-) radiation, and the other for detecting the (second) γ-radiation. Certain conditions must be fulfilled and various small corrections to the observed counting rates must be applied. If N_1 and N_2 are the counting rates of the β (or γ) and of the γ-counters, respectively, and N_{12} is the coincidence rate, the absolute rate of disintegration, $-dN/dt$, of the sample is given by

$$-dN/dt = N_1N_2/N_{12}. \qquad 3.$$

This method can be applied to the determination of the activity of long-lived as well as moderately short-lived nuclides.

The technique of "known geometry" with end-window counting, for example, involves measuring the rate of decay of a sample under conditions in which the counter "sees" a known solid angle at a known distance from the source. In principle the method is simple but corrections must be applied (16) for resolution or dead time losses; for backscattering from the support; for sidescattering from the walls of the shield enclosing the sample, the support and the counter; for absorption by the window of the counter, etc.

The method of end-window counting is applicable preferably to β-emitters with moderate or long half lives. A variation of the method of "known geometry" is that in which the sample to be measured is completely inside the counter or may even be part of the filling gas. This type of counter has been successfully used in measurements involving C^{14} and H^3.

The rate of charge loss has been measured in isolated systems containing a radionuclide by using a Lindemann electrometer and a compensating condenser (17). The method has been applied to P^{32} and Na^{22}.

Internal counters with 4π geometry suggested in 1947 by Borkowski (18) have been refined and used extensively (19a, 19b) for absolute β-measurements. Proportional 4π counters have been widely used in Canada (20), England (21, 22, 23) and in Germany (24, 25) for standardization of both high and low-energy β-emitters.

Panel discussions (16) on the techniques of absolute β-counting by the known geometry method have brought out a number of small, hitherto unsuspected sources of error regarding the effects of backscattering from supports, self-absorption, etc. New measurements have been made of the backscattering of positrons and electrons from various kinds of supporting materials (26, 27). The method of Marinelli (28) can be used for standardization if the decay scheme has been established. The rate of disintegration of a radionuclide can also be determined (29) if the average energy per disintegration, $\overline{E}$, is known.

Calorimetric methods for the determination of activity involve measurement of the rate of heat evolved, dQ/dt, by absorption of the energy emitted during the decay of the radionuclide. The method involves the usual thermal and other corrections applicable to calorimetry and is used preferably for β-emitters or for other isotopes where the radiation to be measured can be completely absorbed in the calorimeter. From the expression

$$dQ/dt = \overline{E}_\beta \, dN/dt \qquad 4.$$

either $-dN/dt$ or $\overline{E}_\beta$, the average energy per β-disintegration, can be computed if one of them is known.

The availability of intense, high specific-activity sources and the development of suitable calorimeters (8, 30) operating at liquid air temperatures has enabled estimation of the half lives of isotopes such as C^{14}.

The consensus presently seems to be (31c) that more reliable measurements can be made by internal 4π and by β-γ (or γ-γ) coincidence counting methods rather than by the method of known geometry. The method using the rate of charge loss (17) probably warrants further investigation.

Decay Schemes

A clearer understanding of the techniques involved and of the errors inherent in coincidence counting (11, 12), the method of "delayed coincidence" counting (32), the development (33, 34) of amplifiers with very short resolving times (10^{-9} sec.), and the virtual elimination of spurious coincidences have permitted closer examination of many complex decay schemes.

A β-β (conversion electron) coincidence spectrometer has been devised (35) in which a Geiger-Mueller counter is placed at the "exit" end of the spectrometer and a scintillation counter is placed near the source. Coincidences are measured between the two counters corresponding to a selected electron "line" of known energy and all other β-radiation. The arrangement is said to be satisfactory for establishing decay schemes by β-β (conversion electron) coincidences.

A new method has been devised (36) for the absolute determination of β-ray energies in which a magnetic electron lens, working at unit modification, uses the image-rotation property to produce two lines by reversal of the current through the lens winding. The specific momentum, $H\rho$, of the focused electrons depends, among other factors, on the angle between the two lines.

Internal conversion coefficients have been measured by γ-x-ray coincidence counting (37, 38) as well as by the double-coil, thin lens, magnetic β-ray spectrometer (39). A revised table of K-shell internal-conversion coefficients is available (40).

Spectrometry

Deutsch (41) has made a critical survey of the techniques of β- and γ-spectroscopy. One paragraph in particular is worth quoting:

> The aim of very high resolution spectrometry in the establishment of decay schemes is twofold: it permits the detection of lines which could otherwise not be resolved either from the continuum or from other neighbouring lines. In some of the more complicated decays the number of identified lines is almost proportional to the resolution used. In addition the use of precision energy measurements permits the application of the combination principle to the location of levels. For example in the decay of I^{131} there are six known γ-ray energies. If these are determined with an uncertainty of 1.5 per cent there appear seven combinations which might be interpreted as alternate decays involving the same initial and final states. With an accuracy of 0.5 per cent four of these remain. In fact, coincidence measurements have shown that only one of these is real, the other accidental.

An automatic count and control mechanism has been devised (42) which stepwise sweeps the β-spectrum automatically and counts the number of impulses received as a function of the focusing magnetic current. The device is said to duplicate with precision the manual control of a β-ray spectrometer.

Crystal spectrometers (43) have been developed for the determination of γ-ray energies to four or more significant figures. Scintillation spectrometers and counters for the measurement of the energy distribution and the half life (1 to 30 sec.) of β-ray emitters have been described (44).

A new type of scintillation spectrometer has been devised (45) in which incident photons are detected in a primary detecting NaI(Tl) crystal; the radiations not completely absorbed in the primary crystal are absorbed in a surrounding cluster of NaI(Tl) crystals which act as an anticoincidence circuit. The arrangement is said to yield the γ-ray spectrum directly without any interpretation of results which might become laborious, particularly if the incident γ-radiation has a complex spectrum. The apparatus has been used to study Cs^{137}, Na^{22}, and other radionuclides.

Pair spectrometers have been constructed (46, 47) in which rotation of the image in a short magnetic lens is used to separate negatrons and positrons by putting the pair converter a little to one side of the optical axis of the lens, from which it is possible to obtain coincidence "lines." With this apparatus the 2.62 Mev γ-ray of ThC'' (Tl^{208}) and the 2.76 Mev γ-ray of Na^{24} have been studied. A recent study has been made of the shapes of β-spectra (48), and tables for the analysis of β-spectra are available (49).

Mass Absorption Coefficients

New measurements have been reported for γ-ray absorption coefficients (50 to 53) over a range of energies from 0.1 to 6 Mev (Co^{60}, I^{131}, and others) in absorbers of atomic number from 13 to 82. The calculated values are in good agreement with those measured experimentally. This information is useful in correcting for the attenuation of the γ-radiation passing through the walls of the G-M counter or ion chamber.

Status of Individual Radionuclides

For the purpose of this presentation, the status of individual radionuclides is divided into three categories: (*a*) nuclides for which standards in the United States are available or are in preparation; (*b*) nuclides for which no standards are available, but for which considerable information on nuclear properties exists; and (*c*) nuclides for which standards would be desirable but for which considerably more information of various kinds is needed.

In each category, the information listed includes (when available): the method of production; method of obtaining radiochemical purity; the half life; the decay scheme; intercomparison of the activity between different laboratories; and the availability of standard samples. The nuclides are listed alphabetically within each category.

Available Standards

Summaries are presented for the following radionuclides: C^{14}, Co^{60}, I^{131}, P^{32}, Ra^{226}, Pb-Bi^{210} (Radium D-E), Sr^{90}, and Tl^{204}.

Carbon-14—Most of the C^{14} produced in the United States is now obtained by neutron irradiation of beryllium nitride, Be_3N_2. The C^{14} is separated as active CO_2 and precipitated as $BaCO_3$. Specific activities of 250 to 1500 mc./gm. of $BaCO_3$ are routinely available (54).

Labeled organic compounds are not suitable as standards for C^{14}. Skraba (55) has found that $C^{14}H_3OH$, for example, decomposes under self-irradiation to methane, ethylene glycol, glycerol, and other compounds to an extent sufficient to render it useless for primary standardization.

Full agreement has not yet been reached for the value of the half life of C^{14}. Because of the long half life of this radionuclide a direct measurement is not possible, and values ranging from a high of 7200 to a low of 4700 years have been obtained by indirect methods. Two general methods have been used: (*a*) end-window counting of solid barium carbonate; and (*b*) counting of gaseous C^{14} either as carbon dioxide or as methane in which the radioactive carbon forms a portion of the filling gas of the counter. Generally speaking, gas-phase counting has proven to be more reliable than the counting of solid barium carbonate.

Anderson (56) reviewed the techniques for detecting and measuring C^{14}, and Broda and co-workers (57) claim to have found it possible to measure as little as 2×10^{-12} curies (4 disintegrations/min.) of C^{14} using CO_2-CS_2 filled counters.

Hawkings *et al.* (58) reported a half life of 6360 ± 200 years using a procedure involving a mass-spectrographic analysis of the active CO_2 and a pair of compensated CO_2-CS_2 filled (59, 60) internal gas counters of varying diameters. Jones (61), using alcohol-argon as a filling gas in an internal G-M counter, obtained 5589 ± 75 yr. for the half life of C^{14}. Libby and co-workers (62, 63) also used alcohol-argon as the filling gas and employed counters of various ratios of length to diameter. The value for the half life first reported, 5720 ± 20 years (62), was lowered to 5580 ± 45 years (63) after further corrections were made for the end- and the wall-effects of the counters. It was assumed that the counting efficiency was 100 per cent.

In 1949 the National Bureau of Standards undertook a cooperative venture to determine the half life of C^{14} and to prepare standard samples of C^{14} for distribution. A sample of specially purified $BaCO_3$ treated to remove silica and other inert impurities was used as the starting point. Details of the NBS measurements have been reported by Manov & Curtiss (64).

The CO_2 from a portion of this active barium carbonate was generated by heating an intimate mixture of $BaCO_3$ with $PbCl_2$ at first to 500° C. and then to 1100° C. The evolved CO_2 was mixed thoroughly by repeated condensation with liquid air and evaporation into a small, closed flask and allowed to stand for several hours. Samples of this CO_2 were sent to several cooperating laboratories for mass spectrographic analysis.

An accurately weighed portion of the same active barium carbonate was mixed with a known weight of inert barium carbonate, the CO_2 evolved with perchloric acid and absorbed in an excess of sodium-hydroxide—sodium carbonate solution. The solution was diluted to a known volume, and samples were distributed to the participating laboratories for counting.

It is to be noted that the problem of determining the half life of C^{14} had been divided into two independent parts: (*a*) a collaborative determination of the isotopic ratio from which N in equation 2 could be calculated; and (*b*) a collaborative determination of $-dN/dt$. The results were reported in February, 1950 (31a, 31b) and later (65) in more detail.

In each case, gas-phase counting was performed with a compensated pair of CO_2-CS_2 filled counters. It is known (59, 60) that the resolving time of the CO_2-CS_2 counters is of the order of 1000 μsec., and at counting rates sufficiently high (50 to 100 counts/sec.) to obtain results of statistical significance in a reasonable length of time, the resolution-time losses are of the order of several per cent. (64)

The counting rates obtained by Chalk River and by MIT[2] were, at the time, provisional values. As an interim value pending further work, it was therefore suggested (31a) that the average isotopic ratio of the active barium carbonate used in the cooperative investigation be considered 3.88 per cent, the activity of the ampoules be tentatively assigned 1280 disintegrations/sec./ml., and the half life of C^{14} be estimated at 5400 years, with an uncertainty of perhaps ± 200 years.

Subsequent to this suggestion, two additional values for the half life using other samples of $BaCO_3$ have been reported by Bernstein & Ballentine (66a) in which it appears that gas-phase counting in the proportional region and in the Geiger-Mueller (G-M) region yield 5513 and 6360 years respectively. This discrepancy appears to have been partially resolved in a later paper (66b) in which the hypothesis was advanced that "over-quenching" of the G-M counter may have occurred which led to a significant loss (13.9 per cent) in the counting rate. Provided this observation and the explanation are correct, it may be appropriate to reduce the value for the half life obtained (66a) in the G-M region to 6360/1.139 or 5580 years. Gas-phase counting would therefore seem to lead to estimates of 5513 and 5580 years for the two sets of measurements. The agreement, however, may be fortuitous.

Evidently the last word on the half life of C^{14} has not yet been said and more experimental work needs be done. There seem to be one set of measurements in the range 5400 to 5600 years and another 6000 to 6200 years.

The maximum energy for the β-spectrum of C^{14} is 155 ± 1 kev (67), and the decay scheme involves only a simple β-emission. Standard samples of C^{14} are available from the National Bureau of Standards.

Cobalt-60.—Co^{60} is generally prepared by neutron absorption in Co^{59}; sample preparation consists of solution in hydrochloric or other acids (with or without added cobalt carrier) and dilution to the appropriate activity.

The value for the half life of Co^{60} is approaching agreement. Recent de-

terminations yield 5.26 ±0.17, 5.27 ±0.07, 5.25 ±0.21, and 5.21 ±0.04 years (6, 68, 69, 70), with an average of 5.25 years.[4]

The decay scheme involves a simple β-decay with $E_{max}^{98} = 0.306 \pm 0.005$ Mev (72), followed by two γ-rays in cascade whose energies (43) are 1.1715 ±0.0010 and 1.331 ±0.0010 Mev, respectively.

The Bureau of Standards has prepared a set of ampoules containing Co^{60} which are dilute with respect to total solids (i.e., approximately 1 μg./ml.) and has measured the activity of these ampoules by β-γ-coincidence, 4π, and other counting methods. Preliminary results were reported by Mann & Seliger (27) and by Putnam (21). The former (27) studied two variations of the 4π β-counter (conducting film and mirror image) and two coincidence-counting methods (β-γ and γ-γ). On the same sample of Co^{60}, the relative results obtained (assigning arbitrarily a value of unity to the first method) were 1.000, 0.996, 1.003, and 1.006.

Iodine-131.—I^{131} is presently separated from fission products by oxidation to elemental iodine and volatilization from an aqueous solution. The radionuclide is distributed in the form of a weakly basic iodide solution containing a trace of $NaHSO_3$ (54).

The half life has been reported by Sreb (73) to be 8.1409 ±0.0062 days; 8.04 ±0.04 days by Sinclair & Halloway (69); 8.06 ±0.02 days by Lockett & Thomas (71); 8.075 ±0.022 days (measured over five half lives), by Seliger, Cavallo & Culpepper (74); and 8.05 ±0.01 days by Hawkings and his co-workers (75). The average value, neglecting (73) is 8.06 days.

Decay schemes for I^{131} have recently been reported by Bell, Cassidy & Kelley (76) and Cork and co-workers (77). Both schemes recognize the existence of the 12 day metastable state of Xe^{131} reported by Zeldes, Brosi & Ketelle (78), but associate it with different β-energies. Additional complexities in the decay scheme have since been discovered. Verster (79), Ketelle (80), Cavanagh (81), and Bell (82) and Kurbatov (83) have confirmed the existence of two additional β-energies, 250 kev (2 per cent), and 807 kev (1 per cent). Rose (84) has measured internal conversion electrons but apparently did not observe the 250 kev β-energy. Bell (85) has recently found a previously unknown γ-energy of about 0.5 Mev that does not fit into the presently accepted decay schemes. Caswell (29) has found the average energy of the β-radiation to be 0.189 ±0.008 Mev.

A number of methods are in use for the standardization of I^{131}; known geometry, coincidence counting, 4π counting, and ionization methods prevail (16). The status of the intercomparison of iodine standards is much more promising than it was six years ago.

The National Bureau of Standards since 1950 has been furnishing on a regular schedule 3-ml. ampoules of I^{131} (and of P^{32}) with a known activity (±3 per cent) in terms of disintegrations per second per milliliter of solution. The activity is of the order of 100,000 disintegrations/sec./ml., with higher

[4] It is understood that the value of 4.95 ±0.04 years (71) has been withdrawn (31c).

activities occasionally available by special arrangement. Provision is made for pH control, the samples are low in total solids (approximately 10 μg./ml.), and instructions for use accompany each sample. 4π proportional counting is used for standardization (19a). The presence of the metastable, 12 day Xe^{131} introduces an error which can be neglected in end-window β-counting or in ionization chamber measurements where an overall accuracy of ± 5 per cent is sufficient. Approximately 200 ampoules are distributed at six-month intervals to users within the United States, Australia, Canada and Great Britain, and frequent inter-checks between NBS,[2] ORNL,[2] and other standardizing laboratories serve to maintain the requisite accuracy in standardization.

An international comparison tabulated by Seliger (19b) for samples distributed by the NBS shows the following relative values (the NBS value is arbitrarily designated as unity): NBS, United States, $4\pi\,\beta$ (1.000); AECL,[2] Canada, 4π (1.022); and two values from Hammersmith Hospital, England, absolute γ-ion chamber (0.997) and 4π G-M (1.030).

Samples of I^{131} are being exchanged in an attempt to establish an international standard. The present agreement appears to be of the order of ± 2 per cent.

Phosphorus-32.—Neutron irradiation of sulfur, followed by chemical oxidation and separation, is used to obtain P^{32} (54). If sulfur-containing compounds are irradiated to form phosphorus, the chemistry of separation is rather involved because of the different radiochemical forms in which the phosphorus may be found. For example, if calcium sulfate is irradiated, metaphosphates (PO_3^-), ortho-phosphates (PO_4^{---}), pyro-phosphates ($P_2O_7^{----}$) and phosphites (HPO_3^{--}) are formed. Failure to recognize the chemistry involved may lead to abnormal tracer behavior (69, 86).

New measurements have been reported for the half life of P^{32}. Using a calorimetric method, Bayly (8) obtained 14.30 ± 0.05 days; Lockett & Thomas (71) used a quartz fibre electroscope and obtained 14.50 ± 0.04 days over a period of five half lives. Neither worker, however, was aware of the possible presence of P^{33} (see below). The maximum β-energy for P^{32} has been found to be 1.704 ± 0.008 Mev (87a).

The existence of P^{33} in reactor-produced P^{32} has been reported by Jensen (87a, 88) and confirmed by Sheline (89) and others. The half life is 2.44 ± 0.2 days, and the maximum β-energy is 0.249 ± 0.002 (87b).

Collaborative determinations of the absolute strength of P^{32} samples have been carried out for a number of years between several standardizing laboratories, and the results have recently been summarized by Seliger (19b). The laboratories reporting, the methods used and the relative values obtained (19b) are as follows: United States NBS, 4π β-counter (1.000); ORNL, defined solid angle (0.986); Columbia University, parallel plate counter (1.006); AECL-Canada, 4π β-counter (1.002); Hammersmith Hospital, England, absolute β-ion chamber (0.971).

Ampoules containing known amounts of P^{32} have been available since

1950 from the National Bureau of Standards. These ampoules contain approximately 100,000 disintegrations/sec./ml. of P^{32} with 0.001 M H_3PO_4 added as carrier. The effect of P^{33} on the measurements is considered to be negligible if the time interval between NBS standardization and use involves less than two half lives. 4π proportional counting is used (19b). The availability and the method of distribution[5] for P^{32} and I^{131} are identical.

Radium-226.—Radium standards have been available for many years, but minor uncertainties still persist in determining the activity of one gram of radium. Careful measurements of the specific activity of radium were made by Kohman (91) in 1947, yielding $(3.608 \pm 0.028) \times 10^{10}$ α-disintegrations per second per gram of radium, and a half life of 1620 ± 13 years. One curie (of radium or of any other nuclide) was redefined in 1950 to be equivalent to 3.700×10^{10} disintegrations per second (1b, 2).

Lead-Bismuth-210 (*Ra D-E*).—Pb^{210} (RaD) is obtained by chemical separation from the equilibrium radium mixture, and an organic reagent, dithizone, is useful (92) for this purpose. Electroplating under carefully controlled conditions (93) is also employed to effect the separation. Bi^{210} (RaE) is obtained as the daughter product of Pb^{210}, and values of 5.02 ± 0.02 and 4.989 ± 0.013 days have been reported (71, 94) for the half life.

The original method for preparing standards of RaE was the subject of discussion between the National Bureau of Standards and the National Research Council, and the method decided upon at the time, early in 1946, was a compromise between (*a*) accurate standards desirable for the future, and (*b*) the immediate need for a fairly large number of reproducible standards with a somewhat lesser degree of accuracy. The NBS standards are composed of a circular deposit of active and inert PbO_2 weighing approximately one milligram; the material is deposited electrolytically in the center of a palladium-faced silver disk approximately one inch in diameter and 1/16-inch in thickness. Calibration was initially made by assaying accurately a radium ore for activity, extracting the total lead therefrom, and then electrolytically depositing a portion of the lead as lead peroxide. Several hundred such standards have been prepared and distributed.

In 1950, Burtt (95) and others found that there was a forward scattering of the β-particles from RaE because of the finite thickness of the PbO_2 deposit. The scattering amounted to approximately 7 per cent under the particular conditions of geometry, backscatter, sidescatter, etc., used by him. Seliger (26) has since made additional measurements of the β-particle backscattering from various sources.

These refinements in measurement point up a fact that has long been

[5] Ten microcurie quantities of radionuclides with a half life of less than 30 days and 1 μc. quantities with a half life over 30 days may be interchanged between laboratories without prior approval by the U. S. Atomic Energy Commission (90). This action has served to stimulate intercomparisons not only of materials proposed as standards, but of various intermediate preparations. It applies, however, only to transfers within the United States.

recognized; i.e., that measurements made by comparison of the β-activities between a standard of a given radionuclide and the "unknown" should be made under identical conditions of geometry, thickness of deposit, back-scattering, and that the energies of the standard and of the "unknown" and the shapes of their β-spectra should be as nearly alike as possible.

An independent calibration of the strength of the RaE sources can be obtained by measuring the growth of the α-activity from RaF. Such measurements have been made by Novey (96) and indicate that if proper corrections are applied, the agreement between β- and α-counting is within 2 per cent. National Bureau of Standards Pb^{210}-Bi^{210} standards are available in activities approximating 100, 200, 500, and 1000 disintegrations./sec., and have been widely used in this country and abroad. The international standardization of Pb^{210}-Bi^{210} has not yet been attempted.

Strontium-90.—Sr^{90}, obtained by separation from fission products, is a pure β-ray emitter which decays to Y^{90} and then to stable Zr^{90}. A value of 19.97 $\pm$0.3 years (97) has been reported by Powers and Voigt for the half life, measurements being made over a period of seven years. The heretofore accepted figure is 25 years.

The maximum β-energies of Sr^{90} and Y^{90}, according to Cohn (98), are 0.525 and 2.24 Mev respectively; for Y^{90}, Moreau & Corba (99) found 2.270 $\pm$0.02 Mev. Similar measurements have been made by Shepherd (100) on Y^{90}. The average β-energy of Y^{90} is 0.895 $\pm$0.035 Mev (29).

The National Bureau of Standards has available for distribution standard samples of Sr^{90} in equilibrium with Y^{90}. The activity, approximately 10,000 disintegrations/sec./ml. of solution, is standardized by 2π β-counting, with an accuracy of $\pm$1.5 per cent.

Thallium-204.—Tl^{204} is prepared by neutron irradiation of Tl^{203} and is made available as an aqueous solution of the nitrate. Various difficulties have been encountered in the preparation of samples with reproducible counting rates. Tl^{204} has chemical oxidation states of +1 and +3 in aqueous solution, and it has been reported by Peacock (31b) that electroplating is not satisfactory as a method of separation from other electrolytes. Thallous nitrate solutions in dilute nitric acid have been found by Reynolds (101) to be more stable than neutral or alkaline solutions of thallic ion or halide solutions of thallous ion.

Values for the maximum β-energy of Tl^{204} have been reported to be 0.765 $\pm$0.010 Mev by Lidofsky, Macklin & Wu (102) and 0.760 $\pm$0.01 Mev by der Mateosian & Smith (103). The Kurie plot is linear down to 0.150 Mev (102).

A value of 4.0 $\pm$0.1 years for the half life of Tl^{204} has been obtained by Harbottle (104), and recently Lockett & Thomas (71) found 2.71 $\pm$0.05 years using a quartz fibre electrometer with measurements extending over a period of eight months. Two older values (3) of 2.7 and 3.5 years have also been reported.

Reynolds (105) has recently published the results of a limited intercomparison (six laboratories) of a solution of Tl^{204} whose activity using different

counting methods, was approximately 1×10^{-3} μc./ml. The results appear promising, with an average deviation of ±10 per cent. Further work is under way.

Standard samples of Tl^{204} are available from the National Bureau of Standards in the form of 3-ml. ampoules with an activity of approximately 10,000 disintegrations/sec./ml. Standardization is performed by 2π β-counting with an accuracy between +4 per cent and −2 per cent.

Desirable Standards; Some Nuclear Information Available

Summaries are presented for the following radionuclides: Au^{198}, Fe^{55}, Fe^{59}, Na^{24}, and H^3.

Gold-198.—The half life of Au^{198} has been found to be: 2.69 ±0.01 (5), 2.73 ±0.01 (69), 2.697 ±0.003 (71) and 2.74 ±0.04 (72) days. The decay scheme has been studied recently by a number of workers (72, 106 to 109). The major portion (98 per cent) of the gold decays by a simple β-emission for which values of 0.97 ±0.01 and 0.958 Mev have been found (42, 72). The single γ-ray energy has been measured yielding a value of 0.411770 ±0.000036 and 0.41173 ±0.00007 Mev (110, 111). The minor portion decays with a β-energy of 0.290 Mev and a γ-energy of 1.09 Mev. The Auger spectrum indicates that K capture to Pt^{198} cannot occur in more than 0.5 per cent of the disintegrations (112). The work of Brosi (107) confirms that of Cavanagh (106). It has been determined (34) that the half life of excited (411 kev) Hg^{198} resulting from the β-decay of Au^{198} is less than 3×10^{-11} sec. Hill & Mihelich (109) observed two weak γ-rays of 159 and 209 kev which have been attributed to Au^{199} formed by the successive reactions: Au^{197} (n, γ) Au^{198}; Au^{198} (n, γ) Au^{199}. The half life for Au^{199} was observed to be 3.3 days, the maximum β-energy is 0.32 Mev (3) and the calculated thermal neutron cross section of Au^{198} is estimated to be about 3.5×10^4 barns. The relative proportions of Au^{198}/Au^{199} were estimated[6] to be 95/1 for a sample irradiated for eight days in a flux of 10^{12} n/cm.²/sec. (109).

Standards for Au^{198} are needed. Presently, measurements of the strength of these sources are generally made by comparison with a radium needle using an ionization chamber counter or electroscope. ORNL assays Au^{198} routinely by means of a high pressure ionization chamber calibrated periodically by 4π coincidence counting of the same sample. Because of its comparatively short half life, it is doubtful that standard samples of Au^{198} can be distributed in the usual sense.

From the practical point of view, two courses of action are open: (*a*) standardization of a Au^{198} source by coincidence counting and simultaneous comparison with radium in an ionization chamber under rigidly specified conditions (the gold might then be certified in terms of radium-equivalents); (*b*) search for an isotope of reasonably long half life that has either the same

[6] A private communication from H. H. Seliger of NBS indicates that for an infinitely long irradiation time, the ratio of Au^{198}/Au^{199} should be approximately 1000/1.

β- or γ-energy as Au^{198} (Tm^{170} has been suggested). Secondary standards might then be distributed for comparison of "unknowns" with either the β- or the γ-radiation, as appropriate.

Iron-55.—Fe^{55} is of interest because the decay is thought to proceed almost entirely by K-capture. Scintillation counting (113) has shown that the continuous radiation has an upper limit of 0.205 Mev, and a later value (38) of 0.206 ± 0.020 Mev has been reported. A new value for the half life, 3.0 ± 0.15 years has been found (114) which is in agreement with an earlier one of 2.94 years (68). Preliminary results on intercomparison of samples of Fe^{55} reported by Reynolds (101) indicate that an agreement of the order of ± 15 per cent is possible.

Iron-59.—Fe^{59} is generally produced by cyclotron bombardment. Three values for the half life have been reported: 45.1 ± 0.2, 47.1 ± 0.5, and 45.0 ± 0.2 days (6, 114, 115). The decay scheme has been studied by Rose and co-workers (116) and by Metzger (117).

Sodium-24.—Na^{24} is produced by neutron irradiation of stable sodium. The half life of Na^{24} has been reported by Sreb (118) to be 15.060 ± 0.039 hr., by Lockett and Thomas (71) as 14.97 ± 0.02 hr. and an earlier value of Wilson & Bishop (119) recalculated by Sreb to yield 14.96 ± 0.10 hr. The three values agree within the limits of error.

Considerable interest has been manifested in the decay scheme of Na^{24} Turner & Cavanagh (120) have found evidence for a 4.17 Mev β-group and estimate the branching ratio to be 0.003 per cent. Siegbahn & Johansson (46) have used a new type of pair spectrometer in which rotation of the image in a short magnetic lens is used to separate negatrons from positrons by putting the pair-converter a little aside from the optical axis. The simultaneous emission of three particles (a decay β-ray and an electron-positron pair) from Na^{24} has been examined (121) and the value of the pair-conversion coefficient for the 2.78 Mev γ-ray has been determined to be $(7.6 \pm 1.9) \times 10^{-4}$. A pair conversion coefficient of $(8.25 \pm 1.05) \times 10^{-4}$ was obtained for positrons stopped in Be. Hedgran and Lind (122) have measured the energy of the γ-rays from Na^{24} and report 1.3680 ± 0.0010 and 2.7535 ± 0.0010 Mev.

Absolute measurements of the activity of Na^{24} have been performed by using cavity-type ionization chambers (22) and have been compared with the results of coincidence counting (21). It will be difficult to set up standards for such a short-lived material.

Tritium.—Two recent values for the half life of tritium yield 12.46 ± 0.1 and 12.41 ± 0.20 years (123, 124). Recent measurements of the maximum β-energy by Langer & Moffatt (125) yield 17.95 ± 0.10 kev, while the average energy (123) is 5.69 ± 0.04 kev. A bibliography of literature on tritium has been compiled (126).

The low-energy of the β-radiation from tritium makes quantitative measurements difficult or impractical by ordinary methods such as end-window counting and recourse must be had to gas-phase measurements (119, 127, 128). For samples which are essentially pure tritium, the method

of gas-density (123) can be used and it is claimed that an accuracy of ±0.05 per cent can be attained within the range of 50–100 per cent T_2. A check on the composition of tritium-deuterium-hydrogen mixtures is obtained by mass-spectrographic analysis. (The tritium can be stored on spongy Zr or Pd, and released by gentle heating.)

For lower concentrations of tritium, internal gas-counting can be used. The counters are of brass with flat end-plates similar to those used by Libby (62) with alcohol-argon in the ratio of 1 to 9 at a total pressure of 10 cm. as the filling gas. The tritium is quantitatively diluted with ordinary hydrogen to give a reasonable counting rate in the G-M tube. A counting efficiency of 97 per cent is assumed, and the length of the plateau is approximately 200 volts with a 1000 volt threshold and a slope of approximately 3 per cent per 100 volts. Backgrounds of approximately 200 c/min. on a counter of $1\frac{1}{2}'' \times 12''$ are obtained. Unfortunately, some memory effects are associated with this type of counter, and the background has been found to increase approximately 200 counts/min. for each filling. The counters can, however, be cleaned thoroughly by rinsing with dilute aqueous ammonia and washing with distilled water. Robinson (127) has used a mixture of tritium and methane as a filling gas. The advantage claimed is that the resolving time is very short, that counting can proceed at a high rate of speed without undue coincidence losses, and that the memory effects are smaller.

It should also be possible to use a vibrating-reed electrometer and an ion chamber for routine measurements. Such a chamber could be calibrated at high concentrations of tritium by means of the gas-density balance and at low concentration by G-M gas-phase counting.

It was recently proposed (31b) that standard samples of tritium be prepared in the form of tritiated water with an approximate activity of 10^6 to 10^7 disintegrations/sec./ml. This work is now under way.

Desirable Standards; Little Nuclear Information Available

Summaries are presented for the following radionuclides: Cr^{51} and Zn^{65}.

Chromium-51.—A value of 27.75 ±0.3 days for the half life has been reported recently by Lyon (129) and the decay scheme which is 90 to 92 per cent K capture has been examined more thoroughly (129, 130). Reynolds (101) has measured the disintegration rate of the same sample of Cr^{51} (a) by x-γ-coincidence counting and (b) by x-ray counting with a proportional counter standardized by means of a source of Mn^{54} of known disintegration rate. Results by the two methods agreed within 3 per cent.

Zinc-65.—A new measurement (115) of the half life has yielded 245.0 ±0.8 days. A small percentage of the disintegrations are by positron emission, the main decay process being by K-capture. Furberg (131) has determined the branching ratio $K_2/(K_1+K_2)$ to be 0.44 ±0.03, where K_1 = number of capture processes leading to the ground state, and K_2 = number leading to the excited state. Major (132) has found 0.45 for the branching ratio, and Griffiths (133) by coincidence measurements found that one positron was emitted for every 65 ±5 γ-rays.

Mann and co-workers (134) measured the β-spectrum by means of a thin lens type magnetic spectrometer and found 0.325 ± 0.002 Mev for the positron and 1.38 ± 0.03 Mev for the γ-radiations.

LITERATURE CITED

1. (a) Evans, R. D., *Nucleonics*, **1**(2), 32–43 (1947); (b) Hahn, P. F., *Radioisotope Therapy* (footnote p. 10) (Academic Press, Inc., New York, N. Y., 1951)
2. Paneth, F. A., *Nucleonics*, **8**(5), 38 (1951)
3. (a) Way, K., Fano, L., Scott, M. R., Thew, K., and Wood, M., *National Bureau of Standards Circular 499*, Suppl., 1, 2, 3 (1950)
4. Technical Information Service, Atomic Energy Commission, Washington, D. C.; Radioactive Products Co., 443 West Congress St., Detroit, Michigan
5. Silver, L. M., *Can. J. Phys.*, **29**, 59 (1951)
6. Tubailem, J., *Compt. rend.*, **233**, 1360 (1951)
7. Bartholomew, R. M., Brown, F., Howell, W. D., Shorey, W. R. J., and Yaffe, L., *Can. J. Phys.*, **31**, 714–22 (1953)
8. Bayly, J. G., *Can. J. Research*, **28**[A], 520–29 (1950)
9. *Symposium on Scintillation Counting* (Washington, D. C., Jan. 26–27, 1954)
10. Clark, L. B., Sr., *Rev. Sci. Instr.*, **24**, 641–43 (1953)
11. Bleuler, E., and Goldsmith, G. J., *Experimental Nucleonics* (Reinhardt & Company, New York, N. Y., 393 pp., 1952)
12. Barnothy, J., and Forro, M., *Rev. Sci. Instr.*, **22**, 415 (1951)
13. Mann, W. B., *National Research Council of Canada Report CRM-408* (September 15, 1948)
14. Dunworth, J. V., *Rev. Sci. Instr.*, **11**, 167–80 (1948)
15. Mitchell, A. C. G., *Rev. Mod. Phys.*, **20**, 296–304 (1948)
16. *Conference on Absolute Beta Counting* (National Research Council, U. S. A., Preliminary Report No. 8, October, 1950)
17. Clark, R. K., *Rev. Sci. Instr.*, **21**, 753–59 (1950)
18. Borkowski, C. J., *Conference on Absolute Beta Counting* (National Research Council, U. S. A., Preliminary Report No. 8, Paper 11, October, 1950, unpublished data)
19. (a) Seliger, H. H., and Cavallo, L., *J. Research Natl. Bur. Standards*, **47**, 41 (1951); (b) Seliger, H. H., and Schwebel, A., *Nucleonics*, **12**[7], 54–63 (1954)
20. Hawkings, R. C., Merritt, W. F., and Craven, J. H., *The Maintenance of Radioactive Standards with the 4-pi Proportional Counter* (Symposium held at the National Physical Laboratory, Teddington, England, May, 1951)
21. Putnam, J. L., *Brit. J. Radiol.*, **23**, 46–63 (1950)
22. Gray, L. H., *Brit. J. Radiol.*, **22**, 677–97 (1949)
23. Smith, D. B., *Atomic Energy Research Establishment Report, AERE-I/R-1210* (June 18, 1953)
24. Meyer-Schutzmeister, L., and Vincent, D. H., *Z. Physik*, **134**, 9–20 (1952)
25. Houtermans, F. G., Meyer-Schutzmeister, L., and Vincent, D. H., *Z. Physik*, **134**, 1–8 (1952)
26. Seliger, H. H., *Phys. Rev.*, **98**, 408–12 (1952)
27. Mann, W. B., and Seliger, H. H., *J. Research Natl. Bur. Standards*, **50**, 197–200 (1953)
28. Marinelli, L. D., *Conference on Absolute Beta Counting* (National Research Council, U. S. A., Preliminary Report No. 8, Paper 11, October, 1950)
29. Caswell, R. S., *Phys. Rev.*, **86**, 82 (1952)

30. Jenks, G. H., and Sweeton, F. H., *Phys. Rev.*, **86,** 803 (1952)
31. *Meeting of the Subcommittee on Beta- and Gamma-Ray Measurements and Standards* (National Research Council, U. S. A.); (a) February, 1950; (b) October, 1952; (c) January, 1954
32. Gatti, E., and Germanogli, E., *Nuovo cimento*, **9,** 189 (1952)
33. Bay, Z., *Rev. Sci. Instr.*, **22,** 397 (1951)
34. Bell, R. E., Graham, R. L., and Petch, H. E., *Can. J. Phys.*, **30,** 35 (1952)
35. Huber, O., Humbel, F., Schneider, H., and DeShalit, A., *Helv. Phys. Acta*, **25,** 3–34 (1952)
36. Craig, D. H., and Dietrich, C. F., *Proc. Phys. Soc.* (*London*), **66**[B], 201–15 (1953)
37. Cavanaugh, P. E., *Phil. Mag.*, **43,** 648–58 (1952)
38. Bell, P. R., Jauch, J. M., and Cassidy, J. M., *Science*, **115,** 12–13 (1952)
39. Waggoner, M. A., Moon, M. L., and Roberts, A., *Phys. Rev.*, **80,** 420 (1950)
40. Rose, M. E., Goertzel, G. H., and Perry, C. L., *Oak Ridge National Laboratory Report, ORNL-1023* (June, 1951)
41. Deutsch, M., *Physics*, **18,** 1037–42 (1952)
42. Olsen, J. L., and O'Kelley, G. D., *Automatic Count and Control System for Beta-Ray Spectrometer* (Contract AT11-1-74 MTA-37, California Research and Development Co., Livermore, California)
43. Lind, D. A., Jr., Brown, R., and DuMond, J. W. M., *Phys. Rev.*, **76,** 1838–43 (1949)
44. Boley, F. I., and Zaffarano, D. J., *Iowa State College Report, ISC-154* (July, 1951)
45. Albert, R. D., *Atomic Energy Commission Document, AECD-3330* (September, 1951); *WAPD-42* (September, 1951)
46. Siegbahn, K., and Johansson, S., *Rev. Sci. Instr.*, **21,** 442 (1950)
47. Alburger, D. E., *Rev. Sci. Instr.*, **23,** 671 (1952)
48. Wu, C.-S., *Rev. Mod. Phys.*, **22,** 386–98 (1950)
49. Fano, U., Curtiss, L. F., Feister, I., and Stegun, I. A., *Natl. Bur. Standards U.S.), Appl. Math. Ser.*, No. 13, 61 pp. (1952)
50. Davisson, C. M., and Evans, R. D., *Mass. Inst. Technol., Nuclear Sci. and Eng. Tech. Report No. 37*, NP-1386 (February, 1950)
51. Davisson, C. M., and Evans, R. D., *Rev. Mod. Phys.*, **24,** 79–107 (1952)
52. Wyard, S. S., *Phys. Rev.*, **87,** 165 (1952)
53. Colgate, S. A., *Phys. Rev.*, **87,** 592–601 (1952)
54. *Isotopes, Catalog and Price List* (1953)[7]
55. Skraba, W. J., Burr, J. G., Jr., and Hess, D. N., *J. Chem. Phys.*, **21,** 1296 (1953)
56. Anderson, E. C., *Ann. Rev. Nuclear Sci.*, **2,** 63–78 (1953)
57. Rohinger, G., and Broda, E., *Z. Naturforsch.*, **68,** 159–60 (1953)
58. Hawkings, R. C., Hunter, R. F., Mann, W. B., and Stevens, W. H., *Can. J. Research*, **27**[B], 545 (1949)
59. Hawkings, R. C., Hunter, R. F., and Mann, W. B., *Can. J. Research*, **27**[B], 555 (1949)
60. Brown, S. C., and Miller, W. W., *Rev. Sci. Instr.*, **18,** 496 (1947)
61. Jones, W. M., *Phys. Rev.*, **76,** 885 (1949)
62. Engelkemeir, A. G., Hamill, W. H., Ingraham, M. G., and Libby, W. F., *Phys. Rev.*, **75,** 1825 (1949)
63. Engelkemeir, A. G., and Libby, W. F., *Rev. Sci. Instr.*, **21,** 550 (1950)

[7] Available from Radioisotope Sales Dept., Oak Ridge National Laboratory, Post Office Box P, Oak Ridge, Tenn.

64. Manov, G. G., and Curtiss, L. F., *J. Research Natl. Bur. Standards*, **46,** 328 (1951)
65. Manov, G. G., *National Research Council Publication 270, Preliminary Report 13* (July, 1953)
66. (a) Miller, W. W., Ballentine, R., Bernstein, W., Friedman, L., Nier, A. O., and Evans, R. D., *Phys. Rev.*, **77,** 714 (1950); (b) Bernstein, W., and Ballentine, R., *Rev. Sci. Instr.*, **21,** 158 (1950)
67. Warshaw, S. D., *Phys. Rev.*, **80,** 111 (1950)
68. Brownell, G. L., and Maletskos, C. J., *Phys. Rev.*, **80,** 1102 (1950)
69. Sinclair, W. K., and Halloway, A. F., *Nature*, **167,** 365 (1951)
70. Kastner, J., and Whyte, G. N., *Phys. Rev.*, **91,** 332 (1953)
71. Lockett, E. E., and Thomas, R. H., *Nucleonics*, **11,** No. 3, 14 (1953)
72. Fan, C.-Y., *Phys. Rev.*, **87,** 152–262 (1952)
73. Sreb, J. H., *Phys. Rev.*, **81,** 643 (1951)
74. Seliger, H. H., Cavallo, L., and Culpepper, N., *Phys. Rev.*, **90,** 443 (1953)
75. Bartholomew, R. M., Brown, F., Hawkings, R. C., Merritt, W. F., and Yaffe, L., *Can. J. Chem.*, **31,** 120–25 (1953)
76. Bell, P. R., Cassidy, J. M., and Kelley, G. G., *Phys. Rev.*, **82,** 103 (1951)
77. Cork, J. M., Rutledge, W. C., Stoddard, A. E., Branyan, C. E., and Childs, W. J., *Phys. Rev.*, **81,** 482 (1951)
78. Zeldes, H., Brosi, A. R., and Ketelle, B. H., *Phys. Rev.*, **81,** 642 (1951)
79. Verster, N. F., Nijgh, G. J., Van Lershout, R., and Bakker, C. J., *Physica*, **17,** 637–57 (1951)
80. Ketelle, B. H., Zeldes, H., Brosi, A. R., and Dandl, R. A., *Phys. Rev.*, **84,** 585 (1951)
81. Cavanagh, P. E., *Phil. Mag.*, **43,** 221–30 (1952)
82. Bell, R. E., and Graham, R. L., *Phys. Rev.*, **86,** 212 (1952); *Can. J. Phys.*, **30,** 35 (1952)
83. Haskins, J. R., and Kurbatov, J. D., *Phys. Rev.*, **88,** 884 (1952)
84. Rose, D., Hinman, G., and Lang, L. G., *Phys. Rev.*, **86,** 863 (1952)
85. Bell, P. R., Davis, R. C., Francis, J. E., Cassidy, J., and Jordan, W. H., *Oak Ridge National Laboratory Report, ORNL-1092* (January, 1952)
86. Fiskell, J. G. A., DuLong, W. A., and Oliver, W. F., *Can. J. Chem.*, **30,** 185 (1952)
87. (a) Jensen, E. N., and Nichols, R. T., *Phys. Rev.*, **85,** 112 (1952); (b) Nichols, R. T., and Jensen, E. N., *Iowa State College Report, ISC-352* (June, 1953)
88. Jensen, E. N., and Nichols, R. T., *Atomic Energy Commission Report, AECU-1264* (April, 1951)
89. Sheline, R. K., Holtzman, R. B., and Fan, C. Y., *Phys. Rev.*, **83,** 919–23 (1951)
90. *Radioisotope Distribution*, Code of Federal Regulations: Title 10-Atomic Energy; Part 30-Section 30.71 (1951)
91. Kohman, T. P., Ames, D. P., and Sedlet, J., *National Nuclear Energy Series, NNES*, Div. 4, **14**[5], Part 2, Paper 22.60 (1951)
92. Bouissieres, G., and Ferradini, C., *Anal. Chim. Acta*, **4,** 610–14 (1950)
93. Prestwood, R. J., *Atomic Energy Commission Document, AECD-3380* (May, 1952)
94. Begemann, F., and Houtermans, F. G., *Z. Naturforsch*, **79,** 143–44 (1952)
95. Burtt, B. P., *Conference on Absolute Beta Counting* (National Research Council, U. S. A., Preliminary Report No. 8, Paper No. 1, October, 1950); Nucleonics, **5,** No. 2, 28–43 (1949)

96. Novey, T., *Conference on Absolute Beta Counting* (National Research Council, U. S. A., Preliminary Report No. 8, Paper No. 3, October, 1950)
97. Powers, R. I., and Voight, A. F., *Phys. Rev.*, **79,** 157–75 (1950)
98. Cohn, R. A., (Doctoral thesis, Ohio State University, Columbus, Ohio, 1950)
99. Moreau, J., and Corba, J. P. Y., *Compt. rend.*, **235,** 38–40 (1952)
100. Shepherd, L. R. (Doctoral thesis, University of Cambridge, Cambridge, England, 1950)
101. Reynolds, S. A. (Unpublished data, Oak Ridge National Laboratory, Oak Ridge, Tenn.; *Meeting of the Subcommittee on Beta- and Gamma-Ray Measurements and Standards*, National Research Council, U.S.A. (October, 1952)
102. Lidofsky, L., Macklin, P., and Wu, C. S., *Phys. Rev.*, **87,** 391 (1952)
103. der Mateosian, E., and Smith, A., *Brookhaven National Laboratory Report, BNL-1246* (1952)
104. Harbottle, G., *Brookhaven National Laboratory Report, Report BNL-1441* (1953)
105. Reynolds, S. A., *Nucleonics*, 11(11), 46 (1953)
106. Cavanagh, P. E., *Phys. Rev.*, **82,** 791–95 (1951)
107. Brosi, A. R., Ketelle, B. H., Zeldes, H., and Fairstein, E., *Phys. Rev.*, **84,** 586 (1951)
108. Hubert, P., *Compt. rend.*, **232,** 2201–3 (1951)
109. Hill, R. D., and Mihelich, J. W., *Phys. Rev.*, **79,** 275 (1950)
110. Muller, D. E., Hoyt, H. C., Klein, D. J., and DuMond, J. W. M., *Phys. Rev.*, **88,** 775 (1952)
111. Hedgran, A., and Lind, D., *Arkiv Fysik.*, **5,** 177 (1952)
112. Broyles, C. D., Thomas, D. A., and Haynes, S. K., *Phys. Rev.*, **89,** 715–24 (1953)
113. (a) Maeder, D., and Preiswerk, P., *Phys. Rev.*, **84,** 595–96 (1951); (b) *Helv. Phys. Acta*, **24,** 625–27 (1951)
114. Schuman, R. P., and Camilla, A., *Phys. Rev.*, **84,** 158 (1951)
115. Tobaliem, J., *J. phys. radium*, **14,** 553 (1953)
116. Brower, D., Hinman, G., Lang, G., Leamer, R., and Rose, D., *Phys. Rev.*, **86,** 1054 (1952)
117. Metzger, F. R., *Phys. Rev.*, **88,** 1360–67 (1952)
118. Sreb, J. H., *Phys. Rev.*, **81,** 469 (1951)
119. Wilson, R., and Bishop, G. R., *Proc. Phys. Soc.* (*London*), **62**[A], 457 (1949)
120. Turner, J. F., and Cavanagh, P. E., *Phil. Mag.*, **42,** 636 (1951)
121. Mins, W., Halban, H., and Wilson, R., *Nature*, **166,** 1027 (1950)
122. Hedgran, A., and Lind, D., *Arkiv Fysik*, **5,** 178–90 (1952)
123. Jenks, G. H., Sweeton, F. H., and Ghormley, J. A., *Phys. Rev.*, **86,** 990 (1950)
124. Jones, W. M., *Phys. Rev.*, **83,** 537–39 (1951)
125. Langer, L. M., and Moffatt, R. J. D., *Phys. Rev.*, **88,** 689 (1952)
126. *USAEC Technical Information Division Report, TID-371* (1950)
127. Robinson, C. V., *Rev. Sci. Instr.*, **22,** 353 (1951)
128. Melander, L., *Acta Chem. Scand.*, **2,** 440 (1948)
129. Lyon, W. S., *Phys. Rev.*, **87,** 1126 (1952)
130. Sunyar, A. W. (Unpublished data, Brookhaven National Laboratory, Upton, Long Island, N. Y., 1952)
131. Furberg, S. E., *Nature*, **168,** 1005 (1951)
132. Major, J. K., *Compt. rend.*, **234,** 2276 (1952); *Phys. Rev.*, **86,** 531A (1952)
133. Griffiths, M., *Phys. Rev.*, **83,** 852 (1951)
134. Mann, K. C., Rankin, D., and Kaykin, P. N., *Phys. Rev.*, **76,** 1719 (1949)

FISSION RADIOCHEMISTRY (LOW-ENERGY FISSION)[1]

By L. E. Glendenin and E. P. Steinberg
Chemistry Division, Argonne National Laboratory, Lemont, Illinois

Introduction

Radiochemical studies of fission products not only led to the discovery of nuclear fission [Hahn & Strassmann (1)] but have since played an important role in the detailed characterization of this phenomenon. Through the measurement of fission yields (probabilities of formation for the various fission products), radiochemical research has resulted in a much more accurate picture of the distribution of mass and nuclear charge in fission than could be obtained by purely physical methods. An extensive investigation of fission yields in low-energy neutron induced fission was made by many workers on the Plutonium Project for U^{235}, U^{238}, and Pu^{239} (2), and also for U^{233} [Steinberg *et al.* (3)]. Fission yields in neutron-induced fission of U^{235} and U^{233} were investigated on the Canadian project by Grummitt & Wilkinson (4). The results of these investigations have shown that low-energy fission is predominantly asymmetric, i.e., the mass distribution (yield-mass curve) has two maxima (light and heavy group peaks) and a deep central minimum (trough) showing the low frequency of symmetric fission modes. With increasing mass of the fissioning nucleus the mass distribution becomes wider, and the light group peak shifts toward higher masses while the position of the heavy group peak remains relatively fixed (with perhaps a slight shift in the direction of lower mass). Some evidence was also obtained in comparing thermal neutron with fast pile neutron induced fission of Pu^{239} for an increase in frequency of symmetric fission modes (trough yields) and very asymmetric modes (wing yields) as the excitation energy of the fissioning nucleus is increased (5). Subsequent investigations, showing the marked increase of trough yields with increasing excitation energy, have been reviewed by Spence & Ford (6).

The radiochemical method is of particular value in the study of the problem of nuclear charge distribution in fission. This problem is concerned with finding the most probable mode of charge division as a function of mass split, and the variation of primary formation (or independent fission yield) with nuclear charge among fission fragments of the same mass number. All fission yield data from the Plutonium Project bearing on this question were considered in 1946 by Glendenin, Coryell & Edwards (7) and were shown to be consistent with an empirical hypothesis that the most probable division of nuclear charge (in slow neutron induced fission) is that which leads to equal charge displacements of complementary fission fragments from stabil-

[1] The survey of the literature pertaining to this review was concluded in January, 1954.

ity. This postulate has been of considerable value in predicting many effects in fission product chains, e.g., cases of isomerism and mass assignments, which were later verified. Recent work supporting the equal charge displacement hypothesis is discussed below in the section on Charge Distribution.

A significant contribution to the radiochemical study of fission products was the introduction by Thode and co-workers (8, 9) of the mass spectrometric technique in the determination of relative fission yields. This method is capable of high precision, may be applied to stable as well as radioactive nuclides, and avoids the difficulties involved in β-counting. Investigation of the relative abundances of stable and long-lived fission-produced isotopes of krypton and xenon by this technique (8, 9) revealed for the first time the existence of "fine structure," i.e., fission yields deviating from a smooth yield-mass curve. Recent mass spectrometric investigations have yielded further evidence for fine structure in mass distribution, and are discussed below in the section on Closed Shell Effects.

A review of radiochemical studies of fission yields prior to 1949 has been given by Way & Dismuke (10) covering mass distribution, charge distribution, and changes that occur as the energy of the particle inducing fission is increased. Spence & Ford (6) have recently reviewed investigations on high-energy fission. Whitehouse (11) has given a general survey of the whole field of nuclear fission covering the literature through 1951. Useful bibliographies (12) on fission have been issued by the Information Office of the British Atomic Energy Research Establishment covering the period from January, 1946 to September, 1952. A survey of spontaneous and slow neutron fission properties of heavy nuclei has been given by Huizenga, Manning & Seaborg (13) covering slow neutron fission cross sections, photofission thresholds, neutron fission thresholds, correlation of slow neutron fissionability with fission thresholds and neutron binding energies, and systematics of spontaneous fission half lives as a function of atomic and mass number.

The present review is limited to the period since 1949 and covers only radiochemical investigations of the low-energy fission process, i.e., spontaneous fission and fission induced by neutrons ranging in energy from thermal to a few Mev. Photofission and high-energy particle induced fission are not included, except for the recent interesting observations on the angular distribution of fission fragments. Investigations primarily concerned with the search for and characterization of individual fission products are not reviewed except insofar as they may relate directly to interpretations of the fission process.

Neutron Induced Fission

Mass distribution.—Most of the general features of the low-energy fission yield-mass curves for U^{233}, U^{235}, U^{238}, and Pu^{239} had been fairly well established by 1949. Work in this field has more recently been directed toward refinements in the measurments to establish absolute fission yields and to examine more detailed features of the mass distribution. In addition, the studies have been extended to some other fissionable nuclides.

The relative fission yields of 23 chains in the pile neutron induced fission of Th^{232} were determined radiochemically by Turkevich & Niday (14). A complete yield-mass curve was constructed from the data and compared with the corresponding curves for U^{233}, U^{235}, U^{238}, and Pu^{239} to illustrate the effect of varying the mass of the fissioning nucleus. Fission of Th^{232} is similar to the others in being highly asymmetric, and the yield-mass curve for this nuclide, the lightest mass so far investigated, extends the trends with mass previously noted. The ratio of the most probable yields to yields for symmetrical fission (peak-to-trough ratio) is 110, considerably lower than the corresponding ratio for thermal fission of U^{235} (about 600). The average energy of the neutrons effective in inducing fission in Th^{232} was estimated as 2.6 Mev, appreciably higher than the "threshold" energy of about 1.1 Mev, and the lower peak-to-trough ratio is consistent with the higher energy content of the compound nucleus. The suggestion was made that the observed decrease in the peak-to-trough ratio with increasing energy may be owing to the superposition on the familiar twin-peaked curve of a yield curve with a rather broad maximum at symmetrical fission which increases in magnitude with increasing energy of excitation.

The earlier fission yield-mass curve for pile neutron induced fission of U^{238} [Engelkemeir *et al.* (15)] was in doubt in the region of the trough because of a possible cadmium contamination and not very well defined in the region of the heavy group peak. Keller, Steinberg & Glendenin (16) have reinvestigated the fission of U^{238} with pile neutrons (estimated average effective energy of 2.8 Mev) by the determination of the yields of 15 products. The results are in essential agreement with the earlier work except in the region of the trough, the yield of the mass 115 chain being 0.035 ± 0.007 per cent compared with the former result of 0.059 per cent. The lower yield of symmetrical modes (peak-to-trough ratio of 200) compared with that for Th^{232} is consistent with the relative excitation energies of the compound nuclei as determined by their neutron fission thresholds and binding energies, and the average energy of the neutrons effective in inducing fission in the two cases. The writers note the difficulty of interpreting the effect of energy on the peak-to-trough ratio when fission is induced by a spectrum of neutrons. Comparisons of the yield-mass curve for U^{238} with those for Th^{232} and spontaneous fission of U^{238} (see below) indicate the expected trends with energy of excitation and with mass.

In addition to these rather complete surveys of mass distribution, fission yields for limited mass regions and some individual fission products have been determined utilizing mass spectrometric and improved counting techniques. Some of these investigations were primarily concerned with the nature of fine structure in the fission yield curves and will be discussed below in the section on Closed Shell Effects.

Relative fission yields in the mass region 143 to 160 were obtained by Inghram, Hayden & Hess (17) for pile neutron fission of U^{235} using a mass spectrometric determination of the relative abundances of isotopes of neo-

dymium, samarium, europium, and gadolinium. Difficulties of fitting the relative yields of one element to those of another, and the corrections for large neutron absorption cross sections in this region were examined. The results indicate a smooth yield curve with higher yields than those obtained radiochemically (2) above mass 153. The authors point out that the irradiated sample was a thick uranium slug in which the neutron energy distribution would differ from that occurring in thin sources irradiated with moderated pile neutrons as employed in many radiochemical studies. It should be noted, however, that the deviations from the radiochemical curve may also have been attributable to contributions from Pu^{239} fission in which the fission yields of this mass region are considerably higher (2). The fission yields of Kr^{85}, Kr^{87}, and Kr^{88} in U^{235} fission were investigated mass spectrometrically by Koch *et al.* (18) who observed relative values of 33 ± 10, 70 ± 15, and 100, respectively.

Redeterminations of the yields of several fission products in the slow neutron fission of U^{235} have been made using more accurate techniques for the determination of disintegration rates. Hardwick (19) found yields for Ru^{103} and Ru^{106} of 2.85 ± 0.16 per cent and 0.38 ± 0.03 per cent, respectively, relative to reference values of 6.2 per cent for Ba^{140} and 6.15 per cent for Cs^{137}. These results are significantly lower than the previously accepted values (2) and are more reliable. Bartholomew *et al.* (20) report a value of 3.1 ± 0.1 per cent for the fission yield of I^{131} relative to a reference value of 6.1 per cent for Ba^{140}. Sugarman (21) clarified the genetics of the decay chains of mass numbers 77 and 78 and determined the yields of 12-hr. Ge^{77}, 38-hr. As^{77}, 86-min. Ge^{78}, and total 91-min. As^{78} to be 2.3×10^{-3}, 6.7×10^{-3}, 1.8×10^{-2}, and 2.0×10^{-2} per cent, respectively, relative to a reference value of 6.17 per cent for Ba^{140}. The values for mass 77 are significantly lower than those previously reported (22) while those for mass 78 are in good agreement. No greater accuracy is claimed for these values than for the earlier ones. Ba^{140} has served as a fission monitor in many investigations, and its absolute fission yield is therefore of considerable importance. Unfortunately, the decay scheme is complex and determinations of absolute disintegration rates had not been made with high accuracy. The data of Freedman & Engelkemeir (23) have been reevaluated by Steinberg (24), using a half life of 308 hr. with empirical self-absorption and scattering correction factors. A yield of 6.32 per cent was obtained with an estimated error of about 10 per cent. Yaffe & co-workers (25) have determined the absolute yield of Ba^{140} as 6.26 per cent with an estimated error of about 5 per cent, and Reed & Turkevich (26) obtained a value of 6.3 per cent with an estimated error of less than 6 per cent. These results are in good agreement, and a yield of 6.3 ± 0.3 per cent is suggested as a best value.

For the determination of absolute yields it is, of course, necessary to know the fission rate of the source material as well as the disintegration rate of the product of interest. Accurate fission and β-counting have been employed in some recent absolute yield determinations in the thermal neutron

fission of U^{235}. Katcoff & Rubinson (27) determined the absolute yield of 5.27-day Xe^{133} as 6.62 ± 0.15 per cent and correlated the result with other yields in the mass region 131 to 137. Absolute gas counting and careful fission monitoring were employed in this determination, and the value is probably the best established fission yield yet reported. The absolute yield of Mo^{99} has been studied as a function of the neutron energy inducing fission by Terrell *et al.* (28). A value of 6.14 ± 0.16 per cent was obtained for thermal fission. A number of absolute yields were determined by Reed & Turkevich (26) with an estimated accuracy of 6 per cent. Values of 4.78 per cent for Sr^{89}, 5.1 per cent for Sr^{91}, 5.5 per cent for Zr^{97}, 5.98 per cent for Mo^{99}, 6.4 per cent for Ba^{139}, and 6.3 per cent for Ba^{140} were obtained. These data are in good agreement with previous yields of lower accuracy, but they are lower in some cases than those which were observed in mass spectrometric determinations now being completed (29). The latter investigation encompasses the determination of a rather complete yield-mass curve for the pile neutron fission of U^{235} by absolute radiometric and mass spectrometric measurements correlated with the results of other investigators.

The possibility of ternary fission into two fragments of about mass 100 and one of about mass 40 was investigated radiochemically on the Plutonium Project [Metcalf *et al.* (30); Boyd, Larson & Simon (31)]. Positive identification of fission products in the mass range 35 to 60 was not made, but upper limits of the order of 10^{-4} per cent were set for the fission yields of such products. Partition into two heavy fragments and one light one in the mass range 4 to 13 had been indicated by cloud chamber and photographic plate studies to occur with a frequency of about 1 per cent of binary fissions. Only a few nuclides in this mass range are suitable for radiochemical investigation, and a search for Be^{7} was made by Cook (32) who set an upper limit of 10^{-5} per cent for the yield in uranium fission. A review of the data on such ternary fission was given by de Laboulaye, Tzara & Olkowsky (33), who investigated the short-range particles in a cloud chamber and interpreted them as probably knock-on atoms. The frequency of occurrence was estimated as $1 \pm 3/1000$ binary fissions.

Charge distribution.—The status of the problem of the division of nuclear charge in fission was reviewed by Glendenin (34) in 1949. All pertinent data were shown to be consistent with both the equal charge displacement hypothesis (7), and a theory of charge division developed by Present (35) based on a nuclear model with radially nonuniform charge distribution. In an extensive study of fission yields and closed shell effects in fission, Pappas (36) presented a modification of the equal charge displacement hypothesis which takes into account the discontinuities in the stability valley at shell closures. This modified treatment was shown to bring apparently anomalous independent yields of Nb^{96} [Cook (37)] and As^{78} [Sugarman (21)] into better agreement with the charge distribution curve. Additional data of Cook (37) and Brown & Yaffe (38) were also included in a summary of all available information on independent yields in U^{235}, Pu^{239}, and U^{233}. The data were

shown to be well accounted for by a single charge distribution curve, essentially identical with that given by Glendenin, Coryell & Edwards (7). Pappas also points out that Present's theory, which does not consider nuclear shell structure, cannot be expected to give exact predictions for individual mass numbers, but is nevertheless in fair agreement with the data. Although no definite choice can yet be made between the two postulates of charge division, the equal charge displacement interpretation has been somewhat more successful in the quantitative prediction of independent fission yields.

Some additional independent yield data have been reported. Ford & Stanley (39) found a value of about 2 per cent of the chain yield for La^{141} in the slow neutron fission of U^{235}, and Turkevich & Niday (14) set an upper limit of about 3×10^{-2} per cent of the total chain for Cs^{136} in the pile neutron fission of Th^{232}. These data are consistent with the charge distribution postulates mentioned. Ford (40) has shown that the charge distribution curve for 14 Mev neutron fission of U^{235} is parallel to that for thermal neutron fission of U^{235} with the most probable charge for a given mass split shifted toward stability, i.e., a smaller neutron-to-proton ratio for the primary fragments. Steinberg & Glendenin (41) found the independent yield of Cs^{136} in the spontaneous fission of Cm^{242} to be in agreement with the prediction of the equal charge displacement hypothesis. Thus, it appears that for all fissile nuclides thus far investigated, a single charge distribution curve is applicable over a wide range of excitation energies (0 to 14 Mev). However, in very high-energy fission, e.g., 190-Mev deuteron fission of Bi [Goeckerman & Perlman (42)], the division of nuclear charge is apparently different, the most probable charge of the primary fragments being that which maintains the same neutron-to-proton ratio as the fissioning nucleus. This may indicate that at very high energies the fission process takes place too rapidly to permit any rearrangement of charge.

Closed shell effects.—The early radiochemical investigations (2) of slow neutron induced fission indicated that the yield distributions were rather smooth functions of mass. In fact, when particular determinations did not fit the smooth curve, errors arising from a failure to achieve interchange, the presence of an isomeric state, or difficulties in the measurement of the disintegration rate were suspected and generally found. The concept of a smooth relationship between fission yield and mass proved extremely useful in establishing mass assignments, half lives of long-lived fission products, etc. Marked deviations from a smooth curve relationship were definitely established, however, by the mass spectrometric determinations of the relative abundance of krypton and xenon isotopes produced in U^{235} fission [Thode and co-workers (8, 9)] and later by the radiochemical determination of the yield of I^{136} in the fission of U^{233}, U^{235}, and Pu^{239} [Stanley & Katcoff (43)].

A proposal to explain this fine structure in mass distribution was made by Glendenin (34, 44) on the basis of the stability of nuclear closed shells of 50 and 82 neutrons. Nuclei which contain 51 or 83 neutrons, i.e., one neutron

more than the closed shell, have abnormally low-binding energies (by approximately 2 to 3 Mev) for the extra neutron. It was postulated that a primary fission product (which has already emitted the usual number of prompt neutrons) containing one neutron in excess of the closed shell may emit this neutron in preference to a β-particle or γ ray. This process of extra neutron emission would result in perturbations in fission yields near a closed shell since the loss in yield from a given chain would not always be exactly compensated by the gain in yield from the chain of one higher mass number. Calculations, based on this mechanism and utilizing the primary yields along fission chains as given by the charge distribution function (discussed in the previous section), indicated a fine structure pattern for the krypton and xenon isotopes and an abnormally low yield for I^{136} in qualitative agreement with the experimental observations.

Further mass spectrometric investigations of the fission yields of cesium, rubidium, and strontium isotopes were carried out by Wiles *et al.* (45, 46). In order to account more quantitatively for these results and the earlier investigations of xenon and krypton yields, Wiles (45) suggested that fragments containing 82 neutrons are favored (i.e., occur in abnormally high yield) in the fission process, in addition to the postfission effect proposed by Glendenin. Experimental verification of the preference for an 82-neutron fragment in fission was obtained by Glendenin *et al.* (47), who observed in mass spectrometric studies an abnormally high yield for mass number 100 which is complementary to the 82 neutron containing masses (133 and 134). Relative fission yields for Zr and Mo isotopes, together with those for Xe and Kr (8, 9) and Nd (7), were normalized to give a yield-mass curve differing significantly in shape from the older "smooth" radiochemically-determined curve for U^{235} fission (2). This investigation has been extended (29) to obtain absolute fission yields for a wide range of mass numbers utilizing the isotope dilution technique, and the results clearly indicate perturbations in yield consistent with nuclear structure preference in fission and excessive postfission neutron evaporation.

Radiochemical determinations of fission yields in the regions of fine structure have been made by Pappas (26), Wiles (48), and Yaffe, Day & Greer (49). In general, this work has corroborated the earlier mass spectrometric observations. Pappas (36) extended the concept of extra evaporation of loosely-bound odd neutrons just outside closed shells to include the third, fifth, and seventh such neutrons on the basis of neutron binding energy systematics, and obtained good agreement with the observed fine structure pattern in the region of the 82-neutron shell. Wiles (48) investigated yields in the mass region 99 to 106 for slow neutron and 15-Mev deuteron fission of U^{235} and 15-Mev deuteron and 13-Mev photon fission of U^{238}. Although evidence for fine structure at mass 101 was slight, the results for the deuteron fission of U^{235} and U^{238} and the photofission of U^{238} indicate abnormally high yields at about mass 105. This is ascribed to a selectivity in the fission process for fragments containing 50 protons (analogous to the 82-neutron preference),

mass 105 being the expected complement of the favored fragment. An analysis of the expected mass positions for the fine structure peaks attributable to the 82-neutron and 50-proton preferences in the fission process is given for a number of fissile nuclides.

Further supporting evidence for nuclear closed shell effects in fission is given by the observations of fine structure in spontaneous fission of Th^{232}, U^{238}, and Cm^{242} discussed in the following section. It is interesting to note, for example, that the widely-different mass positions of light group fine structure in U^{235} fission (mass 100) and Cm^{242} fission (mass 105) are both complementary to the mass region (around 134) associated with 82 neutrons. The shift of heavy group fine structure from mass 134 in U^{235} fission to mass 132 in spontaneous fission of Th^{232} and U^{238} is also consistent with the expected mass positions of the 82-neutron shell.

Spontaneous Fission

Information on the mass distribution of the fragments from spontaneous fission was first obtained in ionization chamber studies by Whitehouse & Galbraith (50). It was found that the kinetic energy distributions of the fragments from spontaneous fission of U^{238} and slow neutron induced fission of U^{235} are essentially identical within the limitations of resolution inherent in this method. The spontaneous fission of Cm^{242} was also observed to be asymmetric in similar studies by Shuey (51) and Hanna *et al.* (52).

More accurate information on the mass distribution in spontaneous fission was obtained by Thode and co-workers (53, 54) and by Wetherill (55), using the highly sensitive mass spectrometric technique. These investigators examined the isotopic composition of the rare gases Kr and Xe produced in various minerals by spontaneous fission of U^{238} (53, 54, 55) and Th^{232} (55). The observed abundances of the krypton and xenon isotopes indicate that the mass distribution in spontaneous fission has narrower peaks and probably a lower trough than that in slow neutron induced fission. Evidence was also found for an abnormally high yield (fine structure) at mass 132 for both U^{238} and Th^{232}.

A more complete investigation of the distribution of yields in spontaneous fission was made by Steinberg & Glendenin (41) who determined radiochemically the yields of 21 fission products (ranging in mass number from 91 to 140) from the spontaneous fission of Cm^{242}. The yield-mass curve exhibits somewhat higher and narrower peaks than are observed in neutron-induced fission. Although the amount of Cm^{242} available was not sufficient to produce a measurable activity of fission products in the region of symmetrical fission (mass numbers 116 to 124), the upper limit set at Cd^{117} (<0.01 per cent) and the slope of the curve indicate a peak-to-trough ratio at least as large as that observed in thermal neutron induced fission of U^{235}, and perhaps considerably larger. Rising trough yields and broadening of the mass distribution have been observed with increasing energy of excitation in induced fission (6), and therefore it might be expected that spontaneous fission (no

excitation) would exhibit a lower trough and narrower peaks. Prominent fine structure in the mass distribution was also observed in the regions of mass 105 and 134. The effect in the light group is more pronounced than that in neutron induced fission of U^{235}, indicating that nuclear structure preference in fission may diminish with increasing excitation energy of the fissioning nucleus.

Angular Distribution of Fission Fragments

Although not strictly within the scope of this review, the recent observations of anisotropic angular distribution of fission fragments in photofission and higher energy particle induced fission are of considerable interest. Winhold, Demos & Halpern (56) observed that the fragments from photofission of Th^{232} are emitted preferentially at right angles to the photon beam with an angular distribution of the form $a+b \sin^2 \theta$, and that the amount of anisotropy (ratio b/a) decreases with increasing photon energy from 1.2 at 8 Mev to 0.4 at 16 Mev. In further experiments (57), employing radiochemical determinations of individual fission products from 16 Mev photofission, it was found that the anisotropy is a function of mass split with b/a increasing from zero at a mass ratio of 1.0 to about 0.8 at mass ratio 1.8. Brolley, Dickinson & Henkel (58, 59) investigated the angular distribution of fragments from neutron induced fission of U^{235} for neutron energies between thermal and 20 Mev. It was found that the fission fragments are emitted preferentially in the same direction as the neutron beam with an angular distribution of the form $a+b \cos^2 \theta+d \cos^4 \theta$, and that the anisotropy is a function of neutron energy increasing from zero at thermal energy to a maximum at about 10 Mev and then decreasing at higher energies. The angular distribution of fragments from 22 Mev proton induced fission of Th^{232}, studied by Cohen *et al.* (60), is also of the form $a+b \cos^2 \theta+d \cos^4 \theta$ with anisotropy greater for asymmetric fission than for symmetric fission as shown by radiochemical determination of individual fission products. Adequate theoretical interpretations of these phenomena have not yet been given.

Summary

The radiochemical investigations of the past few years have extended the previously noted trends of the mass distribution with variation in excitation energy and mass of the fissile nucleus, and have established the general applicability of a single charge distribution function. Marked deviations from smooth fission yield-mass curves have been observed and correlated with the influence of nuclear closed shells, giving a plausible picture in terms of preferential formation of and neutron emission from particular fragments.

The pronounced asymmetry of low-energy fission is perhaps the most outstanding feature of the process. Many nuclear models have been invoked in attempts to account for this phenomenon, but there has been no general acceptance of any one theoretical development. The most successful treat-

ments appear to be those of Hill & Wheeler (61) and Fong (62). The former is based on the collective model of the nucleus and, although no quantitative conclusions are drawn, it is stated that the model is not inconsistent with fission asymmetry. Fong's theory is based on the development of a mass equation which takes into account the perturbations attributable to closed shells. The concept of statistical equilibrium is utilized with the probability of formation determined by the number of available quantum states in the excited fragments. Quantitative calculations of the expected mass distribution in slow neutron induced fission of U^{235} are in excellent agreement with the observed fission yield-mass curve. Some other predictions, however, particularly regarding charge distribution, are not in agreement with observation, and further quantitative tests of the applicability of the theory to other fissile nuclides and other features of the fission process are needed.

LITERATURE CITED

1. Hahn, O., and Strassmann, F., *Naturwiss.*, **27,** 11 (1939)
2. *Radiochemical Studies: The Fission Products*, Nat'l Nuclear Energy Ser., Div. IV-9 (Coryell, C. D., and Sugarman, N., Ed., McGraw-Hill Book Co., Inc., New York 18, N. Y., 2086 pp., 1951)
3. Steinberg, E. P., Seiler, J. A., Goldstein, A., and Dudley, A., *U. S. Atomic Energy Commission Document, MDDC-1632* (1948)
4. Grummitt, W. E., and Wilkinson, G., *Nature*, **161,** 520 (1948)
5. Steinberg, E. P., and Freedman, M. S., in *Radiochemical Studies: The Fission Products*, Nat'l Nuclear Energy Ser., Div. IV-9, Paper 219, 1378 (Coryell, C. D., and Sugarman, N., Ed., McGraw-Hill Book Co., Inc., New York 18, N. Y., 2086 pp., 1951)
6. Spence, R. W., and Ford, G. P., *Ann. Rev. Nuclear Sci.*, **2,** 399 (1953)
7. Glendenin, L. E., Coryell, C. D., and Edwards, R. R., in *Radiochemical Studies: The Fission Products*, Nat'l Nuclear Energy Ser., Div. IV-9, Paper 52, 489 (Coryell, C. D., and Sugarman, N., Ed., McGraw-Hill Book Co., Inc., New York 18, N. Y., 2086 pp., 1951)
8. Thode, H. G., and Graham, R. L., *Can. J. Research*, [A]**25,** 1 (1947)
9. Macnamara, J., Collins, C. B., and Thode, H. G., *Phys. Rev.*, **78,** 129 (1950)
10. Way, K., and Dismuke, N., *Oak Ridge National Laboratory Report, ORNL-280* (1950)
11. Whitehouse, W. J., *Prog. Nuclear Phys.*, **2,** 120 (Pergamon Press, Ltd., London, England, 295 pp., 1952)
12. *Bibliography on Fission* (Atomic Energy Research Establishment, Harwell, Berks., England, Inf./Bib. 76, July, 1951; Inf./Bib. 76, Oct., 1952, Suppl. 1)
13. Huizenga, J. R., Manning, W. M., and Seaborg, G. T., in *The Actinide Elements*, Nat'l Nuclear Energy Ser., Chapt. 20, 839 (Seaborg, G. T., and Katz, J. J., Ed., McGraw-Hill Book Co., Inc., New York 18, N. Y., 870 pp., 1954)
14. Turkevich, A., and Niday, J. B., *Phys. Rev.*, **84,** 52 (1951)
15. Engelkemeir, D. W., Seiler, J. A., Steinberg, E. P., and Winsberg, L., in *Radiochemical Studies: The Fission Products*, Nat'l Nuclear Energy Ser., Div. IV-9, Paper 218, 1375 (Coryell, C. D., and Sugarman, N., Ed., McGraw-Hill Book Co., Inc., New York 18, N. Y., 2086 pp., 1951)

16. Keller, R. N., Steinberg, E. P., and Glendenin, L. E., *Phys. Rev.*, **94,** 969 (1954)
17. Inghram, M. G., Hayden, R. J., and Hess, D. C., *Phys. Rev.*, **79,** 271 (1950)
18. Koch, J., Kofoed-Hansen, O., Kristensen, P., and Drost-Hansen, W., *Phys. Rev.*, **76,** 279 (1949)
19. Hardwick, W. H., *Phys. Rev.*, **92,** 1072 (1953)
20. Bartholomew, R. M., Brown, F., Hawkings, R. C., Merritt, W. F., and Yaffe, L., *Can. J. Chem.*, **31,** 120 (1953)
21. Sugarman, N., *Phys. Rev.*, **89,** 570 (1953)
22. Steinberg, E. P., and Engelkemeir, D. W., in *Radiochemical Studies: The Fission Products*, Nat'l Nuclear Energy Ser., Div. IV-9, Paper 54, 566 (Coryell, C. D., and Sugarman, N., Ed., McGraw-Hill Book Co., Inc., New York 18, N. Y., 2086 pp., 1951)
23. Freedman, M. S., and Engelkemeir, D. W., in *Radiochemical Studies: The Fission Products*, Nat'l Nuclear Energy Ser., Div. IV-9, Paper 206, 1344 (Coryell, C. D., and Sugarman, N., Ed., McGraw-Hill Book Co., Inc., New York 18, N. Y., 2086 pp., 1951)
24. Steinberg, E. P. (Unpublished data, October, 1952)
25. Yaffe, L. (Personal communication, October, 1952)
26. Reed, G. W., and Turkevich, A., *Phys. Rev.*, **92,** 1473 (1953)
27. Katcoff, S., and Rubinson, W., *Phys. Rev.*, **91,** 1458 (1953)
28. Terrell, J., Scott, W. E., Gilmore, J. S., and Minkkinen, C. O., *Phys. Rev.*, **92,** 1091 (1953)
29. Glendenin, L. E., Steinberg, E. P., Hayden, R. J., Inghram, M. G., and Flynn, K. F. (To be published in *Phys. Rev.*, 1954)
30. Metcalf, R. P., Seiler, J. A., Steinberg, E. P., and Winsberg, L., in *Radiochemical Studies: The Fission Products*, Nat'l Nuclear Energy Ser., Papers 47-51, 478–88 (Coryell, C. D., and Sugarman, N., Ed., McGraw-Hill Book Co., Inc., New York 18, N. Y., 2086 pp., 1951)
31. Boyd, G. E., Larson, Q. V., and Simon, D. M., *Clinton Laboratories* (*Oak Ridge*) *Reports MonN-311*, 78 (1947); *MonN-370*, 428 (1947)
32. Cook, G. B., *Nature*, **169,** 622 (1952)
33. de Laboulaye, H., Tzara, C., and Olkowsky, J., *Compt. rend.*, **237,** 155 (1953)
34. Glendenin, L. E., *Laboratory for Nuclear Science Technical Report No. 35*, Massachusetts Institute of Technology (1949)
35. Present, R. D., *Phys. Rev.*, **72,** 7 (1947)
36. Pappas, A. C., *Laboratory for Nuclear Science Technical Report No. 63*, Massachusetts Institute of Technology, (1953); Pappas, A. C., and Coryell, C. D., *Phys. Rev.*, **81,** 329 (1951)
37. Cook, G. B. (Personal communication, June, 1953)
38. Brown, F., and Yaffe, L., *Can. J. Chem.*, **31,** 242 (1953)
39. Ford, G. P., and Stanley, C. W., *U. S. Atomic Energy Commission Document, AECD-3551* (1953)
40. Ford, G. P., *U. S. Atomic Energy Commission Document, AECD-3597* (1953)
41. Steinberg, E. P., and Glendenin, L. E., *Radiochemical Investigation of the Spontaneous Fission of* Cm^{242} (Presented at Gordon Research Conference on Nuclear Chemistry, New Hampton, N. H., June 23, 1953); to be published in *Phys. Rev.* (July 15, 1954)
42. Goeckerman, R. A., and Perlman, I., *Phys. Rev.*, **73,** 1127 (1948)
43. Stanley, C. W., and Katcoff, S., *J. Chem. Phys.*, **17,** 653 (1949)

44. Glendenin, L. E., *Phys. Rev.*, **75,** 337 (1949); Glendenin, L. E., and Coryell, C. D., *Phys. Rev.*, **77,** 755 (1950)
45. Wiles, D. R., *Fission Yields of Cesium, Rubidium, and Strontium Isotopes and Their Relation to Fine Structure in Fission* (Master's Thesis, McMaster Univ., Hamilton, Ont., Canada, August, 1950)
46. Wiles, D. R., Smith, B. W., Horsley, R., and Thode, H. G., *Can. J. Phys.*, **31,** 419 (1953)
47. Glendenin, L. E., Steinberg, E. P., Inghram, M. G., and Hess, D. C., *Phys. Rev.*, **84,** 860 (1951)
48. Wiles, D. R., *A Study of Fission-Yield Fine Structure* (Doctoral thesis, Massachusetts Institute of Technology, Cambridge, Mass., 1953)
49. Yaffe, L., Day, A. E., and Greer, B. A., *Can. J. Chem.*, **31,** 48 (1953)
50. Whitehouse, W. J., and Galbraith, W., *Phil. Mag.*, **41,** 429 (1950)
51. Shuey, R. L., *University of California Radiation Laboratory Report, UCRL-959* (1950)
52. Hanna, G. C., Harvey, B. G., Moss, N., and Tunnicliffe, P. R., *Phys. Rev.*, **81,** 466 (1951)
53. Macnamara, J., and Thode, H. G., *Phys. Rev.*, **80,** 471 (1950)
54. Fleming, W. H., and Thode, H. G., *Phys. Rev.*, **92,** 378 (1953)
55. Wetherill, G. W., *Phys. Rev.*, **92,** 907 (1953)
56. Winhold, E. J., Demos, P. T., and Halpern, I., *Phys. Rev.*, **87,** 1139 (1952)
57. Winhold, E. J., Demos, P. T., Halpern, I., and Fairhall, A. W., *Laboratory for Nuclear Science Progress Report,* Massachusetts Institute of Technology (February 28, 1953)
58. Dickinson, W. C., and Brolley, J. E., Jr., *Phys. Rev.*, **90,** 388 (1953)
59. Brolley, J. E., Jr., Dickinson, W. C., and Henkel, R. L. (Personal communication, March, 1954)
60. Cohen, B. L., Jones, W. H., McCormick, G. H., and Ferrell, B. L., *Bull. Am. Phys. Soc.*, **29,** 21 (1954)
61. Hill, D. L., and Wheeler, J. A., *Phys. Rev.*, **89,** 1102 (1953)
62. Fong, P., *A Theory of Nuclear Fission* (Doctoral thesis, University of Chicago, Chicago, Ill., 1953); *Phys. Rev.*, **89,** 332 (1953)

STABLE ISOTOPE DILUTION AS AN ANALYTICAL TOOL[1]

By Mark G. Inghram

Department of Physics, University of Chicago, Chicago, Illinois
Physics Division, Argonne National Laboratory, Lemont, Illinois

Introduction

The physicist engaged in nuclear or solid state work often would like to use a chemical analysis in order to expediently proceed on a research problem. For example, one way to ascertain the branching ratio for the radioactive decay of Cu^{64} is to determine chemically the ratio of the amounts of

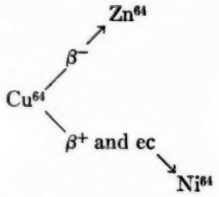

Zn^{64} and Ni^{64} formed from the decay process. In such a determination the branching ratio measured does not involve any assumptions as to decay mechanism, for example, whether the decay to Ni^{64} is by electron capture, positron emission, or both. Unfortunately, in many problems, the amount of the element of interest is below one part in a million (p.p.m.) so that the usual methods of chemical analysis can not be used. One method which can be used to do accurate chemical analysis in the p.p.m. range, and often well below, is that of isotopic dilution in which a tracer isotope is used as an internal standard. Of course, the fact that it is eminently suited to sub p.p.m. determination does not in any way preclude its use in the macro range. In fact, the biologists have been using it for a number of years in these macro ranges for the determination of H, C, and N (1). Its use was limited to these elements until the end of the war (1945) because of the fact that these were the only elements for which samples having stable isotopic composition different from normal (dilutants) were available. In 1946, the U. S. Atomic Energy Commission made available separated stable isotopes of many of the elements, so that the isotopic dilution method now is a practical tool for chemical analysis with sensitivity potentialities far exceeding standard analytical chemistry procedures.

Method

The isotopic dilution method of chemical analysis with a mass spectrometer can be illustrated by outlining the procedure and by giving a hypothetical

[1] The survey of literature pertaining to this review was concluded in March, 1954.

example. It should be kept in mind that the mass spectrometer is the most universal of the isotopic analysis schemes, but that any other method of isotopic analysis can be adapted to yield the same type of result. A typical procedure is as follows:

I. A weighed portion of the sample to be analyzed is dissolved in an appropriate solvent.

II. A weighed amount (usually an aliquot of a stock solution) of a separated isotopic tracer of the element in question is added to the result of Step (*a*).

III. The mixture of the sample and tracer are processed through appropriate steps to insure that the tracer is properly equilibrated with the sample.

IV. The element in question, now consisting of a mixture of normal and dilutant isotope, is extracted chemically (this step is optional depending on the element in question and the sensitivity desired).

V. The change in isotopic composition of the element in question in the sample caused by addition of the tracer isotope is determined mass spectrometrically.

From the change in isotopic composition obtained in Step V the concentration of the element in the original sample can be calculated.

A hypothetical example of such a measurement is the determination of the amount of La in a metal sample. La as it exists in nature consists of two isotopes, La^{139} and La^{138}, with abundances of 99.911 per cent and 0.089 per cent, respectively. To a first approximation it consists only of La^{139}. Suppose that to 1 gm. of the sample to be studied is added 1 μg. of the separated isotope La^{138} and that, after mixing and extracting the La according to Steps I to IV outlined above, one observes the mass spectrum shown in Figure 1, i.e., that the ratio of La^{139} to La^{138} is 1:2. Thus, since the peak height attributable to the tracer added as internal standard is 1 p.p.m., that attributable to the La in the sample is one-half of that or 0.5 p.p.m. (there is a small correction because of the difference in atomic weight of La^{138} and La^{139}). The accuracy is simply the accuracy in the determination of the ratio of the isotopes which, if it were 1 per cent, would yield a final answer of 0.500 $\pm$.005 p.p.m.

In actual practice clear-cut cases such as the hypothetical example given above do not often occur. Both normal and tracer isotopes consist of mixtures of isotopes so that recourse to a simple set of two simultaneous equations is usually necessary. An example is shown in Figure 2. This figure shows an isotopic dilution analysis of the U in a meteor (2). In this particular case the U content was about 0.005 p.p.m. Since both tracer and normal contain a mixture of isotopes, simultaneous equations are necessary. Thus, if

$$R_1 = \left(\frac{U^{235}}{U^{238}}\right)_{\text{normal}} \qquad 1.$$

$$R_2 = \left(\frac{U^{235}}{U^{238}}\right)_{\text{tracer}} \qquad 2.$$

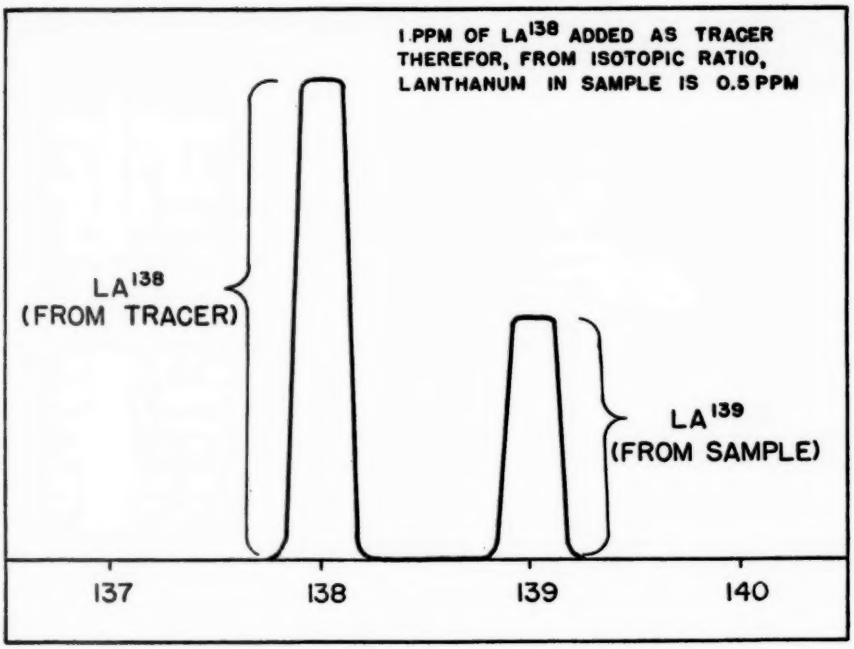

FIG. 1. Hypothetical isotopic dilution measurement of La in a solid sample. One p.p.m. of La^{138} added as tracer gives the peak at mass 138. Since the peak of 139 is one-half of this, the sample contained one-half the weight of tracer added or 0.5 p.p.m.

$$R_3 = \left(\frac{U^{235}}{U^{238}}\right)_{mxture} \qquad 3.$$

$$M_1 = \text{Mass of U in sample} \qquad 4.$$

$$M_2 = \text{Mass of U added as tracer} \qquad 5.$$

solving for the mass M_1 in terms of R_1, R_2, R_3, and M_2 neglecting the difference in atomic weight one finds

$$M_1 = \frac{(R_1 + 1)(1 - R_3/R_2)}{(R_3 - R_1)(1 + 1/R_2)} M_2. \qquad 6.$$

From this equation it is apparent that the best tracer is one which differs from normal by the greatest possible factor so that R_3/R_2 can be very different from one. The ideal tracer is a monoisotope in which case $R_2 = \infty$. As will be seen, this condition is also the one which makes the chemical processing the simplest, because it will in principle allow the addition of a maximal amount of tracer in which case difficulty of separation of the tracer from the sample should be minimal.

DISCUSSION

From the foregoing description of the procedure, one may draw con-

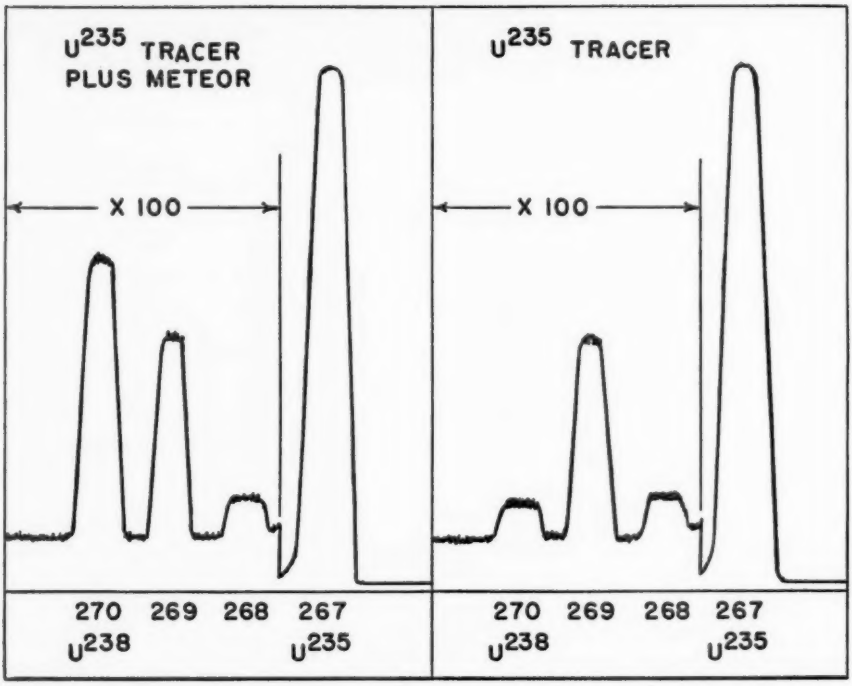

FIG. 2. Mass spectrum illustrating the isotopic dilution method of determination of trace quantities of uranium. This element is analyzed as UO_2 so that the apparent mass of U^{235} is 235+32=267. The peaks at mass 268 and 269 are attributable to O^{17} and O^{18}, respectively. The change of 500 per cent in the U^{238} abundance in the spectrum at the left is attributable to a meteorite containing five p.p.b. of U.

clusions as to the advantages and difficulties with the isotopic dilution method of chemical analysis.

The final result, equation 6, depends only on isotopic ratios. It does not depend on the chemical recovery of the element in question. For example, if in the foregoing example 99 per cent of the La^{138} had been lost, so also would 99 per cent of the La^{139} and the result would have been unchanged. This elimination of the usual requirement of quantitative or known chemical recovery greatly eases the chemistry involved. Chemical recovery is important only in as far as contamination is a factor, as will be discussed later.

The method is absolute, i.e., it requires no calibration with samples of known concentration. There are no undetermined additive factors by which the result must be corrected as in the usual gravimetric methods where solubilities are involved. As long as enough material is recovered to serve for isotopic analysis, the result is correct.

If the isotopic tracer is calibrated by dilution against normal, using the

same mass spectrometer to be used in later measurements, the discrimination of the instrument cancels out to the approximation that it can be considered constant.

Since the method involves only isotopic ratios, any type of mass spectrometer can be applied. Therefore, the instrument having the highest sensitivity for a given element can be used. For many of the elements this means sensitivities of 10^{-12} gm. and for a few, K, Rb, Cs, sensitivities of 10^{-14} gm. The limitation is usually not the mass spectrometer but contamination. For example, how does one handle a K sample without getting many times 10^{-14} gm. of K from reagents or from the air?

If the tracer is good, i.e., very different from normal, one does not have to make a good guess as to the level of the impurity in order to realize the full potentialities of the method. Thus, in the spectrum shown in Figure 2, if, without changing the amount of tracer, the U had been 10 times lower or 10,000 times higher, the accuracy of the analysis would have been unchanged. To go outside this range it would have been necessary to use different amounts of tracer.

The method is useful for only one or at most only a few elements at a time. Different elements involve different procedures. The method is, therefore, not as useful for general chemical analysis as the Dempster vacuum spark or the ion bombardment techniques (3). This difficulty is counterbalanced by the fact that it is many orders of magnitude more sensitive and several times more accurate than these alternative mass spectrometric procedures. It is, therefore, often applicable when all other methods fail.

All methods of trace analysis suffer from problems of contamination. Thus, in a single analysis one can not determine whether the normal material came from the sample or from contamination in reagents. In the mass spectrometric isotopic dilution technique of analysis, this problem is handled by processing two parts of the sample differing in mass by a factor of ten through the same amount of reagents. If contamination is negligible, the two will have the element in question in the ratio of the starting samples. If the ratio is less than this, contamination is present and the reagent corrections can be calculated. Note, however, that corrections can be applied only if the chemical recovery is identical in the two samples. Note further that if the contamination comes in as dust particles and is not introduced from the reagents, then there is no reason to assume that the contamination introduced in one sample is the same as that in the other. The safest way to correct for contamination is to have none present, i.e., use extremely clean laboratory techniques. This problem is, of course, less important when there are large amounts of impurity present in the sample.

The stable isotopic dilution technique is limited in application to those elements which have more than one isotope which can be measured in the mass spectrometer. The scope of the method is given in Table I. This table lists the elements in two columns depending on whether or not they can be analyzed by the isotopic dilution method.

TABLE I

SCOPE OF ISOTOPIC DILUTION METHOD OF CHEMICAL ANALYSIS

Elements Analyzable				Elements Not Analyzable
H	V	Pd	Gd	F
He	Cr	Ag	Dy	Na
Li	Fe	Cd	Er	Al
(Be)	Ni	In	Yb	P
B	Cu	Sn	Lu	Sc
C	Zn	Sb	Hf	Mn
N	Ga	Te	W	Co
O	Ge	(I)	Re	As
Ne	Se	Xe	Os	Y
Mg	Br	(Cs)	Ir	Cb
Si	Kr	Ba	Pt	Rh
S	Rb	La	Hg	Pr
Cl	Sr	Ce	Tl	Tb
A	Zr	Nd	Pb	Ho
Ca	Mo	(Pm)	Th	Tm
Ti	(Tc)	Sm	U	Ta
K	Ru	Eu	(Pu)	Au
Total 68				Total 17

Those elements, in parentheses, listed under those which are analyzable do not have two isotopes in nature but they have a long-lived isotope which can be formed into piles and can be used in a similar way. Note then that these are "perfect" tracers since there is no superposition of peaks. Examples of such tracers are I^{129} and Cs^{137} formed in fission. There are a few elements listed under "not analyzable" which could be analyzed by using very hot tracers, but in general they are more easily handled by other methods.

PREPARATION OF TRACERS

The preparation of tracers for laboratory use is a special problem since all calculations involve a precise knowledge of the amount of tracer added. The most convenient tracer is a well standardized stock solution from which known amounts of tracer can be withdrawn by simply measuring the volume. In some instances it is more convenient to introduce the tracer as a gas. This is the case when one is working with gas samples or with rare gases in solid materials. In either case there is a problem as to purity and amounts.

The simplest method of making up a tracer solution is to add a known weight of a good gravimetric compound of the element to a known volume of water. This procedure, however, is not recommended for two reasons: (*a*) it takes a large amount of sample to make a good gravimetric determination, i.e., of the order of 50 mg.; and (*b*) the result depends on the chemical

purity of the tracer element in question. A typical alternative procedure is as follows:

I. Prepare a solution of the tracer by dissolving about 1 mg. of tracer in solution in a convenient amount of water.

II. Prepare a standard solution of a chemically pure sample of normal isotopic composition by dissolving gram amounts of reagent material in a quantity of water about 1000 times that in Step I.

III. Combine equal aliquots of the solution from Step I and Step II and measure the resulting isotopic composition on the mass spectrometer.

From the isotopic composition observed in Step III, the concentration of the tracer sample can be calculated. The advantages of this technique are: (*a*) large amounts of separated isotope are not necessary for standardization; (*b*) the chemical purity of the tracer does not enter, the result depends only on the purity of the reagent grade normal material used in Step II; and (*c*) the mass spectrometric discrimination introduced in the isotopic measurement of Step III is later cancelled when the isotopic composition resulting from an isotopic dilution analysis is made.

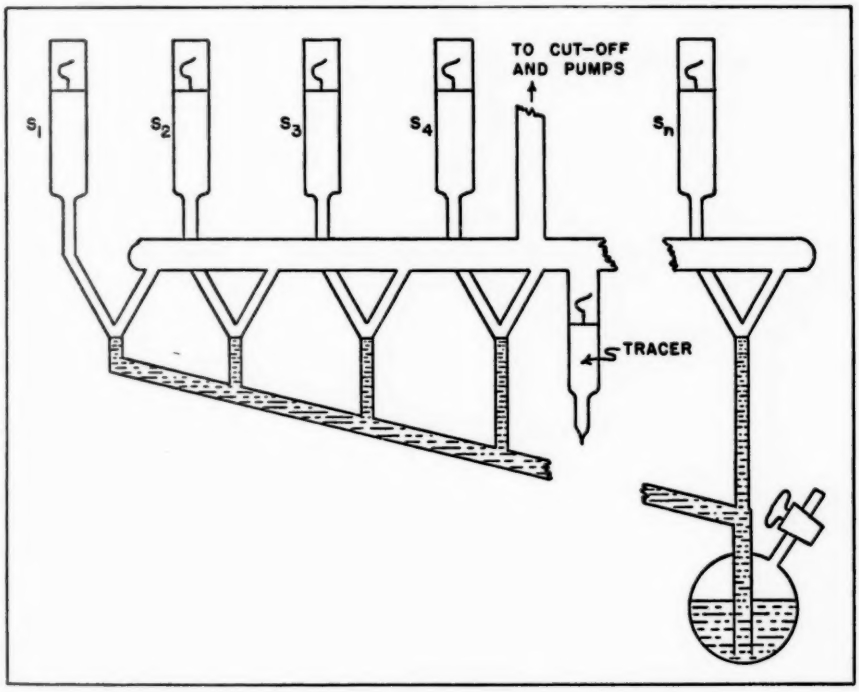

FIG. 3. Apparatus used for preparing gas isotopic tracer for use in isotopic dilution measurements. Three of these tracers are usually used in the apparatus of Figure 4 to determine the amount of tracer in each of the $S \rightarrow S_n$ tubes. This one operation of the apparatus gives $n-3$ tracers containing known amounts of gas.

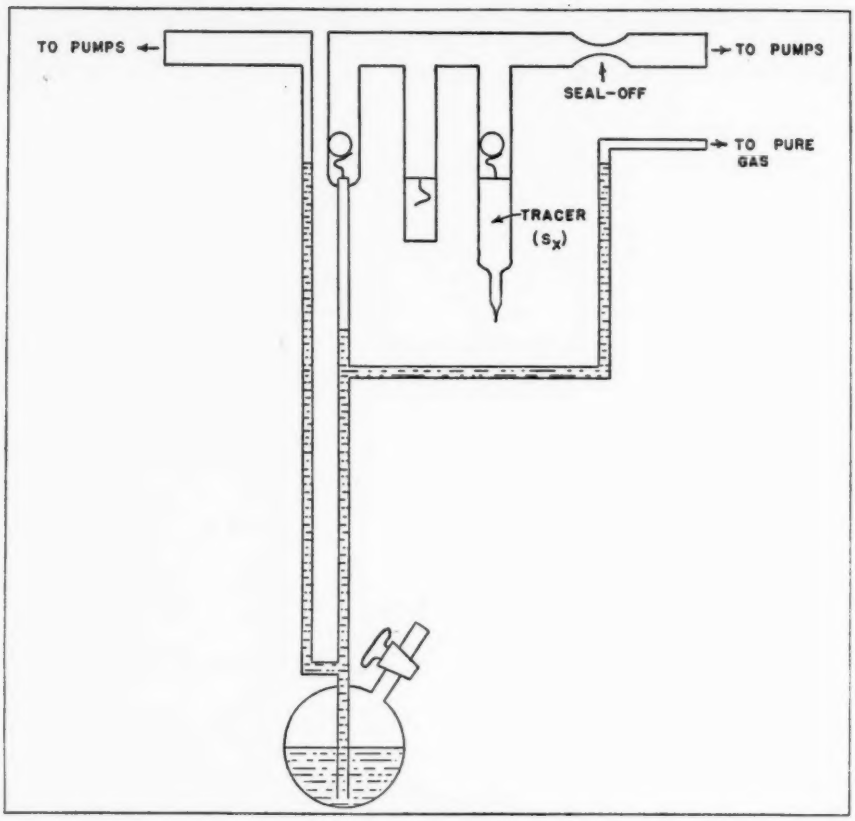

FIG. 4. Apparatus for diluting the tracer samples prepared in the setup shown in Figure 3 with a known amount of reagent grade gas. From the ratio of isotopes observed in the mixed gas, the amount of gas in each of the S_n tubes can be calculated.

Preparation of gas tracers is a somewhat different task since small pure gas aliquots are difficult to prepare. Again, a more satisfactory method is to prepare tracers and determine their concentrations by diluting against reagent grade gases. A procedure which has proved reliable is as follows. I. Subdivision of the tracer is accomplished with the apparatus shown in Figure 3, which consists of a number of sample tubes, S_1, $S_2 \cdots S_n$ of known volume connected to a manifold through a series of Y-shaped capillar cutoffs. The tracer to be divided is connected to the manifold as shown. After the apparatus is evacuated and isolated from the pumps the tracer is broken into the manifold and allowed to equilibrate throughout the system for a number of hours. The mercury in the capillary cutoffs is then raised the 1 or 2 mm. necessary to isolate each of the samples and the individual samples sealed

TABLE II

ISOTOPIC DILUTION ANALYSIS OTHER THAN BIOLOGICAL

Element	Sample	Ref.	Purpose
Gd	Eu	(4)	Branching in radioactivity
Sm	Eu	(4)	Branching in radioactivity
Ca	KCl	(5)	Branching in radioactivity
A	KCl	(5)	Branching in radioactivity
A	Meteor	(6)	Geologic age
Xe	Bu_2Te_3	(7)	Double beta decay
Zn	Cu	(8)	Branching in radioactivity
Ni	Cu	(8)	Branching in radioactivity
Kr	NaBr	(8)	Branching in radioactivity
Se	NaBr	(8)	Branching in radioactivity
Xe	NaI	(8)	Branching in radioactivity
Te	NaI	(8)	Branching in radioactivity
U	Minerals	(2)	Geologic age
Pb	Minerals	(9)	Geologic age
Th	Minerals	(10)	Geologic age
A	Minerals	(11)	Geologic age
Sr	Minerals	(12)	Geologic age
Rb	Minerals	(12)	Geologic age
Kr	Minerals	(13)	Spontaneous fission
Xe	Minerals	(13)	Spontaneous fission
Ne	Minerals	(13)	Neutron flux in geology
Sr	U	(14)	Fission yield
Zr	U	(14)	Fission yield
Mo	U	(14)	Fission yield
Ru	U	(14)	Fission yield
Cs	U	(14)	Fission yield
Ba	U	(14)	Fission yield
Ce	U	(14)	Fission yield
Nd	U	(14)	Fission yield

off. The ratio of the volumes in S_1—S_n to that of the capillary cutoffs is made sufficiently large to give the desired accuracy in the result.

II. Several, usually three, of the tracer tubes are connected successively to an apparatus similar to that shown in Figure 4 for dilution against a known volume of reagent grade gas of normal isotopic composition. The PV in this sample is determined in the modified McLeod. The sample is always released by a break off at the top of McLeod capillary in order to eliminate any absorbed gases from the lower part of the system from being added to the sample. The capillaries are made small so that the pressures used can be high.

III. After an appropriate mixing time (long, since mixing is through a

TABLE III

URANIUM AND THORIUM CONTENT OF VARIOUS GEOLOGIC MATERIAL*

Sample	Uranium in p.p.m.	Thorium in p.p.m.
Zircon	2650 ± 40	2180 ± 20
Sphene	303 ± 5	5375 ± 75
Perthite	$0.22 \pm .03$	$0.410 \pm .008$
Stone Meteor	$0.0054 \pm .0002$	—
Ammonium Nitrate	$0.000075 \pm .000004$	—

* These results are taken from the work of Tilton *et al.* (15) and Tilton (2).

capillary of a break-off) the isotopic composition of the resulting mixture is determined in a mass spectrometer.

From the result observed in Step III above, the amount of gas in each of the tracer tubes used in Step II can be calculated, and since the volume ratios in all tubes, S_1—S_n, is known, the amounts of tracer in each of the remaining tubes is also known. Thus, the setup of Figure 3 will prepare n-3 tracer aliquots for use in isotopic dilution analyses. The advantages of the above method of gas tracer preparation are identical to those listed under liquid tracers with the added advantage that if the ratio of surface to volume of each of the samples, tubes is about the same, the error arising from absorption of gas on walls is greatly reduced. Measurement on rare gas tracers produced in the above way are reproducible to within about 1 per cent.

Sources of tracer isotopes for use in the above preparations are limited. The U. S. Atomic Energy Commission produces the greatest variety. A few comments should be made about these samples. In general, an isotopic tracer made in a pile is better than a tracer made in a calutron. Thus, if one prepares a mercury tracer by slow neutron irradiation of gold, it is pure Hg^{198}, while the best tracer prepared by calutrons is only about 95 per cent pure. Other examples of pile produced tracers are: Xe^{128} from NaI, A^{38} from NaCl, Ba^{134} from Cs, Nd^{142} from Pr, etc. Certainly, of all the isotopes a long-lived fission isotope is the most perfect.

RESULTS

The elements which have been handled with the isotopic dilution technique along with the samples in which the elements have been determined are given in Table II.

To illustrate the range and accuracy of the method, analyses of the U and Th content of some geologic material will be found in Table III.

Using the error as a measure of sensitivity, isotopic dilution analyses of U have been done down to four parts in 10^{12} and on Th to eight parts in 10^9. Both of these are considerably better than the sensitivity obtained with

any other known analytical method. The errors are attributable to contamination and sample inhomogeneity; in no case do they represent the limits of the method.

Conclusions

The isotopic dilution method of chemical analysis is a practical tool for high sensitivity analytical work. The time required for an analysis is variable depending on the sensitivity and the accuracy desired. For example, if one has a vacuum lock equipped mass spectrometer and one wants to determine the amount of Rb in a K salt with a sensitivity of one part in 10^8, one would require less than 30 min. for analysis. On the other hand, if one is working with Th or U in rocks, from three to five days are necessary for each analysis.

The method has been applied to only a limited number of problems since good tracer isotopes have been available through the Atomic Energy Commission only since the war (1945). Applications have been further limited because of the fact that the supply of separated isotopes is extremely limited and there are definite restrictions as to their use. The cost of a 10 μg. tracer for a Pb analysis is about one cent according to Dr. Kern of the Atomic Energy Commission. This is completely negligible in comparison to the total cost of an analysis. It is clear, therefore, that as soon as separated isotopes are produced and supplied by private or public firms on a self-supporting unrestricted basis, the isotopic dilution method of chemical analysis can become a standard tool for trace element work.

LITERATURE CITED

1. Rittenberg, D., *J. Appl. Phys.*, **13**, 561 (1942)
2. Tilton, G. R., *Atomic Energy Commission Report, AECD-3182* (1951)
3. Inghram, M. G., *J. Phys. Chem.*, **57**, 809 (1953)
4. Hayden, R. J., Reynolds, J. H. and Inghram, M. G., *Phys. Rev.*, **75**, 1500 (1949)
5. Inghram, M. G., *Phys. Rev.*, **80**, 916 (1950)
6. Suess, H. E., Hayden, R. J., and Inghram, M. G., *Nature*, **168**, 432 (1951)
7. Hayden, R. J., and Inghram, M. G., *Mass Spectroscopy in Physics Research, Natl. Bur. Standards (U. S.), No. 522*, 189–92 (1953)
8. Reynolds, J. H., *Phys. Rev.*, **79**, 789 (1950)
9. Patterson, C., *Atomic Energy Commission Report, AECD-3180* (1951)
10. Tilton, G. R., Aldrich, L. T., and Inghram, M. G., *Anal. Chem.* (In press)
11. Wasserburg, G. J., and Hayden, R. J., *Phys. Rev.*, **93**, 645 (1954)
12. David, G. L., and Aldrich, L. T., *Bull. Geol. Soc. Amer.*, **64**, 379 (1953)
13. Wetherill, G., *Phys. Rev.*, **92**, 907 (1953)
14. Glendenin, L., Steinberg, E., Hayden, R. J., and Inghram, M. G., *Phys. Rev.* (To be published)
15. Tilton, G. R., Patterson, C., Brown, H., Inghram, M. G., Hayden, R. J., Hess, D. C., and Larsen, E., *Bull. Geol. Soc. Amer.* (In press)

NUCLEAR PARTICLE DETECTION: FAST ELECTRONICS[1]

By R. E. Bell

Chalk River Laboratory, Chalk River, Canada, and Radiation Laboratory, McGill University, Montreal, Canada

Introduction

The great advances in the techniques of nuclear particle detection that have occurred within the last six years are almost entirely attributable to the introduction of the scintillation counter by Kallmann (1) and Deutsch (2) late in 1947. Before 1947 an article with the same title as the present one would have taken the limit of response time as about 10^{-7} sec., with perhaps hopeful references to faster results from electron multipliers in certain special applications. The introduction of the scintillation counter has reduced this limit to a few times 10^{-10} sec. It is therefore appropriate to limit this review almost entirely to scintillation counters; this limitation is indeed not a serious one, since now most experiments involving counting of nuclear particles employ the scintillation method. An appropriate definition of the word "fast" would be "responding in less than 10^{-7} sec." In order to confine this review to a reasonable length, the reader is assumed to be generally familiar with scintillation counting and with electronic pulse techniques.

Scintillation counters may be classified into the usual phosphor type and the Cerenkov type. The former type is usually limited in speed of response by the speed of the phosphor itself. In the latter type the light quanta detected by the photomultiplier are produced instantaneously by the passage of a relativistic particle through the Cerenkov medium, so that the phosphor response time is effectively zero. Cerenkov counters are the subject of a separate chapter in this volume and will not be specifically discussed further.

A fundamental limit on the timing of an event by a counting apparatus is imposed by the size of the apparatus and the speed of light. For example, suppose a 2 cm. cube of phosphor is being used to count γ-rays, one face of the cube being in contact with the photomultiplier. The earliest instant at which light can reach the photomultiplier is later by 10^{-10} sec. (assuming refractive index of 1.5 for the phosphor material) for a γ-ray absorbed far from the photomultiplier than for one absorbed nearby. Good experimental design can only partially overcome this limit, for example, by partially cancelling the light transit time against the time of flight of the γ-ray. The obvious remedy of reducing the apparatus size is not open to us, because of the loss of counting efficiency that such a step would entail. The limit is therefore real and physical, and not merely technical. There is, in addition, the technical limit that electron transit time effects in the best present photo-

[1] The survey of literature pertaining to this review was concluded in January, 1954.

multipliers introduce an uncertainty of a few times 10^{-10} sec. in the timing of an event. Pulse timing with accuracy near the above limits has been repeatedly achieved with scintillation counters (cf. COINCIDENCE TECHNIQUES). Further progress in this direction must therefore await new developments.

Besides the timing of events, scintillation counters yield valuable information through measurement of the amplitudes of their output pulses. It is often desirable to measure the height of a pulse with a minimum of delay in the process. The time necessary to accomplish this measurement is directly dependent on the response time of the scintillation phosphor, since in this case we must observe substantially the whole of the pulse and not merely its beginning. The technique of PULSE HEIGHT ANALYSIS has not been carried as close to its technical limit of speed as that of fast coincidence analysis; a similar remark applies to COUNTING. These topics, together with AMPLIFICATION, are discussed in the sections to follow.

AMPLIFICATION

Conventional linear amplifiers for use in nuclear counting usually have rise times of about 10^{-7} sec. and maximum output pulses of 50 to 100 volts. Such amplifiers just escape the definition of "fast" used for this review. The usual pentode tubes used in these amplifiers have $g_m \backsim 10^4$ μmho, practical total capacity C_T (input plus output) $\backsim 20$ $\mu\mu$f, and maximum plate current $i_m \backsim 20$ m.a. A tube with these parameters used in a resistance coupled circuit has a time constant per unit gain $C_T/g_m = 2\times10^{-9}$ sec. A single stage of gain 10 therefore has a time constant of 2×10^{-8} sec.; four such stages cascaded to give a gain of 10^4 then have a time constant of $\sqrt{4}\times2\times10^{-8}$ sec. $=4\times10^{-8}$ sec. Taking the rise time (10 to 90 per cent) as 2.5 time constants, we arrive at the figure of 10^{-7} sec. mentioned above. The maximum possible rate of rise of the pulse at the output of such an amplifier is $i_m/C_T = 10^9$ v./sec., so that in 10^{-7} sec. the pulse can only rise 100 volts. The above considerations are not influenced by the use of inverse feedback. Thus the limitations of the usual linear amplifier are just those of the vacuum tubes of which it is composed.

Two means of overcoming these limitations are now in use; the distributed amplifier, which is a new way of connecting conventional tubes in an amplifier, and the secondary emission pentode, which is a tube in which g_m is raised without raising C_T.

The distributed amplifier was first put to practical use by Ginzton and his co-workers (3) following the original suggestion by Percival (4). It is, in effect, a method of connecting the g_m's of several tubes in parallel without adding up their parallelled capacities. (The latter effect defeats attempts to achieve better bandwidth performance by simple paralleling of tubes.) The basic circuit is shown in Figure 1, where for simplicity the tubes are shown as triodes and the supplying of d-c voltages to the plate circuit has been ignored. The grids are connected by inductances L_g to form an artificial

transmission line with the capacitances C_g, which are just the grid input capacities of the tubes. The characteristic impedance of the grid line is $R_g = (L_g/C_g)^{\frac{1}{2}}$. The signal travels from left to right along this line, arriving successively at the various grids, and is absorbed by the termination R_g. The time delay between successive grids is $(L_gC_g)^{\frac{1}{2}}$. If the plate transmission line is proportioned so that $(L_pC_p)^{\frac{1}{2}} = (L_gC_g)^{\frac{1}{2}}$, the amplified grid signals will add in phase along the plate line as a wave travelling to the right, and will pass to the output. Backward moving waves of equal amplitude from the individual tubes also exist in the plate line; they are absorbed in the termination $R_p = (L_p/C_p)^{\frac{1}{2}}$ at the left hand end of the plate line. The gain per tube is

$$A_1 = \tfrac{1}{2}g_m(L_p/C_p)^{1/2},$$

the factor $\frac{1}{2}$ being attributable to the wasted backward waves. The total gain is

$$A_n = (n/2)g_m(L_p/C_p)^{\frac{1}{2}},$$

for n tubes so connected if the output load is an impedance equal to R_p. The open-circuit output gain is $2A_n$. Thus the gain per tube A_1 may actually be less than unity, and the whole unit may still have a useful gain. Regarding the plate (or grid) artificial transmission line as a repetitive low-pass filter,

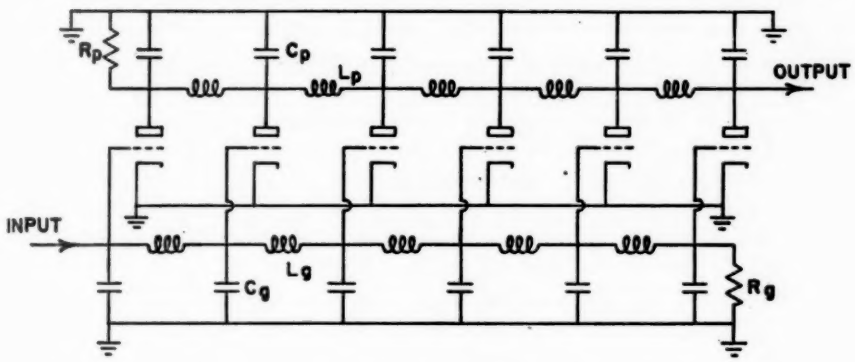

FIG. 1. Schematic diagram of a 6 tube distributed amplifier. The tubes are shown as triodes, though pentodes would invariably be used, and the supplying of d-c voltages to the various electrodes has been ignored.

the cutoff angular frequency is $(L_pC_p)^{-\frac{1}{2}}$, corresponding to a time constant of $(L_pC_p)^{\frac{1}{2}}$. A single tube with resistive plate load equal to $R_p = (L_p/C_p)^{\frac{1}{2}}$ would have a time constant equal to $R_pC_p = (L_pC_p)^{\frac{1}{2}}$, identical with the figure for the distributed amplifier. The distributed amplifier thus has the effect of multiplying the g_m, or gain, of the tube by n, while maintaining the same rise time; the price paid for this is the n-fold increase in tubes used and power dissipated.

A typical set of values is $n = 6$, tube type 6AK5, with $C_g \backsim 5$ $\mu\mu$f and $g_m = 5 \times 10^{-3}$ mhos. With a small capacity added to the plate of each tube,

C_p can be made equal to C_g, so that the plate and grid lines become identical. This step is not always desirable, but is a convenience if distributed stages are to be cascaded. Choosing $R_p = R_g = 200$ ohms, $L_p = L_g$ becomes 0.2 μh. The gain (open circuit) is $ng_mR_p = 6$, and the time constant is $R_pC_p = 10^{-9}$ sec., giving a rise time (10 to 90 per cent) of 2.5×10^{-9} sec. If the plate line of this 6-tube stage is fed into the 200 ohm grid line of the succeeding stage, the stage gain becomes 3. Amplifiers of approximately these specifications, consisting of two cascaded stages, each of 6 type 6AK5 tubes, are available commercially. Their over-all gain is 10 and their quoted rise time 3×10^{-9} sec., in agreement with the above estimates. Other models of this type of amplifier have been designed for providing large output voltages for deflecting oscilloscopes, for example, and a number of commercial oscilloscopes now employ them. Distributed amplifiers have a number of disadvantages, among which may be mentioned the fact that they insert a delay of $n(L_gC_g)^{\frac{1}{2}}$ sec. per stage. (In our example this would be 6×10^{-9} sec. For oscilloscope amplifiers this delay is not necessarily a disadvantage.) In addition, since the input and output voltages are not synchronized, there is no obvious way to apply inverse feedback in order to improve their gain stability and linearity.

Examples of actual distributed amplifier designs are given by Horton *et al.* (5), Yu *et al.* (6), Gérardin (7), and Bassett & Kelly (8). Some of these designs are for surprisingly high gains; the amplifier of Yu *et al.* has a gain of 74 db. (voltage gain 5000, with bandwidth 150 mc/sec. (rise time $\sim 4 \times 10^{-9}$ sec.). A coincidence circuit built in the distributed manner has been described by Wiegand (9), and there does not seem to be any reason why distributed stages should not be coupled together to give very fast trigger circuits, amplitude discriminators, and so on. Little seems to have been done along these lines, probably because in actual experiments the necessity for very fast devices of this kind can usually be avoided.

The second method used for improving the performance of amplifiers involves the secondary emission pentode. This tube consists of a normal pentode with a secondary emitting dynode in place of the usual anode. The grid of the pentode controls the flow of electrons to this dynode in the usual way, and a further electrode, the anode, collects the secondary electrons emitted from the dynode. With a secondary emission ratio of, say, four, the current to the anode is four times that to the dynode, while the net dynode current is a reverse current of three times that incident on it. The addition of the dynode-anode system to an ordinary pentode with transconductance g_m thus yields a tube having two output electrodes with transconductances $4g_m$ and $-3g_m$, with no appreciable change in tube capacities. The idea for this type of tube appears to have originated with Jonker & Overbeek (10). Two available types are the Phillips EFP60 and the Mullard VX5038. Combining figures taken from papers by Moody *et al.* (11) and Wells (12), we may compare these two tubes with the conventional 6AK5 and 6AH6, and with the high performance conventional

pentode type WE-404A. In order to get consistent results, Wells' ratio of VX5038 to 6AK5 has been used to compute values to compare with Moody's absolute values for the other tubes. The results are given in Table I.

TABLE I

COMPARISON OF CONVENTIONAL AND SECONDARY EMISSION PENTODES

Tube type	g_m (μmho)	C_T ($\mu\mu$f)	C_T/g_m = time const./gain (10^{-10} sec.)
6AK5	5,000	6.8	13.6
6AH6	9,000	13.6	15.1
WE 404A	12,500	10.0	8.0
EPF60	25,000	17.7	7.1
VX5038	19,000	11.8	6.2

The superiority of the secondary emission types for fast amplification is at once evident (though as shown by Thompson (13), this superiority does not apply to signal-to-noise ratio). The secondary emission types have the additional advantage of having a dynode with a negative g_m, which can be used as an output electrode in place of the anode to give an output signal of the same sign as the grid input signal. Moody *et al.* (11) describe a simple 4-stage amplifier using EFP60's, giving a gain of 500 and bandwidth of nearly 50 mc/sec. Wells (12) cites an amplifier designed by Borg using 20 VX5038's to give a gain of 1000 and a bandwidth of 150 mc/sec. A combination of the distributed technique with secondary emission tubes should lead to even higher performances than these.

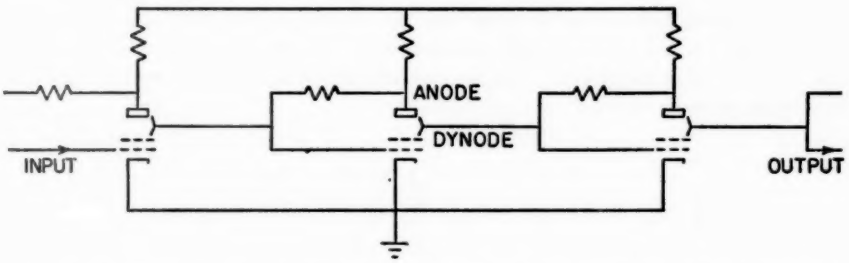

FIG. 2. Diagram of a proposed repetitive feedback amplifier using secondary emission pentodes. The supplying of d-c voltages to the various electrodes has been ignored.

The fact that amplified outputs of both signs are available from the same tube, and that both the anode and dynode currents are larger than the cathode current, makes the tube adaptable to many different positive and negative feedback arrangements. One possibility mentioned by Moody is a dynode-coupled wide band amplifier employing negative feedback from

each anode to the preceding dynode. The arrangement is sketched in Figure 2, where as usual the supplying of d-c operating voltages has been ignored. This amplifier is of the non-phase-inverting type, and for negative input pulses would be free of paralysis effects caused by grid current flow when positive pulses overload. Apparently many possibilities for the use of secondary emission pentodes remain unexplored. A minor disadvantage of these tubes is the tendency for their characteristics to drift with time. Moody *et al.* show that simple d-c stabilizing circuits can overcome this effect (11).

The subject of secondary emission brings us naturally to consider electron multipliers and photomultipliers as amplifiers. The usual photomultiplier has from 9 to 14 stages of secondary emission amplification, with overall gain from 10^5 to 10^9. The rise time varies widely, depending mainly on the dynode structure of the particular tube. The fastest type is the focused 931A structure. Such a structure may, in a 1P21 photomultiplier, give a gain of 10^6 and a rise time less than 10^{-9} sec.; the rise time per unit gain is less than 10^{-15} sec., or at least 10^5 times better than any single amplifier tube so far discussed. It would therefore seem logical to increase the number of dynodes in photomultipliers to the point where external amplification is unnecessary. This has been done in the 16-stage RCA type H-4646 and the 14-stage EMI type 5311. Unfortunately, the dynode structures of these types are such that their rise times are distinctly longer than that of the 931A structure. However, Bell & Petch (14) have shown that 1P21 photomultipliers can be run at an applied voltage of $\backsim$2000 volts, the gain then being $\backsim 10^8$, retaining the short rise time. Table II lists the rise times and nominal gains of some photomultiplier tubes; the data for this table has been collected from various publications and from tube manufacturers' data sheets. The figures given may not be strictly comparable between the types, but will serve to illustrate the differences to be found in practice. The shortcomings of photomultipliers as amplifiers, such as noise, afterpulsing, and instability of gain, are beyond the scope of this summary. A discussion of afterpulsing by several authors is found in reference (15).

TABLE II

AMPLIFYING PROPERTIES OF TYPICAL PHOTOMULTIPLIERS

Photomultiplier	Dynode structure	Gain (10^6)	Rise time (seconds)
RCA 1P21	931A	2.0	10^{-9}
RCA 5819	large cathode+931A	0.6	5×10^{-9}
RCA 6342	large cathode+931A	0.6	5×10^{-9}
RCA H4646	curved dynodes in line	1000	2×10^{-9}
EMI 5311	venetian blind	10	7×10^{-9}
DuMont 6292	quarter-circle boxes	1.0	probably $\sim10^{-8}$

Counting

Experiments where fast pulse response is necessary are often (though not invariably) characterized by high counting rates in one or more counters. In addition, experiments involving particles from pulsed accelerators often involve high instantaneous counting rates during an accelerator pulse, even though the average counting rate is modest. Suppose an accelerator has a duty cycle of 1 per cent, and that an average counting rate of 10^4 per sec. is to be recorded; the instantaneous counting rate during the pulse will be 10^6 per sec., and a system dead time of 10^{-8} sec. or less is necessary to hold the counting losses below 1 per cent. One approach to this problem is to design experiments for lower counting rates; another is to make accurate allowance for counting losses, as discussed at length by Westcott *et al.* (16); the third is to build fast counting systems, including scalers of short dead time.

Owing to the other alternatives mentioned, there has been comparatively little work published on fast scalers ("fast" now meaning having less than 10^{-7} sec. dead time). Scales-of-two using dual triode tubes and diode inter-scale coupling usually have dead times ranging from 2 to 10 μsec. A scale-of-two using two conventional pentodes is easily made to give a dead time less than one microsecond; if the further step is taken of limiting the anode and grid excursions of the tubes (by means of diodes) so that the tubes are always operating in regions of high g_m, dead times near 0.1 μsec. can be realized. An example of such a scaler is found in a paper by Moody *et al.* (17). Schoenwetter (18) has described a scale of four using 6AH6 pentodes and germanium coupling and clamping diodes; the two 6AH6's of the first scale of two are coupled by 6J6 triode cathode followers in order to reduce capacitive loading on the anodes of the 6AH6's. The dead time achieved is 6×10^{-8} sec., but this circuit appears to be expensive and fragile (13 tubes and 20 germanium diodes for a scale of 4). Scalers of 0.1 μsec. dead time are advertised commercially. Wells (19) has described a scale of 10 of 0.25 μsec. dead time involving the step charging of a capacitor with pulses from a discriminator.

A promising truly fast scale of two has been described by Fischer & Marshall (20). The circuit uses two EFP60 secondary emitting pentodes in a symmetrical circuit; the fast switching action between the tubes is assisted by internal feedback from dynode to grid within each tube, so that each tube separately is a trigger circuit, the two being cross connected so that only one can be conducting at a time. Diode clamping of the grids and diode switching of the input pulses is employed. This circuit can resolve two pulses 10^{-8} sec. apart. The pulse shaping stages with which it is fed also use EFP60 tubes. Fischer & Marshall (20) also state that they have built triode scaling pairs of 5×10^{-8} sec. dead time.

We must conclude that there is no reason why very fast scalers should not be built in greater numbers, using either secondary emission tubes or

distributed amplifiers, or both. The lack of such scaler designs is presumably attributable to lack of demand for them.

Pulse Height Analysis

A discussion of fast pulse amplitude ("height") analysis starts with almost the same remarks as those made about fast scalers; the technical resources for pulse height analysis with response times less than 10^{-7} sec. are available, but it is almost never necessary to employ them. As pointed out by Bell & Petch in 1949 (14), if it is necessary to determine accurately both the amplitude of a pulse and its time of occurrence with respect to another pulse, the two measurements may be performed separately and combined afterwards in a relatively slow coincidence operation. A block diagram illustrating the process is given in Figure 3. Counters 1 and 2 deliver their pulses both to the fast coincidence circuit, and to ordinary linear amplifiers feeding pulse height analysers whose speed need not be particularly great. At the output, a triple coincidence unit of modest speed selects, out of

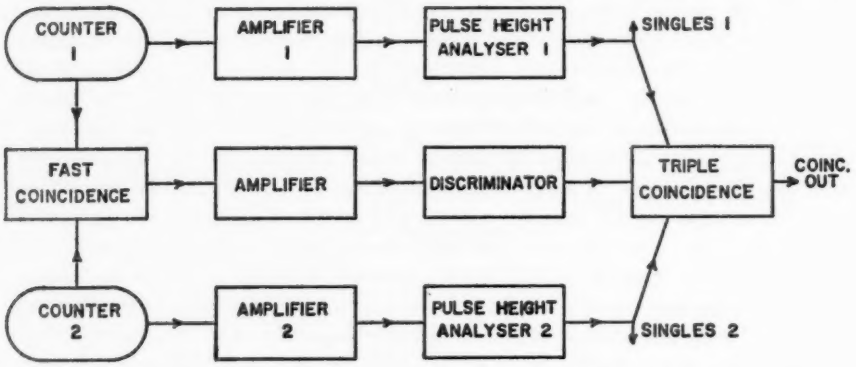

Fig. 3. Block diagram of a circuit arrangement for measuring both the amplitudes of the pulses from two counters, and their relative time of occurrence, without having to perform very fast pulse height analysis. This assembly is sometimes called the "fast-slow" coincidence system.

all the fast coincidences formed initially, only those that correspond to the pulse heights selected in the two selection channels. The pulse height selectors may, with obvious small changes in Figure 3, be of any type, including elaborate multichannel devices. Also, if a delayed coincidence experiment is being performed in the fast coincidence channel, any delay may be inserted between the counters so long as it does not exceed the resolving time of the final triple coincidence circuit. It is easy to see that the final coincidence circuit does not add appreciably to the number of chance coincidences, or otherwise complicate the action of the assembly.

With the circuit of Figure 3 available, the pulse height analyser needs only to be able to handle the counting rate encountered in the experiment. In

addition, a large fraction of all present day pulse height analysis occurs in γ-ray spectroscopy with NaI(Tl) scintillation counters, where the phosphor rise time of 0.25 μsec. controls the response time to be used. The emphasis in pulse height analysis has therefore been on accuracy and flexibility, and a pulse height analyser is considered "fast" if it has a dead time of one or two microseconds.

An excellent series of review articles on existing pulse height analysers has been published by Van Rennes (21). These articles cover simple voltage discriminators, single channel analysers, and multichannel analysers. In the development of such instruments the various government laboratories in the United States, Canada, and Britain have been the most prominent, probably because good pulse height analysers tend to be expensive.

A few efforts have been made to design a truly fast voltage discriminator, i.e., one which will respond to a short pulse and deliver its answer with small delay. Moody *et al.* (11), for example, describe a trigger circuit using an EFP60, and a voltage discriminator circuit derived from it in which the voltage sensing element is a germanium diode. The latter circuit works well on input pulses around 10^{-8} sec. in duration, and with decreasing sensitivity for shorter pulses. The minimum pulse for triggering is 0.1 v., and the output pulse rise time and delay are from 3 to 10 times 10^{-9} sec., depending on the input pulse size and shape. Wells (12) and Garwin (22) have commented adversely on the performance of the usual germanium diodes for short pulses, and it may happen that other devices will have to be used as absolute voltage discriminators for pulse durations less than 10^{-8} sec., e.g., beam deflection devices. Little effort has been directed towards this field, for the reasons given above.

Coincidence Techniques

A coincidence circuit may be defined as a nonlinear circuit having two inputs and one output, such that a pulse is delivered from the output only when the two inputs have received pulses within a short time of each other. This short time is the resolving time of the coincidence circuit. The definition of resolving time has received much attention in the literature; in fast coincidence work it is usually taken as $2\tau_0$, the full width at half height of the prompt coincidence resolution curve (the measured curve of coincidence counting rate as a function of delay time artificially inserted between the pulses from the two counters). The main object of the design of fast coincidence circuits is the reduction of the resolving time, both as an aid in measuring short time intervals between pulses, and as an aid in reducing the number of chance coincidences between causally unrelated events. Experience has shown that it is comparatively easy to build a coincidence circuit whose resolving time is as short as is justified by the performance of the presently available counters. Bell *et al.* (23) have shown how to estimate the minimum resolving time possible with a particular scintillation phosphor, neglecting the time lags of the photomultiplier and associated circuitry. Their result

is based on a calculation by Post & Schiff (24) which shows that the mean time lag for the emission of the first photoelectron from the photocathode, after the excitation of the phosphor by an incident particle, is approximately $\bar{t}=\tau/R$. Here τ is the phosphor decay time and R is the total number of photoelectrons emitted during the pulse. Bell *et al.* (23) show that the minimum resolving time for 90 per cent coincidence efficiency is $2\tau_0=6\tau/R$. For 1P21 tubes with stilbene phosphors excited by 100 kev electrons, they predict and observe $2\tau_0=2\times10^{-9}$ sec.

The resolving time represents the accuracy with which a single coincidence event can be timed. In an actual coincidence experiment many such events are observed, and the mean delay of a given radiation relative to its predecessor can be measured to an accuracy considerably better than 10^{-10} sec. The technique of such measurements is discussed at length by Bell *et al.* (23), and with particular reference to the errors likely to be encountered, by Graham & Bell (25).

In order not to slow up the incident counter pulses, it is necessary to bring them to the actual coincidence detecting circuit with a minimum of pretreatment. This requirement puts a premium on coincidence circuits that will work with the small pulses that the usual scintillation counters are capable of delivering (typically 0.1 to 5 volts). A moderate amount of high speed amplification of the counter pulses, such as may be obtained from distributed amplifiers, has been used successfully. Resolving times in the 10^{-9} sec. range are not usually achieved with coincidence circuits involving the deflection of an oscilloscope, or with arrangements in which the pulses are preshaped before being applied to the coincidence circuit. Such apparatus, excellent for many applications, will not be discussed further here.

A wide variety of coincidence circuits has been published since 1949 in which the above requirements have been met. These circuits may be conveniently classified into three types, viz., parallel, series, and bridge types. In summarizing progress in the various types of circuit, the resolving times quoted will be those achieved with actual counters connected to the circuits, and not with artificial pulses. Coincidence circuits with more than two inputs are not included, since no new principles are involved.

Parallel coincidence circuits.—The parallel coincidence circuit stems from the original Rossi coincidence circuit (26) and its outgrowth, the so called "fast Rossi" circuit. A typical parallel (fast Rossi) circuit is shown in Figure 4. The negative input pulses from the two counters are applied to the two grids of a pair of tubes V_1 and V_2. These tubes are shown as triodes in Figure 4, but may with advantage be pentodes in order to avoid capacity coupling between grid and anode circuits. [Howland *et al.* (27) have shown how diodes may be used in place of V_1 and V_2.] In the quiescent state each of these tubes is conducting a current i, so that there is a voltage drop $2Ri$ across the common anode load R. To achieve fast operation it is necessary to make R smaller than the plate resistances of V_1 and V_2, and the voltage drop $2Ri$ is then small compared with the B+ supply voltage. When a single negative pulse arrives at one grid, it will tend to cut off one anode current and cause the

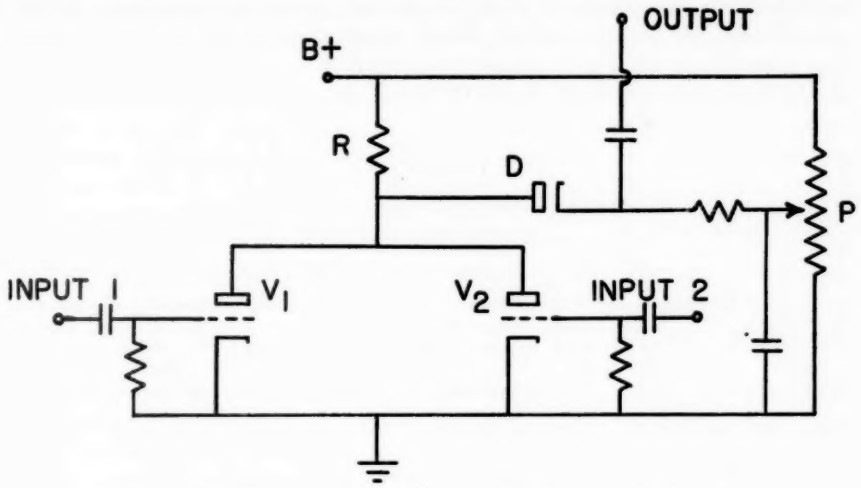

FIG. 4. A typical fast Rossi, or parallel, coincidence circuit.

anode voltage to rise, at most by Ri. Simultaneous pulses arriving at the two grids cause an output of up to $2Ri$. The diode D is biased by means of potentiometer P to pass only those pulses whose amplitudes are greater than Ri. Thus, the output terminal receives a pulse only for overlapping input pulses; the resolving time is set almost entirely by the duration of the input pulses. For best operation the input pulses should cause complete anode current cut off, a typical requirement being three volts.

In order that a short resolving time may be achieved, we must have in addition to short input pulses, an anode circuit that will respond within the duration of the input pulses. If the capacity to ground of the anodes of V_1 and V_2 and associated wiring is, say, 10 $\mu\mu$f, then R can be at most 100 ohms if a time constant of 10^{-9} sec. is desired. The diode D must also respond within this time. The remainder of the circuit beyond D need not have such a fast response, unless for some reason it is necessary to record the fact that a coincidence has occurred with a speed comparable to the resolving time.

In general, a parallel coincidence circuit consists of a pair of pulse size limiters (V_1 and V_2 in Figure 4), an element for adding the equalized pulses (R in Figure 4) and an element for detecting pulses of larger than "single" size (D in Figure 4). The circuit is similar to a pair of switches in parallel (V_1 and V_2), both of which must be opened if the current is to be completely interrupted; hence the classification as a parallel coincidence circuit.

Parallel coincidence circuits designed for short resolving times have appeared in great profusion since 1948. In these circuits many different kinds of elements have been used in place of the triode equalizers and diode coincidence detector of Figure 4, but all can be reduced to essentially the same circuit. Table III lists a number of these circuits, and summarizes their makeup and properties in tabular form. The entries in Table III are

intended only as examples of the faster circuits of this type on which detailed information has been published. Much excellent work has been done using fast coincidence circuits in which the authors give only a passing reference to the actual circuits used. Table III omits all such cases. (Similar remarks apply to Tables IV and V to follow.)

TABLE III

EXAMPLES OF PARALLEL COINCIDENCE CIRCUITS

Authors	Ref. No.	Date	Counters Used	Equalizers	Coincidence Detector	$2\tau_0$ (sec.)
Bay & Papp	28	1948	electron mult.	triodes	biased triode	1×10^{-8}
Bell, Graham, & Petch	14, 23	1949, 1952	scintillation (1P21)	pentodes (6AK5)	germanium diode	2×10^{-9}
Garwin	22	1950	scintillation (5819)	triodes (6J6)	germanium diode	4×10^{-8}
Meyer, Baldinger & Huber	29	1950	electron mult.	triodes, cathode output	germanium diode	4×10^{-9}
De Benedetti & Richings	30	1952	scintillation (5819)	pentodes (6AK5)	germanium diode	3×10^{-9}

The parallel coincidence circuit has an advantage over the series and bridge types for delayed coincidence work, in which a measured variable delay time must be inserted in series with the pulses from each counter in turn. In both the series and bridge types, the fast signals from the two counters are brought to separate terminals of the coincidence circuit. Two separate delay lines, one of which may be of fixed length, are therefore necessary. In the parallel circuit the fast pulses are mixed in the anode circuit of V_1 and V_2 (Figure 4), so that a single delay line may be used. As a result of this advantage, most of the delayed coincidence work at short resolving times has employed the parallel circuit.

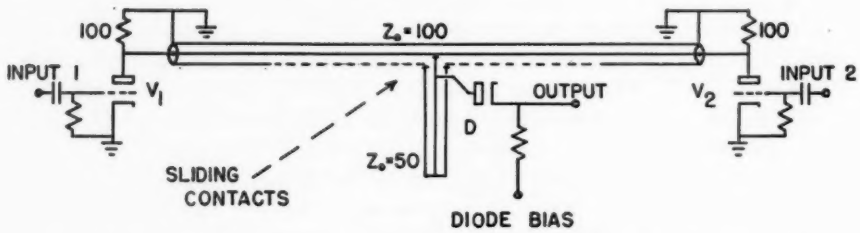

FIG. 5. A parallel coincidence circuit arranged with a delay line for performing delayed coincidence experiments. The supplying of d-c voltages to V_1 and V_2 has been ignored.

The basic arrangement is sketched in Figure 5, as first described by Bell & Petch (14). The tubes V_1 and V_2 are now separated physically (itself an advantage in many experiments) and each has a separate 100 ohm anode load. (The supplying of d-c voltages to V_1 and V_2 has been ignored in Fig.

5, for simplicity.) The two anodes are joined by a long length of cable of characteristic impedance 100 ohms, part of which is provided with a slotted outer shield in the manner of the familiar standing wave detector of high frequency radio work. A 50 ohm clipping cable and the coincidence detecting diode D are slid along the delay line to vary the delay between the two counters. The length of the clipping cable determines the pulse length applied to diode D, thus fixing the resolving time. An incidental benefit of this arrangement is that the delay line length is effectively doubled, because delay removed from one side of the circuit is automatically inserted into the other. Bell, Graham, & Petch (23) have described a delay device based on Figure 5, in which the 100 ohm line is coiled in a helix around a rotating cylinder, along which the clipping cable and diode D are driven by the rotation. Such a device lends itself well to automatic operation.

Series coincidence circuits.—The series coincidence circuit was originated by Bothe (31) in 1930. The basic scheme is illustrated in Figure 6. A multigrid vacuum tube (or two simpler tubes in series) is connected with negative biases on two of its grids such that anode current flow is effectively prevented by both of them. Positive input pulses are applied to the two separate grids, and anode current flows only when two such pulses overlap in time. The circuit is thus the equivalent of two switches in series, both of which must be closed if any current is to flow. Over the years since 1930 the series circuit has seen rather less use than the parallel type. Recently, however, the gated beam tube type 6BN6 has become available, and this type is very suitable

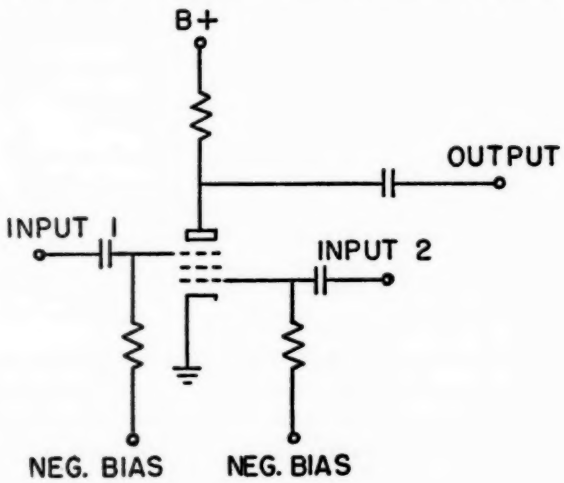

FIG. 6. A typical series coincidence circuit.

for series coincidence use. The tube is described in some detail in connection with a coincidence circuit by Fischer & Marshall (32). The 6BN6 consists of two electrically separated compartments traversed by a common electron

beam; each compartment contains a grid which is capable of preventing the electron beam from reaching the anode. Because of the fact that the electron transit time through a vacuum tube is of the order of 10^{-9} sec., certain troublesome effects occur when a series coincidence circuit is used at resolving times of the order of 10^{-9} sec.; however, Fischer & Marshall have shown that these effects do not destroy the usefulness of the series circuit at these resolving times.

The speed of response of the series circuit need only be maintained up to and including the two grids of Figure 6. The anode load resistor may be large and the following circuitry may be slow. Because of the fact that no anode current can flow in the absence of overlapping input pulses, the series circuit is very positive in its action. It has the further advantage of not requiring equalized input pulses, provided only that complications resulting from grid current flow are avoided in driving the input grids positive. (Some workers have therefore employed pulse equalization.) The series circuit seems likely to see increasing use in future experiments.

Table IV gives a number of examples of recent series circuits of short resolving time, and lists the relevant properties of each. The fact that the series circuit has not been used at resolving times as short as the parallel circuit does not appear to be attributable to any inherent inferiority.

TABLE IV
EXAMPLES OF SERIES COINCIDENCE CIRCUITS

Authors	Ref. No.	Date	Counters Used	Series Tube	$2\tau_0$ (seconds)
Schultz & Beringer	33	1948	proportional	pentode (6AC7)	3×10^{-8}
Wiegand	9	1950	scintillation	distributed pentagrid converters (6BA7)	$\sim2\times10^{-8}$
Smaller & Avery	34	1951	scintillation	6BN6	$\sim4\times10^{-8}$
Fischer & Marshall	32	1952	Cerenkov scintillation (1P28)	6BN6	6×10^{-9}

Bridge coincidence circuits.—Since 1948 a number of bridge type coincidence circuits have been described. These circuits are almost always based on the use of germanium diodes as nonlinear elements. The usual principle is as follows: pulses from one counter are fed to a balanced bridge containing germanium diodes and produce no response at the bridge output; pulses from the second counter are connected to a point in the bridge in such a way that they cannot reach the output (because of the action of a diode) but can upset the balance of the bridge for the first counter. Thus output pulses are produced only when input pulses are present simultaneously. Bridge circuits are simple and compact, and will work with small input pulses. Their main dis-

advantage lies in the difficulty of maintaining the balance of a bridge containing nonlinear elements over a wide range of input pulse amplitudes. Thus there is danger that an exceptionally large single pulse will produce sufficient output to be recorded as a coincidence, and publications on bridge coincidence circuits have paid great attention to the "singles rejection ratio." Careful selection of the germanium diodes in the bridge is usually necessary. The fear of the single pulse effect has perhaps unduly hampered the application of bridge circuits to actual coincidence experiments.

The diode bridge circuit of Bay (35) is shown in Figure 7. The fast pulse part of the circuit is drawn with full lines, and the output circuit with broken lines. Short negative pulses are assumed to be applied to the inputs through 100 ohm cables, the terminating resistors for which are visible in Figure 7. A short negative input pulse applied to input 1 charges up condensers C_1 and C_2 (each 100 $\mu\mu$f) to equal voltages through the germanium diodes D_1 and D_2. After the input pulse has gone, points A and B are left at equal and

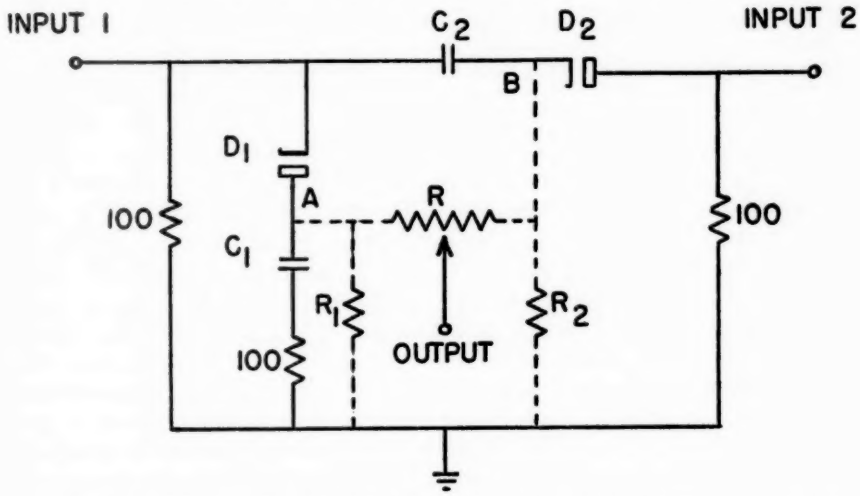

FIG. 7. A bridge coincidence circuit. The diodes D_1 and D_2 are germanium types. Solid lines represent the fast pulse circuit, and broken lines the measuring, or output, circuit.

opposite voltages, negative and positive respectively. (The 100 ohm resistor in series with C_1 maintains the symmetry of the charging circuits.) The charges on C_1 and C_2 leak away slowly ($\backsim$1 μsec.) through the resistors R_1, R_2 ($\backsim 10^4$ ohms). The output terminal is connected to the midpoint of the resistor R ($\backsim 10^6$ ohms), so that no output is produced from a single pulse at input 1. A single negative pulse at input 2 produces no charging effect, and hence no output. The presence of a negative input pulse on input 2 while the charging process is proceeding reduces the voltage available for charging C_2 without appreciably affecting the charging of C_1. In such a case a net

negative output is produced. In practice R_1, R_2, and R may be adjusted to obtain the best balance. If the fast input pulses are to be positive, the diodes of the bridge are reversed.

Other bridge circuits have required opposite polarities for the two counter input pulses, or a differential amplifier at the output, but their action is basically similar. Table V lists the properties of a number of published bridge coincidence circuits. More detailed discussions of the properties of bridge coincidence circuits are given by Bay (35) and Strauch (36).

TABLE V

EXAMPLES OF BRIDGE COINCIDENCE CIRCUITS

Authors	Ref. No.	Date	Counters Used	Input Pulse Polarities	Output amplifier	$2\tau_0$ (sec.)
Meyer, Huber & Baldinger	37, 38	1948	electron mult.	both required	conventional	$\sim 2\times 10^{-8}$
Meyer, Baldinger & Huber	39	1949	scintillation	same	differential	10^{-7}
Morton & Robinson	40	1949	scintillation	both required	conventional	10^{-7}
Shrader	41	1950	scintillation	same	differential	4×10^{-8}
Bay	35	1951	electron mult.	same	conventional	$<10^{-9}$
Strauch	36	1953	scintillation	same	differential	10^{-8}

In all the coincidence circuits so far described (parallel, series, and bridge), the resolving time has been determined mainly by the duration of the individual pulses applied to the coincidence detecting element. Bay, however, has recently shown how to make the resolving time shorter than the input pulse durations (42, 43). The circuit is a kind of bridge circuit involving the pulse timing in the balance conditions. The pulses from the two counters are given two slightly different relative delays, and are then applied to two separate bridge type coincidence detectors. A pair of perfectly coincident input pulses arrives at one detector slightly out of synchronism, and at the other detector out of synchronism by the same amount in the opposite sense. The degree of overlap of the two pulses is therefore the same in both detectors, whose outputs will be equal. A slight lag of one input pulse relative to the other will increase one detector output and decrease the other, so that there is now a finite difference in their outputs. The circuit is so arranged that a coincidence from an auxiliary detector (normally one of those already in use) is recorded only when this difference is small or zero, thus greatly reducing the resolving time of the auxiliary detector. The circuit is called the "differential" coincidence circuit by Bay. The arrangement sounds complex in the above description, but Bay has ingeniously condensed the circuit until it contains only a few more elements than the usual bridge circuit. Using this device with Cerenkov scintillation counters to eliminate the time lags caused by ordinary scintillation phosphors, Bay (44) has demonstrated an over-all resolving time of $2\tau_0 = 8.8\times 10^{-10}$ sec. He further

decomposed this resolving time into two contributions, each of 5×10^{-10} sec., one being the true resolving time of the differential circuit, and the other representing the mean random time delay introduced by the photomultipliers (1P21 tubes operated at 1400 volts). The differential coincidence circuit has not yet seen extensive application in nuclear physics experiments, but there is little doubt that it will prove useful in the future.

LITERATURE CITED

1. Kallmann, H., *Natur. u. Tech.*, July (1947)
2. Deutsch, M., *Nucleonics*, **2**(3), 58 (1948)
3. Ginzton, E. L., Hewlett, W. R., Jasberg, J. H., and Noe, J. D., *Proc. Inst. Radio Engrs.*, **36**, 956 (1948)
4. Percival, W. S., *British Patent, No. 460562* (January 29, 1937)
5. Horton, W. H., Jasberg, J. H., and Noe, J. D., *Proc. Inst. Radio Engrs.*, **38**, 378 (1950)
6. Yu, Y. P., Kallmann, H. E., and Christaldi, P. S., *Electronics*, **24**, 106 (1951)
7. Gérardin, L., *Revue Technique de la Compagnie Francaise Thomson-Houston, No. 15*, 19 (April, 1951)
8. Bassett, H. G., and Kelly, L. C., *Proc. Inst. Elec. Engrs. (London)*, **101, Pt. III**, 5 (1954)
9. Wiegand, C., *Rev. Sci. Instr.*, **21**, 975 (1950)
10. Jonker, J. L. H., and Overbeek, A. J. W. M. v., *Wireless Eng.*, **15**, 150 (1938)
11. Moody, N. F., MacLusky, G. J. R., and Deighton, M. O., *Electronic Eng.*, **24**, 214, 287, 330 (1952)
12. Wells, F. H., *Nucleonics*, **10**(4), 28 (1952)
13. Thompson, B. J., *Proc. Inst. Radio Engrs.*, **29**, 583 (1951)
14. Bell, R. E., and Petch, H. E., *Phys. Rev.*, **76**, 1409 (1949)
15. Scintillation Counter Symposium, *Nucleonics*, **10**(3), 32 (1952)
16. Westcott, C. H., Greenberg, J. S., and Kirkaldy, J. S., *Can. J. Phys.*, **31**, 859 (1953)
17. Moody, N. F., Howell, W. D., Battell, W. J., and Taplin, R. H., *Rev. Sci. Instr.*, **22**, 439 (1951)
18. Schoenwetter, H. K., *Rev. Sci. Instr.*, **24**, 515 (1953)
19. Wells, F. H., *J. Sci. Instr.*, **29**, 111 (1952)
20. Fischer, J., and Marshall, J. (Personal communication, February 10, 1954)
21. Van Rennes, A. B., *Nucleonics*, **10**(7), 20; (8) 22; (9) 32; (10) 50 (1952)
22. Garwin, R. L., *Rev. Sci. Instr.*, **24**, 618 (1953)
23. Bell, R. E., Graham, R. L., and Petch, H. E., *Can. J. Phys.*, **30**, 35 (1952)
24. Post, R. F., and Schiff, L. I., *Phys. Rev.*, **80**, 1113 (1950)
25. Graham, R. L., and Bell, R. E., *Can. J. Phys.*, **31**, 377 (1953)
26. Rossi, B., *Nature*, **125**, 636 (1930)
27. Howland, B., Schroeder, C. A., and Shipman, J. D., Jr., *Rev. Sci. Instr.*, **18**, 551 (1947)
28. Bay, Z., and Papp, G., *Rev. Sci. Instr.*, **19**, 565 (1948)
29. Meyer, K. P., Baldinger, E., and Huber, P., *Helv. Phys. Acta*, **23**(1–2), 121 (1950)
30. DeBenedetti, S., and Richings, H. J., *Rev. Sci. Instr.*, **23**, 37 (1952)
31. Bothe, W., *Z. Physik*, **59**, 1 (1930)
32. Fischer, J., and Marshall, J., *Rev. Sci. Instr.*, **23**, 417 (1952)
33. Schultz, H. L., and Beringer, R., *Rev. Sci. Instr.*, **19**, 424 (1948)

34. Smaller, B., and Avery, E., *Rev. Sci. Instr.*, **22,** 341 (1951)
35. Bay, Z., *Rev. Sci. Instr.*, **22,** 397 (1951)
36. Strauch, K., *Rev. Sci. Instr.*, **24,** 283 (1953)
37. Meyer, K. P., Huber, P., and Baldinger, E., *Helv. Phys. Acta*, **21**(3–4), 188 (1948)
38. Baldinger, E., Huber, P., and Meyer, K. P., *Rev. Sci. Instr.*, **19,** 473 (1948)
39. Meyer, K. P., Baldinger, E., and Huber, P., *Helv. Phys. Acta*, **22**(4), 420 (1949)
40. Morton, G. A., and Robinson, K. W., *Nucleonics*, **4**(2), 25 (1949)
41. Shrader, E. F., *Rev. Sci. Instr.*, **21,** 883 (1950)
42. Bay, Z., *Phys. Rev.*, **83,** 242 (1951)
43. Bay, Z., Meijer, H. R., and Papp, G., *Nucleonics*, **10**(3), 39 (1952)
44. Bay, Z., Cleland, M. R., and McLernon, F., *Phys. Rev.*, **87,** 90 (1952)

CHARACTERISTICS OF SCINTILLATORS[1]

By Robert K. Swank[2]

Argonne National Laboratory, Lemont, Illinois

Introduction

Several reviews of the development, theory, and application of scintillation counters have already appeared. For the convenience of the reader, a few of the most recent and comprehensive reviews are listed in the bibliography (1 to 4). An attempt has been made in this chapter to supplement, rather than duplicate, the previous summaries. The following discussion will be concerned primarily with the scintillator itself and with the scintillations produced in it by high-energy particles. For convenience, the scintillators will be grouped according to their chemical similarity.

The scintillation process.—A description of the scintillation process should tell us the magnitude, the spectral distribution, and the time dependence of the emission of ultraviolet or visible photons resulting from the absorption of a high-energy charged particle by the scintillator. For most of the particles and energies dealt with in nuclear experiments, the energy of the fast charged particle is almost entirely expended in producing electronic excitation and ionization in the absorbing material. Since the energy of the particle is very large, all the possible excited states are produced, including ionization with various amounts of excess kinetic energy. The initial populations of the various excited states are determined mainly by the relative oscillator strengths of the corresponding transitions from the ground state. This follows from the fact that, except for close encounters, the field of the charged particle may be approximated by a "white" electromagnetic spectrum whose shape is given by the Fourier transform of the impulsive field of the fast particle. In a monatomic gas at low pressure, such excitation would be followed by the emission of spectral lines corresponding to various transitions from the excited states to lower states or to the ground state. In the solid or liquid form, most materials show only a negligible luminescence upon irradiation with high-energy charged particles. Furthermore, the spectra of the relatively few materials which do scintillate efficiently indicate emission from only one or at most a few transitions from lower excited states to the ground state. Within the accuracy of available experimental data, the emission spectra for particle excitation and ultraviolet excitation have the same spectral distribution. One might conclude from this that the scintillation phenomenon is merely a variation of the fluorescence phenomenon, in which the excitations are produced by

[1] The survey of literature pertaining to this review was concluded in March, 1954.

[2] The author is indebted to Mr. W. L. Buck of Argonne National Laboratory for valuable suggestions and criticisms of the manuscript, and to Drs. F. N. Hayes and F. B. Harrison of Los Alamos Scientific Laboratory for valuable suggestions.

the impulsive field of a moving charge. However, many factors combine to greatly complicate the scintillation process. A calculation by Harrison (5) has shown that the fluorescence excitations produced in benzene are many times greater than would be predicted by direct excitation of that state by the charged particle. In this case, and probably in many others, the major portion of the particle-induced fluorescence excitations results from decay of higher states into the state from which fluorescence occurs. Aside from the excitation of the fluorescence state by direct and indirect processes, the particle may influence the emission process as well. This influence can result from local effects such as chemical dissociation, heating, electric fields, and mutual quenching by neighboring excited molecules.

In spite of the many factors which serve to distinguish the scintillation process from the fluorescence process, a description of the two phenomena in common terms is not hopeless. By ignoring for the moment the perturbation of the emission process by the products of energy loss, the number of photons emitted in a scintillation may be expressed as

$$N = \frac{E_0 q}{w} \qquad 1.$$

where E_0 is the initial energy of the fast particle stopped in the scintillator, w is the average energy expended for the production of one excitation in the fluorescence state, and q is the fluorescence quantum efficiency. The usefulness of equation 1 will depend upon our ability to modify it suitably to account for the more complicated effects mentioned above. Some of these modifications, to be discussed later, will require that w or q vary with the energy of the particle. In this case, equation 1 must be written in incremental form

$$dN = -(q/w)dE \qquad 2.$$

where dN is the number of photons emitted as the particle energy falls from E to $E-dE$.

Measurement of Scintillation Properties

Scintillation efficiency.—Most of the values of scintillation efficiency reported in the literature are given in terms of the response of a particular photomultiplier tube. This type of measurement frequently leads to unequal weighting of different materials as a result of the wavelength dependence of the photocathode efficiency, i.e., the scintillation amplitude in terms of the number of cathode photoelectrons is

$$\int_0^\infty N\xi(\lambda)\eta(\lambda)d\lambda$$

where $\xi(\lambda)$ is the fraction of the emitted photons whose wavelengths lie between λ and $\lambda+d\lambda$, $\eta(\lambda)$ is the quantum efficiency spectrum of the photocathode, and λ is the wavelength. Fortunately, most of the scintillation efficiencies reported were measured with a Cs_3Sb type photosurface. An illustration of the magnitude of this effect is seen in Figure 1. Here the relative quan-

tum efficiency spectrum of a type 5819 photomultiplier[3] is plotted together with the quantum emission spectra of two plastic scintillators. From Figure 1 it can be calculated that the ratio of photomultiplier pulse heights for the plastic containing terphenyl to that containing tetraphenylbutadiene

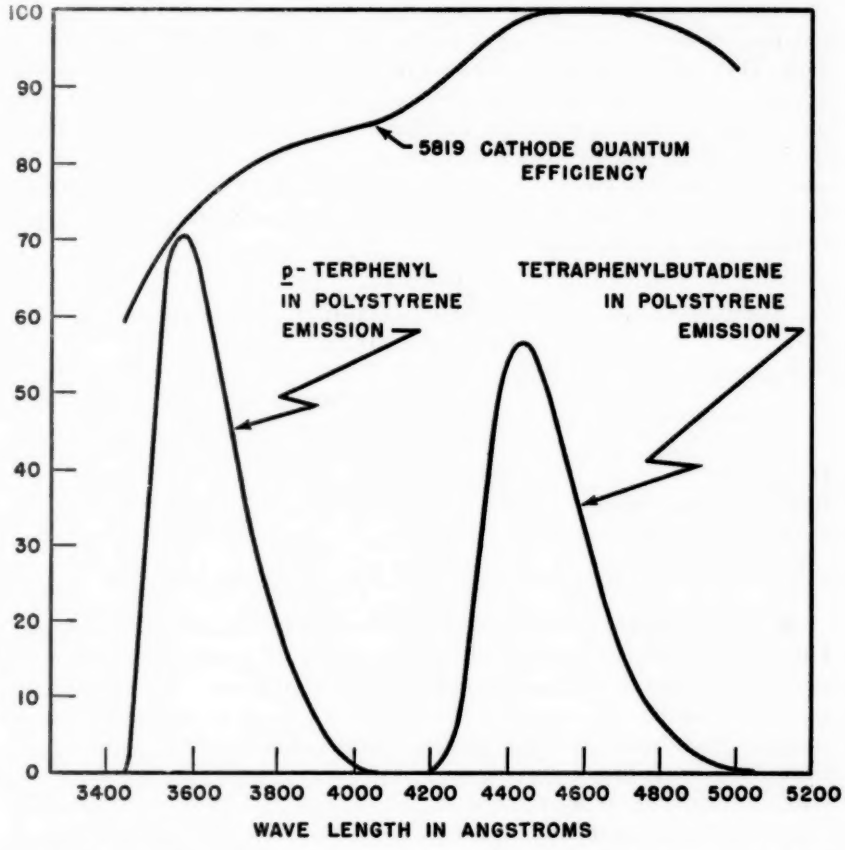

FIG. 1. Quantum efficiency spectrum of a type 5819 photomultiplier with S-9 response, and quantum emission spectra of two plastic scintillators. The light output ratio of the plastic containing terphenyl to the plastic containing tetraphenylbutadiene is 1.10, while the corresponding photomultiplier pulse height ratio is 0.78. The ordinate scale is arbitrary.

is 0.78, while the ratio of light outputs is 1.10. If a reflector is used in making scintillator comparisons, errors may arise from variations in reflectivity with wavelength. Discrepancies may also occur as a result of differences in optical

[3] The response shown is that supplied by the manufacturer, designated as S-9. Recent characteristics supplied by the manufacturer have been given a new designation, S-4, showing a different spectral response.

perfection or index of refraction of the samples. These effects are minimized if one face of the scintillator is in optical contact with the photosurface.

If workers in different laboratories are to compare relative efficiency measurements, it is necessary to establish a reference standard. The material which is most frequently used for such comparisons is the anthracene crystal. This choice is somewhat unfortunate, since anthracene is not easily purified, and the production of perfect crystals is quite difficult. Sangster (6) has shown that with the most careful preparation, different procedures may lead to pulse height variations of 20 per cent. To the extent that accurate reference samples can be produced, it is possible to make an absolute scintillation efficiency measurement from a relative one if the absolute efficiency of the reference sample is known. Several investigators have undertaken recently to measure the absolute efficiency of anthracene. The results of their measurements are given in Table I.

TABLE I

ABSOLUTE SCINTILLATION EFFICIENCY OF ANTHRACENE FOR HIGH-ENERGY β-PARTICLE EXCITATION

Investigators	Date	Efficiency $Nh\nu/E_0 \times 100$ per cent	Energy to Make a Photon (ev)
Harrison (5)	1951	4.2	65
Birks & Szendrei (77)	1953	3.7	70
Furst, Kallmann, & Kramer (78)	1953	10	26

Most scintillators are at least partially transparent to their own radiation. This fortunate circumstance can be understood by considering the fundamental processes of absorption and emission of radiation by a scintillator molecule. The thermal energy of the molecule causes it to oscillate about the position of minimum potential energy. These oscillations are quantized into vibrational levels in the ground state, and vibrational levels in the excited state. At ordinary temperatures, the molecules will come to equilibrium in the lower vibrational states. In general, the position of equilibrium in the excited state will differ from that in the ground state. This fact, together with the Franck-Condon principle, which requires that the nuclear coordinates remain fixed during an electronic transition, means that when a photon is absorbed, the molecule is left in a high vibrational level of the excited state. The molecule is thus momentarily out of thermal equilibrium with its surroundings but adjusts quickly (in 10^{-13} to 10^{-12} sec.) by giving up vibrational energy. A similar thermal readjustment occurs after emission of a fluorescence photon. Thus, the emission spectrum of the molecule is displaced from the absorption spectrum toward longer wavelengths. However, the difference between the wavelengths of the absorbed and emitted quanta is a statistical quantity, dependent on the initial and final thermal states of

the molecule. In a certain number of cases, the emitted quantum may have a shorter wavelength than the absorbed quantum. Furthermore, the shape of the energy configuration is different for different molecules at any one time and for any one molecule at different times, as a result of thermal fluctuations of neighboring molecules. Thus, although the mean wavelength of the emission spectrum is always longer than the mean wavelength of the absorption spectrum, an overlapping of the spectra is frequently observed. This effect is illustrated schematically in Figure 2, where the area designated by a is proportional to the number of photons emitted in a scintillation. However, as a result of the overlap of the spectra, the short wavelengths are selectively

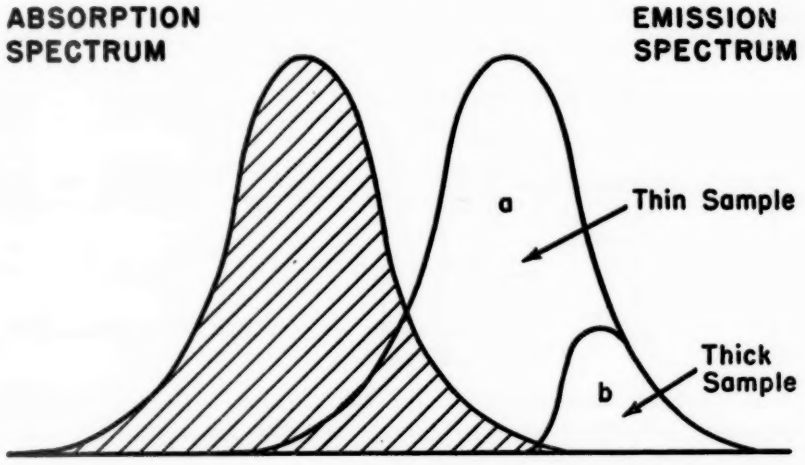

FIG. 2. Schematic representation of the absorption and emission spectra of a scintillator.

self-absorbed, with the result that the smaller number of photons represented by area b are transmitted. Those photons which are reabsorbed will excite other similar molecules to the same state, and a fraction, q, of the reabsorptions will result in a second generation of photons. Since thermal equilibrium is established between absorption and emission, the second generation will have the same spectral distribution as the first. Birks & Little (7) have shown that the number of photons ultimately escaping can be calculated readily if one makes the simplifying assumption that the fraction escaping is the same for each successive generation. This assumption, which neglects diffusion entirely, is a good approximation for many scintillators, since the number of significant generations is not more than ten, and diffusion away from the source is relatively small. If this assumption is made, the ratio of the number of photons observed to the number emitted is found to be

$$\frac{N_{\text{obs.}}}{N} = \frac{b/a}{1 - q(1 - b/a)} \qquad 3.$$

and the spectral distribution of the observed scintillation has the same shape as curve *b*. As might be expected, this ratio approaches b/a if q is very small and approaches unity if q approaches unity. Thus, a thick scintillator with a very high fluorescence quantum efficiency may have considerable self-absorption with only a small loss in pulse height. Self-absorption is much less serious in the case of activated scintillators, since a further degradation of the excitation energy occurs upon transfer of the excitation from the bulk material to the emitting center. The same is true of scintillators employing "wavelength shifters" which absorb the primary fluorescence radiation and re-emit it at a longer wavelength. In three-component scintillators, such as the commonly used liquids and plastics, three successive degradations of the excitation energy occur. As a consequence, scintillators of this type often show a mean free path of several meters for their emitted light.

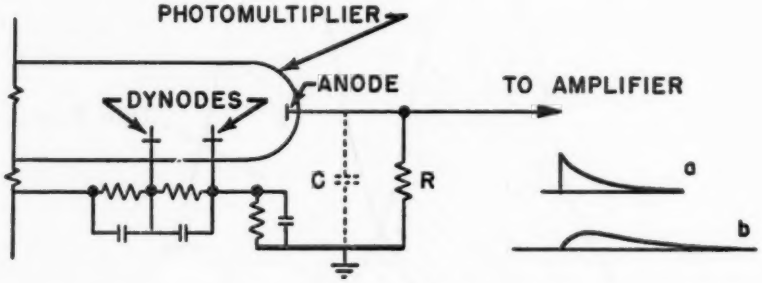

FIG. 3. Typical photomultiplier anode circuit. C usually consists of distributed circuit capacitance. Waveforms a and b represent output pulses (equation 6) from "fast" and "slow" scintillators, respectively.

In the measurement of relative scintillation efficiency, one of two methods is generally used. In the first method the scintillator is irradiated with a source of moderately high intensity. No attempt is made to observe individual light flashes, but a measurement is made of the steady value of the emitted light flux. Measurement of the average or d.c. value of the current from a photomultiplier is a technique often used. If, under constant irradiation, a reading of the equilibrium current is made, the reading will be proportional to the average total light emitted per scintillation, irrespective of the time delay between the exciting event and the completion of the light emission process. In the other method of measuring scintillation efficiency, a measurement is made of the amplitudes of the light pulses corresponding to absorption of individual fast particles by the scintillator. If a reasonable number of pulses are to be observed per unit time, the time of observation of each pulse is necessarily limited. The observation time or "integration time" of the pulse recording system can be illustrated with the aid of Figure 3. This figure shows a typical photomultiplier anode circuit, and the kinds of wave forms usually observed. The wave form is determined partly by the

anode time constant RC and partly by the scintillator decay characteristic. To illustrate this, assume that the scintillator is excited instantaneously at $t=0$ by a high-energy charged particle, and that the fraction (of all the fluorescence photons produced) emitted between t and $t+dt$ may be expressed by a function $f(t)dt$. Then the rate of photon emission for $t>0$ is $Nf(t)$, and the photomultiplier anode current (neglecting time dispersion in the multiplier) will be

$$I(t) = Ng\bar{\eta}Gef(t) \qquad 4.$$

where g is the fraction of the emitted light which is collected by the photocathode, $\bar{\eta}$ is the average quantum efficiency of the photocathode for the emitted spectrum, and G is the multiplication factor of the multiplier. Since the anode current is split between R and C, the anode voltage will be given by the solution of the differential equation.

$$I(t) = \frac{V}{R} + C\frac{dV}{dt}. \qquad 5.$$

For the simple case where $f(t)$ is given by the exponential function $(1/\tau)$ exp $(-t/\tau)$ the voltage pulse will have the form

$$V(t) = \frac{Ng\bar{\eta}Ge}{C}\left(\frac{RC}{RC-\tau}\right)(e^{-t/RC} - e^{-t/\tau}) \qquad 6.$$

and the pulse amplitude will be

$$V_{\max} = (Ng\bar{\eta}G/C)\gamma^{1/1-\gamma}$$

where

$$\gamma \equiv RC/\tau. \qquad 7.$$

Thus, the observed amplitude of the pulse is dependent on the decay parameter of the scintillator (τ in this case) and the circuit integration time (RC in this case). If in equation 7, $RC \gg \tau$, then the pulse amplitude is independent of τ. Unless this condition is satisfied i.e., the emission process is completed in a time short compared to the circuit integration time, scintillation efficiencies determined from pulse amplitudes will not correspond to efficiencies measured by the d.c. technique. The situation is complicated in practice because of the complex form of the scintillation decay. Frequently, the decay will have a short exponential portion followed by one or more long components. The contribution of such long components to the pulse amplitude for different values of R has been studied by Kallmann (8) and Bittman, Furst, & Kallmann (9). A novel method for the study of long components in the scintillation decay has been devised by Jackson & Harrison (10). In this method the scintillator, viewed by a photomultiplier, is irradiated continuously with x-rays, except for short intervals during which the x-ray tube is gated off. Immediately prior to the gating off of the x-ray tube, the photomultiplier is gated on. In this way, long components build up to equilibrium, and, from the decay viewed during the off period of the x-ray tube, one can calculate the relative contributions of the various decay components to the total scintillation. Jackson & Harrison (10) and Harrison (11)

have observed components longer than the initial decay period for most organic crystal scintillators, as well as NaI(Tl), but report no long components in organic liquid scintillators. This suggests that long components in other materials may be detected by comparing their d.c. outputs and pulse heights with those of a liquid scintillator.

In measuring scintillation efficiency, the choice of a suitable exciting source is important. If one wishes to measure the response of a scintillator to fast electrons, one may use a source of β-rays or high-energy electrons, or produce high-energy electrons within the scintillator by irradiating it with γ-rays. For scintillators of low atomic number, irradiation by an external source of "internal conversion" electrons gives a pulse height distribution with a sharp peak, so that pulse height measurements are readily made. However, scintillators containing elements of high atomic number will backscatter the electrons strongly and distort the pulse height distribution. In this case an external γ-ray source is more desirable, since it produces a sharp peak in the pulse height distribution as a result of photoelectric absorption of the γ-rays. A Cs^{137} source is very convenient since it has both internal conversion electrons (624 kev) and γ-rays (662 kev). A method has frequently been used in which the d.c. output resulting from γ-ray excitation is measured. This method can be quite accurate, but under certain circumstances may lead to considerable ambiguity. If the scintillator contains only light elements, and the γ-ray energy is sufficiently high, only Compton electrons are formed. The absorbing power of a small scintillator is then proportional to the number of electrons it contains. If the walls surrounding the scintillator are also made of materials of low atomic number, scintillators of somewhat different size and density can be standardized by dividing the meter reading by the number of electrons in the scintillator. If the density and atomic number of the scintillator are very high, and the γ-ray energy is low, then the radiation will be totally absorbed by the scintillator, and the readings must be corrected for the solid angle subtended from the source by the scintillator. For intermediate energies or atomic numbers, the situation is much more complicated, for the readings must be corrected for the energy actually absorbed by the scintillator.

Scintillation efficiency is a function of the temperature of the scintillator. In most cases, the efficiency decreases with increasing temperature. Kallmann (12) has shown that the efficiency of organic crystals decreases gradually with increasing temperature up to the melting point, at which temperature the efficiency falls to approximately zero. For inorganic scintillators, the efficiency is only slightly temperature dependent up to a certain critical temperature region at which point the efficiency falls rapidly with increasing temperature. In many cases, this sharp decrease in efficiency seems to fit an expression of the form

$$N = \frac{N_0}{1 + \alpha \exp(-\epsilon/kT)} \qquad 8.$$

where N_0 is the number of photons emitted at low temperature, ϵ is the

activation energy associated with quenching, k is Boltzmann's constant, and α a constant. Bonanomi & Rossel (13, 14) have shown that the variation of the scintillation efficiency of several alkali halide scintillators with temperature is accurately described by equation 8. One way in which an expression of this form can arise is the following: If the molecule in the excited state (electronic) can oscillate with sufficient amplitude, it may reach a point where the excited state and ground state differ by an amount so small that the transition may take place with the emission of elastic waves instead of light. The probability of such an event is proportional to $\exp(-\epsilon/kT)$ where ϵ is the energy required to reach the quenching configuration. The competition between this process and the emission process leads directly to an expression of the form given in equation 8. Some scintillators, such as calcium tungstate, are in the critical region at room temperature. Some other materials have critical regions below room temperature and consequently are not ordinarily considered as scintillators.

Scintillation spectra.—A knowledge of the emission spectra of scintillators is useful in selecting the proper photodetector for use with the scintillator and for arriving at specifications for the optical system. For example, it is necessary to know whether a certain liquid scintillator must be used in a quartz container or whether glass is adequate. On the other hand, a knowledge of emission spectra is useful in connection with investigations of the fundamental principles of the scintillation process. The requirements for measurement of the emission spectra are entirely different for these two purposes. For use in fundamental investigations, one must know the spectrum actually emitted by the molecules. Any distortion by selective self-absorption is intolerable. For this purpose, one must make measurements on extremely thin samples or on dilute solutions. This differs from the practical requirements in which one generally wants to know the spectrum that emerges from a thickness of the magnitude to be used in the scintillation counter under consideration. If ultraviolet excitation is used in determining the emission spectrum, one can simulate the practical spectrum by using a "back surface" excitation, in which the fluorescence radiation passes through the scintillator to reach the spectrometer. On the other hand, if one uses a "front surface" excitation with ultraviolet of a wavelength corresponding to the peak of an absorption band, the self-absorption is small, and the observed spectrum approaches the molecular spectrum. In some cases where spectra have been reported, it is not clear to what degree self-absorption was a factor.

Scintillation decay times.—The presence of impurities can affect the scintillation decay time by as great a factor as it affects the efficiency. The impurity may act as a quencher, in which case the decay time will be reduced, or it may fluoresce, giving a decay time characteristic of the impurity. In other cases, the impurity may provide electron traps and lead to phosphorescence.

Repeated self-absorption may alter the observed decay time of a scintillator. It is well known that the radiations from monatomic gases may be

imprisoned for long periods of time by repeated self-absorption [see for example, Mitchell & Zemansky (15)]. Such imprisonment is enormously reduced in solids, as a result of the principles described earlier which cause the emission spectrum to be shifted to longer wavelengths relative to the absorption spectrum. However, as a result of the overlapping of these broad bands, the radiation may still undergo considerable self-absorption before emerging from a thick sample. Birks & Little (7) have shown that the decay time observed for thick organic crystals may be several times longer than the true molecular lifetime, as a result of this effect. By making the same assumptions that were made in the derivation of equation 3, the decay time of a thick scintillator is found to be

$$\tau = \frac{\tau_0}{1 - q(1 - b/a)} \qquad 9.$$

where τ_0 is the molecular lifetime and b and a are the areas under the thick sample emission spectrum and the molecular emission spectrum respectively (the two spectra must be normalized to coincide at the longest wavelengths). The ratio b/a is also the probability that an emitted photon will escape the scintillator without being reabsorbed. For practical applications, a measurement of τ is important, but for interpretive use it is necessary to determine τ_0.

Nearly all the decay time measurements reported so far have been made with a photomultiplier. The high gain and wide frequency response of this device make possible the measurement of scintillation decay with considerable accuracy for periods down to 10^{-8} sec. Below this period, the contribution of the photomultiplier to the observed decay becomes increasingly important, and for scintillation lifetimes below 3×10^{-9} sec., the multiplier may contribute a major portion of the observed decay. The time spread introduced by the photomultiplier is principally attributable to the transit time spread of the electron avalanche. This spread is determined by many factors such as the number of multiplying stages, the degree of focusing, the distance between stages, and the applied voltage. For photomultipliers and operating voltages customarily used in scintillation counting, the transit time spread (width at one-half maximum of the output pulse for an infinitely narrow light pulse) ranges between 10^{-9} and 2×10^{-8} sec.

Since the scintillation resulting from a single ionizing event may often produce only a few hundred photoelectrons at the photocathode, an accurate measurement of the decay time from one pulse is not possible. The problem is analogous to the measurement of the half-life of a short-lived radioisotope where the activity available provides a total of only a few hundred counts. The accuracy of measurement can be increased by averaging the ordinates of many pulses, by increasing the energy of the ionizing particle, or by using artificial excitation, consisting of a short burst containing many high-energy particles.

There are three fundamental processes which have been used to describe the decay of luminescence. The first process is "fluorescence" decay which follows the law given by

$$f(t) = (1/\tau) \exp(-t/\tau). \quad 10.$$

The decay parameter τ is independent of temperature and excitation density, except for a temperature dependence which may occur at the point where strong temperature quenching takes place. The second process, known as "phosphorescence" decay, follows the decay law given by equation 10, but the decay parameter is extremely temperature dependent, obeying the relation

$$(1/\tau) = s \exp(-\epsilon/kT). \quad 11.$$

The third process of decay may be referred to as "bimolecular" decay. It is characterized by the fact that the decay rate is more rapid the greater the density of excitation. The decay follows the form

$$f(t) = \alpha/(1 + \alpha t)^2. \quad 12.$$

The parameter α is proportional to excitation density and in some cases is also temperature dependent according to a relation of the form given by equation 11. For a complete discussion and derivation of these relations see Randall & Wilkins (16) or Garlick (17).

Three general methods have been used for the measurement of scintillation decay. In the first method, the photomultiplier anode (or last dynode) pulse is viewed on a cathode-ray oscilloscope. This method has been used most frequently. The anode time constant RC can be long compared to the decay characteristic, in which case the anode voltage will be proportional to the time integral of the anode current $I(t)$ (given by equation 4), or RC can be made much shorter than the decay time so that the anode voltage is proportional to the anode current. Post & Shiren (18) have greatly improved the time resolution of the method by applying very high voltages to the photomultiplier, breakdown being avoided by applying the voltage for only a few microseconds at a time. Phillips & Swank (19) have increased the statistical accuracy by using pulsed x-ray excitation.

In the second method, used by Liebson, Bishop, & Elliot (20), the scintillator is excited by a periodically pulsating source of ultraviolet or x-rays. The exciting ultraviolet light is modulated by diffraction from an oscillating quartz crystal. If the number of ultraviolet photons absorbed per second by the scintillator is $J_0 \sin \omega t$, then after equilibrium is established, the number of fluorescence photons emitted per second will be given by

$$F(t) = qJ_0 \int_{-\infty}^{t} f(t - t_0) \sin \omega t_0 dt_0 \quad 13.$$

where it is assumed that the principle of superposition applies. For the simple case where $f(t)$ is exponential (equation 10)

$$F(t) = \frac{qJ_0}{\sqrt{1 + \omega^2\tau^2}} \sin(\omega t - \theta)$$

where

$$\tan \theta = \omega\tau. \quad 14.$$

The fluorescence light $F(t)$ will pulsate at the same frequency as the exciting light but will be reduced in amplitude and shifted in phase. From the phase difference between the exciting light and the fluorescent light, one obtains the decay parameter, if the form of $f(t)$ is known. This method was modified by Birks & Little, who used a gas discharge tube as the source of exciting light (7).

A third method for measuring decay times has been described by Elliot *et al.* (21). The principle of this method is illustrated by Figure 4. The photomultiplier pulse *a* is superimposed on its delayed reflection *b*. A crystal diode

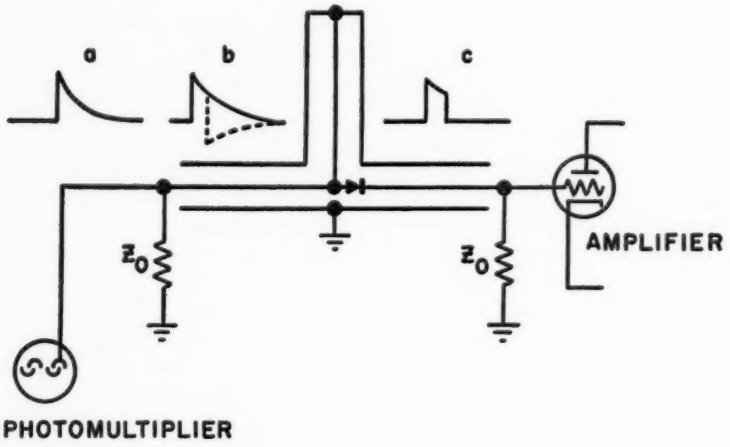

FIG. 4. Circuit diagram for the "shorted line" method of measuring scintillation decay time. z_0 is the characteristic impedance of the line used. [After Elliot *et al.* (21).]

passes only the positive portion, *c*. The pulse *c* is fed into a "slow" amplifier which delivers an output pulse proportional to the area under *c*, so that the output pulse amplitude (for an ideal diode) is

$$A(t_1) = \int_0^{t_1} f(t)dt \qquad 15.$$

where t_1 is the transit time down and back from the shorted stub. $f(t)$ may be obtained from equation 15 by differentiation with respect to t_1. Elliott *et al.* assumed the exponential form for $f(t)$ and measured the change in t_1 necessary to reduce $A(t_1)$ by a certain factor. They found that the nonideal response of the diode could be corrected by a factor which was relatively constant over the range of decay times examined.

Two other methods have been used which are somewhat analogous to the above method, and could be considered to be variations of it. The first method, used by Lundby (22), consists of determining the decay time of a scintillator from its performance in a coincidence circuit. The other method,

used by Bittman *et al.* (9), consists of determining the amplitude of the photomultiplier anode pulse as a function of the shunt resistance, R. In this method, a qualitative determination of the form of $f(t)$ is obtained.

Organic Scintillators

The presently known organic scintillators are compounds whose molecules contain one or more benzene rings. They comprise the largest and one of the best-known families of fluorescent materials. For a complete survey of their fluorescence properties see Pringsheim (23).

Organic crystals.—The organic scintillators form molecular crystals with low cohesive energy. The absorption and emission spectra are shifted only slightly (~200 Å) in the crystalline state, compared with the free molecules. Relationships between chemical structure and scintillation efficiency have been studied by Kallmann (8), Sangster (6), and Koski & Thomas (24). No reliable system has been found for predicting scintillation efficiencies, but a few general relationships have been noted, such as the desirability of a symmetrical molecule with a large number of conjugated double bonds, and the undesirability of steric hindrance or of the substitution of sulfur or halogens. The emission spectra of these compounds extend from about 3000 Å for solid benzene to 6000 Å for materials like pentacene and diphenyloctatetraene. A more or less uniform increase in emission wavelength occurs with an increase in the number of double bonds.

Organic scintillators are characterized by their short decay times, which are of the order of 10^{-8} sec. Recent observations by Jackson & Harrison (10) and Harrison (11), however, have shown that metastable states exist which give minor decay components up to about 100 μ sec. The decay times of organic scintillators decrease with decreasing temperature. Figure 5 shows

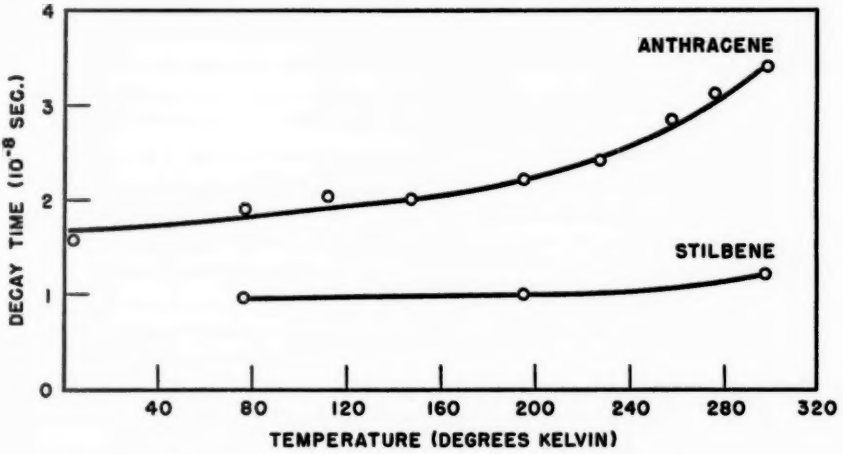

FIG. 5. Scintillation decay times of anthracene and stilbene versus temperature. [After Elliot *et al.* (25).]

the results reported by Elliot *et al.* (25) for anthracene and stilbene, measured by the "shorted line" technique. The effect shown is opposite to that characteristic of phosphorescence decay (equation 11). Birks (1) has suggested that these results may be explained by self-absorption (equation 9). An increase of τ with increasing temperature could result from the fact that the photon escape probability b/a decreases with increasing broadening of the spectra at higher temperatures.

There has been considerable disagreement among various investigators concerning the values for efficiency, emission spectra, and decay times of various organic crystals. Aside from effects associated with sample thickness, already described, this disagreement is probably attributable in large measure to the effects of impurities. There are three ways in which an impurity may influence the properties of an organic crystal: (*a*) by perturbing the fluorescent molecules adjacent to it, the impurity may alter their fluorescence properties; (*b*) the impurity may absorb the radiation emitted by the fluorescent molecules; and (*c*) the fluorescence excitation may migrate without radiation, some of it being captured by the impurity. Operation of mechanism (*a*) alone would require concentrations of the order of 5 to 10 per cent to significantly alter the fluorescence properties, since only the molecules adjacent to the impurity are affected. Therefore, the effects often observed wherein the scintillator is affected by impurity concentrations of 0.1 per cent or smaller must be attributable to (*b*) or (*c*).

An extensive investigation of the effect of small amounts of impurity on the fluorescence of organic crystals was carried out by Bowen *et al.* (26, 27, 28). It was found that the fluorescent crystal was most sensitive to those impurities which absorbed strongly in the region of the fluorescence spectrum, an observation that would seem to indicate that the radiation emitted by the fluorescent crystal was being reabsorbed by the impurity. However, as a result of other observations, Bowen was led to the conclusion that the excitation energy was able to diffuse through the crystal and be captured by the impurity without radiation taking place. A theoretical basis for such processes has been given by Kallmann & London (29), by Frenkel (30), and by Förster (31). These conclusions, derived from experiments with ultraviolet excitation, have a very important bearing on our understanding of the scintillation process. Later experiments with liquid and plastic scintillating solutions tend to support the notion of nonradiative energy migration in organic scintillators. However, it should be pointed out that the validity of Bowen's conclusions has recently been questioned by Birks (1), who shows that many observations which at first appear to demand a nonradiative transfer mechanism can be explained equally well by a radiative transfer mechanism.

Based on the assumption of nonradiative energy migration and transfer, Bowen derived equations to express the dependence of the fluorescence output of the host crystal, and in the case of fluorescent impurities, the dependence of the impurity fluorescence on the concentration of the impurity. Using a slight modification of Bowen's terminology, the equations are

$$q_A = \frac{k_1}{k_1 + k_2 + k_3c + k_7c} \tag{16.}$$

$$q_B = \frac{k_3k_4c}{(k_1 + k_2 + k_3c + k_7c)(k_4 + k_5 + k_6c)} \tag{17.}$$

where q_A and q_B are the quantum efficiencies for the host crystal A and the solute substance B, respectively, for radiation "absorbed by the host crystal" and

(*a*) k_1 is the reaction probability for fluorescence of A
(*b*) k_2 is the reaction probability for self-quenching of A
(*c*) ck_3 is the reaction probability for transfer of excitation from A to B
(*d*) k_4 is the reaction probability for fluorescence of B
(*e*) k_5 is the reaction probability for internal quenching of B
(*f*) ck_6 is the reaction probability for self-quenching of B
(*g*) ck_7 is the reaction probability for quenching of A by B

and c is the concentration of B in A. For low concentrations process (*g*) may be neglected since quenching at low concentrations takes place as a result of process (*c*) followed by (*e*) and (*f*). Then equations 16 and 17 may be written

$$q_A = \frac{q_0}{(1 + \sigma c)} \tag{18.}$$

$$q_B = \left(\frac{\sigma c}{1 + \sigma c}\right)\left(\frac{q_1}{1 + mc}\right) \tag{19.}$$

where

$$q_0 = \frac{k_1}{k_1 + k_2}, \qquad q_1 = \frac{k_4}{k_4 + k_5}$$

$$\sigma = \frac{k_3}{k_1 + k_2}, \qquad m = \frac{k_6}{k_4 + k_5}.$$

If the impurity is fluorescent, its emission, given by equation 19, rises to a maximum at $c = 1/\sqrt{\sigma m}$ and then declines. If the impurity is nonfluorescent ($q_1 = 0$), then $q_B = 0$ and the quenching of A is given by equation 18. Successful application of these principles has been found in the use of naphthalene crystals containing small amounts of anthracene as an impurity. The crystals are as easy to grow as pure naphthalene, but give a greater scintillation response.

As was mentioned above, deviations from the simple linear relationship given by equation 1 between the scintillation magnitude and the energy of the particle stopped in the scintillator are to be expected as a result of interactions of excited molecules with other nearby excited molecules, or with other products created by the dissipation of the particle's energy. Such an effect was first noticed by Kallmann (12), who observed that the light output from organic crystals per unit energy expended was much smaller for α-particles than for β-particles. The effect was also evident in the results of Hopkins (32), who found that the pulse height from electrons on anthracene

was proportional to energy above 125 kev, but deviated from proportionality below this energy. Recently, the dependence of scintillation efficiency on the energy and nature of the exciting particle has been studied by several investigators. The results of Taylor *et al.* (33), Frey *et al.* (34), and Birks (35) for anthracene have been combined in the curves shown in Figure 6. It is readily seen that the ratio of the scintillation pulse height to the energy of the particle stopped in the scintillator is smaller the larger the specific energy loss of

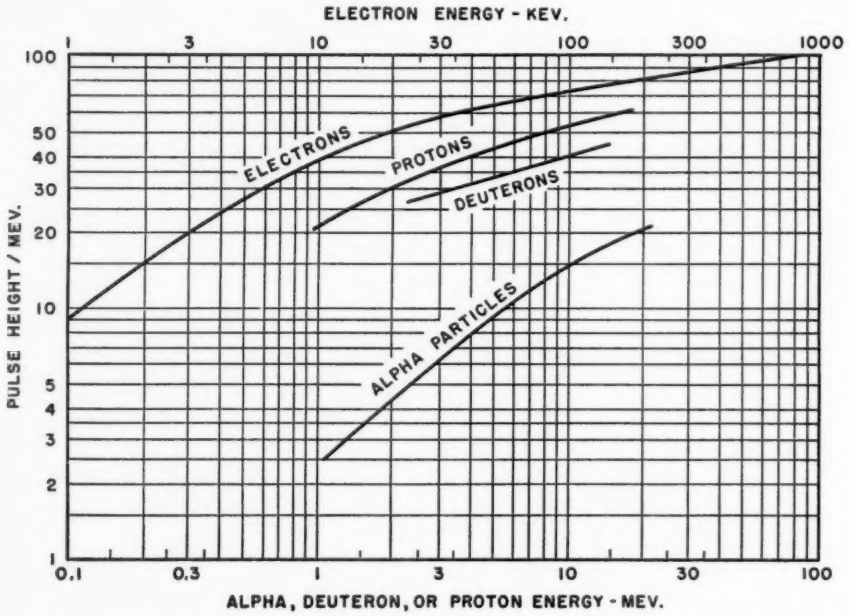

FIG. 6. Pulse height/energy ratio versus energy for several particles on anthracene, from the data of Taylor *et al.* (33), Frey *et al.* (34), and Birks (35).

the particle. This effect is seen more clearly in Figure 7, where the specific efficiency dN/dx and the incremental efficiency dN/dE are plotted (from the data of Taylor *et al.*) against the specific energy loss of the particle. dN/dx is the number of photons emitted per unit distance traveled by the particle (the units in Figure 7 are arbitrary). Figure 7 shows that the scintillation efficiency of anthracene is a function of the specific energy loss, irrespective of the mass or charge of the particle. The deviation of the low-energy electron data from the curve has been explained by Birks (36) as a surface effect which becomes significant when the range of the particle in the scintillator is less than about seven microns. Birks (37) has derived a theoretical formula to account for the results shown in Figure 7, based on the assumption of quenching by "impurities" resulting from radiation damage. Thus the quenching

formula (equation 18) applies, and since the quenchers are formed by the dissipation of the particle's energy, $c = BdE/dx$, so that

$$\frac{dN}{dE} = \frac{q}{w}\left(\frac{1}{1 + kBdE/dx}\right). \qquad 20.$$

Birks has shown that the values of scintillation amplitude obtained from equation 20 by integrating over the range of the particle give excellent agree-

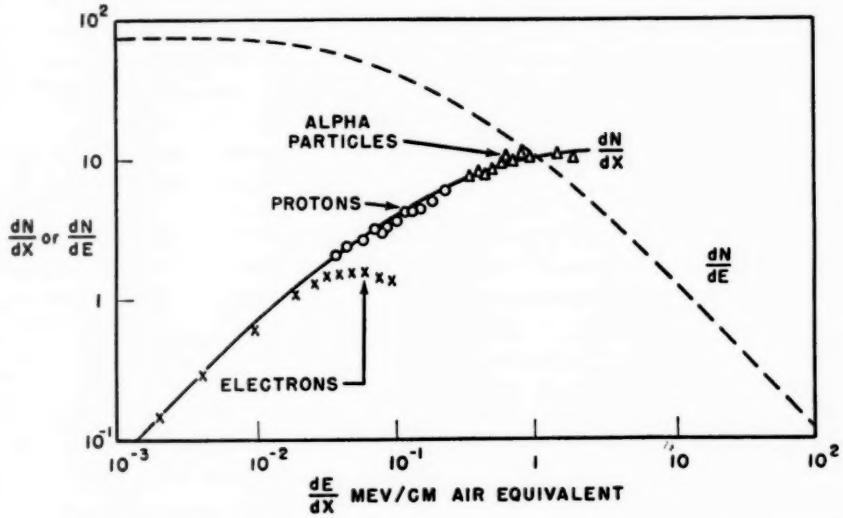

FIG. 7. Specific photon emission, dN/dx and incremental photon emission dN/dE versus specific energy loss of the exciting particle on anthracene. [After Taylor *et al.* (33).]

ment with experimental data for electrons, protons, deuterons, and α-particles on anthracene.

Another theory was developed by Wright (38) in which the quenching is assumed to result from interactions between similar excited molecules. This theory leads to a bimolecular decay law, which reverts to an exponential at long times, and gives for the scintillation efficiency

$$\frac{dN}{dE} = \frac{q}{w}\,\frac{\ln(1 + MdE/dx)}{MdE/dx} \qquad 21.$$

where M is a constant. The shapes of equations 20 and 21 are not sufficiently different to decide between them on the basis of present experimental data. The data of Bittman *et al.* (9) on decay times favor Wright's theory, however.

A convenient measure of the effect of the specific energy loss of the exciting particle on the efficiency of a particular scintillator is obtained by com-

paring the ratio of pulse height to energy for polonium α-particles ($E_0 = 5.3$ Mev) with that of a high-energy electron ($E_0 \geqq 1.0$ Mev). This measurement is frequently referred to as the α-to-β ratio. It is very close to 0.10 for anthracene and is remarkably similar for other organic scintillators.

Table II gives some properties of the commonly used organic crystal scintillators.

TABLE II

ORGANIC SCINTILLATION CRYSTALS

Material, Empirical Formula	Density (gm./cm.^{3}) Melting Point (°C.)	Wavelength of Maximum Emission (Å)	β-Particle Pulse Height*	Linearity α/β Ratio	Decay Constant† $\times 10^9$ (sec.)	Miscellaneous
Anthracene $C_{14}H_{10}$	1.25 217	4400	100	Linear $\beta >$ 125 kev $\alpha/\beta = 0.10$	32	Large crystals difficult to grow
trans-Stilbene $C_{14}H_{12}$	1.16 124	4100	60	$\alpha/\beta = 0.1$	6.4	Good crystals readily obtained; very fragile
Diphenylacetylene $C_{14}H_{10}$	1.18 62.5	3900	45		5.4	Good crys- readily obtained
p-Terphenyl $C_{18}H_{14}$	1.23 213	4000	40		5.0	Fair crystals readily obtained; rugged
p,p'-Quaterphenyl $C_{24}H_{18}$	— 318	4200	85		7	Good crystals difficult to grow

* 5819 or 6292 photomultiplier response, relative to anthracene crystal = 100.
† Time for light intensity to fall to $1/e$ of initial intensity.

Liquid scintillators.—Following the report of Reynolds *et al.* (39), that scintillation pulses could be obtained from solutions of *p*-terphenyl in xylene comparable to those from crystals, the application of these scintillators spread rapidly. An extensive investigation of these materials has been carried out by Kallmann & Furst (40, 41, 42). Most of our present understanding of the basic principles of this type of scintillator is a result of their investigations. They have shown that a transfer of excitation energy from solvent to solute occurs in these solutions very similar to that observed by Bowen in crystalline solid solutions. In the case of the liquids, however, almost no fluorescence output is observed for the pure substances, i.e. $q_A = 0$. It is the fact that the excitation energy is transferred to the solute before quenching can occur that makes possible a reasonable efficiency. Using a similar analysis Kallmann & Furst have derived an equation of the same form as equation 19

to express the luminescence output as a function of concentration. The agreement of this equation with observation has been verified with many different solvents and solutes. In addition to the use of a fluorescent solute as activator, Kallmann & Furst found that a highly fluorescent solute in very low concentration could absorb the fluorescence from the primary solute and re-emit it at a longer wavelength. Such secondary solutes, now commonly referred to as "wavelength shifters," have become very useful in obtaining a better match to the photomultiplier sensitivity spectrum and in reducing self-absorption in the scintillator.

A new series of fluorescent solutes for liquid scintillators has been developed by Hayes (43). These compounds, which might be referred to as the "phenyloxazoles," are far more soluble than *p*-terphenyl. They are the only known solutes which may be used successfully at low temperatures. Various members of this family of compounds are suitable for primary solutes or "wavelength shifters."

Reynolds (74) has studied the response of liquid scintillators to α-particles. For a solution of five grams per liter of terphenyl in toluene, the response is very similar to that of anthracene. However, the α-to-β ratio decreases rapidly with decreasing terphenyl concentrations. The response of these solutions to various particles has been discussed by Harrison (75).

Liquid scintillators are very subject to poisoning by impurities, particularly organic sulfur and halogen compounds. A special kind of poisoning which has been studied by Pringle *et al.* (44) is that resulting from oxygen. Pringle has shown that the effect of dissolved oxygen is reversible, and that the scintillation efficiency may be restored by bubbling nitrogen through the liquid. Formulas and characteristics of a number of liquid scintillating solutions are given in Table III.

Plastic scintillators.—Since the report by Schorr & Torney (45) that scintillations had been observed in solid solutions of terphenyl in polystyrene, interest in these materials has centered around the development of larger light output and in investigating the nature of the energy transfer processes. Koski (46) has studied the spectra and pulse heights of several solid solutions. Pichat *et al.* (47, 48) developed plastic scintillators containing 1,1,4,4-tetraphenyl-1,3-butadiene and reported pulse height and spectra of various solutions, together with experiments which indicated that a nonradiative energy transfer mechanism was involved in the scintillation process. Buck & Swank (49, 50) studied pulse heights, spectra, and decay times of several solutes in polystyrene and polyvinyltoluene. Curves of pulse height versus concentration (Fig. 8) were found to agree very well with the form given by equations 18 and 19. A study of the propagation of energy through thin films and of decay time versus solute concentration led to the conclusion that about 20 per cent of the solvent excitation energy was transmitted to the solute by radiation and 80 per cent by a nonradiative mechanism. A summary of the available data for several plastic scintillator formulas is given in Table IV.

TABLE III

Liquid Scintillators

Solvent	Solute* (grams/liter)	Second Solute* (grams/liter)	Wavelength of Maximum Emission (Å)	β-Particle Pulse Height†	α/β Ratio	Decay Constant‡ ×10⁹ (sec.)	Miscellaneous
Toluene§	TP, 5	0	3550	0.35	0.09	2.2	
Phenylcyclohexane‖	TP, 3	0	3550	0.27		<2.9	Can be used in Lucite containers
Phenylcyclohexane‖	TP, 3	DPH, 0.01	4500	0.35		8.0	Can be used in Lucite containers
Toluene§	TP, 5	αNPO, 0.02	4150	0.42		≦3.2	Photon mean free path ∼2 meters
Toluene§	PPO, 3	0	3820	0.40		≦3.0	Useful at low temperatures
Toluene§	PBD, 8	0	3700	0.49		<2.8	

* Solute abbreviations: TP = *p*-terphenyl; DPH = 1,6-diphenyl-1,3,5-hexatriene; αNPO = 2-(1-naphthyl)-5-phenyloxazole; PPO = 2,5-diphenyloxazole; PBD = 2-phenyl-5-(4-biphenylyl)-1,3,4-oxadiazole.

† 5819 or 6292 photomultiplier responses, relative to anthracene crystal = 1.00.

‡ Time for light intensity to fall to $1/e$ of initial value.

§ Specially purified by Dr. F. N. Hayes, Los Alamos Scientific Laboratory.

‖ Eastman Kodak Co. No. 1502.

TABLE IV

Plastic Scintillators

Solvent	Solute* (grams/liter of monomer)	Second Solute* (grams/liter of monomer)	Wavelength of Maximum Emission (Å)	β-Particle Pulse Height†	α/β Ratio	Decay Constant‡ ×10⁹ (sec.)	Miscellaneous
Polystyrene	TP, 36	0	3550	0.28	0.10	≦3.0	
Polystyrene	TPB, 16	0	4500	0.36	0.08	4.6	
Polystyrene	TP, 36	TPB, 0.2	4450	0.39	0.10	4.0	
Polyvinyltoluene	TPB, 16	0	4500	0.37	0.08	4.6	
Polyvinyltoluene	TP, 36	TPB, 0.2	4450	0.45	0.10	4.0	Photon mean free path ∼2 meters
Polyvinyltoluene	TP, 36	DPS, 0.9	∼3800	0.48	0.10	≦3.0	

* Solute abbreviations: TP = *p*-terphenyl; TPB = 1,1,4,4-tetraphenyl-1,3-butadiene; DPS = *p,p'*-diphenylstilbene.

† 5819 or 6292 photomultiplier responses, relative to anthracene crystal = 1.00.

‡ Time for light intensity to fall to $1/e$ of initial value.

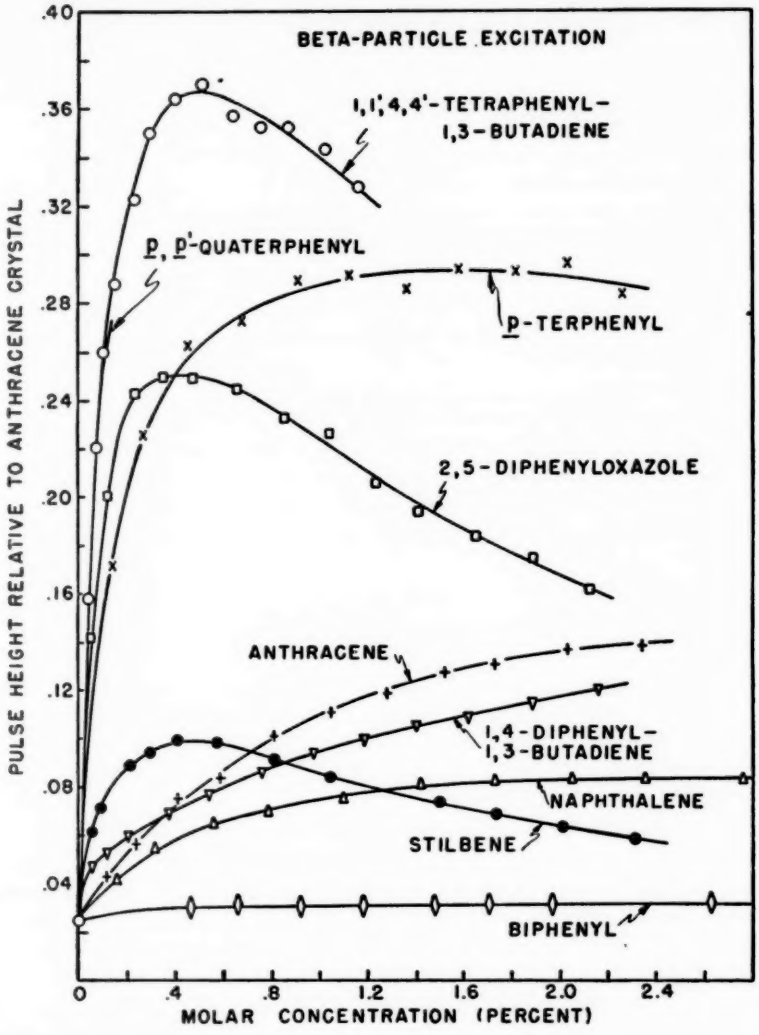

FIG. 8. Pulse height versus concentration for several plastic scintillators. Solid lines are theoretical curves (equations 18 and 19) fitted to the experimental points. [After Swank & Buck (50).]

INORGANIC SCINTILLATORS

Most of the available information concerning the behavior of inorganic scintillators stems from earlier investigations of the ultraviolet fluorescence and the cathodoluminescence of these materials. [For a summary see Fonda & Seitz (51), Kröger (52), Leverenz (53), Garlick (17), Pringsheim (23).]

Those compounds which are of current interest form ionic crystals. The large forces which exist between ions cause a convergence of the individual molecular orbits of the valence electrons into diffuse bands belonging to the entire crystal. These energy bands are illustrated in the diagram shown in Figure 9.

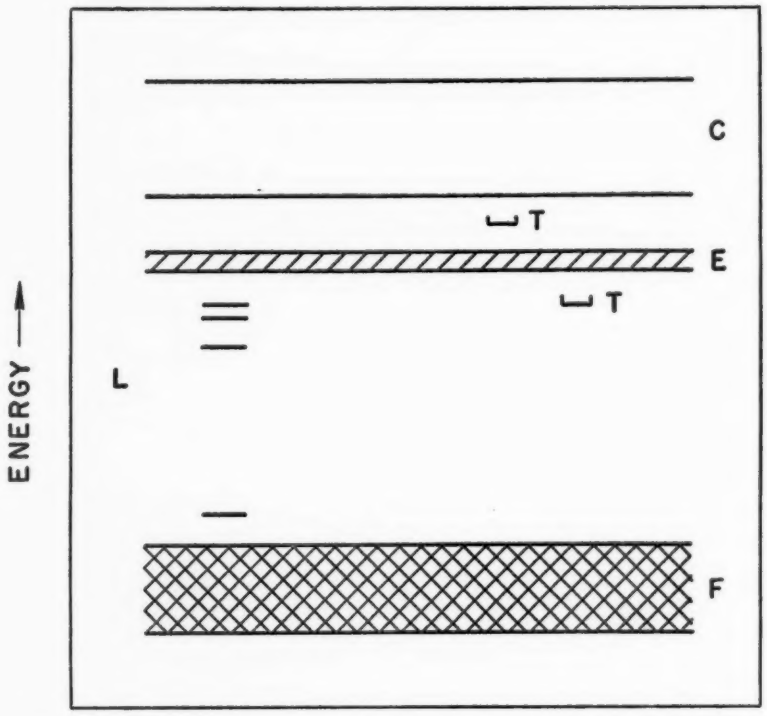

FIG. 9. Energy level diagram for an activated crystalline scintillator. F is the highest filled band, C the conduction band, E an exciton band. T designates electron traps and L designates levels in the luminescent center.

In the unexcited crystal, the highest occupied band is completely filled according to the Pauli exclusion principle. Upon absorption of a quantum of energy by the crystal, an electron may be raised from the filled band F into the conduction band C, whereupon the electron and the hole it leaves in the filled band may move independently through the crystal, at least until they are captured by an impurity or imperfection in the crystal. It may also be possible for the absorbed quantum to excite the crystal without ionization (band E). Again, however, the excitation energy is not localized but moves rapidly through the crystal in the form of excitation waves [Frenkel (30), Franck & Teller (54)]. These excitation waves also exhibit corpuscular properties, and the associated particle is referred to as the exciton. The exciton

diffuses rapidly through the crystal, passing a molecule in a time shorter than the molecular vibrational period. It may arrive at a crystal imperfection and radiate its energy as elastic waves, or may be captured by an impurity, causing the impurity to become excited. It is through the latter process that exciton waves may be important to the scintillation phenomenon.

Alkali halides.—These crystals, containing small amounts of thallium halide, are among the oldest and best-known inorganic phosphors. A summary and interpretation of the properties of these phosphors has been given by Seitz (55). Seitz considers the activation by thallium to consist primarily of substitution of Tl^+ for alkali ions. This introduces new absorption bands at longer wavelengths than the fundamental absorption of the crystal. The absorption levels observed can be correlated with levels in the free Tl atom. Experiments with excitation of KCl(Tl) by ultraviolet show that: (*a*) the Tl fluoresces with a high efficiency when irradiated in its "characteristic" absorption bands but with a much lower efficiency when the crystal is irradiated in the "fundamental" absorption band; and (*b*) photoconduction is not produced in either case. Observation (*b*) indicates that the fundamental absorption must create an exciton rather than a conduction electron, and (*a*) indicates that transfer of the exciton energy to the emitting center is inefficient.

The high scintillation efficiency of NaI(Tl) and KI(Tl) indicates that excitations produced in the lattice must be transmitted to the emitting center with a high efficiency. The available energy of the ionizing particle is much larger than that of the quanta used in experiments with ultraviolet, so it may be assumed that the major portion of the particle's energy goes into ionization. Emission can then result from the recombination of electrons and holes in the activator center.

The Tl-activated alkali halides exhibit a phosphorescent scintillation decay, consisting of one or more components of the form given by equations 10 and 11. A study of the decay parameters has been carried out recently by Bonanomi & Rossel (13, 14).

The Tl-activated alkali halides are striking because of their high transparency to their own radiation. The longest absorption wavelength is below 3000 Å whereas the emission is almost entirely above 3000 Å in all cases, and mostly above 4000 Å for the iodides. The situation is much less favorable in the case of activation by Sn or Eu.

The most useful alkali halide scintillator has been NaI(Tl). The use of this scintillator was reported by Hofstadter (56, 57, 58). Most of the scintillation energy is emitted in a phosphorescent component having a very short lifetime (0.25 μ sec. at room temperature). Aside from the high efficiency and transparency it is also a fortunate property of this scintillator that self-quenching by the activator ions is very small. As a result, it is possible to obtain optimum efficiency (for electrons) over a wide range of activator concentrations. Harshaw *et al.* (59) have found that although the thallium concentration may vary by more than a factor of two over a large boule grown

from the melt, the pulse height variation is negligible. Their data for pulse height versus thallium concentration are shown in Figure 10.

Investigations by Taylor *et al.* have shown that NaI(Tl) shows a linear relationship of pulse height versus energy for electrons and protons over a wide range of energies, but shows a deviation from linearity for α-particles below 20 Mev. Similarly, the pulse height per unit energy is the same for protons and electrons but smaller for α-particles. Lovberg (60) has reported

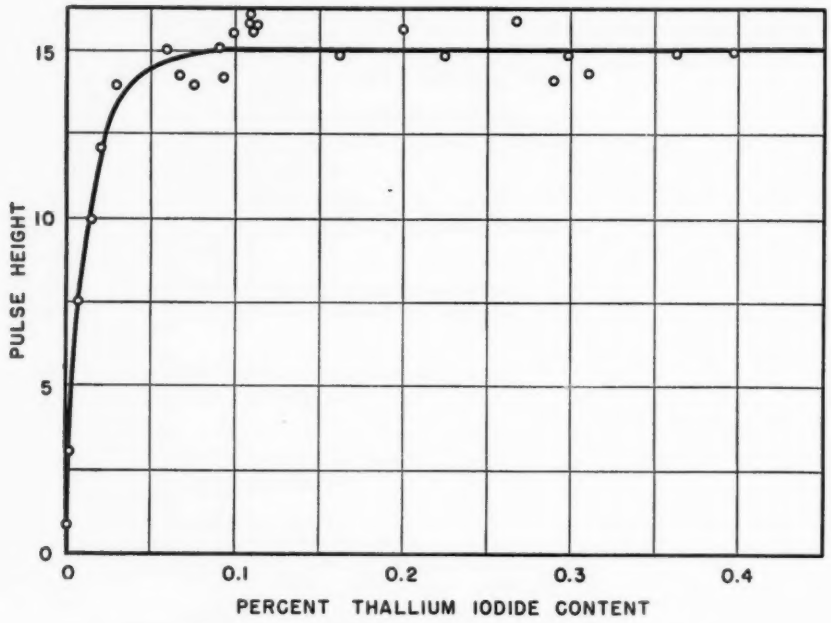

FIG. 10. Fast electron pulse height versus Tl concentration in NaI(Tl). [After Harshaw *et al.* (59).]

results of relative pulse height versus energy for α-particles below 10 Mev. These results are shown in Figure 11. Curves similar to those shown in Figure 6 cannot yet be constructed for NaI(Tl) because of the observation made by Eby *et al.* (61) that the relative response versus energy is different for different Tl concentrations. Hence the work of different investigators cannot be compared unless the activator concentrations are given.

Detection of slow neutrons by means of the Li^6 (n,α) H^3 reaction in LiI(Tl) was reported by Hofstadter *et al.* (62). Later experiments by Schardt & Bernstein (63) showed that these crystals grown from the melt exhibited variations in pulse height over the crystal volume as a result of large variations in Tl concentration. They found that Sn was more easily incorporated with good uniformity. Schenck (64) obtained larger pulse heights by activation with Eu. He found that the slow-neutron pulse height divided by the reac-

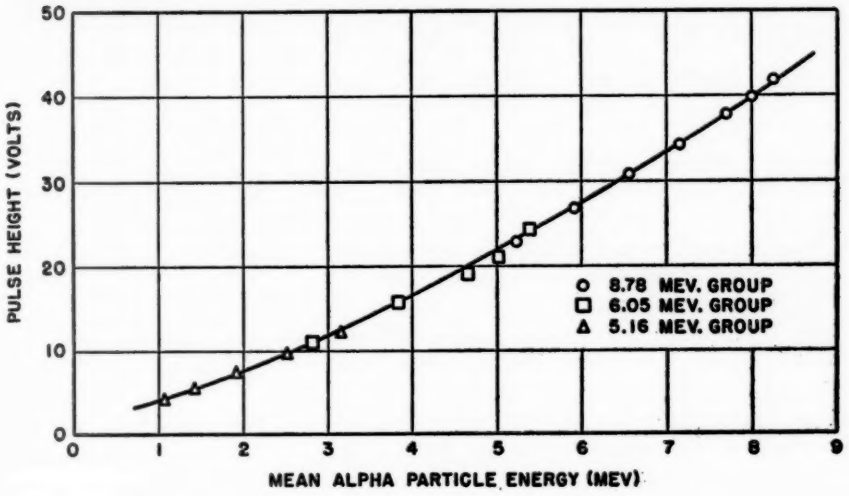

FIG. 11. Relative pulse height versus energy of α-particles on NaI(Tl). [After Lovberg (60).]

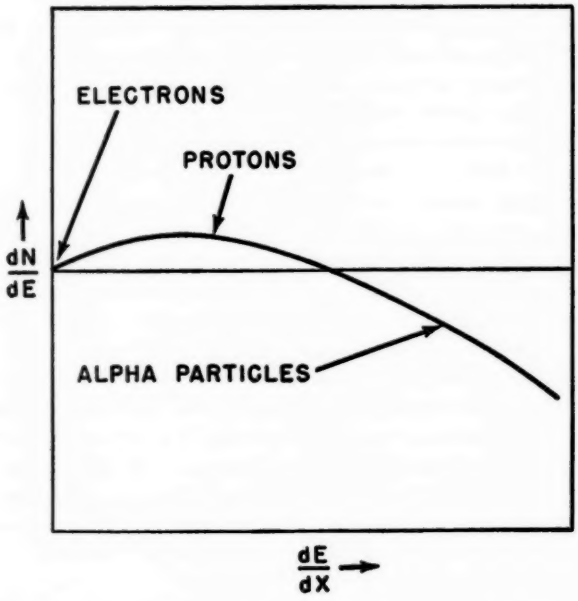

FIG. 12. Proposed shape of the curve of incremental efficiency versus specific energy loss for LiI(Eu).

tion energy was equal to 95 per cent of the pulse height per unit energy obtained with fast electrons. The natural conclusion was that this scintillator had an efficiency which was almost independent of the nature and energy of the exciting particle. This conclusion later proved to be wrong [Schenck & Neiler (65)]. The pulse height per unit energy for protons was found to be greater than for electrons. This and other observations led to the conclusion that the α-particle efficiency was appreciably smaller than the corresponding electron efficiency. From this, one might construct a hypothetical curve of efficiency versus specific energy loss similar to that shown in Figure 12. An explanation of this behavior has not been given.

Scintillation properties for $CaI_2(Tl)$ and CsI(Tl) (66), and CsF (67) have been reported by Van Sciver & Hofstadter. Small, transparent crystals of $NH_4I(Tl)$ were grown by Gugelot (76). The pulse heights from electrons were only 1/15 as large as those from NaI(Tl), and the response to α-particles was nonlinear.

Experiments with unactivated crystals of CsI at low temperatures have been reported by Hahn (68). At 77° K these crystals give a large scintillation response to α-particles and show better proportionality than NaI(Tl) or KI(Tl). A summary of data for alkali halide scintillators is given in Table V.

Zinc sulfide.—Unactivated ZnS shows a blue emission immediately outside its absorption edge. Whether the emission is characteristic of "pure" ZnS or of ZnS activated by excess Zn is not known. When Ag is incorporated as an impurity in amounts of the order of 0.01 per cent, the blue emission is greatly enhanced, and the scintillation efficiency is very high.

There are no pure excitation bands in ZnS. Irradiation in the first absorption band produces photoconduction. Similarly, absorption of a high-energy particle produces conduction electrons with a high efficiency. Luminescence is then produced when the electrons and holes recombine at the luminescence centers. However, recombination is retarded by trapping of electrons in the lattice. Observations by Bube (69) indicate that as many as sixteen different trapping levels may be present in the ZnS lattice. Since luminescence results from recombination, the decay is of the bimolecular form (equation 12); and since the recombination rate is determined by release from traps, it is strongly temperature dependent.

Although ZnS(Ag) is one of the most efficient known scintillators and has an emission spectrum ideally suited to the best photomultipliers, its use in scintillation counters has been very limited for three reasons: (*a*) Large single crystals are extremely difficult to prepare; (*b*) the crystal is only partially transparent to its own radiation; and (*c*) most of the luminescence energy is emitted too slowly for use in pulse counters. Nevertheless, ZnS(Ag) has been found useful for counting heavy charged particles as well as fast and slow neutrons.

Kallmann (70) has reported that while the response of ZnS(Ag) to α-particles (per unit energy absorbed) is greater than to electrons, the response to fission fragments is considerably smaller. This suggests that perhaps a

TABLE V

ALKALI HALIDE SCINTILLATORS

Material	Density (gm./cm.³) Melting Point (°C.)	Wavelength of Maximum Emission (Å)	β-Particle Pulse Height* (10μ sec.)	β-Particle Light Output† (D.C.)	Linearity, Response to Heavy Particles	Initial Decay Period‡ (μ sec)	Miscellaneous
NaI(Tl)	3.67 651	4100	210	210	Linear β, p $\alpha/\beta=0.5$	0.25	Hygroscopic, excellent transparency
KI(Tl)	3.13 582	4100	~50	~200	Linear β, p $\alpha/\beta=1.0$	1.0	Excellent transparency
CsI(Tl)	4.51 621	(blue)	55	~130	$\alpha/\beta=0.5$	1.1	
LiI(Tl)	4.06 446	~4500	20		$n/\beta=0.65$§	1.2	Nonuniform, very hygroscopic
LiI(Sn)	4.06 446	5300	12		Linear β, p $n/\beta=0.93$§	0.7	Pale yellow, very hygroscopic
LiI(Eu)	4.06 446	~4400	75		Linear β, p $n/\beta=0.95$§	2.0	Almost colorless, very hygroscopic
CsF	3.59 684	~4000	5–10		$\alpha/\beta=0.25$	0.005	
CsI (77° K)	4.51 621				Linear $\alpha \geqq 3$ Mev	0.5	35 per cent efficiency for α-excit.

* 5819 or 6292 photomultiplier response with ~10μ sec. anode time constant, relative to anthracene crystal = 100.

† Photomultiplier anode current, relative to anthracene crystal = 100.

‡ Time for light intensity to fall to $1/e$ of initial value.

§ Thermal neutron pulse height/4.785 Mev ÷ electron pulse height/energy.

characteristic of the general shape shown in Figure 12 applies to this scintillator.

Alkaline earth tungstates.—The tungstates of Mg, Ca, Sr, and Cd all make efficient phosphors. Incorporation of an activator is not necessary for the fluorescence of these compounds. However, the chemically-prepared powders are not luminescent, and it is necessary to "activate" them by heating. This has sometimes been considered to involve incorporation of an activator center through a deviation from stoichiometric proportions. However, increasing the size and perfection of the crystals by heating may remove or reduce quenching defects. Experiments by Kröger (52) strongly indicate that the fluorescence of these compounds is a molecular phenomenon, not involving transfer of energy to an activator center.

Observation of scintillations in natural scheelite ($CaWO_4$) by Moon (71) aroused considerable interest because of the very high sensitivity of these crystals to γ-rays. Gillette (72) produced small synthetic $CaWO_4$ and $CdWO_4$ crystals. Although the high melting point of $CaWO_4$ makes the growing of crystals from the melt difficult, this would probably not present an

insurmountable obstacle to the preparation of large crystals. The decline of technical interest in this material is not attributable to this difficulty but to the displacement of the scintillator by NaI(Tl), which produces larger pulses of shorter decay times.

Miscellaneous scintillators.—Scintillations in CaF_2 and other minerals were reported by Moon (71). The decay time of CaF_2 has been reported by MacIntyre (73). See Table VI.

TABLE VI

MISCELLANEOUS INORGANIC SCINTILLATORS

Material	Density (gm./cm.³) Melting Point (°C.)	Wavelength of Maximum Emission (Å)	β-Particle Pulse Height* (10μ sec.)	β-Particle Light Output† (D.C.)	Linearity, Response to Heavy Particles	Initial Decay Period‡ (μsec.)	Miscellaneous
ZnS(Ag)	4.09 1850	4500	~100	~400	$\alpha/\beta = 2.0$	~10	Crystalline powders
$CaWO_4$	6.1 1535	4300	36		Linear β $\alpha/\beta \approx 0.2$	6	Small crystals. Chemically inert
$CdWO_4$	7.90 1325	5300	21			8	Small crystals. Pale yellow
CaF_2	3.18 1360	~2500	~25§		Linear β $\alpha/\beta < 1.0$	0.2	Large crystals. Chemically inert
$CaI_2(Tl)$	3.96 575	~4000	230			1.1	Hygroscopic

* 5819 or 6292 photomultiplier response with ~10μ sec. anode time constant, relative to anthracene crystal = 100.

† Photomultiplier anode current, relative to anthracene = 100.

‡ Time for light intensity to decay to $1/e$ of initial value.

§ With external plastic "wavelength shifter."

LITERATURE CITED

1. Birks, J. B., *Scintillation Counters* (Pergamon Press Ltd., London, England and McGraw-Hill Book Co., Inc., New York, N. Y., 148 pp., 1953)
2. Curran, S. C., *Luminescence and the Scintillation Counter* (Butterworths Scientific Publications, London, England and Academic Press Inc., New York, N. Y., 219 pp., 1953)
3. Garlick, G. F. J., *Progress in Nuclear Physics*, **2**, 51–88 (Pergamon Press Ltd., London, England and Academic Press, Inc., New York, N. Y., 295 pp., 1952)
4. Jordan, W. H., *Ann. Rev. Nuclear Sci.*, **1**, 207–44 (1952)
5. Harrison, F. B., *Liquid Scintillation Counters and Their Application to the Measurement of the Negative μ-Meson Capture Probability in the Heavy Elements* (Doctoral thesis, Princeton University, Princeton, N. J., 1951)
6. Sangster, R. C., *Massachusetts Institute of Technology Technical Report No. 55* (1952)

7. Birks, J. B., and Little, W. A., *Proc. Phys. Soc.* (*London*), [A]**66,** 921 (1953)
8. Kallmann, H., New York University, *Progress Report No. 6,* Contract No. DA 36-039 SC-5487 (1952)
9. Bittman, L., Furst, M., and Kallmann, H., *Phys. Rev.*, **87,** 83 (1952)
10. Jackson, J. A., and Harrison, F. B., *Phys. Rev.*, **89,** 322 (1953)
11. Harrison, F. B., Scintillation Counter Symposium (Washington, D. C., 1954); *Nucleonics,* **12**(3), 24 (1954)
12. Kallmann, H., Scintillation Counter Symposium (Oak Ridge, Tenn., 1949); *Atomic Energy Commission Report AECU-583* (1949)
13. Bonanomi, J., and Rossel, J., *Physica,* **18,** 486 (1952)
14. Bonanomi, J., and Rossel, J., *Helvetica Phys. Acta,* **25,** 725 (1952)
15. Mitchell, A. C. G., and Zemansky, M. W., *Resonance Radiation and Excited Atoms* (The University Press, Cambridge, Mass., 338 pp., 1934)
16. Randall, J. T., and Wilkins, M. H. F., *Proc. Roy. Soc.* (*London*), [A]**184,** 347 (1945)
17. Garlick, G. F. J., *Luminescent Materials* (Oxford University Press, London, England, 254 pp., 1949)
18. Post, R. F., and Shiren, N. S., *Phys. Rev.*, **78,** 81 (1950)
19. Phillips, H. B., and Swank, R. K., *Rev. Sci. Instr.*, **24,** 611 (1953)
20. Liebson, S. H., Bishop, M. E., and Elliot, J. O., *Phys. Rev.*, **80,** 907 (1950)
21. Elliot, J. O., Liebson, S. H., Meyers, R. D., and Ravilious, C. F., *Rev. Sci. Instr.*, **21,** 631 (1950)
22. Lundby, A., *Phys. Rev.*, **81,** 324 (1951)
23. Pringsheim, P., *Fluorescence and Phosphorescence* (Interscience Publishers, New York, N. Y., 794 pp., 1949)
24. Koski, W. S., and Thomas, C. O., *J. Chem. Phys.*, **19,** 1286 (1951)
25. Elliot, J. O., Liebson, S. H., and Ravilious, C. F., *Phys. Rev.*, **79,** 393 (1950)
26. Bowen, E. J., and Mikiewicz, E., *Nature,* **159,** 706 (1947)
27. Bowen, E. J., and Lawley, P. D., *Nature,* **164,** 572 (1949)
28. Bowen, E. J., Mikiewicz, E., and Smith, F. W., *Proc. Phys. Soc.* (*London*), [A]**62,** 26 (1949)
29. Kallmann, H., and London, F., *Z. Physik,* [B]**2,** 207 (1929)
30. Frenkel, J., *Phys. Rev.*, **37,** 17, 1276 (1931)
31. Förster, T., *Ann. Physik,* **2,** 55 (1948)
32. Hopkins, J. I., *Rev. Sci. Instr.*, **22,** 29 (1951)
33. Taylor, C. J., Jentschke, W. K., Remley, M. E., Eby, F. S., and Kruger, P. G., *Phys. Rev.*, **84,** 1034 (1951)
34. Frey, H. B., Grim, W. M., Preston, W. M., and Gray, T. S., *Phys. Rev.*, **82,** 372 (1951)
35. Birks, J. B., *Proc. Phys. Soc.*, [A]**63,** 1294 (1950)
36. Birks, J. B., *Phys. Rev.*, **86,** 569 (1952)
37. Birks, J. B., *Phys. Rev.*, **84,** 364 (1951)
38. Wright, G. T., *Phys. Rev.*, **91,** 1282 (1953)
39. Reynolds, G. T., Harrison, F. B., and Salvani, G., *Phys. Rev.*, **78,** 488 (1950)
40. Kallmann, H., and Furst, M., *Phys. Rev.*, **79,** 857 (1950)
41. Kallmann, H., and Furst, M., *Phys. Rev.*, **81,** 853 (1951)
42. Furst, M., and Kallmann, H., *Phys. Rev.*, **85,** 816 (1952)
43. Hayes, F. N., Scintillation Counter Symposium (Washington, D. C., 1954); *Nucleonics,* **11**(3), 27 (1954)

44. Pringle, R. W., Black, L. D., Funt, B. L., and Sobering, S., *Phys. Rev.*, **92**, 1582 (1953)
45. Schorr, M., and Torney, F., *Phys. Rev.*, **80**, 474 (1950)
46. Koski, W. S., *Phys. Rev.*, **82**, 230 (1951)
47. Pichat, L., and Koechlin, Y., *J. chim. phys.*, **48**, 225 (1951)
48. Pichat, L., Pesteil, P., and Clement, J., *J. chim. phys.*, **50**, 26 (1953)
49. Buck, W. L., and Swank, R. K., *Nucleonics*, **11**(11), 48 (1953)
50. Swank, R. K., and Buck, W. L., *Phys. Rev.*, **91**, 927 (1953)
51. Fonda, G. R., and Seitz, F., *Preparation and Characteristics of Solid Luminescent Materials* (John Wiley & Sons, Inc., New York, N. Y., 459 pp., 1948)
52. Kröger, F., *Some Aspects of Luminescence in Solids* (Elsevier Publishing Co., New York, N. Y., 310 pp., 1948)
53. Leverenz, H. W., *An Introduction to Luminescence of Solids* (John Wiley & Sons, Inc., New York, N. Y., 569 pp., 1950)
54. Franck, J., and Teller, E., *J. Chem. Phys.*, **6**, 861 (1938)
55. Seitz, F., *J. Chem. Phys.*, **6**, 150 (1938)
56. Hofstadter, R., *Phys. Rev.*, **74**, 100 (1948)
57. Hofstadter, R., *Phys. Rev.*, **75**, 796 (1949)
58. Hofstadter, R., *Phys. Rev.*, **79** 389 (1950)
59. Harshaw, J. A., Kremers, H. C., Stewart, E. C., Warburton, E. K., and Hay, J. O., *Atomic Energy Commission Report No. NYO-1577* (1952)
60. Lovberg, R. H., *Phys. Rev.*, **84**, 852 (1951)
61. Eby, F. S., Jentschke, W. K., and De Pasquali, G., *Phys. Rev.*, **91**, 495 (1953)
62. Hofstadter, R., McIntyre, J. A., and West, H. I., *Phys. Rev.*, **82**, 749 (1951)
63. Schardt, A. W., and Bernstein, W., *Atomic Energy Commission Report BNL-1156* (1953)
64. Schenck, J., *Nature*, **171**, 518 (1953)
65. Schenck, J., and Neiler, J. H., Scintillation Counter Symposium (Washington, D. C., 1954); *Nucleonics*, **11**(3), 28 (1954)
66. Van Sciver, W., and Hofstadter, R., *Phys. Rev.*, **87**, 522 (1952)
67. Van Sciver, W., and Hofstadter, R., *Phys. Rev.*, **87**, 522 (1952)
68. Hahn, B., *Phys. Rev.*, **91**, 772 (1953)
69. Bube, R. H., *Phys. Rev.*, **78**, 349 (1950)
70. Kallmann, H., *Signal Corps Engineering Report No. E-1044* (Fort Monmouth, N. J., 1950)
71. Moon, R. J., *Phys. Rev.*, **73**, 1210 (1948)
72. Gillette, R. H., *Rev. Sci. Instr.*, **21**, 294 (1950)
73. MacIntyre, W. J., *Phys. Rev.*, **75**, 1439 (1949)
74. Reynolds, G. T., *Nucleonics*, **10**(7), 46 (1952)
75. Harrison, F. B., *Nucleonics*, **10**(6), 40 (1952)
76. Gugelot, P. C., *Atomic Energy Commission Report NYO-973* (1951)
77. Birks, J. B., and Szendrei, M. E., *Phys. Rev.*, **91**, 197 (1953)
78. Furst, M., Kallmann, H., and Kramer, B., *Phys. Rev.*, **89**, 416 (1953)

ČERENKOV COUNTERS[1]

By John Marshall

Institute for Nuclear Studies, University of Chicago, Chicago, Illinois

It was recognized early in the study of radioactivity that there are a number of substances which luminesce strongly under the influence of α-, β-, and γ-radiation. A much larger class of substances was known to luminesce only very feebly under radiation, and it was this feeble luminescence which Čerenkov undertook to investigate in 1934 (1). Čerenkov studied the visible light produced in water by an intense beam of γ-radiation. He was able to photograph this light and found a most unexpected angular distribution. The maximum intensity was in a cone of approximately 40° half angle from the direction of the γ-radiation producing the effect. Čerenkov found also that, when the water was replaced by benzene, the effect persisted, but the angle of the cone was larger by a few degrees.

The effect was not understood, although Čerenkov continued to study it to some extent, until 1937 (2) when Frank & Tamm (3) published a paper in which they explained it satisfactorily on the basis of classical electromagnetic theory. According to the analysis of Frank & Tamm the effect can be considered to be an electromagnetic shock wave produced when a charged particle traverses a dielectric medium at a speed greater than that of light in the medium. The spectrum extends over all frequencies for which the velocity of the electromagnetic radiation is less than that of the particle, with an intensity and angular distribution given by equations 1 and 2:

$$I = \frac{4\pi^2 e^2 Z^2}{hc^2}\Delta\nu\left(1 - \frac{1}{\beta^2 n^2}\right)$$

$$= \frac{2\pi Z^2 \Delta\nu}{137c}\sin^2\theta \qquad 1.$$

$$= \frac{2\pi Z^2}{137}\left(\frac{1}{\lambda_1} - \frac{1}{\lambda_2}\right)\sin^2\theta.$$

$$\cos\theta = \frac{1}{\beta n}. \qquad 2.$$

In equations 1 and 2: I = number of photons emitted per centimeter of path; $\Delta\nu$ = the frequency interval of the photons emitted; λ_1 and λ_2 are the limits of the interval of wave length considered; Z is the charge of the particle in units of the electronic charge; β is the ratio of the speed of the particle to that of light in vacuo; n is the index of refraction of the dielectric medium in the frequency interval considered; θ is the direction of the Čerenkov radiation measured from the direction of the charged particle; h = Planck's constant; c = velocity of light.

[1] The survey of literature pertaining to this review was concluded in April, 1954.

In 1938 Collins & Reiling (4) repeated Čerenkov's original experiment with a considerably improved technique. They used monoenergetic (2 Mev) electrons from an electrostatic accelerator and photographed the light produced when these electrons passed through thin layers of glass, cellophane, and mica. They found the angular distribution of the light to agree well with the predictions of the theory. In 1943 Wyckoff & Henderson (5), using an electron beam of variable energy studied the variations of the Čerenkov angle, θ, with velocity of the electrons and found complete agreement.

Since the Čerenkov radiation is a shock wave, it contains components of all frequencies for which the index of refraction is large enough to give a real value of θ in equation 2. In ordinary optical materials the radiation includes the visible spectrum with energy flux larger toward the violet end. It may be observed visually when, for example, a strong source of reasonably energetic β-radiation is immersed in water and has a bluish white appearance to the eye. It is a well-known phenomenon in water used either as a moderator or a shield around nuclear reactors (6).

Equation 2 is easy to derive by use of a Huygens construction (Fig. 1). The direction of the electromagnetic shock wave is quite analogous to the di-

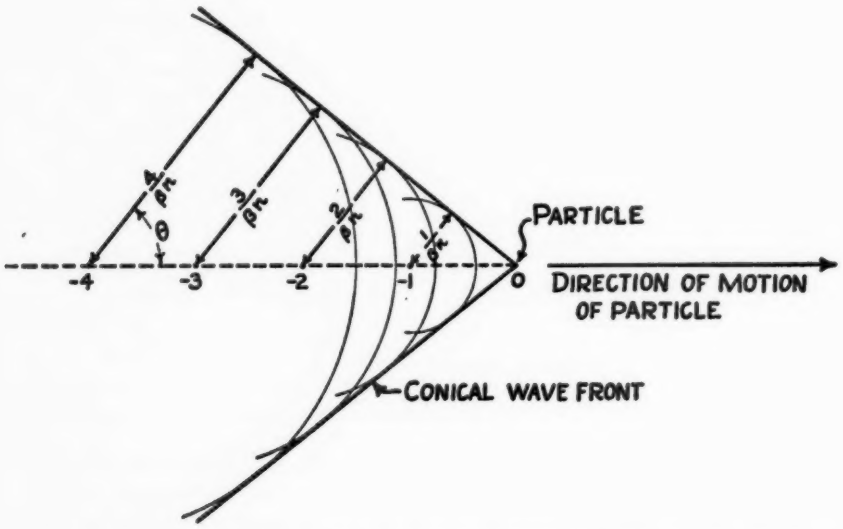

FIG. 1. Huygens construction of Čerenkov wave front. Charged particle moving in positive x direction at velocity $v=\beta c$. Time required for particle to move to 0 from -4 cm. $\tau=4/\beta c$. In time $\tau=4/\beta c$ light travels $r=(c/n)\,\tau=4/\beta n$ cm. Therefore wavelet starting when particle was at -4 cm. has radius $4/\beta n$ when particle reaches 0. Similarly wavelet starting when particle was at $-M$ cm. has radius $M/\beta n$ when particle reaches 0. Wavelets reinforce along conical wave front propagated in direction θ relative to moving particle. $\cos\theta=(M/\beta n)/M=1\beta/n$.

rection of the shock wave produced when a bullet travels through air at a speed greater than that of sound. The shock wave is conical, with its direction of propagation, of course, normal to the wave in the forward direction. The apex of the cone is coincident with the particle producing the disturbance. The half angle of the cone is θ in equation 2. If the particle moves at a speed smaller than that of light in the radiating medium it produces no Čerenkov light. If it is moving just above the speed of light in the medium, the direction of the radiation is almost straight forward. If the speed of the particle is increased, the angle θ also increases, reaching a limiting value for very relativistic particles given by the relation $\cos \theta = 1/n$.

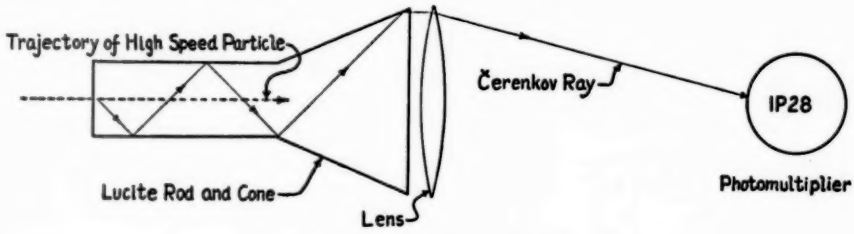

FIG. 2. Getting-Dicke focusing counter.

The Čerenkov radiation is polarized with the electric vector in the radial direction. In other words, the electric vector lies in the shock wave front and points toward or away from the particle responsible for the radiation.

The advent of the photomultiplier tube made it practical to use the Čerenkov radiation as a means of counting individual particles. The techniques of particle counting by the scintillation of luminescent materials were directly applicable, except for the facts that the intensity of the Čerenkov radiation was considerably smaller than that of the phosphors and that there was a doubt in the minds of the experimenters that the Čerenkov radiation could be distinguished from weak luminescence which might be found in almost any material.

Čerenkov counters fall into two main types: focusing and nonfocusing. Historically, the focusing type came first, although it is more complicated and probably less useful than the nonfocusing type. The reason for the development of the more complicated type first was that the experimenters were afraid that the weak Čerenkov radiation would be masked by ordinary fluorescence or phosphorescence. Also, they felt called upon to prove that what they were observing was Čerenkov radiation, and focusing counters are especially suitable for this purpose.

Dicke (7) is the first person to have built a Čerenkov counter. His counter (Fig. 2) was of the focusing type and had an uncomfortably small sensitive area and angular acceptance. At the time of his tests (1946) large accelerators producing beams of relativistic particles were not so readily available as today, and Dicke was forced to use a 20 Mev betatron as a source of radia-

tion. The conditions of the experiment were such that he was not completely certain that the counts he had obtained resulted from Čerenkov light. Slightly before Dicke's publication, Getting (8) published a proposal for a similar type of Čerenkov counter. Getting, however, reported no experimental work.

After Dicke & Getting, the development of Čerenkov counters lagged until 1950, when Jelley (9) reported at the Harwell Nuclear Physics Conference the success of a nonfocusing counter (Fig. 3). The success of Jelley's counter stimulated work by a number of other people and since then development has been rapid.

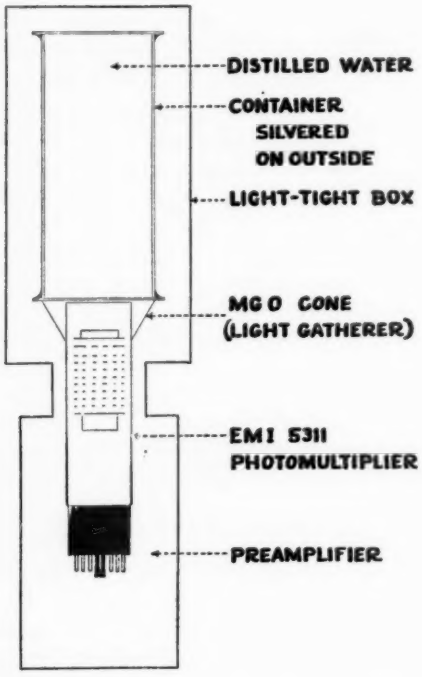

FIG. 3. Jelley's nonfocusing water Čerenkov counter. The first really successful Čerenkov counter. The MgO cone allows light to strike the photocathode from the back side. The black paint on the outside of the tube must be removed for this purpose.

NONFOCUSING COUNTERS

In principle, a nonfocusing Čerenkov counter consists simply of a container filled with a transparent substance, the photocathode of a multiplier tube being exposed to any light which is produced therein. The walls of the container should have as high a reflectivity as possible to prevent loss of light, and for the same reason the cathode of the multiplier should occupy as

large a proportion as possible of the walls of the container. It is necessary, of course, if the device is rightly to be called a Čerenkov counter, that the material forming the radiator should produce a negligible quantity of light by processes other than the Čerenkov radiation.

It is obvious that a counter of this type will be most successful if the photomultiplier cathode has a large area. As a matter of fact, the development of the nonfocusing Čerenkov counter followed closely after the development of the large-cathode end-on photomultipliers E.M.I. 5311 and R.C.A. 5819.

Jelley's original counter and the counters of a number of other workers make use of the directional properties of the Čerenkov radiation as an aid in light collection. The typical design is a relatively long radiator, the charged particle passing more or less lengthwise through it and the light being collected at the exit end. The walls are made reflecting either through the use of a specular metal coating or through total internal reflection. In many of the counters the entrance end of the radiator is blackened so that the radiation from a particle passing in the reverse direction through the tube is absorbed and does not lead to a count.

The exact design of the counter depends on the use to which it is to be put. The principal uses of the nonfocusing counter are explained in the following paragraphs.

Simply as a counter.—The particles, of course, must be fast enough so that they produce Čerenkov radiation in the radiator. Thus the counter is applicable to any particle that has a long enough range in the particular radiator used and a high enough velocity to produce a usable number of photons at the cathode of the multiplier. In general, a scintillation counter using a conventional phosphor is probably better for this unspecialized use than is a Čerenkov counter. A possible exception is the case where an exceptionally short pulse is required. The light pulse from a Čerenkov radiator is usually shorter than 10^{-9} sec. and is often much shorter than even this. Thus a Čerenkov counter may be called for when exceptionally short time resolution is required (10).

As a threshold counter.—Čerenkov counters may be used by suitable choice of radiator material as velocity threshold counters. For instance, a counter with a Lucite radiator ($n = 1.50$) has been used to respond to protons of greater than 325 Mev energy ($\beta = .67$) while being insensitive to slower particles (11). Similarly, a counter employing a water radiator has been used to count high-energy electrons in the presence of large quantities of neutrons of up to 450 Mev energy (12, 13, 14). In Figures 3 and 4 there are shown designs of two nonfocusing counters. Quite satisfactory pulse heights are available from these counters because of the efficient light collection and long particle path in the radiator. Such counters are readily applicable only to rather high-energy particles (more than about 10 Mev for electrons) because of the rather long range at high velocity required to produce a reasonable number of photons.

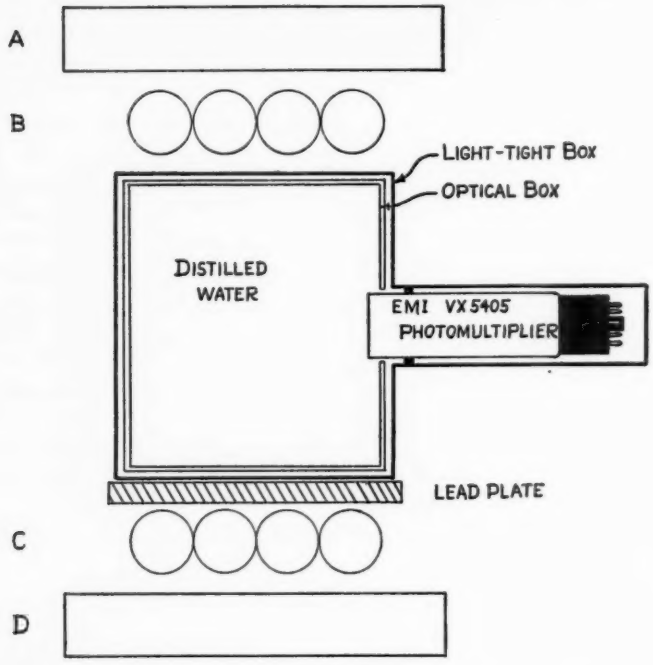

FIG. 4. Čerenkov counter used by Duerden & Hyams for distinguishing protons from μ-mesons by pulse height. *A*, *B*, *C*, *D* are counter trays in quadruple coincidence. Optical box is 24 cm. cube. Walls of optical box are made by constructing a water tight sandwich of 1 mm. plexiglass sheet cemented together around the edge with 1 mm. plexiglass spacers. Occasional pillars are put in the middle to prevent collapse. The walls are then filled with MgO of highest chemical purity. A water tight seal is provided around the end of the photomultiplier tube. Three cm. Pb plate below Čerenkov counter prevents μ-decay electrons from reaching counter trays *C* and *D*.

With pulse height analyzer for identification of particles.—A singly charged particle of a given velocity produces, according to equation 1, a well-defined intensity of Čerenkov radiation in a given radiator. If some other property such as the energy or momentum can be measured in addition to the Čerenkov intensity, it is possible under certain conditions to identify the particle. This has been done by Duerden & Hyams (15). Using the counter, as shown in Figure 4, they connected the output of their counter through a pulse height discriminator onto an anticoincidence circuit so that it rejected particles passing through their apparatus which produced Čerenkov pulses larger than one tenth that of the average relativistic particle. When this condition was taken in conjunction with a minimum range requirement, they were able to pick out protons of a certain energy range and to record them in a cloud chamber.

While Duerden & Hyams' counter was used essentially as a velocity selector, Winckler & Anderson (16, 17) have shown that it is possible to use a Čerenkov counter for the identification of particles of atomic number different from 1. Since equation 1 shows that the intensity for a given velocity varies as Z^2, one would expect that relativistic He nuclei would produce intensities four times as large as relativistic protons or mesons, and that relativistic Li nuclei would produce nine times as much light. In Figure 5 there is

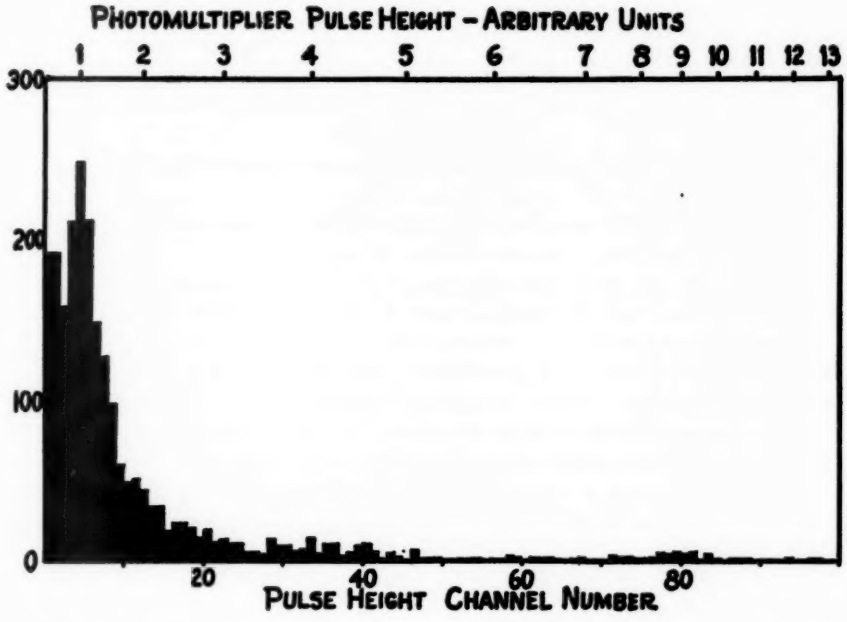

FIG. 5. Pulse height distribution obtained at top of atmosphere by Winckler & Anderson with nonfocusing Čerenkov counter. Small peaks are visible at four and nine times the proton pulse height corresponding to relativistic He and Li nuclei.

reproduced their pulse height analysis curve obtained from a balloon flight at high altitude. Peaks are observable both from relativistic He nuclei and Li nuclei.

Lindenbaum & Pevsner (26) have recently reported a nonfocusing counter of a transmission type. Here a relatively thin cell of the material to be used for a Čerenkov radiator is enclosed with a specularly reflecting envelope and is viewed from the two sides by photomultiplier tubes. The advantage of this type of counter is that the particle passes through a definite thickness of counter and can be used afterward. The normal end-on type of nonfocusing counter is geometrically of a rather poor shape for this use and is best applied at the last element in an experimental array.

Intensity

In the operation of an actual counter the intensity that must be considered is not, for instance, the number of photons emitted in the visible, but rather the number of electrons that the photons can liberate from the cathode of a photomultiplier tube or other light-sensitive device. One must then consider the photoefficiency of the cathode, its response to light of various frequencies, and the spectral distribution of the Čerenkov light. In addition one must consider the optical collection efficiency of the photocathode.

Taking the last consideration first, it is possible with a tube having its photocathode deposited on the inside of the glass envelope in a semitransparent layer to achieve very high collection efficiencies. The Čerenkov light is emitted by a relativistic particle at an angle such that the angle of incidence with the wall of the cylindrical radiator cannot be smaller than the critical value for total-internal reflection. It can be shown, in fact, that always more than half of the light strikes the walls so as to be totally reflected. Under reasonably favorable conditions, almost 100 per cent of the light reaches the collection end of the radiator. If the photocathode is deposited on the envelope of the multiplier tube it may be put in optical contact with the radiator by the use of transparent optical cement, liquid, or grease. Finally, if the sensitive area of the photocathode is as large as or larger than the cross section of the radiator, practically every photon that is formed reaches the cathode and has a chance to produce a photoelectron.

The spectral distribution of the Čerenkov light, if plotted in the usual way as power radiated per unit wave length, is strongly shifted towards the violet. If it is plotted as number of photons per unit frequency interval, it is uniform at all frequencies so long as the index of refraction can be considered to be constant.

In Figure 6 are plotted photon yield curves of several photomultipliers as a function of frequency. It will be seen that although there is considerable difference between the sensitivity curves of the bare photomultipliers, this difference disappears to some extent when the light is filtered through two inches of Lucite. For practical purposes one can say that, for the computation of Čerenkov pulse heights, one can consider the sensitivity of each of the multiplier cathodes plotted to be constant at its maximum value over a frequency range of about 2.9×10^{14} c.p.s. This is just about the frequency range of the visible spectrum, so, for a rough idea of the number of photoelectrons produced, one can simply compute the number of photons in the visible region which strike the cathode and multiply this number by .06, or whatever the maximum yield of electrons per photon is for the particular multiplier in question.

For example, the yield of photons in Lucite ($n=1.50$) traversed by a relativistic particle of one electronic charge is:

$$\frac{2\pi\Delta\nu}{137\times3\times10^{10}}\left(1-\frac{1}{1.5^2}\right)=\frac{2\pi\times2.9\times10^{14}\times.5555}{137\times3\times10^{10}}=246 \text{ photons/cm.}$$

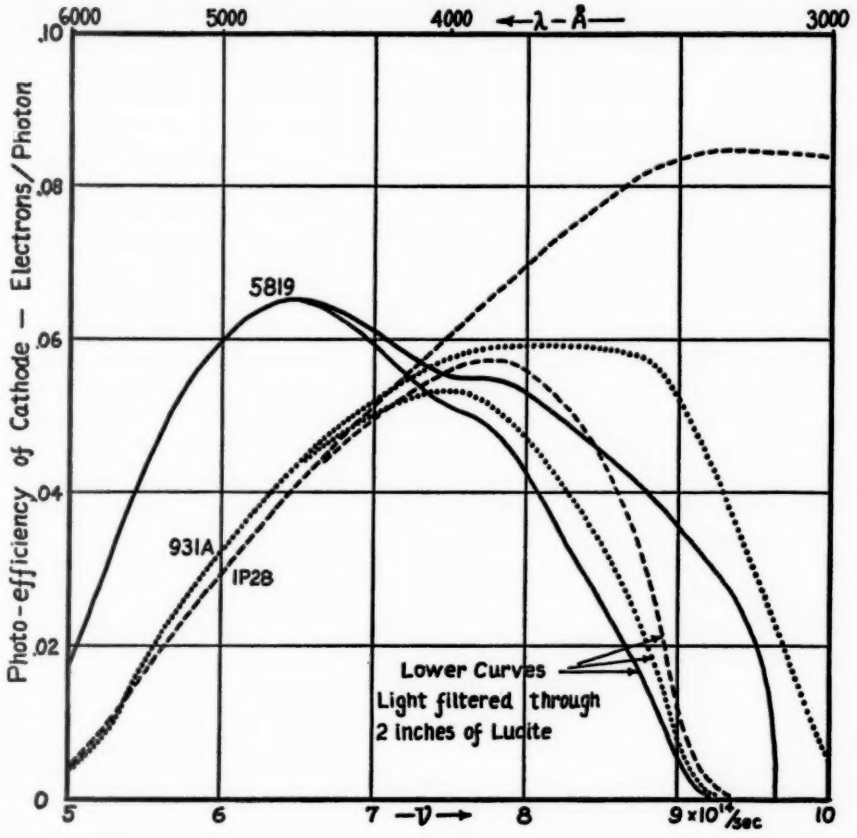

FIG. 6. Cathode efficiency curves for photomultipliers. These curves are computed from data published by the manufacturer. Upper curves represent number of electrons emitted by the photocathode of each tube type for one photon of the indicated frequency incident on its sensitive region. Lower curves are the same thing for light that has been passed through two inches of Lucite. Assumed no light loss from reflection at surfaces of Lucite.

If this is multiplied by .06, one obtains about 15 electrons produced at the photocathode per centimeter traversed by the relativistic particle. The assumption is made that all photons produced strike the photocathode. It is obvious that with photon collection efficiencies often considerably less than unity, one must use fairly thick radiators in order to achieve pulses of enough electrons so that pulse heights can be measured with reasonable statistics.

One difficulty with the use of thick radiators is that the particle being counted may undergo a nuclear collision in passing through and thereby change its velocity and perhaps produce secondary particles so that the

pulse height recorded will be different from what was expected. The resultant pulse may be either larger or smaller than it would have been with no collision. Thick radiators are quite satisfactory in studying cosmic-ray μ-mesons since they undergo essentially no nuclear collisions at all. This difference can be seen in the work of Winckler & Anderson (16, 17) who get quite a sharp pulse height resolution curve from μ-mesons at sea level although a curve taken with the same apparatus at balloon altitudes is very broad, a good number of the particles being protons, or π-mesons.

Another use of thick radiators is in the detection of high-energy γ-rays and the measurement of their energies by collection of all Čerenkov light from an entire electron shower. This type of work has been undertaken by several workers (18), but the only publication on the subject known to the author is that of Kantz & Hofstadter (19). They have investigated experimentally the distribution of energy in a shower produced by a high-energy electron or photon in materials of a variety of radiation lengths. They report work of Fregeau & Hofstadter who obtained pulse height distributions having a full width at half maximum of 30 to 40 per cent of the mean pulse height using a single crystal of thallium chloride which has a density of 7 gm./cm.^{3} as a converter and radiator. The crystal was 3.5 in. in diameter and 5 in. long and was exposed presumably to electrons of various energies from the Stanford linear accelerator, although this is not clear from the publication. The method shows promise, although it suffers from competition with large crystals of NaI(Tl) scintillator.

Gas Čerenkov Counters

Čerenkov radiation can be produced in gases just as in other materials, provided that the particle producing the radiation has a high enough velocity that the product βn is larger than unity. The difficulties of using counters with gas radiators are easily seen when one computes the intensity. For index of refraction n, just greater than one, the intensity is given approximately by the following formula: $I = 900\ (\beta n - 1)$ photons in the visible/(cm. of path). In the case of air at one atmosphere the index of refraction is 1.0003 so that $n - 1 = 3 \times 10^{-4}$. The intensity then is: $I = 900 \times 3 \times 10^{-4} = 27 \times 10^{-2} = 0.27$ photons/cm. for a completely relativistic particle of one electronic charge. For any Čerenkov radiation to be given off at all, the speed of the particle must be at least .9997 c. This implies a particle energy of more than 40 times the rest mass, and to obtain a reasonable intensity of Čerenkov radiation the particle should have even more energy. A particle with energy 60 times its rest mass has β equal to $1 - 1.4 \times 10^{-4}$ so that βn is $1 + 1.6 \times 10^{-4}$ and $I = 1.6 \times 10^{-4} \times 900 = .14$ photons per cm.

The Čerenkov radiation produced in a material with index of refraction as small as this has a direction almost parallel with the particle producing the radiation. Approximately the angle in radians is $\sqrt{2(\beta n - 1)}$. So in air a completely relativistic particle gives an angle of about 0.25 radian or 1.4°.

A device using the Čerenkov radiation in a gas has been constructed by Tollestrup & Wentzel (20), who use a one meter long brass tube filled with He as a radiator to detect high-energy electrons produced by the *bremsstrahlung* from a synchrotron. The device has a threshold of 20 Mev when filled with air and of 60 Mev when filled with He, both at standard temperature and pressure. The light is led to a photomultiplier tube by reflection on a first surface mirror mounted at 45° to the beam. The photomultiplier is one meter to the side and is shielded with Pb against the effects of radiation directly on it. Reversing the direction of the radiation reduces the intensity by a factor 100. This shows that the effect results from Čerenkov radiation and that very little of the light that reaches the multiplier is attributable to ionization luminescence. The device is easily gated by the use of a rectangular pulse on one of the dynodes of the multiplier. This monitoring device of Tolerstrup & Wentzel can hardly be called a counter. On the average, if the light collection is efficient, the pulses produced at the photomultiplier can hardly be of more than one electron from the cathode. They measure actually the d.c. current and discriminate against dark current by gating on only during the synchrotron pulse.

Galbraith & Jelley (21) have performed an interesting experiment where they have detected the Čerenkov light produced by large cosmic-ray showers in the air of the atmosphere. Obviously their equipment will work only at night. They used an end window photomultiplier at the focus of a 10 in. paraboloid mirror with an acceptance cone for light within 12° of the zenith. They surrounded the light detector with an array of sixteen 200 cm^2 Geiger-Mueller (hereafter G-M) tubes arranged in a 180 m. square array and used large pulses from the photomultiplier to trigger the sweep of an oscilloscope which displayed G-M pulses. Out of 50 such sweeps they found 18 where at least one G-M tube went off simultaneously. The inference is that the large large light pulses from the night sky are largely attributable to extensive cosmic-ray showers. The experiment was tried on a cloudy night with a heavy cloud layer at somewhere between 4000 and 9000 ft. The frequency of large pulses was reduced by about a factor two, which, together with the pulse height distribution they found, indicates that of the order of one-half of the light from such a shower came from above this altitude.

Ascoli Balzanelli & Ascoli (22) have performed an experiment in which they demonstrated that some cosmic rays could be counted by the light produced when they passed through about one meter of air. The light was collected by a specularly reflecting cone onto the cathode of an E.M.I. 6260 photomultiplier and counts were taken in coincidence with a Geiger counter telescope. They found about a 30 per cent reduction in counting rate when an opaque screen was introduced so that light could not reach the photocathode. Probably a large part of their background was attributable to cosmic rays passing through the multiplier tube where Čerenkov radiation may have been produced in the glass of the envelope or where there may have been a few secondary electrons produced directly in the multiplier structure.

Focusing Counters

A focusing Čerenkov counter is defined for the purpose of this discussion as one in which the light of one particular Čerenkov angle is focused through a diaphragm of some sort so it can be directed onto a photomultiplier cathode while light of other angles is directed elsewhere. Such a counter is capable, then, of recording particles of a narrow band of velocities and of rejecting particles of other velocities.

In all the focusing counters known to the writer, the focusing part of the counter consists essentially of a cylindrically symmetrical assembly of optical parts designed to focus light from a parallel beam of particles of one velocity onto the cathode of a photomultiplier. In some of the counters the light is split before the final focus into two or more converging beams by the use of plane mirrors. These two or more beams are brought to two or more photomultiplier cathodes, the outputs of the multipliers being connected in coincidence.

It can be shown (23) that it is impossible to focus all of the light generated by a bundle of parallel particles to a sharp point. The argument hinges on the conservation of angular momentum of photons in a cylindrically symmetrical system, the angular momentum being taken around the cylindrical axis. Skew rays of light coming from particles parallel to but not on the axis do not pass through the axis and can never be made to do so by a cylindrically symmetric system. This angular momentum limitation is a serious one in that the diameter of the image circle in practical cases is somewhat larger than the diameter of the bundle of particles. The angular momentum limitation is not necessarily a limitation on the velocity resolution obtainable. Even though it is impossible to focus to a point on the axis, it can be possible under certain conditions to focus to a sharp ring around the axis, and to pass the light through an annular slit to obtain velocity resolution.

The Getting-Dicke Focusing Counter (7, 8)

This is the earliest type of focusing counter and incidentally the first Čerenkov counter of any type. It has since been used by other workers (10) and is applicable to cases where it is possible to collimate the incident particles into a very narrow beam. It suffers, in its usual form, from a least image size many times larger than the bundle of incident particles. This is attributable to the fact that the angle of convergence of light to the focus is small compared to the Čerenkov angle so that, to conserve angular momentum of photons around the axis, the light must pass much farther from the axis at the focus than the distance at which it was produced.

Dicke reported what must now be considered to have been successful operation of a Čerenkov counter of this general type (see Fig. 2) with radiation from a 20 Mev betatron. His publication indicated that he was not completely sure that he had observed Čerenkov light.

A counter of the same general type has been reported by Birge (24) and one has been used by Bay (10) to produce very short pulses for testing a co-

incidence circuit. In most cases, with this type of counter a Pb collimator has been used to limit the incident particles to a very small region around the axis.

Focusing Counters Employing Cylindrical Mirror

The writer (23, 25) has reported the construction of several focusing counters which use a cylindrical mirror to return the divergent Čerenkov light to the axis where it can be focused on a photomultiplier cathode. These counters suffer to some extent from the same defocusing because of skew rays which limit the useful aperture of the Getting-Dicke counter. However, since the convergent angle to the focus is equal to the divergent angle of the Čerenkov radiation, the defocusing is only by a factor equal to the index of refraction of the radiator. Thus the image of a radiator one centimeter in diameter is 1.5 cm. in diameter if the radiator is of Lucite with index 1.5.

In the focusing counters constructed by the writer, (See Figures 7, 8),

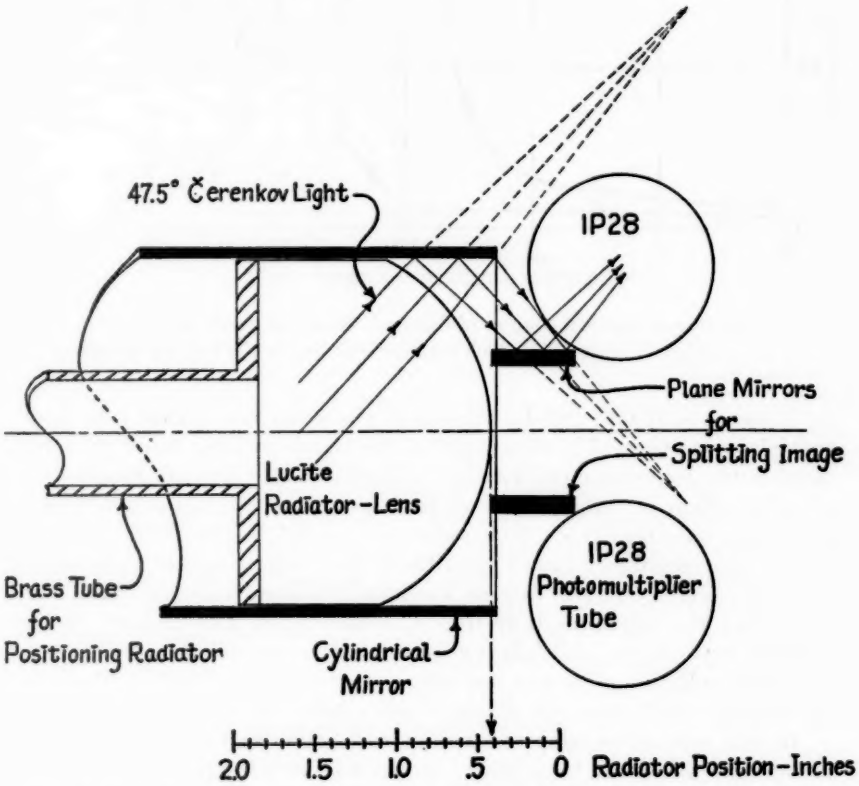

Fig. 7. Focusing counter with small sensitive area used by Marshall for analysis of meson beams. Radiator in this counter is integral with the lens.

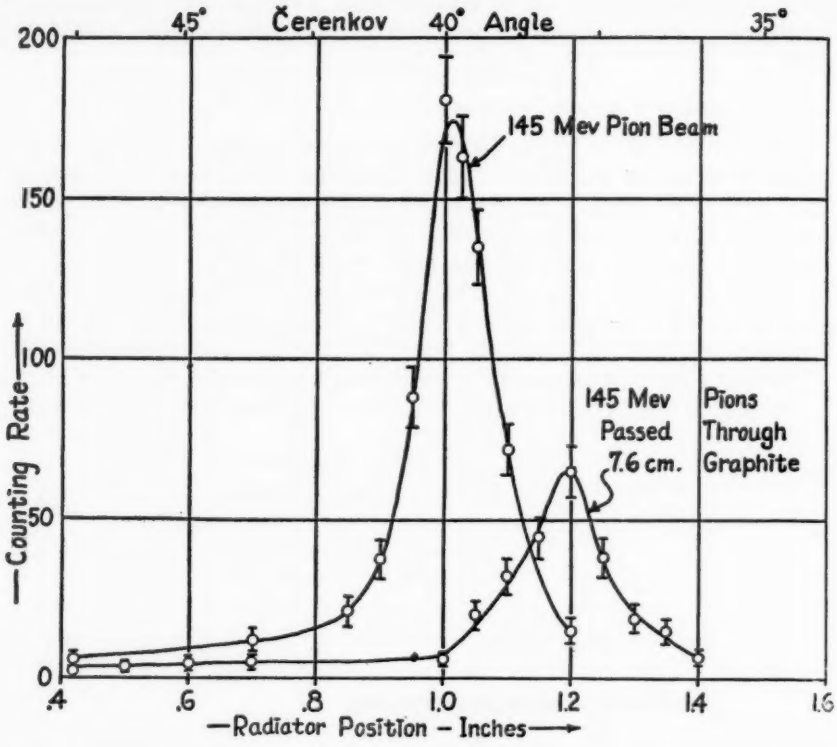

FIG. 8. Velocity resolution of counter of Figure 7. Radiator position scale corresponds to inch scale of Figure 7, in which counter is shown in the 0.42-in. position.

the image is split into two by the use of plane mirrors so that two photomultipliers can be used in coincidence. Coincidence techniques are extremely useful in the application of Čerenkov counters; in fact they are almost indispensable except in the case of very large pulses such as are available with good light collection from thick radiators exposed to relativistic particles. Coincidence techniques make it possible to discriminate against noise pulses, which particularly in the case of Čerenkov counters may occasionally be larger than the pulses resulting from Čerenkov light. The coincidence may be either between two multipliers exposed to the same radiator, or between a Čerenkov radiation pulse and one from a separate counter which may be of the Čerenkov radiation type or which may employ an ordinary phosphor.

In this type of focusing counter, as well as in the Getting-Dicke type, background pulses can be produced by particles striking parts of the optical system not normally intended to serve as radiator.

These background pulses smear out the resolution of the counter to particles of varying velocity. This type of background can be eliminated by split-

ting the optical system just at the place where the light leaves the radiator and enters the focusing device. An arrangement for this purpose is shown in Figure 9.

With a focusing counter of this type it is possible to analyze a beam of particles to find what speeds it includes. This is possible because the angle of the focused light can be varied between reasonable limits by varying the position of the photomultipliers relative to the lens. The sensitive area is rather small which tends to make the counter unsuitable for general experimental use, but the general design has been used by Mather & Martinelli (27) to detect electrons produced by the decay γ-rays from π^0 mesons and thereby to measure the production cross section of the mesons.

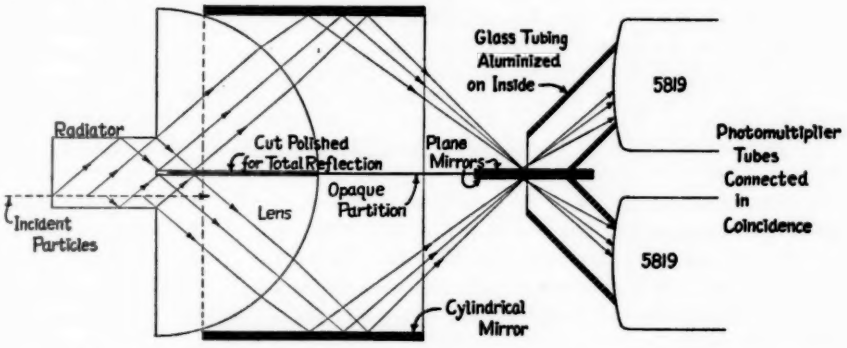

FIG. 9. Split lens focusing counter. Optical system divided beyond end of radiator to reduce background from Čerenkov radiation in the lens.

Bassi (28) proposed a counter which seems to involve some of the principles of a focusing counter, but the author knows of no publications describing the use of the counter. Instead, he and co-workers (29, 30) have used nonfocusing counters in a series of experiments of rather exploratory nature. They report the observations of an anomalous increase of Čerenkov radiation intensity for very relativistic particles (this might be a result of knock-on electrons). Bassi *et al.* also report a phosphorescence in water and Lucite which, in the opinion of the author, was attributable to light reflected from the opposite end of a radiator blackened by placing a black cavity outside the surface. This method of blackening is reduced in efficiency by internal reflection which, in some cases, can even be total. Efficient blackening can be achieved with black paint applied directly to the outer surface of the radiator. In this case the blackening is in optical contact with the surface, and internal reflection becomes important only with an unfortunate combination of indices of refraction.

Space limitations have prevented the inclusion in this chapter of details of many interesting experiments and devices. The bibliography covers every published Čerenkov counter known to the author. In the majority of cases

where two or more articles have been published on the same subject by the same author, the most complete alone has been included. A short review article on the subject has been published by Jelley (32).

LITERATURE CITED

1. Čerenkov, P. A., *Compt. rend. acad. sci. U.R.S.S.*, **2**, 451 (1934)
2. Čerenkov, P. A., *Phys. Rev.*, **52**, 378 (1937)
3. Frank, I., and Tamm, I., *Compt. rend. acad. sci. U.R.S.S.*, **14**, 109 (1937)
4. Collins, G. B., and Reiling, V. G., *Phys. Rev.*, **54**, 499 (1938)
5. Wyckoff, H. O., and Henderson, J. E., *Phys. Rev.*, **64**, 1 (1938)
6. Skarsvåg, K., and Lundby, A., *Joint Establishment for Nuclear Energy Research Report No. 22* (1953) (Kjeller, Lillestrøm, Norway)
7. Dicke, R. H., *Phys. Rev.*, **71**, 737 (1947)
8. Getting, I. A., *Phys. Rev.*, **71**, 123 (1947)
9. Jelley, J. V., *Proc. Phys. Soc.* (*London*), [A]**64**, 82 (1951)
10. Bay, Z., Cleland, M. R., and McLernon, F., *Phys. Rev.*, **87**, 901 (1952)
11. Nedzel, V. A., *Phys. Rev.*, **94**, 174 (1954)
12. Marshall, J., Marshall, L., Nedzel, V. A., and Warshaw, S. D., *Phys. Rev.*, **88**, 632 (1952)
13. Hildebrand, R. H., *Phys. Rev.*, **89**, 1090 (1953)
14. Hildebrand, R. H., *Rev. Sci. Instr.*, **24**, 463 (1953)
15. Duerden, T., and Hyams, B. D., *Phil. Mag.*, [7]**43**, 717 (1952)
16. Winckler, J. R., and Anderson, K., *Rev. Sci. Instr.*, **23**, 765 (1952)
17. Winckler, J. R., and Anderson, K., *Phys. Rev.*, **93**, 596 (1954)
18. Yuan, L. C. L. (Private communication, December, 1953)
19. Kantz, A., and Hofstadter, R., *Nucleonics*, **12**, 36 (1954)
20. Tollestrup, A. V., and Wentzel, W. A., *Phys. Rev.*, **93**, 950 (1954)
21. Galbraith, W., and Jelley, J. V., *Nature*, **171**, 349 (1953)
22. Ascoli Balzanelli, A., and Ascoli, R., *Nuovo cimento*, **10**, 1345 (1953)
23. Marshall, J., *Phys. Rev.*, **86**, 685 (1952)
24. Birge, R. W., *Phys. Rev.*, **85**, 766a (1952)
25. Marshall, J., *Phys. Rev.*, **81**, 275 (1951)
26. Lindenbaum, S. J., and Pevsner, A., *Rev. Sci. Instr.*, **25**, 285 (1954)
27. Mather, J. W., and Martinelli, E. A., *Phys. Rev.*, **92**, 780 (1953)
28. Bassi, P., *Nuovo cimento*, **8**, 807 (1951)
29. Bassi, P., Bianchi, A. M., and Manduchi, C., *Nuovo cimento*, **9**, 861 (1952)
30. Bassi, P., and Bianchi, A. M., *Nuovo cimento*, **9**, 1087 (1952)
31. Hofstadter, R., Fechter, H. R., and McIntyre, J. A., *Phys. Rev.*, **92**, 978–97 (1953)
32. Jelley, J. V., *Atomics*, **4**, 81 (1953)

ALPHA RADIOACTIVITY[1]

By I. Perlman and Frank Asaro

Radiation Laboratory and Department of Chemistry, University of California, Berkeley, California

Introduction

A comparison of the number of α-emitters known at present with those known a few years ago serves as a rough index of the comparative research activity on α-radioactivity and associated problems. By 1944 just 26 α-emitters had been definitely identified and reported, and of these all but one were members of the natural radioactive families. (Some others were found during the war years but publication was delayed.) In 1948 the total number of α-emitters had climbed to nearly 90, and at the end of 1953 there were more than 160 known. The increase in numbers of α-emitters has been accompanied by diversification of the information attainable by the treatment of α-decay data as well as a better insight into those features of α-radioactivity already recognized. It is perhaps worth recalling, however, that the basic α-decay theory (1, 2) was developed in the "days of the natural radioactivities" and precise absolute α-energies were determined during this period (3).

The huge increase in numbers of α-emitters is a result of several stimuli. The wartime military efforts in atomic energy were directly concerned with several new α-emitters, and as a result of their preparation a number of others appeared as by-products. This work stimulated the desire to know the nuclear properties of other isotopes of these elements and developed into a search for higher transuranium elements as well. It is interesting to note that at present there are as many elements known above U as there are between U and Bi. Another important source of α-emitters came with the construction of particle accelerators operating in a new high-energy range. With the use of such instruments (particularly the Berkeley 184-inch cyclotron), exploration into the region of neutron deficient isotopes became possible and resulted in the discovery of a wide range of new α-emitters including a group among the rare earth elements.

This review will be confined in large measure to the development of a few topics which have stemmed from the investigations of the past several years. The classical work on α-radioactivity will not be covered, and no special treatment will be given to the natural α-emitters.

A few brief statements outlining these newer developments are given in the following:

(*a*) Regularities in α-decay energy.—It is possible to correlate decay energies on a semi-empirical basis, and the observed regularities make it possible to predict rather closely the decay energies of unknown species.

[1] The survey of the literature pertaining to this review was concluded in April, 1954.

(*b*) Regularities of decay lifetimes.—It is now known that one-body α-decay theory, not far different in form from that originally proposed, is capable of yielding precise lifetime values for most even-even nuclei but not for other types. Lifetimes can be predicted on a semi-empirical basis for almost all cases.

(*c*) New developments in α-decay theory.—The results to be cited on odd nucleon types and on the complex spectra of all types serve to delimit the applicability of present α-decay theory and to define the problems which must be solved by a more comprehensive theory. Some attempts to build upon the classical theory will be mentioned.

(*d*) Spectroscopic states deduced from alpha decay.—Almost all α-emitters show complex spectra when examined with instruments of high resolution. The mapping of nuclear spectroscopic states populated in the α-decay process has yielded substantial information on the general picture of energy levels in the heavy element region.

Unfortunately, it will not be possible in this review to discuss the important advances in detection and energy determination of α-particles. Also omitted are the means for producing the many α-emitters and any individual discussion of many of the interesting new species.

Alpha Decay Energy

Somewhat beyond the middle of the periodic system α-emission becomes energetically possible for all nuclides along the band of β-stability. Alpha decay lifetimes are, however, strongly dependent upon α-decay energies, and only when the decay energy exceeds a certain value do the lifetimes decrease into the range where radioactivity can be detected. Since the potential barrier against α-decay increases with atomic number, the "critical" α-decay energy increases with atomic number. As a rough gauge of this effect we may say that the energy required for a half life of 10^{12} years is 2 Mev in the region of Sm (atomic number 62) and 4 Mev in the region of U (atomic number 92). The energy dependence in the heavy element region is such that doubling the energy (4 Mev to 8 Mev) decreases the half life by a factor of more than 10^{20}.

The general energy trends along the line of maximum β-stability are indicated in Figure 1 which is similar to a drawing published by Kohman (4). The curve was constructed by making use of available mass data in the region in which α-emission is not discernible. Aside from the smooth curve showing α-decay energies, three other lines are shown. One of these simply shows the line of demarcation between stability and instability toward α-emission, and the other two show the approximate positions at which half lives would be 10^{8} years and 10^{-4} years ($\sim$1 hr.). As mentioned, the smooth curve goes through the center of β-stability for each mass number. If we also consider neutron deficient isotopes of each element, it will be found that their α-decay energies are greater, a point which will be considered in more detail presently. Two such series of isotopes (for Gd and U) are indicated by points and segments of curves crossing the main curve. The position of shell

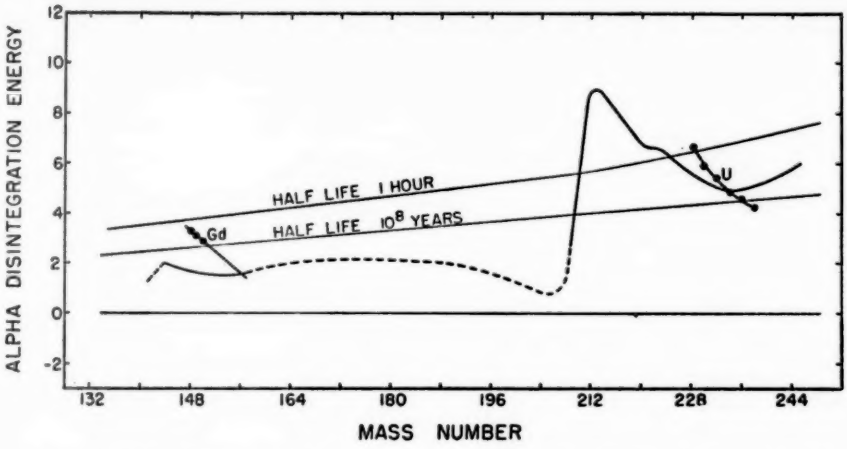

FIG. 1. Alpha decay energy profile. Broken line portion of curve indicates region where direct α-decay measurements are absent. Plotted points on segments of crossing curves pertain to known α-emitters of Gd and U. Half life guide lines indicate positions of applicable lifetimes as a function of mass number.

closures at 82 protons and 126 neutrons is readily seen through its influence on α-decay energy.

The mass data available are not nearly accurate enough to define the curve of Figure 1 with the precision required to be useful as a guide for α-decay properties. Uncertainties of several Mev are present in most of the data while a fraction of a Mev is sufficient to change a lifetime from the region of easy observation to that of extremely long periods. The curve is consistent with known α-decay properties and can be altered in detail as more precise data become available.

Summary of alpha energies.—A compilation of all α-energies in the heavy element region is given in Table I.[2] The data shown for each α-emitter represent what is considered to be the most reliable set. In general, only those α-groups actually measured are included, although from γ-ray and conversion electron data there may be evidence for other α-groups. In a few cases α-γ coincidence measurements showed the presence of a new α-group in coincidence with a specific γ-ray, but the α-energy could be better defined from that of the γ-ray. Where the interpretation was unambiguous such

[2] Most of the references for data shown here and in Figure 2 will be found in the 1953 Table of Isotopes (reference 25). For newer data consult the following: Po^{206} (5), Em^{211} (6), Em^{218} (7), Em^{220} (8), Ra^{222} (7), Ra^{224} (9), Th^{226} (7), Th^{228} (9), Th^{230} (10, 113), Th^{232} (11), Pa^{231} (114), U^{230} (7), U^{232} (8), U^{234} (12), U^{238} (11), Pu^{234} (115), Pu^{238} (13), Pu^{240} (8), Pu^{241} (8), Pu^{242} (8), Am^{241} (14), Am^{243} (14), Cm^{245} (116), Cm^{243} (8, 15), Cm^{241} (16), Bk^{249} (17), Cf^{246} (18), Cf^{248} (19), Cf^{249} (17, 19, 20), Cf^{250} (17, 19, 20), Cf^{252} (17, 19, 20), 99^{247} (21), 99^{253} (19, 20, 22, 23), 100^{254} (19, 22, 23, 24) and 100^{255} (19).

TABLE I

ALPHA PARTICLE ENERGIES AND ABUNDANCES

Alpha emitter	Alpha particle energy (Mev)	Relative abundances (%)	Type of measurement
$Bi^{<198}$ (1.7 m.)	6.2		ion ch
Bi^{198}	5.83		ion ch
Bi^{199}	5.47		ion ch
Bi^{201}	5.15		ion ch
Bi^{203}	4.85		range
Bi^{209}	~3.15		range
Bi^{210} (~10^6 y)	4.93		ion ch
Bi^{211}	6.272	16	spect
	6.618	84	spect
Bi^{212}	5.481	0.016	spect
	5.603	1.1	spect
	5.622	0.15	spect
	5.765	1.7	spect
	6.047	69.9	spect
	6.086	27.2	spect
Bi^{213}	5.86		ion ch
Bi^{214}	5.444	55	spect
	5.505	45	spect
Po^{200}	5.84		ion ch
Po^{201}	5.70		ion ch
Po^{202}	5.59		ion ch
Po^{204}	5.37		ion ch
Po^{205}	5.2		ion ch
Po^{206}	5.064	4	spect
	5.218	96	spect
Po^{207}	5.10		ion ch
Po^{208}	5.108		spect
Po^{209}	4.877		spect
Po^{210}	4.5	weak	α-γ coinc.
	5.299	100	spect
Po^{211} (0.52 s)	6.56	0.53	spect
	6.88	0.50	spect
	7.434	99	range
Po^{211}? (25 s)	7.14		ion ch
Po^{212}	8.776		spect
Po^{213}	8.336		ion ch
Po^{214}	7.680		spect
Po^{215}	7.365		range
Po^{216}	6.774		spect
Po^{217}	6.5		ion ch
Po^{218}	5.998		spect
$At^{<202}$	6.50		ion ch
$At^{<203}$	6.35		ion ch

TABLE I—*Continued*

Alpha emitter	Alpha particle energy (Mev)	Relative abundances (%)	Type of measurement
At^{203}	6.10		ion ch
At^{205}	5.90		ion ch
At^{207}	5.75		ion ch
At^{208} (1.7 h)	5.65		ion ch
At^{209}	5.65		ion ch
At^{210}	5.355	37	spect
	5.437	31	spect
	5.519	32	spect
At^{211}	5.862		spect
At^{213}	9.2		range
At^{214}	8.78		ion ch
At^{215}	8.00		ion ch
At^{216}	7.79		ion ch
At^{217}	7.02		ion ch
At^{218}	6.63		range
At^{219}	6.27		ion ch
Em^{208}	6.138		spect
Em^{209}	6.02		ion ch
Em^{210}	6.036		spect
Em^{211}	5.605	~1.5	spect
	5.778	67	spect
	5.847	33	spect
Em^{212}	6.262		spect
Em^{215}	8.6		ion ch
Em^{216}	8.01		ion ch
Em^{217}	7.74		ion ch
Em^{218}	6.53	weak	α-γ coinc
	7.127	100	spect
Em^{219}	6.214	4	spect
	6.434	12	spect
	6.559	15	spect
	6.824	69	spect
Em^{220}	5.747	~0.3	spect
	6.282	100	spect
Em^{222}	5.486		spect
Fr^{212}	6.339	24	spect
	6.387	39	spect
	6.409	37	spect
Fr^{217}	8.3		range
Fr^{218}	7.85		ion ch
Fr^{219}	7.30		ion ch
Fr^{220}	6.69		ion ch
Fr^{221}	6.05	~25	ion ch
	6.30	~75	ion ch
Ra^{213}	6.90		ion ch

TABLE I—*Continued*

Alpha emitter	Alpha particle energy (Mev)	Relative abundances (%)	Type of measurement
Ra^{219}	8.0		ion ch
Ra^{220}	7.43		ion ch
Ra^{221}	6.71		ion ch
Ra^{222}	6.23	weak	α-γ coinc
	6.554	100	spect
Ra^{223}	5.419	3	spect
	5.487	2	spect
	5.528	9	spect
	5.596	24	spect
	5.704	53	spect
	5.730	9	spect
	5.860	weak	spect
Ra^{224}	5.445	5.2	spect
	5.681	95	spect
Ra^{226}	4.592	5.7	spect
	4.777	94	spect
Ac^{221}	7.6		range
Ac^{222}	6.96		ion ch
Ac^{223}	6.64		ion ch
Ac^{224}	6.17		ion ch
Ac^{225}	5.80		ion ch
Ac^{227}	4.942		spect
Th^{223}	7.55		ion ch
Th^{224}	7.13		ion ch
Th^{225}	6.57		ion ch
Th^{226}	6.037	0.6	spect
	6.100	1.8	spect
	6.228	21	spect
	6.336	77	spect
Th^{227}	5.651	~2	spect
	5.704	15	spect
	5.728	~1	spect
	5.749	17	spect
	5.796	2	spect
	5.860	4	spect
	5.922	~2	spect
	5.952	13	spect
	5.972	21	spect
	6.001	5	spect
	6.030	19	spect
Th^{228}	5.173	0.2	spect
	5.208	0.4	spect
	5.338	28	spect
	5.421	71	spect

TABLE I—*Continued*

Alpha emitter	Alpha particle energy (Mev)	Relative abundances (%)	Type of measurement
Th^{229}	4.85	~70	ion ch
	4.94	~20	ion ch
	5.02	~10	ion ch
Th^{230}	4.437	0.07	spect
	4.471	0.2	spect
	4.613	23.4	spect
	4.682	76.3	spect
Th^{232}	(3.93)	24	γ energy
	3.994	76	ion ch
Pa^{226}	6.81		ion ch
Pa^{227}	6.46		ion ch
Pa^{228}	5.85	25	ion ch
	6.09	75	ion ch
Pa^{229}	5.69		ion ch
Pa^{231}	4.660	1–3	spect
	4.720	11	spect
	4.838	3	spect
	4.938	25	spect
	4.998	23	spect
	5.015	23	spect
	5.042	11	spect
U^{227}	6.8		ion ch
U^{228}	6.67		ion ch
U^{229}	6.42		ion ch
U^{230}	5.662	0.8	spect
	5.819	31	spect
	5.888	68	spect
U^{231}	5.45		ion ch
U^{232}	5.132	0.3	spect
	5.261	32	spect
	5.318	68	spect
U^{233}	4.731	2	spect
	4.780	15	spect
	4.823	83	ion ch
U^{234}	4.59	~0.3	α-γ coinc
	4.714	26	spect
	4.763	74	ion ch
U^{235}	4.20	4	ion ch
	4.40	83	ion ch
	4.47?	~3	ion ch
	4.58	10	ion ch
U^{236}	(4.45)	27	γ energy
	4.499	73	ion ch
U^{238}	(4.135)	23	γ energy

TABLE I—*Continued*

Alpha emitter	Alpha particle energy (Mev)	Relative abundances (%)	Type of measurement
	4.182	77	ion ch
Np^{231}	6.28		ion ch
Np^{233}	5.53		ion ch
Np^{235}	5.06		ion ch
Np^{237}	4.77		ion ch
Pu^{232}	6.58		ion ch
Pu^{234}	(6.14)	14	γ energy
	6.19	86	ion ch
Pu^{235}	5.85		ion ch
Pu^{236}	(5.71)	20	γ energy
	5.75	80	ion ch
Pu^{238}	5.352	0.1	spect
	5.452	28	spect
	5.495	72	spect
Pu^{239}	5.099	11	spect
	5.137	20	spect
	5.150	69	spect
Pu^{240}	5.014	0.1	spect
	5.118	24	spect
	5.162	76	spect
Pu^{241}	4.848	25	spect
	4.893	75	spect
Pu^{242}	4.854	20	spect
	4.898	80	spect
Am^{237}	6.01		ion ch
Am^{239}	5.75		ion ch
Am^{241}	5.379	1.4	spect
	5.433	13.6	spect
	5.476	84	spect
	5.503	0.2	spect
	5.535	0.3	spect
Am^{243}	5.171	$\sim$3	spect
	5.225	13	spect
	5.267	84	spect
Cm^{238}	6.50		ion ch
Cm^{240}	6.25		ion ch
Cm^{241}	5.95		ion ch
Cm^{242}	5.965	0.035	spect
	6.066	26.3	spect
	6.110	73.7	spect
Cm^{243}	5.679	3	spect
	5.732	13	spect
	5.777	78	spect
	5.985	6	spect

TABLE I—*Continued*

Alpha emitter	Alpha particle energy (Mev)	Relative abundances (%)	Type of measurement
Cm^{244}	5.755	25	spect
	5.798	75	spect
Cm^{245}	5.34		ion ch
Bk^{243}	6.20	17	ion ch
	6.55	53	ion ch
	6.72	30	ion ch
Bk^{245}	5.90	34	ion ch
	6.15	48	ion ch
	6.33	18	ion ch
Bk^{249}	5.4		ion ch
Cf^{244}	7.15		ion ch
Cf^{246}	6.711	22	spect
	6.753	78	spect
Cf^{248}	6.26		ion ch
Cf^{249}	5.82	90	ion ch
	6.00	10	ion ch
Cf^{250}	6.04		ion ch
Cf^{252}	6.13		ion ch
99^{247}	7.35		ion ch
99^{253}	6.62		ion ch
100^{254}	7.20		ion ch
100^{255}	7.1		ion ch

α-groups are included. Similarly, an α-group may be included which is not directly observed because it cannot be resolved from a neighboring intense group, but for which γ-rays or conversion electrons define this group unambiguously. Such α-energies are enclosed in parentheses and the type of measurement designated as "γ energy." We have arbitrarily omitted the so-called "long range α-particles" of Po^{212} and Po^{214} (even though they do appear in low abundance in the spectra) since these are not transitions from the ground states or from measurable metastable states.

It is difficult to assign meaningful limits of error for the individual measurements and they are omitted. In general, those made with a spectrograph may be in error by as much as 15 kev, but a large number are perhaps accurate to less than 5 kev; those made by the ionization chamber method will vary in accuracy from 10 to 75 kev; and range measurements in photographic emulsions are even more difficult to assess. Energy differences between groups in a particular spectrum are in general more accurate than the absolute α-energy. Most energies determined are not absolute but depend upon comparison with standards, so a list of some of the most accurate values (absolute and comparative) suitable for standards are shown in Table II.

TABLE II

ABSOLUTE ALPHA PARTICLE ENERGY DETERMINATIONS INCLUDING SOME VALUES MEASURED RELATIVE TO RaC'*

Alpha emitter	Briggs (3)	Sturm and Johnson (27)	Rosenblum, Dupouy (28)	Lewis, Bowden (29)	Collins, McKenzie, and Ramm (30)	Best value, Briggs (26)
RaC' (Po^{214})	7.680	7.683				7.680
ThC' (Po^{212})	8.776†		8.780	8.776†	8.786	8.780
Po^{210}		5.298	5.299	5.299†	5.305	5.301
ThC ($Bi^{212})\alpha_0$	6.082†		6.087	6.082†	6.090	6.086
ThC ($Bi^{212})\alpha_{40}$	6.043†		6.048	6.042†	6.050	6.047

* All measurements cited were made with magnetic spectrographs except those of Sturm & Johnson (27) who used an electrostatic device. The values listed for the magnetic measurements were corrected as done by Briggs (26) in terms of slight revisions of fundamental constants used in the conversion of $H\rho$ to energy.

† Measured relative to RaC'.

Alpha decay energy systematics.—The value of a curve such as that in Figure 1 is to help visualize in broad outline the conditions and regions of α-instability. A good deal more is to be learned from a more detailed examination of the regions where α-radioactivity is prominent. It is observed that α-decay energies[3] fall into well behaved patterns, the recognition of which has proved considerably useful for a number of purposes. Two of the functions of these correlations will be mentioned.

Alpha decay series (containing relatively few β-decay steps) provide a continuous series of energy increments from the region of the element Pb to the highest elements possible. The many decay chains either combine through decay or can be related energetically by measured neutron binding energies. By analyzing these data, it is possible to obtain a rather detailed picture of the energy surface[4] in the heavy element region. The shape of the

[3] Alpha decay energy or simply decay energy will refer to the Q value for the α-emission process and is therefore immediately transferable into a mass of energy difference between ground states of parent and daughter. The actual α-particle measured for the ground state transition is of appreciably lower energy because of the energy carried off by the recoil atom. Of course, the α-groups leading to excited states are of still lower energy. The measured energies of α-groups will be referred to as "α-particle energies" or "particle energies" to distinguish them from "decay energies."

[4] "Energy surface" refers to a surface defined by the energy contents or masses of the nuclides.

energy surface is readily delineated from these data, and regions of greater or lesser stability stand out clearly. A schematic representation of such a surface, exaggerated for purposes of illustration, was given by Perlman, Ghiorso & Seaborg (31). A complete and critical compilation of all decay energy data, and the atomic masses calculated from these has been made by Seaborg & Glass (32). The data include masses of nuclides not yet prepared and these were derived from decay energies estimated by methods which will be indicated below.

Of great value to the experimentalist has been the ability to predict α-energies, and the agreement between predicted and measured values often serves

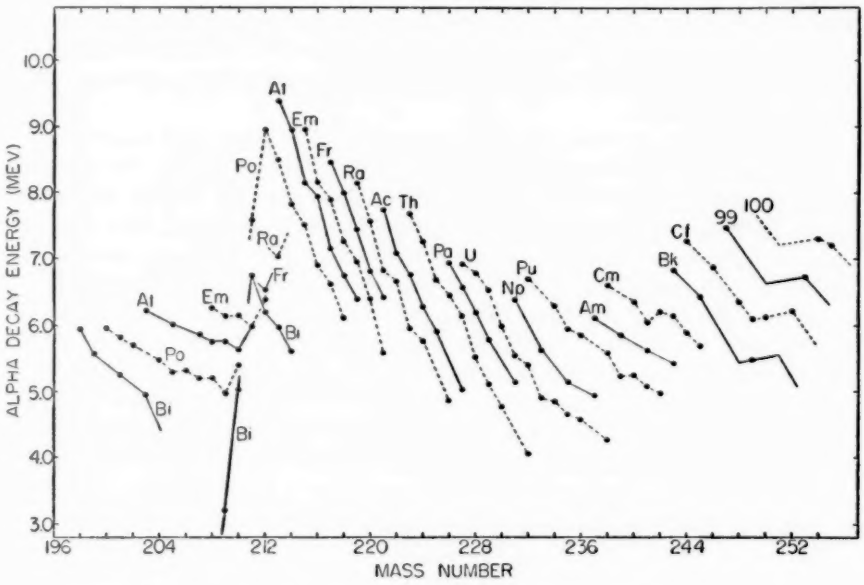

FIG. 2. Alpha decay energy versus mass number.

as a criterion for isotopic assignment. Furthermore, if the energy can be predicted, the half life can be calculated. The forecasting of both α-energy and half life has been of inestimable value in the preparation and identification of higher and higher elements.

A number of systems for correlating α-decay energies have been employed and perhaps that most widely used is illustrated in Figure 2. Here, the isotopes of each element on a mass number versus energy plot are joined, resulting in a family of curves which over a wide region comprise a series of nearly parallel lines. It will be noted that in this region (above mass number $\sim$212) α-energies decrease with increasing mass number for each element; that is, with increasing neutron number. This system in some modification

has been used by a number of workers (31, 33 to 37), while others have used contour map presentation (38, 39) and still different methods (40).

Before turning to the regions in Figure 2 where sharp changes in the lines occur, let us consider the broad region of regular behavior. The semi-empirical method of calculating atomic masses of Weizsäcker (41), as developed further by Bethe & Bacher (42) and by Bohr & Wheeler (43), pictures the energy surface as a trough having parabolic sections at constant mass number, A. The bottom of the trough goes through the β-stable nuclides and if the energy coordinate is expressed in terms of the mass defect, the line along the bottom becomes the familiar "best" mass defect curve. It can be shown graphically (31) or analytically (4) that the observed trend of α-energy with mass number (Fig. 2) is to be expected from this picture. Differences in slope and spacing of the lines can be interpreted in terms of departures from extreme regularity of the trough such as small changes in curvature of the trough or of its slope.

The dramatic inversion in the α-energy trend around mass number 212 is a consequence of the major closed shells in this region (37, 44). We can see what happens more precisely by following the curve for the Po isotopes. From Po^{218} down to Po^{212} the curve follows the normal trend; then Po^{211} is seen to have considerably lower α-energy than Po^{212}. This can readily be shown to be a reflection of the fact that the binding energy of the 126th neutron in Pb (Pb^{207}–Pb^{208}) is greater than that of the 128th neutron in Po (Po^{211}–Po^{212}). Similarly, since the binding energy of the 125th neutron in Pb (Pb^{206}–Pb^{207}) is greater than that of the 127th neutron in Po (Po^{210}–Po^{211}), the α-energy of Po^{210} is lower than that of Po^{211}. After the neutron shell of 126 is well passed and the neutron binding energies change monotonically for both parents and daughters, the regular trend of increasing α-energy with decreasing neutron number is resumed (see region between Po^{203} and Po^{203}).

The curve for Bi is seen to parallel the Po curve with a wide energy spacing between them. This energy spacing is presumably a consequence of the 82 proton shell. The reappearance of α-radioactivity in highly neutron deficient isotopes of Bi (45) was the clue needed to establish the generalness of this effect of crossing the region of 126 neutrons (44 to 52).

It will be noted that the α-energies for the isotopes with 128 neutrons would be expected to become progressively greater for each higher proton number. Half lives will accordingly be very short in this region so that preparation and identification of such nuclides would be difficult. However, more neutron deficient isotopes should be more stable just as Po^{210} is more stable than Po^{212}. Such a region has been found for At, Em, and even for Ra, showing that the effect of 126 neutrons extends at least this high (51, 52). Undoubtedly these points shown on Figure 2 join to those of higher neutron number by going through sharp peaks higher than those shown for Po and At.

The question arises as to whether or not there is evidence for other closed shells or subshells on the basis of α-decay data. A situation similar to that

at 126 neutrons, but considerably more subdued, seems to occur at neutron number 152 (19). The evidence comes principally from the α-energy trend of Cf isotopes (element 98) as seen in Figure 2 showing that the Cf isotope with 154 neutrons has a higher energy than those of the next few isotopes of lower mass number. The fragmentary data on elements 99 and 100 are not out of line with this concept and the lines are drawn in Figure 2 according to expectations. As will be explained later, the positions of closed shells can be correlated with energy level spacings between certain excited states and their ground states but, in this respect, the single nuclide known with 152 neutrons (Cm^{248} from α-decay of Cf^{252}) does not reflect a closed shell configuration (53, 54).

It will be noted in Figure 2 that the energy increments from isotope to isotope along many of the curves are not very uniform. Aside from the marked inversion in trend in the region of Pb and the probable small inversion in con-

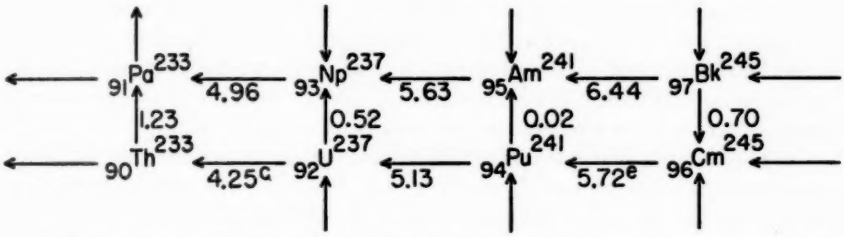

FIG. 3. Decay cycles for part of $4n+1$ family. Code: ← α-decay, ↑ negative β-decay, ↓ electron capture decay. Numerals indicate energies in Mev; those with superscript "*c*" are calculated by closing the cycles; those with superscript "*e*" are estimated as by the use of Figure 2; those unmarked are measured values.

junction with 152 neutrons, it is seen that in some places the isotopes seem bunched and in others relatively spread out. It has been suggested that there are subshells at 92 protons (55, 56) and at 88 protons (56) in explanation of some of these irregularities. Other inferences of α-decay energies on possible subshells have been discussed by Broneiwski (57).

Decay energies from energy-balance cycles.—As a guide in research on new heavy isotopes, the ability to predict decay properties is of great value. By interpolation and extrapolation, the curves of Figure 2 may be used to estimate α-energies and these as well as measured values can be used in constructing a self-consistent system of energy-balance cycles which can be used in turn to calculate degrees of β^- instability and other α-energies.

To illustrate this method of correlating decay energies (32), a segment of the decay cycle representation of $4n+1$ type[5] nuclei is shown in Figure 3. A few examples of the uses of these cycles will be mentioned. It is noted that by making use of three measured decay energies the α-energy of the 6.8 day

[5] The type "$4n+1$" means that all mass numbers are divisible by 4 with remainder 1. All nuclei connected by α- and β-decay processes are of the same type.

β^- emitter U^{237} is calculated to be 4.25 Mev. This is almost identical with the decay energy of U^{238} which has a half life of 4.5×10^9 years. The partial α-decay half life of U^{237} would be expected to be at least as long. Accordingly, the α-branching of U^{237} would be only of the order of 10^{-12} so that this mode of decay would be most difficult to observe. On the contrary, the α-branching of Pu^{241} was similarly estimated to be about 10^{-5} which was within reach for measurement and the α-energy as subsequently measured is shown in Figure 3.

Another use of these cycles has to do with predictions of β-stability. If one considers the possibility that Cm^{245} is a β^--emitter and that its preparation would therefore also produce Bk^{245}, the idea should be rejected because it is seen that Bk^{245} is unstable with respect to Cm^{245} by about 0.7 Mev. The estimated α-energy of Cm^{245} which goes into this calculation cannot possibly be in error by an amount to reverse this conclusion.

An extension of these cycles to still higher elements gives a means of making predictions into a region where measurements have not been made, and these predictions serve as an important guide to the experiments. Other cycles can be devised to join different nuclear types through measured binding energies. With a single neutron binding energy measurement joining two series, other neutron binding energies can be calculated (32).

Alpha emitters just below lead.—The removal of neutrons from any element increases the potential toward α-decay and this is the basis for the main trend in Figure 2. Alpha active nuclides of Au and Hg have been prepared by removing many neutrons from the stable isotopes (58). In the case of Au, the stable isotope Au^{197} is estimated to have an α-decay energy of only 1 to 2 Mev, while the isotope observed with an α-energy of 5.1 Mev is believed to lie in the mass number range 183 to 187. As neutrons are removed, successive isotopes become more unstable toward orbital electron capture also, but since α-decay lifetimes are extremely sensitive to energy, this mode of decay should at some point become discernible.

One other α-emitter in this region has been reported (59), a component of natural W. The extremely low specific activity seems out of line with the measured energy (3.2 Mev) if the emitter has the abundance of one of the known W isotopes, so the authors postulate the existence of a rare isotope (W^{178}) in the natural mixture in amounts too small to detect by mass spectroscopy.

Rare earth alpha emitters.—Among the rare earth elements we pass through a region where stable or slightly deficient nuclides can decay by α-emission to the closed shell of 82 neutrons. Such a nuclide with 84 neutrons is Sm^{146} which is β-stable but missing in nature because of its relatively short α-half life ($\sim5\times10^7$ years) (60). The α-energies are summarized in Figure 4 and although the curves are fragmentary as compared with those in the heavy element region, the basic structure as related to the 82 neutron shell is unmistakable. The point assigned to Nd^{144} is of special interest because Nd^{144} is a component of natural Nd (61).

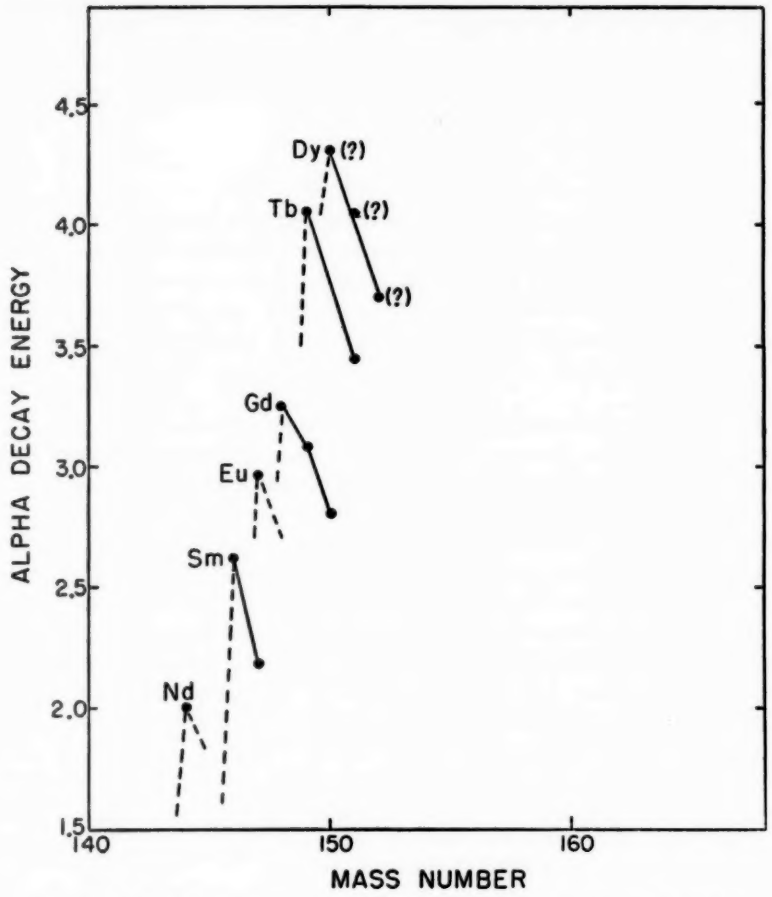

FIG. 4. Alpha decay energy versus mass number in the rare earth region.

COMPLEX ALPHA SPECTRA

As in other decay processes, the appearance of multiple groups in the α-emission process may be considered as the result of competition in populating available energy levels. It will be seen that α-decay lifetimes are influenced by a number of factors and among these is the sharp dependence of lifetime with decay energy. Consequently, it would not be expected that transitions to high-lying levels (say 1 Mev) would be readily observed. There are, however, selection processes operating which can delay the highest energy group and cause lower energy groups to be the most prominent. As yet, there is no systematic formulation of "selection rules" for the α-decay process. The development of α-decay theory with this as an objective is undoubtedly the most important step now faced.

The present discussion will be concerned largely with the regularities which are appearing with respect to the location of energy levels, their spectroscopic designation, and in the degree to which these states are populated. As already stated, only a start has been made in developing reasons for preference in populating certain states.

Even-Even Alpha Emitters

Principal alpha groups (the ground state and first excited state).—With a high degree of certainty it can be said that the transition to the ground state is the most abundant for this nuclear type. In each of the many cases which have been examined in detail, the main α-group is that of highest energy and there is no evidence that the group is followed by γ-radiation. To this extent at least the even-even α-emitters are well behaved according to existing α-decay theory.

In examining a number of even-even α-emitters around U and in the transuranium region, it was noted that each had a second prominent α-group of some 40 to 50 kev lower energy than the ground state transition (62). The abundance of this group was always in the range 15 to 30 per cent.[6] (We shall see presently that the states reached by these α-groups apparently all have spin 2 and even parity and we shall call each the "first even spin state" or simply the "first even state.")[7] When lower elements or lower neutron numbers of a particular element are considered, the same states are identified but the energy level spacings above the ground states become progressively greater and the abundances of the α-groups populating these states progressively lower. A summary of the energy spacings between the ground state and first even state as a function of neutron number and proton number is shown in Figure 5. The points divide into families according to atomic number and appear to reach maxima for nuclei with 126 neutrons. In some cases, the points in Figure 5 were determined from γ-ray spectra rather than from observation of the α-groups.

It has already been deduced by several authors (63, 64, 65) that the first excited states of even-even nuclei in general are 2+ states and this applies to regions other than that of the heavy elements and irrespective of the particular energy spacing of the levels. There is theoretical justification for the 2+ assignment both from modifications of the independent particle model (66, 67) and from the collective model (68, 69). There is also theoretical explanation (67, 69) and empirical proof (62, 65, 70, 71) that the energy

[6] We shall define "abundance" to indicate the number of α-particles in a particular group relative to the total number of α-particles.

[7] It is worth recalling that in conserving parity in the α-decay of an even-even emitter, the even spin states must have even parity and the odd spin states odd parity. A corollary is that γ-ray transitions from any of these excited states to the ground state must be electric transitions and not magnetic.

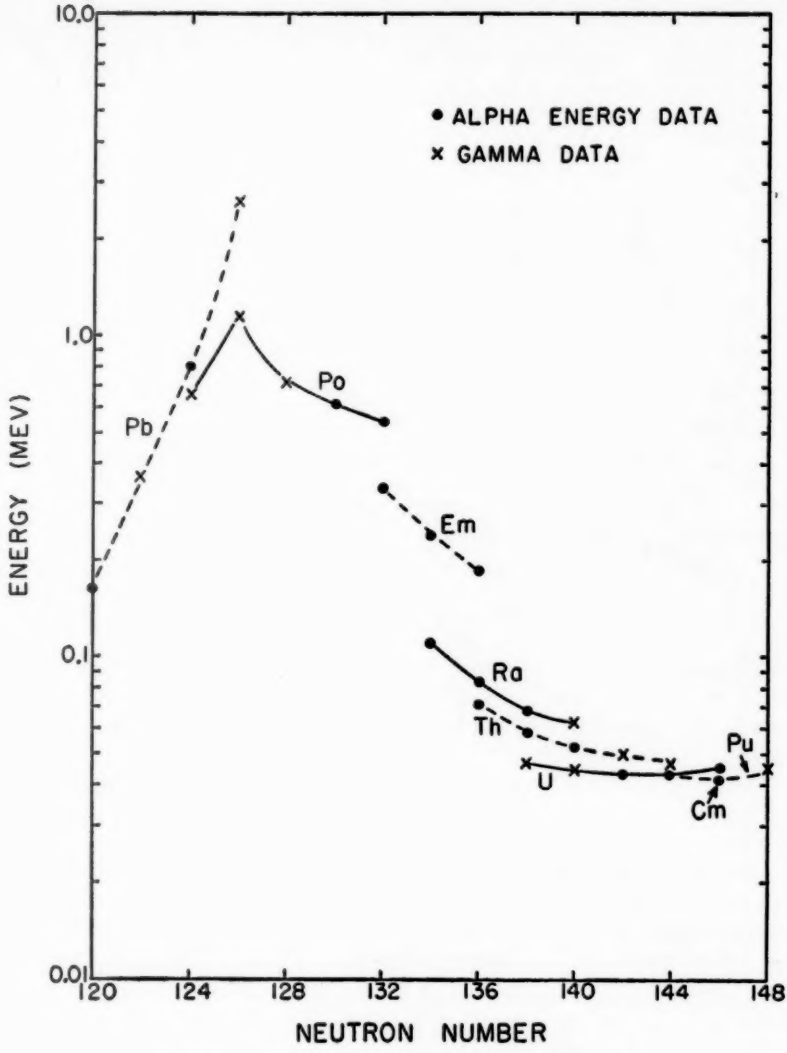

FIG. 5. First excited state energies of even-even nuclei in the heavy element region.

level spacing for the first excited state goes through a maximum at each closed shell as is seen in Figure 5 for the 126 neutron shell.

Two typical even-even α-spectra are shown in Figure 6 and for the present we shall focus attention on the two lowest states corresponding to the two α-groups considered. The states assigned 2+ are the "first even states"

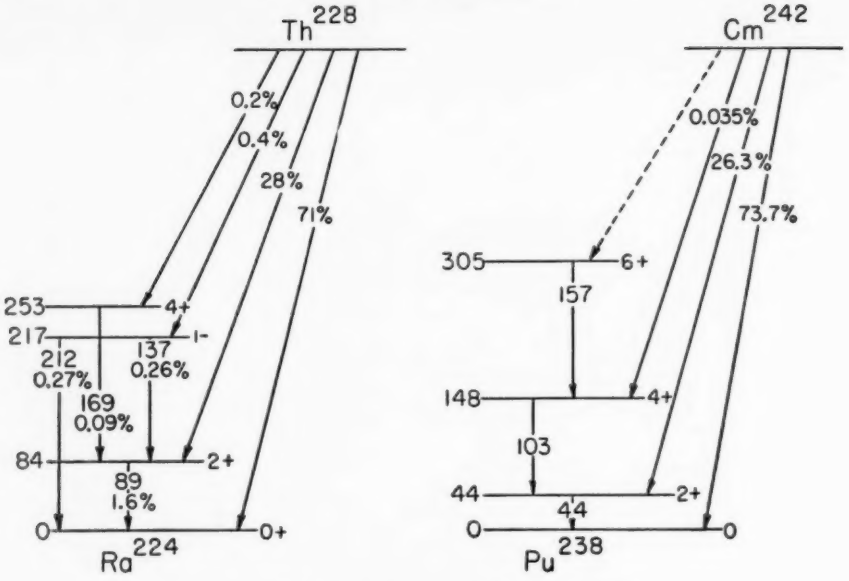

FIG. 6. Decay schemes of Th^{228} and Cm^{242}.

already mentioned and are designated so because they de-excite to the ground state by electric quadrupole (E2) transitions.[8] Since there is no evidence to the contrary, we shall assume that the "first even state" is in each case the "first excited state."

Rare alpha groups (higher even states and first odd state).—Many of the α-emitters which have lent themselves to detailed analysis have proved to have one or more additional groups of lower energy and in low intensity. The low intensities of these groups are not attributable alone to lower energy than the two main groups. If we calculate the lifetimes for the ground state transition and that to the first excited state according to current α-decay theory, the results are in substantial agreement with the measured lifetimes. However, the measured partial half lives for the higher transitions are considerably longer than the calculated values and we refer to such transitions as "hindered." This subject will be dealt with under the section on α-decay theory, and for the present we will consider only the energy level spacings and spectroscopic assignments.

In each case which could be examined in the necessary detail, there was

[8] The nature of the transition has been deduced from measurements of absolute conversion coefficients, relative L subshell conversion coefficients and α-γ angular correlations. The cases studied are the α-emitters Po^{210} (72), Ra^{222} (7), Ra^{224} (73, 74, 75), Ra^{226} (75), Th^{226} (7), Th^{228} (9, 76, 77, 78), Th^{230} (77, 79), U^{230} (7), U^{232} (8), U^{234} (8), U^{236} (80), Pu^{238} (13), Cm^{242} (15), and Cf^{246} (89). The excited states in question belong, of course, to the α-decay products.

found a rare α-group going to a state which decays by an E2 transition only to the 2+ state.[9] These states are those designated as 4+ in Figure 6 and will be known as the "second even states." From the nature of the γ-ray transition, the second state could be 0+, 2+ or 4+; the 4+ assignment is made largely from a theory to be mentioned presently which fixes it as a member of a rotational band of states 0+, 2+, 4+ $\cdots$. The fact that no crossover transition is seen from the second even state to the ground state may also be taken as partial evidence for the assignment.

In a few cases, very rare γ-rays have been seen (the α-groups would be below the limits for detection) and are assigned to transitions between the third and second even states (13, 15). In the case of Pu^{238} decay (13), the γ-ray was shown to be in coincidence with that between the 4+ and 2+ states. Since the energy of the state defined by the γ-ray corresponds closely with expectations if it were the third "even state" (6+) of the rotational band, it has been so designated (see Cm^{242} spectrum, Fig. 6). The theory behind these assignments will now be examined.

According to a theory of Bohr and Mottelson (68, 82), collective aspects of nuclear motion and individual particle aspects are coupled. In a "region well removed from a closed shell" there should be a series of energy levels corresponding to a rotational band in which only even states (0+, 2+, 4+ $\cdots$) appear for an even-even nucleus. On this basis, electric quadrupole transitions should predominate. Another requirement of the rotational spectrum in this region is that the states lie at energies proportional to $I_j(I_j+1)$, where I_j is the spin of the jth even state. For the levels 0+, 2+, 4+, 6+, the ratios of 4+/2+ and 6+/2+ would therefore be respectively 3.3 and 7.0. Figure 7 shows an extensive set of these ratios of the first and second even states, and it is seen that the agreement with expectations is excellent for the higher neutron numbers but gradually departs as the region of 126 neutrons is approached. Apparently the same behavior can be noted for even-even nuclei in the rare earth region in reference to the 82 neutron shell (83). The point for Pb^{208} in Figure 7 is of questionable significance since it is not at all certain that the first two excited states as deduced from Tl^{208} β^--decay are indeed 2+ and 4+. As an example of this uncertainty, a number of different measurements concerning the first excited state have resulted in different assignments: 1+ or 2+ (84), 2+ (85, 86, 87), 3− (88). In two cases, Pu^{238} and U^{234}, (α-decay of Cm^{242} and Pu^{238}) where a third even state is inferred, the energy ratio of this level to the 2+ level is indeed close to 7.0. The evidence for the higher state in the case of Pu^{238} decay is that the γ-ray used to define it is in coincidence with the γ-ray from the 4+ to the 2+ states (13).

[9] Conversion coefficient data defining the transition as E2 have been obtained in the α-decay of Cm^{242} (15) Pu^{238} (13, 81), U^{232} (8), Th^{228} (9). For other cases there is no direct information, but other regularities to be discussed presently make it highly likely that comparable states are being considered.

UNIVERSITY OF MICHIGAN LIBRARIES

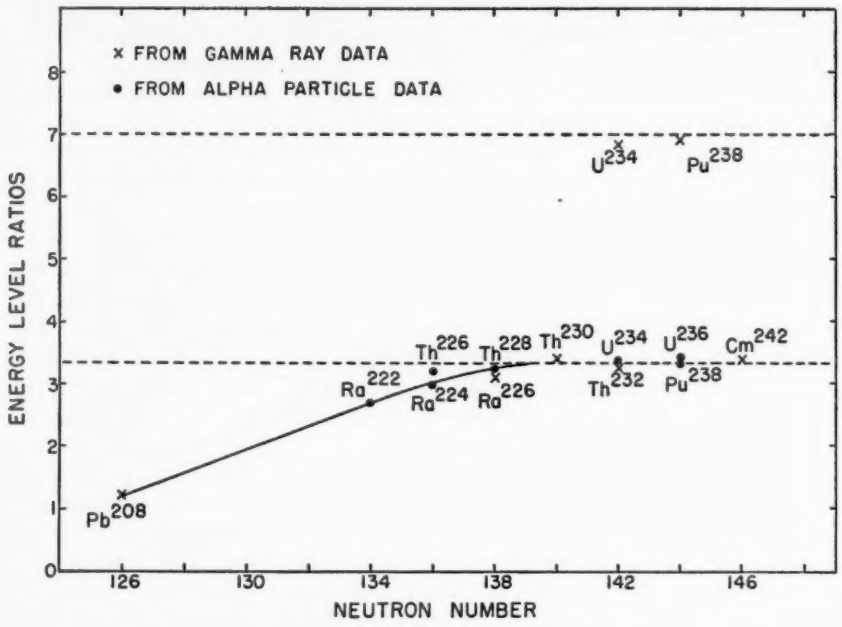

FIG. 7. Ratios of energies of the second and third even spin state to the first excited state. The broken lines represent the expected values from the Bohr-Mottelson theory for rotational levels in regions removed from closed shells.

In a number of cases, a state believed to be 1− has entered among the low-lying even states. The spectrum for Th^{228} which is typical of this type is shown in Figure 6 (9). In contrast to the second even state, this state always decays both to the first even state and to the ground state. The conversion coefficients of both conform with E1 transitions (9) as do more recent α-γ angular correlations made on Th^{226}, Th^{228} and U^{230} (89).

The 1− state has probably been identified in the decay of Th^{230} and U^{232} as well as for the three cases just mentioned. Significantly this state has been identified only among the low-lying excited states of nuclei of neutron numbers in the range 134 to 138 neutrons. From the fragmentary evidence at hand it seems possible that the state has a minimum energy at 136 neutrons and rises at both lower and higher neutron numbers.

With respect to the degree of population of the 1− state in the α-decay process, the data are too few to arrive at any generalizations. In the cases studied, the process seems to be competitive with that leading to the 4+ state for comparable energies.

Finally, it should be remarked that there is no ready explanation for a low-lying odd parity state such as this. Neither the independent particle model nor the collective model would predict such states in any straightforward manner.

Odd Nucleon Alpha Emitters

The α-spectra of nuclei having odd nucleons are in general considerably more complex than those of even-even nuclei and consequently have not been worked out with the same degree of certainty. Also, they may differ from each other considerably and have not yet yielded to a comprehensive generalized picture such as applies to the even-even nuclei.

Nevertheless, some regularities can be discerned, and among these is the appearance of rotational bands (14, 90) closely similar to those of the even-even nuclei. Interestingly enough, the fundamental state of the rotational band (where such a band shows up distinctly) is that populated in highest abundance, but it need not be the ground state and perhaps usually is not. The important implication of such spectra with respect to α-decay theory is that powerful "selection rules" are in force since the highest energy transition (that to the ground state) is often in very low intensity (91).

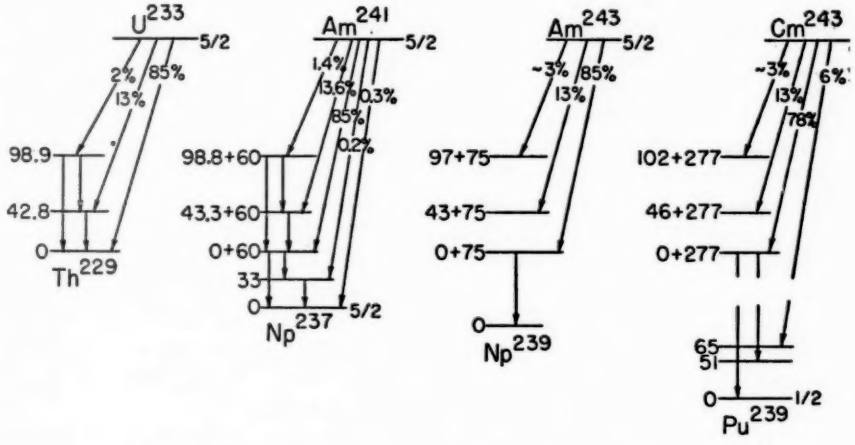

FIG. 8. Decay schemes of some odd-nucleon α-emitters.

Figure 8 shows some spectra which were selected to illustrate some of the regularities noted.[10] (Obviously it is not possible to discuss all spectra of these types and some, such as that for Th^{227} with eleven reported groups (92), are too complex for analysis at present.)

The partial spectrum for U^{233} is not representative of most of those examined in that it looks much like that of an even-even α-emitter. The energy level spacings for these states are much like those of Cm^{242} (see Fig. 6) and the relative populations of the states are roughly comparable, but an important difference to be noted is that the second excited state decays both to the first excited state and directly to the ground state. A possible explana-

[10] The references for the data comprising these α-spectra are Am^{241} (14, 91) Am^{243} (14), Cm^{243} (8, 15), U^{233} (8).

tion of this spectrum lies in its interpretation as a rotational band, the grounds for which are now sketched.

According to Bohr & Mottelson (68), the rotational band for a nucleus with an odd nucleon will have a fundamental state of spin I_0 and higher states of spins I_0+1, I_0+2, $\cdots$, all with the same parity. The spacings of these levels will go as $W+CI(I+1)$, where W and C are constants for a particular level sequence. For the U^{233} case the following equations may be set up:

$$E_{98.9} - E_{42.8} = C(I_0+2)(I_0+3) - C(I_0+1)(I_0+2) = 56.1$$
$$2C(I_0+2) = 56.1$$
$$E_{42.8} - E_0 = C(I_0+1)(I_0+2) - CI_0(I_0+1) = 42.8$$
$$2C(I_0+1) = 42.8.$$

The solution of the simultaneous equations gives $I_0=2.2$ and since the spin must be half integral we take the closest value, $I_0=5/2$. It should be mentioned that this analysis is extremely sensitive to the accuracy of the data; an error of only 0.5 kev in the 42.8 kev level, making it 43.3 kev, would change the calculated value of I_0 to exactly 2.5. If we accept 5/2 for the fundamental state, the spins of the other two levels become 7/2 and 9/2. The cascading γ-ray transitions could then be M1 and/or E2 and the cross over transition E2, which assignments are not out of order with the fact that both crossover and cascade γ-rays are observed.

The spectra for Am^{241}, Am^{243}, and Cm^{243} α-decay show quite similar rotational bands with calculated fundamental state spins of 5/2, but the fundamental states in these cases are not the ground states. Americium 241 and Am^{243} differ only in that this state is respectively 60 and 75 kev above the ground state. For Cm^{243}, the ground state transition has not yet been observed even though it has 277 kev higher decay energy than the main group, a fact established by α-γ coincidence counting (15).

It is perhaps not profitable at present to speculate in detail on the meaning of the complex spectra of the nuclear types under discussion. We believe that rotational bands which can be explained as a consequence of collective modes of nuclear motion are discernible. It is also probable that other important features of the spectra must bring in the concept of single particle states. Just what these states are and what guides the α-decay process to some and not others is still obscure. Some speculations on these matters as they apply to α-decay theory will be brought out in the section on this subject. It is worth reiterating here that no simple criterion or rule is likely to explain the spectra shown in Figure 8 as well as the extremely complex spectrum of Th^{227} and that of Pu^{239} which is a good deal simpler but different from both types.

Alpha Decay Lifetimes and Theory

It is possible to correlate α-decay lifetimes empirically and to arrive at systems which can be used to predict half lives. For example, regularities can

be observed in plotting the half life with the mass number for successive elements. However, it is also possible to systematize the half lives in terms of parameters which are involved in current α-decay theory and thereby also obtain some information on the status of the theory.

It will be seen that the ground state transitions of even-even α-emitters are treated with extraordinary precision by basic one-body α-decay theory. However, analysis of the many α-spectra obtained during the past few years has shown clearly that more elaborate theory is required to account for the behavior of other nuclear types as well as for certain of the transitions to excited states of the even-even nuclei. The development of new approaches to cover these cases is currently in a formative stage. It will not be possible in this review to cover in detail either the old theory or the new approaches; rather, we shall emphasize those aspects of α-spectra which appear to require new forms for expression and indicate the direction some of these new forms are taking.

Basis for one body theory.—The initial conception by Gamow (1) and by Condon & Gurney (2) of the α-decay process as a barrier penetration problem has been cast into a number of forms differing in detail but basically all ending up with the decay rate expressed as the product of two factors: (*a*) a "frequency factor" which may be considered as the decay rate without the barrier; and (*b*) a "penetration factor" which expresses the probability of an α-particle emerging through the negative energy region of the coulombic potential barrier. The various solutions to the problem differ in the degree of rigor which is applied, and it might be stated that the sensitive portion is the "penetration factor" which is exponential in form and is handled virtually identically in the several treatments. (See, for example, references 93 to 97.)

The parameters which enter into the penetration factor are those which define the barrier for the α-particle of energy E and these are the nuclear charge and the effective nuclear radius. The frequency factor, likewise, is a function of the energy of the α-particle and nuclear radius and although approximations are introduced in its evaluation, this factor is relatively insensitive and does not strongly influence the results. It is probably here, however that the one body model breaks down as a representation of decay processes, that is, where single particle states are of importance.

It will be noted that of these parameters the nuclear charge has explicit meaning dissociated from the α-decay process and the α-energy and decay constant are subject to precise measurement, but the effective nuclear radius is a quantity which is not obviously meaningful for this process when determined from other nuclear phenomena, nor do such independent methods of measuring the radius give the desired precision for testing α-decay theory. The procedure to test the theory is therefore confined at present to see if calculated nuclear radii fall into a reasonable range and pattern of values or fluctuate in an unreasonable fashion (58, 93 to 100). Conversely, one may assume some function for nuclear radii, from this derive theoretical curves

UNIVERSITY OF MICHIGAN LIBRARIES

to express the decay constant in terms of the other parameters, and test the agreement with the measured decay constants (31, 98, 99, 101, 102). It is this second approach which has proved most useful in correlating a large number of data. Further discussion of this matter will follow as the data for even-even α-emitters are examined.

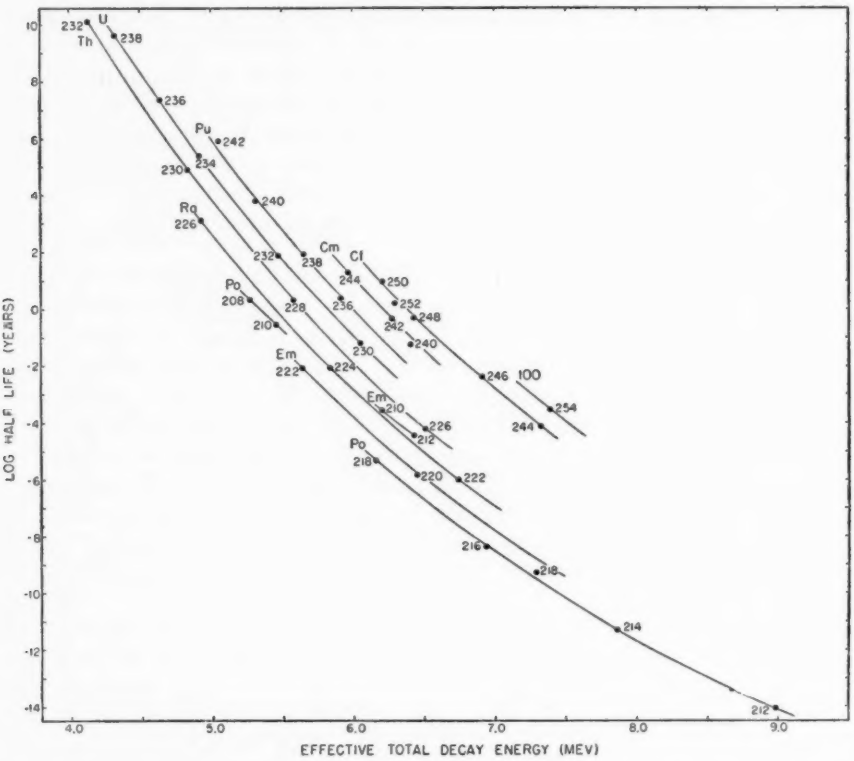

FIG. 9. Experimental values of log half life versus α-energy. ("Effective α-energy" includes correction of particle energy for recoil and electron screening—see text.)

Even-even alpha emitters: ground state transitions.—Figure 9 shows a plot of the half life versus energy relationship as a family of curves. The curves are defined by the experimental half lives and are in this respect empirical. If, however, we were to calculate half lives with the Kaplan (99) modification of the Preston (95) formula, by using the measured α-energy for each point and assuming a function for the nuclear radius, $1.52\times10^{-13}A^{1/3}$, the resulting curves would lie close to those of Figure 9. In detail, the calculated curves of the lower elements (Po, Em) would lie somewhat below the corresponding curves of Figure 9 and for the higher elements (Cm, Cf) the calculated curves would lie slightly above those shown in Figure 9. (The segments of

curves shown for Po^{210} and Po^{208} and for Em^{210} and Em^{208} should be considered as special cases in which effective nuclear radii suffer a discontinuity and these are nuclei with 126 neutrons and fewer.) To bring about more exact agreement one can bring in a second order effect by assuming that the nuclear radius parameter should not be a constant, 1.52, but should vary in some fashion, say with atomic number. To see what is required, a calculation was made for the effective radius of each nucleus using measured values of both energy and half life and the results are shown in Figure 10. The sharp

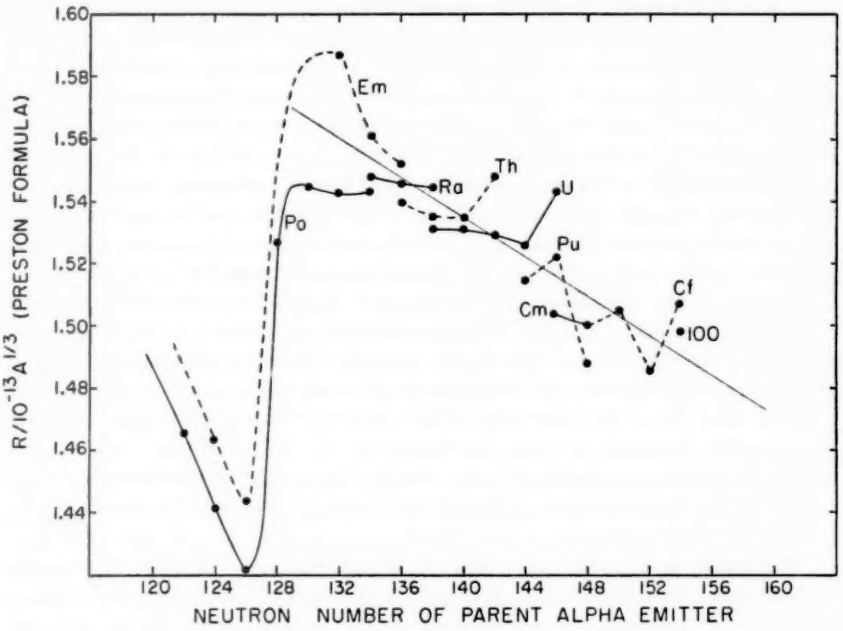

FIG. 10. Nuclear radius parameter.

break at 126 neutrons is apparent but, in addition, there seems to be general decrease in radius parameter with increase in atomic number. This, of course, is a restatement of the relation mentioned between the empirical curves and those calculated on the basis of a single average value for the radius parameter. With reference to the data of Figure 10, it should be pointed out that there is sufficient experimental uncertainty in some of the values which went into these calculations to shift the points by 0.02 unit of radius parameter or even more.

In summary, we can say that the basic one body theory of α-decay applied to the ground state transitions of even-even α-emitters gives a remarkably consistent picture. By using reasonable and consistent assumptions for the values of the nuclear radii, the theory explains observed half lives which

differ by a factor of 10^{24}. It should be pointed out that different formulations of the theory will give somewhat different "best values" for the radius parameter, but each is internally consistent.

Two further points should be mentioned with respect to the curves of Figure 9. It may be noted that the energy values listed are somewhat higher than measured particle energies. The α-energy pertinent to α-decay theory is based on its center of mass velocity and therefore the particle energy must be increased by the energy of the recoil nucleus. This correction amounts to $\sim$100 kev for a 6 Mev α-particle in this region.

An additive correction to the α-particle energy so far overlooked has been suggested by Ambrosino & Piatier (103) and has to do with the lowering of the potential barrier by the electron cloud. As discussed by Rasmussen (104) this correction should be applied as an added α-energy amounting to about the difference of total electron binding energies between parent and daughter in the particular α-decay process. This amounts to $\sim$38 kev in the region of U and is smaller for lighter elements. This latter "screening correction" to the particle energies does not have a profound effect on the agreement of theory and experiment which is under discussion, but it does have the effect of giving somewhat smaller values of nuclear radii than if it were ignored.

The other item concerning Figure 9 has to do with the reason that smooth curves can be drawn at all because, in principle, each curve is not continuous if the nuclear radius is an independent variable. However, as seen in Figure 2, α-energies vary more or less monotonically with mass number A and since nuclear radii do so likewise, each value of energy (for a particular element) does localize the mass number and therefore the radius. Where two isotopes within the same energy range do have large differences in effective radii they do not lie on the same curve. This effect is seen for Po and Em curves on the two sides of 126 neutrons.

Even-even alpha emitters: transitions to excited states.—For any particular ground state transition, one can calculate the partial half life to any excited state under the assumption that the only factor influencing the relative decay rates is the energy function. Let us first consider transitions to the first excited state (2+). The effective radius as determined from the ground state transition process is adopted and it is assumed that the spin change, whether $\Delta I=0$ or $\Delta I=2$, will not affect the decay rates very much. This latter assumption has the theoretical justification of the calculations of Preston (95, 96) which show that contrary to previous treatments, a $\Delta I=2$ transition should be some 1.5 times faster than a $\Delta I=0$ transition and that only when $\Delta I=4$ does the function take the direction of delaying the transition.

The ratios of expected abundances (solely from energy difference) to experimental abundances are shown in Table III. Around Ra, Th, and U the ratios are seen to be close to unity and perhaps to rise significantly for the heavier elements. Some recent ideas on the population of these states will be mentioned below where transitions to the 4+ state are discussed.

One apparent anomaly is Po^{208}, for which no α-group has yet been seen

TABLE III

POPULATION OF FIRST EVEN STATE (2+) BY ALPHA DECAY OF EVEN-EVEN NUCLEI

Alpha emitter	Energy level (kev)*	Departure factor†	Alpha emitter	Energy level (kev)*	Departure factor†
Po^{206}	163	3.1	U^{234}	52	1.2
Po^{208}	374	>32	U^{236}‡	50	1.1
Po^{210}‡	800	1.6	U^{238}‡	45	1.5
Ra^{224}	240	1.2	Pu^{234}‡	45	3.5
Ra^{226}	188	0.9	Pu^{236}‡	47	2.2
Th^{226}	110	1.2	Pu^{238}	43	1.6
Th^{228}	84	0.9	Pu^{240}	44	1.7
Th^{230}	68	1.0	Pu^{242}‡	45	2.2
Th^{232}‡	65	0.8	Cm^{242}	44	1.7
U^{230}	70	1.1	Cm^{244}	43	1.8
U^{232}	58	1.1	Cf^{246}	42	2.7

* Energy level of the 2+ state of the daughter nucleus.

† Ratio of calculated abundance (solely from energy difference) to experimental abundance. A factor of unity means that the lifetime for the decay to this state (in this case 2+) is according to expectations from α-decay theory using the ground state transition to define the nuclear radius and neglecting any effect of spin change.

‡ The experimental abundances or energies may be suspect.

leading to the 374 kev 2+ state, and the partial half life is at least thirty-two-fold greater than that calculated. It is significant that there is other evidence (68, 105) that the first excited state of Pb^{204} is not a rotational state. Here, it seems, is a presently isolated but important item which must be included in a comprehensive α-decay theory. If we may generalize from this single case, we may postulate that a 2+ state of an even-even nucleus is populated "normally" only if it is a collective state of the type discussed.

The examination of transitions to the 4+ state gives a totally different and unique picture (106). Here, if the partial half lives are calculated as above, it is found that they are much shorter than the measured values; that is, the 4+ states are populated much more sparsely than would be expected on the basis of α-energy alone. Furthermore, the ratio of measured half life to calculated half life varies considerably and in a more or less regular way with atomic number as shown in Figure 11. It is seen that for Cm^{242} the second even state is hindered in its population by a factor of 400 (compare with factor 1.7 for first even state, Table III), while for Th isotopes this factor is of the order of 10. There is no a priori justification for plotting the data of Figure 11 in the manner shown; for the present it merely serves the purpose of giving visual expression to the considerable range encountered in the population of apparently identical spectroscopic states.

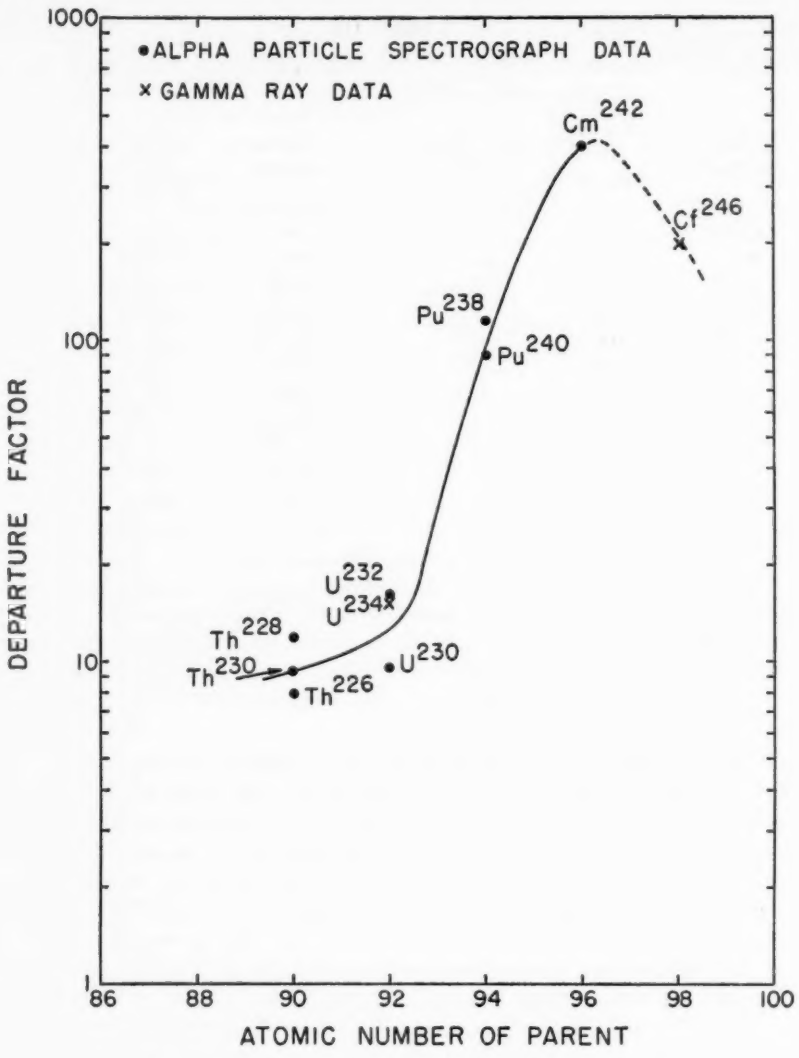

FIG. 11. Departure factors for α-groups to the second even spin state of even-even nuclides.

Recently, an attack has been made on this problem which appears fruitful. The basic idea developed by Preston (107) is that the α-particle emerging through the coulomb potential region and beyond the range of nuclear forces can couple with a noncentral electric field of the nucleus in such a way as to change its energy. Such fields would be associated with spheroidal distortions

in nuclei as discussed by Bohr & Mottelson (68) and Hill & Wheeler (108). The distortion would be described by the intrinsic quadrupole moment which Ford (69) has shown by calculations to be increasing with mass number in the region above Pb and would presumably continue until the approach to a new shell is felt.

The mechanism of quadrupole interaction with the emerging α-particle wave to explain the population of the first two excited states in a rotational band has been explored in detail by Rasmussen (109). For the case of Cm^{242} decay, for which approximate numerical integrations have been carried out (assuming an intrinsic quadrupole moment, Q_0, in Pu^{238} of $+17\times10^{-24}$ cm.^{2}), he found that the population of the 2+ state should be relatively unaffected, but that the population of the 4+ state should be strongly depressed in essential agreement with the experimental observations. The assumed value for Q_0 seems reasonable for a nucleus in this region in view of the recent measurement of the quadrupole moment of U^{235} as $+8\times10^{-24}$ cm.^{2} (112), which with the spin of 5/2 corresponds to a value for Q_0 of $+22\times10^{-24}$ cm.^{2}. The quadrupole moment for even-even nuclei cannot, of course, be measured by spectroscopic means, but there is the possibility of obtaining information through coulomb excitation cross sections and γ-ray lifetimes.

Since this approach in explaining certain features of α-spectra is in an incomplete state of development, it is not worthwhile to speculate on the possible significance of the downturn of the curve of Figure 11 between Cm^{242} and Cf^{246}, nor to discuss a number of other ramifications of the mechanism.

We shall just recall that other low-lying states in even-even nuclei have been identified, but for which detailed information is lacking. There is the third even state (6+?) which is a member of the well-defined rotational band. Also, in a limited region there appear 1− states which are populated roughly to the same extent as the 4+ states in the same region. It is not clear what type of nuclear configuration would give rise to such states.

Odd nucleon alpha emitters.—The most obvious question concerning this category of α-emitters is why the ground state transition is often highly hindered and why the hindrance is so irregular. Table IV shows the data for such α-emitters and the last column contains the "departure factor" which, as before, is the ratio of the measured partial half life for a transition to the half life which would be calculated from one body α-decay theory. We note that for the four species shown in Figure 8 the departure factors for the apparent ground state transitions are: U^{233}—1.4, Am^{241}—1000, Am^{243}—700, Cm^{243}—>26. It is not certain that for each case in Table IV the ground state transition has been identified and where this should prove to be the case the departure factor would be larger.

The first point to be disposed of is the effect of spin change. As already pointed out in a number of instances, both theoretical and experimental appraisal indicates that the lifetime is relatively insensitive to spin change, per

TABLE IV

POPULATION OF GROUND STATE BY ALPHA DECAY OF ODD-NUCLEON EMITTERS

Alpha emitter	Particle energy*	Abundance†	Departure factor‡
Cf^{249}	6.00	0.10	300
Bk^{245}	6.33	0.18	700
Bk^{243}	6.72	0.30	900
Cm^{243}	6.049	<0.5	>26
Am^{243}	5.341	$\lesssim$0.003	$\leq$1000
Am^{241}	5.535	0.0034	700
Pu^{241}	5.01	<0.11	>30
Pu^{239}	5.150	0.69	3
Np^{237}	4.86	<0.15	>50
U^{235}	4.58	0.10	900
U^{233}	4.823	0.83	1.4
Pa^{231}	5.042	0.11	220
Th^{229}	5.02	0.10	100
Th^{227}	6.030	0.19	130
Ra^{223}	5.730	0.09	50
Fr^{212}	6.409	0.37	10
Em^{219}	6.824	0.69	18
Em^{211}	5.847	0.33	8
At^{211}	5.862	1.00	3
At^{210}	5.519	0.32	2
Po^{213}	8.336		1.5
Po^{211}	7.434	0.99	100
Po^{209}	4.877		2

* Particle energy of α-group believed to lead to the ground state. In some instances it is possible that the groups selected are not the ground state transitions in which cases the "departure factors" would be greater than those shown.

† Abundances are based on observed α-groups except where the highest energy group is known to be followed by γ-radiation.

‡ Defined in Table III.

se, certainly within the framework of reasonable spin changes. Conversely, we know that the ground states of Am^{241} and Np^{237} both have spin 5/2 (110, 111) yet the transition between these states is hindered 1000 fold.

Other ideas, not yet formulated quantitatively, appear to be more promising. One suggestion (31) has to do with the breakdown of the one body model in its implication that α-particles exist as discrete entities within the nucleus and that the probability of α-emission depends only upon the frequency factor of this preformed α-particle in encountering the coulomb barrier and upon the rate of barrier penetration. We have seen that for ground state transitions of even-even nuclei the evidence for this extreme simplification indicates that it is substantially correct. For ground state

transitions of odd nucleon emitters, however, it is suggested (31) that there can be a considerable time involved in assembling the components of the α-particle. Such would be the description if the mixture of configurations which constitutes the emitting nucleus contained only as a minor component the configuration with the odd particle as a constituent of an incipient α-particle. Rasmussen (90) has pointed out further that nuclear spins need not give a true picture of the nucleon states of the parent and daughter nuclei. In a region well away from a closed shell where large spheroidal distortions are expected, the strong-coupling configurations may predominate and the nuclear spin can be different from and lower than the j-value for the single odd nucleon. On this basis, the spectroscopic state of the odd proton in Am^{241} may be quite different from that in Np^{237} even though both nuclear spins are 5/2. If such were the case, the change in wave functions could properly introduce a hindrance to the α-decay. Only for those transitions where the single particle wave function remains unaltered would one expect unhindered α-decay. Significantly, it appears that such transitions can be found in the spectra of the odd nucleon emitters, but in general these are not the ground state transitions. This subject will now be examined.

In Figure 8 it is seen that the most abundant groups of Am^{241} and Am^{243} lead to states which are 60 and 75 kev respectively above the ground state. Furthermore, for the particular energies of these α-transitions, the hindrance or departure factors are only of the order of unity (in contrast to 1000 for the ground state transitions) and, in this respect, appear to be like the ground state transitions of even-even nuclei. By making certain assumptions it is possible to deduce the spins for these excited states (60 and 75 kev states). The analysis has already been carried out on page 178 and is based on the recognition of three excited states as members of a rotational band from which the spins of these states can be deduced. In this case, the spins for the 60 kev excited state of Np^{237} and the 75 kev state for Am^{243} are deduced to be 5/2 (14, 90). It is suggested (90) then that these states may be those in which the odd particle wave function rearrangement is a minimum and that the transition is therefore relatively unhindered.

As already discussed under even-even nuclei, the splitting of α-groups into a rotational spectrum may involve the effect of electric field interactions. The appearance of what looks like rotational bands in these odd nucleon species implies, of course, that the same mechanism is in play here.

It seems apparent that the past few years have seen a departure from classical α-decay theory as well as a reinforcement in our confidence in some of its aspects. It also seems likely that some of the new ideas when further developed will add appreciably to the explanation of the α-decay process, and that the ramifications of these ideas will provide a better understanding of nuclear structure.

LITERATURE CITED

1. Gamow, G., *Z. Physik*, **51**, 204 (1928)
2. Condon, E. U., and Gurney, R. W., *Phys. Rev.*, **33**, 127 (1929); *Nature* **122**, 439 (1928)

3. Briggs, G. H., *Proc. Roy Soc.* (*London*), **157**[A], 183 (1936)
4. Kohman, T. P., *Phys. Rev.*, **76,** 448 (1949)
5. Rosenblum, S., and Valadares, M., *Compt. rend.*, **236,** 196 (1953)
6. Stoner, A., Hyde, E. K., and Asaro, F. (Unpublished data, 1953)
7. Asaro, F., Slater, L. M., Stephens, F., and Perlman, I. (Unpublished data, 1953)
8. Asaro, F., and Perlman, I. (Unpublished data, 1953)
9. Asaro, F., Stephens, F., and Perlman, I., *Phys. Rev.*, **92,** 1495 (1953)
10. Valladas, G., and Bernas, R., *Compt. rend.*, **236,** 2230 (1953)
11. Jackson, H. G., and Harvey, B. G. (Private communication, October, 1953)
12. Valladas, G., *Compt. rend.*, **237,** 1673 (1953)
13. Asaro, F., and Perlman, I., *Phys. Rev.*, **94,** 381 (1954)
14. Asaro, F., and Perlman, I., *Phys. Rev.*, **93,** 1423 (1954)
15. Asaro, F., Thompson, S. G., and Perlman, I., *Phys. Rev.*, **92,** 694 (1953)
16. Glass, R. A., *University of California Radiation Laboratory Unclassified Document UCRL-2560* (Doctoral thesis, Univ. of California, Calif., April, 1954)
17. Diamond, H., Magnusson, L. B., Mech, J. F., Stevens, C. M., Friedman, A. M., Studier, M. H., Fields, P. R., and Huizenga, J. R., *Phys. Rev.*, **94,** 1083 (1954)
18. Hummel, J. P., Chetham-Strode, A., Asaro, F., and Perlman, I. (Unpublished data)
19. Ghiorso, A., Thompson, S. G., Higgins, G. H., Harvey, B. G., and Seaborg, G. T., *Phys. Rev.*, **95,** 293 (1954)
20. Thompson, S. G., Ghiorso, A., Harvey, B. G., and Choppin, G. R., *Phys. Rev.*, **93,** 908 (1954)
21. Ghiorso, A., Rossi, G. B., Harvey, B. G., and Thompson, S. G., *Phys. Rev.*, **93,** 257 (1954)
22. Studier, M. H., Fields, P. R., Diamond, H., Mech, J. F., Friedman, A. M., Sellers, P. A., Pyle, G., Stevens, C. M., Magnusson, L. B., and Huizenga, J. R., *Phys. Rev.*, **93,** 1428 (1954)
23. Fields, P. R., Studier, M. H., Mech, J. R., Diamond, H., Friedman, A. M., Magnusson, L. B., and Huizenga, J. R., *Phys. Rev.*, **94,** 209 (1954)
24. Harvey, B. G., Thompson, S. G., Ghiorso, A., and Choppin, G. R., *Phys. Rev.*, **93,** 1129 (1954)
25. Hollander, J. M., Perlman, I., and Seaborg, G. T., *Revs. Mod. Phys.*, **25,** 469 (1953)
26. Briggs, G. H., *Revs. Mod. Phys.*, **26,** 1 (1954)
27. Sturm, W. J., and Johnson, V., *Phys. Rev.*, **83,** 542 (1951)
28. Rosenblum, S., and Dupouy, G., *Compt. rend.*, **194,** 1919 (1932); *J. Phys. radium*, **4,** 262 (1933)
29. Lewis, W. B., and Bowden, B. V., *Proc. Roy. Soc.* (*London*), [A] **145,** 235 (1934)
30. Collins, E. R., McKenzie, C. D., and Ramm, C. A., *Proc. Roy. Soc.* (*London*), [A]**216,** 219 (1953)
31. Perlman, I., Ghiorso, A., and Seaborg, G. T., *Phys. Rev.*, **77,** 26 (1950)
32. [11]Seaborg, G. T., and Glass, R. A. (To be published)
33. Fournier, G., *Compt. rend.*, **184,** 878 (1927)
34. Elsasser, W., *J. Phys. radium*, **4,** 635 (1934)
35. Berthelot, A., *J. Phys. radium*, **3,** 17 (1942)
36. Schintlmeister, J., *Wien. Chem. Ztg.*, **46,** 106 (1943)

[11] Preliminary editions of this compilation have been given by Seaborg (*Phi Lambda Upsilon Third Annual Lecture Series for 1952*, Ohio State University, Columbus, Ohio) and by Glass (16).

37. Karlik, B., *Acta Phys. Austriaca*, **2**, 182 (1948)
38. Wapstra, A. H., *Nature*, **161**, 529 (1948)
39. Glueckauf, E., *Proc. Phys. Soc.* (*London*), **61**[A], 25 (1948)
40. Pryce, M. H. L., *Proc. Phys. Soc.* (*London*), **63**[A], 692 (1950)
41. Weizsäcker, C. F., *Z. Physik*, **96**, 431 (1935)
42. Bethe, H. A., and Bacher, R. F., *Revs. Mod. Phys.*, **8**, 82, 104, 165 (1936)
43. Bohr, N., and Wheeler, J. A., *Phys. Rev.*, **56**, 426 (1939)
44. Perlman, I., Ghiorso, A., and Seaborg, G. T., *Phys. Rev.*, **74**, 1730 (1948)
45. Templeton, D. H., and Perlman, I., *Phys. Rev.*, **73**, 1211 (1948)
46. Templeton, D. H., Howland, J. J., and Perlman, I., *Phys. Rev.*, **72**, 758 (1947)
47. Neumann, H. M., and Perlman, I., *Phys. Rev.*, **78**, 191 (1950)
48. Barton, G. W., Ghiorso, A., and Perlman, I., *Phys. Rev.*, **82**, 13 (1951)
49. Karraker, D. G., and Templeton, D. H., *Phys. Rev.*, **81**, 510 (1951)
50. Karraker, D. G., Ghiorso, A., and Templeton, D. H., *Phys. Rev.*, **83**, 390 (1951)
51. Momyer, F. F., Hyde, E. K., Ghiorso, A., and Glenn, W. E., *Phys. Rev.*, **86**, 805 (1952)
52. Momyer, F. F., and Hyde E. K. (To be published); Momyer, F. F., *University of California Radiation Laboratory Unclassified Report UCRL-2060* (Doctoral thesis, December, 1952)
53. Huizenga, J. R., and Magnusson, L. B. (Private communication, April, 1954)
54. Ghiorso, A., Thompson, S. G., Harvey, B. G., and Choppin, G. R. (Unpublished data)
55. Stähelin, P., and Preiswerk, P., *Helv. Phys. Acta*, **24**, 623 (1951)
56. Sengupta, S., *Phys. Rev.*, **87**, 1136 (1952)
57. Broniewski, A., *Can. J. Phys.*, **29**, 193 (1951)
58. Rasmussen, J. O., Thompson, S. G., and Ghiorso, A., *Phys. Rev.*, **89**, 33 (1953)
59. Porschen, W., and Riezler, W., *Z. Naturforsch.*, **8a**, 502 (1953)
60. Dunlavey, D. C., and Seaborg, G. T., *Phys. Rev.*, **92**, 206 (1953)
61. Waldron, E. C., Schultz, V. A., and Kohman, T. P., *Phys. Rev.*, **93**, 254 (1954)
62. Asaro, F., and Perlman, I., *Phys. Rev.*, **87**, 393 (1952)
63. Goldhaber, M., and Sunyar, A. W., *Phys. Rev.*, **83**, 906 (1951)
64. Horie, H., Umezawa, M., Yamaguchi, Y., and Yoshida, S., *Progr. Theoret. Phys.* (*Japan*), **6**, 254 (1951)
65. Scharff-Goldhaber, G., *Phys. Rev.*, **90**, 587 (1953)
66. Flowers, B. H., *Phys. Rev.*, **86**, 254 (1952)
67. De Shalit, A., and Goldhaber, M., *Phys. Rev.*, **92**, 1211 (1953)
68. Bohr, A., and Mottelson, B. R., *Kgl. Danske Videnskab. Selskab, Mat.-fys. Medd.*, **27**, No. 16 (1953)
69. Ford, K. W., *Phys. Rev.*, **90**, 29 (1953)
70. Stähelin, P., and Preiswerk, P., *Helv. Phys. Acta*, **24**, 623 (1951)
71. Rosenblum, S., and Valadares, M., *Compt. rend.*, **235**, 711 (1952)
72. DeBenedetti, S., and Minton, G. H., *Phys. Rev.*, **85**, 944 (1952)
73. Rosenblum, S., Valadares, M., and Guillot, M., *J. Phys. radium*, **15**, 129 (1954)
74. Rosenblum, S., Valadares M., and Guillot, M., *Compt. rend.*, **234**, 1767 (1952)
75. Milton, J. C. D., and Frazer, J. S., *Bull. Am. Phys. Soc.*, **29**, 40 (1954)
76. Battey, J., Madansky, L., and Rasetti, F., *Phys. Rev.*, **89**, 182 (1953)
77. Rosenblum, S., Valadares, M., and Guillot, M., *Compt. rend.*, **235**, 238 (1952)
78. Beling, J. K., Feld, B. T., and Halpern, I., *Phys. Rev.*, **84**, 155 (1951)
79. Temmer, G. M., and Wyckoff, J. M., *Phys. Rev.*, **92**, 913 (1953)
80. Grover, J. R., and Seaborg, G. T. (Unpublished data)
81. Church, E. L. (Private communication, Dec., 1953)

82. Bohr, A., and Mottelson, B. R., *Phys. Rev.*, **89,** 316 (1953); **90,** 717 (1953)
83. Church, E. L., and Goldhaber, M., *Bull. Am. Phys. Soc.*, **29,** 38 (1953)
84. Martin, D. G. E., and Richardson, H. O. W., *Proc. Phys. Soc. (London)*, **63**[A], 223 (1950)
85. Petch, H. E., and Johns, M. W., *Phys. Rev.*, **80,** 478 (1950)
86. Kraushaar, J. J., and Goldhaber, M., *Phys. Rev.*, **89,** 1081 (1953)
87. Slätis, H., and Siegbahn, K., *Determination of Multipole Orders from Internal Pair Formation*, p. 153 (M. Siegbahn Commemorative Volume, Almqvist and Wiksells Boktryckeri AB, Uppsala, Sweden, 845 pp., 1951)
88. Elliott, L. G., Graham, R. L., Walker, J., and Wolfson, J. L., *Phys. Rev.*, **93,** 356 (1954)
89. Stephens, F., Asaro, F., and Perlman, I. (Unpublished data)
90. Rasmussen, J. O., *Arkiv. Fysik*, **7,** 185 (1953)
91. Asaro, F., Reynolds, F. L., and Perlman, I., *Phys. Rev.*, **87,** 277 (1952)
92. Rosenblum, S., Perey, M., Valadares, M., and Guillot, M. (Private communication, October, 1952)
93. Bethe, H. A., *Revs. Mod. Phys.*, **9,** 69 (1937)
94. Gamow, G., and Critchfield, C. L., *Atomic Nucleus and Nuclear Energy Sources*, Chapt. VI (Oxford University Press, New York, 11 N. Y., 344 pp., 1949)
95. Preston, M. A., *Phys. Rev.*, **71,** 865 (1947)
96. Winslow, G. H., and Simpson, O. C., *Argonne National Laboratory Unclassified Reports ANL-4841* (June, 1952); *ANL-4901* (December, 1952); *ANL-4910* (January 1953)
97. Devaney, J. J., *Phys. Rev.*, **91,** 587 (1953)
98. Perlman, I., and Ypsilantis, T. J., *Phys. Rev.*, **79,** 30 (1950)
99. Kaplan, J., *Phys. Rev.*, **81,** 962 (1951)
100. Biswas, S., and Patro, A. P., *Indian J. Phys.*, **22,** 539 (1948)
101. Berthelot, A., *J. Phys. radium*, **3,** 52 (1942)
102. Biswas, S., *Indian J. Phys.*, **23,** 51 (1949)
103. Ambrosino, G., and Piatier, H., *Compt. rend.*, **232,** 400 (1951)
104. Rasmussen, J. O., *University of California Radiation Laboratory Unclassified Document UCRL-1473* (Doctoral thesis, Univ. of California, Calif., January, 1952)
105. Frauenfelder, H., Lawson, J. S., Jr., and Jentschke, W., *Phys. Rev.*, **93,** 1126 (1954)
106. Asaro F., and Perlman, I., *Phys. Rev.*, **91,** 763 (1953)
107. Preston, M. A., *Phys. Rev.*, **75,** 90 (1949)
108. Hill, D. L., and Wheeler, J. A., *Phys. Rev.*, **89,** 1102 (1953)
109. Rasmussen, J. O., *University of California Radiation Laboratory Unclassified Document UCRL-2431* (December, 1953)
110. Fred, M., and Tomkins, F. S., *Phys. Rev.*, **89,** 318 (1953)
111. Tomkins, F. S., *Phys. Rev.*, **73,** 1214 (1948)
112. Vander Sluis, K. L., and McNally, J. R., Jr., *J. Opt. Soc. Amer.*, **44,** 87 (1954)
113. Rosenblum, S., Valadares, M., Blandin-Vial, J., and Bernas, R., *Compt. rend.*, **238,** 1496 (1954)
114. Hummel, J. P., Asaro, F., and Perlman, I. (Unpublished data)
115. Dunlavey, D. C., and Seaborg, G. T. (Private communication, 1953)
116. Hulet, E. K., Univ. of California Radiation Lab. Unclassified Doc. UCRL-2283 (July, 1953); *An Investigation of the Isotopes of Berkelium and Californium* (Doctoral thesis, University of California, Berkeley, Calif., 1953)

POSITRONIUM[1]

By S. DeBenedetti and H. C. Corben
Carnegie Institute of Technology, Pittsburgh, Pennsylvania

In these days when the attention of the physicist is concentrated on the study of queer particles and of interactions which escape our comprehension, it is somewhat refreshing to turn our minds towards a subject which does not lack of fundamental importance and about which we can claim a certain amount of understanding. Such a subject is the behavior of electrons and positrons and their interaction with electromagnetic radiation. In this article we consider a particular example in this field: the annihilation of positron-electron pairs and the formation of the quasi-stable atom of positronium. Although such studies cannot be said to have brought basic changes in our thinking, they have resulted in a well organized body of information which can be regarded with a sense of aesthetic satisfaction.

Introduction

The discovery of positive electrons (1) was immediately followed by a series of investigations in order to prove that these particles exhibited the properties predicted by Dirac theory (2). It was found that positrons were produced in cosmic ray showers (3) and could be created by γ-rays from radioactive sources (4). Such creation occurred, as required for the simultaneous conservation of energy and momentum, in the vicinity of an atomic nucleus; its cross section was proportional to the square of the atomic number (5), as the theory predicted. Eventually, the production of positron-electron pairs was observed in the gas of a cloud chamber (6).

The ratio e/m of electrons and positrons was compared experimentally and found to be the same, first within an error of 15 per cent (7), then within 2 per cent (8), and finally within 0.01 per cent (9).

As a direct consequence of the interaction of electrons and electromagnetic field it was anticipated that the rest mass of a pair of positive and negative electrons could be radiated in the form of electromagnetic energy. From the condition of momentum conservation it follows that at least two quanta must be emitted unless the electron is strongly bound to a nucleus or is very near to another electron. The most probable process is that in which the positron comes to rest before annihilating with the emission of two quanta which then move in opposite directions, each with an energy mc^2.

The phenomenon of positron annihilation has been experimentally verified in considerable detail. In the pioneering work of Thibaud (7) positrons produced by γ-rays from a radioactive source were concentrated with a trochoidal method on an absorber where they came to rest. From this absorber γ-rays of about 0.5 Mev emerged and could be identified with the annihila-

[1] The survey of literature pertaining to this review was concluded in April, 1954.

tion radiation. With the discovery of artificial radioactive β^+ emitters, more convenient sources of positrons became available. Performing with these sources an experiment similar to that of Thibaud, Joliot (10) proved that the positrons of β-decay are of the same nature as those produced by the materialization of γ-rays. Klemperer (11) was the first to prove with a coincidence experiment that two simultaneous γ-rays resulted from the annihilation process. More recently, Beringer & Montgomery (12) demonstrated that the two quanta are emitted in opposite directions within one degree. Concerning the energy of the annihilation line, recent studies (13, 14) have confirmed the expected value with such accuracy that one may state that the rest energies of the positron and electron are the same within one part in 10^4. Thus, all experimental results are in good agreement with the view that positive and negative electrons are "anti-particles" in the sense of Dirac theory.

However, before annihilation takes place, positive and negative electrons behave as stable particles which attract each other because of their opposite charges. As a result they may form a bound system, in many ways similar to an atom. The possible existence of such a quasi-stable system was first suggested by Mohorovičić (15) in 1934. Later, Ruark (16) introduced the name of positronium.

If positronium is formed its states would be similar to those of hydrogen, the main difference being that the reduced mass is one-half the electron's mass. The reduced mass correction decreases the energy of the states to about one half of that of hydrogen and increases by a factor two the linear dimensions of the wave functions.

If formed in an excited $l \neq 0$ state, positronium survives long enough to emit a line of the characteristic optical spectrum, until it reaches one of the S states, from which it annihilates rather than radiating optically. In the ground state the spins of the two electrons can be parallel (1^3S triplet positronium or orthopositronium) or antiparallel (1^1S, singlet positronium or parapositronium). These two states are substantially different in their annihilation properties because of the existence of selection rules preventing the annihilation of the ^3S state with the emission of only two γ-rays. Thus, the annihilation of parapositronium is the usual two-quantum or singlet annihilation, whilst that of orthopositronium is the higher order process of three-quantum or triplet annihilation.

Though positronium can be observed in principle through the emission of its spectral lines, its existence has so far been established only through the annihilation behavior of its triplet state.

Although theoretically the systems $2e^+ + e^-$, $2e^- + e^+$ and $2e^+ + 2e^-$ also have small positive binding energies (17 to 20), they have not yet been observed and we shall not discuss them in this article. Systems arising by attachment of a positron to an atom, ion or molecule may well be stable apart from the annihilation process (21, 22), and indeed such dynamical stability has been established theoretically for the system $P + e^- + e^+$ (P = proton) (23, 24). In this paper, however, we shall be concerned almost exclusively with the positronium atom $e^+ + e^-$.

Before proceeding to a more detailed discussion of recent experimental work it will be necessary to present an outline of the theory of the annihilation process.

Theory of the Annihilation Process

General arguments and selection rules.—Although the theory of annihilation can be developed without ambiguity from the knowledge of the fields involved and of their interaction, it is of interest to start by studying the consequences of the invariance properties of the initial and final states under rotation, reflection, and charge conjugation. For this, we shall follow considerations which several authors (25 to 31) have developed mainly in connection with the disintegration properties of particles for which a field theory has not been developed. The use of this method, in our case, has the advantage of simplicity compared to the cumbersome complete treatment. Naturally, the generality of the method is also its limitation.

Let us confine our attention to annihilation at low relative kinetic energy: in this case only the S states of the pair (and in particular of positronium) are of interest since for higher angular momenta the wave function of positron and electron do not overlap sufficiently. The cases of ^1S and ^3S, however, will have to be considered separately.

The ^1S state, having total angular momentum 0 is described by a single wave function, which a priori could have either even or odd parity (scalar or pseudoscalar); the ^3S state, of $J=1$, requires for its representation three functions (related to the three m states) which transform as the components of a vector or of a pseudovector. (The components of a vector have odd parity, changing their sign under inversion of the coordinate axes, and those of a pseudovector have even parity.)

If an isolated system undergoes a change, its parity as well as its angular momentum remains unchanged. Thus, for instance, if the state of a pair is pseudoscalar, the state of the resulting annihilation radiation must also be pseudoscalar.

Let us now consider the state resulting from the process of two quantum annihilation. This is characterized by three vectors, the momentum $\mathbf{p}$ of one quantum and the two polarization vectors $\boldsymbol{\varepsilon}_1$ and $\boldsymbol{\varepsilon}_2$. Since the operator representing the creation of a photon in the polarization state $\boldsymbol{\varepsilon}$ is proportional to $\boldsymbol{\varepsilon}$, the state as a whole must be a linear function of the two vectors $\boldsymbol{\varepsilon}_1$ and $\boldsymbol{\varepsilon}_2$. Considering the limitation $\mathbf{p}\cdot\boldsymbol{\varepsilon}_1=o=\mathbf{p}\cdot\boldsymbol{\varepsilon}_2$, it can have one of the following forms:

$\boldsymbol{\varepsilon}_1\cdot\boldsymbol{\varepsilon}_2$	$f(\lvert\mathbf{p}\rvert)$	(scalar)
$\boldsymbol{\varepsilon}_1\times\boldsymbol{\varepsilon}_2\cdot\mathbf{p}$	$f(\lvert\mathbf{p}\rvert)$	(pseudoscalar)
$(\boldsymbol{\varepsilon}_1\cdot\boldsymbol{\varepsilon}_2)\mathbf{p}$	$f(\lvert\mathbf{p}\rvert)$	(vector)
$\boldsymbol{\varepsilon}_1\times\boldsymbol{\varepsilon}_2$	$f(\lvert\mathbf{p}\rvert)$	(pseudovector)
$(\boldsymbol{\varepsilon}_1\times\boldsymbol{\varepsilon}_2\cdot\mathbf{p})\mathbf{p}$	$f(\lvert\mathbf{p}\rvert)$	(pseudovector)

where the $f(|\mathbf{p}|)$ are unspecified functions of $|\mathbf{p}|$. If one now considers the restrictions imposed by the Bose statistics of the quanta, which require that

the state be symmetrical with respect to the exchange of the two photons ($\boldsymbol{\varepsilon}_1 \rightarrow \boldsymbol{\varepsilon}_2$, $\boldsymbol{\varepsilon}_2 \rightarrow \boldsymbol{\varepsilon}_1$, $\mathbf{p} \rightarrow -\mathbf{p}$), one finds immediately that the last three of the above forms are not allowed.

Since neither vector nor pseudovector states are permitted for two quanta traveling in opposite directions, it follows that the $J=1$, ^3S state of the pair cannot annihilate with the emission of two γ-rays. The most probable way of annihilation of a ^3S state is therefore the three quantum annihilation process.

Turning now to the annihilation from the ^1S state (which is therefore the state which must give rise to the two quanta), we are left with two possibilities, scalar and pseudoscalar. Experimentally, the two possibilities are distinguishable because the first corresponds to γ-rays plane polarized in the same plane, the second to γ-rays plane polarized in perpendicular planes. In agreement with the prediction of the complete theory, experiment shows that the annihilation quanta are polarized in perpendicular directions. Thus, the ^1S state is pseudoscalar; or, in other words, the parity of the electron is opposite to that of the positron.

The experimental work on this problem followed the suggestion (17, 32, 33) that if the photons are Compton scattered, their relative polarization would be revealed by the angular distribution of the coincidences between the two scattered radiations. For cross-polarized quanta at 82° scattering angle for each photon, the number of coincidences between counters placed to detect them is in the ratio 2.85 for counters of azimuth differing by $\pi/2$, to unity for counters with the same azimuth. The effect has been observed (34, 35, 36) and, when one takes into account the finite solid angle subtended by the counters, the results are in agreement with theory. Photo-electrons ejected by the two quanta also show an azimuthal correlation (32) which has been observed (37).

For the sake of completeness it is worth proving that the ^1S state cannot annihilate with the emission of three or any other odd number of γ-rays. This proof can be obtained by considering the operation of charge conjugation which consists in the change in sign of all electric charges and electromagnetic fields. For a positron-electron pair, this operator is equivalent to charge exchange which in turn equals parity $\times$ spin exchange.[2] Since a singlet state is odd with respect to spin exchange, it is therefore even with respect to charge conjugation. As to the final state, the charge conjugation operator reverses the sign of each vector $\boldsymbol{\varepsilon}$, and thus has the eigenvalue $(-1)^n$ for a state consisting of n quanta. Finally, since the charge conjugation operator is a constant of the motion, the ^1S state can annihilate only into an even number of quanta. Similarly, the ^3S state can annihilate only into an odd number of quanta.

[2] Consider the state: electron at $\mathbf{r}$ with spin α, positron at $-\mathbf{r}$ with spin β. Under reflection in the origin, this becomes: electron at $-\mathbf{r}$ with spin α, positron at $\mathbf{r}$ with spin β, since the spins being axial vectors are not changed by reflection. Under spin exchange this latter state becomes: electron at $-\mathbf{r}$ with spin β, positron at $\mathbf{r}$ with spin α; i.e., charge exchange = spin exchange $\times$ parity = parity $\times$ spin exchange.

Two quantum annihilation.—In the lowest approximation the annihilation of a free positron-electron pair is a second order process which may be represented by the Feynman diagram of Figure 1. The order of magnitude of the cross section for this phenomenon can be obtained from the following simple dimensional argument. If one neglects the Coulomb attraction between the members of the pair (an approximation equivalent to the "plane wave" quantum mechanical treatment) the transition probability will be proportional to the fourth power of e; if one considers relative velocities $v \ll c$,

FIG. 1. Feynman diagram for the process of two quantum annihilation.

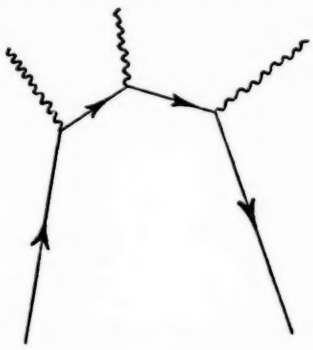

FIG. 2. Feynman diagram for the process of three quantum annihilation.

the transition probability will be independent of v (and the cross section will vary as $1/v$), since the initial kinetic energy is negligible compared to the energy available for the process. Thus we can write

$$\sigma_{2\gamma} \approx (\alpha^2/\beta) f(\hbar, c, m) \quad \text{where} \quad \alpha = e^2/\hbar c, \ \beta = v/c.$$

Since f must have the dimensions of an area we have no other choice but

$$\sigma_{2\gamma} \approx (\alpha^2/\beta)(\hbar/mc)^2 = r_0^2 c/v \quad \text{with} \quad r_0 = e^2/mc^2 = 2.8 \times 10^{-13} \text{ cm}.$$

Detailed calculation in the plane wave approximation (38) gives the result:

$$\sigma_{2\gamma} = \frac{\pi r_0^2}{\gamma + 1}\left[\frac{\gamma^2 + 4\gamma + 1}{\gamma^2 - 1} \ln (\gamma + \sqrt{\gamma^2 - 1}) - \frac{\gamma + 3}{\sqrt{\gamma^2 - 1}}\right]$$

for a positron of energy γmc^2. In the limit $\gamma \to 1 (v \ll c)$, this becomes

$$\sigma_{2\gamma} = \pi r_0^2 c/v \qquad 1.$$

in order of magnitude agreement with the value estimated above.

These cross sections represent an average over initial spin states. Otherwise one would have

$$\begin{aligned} {}^3\sigma_{2\gamma} &= 0 \quad \text{for triplet collisions,} \\ {}^1\sigma_{2\gamma} &= 4\sigma_{2\gamma} \quad \text{for singlet collisions.} \end{aligned} \qquad 2.$$

The effect of Coulomb attraction can be included considering that this results in a distortion of the wave function which brings the positron and

the electron closer to each other. Since the rate of transition is proportional to the probability of finding the positron at the position of the electron, the above cross sections must be multiplied by a factor $|\psi(0)|^2$, where ψ is a properly normalized Coulomb wave function. For positive energy states one has (ref. 2, page 84)

$$|\psi(0)|^2 = 2\pi\xi[1 - \exp(-2\pi\xi)]^{-1} \qquad \xi = \frac{\alpha}{\beta} = \frac{c}{137v} \tag{3.}$$

But it is the bound negative energy states which are of special importance to us, since they describe the atom of positronium. For an S state of positronium of total quantum number n, $|\psi(0)|^2 = 1/\pi(2na_0)^{-3}$ where $a_0 = r_0/\alpha^2$ is Bohr's radius, and the factor 2 arises from the reduced mass correction. Thus the mean lives ${}^1\tau_{2\gamma}$ of the ${}^1S$ positronium states are given by

$$\frac{1}{{}^1\tau_{2\gamma}} = {}^1\sigma_{2\gamma} v |\psi(0)|^2 = \frac{1}{2}\frac{\alpha^5}{n^3}\frac{mc^2}{\hbar} \tag{4.}$$

Numerically:

$${}^1\tau_{2\gamma} = 1.25 \times 10^{-10} n^3 \text{ sec.} \tag{5.}$$

For comparison, one notes that the mean lives for the emission of optical radiation of the S states of positronium (twice as long as those of the corresponding terms of the hydrogen atom) are: $2S$: ∞ (metastable); $3S$:3.2 10^{-7} sec.; $4S$:4.6 10^{-7} sec., etc. Thus, positronium will annihilate rather than emit an optical line from its ${}^1S$ states. For state of nonvanishing angular momenta, on the other hand, the annihilation probability is negligible compared to the probability of optical transition.

Three-quantum annihilation.—If a pair is in a ${}^3S$ state the most probable process leading to its annihilation is that in which three quanta are emitted. From the corresponding lowest order Feynman diagram (Figure 2) it would appear that, for given n,

$$\frac{1}{{}^3\tau_{3\gamma}} \approx \alpha \frac{1}{{}^1\tau_{2\gamma}}$$

since this process is of one higher order. Detailed calculations (39, 40, 41) yield the result, first given by Ore & Powell:

$${}^1\tau_{2\gamma}/{}^3\tau_{3\gamma} = (4/9\pi)(\pi^2 - 9)\alpha = 1/1115 \approx \alpha/8 \tag{6.}$$

or numerically:

$${}^3\tau_{3\gamma} = 1.4 \times 10^{-7} n^3 \text{ sec.} \tag{7.}$$

For the ratio of the spin averaged cross sections one obtains

$$\frac{\sigma_{3\gamma}}{\sigma_{2\gamma}} = \frac{\frac{3}{4}{}^3\sigma_{3\gamma}}{\frac{1}{4}{}^1\sigma_{2\gamma}} = 3({}^1\tau_{2\gamma}/{}^3\tau_{3\gamma}) = 1/372 \tag{8.}$$

or

$$\sigma_{3\gamma} = (4/3)(\pi^2 - 9)\alpha r_0^2 c/v.$$

These results imply that a ^1S state annihilates 1115 times faster than the corresponding ^3S state, and that the ratio of the numbers of three-quantum to two quantum events in collisions with statistically distributed spins is 1/372.

The energy spectrum of the photons emitted in the three quantum annihilation process has been calculated by Ore & Powell and is shown in Figure 3, where the dotted curve represents the statistical estimate obtained by considering the available volume in momentum space.

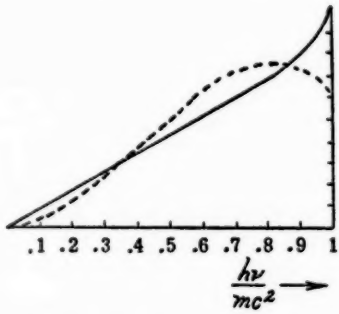

FIG. 3. Theoretical spectrum of the gamma rays from the three quantum annihilation process. Full curve: complete theory; dotted curve: statistical theory. [Ore, A., and Powell, J. L., *Phys. Rev.*, **75**, 1696 (1949).]

General arguments such as those previously discussed may also be applied to the special case of symmetric disintegration into three photons of equal energy, at 120° to each other. From the rotational symmetry properties of this final state it has been shown (31) that the ^1S state cannot decay into three such photons [that it cannot decay into any state of three photons has already been shown in another section (i.e., *General arguments and selection rules*) to result from the condition of invariance under charge conjugation]. For the $m = \pm 1$ levels of the ^3S state, it follows by such arguments that if two quanta are right circularly polarized the other is left circularly polarized, and that for symmetric annihilation from these levels the ratio of the number of quanta polarized perpendicular to their plane of detection to those polarized in this plane is 2.

These results, which apply only to the symmetrical case, are naturally in agreement with the consequences of perturbation theory, on the basis of which they may be extended by avoiding the spin averaging and polarization summing processes performed in the computation of $^3\tau_{3\gamma}$. In this way, it has been shown by Drisko (41) that, to the lowest order of perturbation theory, in the case of symmetric disintegration the ratio of the number of quanta polarized perpendicular to their plane of detection to those polarized in this plane is 5/1 for the state $m=0$ and 2/1 for the states $m = \pm 1$. Thus, for unpolarized positronium this ratio is

$$\frac{n_\perp}{n_\parallel} = \frac{1}{3}\left(\frac{5}{1}\right) + \frac{2}{3}\left(\frac{2}{1}\right) = \frac{3}{1} \qquad 9.$$

If the three quanta emerging from the ^3S state are observed in the plane perpendicular to the axis of quantization, it also follows from Drisko's calculations that, of the triple coincidences recorded, a fraction $f = 1/2$ (instead of the statistical value 1/3) come from the $m = 0$ substate. If only one of the quanta is observed, an integration over the angles and momenta consistent with energy and momentum conservation yields the result that of the total number of quanta emitted at an angle θ with the direction of quantization, the fraction

$$f(\theta) = \frac{(\pi^2 - 19/2)\sin^2\theta + 1/3}{2(\pi^2 - 9)} \qquad 10.$$

comes from the $m = 0$ state. Thus at 90°, the $m = 0$ state contributes

$$\frac{\pi^2 - 55/6}{2(\pi^2 - 9)} \doteq 40\% \qquad 11.$$

of the quanta (instead, again, of the statistical value of 1/3).

A comparison with experimental results of these theoretical predictions, as well as those of equations 8 and 9, is discussed in later sections of this article (pages 201–2 and 213–15).

The Formation of Positronium in Gases

Discovery of positronium.—We have seen that if the spins of the positive and negative electrons are randomly oriented, triplet annihilation is expected to be much less frequent than singlet annihilation, the frequency ratio being of the order of α. However, the formation of positronium basically changes this state of affairs, as may be easily seen from the following considerations.

We should expect that this atom is formed in the triplet state three times as frequently as in the singlet. Then, the ratio 3/1 in the abundance of the two spin states is maintained until annihilation occurs (unless altered, as discussed later, by external causes, such as collisions capable of inducing spin flips). Thus, if all the positrons from a given source produced positronium, three-fourths of them (instead of 1/372) would annihilate with the emission of three γ-rays. The small probability of triplet annihilation will not affect the frequency of its occurrence, but will be revealed through the long mean life of the orthopositronium atoms.

It is evident that, in order to reduce the collisions which may decompose positronium or convert triplet into singlet, it is desirable to work in a rarefied medium, such as a gas. At small densities, however, the probability of annihilation of free positrons is also reduced, giving rise to a longer mean life independently of positronium formation. The annihilation probability of the free positrons, however, is proportional to the gas pressure, while that of triplet positronium should be pressure independent.

The first observations indicating that the mean life of positrons in certain gases was not inversely proportional to pressure were made by Shearer & Deutsch (42). This work was followed by experiments of Deutsch (21, 43) which resulted in the discovery of positronium.

The method consisted in the measurement of the positron lives in gases by means of the technique of delayed coincidences. The source used was the isotope Na^{22} which emits positrons and, practically simultaneously with each positron, a γ-ray of 1.3 Mev. The source was mounted on the face of a scintillation counter (see Figure 4) which detected the 1.3 Mev γ-rays, giving a signal simultaneous with the birth of the positrons. The positrons were made

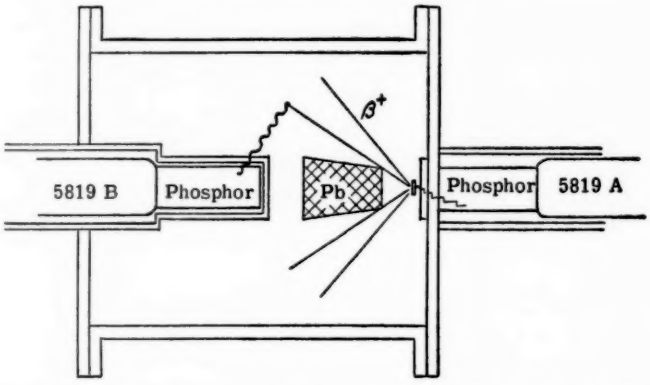

FIG. 4. Apparatus to measure the lifetime of positrons in gases [Deutsch, M., Annihilation of positrons, Progress in Nuclear Physics, **3**, 141, Academic Press, New York, New York, (1953).]

to travel in a gas container where some stopped and annihilated; a second counter, shielded from the direct radiation of the source, detected the annihilation radiation, thus providing a signal simultaneous with the positron's death. The time between these two signals, and thus the positron decay curve was measured with a multi-channel coincidence circuit.

The resolution of the decay curves into the component resulting from positronium triplet and the component resulting from annihilations from free collisions, was made possible by the discovery that traces of nitric oxide vapors suppress the delayed coincidences attributable to the triplet positronium. The explanation of this effect is related to the fact that the NO molecule contains an odd number of electrons, and therefore possesses an unpaired electron whose spin can be flipped without requiring appreciable energy. When a positronium atom collides with this molecule, the two bodies can exchange an electron. If the electron exchanged is the unpaired one, this can be replaced in the molecule by an electron of opposite spin with the conversion of orthopositronium into parapositronium.

Deutsch found that the number of delayed coincidences in nitrogen gas

was decreased by about a factor three with the addition of 3 per cent NO, the remaining coincidences presumably resulting from annihilation of free positrons. But in dichlorodifluoromethane ("Freon 12") vapors, the addition of NO entirely eliminated the long life, indicating that in this substance, this was exclusively attributable to triplet positronium. From the value of the mean life extrapolated to zero pressure (Fig. 5) the rate of annihilation of triplet positronium was found to be $(6.8 \pm 0.7)\ 10^6$ sec.$^{-1}$ corresponding to a mean life of 1.5×10^{-7} sec., in excellent agreement with the computation of Ore & Powell (equation 7).

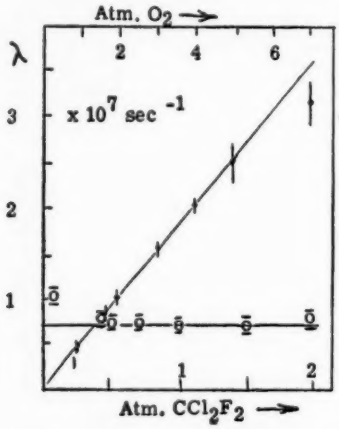

FIG. 5. Pressure dependence of annihilation probability for O_2 (points) and CCl_2F_2 (open circles) in apparatus of Fig. 4. [Deutsch, M., *Phys. Rev.*, **83**, 866 (1951).]

The pressure independence of the annihilation probability and the NO effect can be considered as very conclusive evidence of the existence of positronium. The numerical agreement between the experimental mean life and the computation of Ore & Powell is of considerable importance, being the first verification of a real third order process in the coupling of Dirac particles with the radiation field.

Methods for the detection of positronium.—The method of delayed coincidence described above is not the only nor the simplest technique which can be used for detecting the presence of positronium. Another method widely used by Deutsch in his later work consists in a measurement of the energy of the annihilation radiation by means of the pulse height analysis of the signals from a NaI(Tl) scintillation counter. For the 510 Kev line of the two quantum annihilation radiation, the pulse height distribution shows a peak resulting from photoelectrons and a continuum attributable to Compton electrons, separated by a well defined valley. The presence of γ-rays from three quantum annihilation, which are distributed continuously between 0 and 510 Kev (see theoretical distribution in Figure 3), results in a decrease of the

mc^2 photopeak and in an increase of the counting rate in the valley. This effect (Fig. 6) may be used to indicate the presence of positronium.

Another simple method was used by Pond (44), who detected the formation of positronium by observing the decrease in the number of double coincidences induced in two counters at 180° by the two γ-rays of the singlet annihilation radiation.

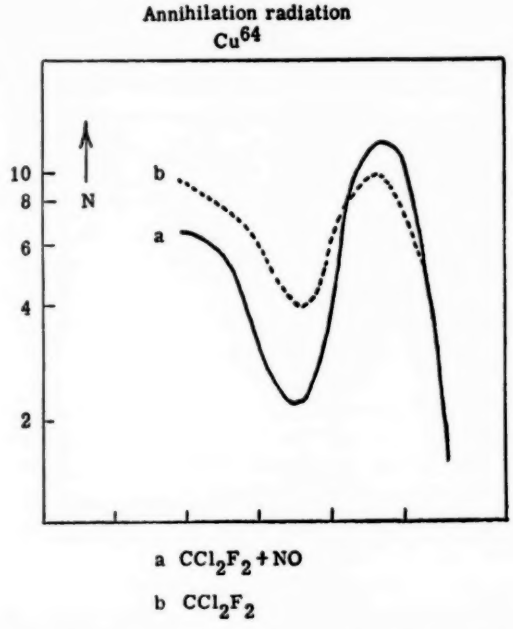

FIG. 6. Annihilation spectrum for positrons stopping in CCl_2F_2 with and without the addition of NO showing how one can distinguish singlet and triplet annihilation. [Deutsch, M., and Dulit, E., *Phys. Rev.*, **84**, 601 (1951).]

The most direct method of detecting the three quantum annihilation from orthopositronium is, obviously, a measurement of coincidences between the three γ-rays. Some experiments conducted with this method will be described in later sections.

Properties of the annihilation radiation from orthopositronium.—The triple coincidence method has been used to investigate experimentally the properties of the γ-rays emitted in triplet annihilation as well as to detect the presence of orthopositronium. In experiments conducted at the Carnegie Institute of Technology (45) the source consisted of a small bell-shaped container holding SF_6 vapors at different pressures up to 10 atmospheres; the Na^{22} activity was deposited on a thin support at the center of the container, in such a manner that most positrons stopped in the vapor where the formation of positronium was favored. Three NaI(Tl) scintillation counters, coplanar

with the source, were used in the measurement of triplet annihilation; the angular correlation was studied by varying their angle within the plane, and the background was determined by removing one counter from the plane. The counters were connected in coincidence, and their pulses were fed to separate differential pulse height selectors, so that each counter operated as a scintillation spectrometer for the coincident radiations.

After obtaining proof of the formation of positronium in the SF_6 vapor by observing the increase in the number of triple coincidences with the pressure of the gas in the container (Fig. 7), the energies of the coincident γ-rays were measured for a variety of angular arrangements. These were found to be in agreement with conservation of energy and momentum for the phenomenon of three quantum annihilation (Fig. 8).

Next, the angular dependence of the coincidences was studied. Since for each configuration of the counters the energy of the γ-rays is determined by the conservation laws, a measurement of angular distribution is equivalent to a measurement of the energy spectrum. The spectral distribution obtained from the experiments agreed with that computed by Ore & Powell. The errors of the measurements were small enough to distinguish between the statistical treatment (dotted curve, Figure 3) and the complete theory (full curve, Figure 3).

Finally, the polarization of one of the quanta was measured in relation to the plane of emission of the three photons (46). For this purpose one of the counters was protected from the direct radiation of the source by means of a lead wall. This counter was placed so that it could detect a triplet annihilation quantum only after this had been scattered (alternatively parallel and perpendicular to the plane of emission) by a polystyrene cylinder. The result showed predominance for polarization with the electric vector perpendicular to the plane, as expected from the theory (equation 9). Unfortunately, in order to get a reasonable counting rate it was necessary to make the counters and scatterer so large that it became difficult to make precise theoretical corrections for their finite size. With this limitation, the measured results were in agreement with the value given by equation 9. Thus these experiments provide an independent proof of the triplet annihilation of orthopositronium and confirm some details of the theoretical predictions.

Formation and decomposition of positronium.—The percentage of positrons forming positronium has been measured for various gases (44, 45, 47), including H_2, He, N_2, A, Freon, SF_6, and found to be of the order of 20 per cent; however, if these gases are contaminated with NO or with O_2 no positronium is observed.

The yield of positronium is increased by the application of electric fields (48); in A, the yield becomes 100 per cent for d.c. fields of 300 volts/cm. per atmosphere (49), or for sufficiently strong radio frequency fields. Addition of a few per cent CO_2 suppresses the effect of the electric field (22).

These phenomena can be understood considering that the binding energy of positronium (6.8 ev), is smaller than that of the electrons in most other

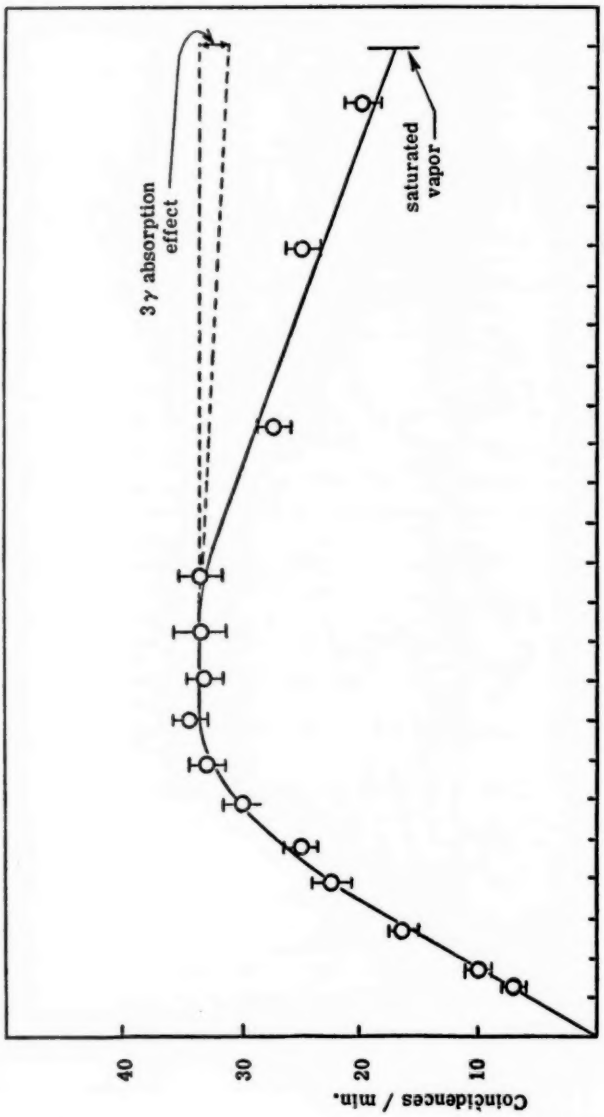

FIG. 7. Triple coincidences from SF_6 as a function of pressure. [DeBenedetti, S., and Siegel, R. T., *Phys. Rev.*, **94**, 955 (1954)].

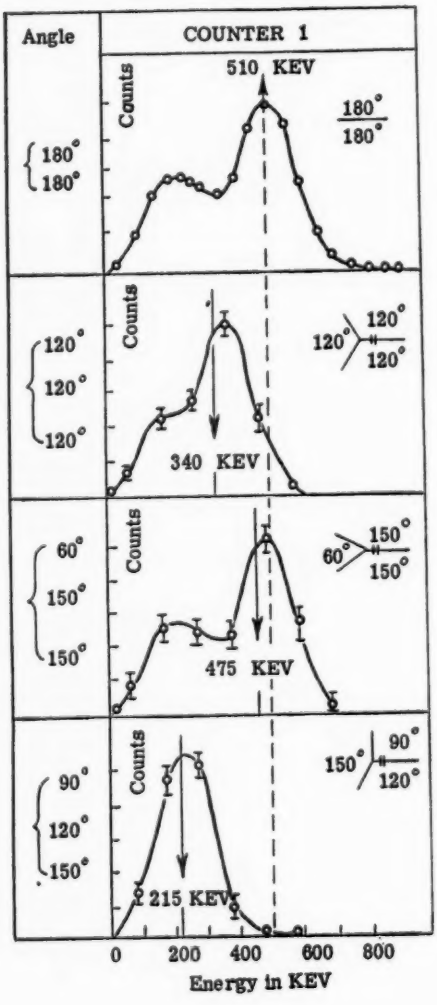

FIG. 8. Energy of γ-rays from three quantum annihilation. [S. DeBenedetti and R. T. Siegel, *Phys. Rev.*, **94**, 955 (1954)].

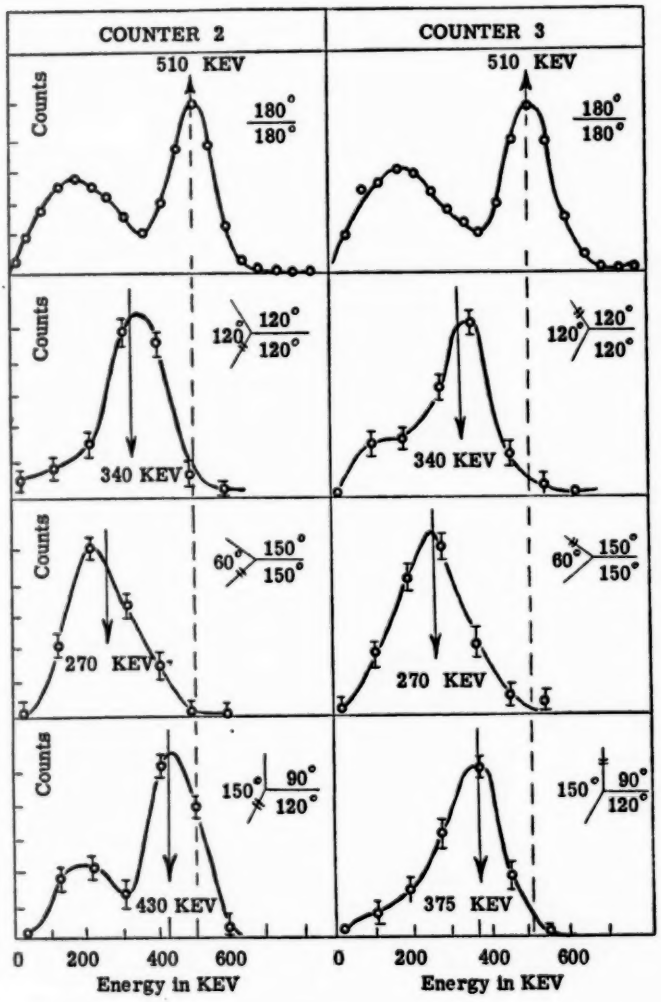
COUNTER 2
COUNTER 3
510 KEV
Counts
180°
180°
120°
120°
120°
340 KEV
60°
150°
150°
270 KEV
150°
90°
120°
430 KEV
375 KEV
0
200
400
600
Energy in KEV

molecules. Thus, only positrons of kinetic energy greater than the difference between the ionization potentials of the molecule and of positronium are energetically capable of capturing an electron to form positronium. On the other hand, if the energy of the positrons is large enough to excite or to ionize the molecule, positronium formation becomes negligible compared to these effects. There is, therefore, only a small kinetic energy band in which the positrons can form positronium. Semiquantitative development of these ideas (47, 50) leads to estimated yields in rough agreement with the observed ones.

The electric field increases the yield because it accelerates the slow positrons, bringing them back into the useful energy band. The addition of CO_2 suppresses this effect because inelastic collisions with this molecule prevent the acceleration of the positrons.

Once positronium is formed, it behaves like any other gaseous molecule up to the time of annihilation. It can be decomposed, or converted from its ortho to its para state (50) in molecular collisions. Typical in this respect is the conversion in collision with NO molecules, which occurs with a cross section of 8×10^{-17} cm^2. (22), and whose mechanism has already been discussed. It is interesting to note that NO_2 is also effective in producing ortho-para conversion, but not N_2O, which has an even number of electrons.

Collisions with O_2 induce ortho-para conversion with a cross section of 4.0×10^{-19} cm^2. (22). Here, the conversion is not related to exchange of electrons, but is produced by the magnetic field of the O_2 molecule.

Deutsch observed that Cl_2 and Br_2 suppress positronium with a cross section of the order of 10^{-16} cm^2. (22). In all probability one is faced in this case with a real chemical reaction in which a positronium halide is formed.

Even the gases which are efficient for positronium production seem to be somewhat effective for its destruction. The slight decrease in the mean life of orthopositronium with increasing pressure of Freon (Fig. 5) and the decrease in the number of triplet annihilations for high density of SF_6 vapors (Fig. 7), show this effect. The cross section is relatively small (9.7×10^{-22} cm^2. for SF_6) (45, 51), but still large enough to account for the almost complete quenching of orthopositronium in the liquid state, which has been observed in experiments with liquid N_2 and liquid Freon.

It appears from these studies that the formation and decomposition of positronium is related to the properties of the molecules of the surrounding gas; in a sense, it can be regarded as a chemical problem. Some scattered information has been found by physicists, as a byproduct of their interest in the physical properties of positronium and of its annihilation radiation. It would seem natural that the work should be continued by chemists, to whom positronium should present the challenge of a new element whose chemical properties have to be classified; and, owing to its extreme simplicity, it may be an element of particular value for the understanding of the mechanism of chemical reactions and for the study of the nature of the chemical bond.

Positron Annihilation and Positronium Formation in Condensed Materials

Momentum of the annihilating pairs.—A comparison of the annihilation probability with the rate of energy loss by ionization shows that most positrons should reach the end of their ionized path before annihilating, in condensed materials as well as in gases. Though the phenomenon of annihilation "in flight" has been observed (52, 53), it is a rare occurrence. More detailed considerations (54, 55) indicate that most .positrons should survive long enough to reach actual thermal equilibrium with the lattice of a solid absorber.

Positrons of such low-energy are effectively repelled by the atomic nuclei; as a consequence their wave function overlaps the wave function of atomic electrons only at the periphery of the atoms, and annihilation will take place mainly with the external valence electrons or, in the case of a conductor, with the free electrons. Since the momenta of these electrons are of the order of $mc/137$, and their energies of the order of 10 ev, the γ-rays of two quantum annihilation should have a spread of about 1/137 of a radian around 180°, and the mc^2 annihilation line should have a width of around 10 ev.

In agreement with these expectations, a departure from perfect antiparallelism of the two annihilation γ-rays was detected with a coincidence experiment (54). The result indicates that the average momentum of pairs annihilating in a Au absorber is 1.2 $mc/137$. Essentially the same value was obtained (for a Cu absorber) from the measurement, with a curved γ-ray spectrometer, of the Doppler width of the annihilation line (14, 56). A line width measurement with a β-spectrometer (57) gave a somewhat smaller value (0.52 $mc/137$), but still of the same order of magnitude.

These observations support the following points: (*a*) the positrons reach very low (possibly thermal) energy before annihilating; (*b*) only the external atomic electrons (the free electrons in the case of a conductor) participate appreciably in the annihilation.

More detailed studies of the angular spread of the annihilation radiation might eventually yield information on electronic states in solids. The work done thus far on the measurements of angular distributions from different absorbers (58, 59) has shown some interesting trends, but further investigations seem to be required before the usefulness of this approach to solid state problems can be assessed.

Mean lives of positrons in solids.—The experiments described so far are not sufficient to decide whether the slow positrons end their lives diffusing in a solid as free particles, or whether some bound system, possibly positronium, is formed previous to their annihilation.

A first experiment bearing on this point was performed by Madansky & Rasetti (60) who, assuming the first point of view, tried to measure the slow positrons' diffusion length. For this purpose they attempted to collect on a negatively charged electrode the slow positrons which should emerge from a solid absorber. This attempt was not successful, and it is possible that

its failure is attributable to the capture of positrons in bound states within the solids.

This possibility is corroborated by the work on positron mean lives in condensed materials. If the positrons annihilate in free collisions their mean life can be computed from the formula $\tau^{-1}=\sigma v N_e$ where σ is the annihilation cross section and N_e the number of electrons per unit volume. Care must be used in applying this expression, however, since because of the low energy of the positrons (*a*) the Coulomb attraction between the members of the pair should be included in the computation of σ and (*b*) the nuclear repulsion confines the positron to a region where the electron density is not equal to its average value.

For the case of the monovalent alkali metals one can reach what seem to be reasonable upper and lower limits of the annihilation life, assuming that free positrons annihilate against the conduction electrons only. For this case, the upper limit of the mean life may be obtained using the plane wave value of the annihilation cross section (equation 1). Since the probability of finding the conduction electrons anywhere in the solid is approximately constant, we can write $(\tau_{\max})^{-1}=\pi r_0^2 c N_A$ where N_A is the number of atoms per unit volume.

The lower limit of the mean life can be obtained including positron-electron attraction in the cross section (correction factor of formula 3 for $\xi \gg 1$) and using a model where the positron is at rest in a Fermi electron-gas of density N_A. After averaging over the electrons' velocities, one obtains $(\tau_{\min})^{-1}=[3\pi mc/(137 p_{\max})]\pi r_0^2 c N_A$ where $p_{\max}$ is the maximum momentum of the Fermi electron gas. The value $\tau_{\min}$ should be a lower limit since we have neglected the modulation of the wave functions in the crystal lattice, the positron's velocity and the dielectric constant of the medium.

The values of $\tau_{\min}$ and $\tau_{\max}$ in units of 10^{-10} sec. are shown below:

	Li	K	Cs
$\tau_{\max}$	29	102	160
$\tau_{\min}$	1.7	4.2	5.6

One expects from these considerations that the positron mean life in K should be at least 2.5×10^{-10} sec. longer than the mean life in Li. The experimental results contradict this expectation. Comparison measurements (61) indicated that, not only the mean lives in Li and K, but also those in all other conductors, including Al, Cu, Pb, were the same within 0.7×10^{-10} sec. These results were confirmed by Bell & Graham (62) who measured the absolute value of positron mean lives in different substances and found the value $(1.5\pm0.5)\ 10^{-10}$ sec. for all metals. A small difference between Pb and Al has been reported recently by Minton (63) who gives the value $(2.9\pm0.3)\ 10^{-10}$ sec. for Al and $(3.5\pm0.3)\ 10^{-10}$ sec. for Pb.

The small values of positron mean lives in conductors and their apparent equality for all metals are difficult to reconcile with the picture of freely diffusing positrons annihilating in collisions with the conduction electrons. Although the available theoretical and experimental evidence does not completely rule out the possibility of annihilation with the bound elec-

trons of the atomic cores, this effect has been disregarded in the interpretation of the mean lives, in view of the information reported in the preceding (page 207) section; instead, it has been assumed that the positrons do not end their lives diffusing freely. Thus, DeBenedetti & Richings suggest that the positron and conduction electrons form "some kind" of fast annihilating state, making the lifetime independent of the metal. More specifically, Bell & Graham are led to speak about positronium formation because of the apparent equality of the mean life of singlet positronium and that observed for positrons in metals.

On the other hand, several experiments have been performed in order to measure the ratio of three quantum to two quantum annihilation (45, 64, 65) in metals, and these have all given results near to the value 1/372 expected theoretically for randomly distributed spins. This fact implies that, if positronium is formed, rapid conversions from the *ortho* to the *para* states resulting from exchange collisions with the Fermi electrons reestablish statistical equilibrium.

Although in some metals, such as the alkali, the interstitial spaces would provide sufficient volume for positronium to exist virtually undistorted, in other tightly packed crystals the positronium wave function would have to be so distorted as to make doubtful the possibility of binding. Even in the most favorable cases the existence of positronium in a metal should not be regarded in a static sense, like the presence of an atom fixed in an interstitial space. Rather, it must be understood in conjunction with the continuous exchange of the electron partner, and with the possibility of migration across the lattice, accompanied by considerable deformation of the wave function. Thus, though it is possible that positronium might emerge as a neutral atom from a metal surface [as it has been suggested (55)], its existence within the metal itself would have to be regarded in a very general sense.

In connection with the mean lives of positrons in metals it seems appropriate to mention some recent communications (66, 67) according to which the life in superconducting Pb is considerably longer than that in Pb at normal temperatures.

In a number of insulators the positron lives are longer than in metals. This effect, first detected by the Carnegie group, was studied in greater detail by Bell & Graham. These authors discovered that, in certain materials such as quartz and Teflon, the positron decay curves could not be interpreted in terms of a single life, but resulted from the composite effect of two different lives. The short lived component is of the order of 10^{-10} sec. and accounts for about two-thirds of the positrons, while the remaining one-third decay with a mean life of the order of 10^{-9} sec. The percentage of the positrons in the two groups depends on the crystal structure and is different for crystalline and fused quartz.

In order to explain the presence of the two mean lives, Bell & Graham suggest that positronium is formed in these insulators. Parapositronium decays promptly and accounts for the short life, orthopositronium accounts for the longer life, which is a measure of the rate at which it is destroyed in

molecular collisions. In agreement with this view, the frequency of 3-quantum annihilation is noticeably greater in the insulators which exhibit the longer positron life (68, 69, 70). From this work, one feels justified in concluding that positronium, or something very similar to it, exists for a short time as a free atom in certain insulators.

Many features of the behavior of positrons in condensed materials remain to be investigated more completely before a detailed explanation of these observations can be found. It is possible that the continuation of this work may be of interest for the study of the physics of the solid state.

FINE STRUCTURE AND ZEEMAN EFFECT

Fine structure.—In discussing the fine structure of the levels of positronium, one notes immediately that terms which correspond in hydrogen to the hyperfine structure are in this case of the same order as those describing the fine structure, since the magnetic moment of the positron is so much greater than that of the proton. The magnetic interaction energy for positronium is, to the lowest order,

$$W_m = -\mu^2 \left\langle \frac{\boldsymbol{\sigma}_1 \cdot \boldsymbol{\sigma}_2}{r^3} - \frac{3\boldsymbol{\sigma}_1 \cdot \mathbf{r}\, \boldsymbol{\sigma}_2 \cdot \mathbf{r}}{r^5} \right\rangle$$

where $\mu = e\hbar/2mc$ and $\boldsymbol{\sigma}_1$, $\boldsymbol{\sigma}_2$ denote the spin states of the two particles. In the limit $r \longrightarrow 0$, this expression becomes, for S states (71),

$$W_m = (8\pi/3)\mu^2 \langle \boldsymbol{\sigma}_1 \cdot \boldsymbol{\sigma}_2 \rangle \langle \delta(\mathbf{r}) \rangle$$

i.e.

$$W_m = (8\pi/3)\mu^2 \boldsymbol{\sigma}_1 \cdot \boldsymbol{\sigma}_2 \, |\, \psi(0) \,|^2$$

with

$$\begin{aligned} \boldsymbol{\sigma}_1 \cdot \boldsymbol{\sigma}_2 &= \quad 1 \text{ (triplet states)} \\ &= -3 \text{ (singlet states)} \end{aligned}$$

and

$$|\, \psi(0) \,|^2 = \frac{1}{\pi} \left(\frac{me^2}{2\hbar^2 n} \right)^3 .$$

Thus

$$\begin{aligned} W_m &= \quad \frac{\alpha^4}{12} \frac{mc^2}{n^3} \text{ (triplet states)} \\ &= -\frac{\alpha^4}{4} \frac{mc^2}{n^3} \text{ (singlet states)} \end{aligned} \qquad 12.$$

However, also of the same order of magnitude is the annihilation force, absent in the case of ordinary atoms, arising from the process indicated by the second Feynman diagram of Figure 9. This corresponds to the fact that positronium spends part of the time in a virtual one-photon state. Since the general selection rules mentioned at the beginning of this article are also applicable to the virtual states, Figure 9(b) gives a contribution only for a state which is odd under charge conjugation, and in particular it modifies the ^3S level, leaving the ^1S level unchanged. Since the electron and positron charges are not always effective, the ^3S level is raised.

The process of virtual one-quantum annihilation introduces a correction W_a of order α^2 to the energy levels, themselves of order $\alpha^2 mc^2$. Thus we should

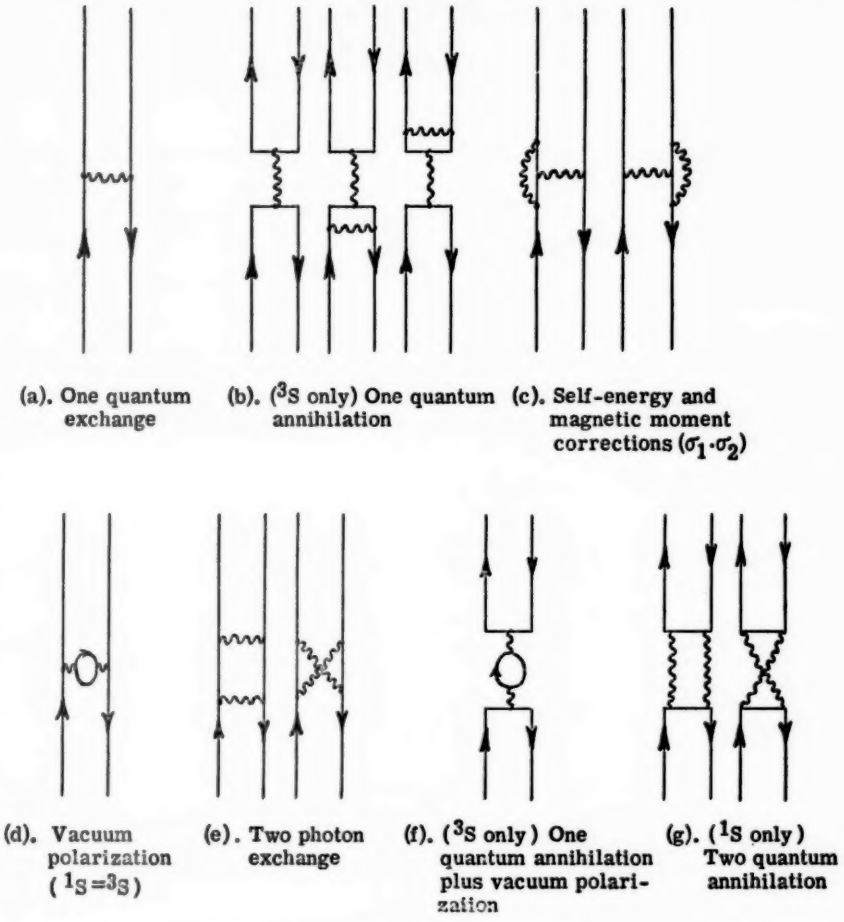
(a). One quantum exchange
(b). (^{3}S only) One quantum annihilation
(c). Self-energy and magnetic moment corrections ($\sigma_1 \cdot \sigma_2$)
(d). Vacuum polarization (^{1}S=^{3}S)
(e). Two photon exchange
(f). (^{3}S only) One quantum annihilation plus vacuum polarization
(g). (^{1}S only) Two quantum annihilation

FIG. 9. Feynman diagrams for the fine structure of the ground state of positronium.

expect that $Wa \sim \alpha^4 mc^2$, and indeed detailed calculations (72 to 76) yield the result

$$W_a = \frac{\alpha^4 mc^2}{4n^3} \quad (^3S) \qquad = 0 \quad (^1S) \tag{13.}$$

To this order, there are other relativistic effects which do not shift the ^1S level relative to the ^3S level, the complete results, for $l=0$, therefore being, apart from the obvious term in α^2,

$$W(^3S) = \frac{\alpha^4 mc^2}{n^3}\left(\epsilon + \frac{1}{12} + \frac{1}{4}\right)$$

$$W(^1S) = \frac{\alpha^4 mc^2}{n^3}\left(\epsilon - \frac{1}{4}\right)$$

with $\epsilon = -1/4 + (11/64n)$. The splitting of the 1^3S, 1^1S levels is thus, to terms of order α^4,

$$\Delta W = (7/12)\alpha^4 mc^2 = 8.45 \times 10^{-4} \text{ ev} = 2.044 \times 10^5 \text{ Mc./sec.} \qquad 14.$$

For $l \neq 0$, the splitting of the levels is much less (75).

The terms of order α^5 have been computed by Karplus & Klein (76) by approximating to the exact equation for positronium developed by Schwinger (77). The corrections to the energy up to terms of order α^5 arise from the diagrams of Figure 9. The results for the splitting of the $n=1$ state $W(^3S) - W(^1S)$ are

$$\Delta W_1 = \alpha^4 mc^2 \left[\frac{1}{3}\left(1 - \frac{3\alpha}{2\pi}\right)\right] \quad \text{Diagrams 9}(a), 9(e)$$

$$\Delta W_2 = \alpha^4 mc^2 \left[\frac{\alpha}{3\pi}\right] \quad \text{Diagrams 9}(c)$$

$$\Delta W_3 = 0 \quad \text{Diagrams 9}(d)$$

$$\Delta W_4 = \alpha^4 mc^2 \left[\frac{1}{4} - \frac{\alpha}{\pi}\right] \quad \text{Diagrams 9}(b)$$

$$\Delta W_5 = \alpha^4 mc^2 \left[-\frac{2\alpha}{9\pi}\right] \quad \text{Diagrams 9}(f)$$

$$\Delta W_6 = \frac{\alpha^5 mc^2}{2\pi}\left[1 - \ln 2 + \frac{i\pi}{2}\right] \quad \text{Diagrams 9}(g)$$

or

$$\Delta W = \frac{\alpha^4 mc^2}{4}\left[\frac{7}{3} - \frac{\alpha}{\pi}\left(\frac{32}{9} + 2\ln 2\right)\right] + \frac{i\alpha^5 mc^2}{4}.$$

The imaginary term, arising from two quantum annihilation, is equivalent to a term in the wave function of the ^1S state proportional to $\exp(-t/2\tau)$ with $\tau = 2\hbar/\alpha^5 mc^2$, which corresponds to the lifetime for real two quantum annihilation already deduced (equation 4). The real part of ΔW is

$$\Delta W = 2.0337 \times 10^5 \text{ Mc./sec.} \qquad 15.$$

in excellent agreement with the experimental values discussed in the following sections (equations 20, 23, 24). The splitting of the $n=2$ levels has also been computed to terms of order α^5 (78).

Zeeman effect.—If a constant magnetic field $\boldsymbol{H}$ be applied to a positronium atom, the ^1S and ^3S levels split further (72 to 75) in the manner shown in Figure 10. Indeed, since

$$\begin{aligned}(\boldsymbol{\sigma}_1 - \boldsymbol{\sigma}_2)_z\, {}^3\psi_{\pm 1} &= 0 \\ (\boldsymbol{\sigma}_1 - \boldsymbol{\sigma}_2)_z\, {}^3\psi_0 &= 2\, {}^1\psi_0 \\ (\boldsymbol{\sigma}_1 - \boldsymbol{\sigma}_2)_z\, {}^1\psi_0 &= 2\, {}^3\psi_0\end{aligned} \qquad 16.$$

and since the magnetic moment of the atom is given by $\boldsymbol{\mu} = e\hbar/2mc(\boldsymbol{\sigma}_1 - \boldsymbol{\sigma}_2)$ approximately, it follows that the perturbing energy $V = -\boldsymbol{\mu} \cdot \boldsymbol{H}$ does not affect the levels $m = \pm 1$, and that it mixes the states $^3\psi_0$, $^1\psi_0$. If $\mathcal{H} = \mathcal{H}_0 + V$, we have

$$(\mathcal{H} - {}^3W)\,{}^3\psi_0 = -(e\hbar/mc)H\,{}^1\psi_0$$
$$(\mathcal{H} - {}^1W)\,{}^1\psi_0 = -(e\hbar/mc)H\,{}^3\psi_0$$

the characteristic values of which are

$${}^3E = \frac{{}^1W + {}^3W}{2} + \frac{\Delta W}{2}(1 + x^2)^{1/2} \qquad 17.$$

and

$${}^1E = \frac{{}^1W + {}^3W}{2} - \frac{\Delta W}{2}(1 + x^2)^{1/2}$$

where ${}^1W$, ${}^3W$ are the unperturbed ${}^1S$, ${}^3S$ energies respectively, $\Delta W = {}^3W - {}^1W$ and $x = 2e\hbar H/(mc\Delta W)$.

To this order of approximation there is no linear Zeeman effect, since x does not appear linearly in equation 17. This corresponds to the fact that, from equation 16 the expectation value of μ for either of the states ${}^3S$, ${}^1S$

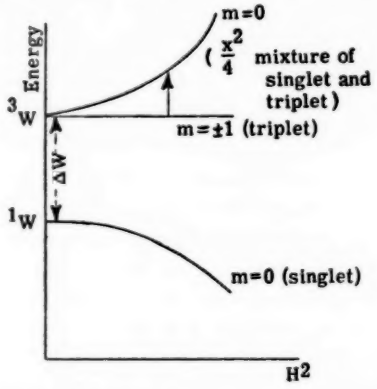

FIG. 10. ${}^3S$-${}^1S$ splitting of positronium in a magnetic field (Equation 17).

is zero. By general arguments similar to those developed on page 192, it may be shown that in positronium there is no linear Zeeman effect to any order. This follows because under the operation of charge conjugation the Hamiltonian of the system is invariant, so that the energy levels are unchanged by this operation. Since charge conjugation reverses the sign of the magnetic field $\boldsymbol{H}$, it then follows that the energy cannot depend linearly on H.

It also follows from general arguments that the $m = \pm 1$ substates of the ${}^3S$ state are not split by a magnetic field (31). This may be deduced by considering a rotation through 180° about an axis perpendicular to $\boldsymbol{H}$, an operation which has the consequence of interchanging the $m = \pm 1$ levels and reversing the sign of $\boldsymbol{H}$. Since $\boldsymbol{H}$ may then be brought back to its original direction by means of the charge conjugation operator, under which the Hamiltonian is invariant, it follows that in the presence of a magnetic field ${}^3W_{m=1} = {}^3W_{m=-1}$ to all orders in H^2.

Magnetic quenching.—Since a magnetic field mixes the states ${}^3S_0$ and ${}^1S_0$,

and since the lifetime of the latter state is approximately 10^{-3} times that of the former, it follows that the $^3S_0$ state is quenched by the application of such a field. The ratio of the number of two quantum decays (from the $^1S_0$ part of the mixture) to the number of three quantum decays (from the $^3S_0$ part) is thus $(x^2/4)(^3\tau/^1\tau)$ where $(x^2/4)$ is the mixing ratio. Thus, the fraction of annihilation processes from the mixed state which result in the emission of three quanta is $[1+(x^2/4)(^3\tau/^1\tau)]^{-1}$. The fraction of all annihilation processes from the original ^3S state which result in three quantum emission is therefore

$$n = 2/3 + (1/3)[1 + (e\hbar H/mc\Delta W)^2 (^3\tau/^1\tau)]^{-1} \qquad 18.$$

since the $m = \pm 1$ states always produce three quanta.

By measuring the number of three quantum annihilations as a function of H it is therefore possible to measure ΔW. However, as noted in equation 10, the angular distribution of the quanta from the partially quenched $^3S_0$ state is different from that of the quanta from the states $m = \pm 1$. Thus, equation 18 is applicable only if the experiment is such that the detectors respond with equal efficiency to the radiation emitted in all directions relative to the magnetic field. Otherwise, the efficiency f of detecting the three quantum annihilation must be included in equation 18, to yield

$$n = 1 - f + f[1 + (e\hbar H/mc\Delta W)^2 (^3\tau/^1\tau)]^{-1}. \qquad 19.$$

The fraction f depends on the geometry of the counters relative to $\boldsymbol{H}$, as we have seen in the section on the *Theory of the Annihilation Process* (page 192). In particular, the value of f depends on whether the experiment consists of measuring all three annihilation quanta by triple coincidence or of measuring the total annihilation radiation spectrum.

The latter method was used by Deutsch & Dulit (79), the annihilation radiation emerging at right angles to the field being observed by means of a scintillation spectrometer. Thus the value $f = 0.4$ given by equation 11 is applicable to this experiment. Their experimental data are shown in Figure 11, the corresponding theoretical curves for different values of ΔW having been calculated from equation 18 instead of equation 19 since at that time the theory of equation 11 had not been developed. However, this correction affects the result, which was

$$\Delta W = 9.4 \times 10^{-4} \text{ ev} \pm 15 \text{ per cent} \qquad 20.$$

by less than the probable error. Thus the reality of the virtual annihilation term 13 included in 14 was fully established, for in its absence the theoretical curve would have been the dotted curve of Figure 11, well outside the probable error of the experiment.

These and other results have been confirmed by various groups (51, 65, 80) using somewhat similar methods. Such measurements give a value for $(^3\tau/^1\tau)(\Delta W)^{-2}$, and if one takes the well-verified value (equation 15) for ΔW, Marder, Hughes & Wu (65) have obtained the value

$$(^3\tau/^1\tau) = 1289 \pm 14 \text{ per cent}$$

in agreement with the theoretical value (equation 6) of 1115.

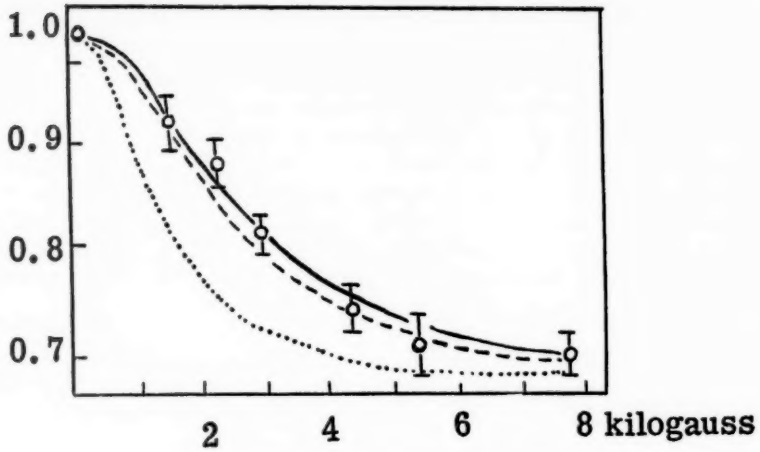

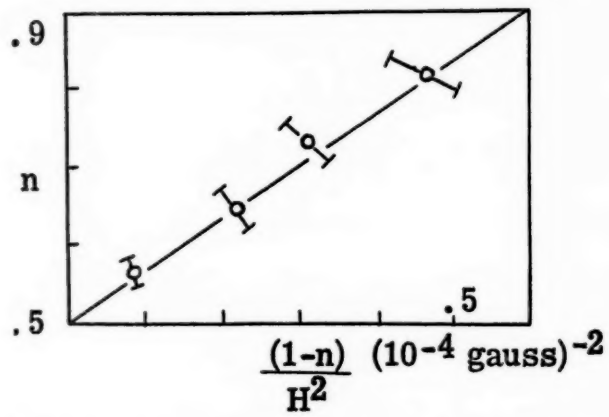

FIG. 11 (above). Relative probability of three quantum annihilation as a function of the magnetic field. [M. Deutsch and E. Dulit, *Phys. Rev.*, **84**, 601 (1951).]

FIG. 12 (below). Graph of n against $(1-n)/H^2$. Equation 21. [J. Wheatley and D. Halliday, *Phys. Rev.*, **88**, 424 (1952).]

Rewriting equation 19 thus

$$n = 1 - f + (1 - n)/aH^2 \quad \text{with} \quad a = (e\hbar/mc\Delta W)^2\,(^3\tau/^1\tau) \qquad 21.$$

one sees that the graph of n against $(1-n)/H^2$ should be a straight line. In an experiment by Wheatley & Halliday (51) the $^3S_1$ decay was detected by three scintillation counters placed symmetrically in the plane perpendicular to the magnetic field. As noted (pp. 196–98) the relevant value of f is 0.5, a result which was verified by extrapolating the experimental curve to large H (Fig. 12). Equation 21 should also be modified to take into account the transitions between triplet and singlet states induced by collisions with the (SF_6) molecules of the gas. Since this is pressure sensitive, measurements at

different pressures may be extrapolated to zero pressure to give $({}^3\tau/{}^1\tau)(\Delta W)^{-2}$.

Resonance quenching.—The experiment reported in the previous section was sufficiently accurate to verify the theory up to terms of order α^4. The terms of order α^5 were measured, before the theory had been developed, by Deutsch & Brown (48). These authors placed positronium in a constant magnetic field of 9000 gauss, which suppressed the three quantum annihilation from the $m=0$ levels. A further quenching was observed when positronium was exposed to a r. f. field of the resonant frequency to induce transitions from the $m=\pm 1$ level to the level $m=0$. From equation 17 this resonant frequency is (cf. arrow on Figure 10)

$$\nu = (\Delta W/2\hbar)[(1+x^2)^{1/2}-1]. \qquad 22.$$

Since ν may be measured with great precision, this method has resulted in a very accurate determination of ΔW. The essential limitation in the measurement of ν is the natural width of the $m=0$ level, which for large H is $\hbar/{}^1\tau$, leading to a fractional error in ν of $\hbar/({}^1\tau\Delta W)=6.2\times 10^{-3}$.

If the measurements of Deutsch & Brown are corrected for the anomalous magnetic moment of the electron [so that $x\rightarrow(2e\hbar/mc)H(1+\alpha/2\pi)$] the result is

$$\Delta W = (2.035 \pm .003)10^5 \text{ Mc./sec.} \qquad 23.$$

Figure 13 shows the resonance curve obtained in more recent measurements by Weinstein, Deutsch & Brown (81). For $\nu=3012.9$ Mc the resonance

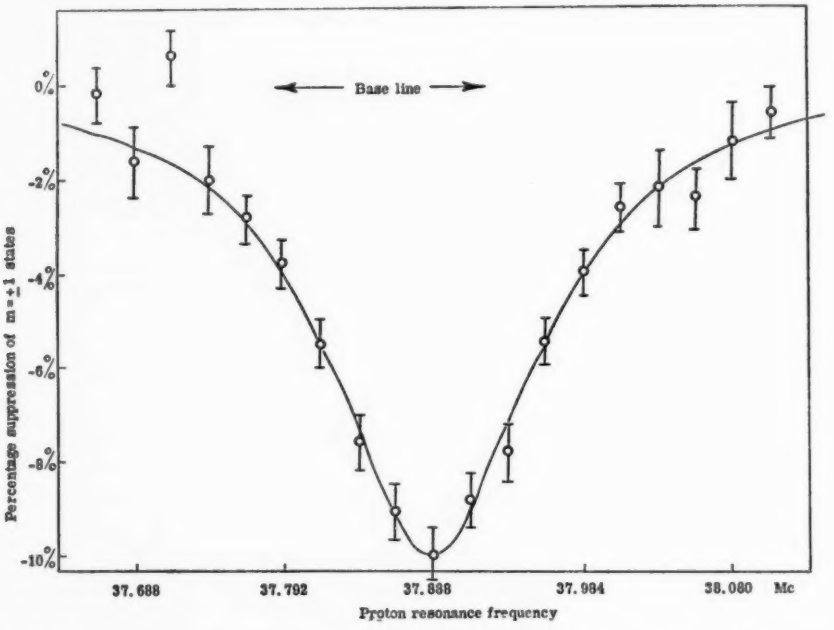

FIG. 13. Resonance absorption in a magnetic field, which is measured by proton resonance. (Frequency in positronium cavity 3012.9 Mc.)

was found for a magnetic field corresponding to a proton resonance of 37.8875 Mc. This is equivalent to a $^3S-^1S$ splitting of

$$\Delta W = 203350 \pm 50 \text{ Mc./sec.} \qquad 24.$$

in excellent agreement with the theoretical value of equation 15. This remarkable agreement may be regarded as a real triumph for the theory of quantum electrodynamics and as one of the major achievements of theoretical and experimental physics in recent years.

LITERATURE CITED

1. Anderson, C. D., *Phys. Rev.*, **43,** 491 (1933)
2. Heitler, W., *The Quantum Theory of Radiation* (Oxford University Press, Oxford, England, 272 pp., 1944)
3. Blackett, P. M. S., and Occhialini, G. P. S., *Proc. Roy. Soc.* (*London*), [A]**139,** 699 (1933)
4. Blackett, P. M. S., Chadwick, J., and Occhialini, G. P. S., *Proc. Roy. Soc.* (*London*), [A]**144,** 235 (1934)
5. DeBenedetti, S., *Compt. rend.*, **200,** 1389 (1935)
6. Simons, L., and Zuber, K., *Proc. Roy. Soc.* (*London*), [A]**159,** 383 (1937)
7. Thibaud, J., *Compt. rend.*, **197,** 1629 (1933); *Phys. Rev.*, **45,** 781 (1934)
8. Spees, A. H., and Zahn, C. T., *Phys. Rev.*, **58,** 861 (1940)
9. Page, L. A., Stehle, P., and Gunst, S. B., *Phys. Rev.*, **89,** 1273 (1953)
10. Joliot, F., *Compt. rend.*, **197,** 1622 (1933); *Compt. rend.*, **198,** 81 (1934)
11. Klemperer, O., *Proc. Cambridge Phil. Soc.*, **26,** 361 (1930)
12. Beringer, R., and Montgomery, C. G., *Phys. Rev.*, **61,** 222 (1942)
13. Muller, D. E., Hoyt, H. C., Klein, D. J., DuMond, J. W. M., *Phys. Rev.*, **88,** 775 (1952)
14. Hedgran, A., *Phys. Rev.*, **82,** 128 (1951); Lindström, G., *Phys. Rev.*, **83,** 465 (1951)
15. Mohorovičić, S., *Astron. Nacht.*, **253,** 94 (1934)
16. Ruark, A. E., *Phys. Rev.*, **68,** 278 (1945)
17. Wheeler, J. A., *Ann. N. Y. Acad. Sci.*, **48,** 219 (1946)
18. Hylleraas, E., *Phys. Rev.*, **71,** 491 (1947)
19. Hylleraas, E. A., and Ore, A., *Phys. Rev.*, **71,** 493 (1947)
20. Ore, A., *Phys. Rev.*, **71,** 913 (1947)
21. Deutsch, M., *Phys. Rev.*, **83,** 866 (1951)
22. Deutsch, M., *Mass. Inst. Technol., Lab. Nuclear Sci. and Engr. Progress Report,* p. 174 (May, 1952)
23. Ore, A., *Phys. Rev.*, **83,** 665 (1951)
24. Ore, A., *Univ. of Bergen Yearbook No. 5* (Bergen, Norway, 1952)
25. Landau, L. D., and Pomeranchuk, I., *Doklady Akad. Nauk S. S. S. R.*, **60,** 207, 213 (1948); *Science Abstr.*, [A]**52,** 1005, 1007 (1949)
26. Yang, C., *Phys. Rev.*, **77,** 262 (1950)
27. Peaslee, D., *Helv. Phys. Acta*, **23,** 845 (1950)
28. Wolfenstein, L., and Ravenhall, D. G., *Phys. Rev.*, **88,** 279 (1952)
29. Michel, L., *Compt. rend.*, **234,** 703 (1952)
30. Michel, L., *Nuovo cimento*, **10,** 319 (1953)
31. Fumi, F. G., and Wolfenstein, L., *Phys. Rev.*, **90,** 498 (1953)
32. Pryce, M. H. L., and Ward, J. C., *Nature*, **160,** 435 (1947)
33. Snyder, H. S., Pasternack, S., and Hornbostel, J., *Phys. Rev.*, **73,** 440 (1948)
34. Bleuler, E., and Bradt, H. L., *Phys. Rev.*, **73,** 1398 (1948)
35. Hanna, R. C., *Nature*, **162,** 332 (1948)

36. Wu, C. S., and Shaknov, I., *Phys. Rev.*, **77,** 136 (1950)
37. Hereford, F. L., *Phys. Rev.*, **81,** 482 (1951)
38. Dirac, P. A. M., *Proc. Cambridge Phil. Soc.*, **26,** 361 (1930)
39. Ore, A., and Powell, J. L., *Phys. Rev.*, **75,** 1696, 1963 (1949)
40. Radcliffe, J. M., *Phil. Mag.*, **42,** 1334 (1951)
41. Drisko, R. M., *Phys. Rev.*, **95,** 611 (1954); *Phys. Rev.* (In press)
42. Shearer, J. W., and Deutsch, M., *Phys. Rev.*, **76,** 462 (1949)
43. Deutsch, M., *Phys. Rev.*, **82,** 455 (1951)
44. Pond, T. A., *Phys. Rev.*, **85,** 489 (1952)
45. DeBenedetti, S., and Siegel, R., *Phys. Rev.*, **85,** 371 (1952); **94,** 955 (1954)
46. Leipuner, L., Siegel, R., and DeBenedetti, S., *Phys. Rev.*, **91,** 198 (1953)
47. Deutsch, M., *Progr. Nuclear Phys.*, **3,** 131 (1953)
48. Deutsch, M., and Brown, S. C., *Phys. Rev.*, **85,** 1047 (1952)
49. Deutsch, M., *Mass. Inst. Technol., Lab. Nuclear Sci. and Engr. Progress Report,* p. 143 (May, 1953)
50. Ore, A., *Univ. of Bergen Yearbook No.'s 9, 12* (Bergen, Norway, 1949)
51. Wheatley, J., and Halliday, D., *Phys. Rev.*, **88,** 424 (1952)
52. Shearer, J. W., and Deutsch, M., *Phys. Rev.*, **82,** 336 (1951)
53. Gerhart, J. B., Carlson, B. C., and Sherr, R., *Phys. Rev.*, **94,** 917 (1954)
54. DeBenedetti, S., Cowan, C. E., Konneker, W. R., and Primakoff, H., *Phys. Rev.*, **77,** 205 (1950)
55. Garwin, R. L., *Phys. Rev.*, **91,** 1571 (1953)
56. DuMond, J. W. M., Lind, D. A., and Watson, B. B., *Phys. Rev.*, **75,** 1226 (1949)
57. Hedgran, A., and Lind, D. A., *Ark. Fysik.*, **5,** No. 2 (1952); *Phys. Rev.*, **82,** 126 (1951)
58. Warren, J. B., and Griffiths, G. M., *Can. J. Phys.*, **29,** 325 (1951)
59. Mayer-Leibnitz, H., *Z. Naturforsch.*, **6[a],** 663 (1951)
60. Madansky, E., and Rasetti, F., *Phys. Rev.*, **75,** 397 (1950)
61. DeBenedetti, S., and Richings, H. J., *Phys. Rev.*, **85,** 377 (1952)
62. Bell, R. E., and Graham, R. L., *Phys. Rev.*, **90,** 644 (1953)
63. Minton, G. E., *Phys. Rev.*, **94,** 758 (1954)
64. Rich, J. A., *Phys. Rev.*, **81,** 140 (1951)
65. Marder, S., Hughes, V., and Wu, C. S., *Phys. Rev.*, **95,** 611 (1954)
66. Millet, W. E., *Phys. Rev.*, **94,** 809 (1954)
67. Talley, H., and Stump, R., *Phys. Rev.*, **94,** 809 (1954)
68. Pond, T. A., *Phys. Rev.*, **93,** 478 (1954)
69. Stewart, A. T. (Private communication, 1953)
70. Leipuner, L. (Private communication)
71. Fermi, E., *Z. Phys.*, **60,** 320 (1930)
72. Berestetski, V. B., and Landau, L. D., *Zhur. Exsptl. i Teort. Fiz.*, **19,** 673 (1949)
73. Berestetski, V. B., *Zhur. Exsptl. i Teort. Fiz.*, **19,** 1130 (1949)
74. Pirenne, J., *Arch. sci. phys. et nat.*, **28,** 273 (1946); **29,** 121, 207 (1947)
75. Ferrell, R. A., *Phys. Rev.*, **84,** 858 (1951); *The Fine Structure of Positronium* (Doctoral thesis, Princeton University, Princeton, N. J., 1951)
76. Karplus, R., and Klein, A., *Phys. Rev.*, **87,** 848 (1952); Fulton, T., and Karplus, R., *Phys. Rev.*, **93,** 1109 (1954)
77. Schwinger, J., *Proc. Natl. Acad. Sci. U. S.*, **37,** 452, 455 (1951)
78. Fulton, T., and Martin, P. C., *Phys. Rev.*, **93,** 903 (1954)
79. Deutsch, M., and Dulit, E., *Phys. Rev.*, **84,** 601 (1951)
80. Pond, T. A., and Dicke, R. H., *Phys. Rev.*, **85,** 489 (1952)
81. Weinstein, R., Deutsch, M., and Brown, S., *Phys. Rev.*, **94,** 758 (1954)

THE INTERACTIONS BETWEEN π-MESONS AND NUCLEONS[1,2,3]

By Murray Gell-Mann

Department of Physics and Institute for Nuclear Studies, University of Chicago, Chicago, Illinois

AND

Kenneth M. Watson

Department of Physics, University of Wisconsin, Madison, Wisconsin

Introduction

During the some seven years which have elapsed since the first observation of artificially produced π-mesons at Berkeley, we have seen a very rapid development of elementary particle physics. There are now at least a dozen accelerators capable of producing π-mesons, including several which have created or are expected to create heavier particles. As a result of the work done with these machines, it is perhaps fair to say that we have at least a qualitative knowledge of the elementary interactions of mesons with nucleons at low energies.

On the other hand, our understanding of the π-meson interactions has in no sense kept pace with our knowledge of these phenomena. The lack of marked success of the purely field theoretic approaches to pion-nucleon processes should probably have been anticipated. Indeed, the very existence of the multitude of heavier unstable particles casts doubt on the hope for success of present day field theories.

In spite of these difficulties of a more fundamental approach, it has been found possible to simplify greatly the experimental data by applying to pion reactions various levels of phenomenological discussion. In many cases this has involved no more than the use of a few general quantum mechanical principles combined with some physical concepts borrowed from the more familiar field of nuclear physics. In other cases, more elaborate models have been suggested, and some of these have proven quite useful.

It will be our primary purpose in the present article to attempt to summarize these theoretical concepts, which have been employed in the study of meson properties. Our model is based on three assumptions:

(*a*) The pion-nucleon interactions have a finite range.

(*b*) Charge independence is valid for these phenomena (i.e., I-spin is conserved).

[1] The survey of literature pertaining to this review was completed in June, 1954.

[2] C.I.T. as used in this article refers to California Institute of Technology; Carnegie Institute of Technology is referred to as Carnegie Tech.

[3] Research for this work was supported by grant from the Atomic Energy Commission.

(*c*) The state ($I=3/2$, $j=3/2$, $l=1$) of the pion-nucleon system is one of especially strong ("attractive") interaction.

The good agreement of this model with present experiments for "low energies" is noted, and the relations of more detailed and basic theories to this model and to the data are discussed.

We shall begin on an almost purely phenomenological level, combining a few general principles of quantum mechanics with some simple physical ideas (see the next section). The presently available experimental data are discussed in terms of their relation to these principles. Finally, the successes of the more sophisticated approaches will be studied.

Some Physical Concepts Applying to Pions

General principles.—We shall be primarily concerned with two-body collisions involving the production (and absorption) and scattering of π-mesons from nucleons. The most studied of these processes fall into three classes:

[Scattering:—(S)]

[6] $$\pi + N \rightarrow \pi + N.$$

(We use π and N to denote pions and nucleons, respectively, irrespectively of their charge states.)

[Photoproduction:—(P_γ)]

[4] $$\gamma + N(\rightleftarrows)\pi + N$$

[Production in Nucleon-Nucleon Collisions:—(P_n)]

[7] $$N + N(\rightleftarrows)\pi + N + N.$$

At sufficiently high energies we may expect additional pions to be produced in each of these processes. Also, other unstable particles may appear (1). The number in brackets at the left of these reaction equations indicates the number of reactions which are obtained by enumerating the possible pion and nucleon charge states.

We shall be most concerned with these reactions at low energies. By "low energies" we specifically mean energies such that the de Broglie wavelength, $\lambda\!\!\!^{-}$, of the meson (in the barycentric system) is not small compared to the range of the interaction involved. We do not expect this range to be much greater (except for Coulomb interactions) than the Compton wavelength

$$\hbar/\mu c,$$

where μ is the rest-mass of the meson. As a result of this, we may suppose that orbital angular momenta greater than $l\hbar$, where

$$l = (1/\lambda\!\!\!^{-})\left(\frac{\hbar}{\mu c}\right) \qquad 1.$$

will not play an important role in the reactions considered.

To illustrate this, in Figure 1 we plot l as determined from Equations 1

versus the meson energy in the laboratory frame of reference for the scattering process (S) above. It is evident that for many processes at most one

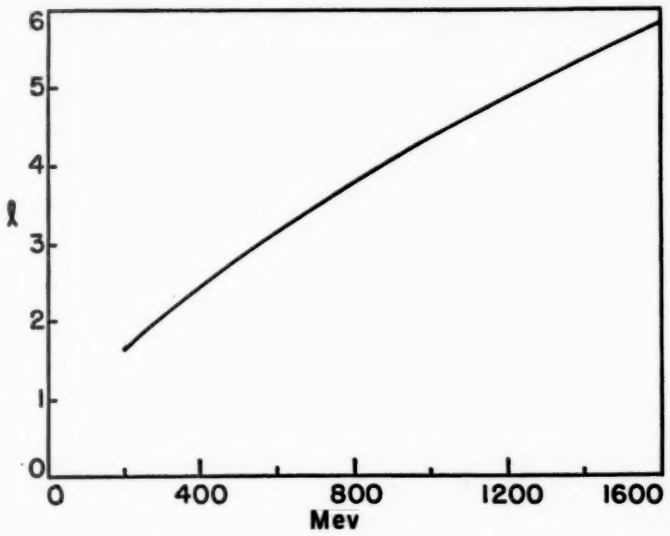

FIG. 1. The highest value of the angular momentum in units of $\hbar$ which is expected for pion-nucleon scattering, versus the pion energy in the laboratory system.

or two values of l need be considered for fair ranges of energy if our supposition concerning the range of the interaction is correct. From the subsequent discussion it will appear that this conclusion seems to be quite correct, with a single state of unit orbital angular momentum (P-state) playing a very important part.

Just as in nuclear physics, the conclusion that the range of interaction is of limited extent has specific consequences. For instance, when only one state of orbital angular momentum is important for an emitted (or absorbed) particle, the energy dependence of the cross section is uniquely determined at "low energies."[4] The energy dependence is summarized for the processes of interest to us in Table I. Here q is the momentum of the meson in the barycentric system. When at most one or two states of angular momentum are important we are led to expect a simple dependence of the cross sections on

[4] To see this, let $T(r)$ be the scattering matrix for the emission of a particle whose space coordinate is r. Also let $T(r)$ vanish for $r>R$ and suppose that only the angular momentum l is of importance. Then the amplitude for emitting the particle into a plane wave state $\phi_q(\mathbf{r})$, where q is the momentum, is

$$A = \int \phi_q^*(r) T(r) d^3r.$$

Since the lth partial wave of ϕ_q varies as $(qr/\hbar)^l$ for $r<\hbar/q$, we have $A \sim q^l$ for $\hbar/q > R$.

TABLE I

THE DEPENDENCE OF THE CROSS SECTION AT "LOW ENERGY" ON THE MOMENTUM OF THE MESON WHICH IS ABSORBED, EMITTED, OR SCATTERED*†

Type of cross section	Absorption	Emission into two particle state	Emission into three particle state	Scattering
Dependence of cross section on momentum	q^{2l-1}	q^{2l+1}	q^{2l+4}	q^{4l}
Dependence of "matrix element" T, on momentum	q^l	q^l	q^l	q^{2l}

* q is the momentum of the meson, l is its angular momentum.

† When some of the emitted particles interact strongly, the q-dependence may be modified, but often in a simple manner. (See section on π-MESON PRODUCTION IN NUCLEON-NUCLEON COLLISIONS.)

energy. (For more than one l-state, we expect linear combinations of the corresponding terms in Table I.) In Figure 2 we present a comparison of several experimental total cross sections with some simple power law curves. Except for the process (P_γ: $\gamma+p\rightarrow\pi^++n$) a P-state power law appears reasonably satisfactory. In the latter case a linear combination of S- and P-waves is required even for rather low γ-ray energies. We shall develop these considerations in more detail in subsequent sections.

A second consequence of our conclusion that few orbital angular momentum states are expected to be important at low energies is that angular momentum and parity conservation will be significant for our considerations. This point will be developed in more detail as we discuss the reactions individually.

There is, however, one particularly important aspect of angular momentum and parity conservation which we now describe. The π-meson is pseudoscalar (2, 3) which implies (by definition) that the emission of a single meson by a single nucleon must be into a state of odd orbital angular mo-

FIG. 2. [*a*] π^+-proton scattering compared to $\sigma\sim q^4$, where q is the meson momentum in the barycentric system. The points are from: Φ—Leonard, S., and Stork, D., *Phys. Rev.* **93,** 568 (1954). The remaining are from Table III: [$\frac{5}{2}$ (*d*), $\frac{7}{2}$ (*e*); $\frac{9}{2}$ (*g*)].

[*b*] $\pi^++d\rightarrow p+p$. The Durbin, R., Loar, H., and Steinberger, J., [*Phys. Rev.* **84,** 581 (1951)] measurements are compared with $\sigma\sim q$.

[*c*] $\sigma(\gamma+p\rightarrow\pi^0+p)$ as measured by Goldschmidt-Clermont, Y., Osborne, L., and Scott, M., *Phys. Rev.* **89,** 329 (1953) is compared with $\sigma\sim q^3$.

[*d*] —experimental $\sigma[\gamma+p\rightarrow\pi^++n]$ compared with $\sigma\sim q$ (- - - - -) and $\sigma\sim q^3$ (— · — · —). See Section on PHOTOPRODUCTION OF π-MESONS FROM NUCLEONS for details.

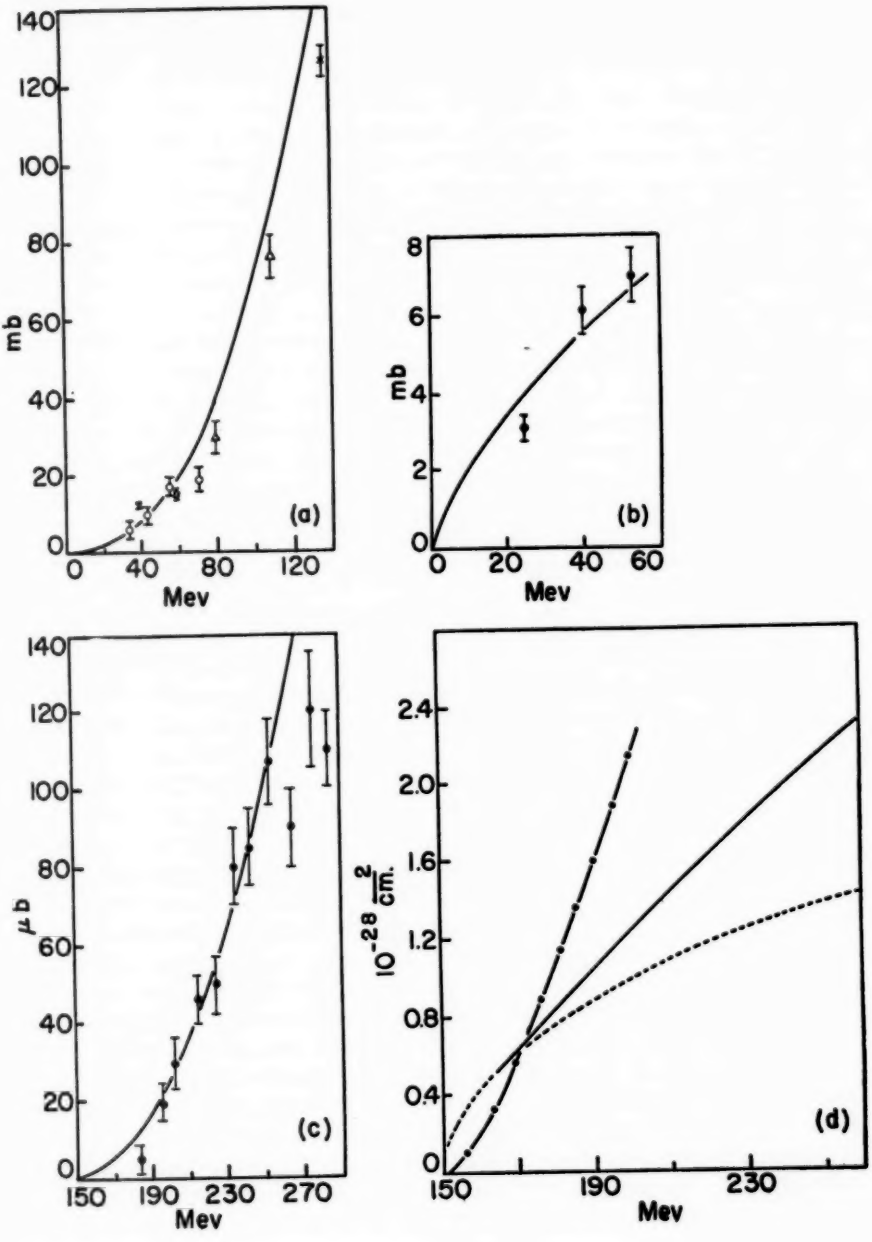
140
120
100
80
60
40
20
0
mb
0 40 80 120
Mev
(a)
8
6
4
2
0
mb
0 20 40 60
Mev
(b)
140
120
100
80
60
40
20
0
μb
150 190 230 270
Mev
(c)
2.4
2.0
1.6
1.2
0.8
0.4
0
10^{-28} cm.^{2}
150 190 230
Mev
(d)

mentum. The total angular momentum must remain $j=1/2$, however, since this is the value for the nucleon initially. The only odd orbital state of the meson-nucleon system with $j=1/2$ is the $l=1$, or P-state. Thus the simple emission (or absorption) process must always lead to (or from) a P-state.

This naturally does not represent a selection rule for physical processes, since simple emission or absorption cannot occur alone. On the other hand, if these simple emission and absorption processes represent the important steps in developing a physical emission or absorption, then it is quite reasonable that the P-state should be predominant (at low energies). This is certainly suggested by the experiments (see Fig. 2 and the subsequent sections) and is not at all incompatible with many expectations from field theory.

We may now summarize the arguments of the present section. Admitting the possibility of exceptional cases, we suppose meson reactions to take place predominantly in P-states at "low energies." Smaller admixtures of other orbital states are of course expected. The dependence of the cross section on energy is uniquely determined at sufficiently low energies by the relevant states of orbital angular momentum. Finally, we must consider selection rules and other consequences of angular momentum and parity conservation. The purpose of most phenomenological analyses of meson properties has been to determine to what extent this simplified model is (or is not) adequate.

The hypothesis of charge independence.—The hypothesis of charge independence has provided a useful simplification for the study of pion phenomena. This principle seems to have had its origin in a suggestion of Breit & Feenberg (4), who proposed in 1936 that the n-n, p-p and n-p nuclear forces might be the same for states of equal angular momentum and parity (which we now know to be at least approximately correct at low energies). This suggestion was based on the similar binding energies and scattering properties of neutrons and protons. To be more specific, we note that a state of the two-body system may be labeled by the quantum numbers[5] (j, S, π, Q), where Q is the charge, S the spin, j the total angular momentum and π the parity. The charge independence hypothesis asserts that the interaction in this state is independent of Q.

Kemmer (5) showed how to construct a meson theory which would always lead to charge independent nuclear forces. Heitler (6) later showed that the Kemmer theory should lead to selection and intensity rules for meson reactions. In view of the uncertainty of meson theories it is desirable to divorce the charge independence hypothesis from meson theory. This may be readily done in a manner which gives a simple interpretation to charge independence (7). In its broadest form (proposed to date) we may say that charge independence implies that neutrons and protons are completely equivalent physically, to the extent that the "weak interactions" (for example, elec-

[5] The spin S must be conserved if we accept charge independence.

tromagnetic and β-decay interactions) are of negligible importance. This means that a wave function which is constructed as a linear combination of neutron and proton wave functions must be physically equivalent to the wave function of either a neutron or proton.

Expressed in mathematical form, we may say that a general unitary transformation which replaces the wave function of each neutron or proton of a system by a linear combination of neutron and proton wave functions must leave the physical properties of the system unchanged. Except for a phase factor, this transformation is equivalent to (isomorphic to) a spin representation of the rotation group in three dimensions (this space has been called "charge space"). At this point we may draw a useful analogy. The invariance of a physical system with respect to rotations in ordinary space implies the conservation of angular momentum, whose operators are the generators of the rotation and whose eigenvalues are called the "isotopic spin." It is evident from the invariance with respect to "charge rotations," as just discussed, that the generators of these rotations will also be conserved. From the analogy to angular momentum, it is clear that these "charge rotation operators" will be formally identical to the angular momentum operators, so we may use the mathematical apparatus for the latter without modification.

In particular, we may introduce a two-component wave function for the "nucleon," its components referring to neutron and proton states. The "charge rotations" are induced by three two-dimensional matrices, τ_1, τ_2, and τ_3, which are formally equivalent to the Pauli-spin matrices. The τ's are components of a vector $\boldsymbol{\tau}$ (with respect to charge rotations) in the three dimensional charge space. For a system of several nucleons a total isotopic spin I may be constructed just as can a total spin S for their ordinary spin. To use a definite representation, we shall suppose that a proton has isotopic spin "up" and a neutron isotopic spin "down." (This assignment is of course arbitrary and is often inverted.)

The principle extends itself uniquely to unstable particles which may be emitted or absorbed singly by nucleons. For instance, consider the emission of a π^+-meson by a proton. Charge independence states that this emission process is unchanged when by the "rotation" the proton wave function is replaced by a linear combination of proton and neutron wave functions. It is evident that this "rotation" must replace the π^+ eigenfunction by a linear combination of π^+, π^-, and π^0 wave functions, since a neutron cannot emit a π^+-meson. This is a three dimensional [irreducible (7)] representation of the rotation group in three dimensions, so the meson has an "isotopic spin" of unity with an isotopic angular momentum operator $\boldsymbol{\tau}$. To summarize, each meson has an isotopic spin of unity, each nucleon an isotopic spin of one-half. A system containing several nucleons and mesons may be resolved into states of total isotopic spin I, in exact analogy with the corresponding problem for ordinary angular momentum. The state I is $(2I+1)$-fold degenerate, the substates being dynamically equivalent.

If the third component of τ is diagonal, the meson wave functions transform under rotations as the spherical harmonics of order unity in charge space:

$$\begin{aligned} \phi(\pi^+) &\rightarrow Y_1^1 \\ \phi(\pi^0) &\rightarrow Y_1^0 \\ \phi(\pi^-) &\rightarrow Y_1^{-1}. \end{aligned} \qquad 2.$$

The meson and nucleonic charge operators are, respectively,

$$Q_\pi = \tau_3, \qquad Q_N = \tfrac{1}{2}[1 + \tau_3], \qquad 3.$$

in units of the charge on the proton.

The total I-spins ("isotopic spins") of some simple meson-nucleon systems are listed in Table II. Each of these I-states represents a constant of

TABLE II

POSSIBLE VALUES OF THE I-SPIN FOR SOME MESON-NUCLEON SYSTEMS

System	Single nucleon	Single pion	Two nucleon	Pion—nucleon	Pion—Two nucleon	Two pions	Two pions—One nucleon
I-spin values	1/2	1	0, 1	1/2, 3/2	0, 1, 1, 2	0, 1, 2	1/2, 1/2, 3/2 3/2, 5/2

the motion for the dynamical behavior of the corresponding system. The $(2I+1)$ substates for each of these are equivalent, which means that the total number of different reactions is greatly reduced. For instance, in the first part of this section (see *General principles*) it was stated that there were six scattering cross sections (S). Reference to Table II indicates only two I-states; therefore only two, rather than six, reactions need be found. For processes P_n Table II indicates that $I=0$, 1, 1 and there are consequently only three, rather than seven, independent processes.

We must finally observe that charge independence in its present form is not rigorous because of the "weak interactions" which violate it (electromagnetic interactions imply a preferred direction in charge space, which keeps us from losing track of the distinction between neutrons and protons, etc.). This means that transitions between different I-states will occur; however, these are presumably of only secondary importance for the phenomena which we are considering (with the exception of the specifically electromagnetic interactions such as photoproduction of pions).

The hypothetical state of strong interaction for the meson-nucleon system.—It is convenient to label states of the one meson-one nucleon system by the isotopic spin I, the angular momentum j, and the orbital angular momentum l, as (I, j, l). There is a suggestion from meson theory that the (3/2, 3/2, 1)-state should be one of particularly strong interaction at certain energies.

Brueckner (8) has put this into the form of an explicit hypothesis by assuming that the scattering in this state passes through a resonance at a meson energy of about 200 Mev in the laboratory system. This hypothesis leads to a variety of implications for pion phenomena which will subsequently be discussed in more detail. There is an increasing amount of evidence that the resonance does indeed exist.

The Scattering of Pions by Nucleons

The elementary scattering processes which have been studied are:

$$\pi^+ + p \rightarrow \pi^+ + p \qquad (S_+)$$
$$\pi^- + p \rightarrow \pi^- + p \qquad (S_-)$$
$$\pi^- + p \rightarrow \pi^0 + n. \qquad (S_e)$$

The differential cross sections for these processes we shall designate by σ^+, σ^- and σ^e, respectively, whereas we shall use $\sigma_T{}^+$, $\sigma_T{}^-$, $\sigma_T{}^e$ for the total cross section. (We shall consistently represent differential and total cross sections by σ and σ_T, respectively.)

We have indicated in Figure 2 that P-wave scattering plays a dominant role in the pion scattering over a considerable energy range. This does not in any way imply that other partial waves are negligible, a point to which we shall return.

A great deal of effort has been put into the experimental study of the pion-proton scattering. The presently available total cross sections are summarized in Figure 3. In Table III we give the experiments and references from which these points are obtained.[6] Of particular interest are the cross sections in the vicinity of 200 Mev recently obtained at Carnegie Institute of Technology [Table III, references (*f*) and (*g*)] and those above 300 Mev measured at Brookhaven [Table III, references (*h*), (*j*) and (*k*)]. The cross sections plotted are σ^+ and $\sigma_T{}^{(-)} \equiv \sigma_T{}^- + \sigma_T{}^e$.

It should be mentioned that the cross sections of Figure 3 include inelastic scattering (*i.e.*, with the production of one or more additional mesons). This becomes energetically possible for pion energies above 200 Mev in the laboratory system. In the vicinity of one Bev the cross sections are probably largely inelastic (9).

It is instructive to resolve the cross sections of Figure 3 into cross sections $\sigma_{1/2}$ and $\sigma_{3/2}$ for the pure isotopic spin substates $I = 1/2$ and $3/2$, respectively. This is easily done using the relations

$$\begin{aligned} \sigma_T{}^+ &= \sigma_{3/2} \\ \sigma_T{}^{(-)} &= \tfrac{1}{3}[\sigma_{3/2} + 2\sigma_{1/2}], \end{aligned} \qquad 5.$$

or

[6] We are deeply indebted to those workers who have supplied us with detailed information of their unpublished experiments. In particular we should like to thank Drs. J. Ashkin., O. Piccioni, and their collaborators.

TABLE III

REFERENCES TO THE EXPERIMENTAL POINTS OF FIGURE 3*

Pion energy in lab system in mev	Reference	Experiment (measured cross sections are indicated)
40	(*a*)	Perry, J. P., and Angell, C. E., *Phys. Rev.*, **91**, 1289 (1953) [σ^+: counter telescope in coincidence with beam defining telescope]
40	(*b*)	Barnes, S., Angell, C., Perry, J., Miller, D., Ring, J., and Nelson, D., *Phys. Rev.*, **92**, 1327 (1953) [σ^-; counter telescope]
34	(*c*)	Roberts, A., and Tinlot, J., *Phys. Rev.* **90**, 951 (1953) [σ^e, γ-rays counted singly and in coincidence]
58, 65	(*d*)	Bodansky, D., Sachs, A., and Steinberger, J., *Phys. Rev.*, **93**, 1367 (1954) [σ^+, σ^-, σ^e; scintillation counters, liquid hydrogen target]
78, 110, 120	(*e*)	Anderson, H., Fermi, E., Martin, R., and Nagle, D., *Phys. Rev.*, **91**, 155 (1953) [σ^+, σ^-, σ^e; scintillation counters, liquid hydrogen target]
135 to 250	(*f*)	Ashkin, J., Blaser, J., Feiner, F., Gorman, J., and Stern, M., *Phys. Rev.*, **93**, 1129 (1954). [$\sigma_T^{(-)}$ transmission, using liquid hydrogen]
135 to 196	(*g*)	Ashkin, J., Blaser, J., Feiner, F., Gorman, J., and Stern, M., *Phys. Rev.*, **93**, 1129 (1954) [σ_T^+; as above]
28, 340, 450	(*h*)	Lindenbaum, S. J., and Yuan, L. C., *Phys. Rev.* (In press), also *Proceedings of 1954 Rochester Conference* [σ_T^+; transmission, $C-CH_2$ subtraction]
340, 450	(*j*)	Lindenbaum, S. J., and Yuan, L. C., *Phys. Rev.* (In press), [$\sigma_T^{(-)}$; see above]
500 to 1500	(*k*)	Cool, R., Madansky, L., and Piccioni, O., *Phys. Rev.* (To be published.) [σ_T^+ and $\sigma_T^{(-)}$; transmission, $C-CH_2$ and $C-CD_2$ subtraction]

* This is not in any sense intended to be a complete list, but rather tends to emphasize recent work. Further references can be found in Ruderman, M. A., Henley, E. M. & Steinberger, J., *Ann. Rev. Nuclear Sci.*, **3** (1953).

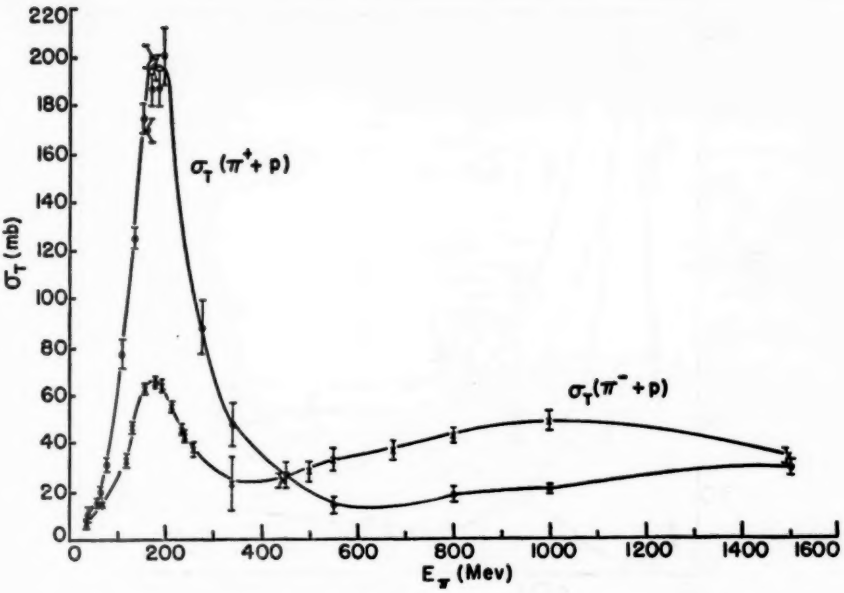

FIG. 3. Total cross section for π^+-mesons and for π^--mesons scattered by protons as a function of the meson energy in the laboratory system. The experimenters whose points are shown may be obtained from Table III by comparing energies. The π^+ points at 1.0 and 1.5 Bev. were obtained from $[\sigma(\pi^-, d) - \sigma(\pi^-, p)]$—see reference (*k*) of Table III. The solid curves are drawn to fit as well as possible the experimental data.

$$\sigma_{1/2} = \tfrac{1}{2}[3\sigma_T{}^{(-)} - \sigma_T{}^{+}]. \qquad 6.$$

It should be noted that these relations hold even when the cross sections are inelastic.

Using the experimental values for $\sigma_T{}^+$ and $\sigma_T{}^{(-)}$ from Figure 3 we have obtained $\sigma_{3/2}$ and $\sigma_{1/2}$ as shown in Figure 4. The solid curves represent a fit to the points shown. The dashed curves represent the upper limit to the scattering in pure states of j and l. They are given by

$$\sigma(j, l) = 2\pi \left(\frac{\hbar}{q}\right)^2 [2j + 1] \qquad 7.$$

where q is the momentum of the pion in the barycentric system. The presence of the peak at 200 Mev in $\sigma_{3/2}$ and its absence in $\sigma_{1/2}$ is quite striking and would seem to provide excellent evidence for the charge independence hypothesis as well as for Brueckner's (8) hypothesis of a resonance in the $(I=3/2, j=3/2, l=1)$ state. In particular, the peak height should be compared with the value of $\sigma(3/2, 1)$ as obtained from Equation (7).

If the peak in $\sigma_{1/2}$ at about one Bev were attributable to scattering in only one angular momentum state, this would require $j \cong 5$ [see also Fig. 1]. This

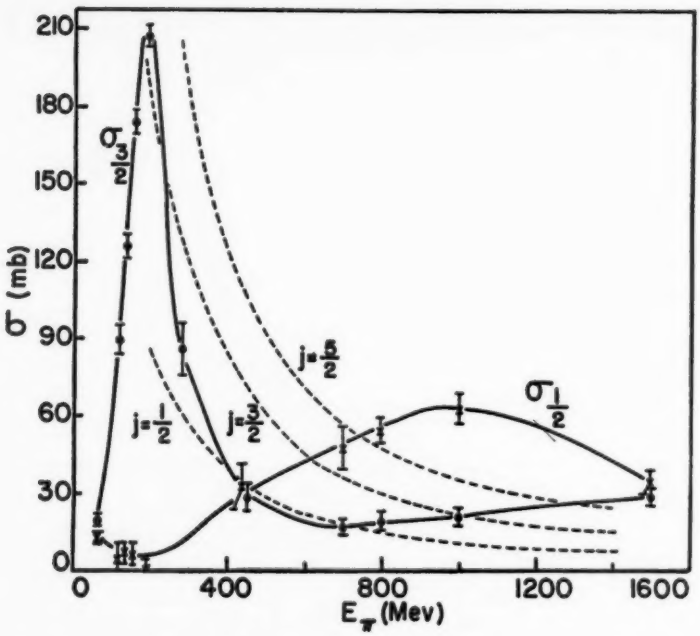

FIG. 4. The experimental values for the pion-nucleon scattering in the states of pure I-spin, 1/2 and 3/2. The dashed curves represent the upper limits on the cross sections for scattering in pure states (j, l) as given by Equation 7.

seems rather unlikely, especially since the cross section appears to be largely inelastic. On the other hand, this peak does perhaps suggest the possibility that at one Bev the inelastic (*i.e.*, meson-production) cross section may be predominantly in the $I=1/2$ state. If this were true, charge independence gives the relations:

$$\sigma(p+\pi^-\to n+\pi^-+\pi^+)+\sigma(p+\pi^-\to n+\pi^++\pi^-)$$
$$=2\sigma(p+\pi^-\to n+\pi^0+\pi^0)+\sigma(p+\pi^-\to p+\pi^-+\pi^0) \qquad 8.$$

and

$$\sigma(p+\pi^-\to p+\pi^0+\pi^-)=\sigma(p+\pi^-\to p+\pi^-+\pi^0).$$

These are differential cross sections. For the total cross sections we have

$$2\sigma_T(p+\pi^-\to n+\pi^-+\pi^+)=\sigma_T(p+\pi^-\to n+\pi^0+\pi^0)$$
$$+\sigma_T(p+\pi^-\to p+\pi^-+\pi^0). \qquad 9.$$

These relations will be valid only when (and if) the production cross sections for π^+-mesons striking protons are small, as stated above.

The smallness of the $I=1/2$ scattering below 400 Mev has been noted by Ashkin (10). The Carnegie Tech[2] data shows this rather strikingly if we plot $3\sigma_T^{(-)}$ and σ_T^+ to the same scale, as is done in Figure 5.

Brueckner (8) proposed fitting the ($j=3/2$, $l=1$, $I=3/2$) state to a one-level resonance formula. Let us suppose that the entire $\sigma_T{}^+ = \sigma_{3/2}$ cross section arises from this state. Then

$$\sigma_T{}^+ = \frac{2\pi\hbar^2}{q^2} \frac{\Gamma^2}{(E - E_0)^2 + \frac{\Gamma^2}{4}}, \tag{10.}$$

where

$$\Gamma = \left[\frac{2\left(\frac{qa}{\hbar}\right)^2}{1 + \left(\frac{qa}{\hbar}\right)^2} \right] \gamma_\lambda{}^2. \tag{11.}$$

Here E_0 is the "resonance energy" in the barycentric system, $\gamma_\lambda{}^2$ is the reduced width, and a is the channel radius. E is the energy of the meson and nucleon in the barycentric system. We have chosen

$$\begin{aligned} E_0 &= 159 \text{ mev} \\ \gamma_\lambda{}^2 &= 58 \text{ mev} \\ a &= 0.88\left(\frac{\hbar}{\mu c}\right). \end{aligned} \tag{12.}$$

The resulting value of σ^+ as calculated from Equation 10 is compared with the experimental cross sections in Figure 5. The fit is evidently excellent.

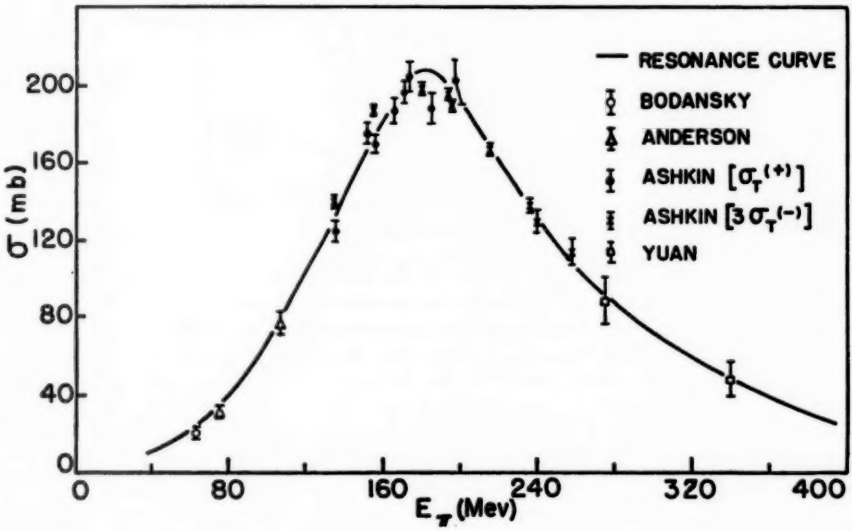

FIG. 5. A one-level resonance formula for the σ^+ scattering as calculated from Equation 10 is compared to the experimental cross sections. The references are given in Table III. The points (⧓) are $3\sigma_T{}^{(-)}$, as measured by Ashkin, *et al.* (10).

Angular distributions for pion scattering are also available (see the references of Table III). Here the experimental information is much less complete than for the total cross sections. Were the scattering entirely in the $(I=3/2,\ j=3/2,\ l=1)$ state all the angular distributions would be of the form

$$(1+3\cos^2\theta), \tag{13.}$$

where θ is the scattering angle in the barycentric system. Some measured angular distributions for σ^+ are presented in Figure 6. The asymmetry about 90° is evidently incompatible with the expression 13. On the other hand, a

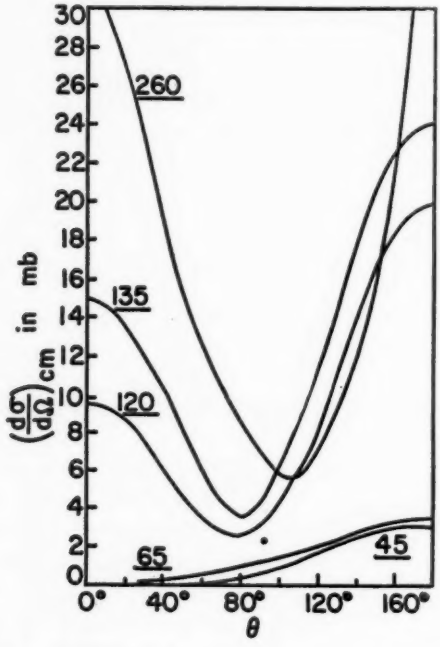

FIG. 6. Some angular distributions in the barycentric system for the scattering $\pi^+ + p \rightarrow \pi^+ + p$. The meson energies in the laboratory system are indicated in Mev. No attempt is made to indicate the experimental errors. The 45 Mev curve is that of Orear, J., Lord, J., and Weaver, A., *Phys. Rev.* **93,** 575 (1954); the 65 Mev curve is taken from reference (*d*) of Table III; the 120 and 135 Mev cross sections are those of reference (*e*) of Table III; the 260 Mev curve is that of Fowler, W. B., Lea, R., Shepard, W. D., Shutt, R. P., Thorndike, A. M., and Whittemore, W. L., *Phys. Rev.* **92,** 832 (1953).

relatively small admixture of *S*-state scattering can lead to the observed asymmetry. The general expression for a cross section with only *S*- and *P*-wave scattering is

$$\sigma = a + b\cos\theta + c\cos^2\theta \tag{14.}$$

which seems to be compatible with available pion scattering angular distributions. Indeed, it appears possible to fit the presently known angular distribution with P-wave scattering only in the $(I=3/2, j=3/2)$ state and with an admixture of S-wave scattering (11).

A great deal of effort has been expended in trying to determine the phase shifts for pion-nucleon scattering. According to charge independence there should be a total of six for energies such that only S- and P-waves contribute. Following the notation of Anderson *et al.*[7] we shall designate the S-wave phase shifts as α_3 and α_1 for the $I=3/2$ and $1/2$ states, respectively. The four P-wave phase shifts are designated by α_{33}, α_{13}, α_{31}, and α_{11}, where the first index is twice I and the second is twice j. The determination of these six phase shifts from the experimental data is very ambiguous at present and various solutions have been obtained (12), so we prefer not to engage in a detailed discussion.

The simplest set of phase shifts (and from the present theoretical point of view perhaps the most reasonable) is that of Bethe [with de Hoffmann *et al.* (see 11)], for which α_{13}, α_{31}, and α_{11} are small and α_{33} passes through

TABLE IV

MESON-NUCLEON SCATTERING PHASE SHIFTS*

E_Π Mev	α_{33}	α_3	α_1
120	30°	−12°	8°
217	107°	−20°	−4°

For $E_\Pi < 120$ Mev,

$$\alpha_{33} \cong 16^0 \left(\frac{q}{\mu_c}\right)^3$$

* Values of Bethe *et al.* (11) are given for the pion-nucleon scattering phase shifts α_{33}, α_3 and α_1; α_{33} and α_3 can be extrapolated linearly in the energy range from 120 to 217 Mev. α_1 should be extrapolated as a parabola with zero slope at 120 Mev in this energy range.

90° for the meson energy $E_\pi = 195$ Mev (in the laboratory system). Values for these phase shifts are given in Table IV. Some arguments in favor of this set are:

(*a*). The very good fit of $\sigma_{3/2}$ to the resonance formula 10 [see Fig. 5]. Were α_{33} not to pass through 90° it would probably be necessary to have a peak in at least two phase shifts at $E_\pi \cong 200$ Mev (11). For this argument not only the shape, but also the magnitude of the cross section is important [see also Fig. 4].

(*b*). The coefficient b in equation 14 changes sign in the vicinity of $E \cong 180$

[7] See Table III, reference (*e*).

Mev [see Fig. 6]. This is certainly compatible with an α_{33} which passes through 90° at about this energy.

(*c*). This behavior is strongly suggested by meson theory and is suggestive of the reason for the lack of a peak in $\sigma_{1/2}$ at 300 Mev [see Fig. 4].

(*d*). The energy dependence and the change in sign of the interference term for π^+-photoproduction (see the section on PHOTOPRODUCTION OF π-MESONS FROM NUCLEONS) strongly suggest "resonant" scattering.

Some further discussion of the scattering phase shifts along with their interpretation is given in the section on MESON THEORY.

THE PHOTOPRODUCTION OF π-MESONS FROM NUCLEONS

Here there are four photo-processes which can occur (along with their inverses):

$$\gamma + p \rightarrow \pi^+ + n \qquad (P_{\gamma+})$$
$$\gamma + n \rightarrow \pi^- + p \qquad (P_{\gamma-})$$
$$\gamma + p \rightarrow \pi^0 + p \qquad (P_{\gamma 0})$$
$$\gamma + n \rightarrow \pi^0 + n. \qquad (P_{\gamma n 0_c})$$

The reactions $P_{\gamma-}$ and $P_{\gamma(n0)}$ must be studied using bound neutrons (preferably in deuterium), so their measurement is more difficult and uncertain.

We shall tentatively assume that for E_γ (the γ-ray energy in the laboratory system) <300 to 400 Mev the meson is emitted with appreciable probability only into S- and P-states with respect to the nucleon. The arguments in favor of this point of view were described in the section, SOME PHYSICAL CONCEPTS APPLYING TO PIONS. From Figure 2 we concluded that the process $P_{\gamma 0}$ involved mostly P-state emission, whereas $P_{\gamma+}$ involved an admixture of S- and P-states at "low energies." The differential cross sections will then have the general form (in the barycentric system)

$$\sigma = A_0 + A_1 \cos\theta + A_2 \cos^2 6. \qquad 15.$$

We shall designate the individual differential cross sections for the four reactions listed above as

$$\sigma(\gamma^+),\ \sigma(\gamma^-),\ \ \sigma(\gamma^0),\ \text{and}\ \sigma(\gamma^{n0}),$$

respectively. The total cross sections will be written as $\sigma_T(\gamma^+)$, etc. The quantity A_0 contains in general contributions from both S- and P-waves and can thus be written as

$$A_0 = A_0(S) + A_0(P), \qquad 16.$$

where $A_0(S)$ and $A_0(P)$ refer respectively to S- and P-states. The energy dependence of the A's may be obtained from Table I at "low energies." (We tentatively take this to mean that $E_\gamma <250$ Mev. The upper limit for "low energy" is not, of course, known *a priori*.) For such energies we write

$$A_0(S) = \frac{\eta}{\nu} g_{0S}$$
$$A_0(P) = \eta^2 \nu g_{0P}$$
$$A_1 = -\eta^2 g_1$$
$$A_2 = -\eta^2 \nu g_2, \qquad 17.$$

where η is the momentum of the meson and ν is that of the photon in units of μc in the barycentric system. This dependence on ν is not determined from general considerations but is a guess based on meson theory. For energies sufficiently close to the energetic threshold the actual ν dependence is not important.

Cross sections for P_{γ^0} at about 90° in the laboratory frame of reference were measured by Silverman & Stearns (13) at Cornell, who observed the energy and angle of the recoil proton for E_γ between 200 and 300 Mev. A similar study has been made at Massachusetts Institute of Technology by Osborne *et al.* (14), who included an analysis of the angular distribution; some of these data are shown in Figure 2. At California Institute of Technology the cross section for P_{γ^0} has been studied for several angles and values of E_γ between 270 and 450 Mev. This work has been done by Walker, Oakley & Tollestrop (15), and more recently some further preliminary information has been obtained by these workers.[8] The method used was similar to that of the Cornell group, the pulse height and range of the recoil protons being observed in coincidence with a decay γ-ray of the π^0.

The differential cross sections for P_{γ^+} have recently been studied by Bernardini & Goldwasser (16)[9] for $E_\gamma < 200$ Mev. The cross sections at low energies are evidently of particular importance for the determination of the g's of Equation 17 (and the multipole moments, as discussed in the part on *The angular distributions* of this section).

At CIT[2] the reaction P_{γ^+} has been studied for E_γ between 200 and 400 Mev. Tollestrop, Keck & Worlock (17) have used a scintillation counter telescope to measure ionization versus residual range for the π^+-mesons. Walker *et al.* (18) have measured the same cross sections, determining the pion energy and angle by a magnetic spectrometer. The CIT data concerning P_{γ^+} have been analyzed in the form of Equation 15 by Bacher *et al.* (19).[10]

The total cross sections.—We consider first the total cross sections for photomeson production. At sufficiently low energies the meson should be emitted into an S-state; however, as noted above, the S-wave amplitude seems to be quite small for π^0-production. This may be qualitatively understood on the basis of a simple model. Emission of a pseudoscalar pion into an S-state must occur only via electric dipole absorption of the photon (20, 21). If we suppose the amplitude for this to be proportional to the static electric dipole moment (with respect to the center-of-mass) for the appropriate meson-nucleon system in the final state, then

[8] Personal communication. We are much indebted to Professor Walker for informing us of this work.

[9] We are deeply indebted to Professors Bernardini and Goldwasser for discussions in advance of publication of their work.

[10] We should emphasize that the π^+ data and their analysis are still somewhat preliminary. We are greatly indebted to the CIT group for permission to quote their work.

$$\sigma(\gamma^-):\sigma(\gamma^+):\sigma(\gamma^0):\sigma(\gamma^{n0}) = [1+\mu/M]^2:1:1/2\left(\frac{\mu}{M}\right)^2:0 \qquad 18.$$

as long as only S-waves need be considered; here, M is the nucleonic mass.

This is in agreement with the observed smallness of the S-wave term for π^0-production. Also

$$\frac{\sigma(\gamma^-)}{\sigma(\gamma^+)} = [1+\mu/M]^2 = 1.32, \qquad 19.$$

on the basis of Equation 18. This is compatible with recent measurements by Sands *et al.* (22) which appear to give

$$\frac{\sigma(\gamma^-)}{\sigma(\gamma^+)} \simeq 1.4 \qquad 20.$$

for very low energy pions.

In view of the successful application of the one-level resonance formula of Equation 10 to the scattering (Fig. 5) it is natural to try the same approach here, considering photoproduction as the reaction channel of the scattering. To the extent that emission of the pion into the $(I=3/2, j=3/2)$ state is predominant, this should be a satisfactory approximation for energies near the "resonance" which occurs for $E_\gamma \cong 340$ Mev. Then (13, 23) (κ is the photon momentum in the barycentric system)

$$\sigma_T(\gamma^0) = 2\pi\left(\frac{\hbar}{\kappa}\right)^2 \frac{\Gamma_\gamma \Gamma}{(E-E_0)^2+\frac{\Gamma^2}{4}}, \qquad 21.$$

where Γ, E, and E_0 were defined in connection with Equation 10. For the reaction width Γ_γ we have $[\nu=\kappa/\mu c]$

$$\Gamma_\gamma = \frac{\nu^2 f_\gamma}{1+\left(\frac{a\kappa}{\hbar}\right)^2} \qquad 22.$$

with the channel radius a given by Equation 12. Here f_γ plays the role of a reduced width and is the only arbitrary parameter in Equation 21. We choose f_γ to be constant and to have the value

$$f_\gamma = 0.10 \text{ Mev}. \qquad 23.$$

In Figure 7 $\sigma_T(\gamma^0)$ as calculated from Equation 21 is compared with the experimental cross sections. [The "experimental" values of σ_T were obtained from the observed differential cross sections on the assumption that the angular distribution is of the form of expression 39 (see *The angular distributions* in this section).] Accepting our determination of $\sigma_T(\gamma^0)$ from the experimental data, one can hardly find any fault with the fit of Equation 21 to this for $0 < E_\gamma < 450$ Mev. The possible validity of Equation 21 is especially interesting in view of the fact that f_γ was our only free parameter.

Let us now investigate the total cross section for P_γ^+; *i.e.*, $\sigma_T(\gamma^+)$. Here the low energy cross sections indicate that an S-wave term is required (see

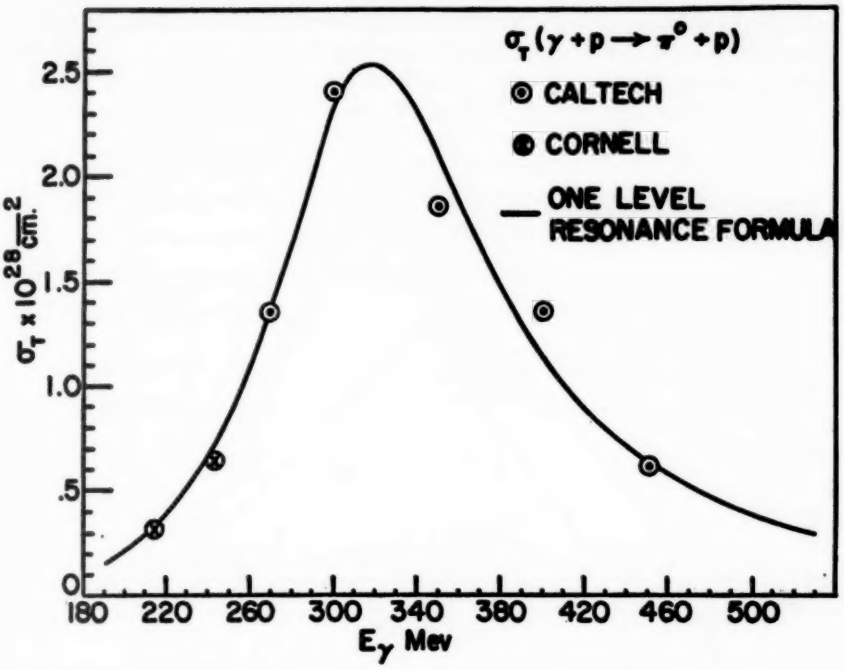

FIG. 7. A comparison of $\sigma_T(\gamma+p\rightarrow\pi^0+n)$ as calculated using the "resonance equation" 21 with experiment. The first two points are those of Equations 17 and the remainder are from Equations 19 and 20.

Fig. 2 and reference 16). We shall assume that the only modification of Equation 21 is in the appearance of an S-wave term as given by pseudoscalar meson theory [except that the P-wave contribution to $\sigma_T(\gamma^+)$ is only one half as great as it is for $\sigma_T(\gamma^0)$ by charge independence (20)]. Then

$$\sigma_T(\gamma^+) = \sigma_0\left(\frac{q}{\kappa}\right)\left[\frac{1-\frac{\kappa}{Mc}}{\left(1+\frac{\kappa}{Mc}\right)^2}\right]+\frac{1}{2}\sigma_T(\gamma^0). \qquad 24.$$

As mentioned above, the first term has the energy dependence expected from meson theory. We choose σ_0 to be constant and equal to

$$\sigma_0 = 2.5\ (10)^{-28}\ \text{cm}^2. \qquad 25.$$

In Figure 8 we compare Equation 24 with the experimental values for $\sigma_T(\gamma^+)$. The agreement is clearly not as good as it seemed to be for $\sigma_T(\gamma^0)$. The calculated curve does not fall off rapidly enough at high energies, but this may very well be the fault of the S-wave term in Equation 32, which by itself is larger than the experimental cross sections above 400 Mev. Also the

peak in the calculated curve seems to come at somewhat too high an energy. When we discuss the angular distribution in the following part it will become apparent that Equations 21 and 24 are oversimplifications. On the other hand, the agreement of these equations with experiment, as evidenced in Figures 7 and 8, is fairly good. Consequently, it is not at all unlikely that (except for finer details) the $(I=3/2,\ j=3/2)$ state is quite significant for photoproduction and indeed Equations 21 and 24 may be reasonable approximations to the actual cross sections.

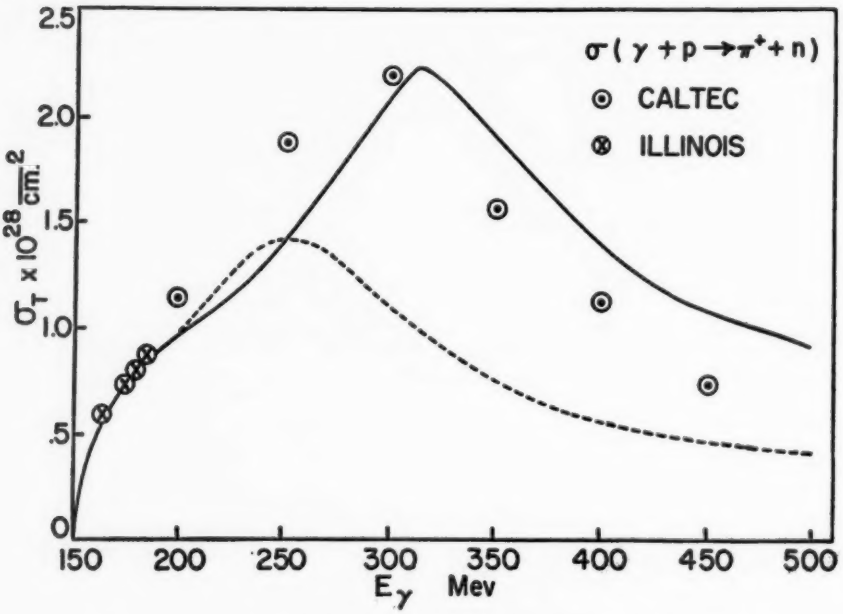

FIG. 8. A comparison of $\sigma_T(\gamma+p\to\pi^++n)$ as calculated from Equation 32 with experiment. The first three points are those of reference (16); the remainder are from references (17), (18) and (19). The dotted curve represents $[\sigma_T(\gamma^+)-\frac{1}{2}\sigma_T(\gamma^0)]$.

There is evidently no *a priori* justification for choosing the γ-ray channel radius a in Equation 22 the same as that for the meson (Equation 11). Indeed, in Equation 17 we have taken this radius for the γ-ray equal to zero. The finite value used in Equation 22 was of some help in bringing the cross sections down rapidly above the resonance peak. We do not, of course, even know that f_γ should remain constant over an appreciable energy interval, so it is not possible at present to say very much about the κ-dependence of the cross sections (except that it should not be important at "low energies").

We must also observe that the term "resonance" as applied to the scattering and photoproduction has not been precisely defined by our discussion. Aside from the statement that α_{33} passes through 90° for $\epsilon_\pi\cong 195$ Mev,

one would desire its energy dependence in this energy region. The Equations 10 and 21 are based on the analogy to resonant nuclear reactions, but probably cannot be justified in detail at relativistic energies (24). The most satisfactory study of resonant reactions involving relativistic pions seems to be that recently proposed by Sachs (24). His expression for a "resonant" cross section is rather similar to Equation 10.

The angular distributions.—The angular distribution for the cross section $\sigma(\gamma^+)$ has been analyzed in the form of Equation 15 by Bacher *et al.* (19) for

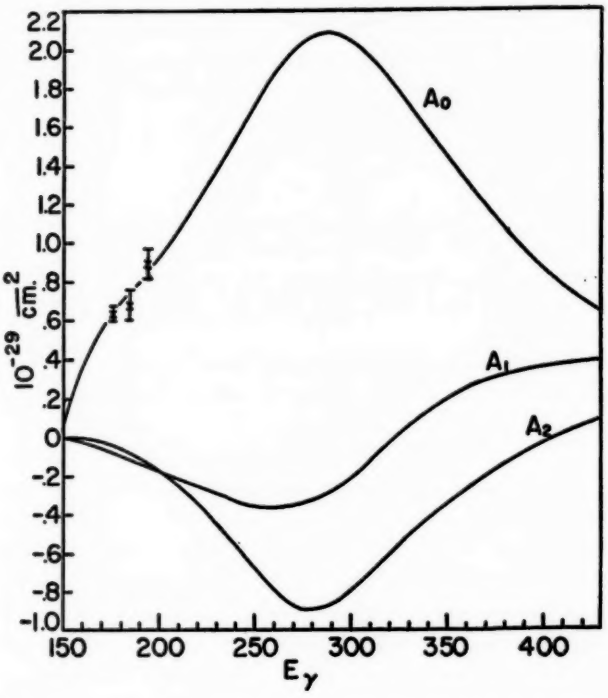

FIG. 9. Experimental values of the coefficients A_0, A_1, and A_2 in the angular distribution for $\gamma+p\rightarrow\pi^++n$. (See Equation 21.) The three indicated points are taken from reference (16); the curves above 250 Mev. are those of reference (19).

E_γ between 250 and 450 Mev. A similar analysis has been made by Bernardini & Goldwasser (25) for $E_\gamma<250$ Mev. The resulting coefficients in Equation 15 are plotted versus energy in Figure 9. Our coefficients in Figure 9 actually differ somewhat from those of the above references in that we have imposed on them the energy dependence implied by Equations 17 for $E_\gamma<250$ Mev. This change is compatible with present experimental uncertainties. The values which we have used for the coefficients g of Equations 17 are given in Table V.

TABLE V

THE COEFFICIENTS g OF EQUATIONS 17 FOR THE ANGULAR DISTRIBUTION FOR PHOTOMESON PRODUCTION*†

Process	$\gamma+p\rightarrow\pi^+ +n$	$\gamma+p\rightarrow\pi^0+p$
g_{0s}	10.5	—
g_{0p}	4.0	8.5
g_1	3.0	—
g_2	3.5	7.3

* The g's are given in units of 10^{-30} cm². g_{0s} is probably accurate to within 10 per cent. The remaining g's may be in error by as much as 25 per cent, although their relative values are probably much more accurate.

† The π^0 data are those of Oakley, D., and Walker, R. L. (24a) and of Osborne *et al.* (26).

The available information concerning the angular distribution $\sigma(\gamma^0)$ is still meager. In Table VI we give the values deduced by Osborne *et al.* (26) for the coefficients of Equation 15. Values for the g_{0P} and g_2 of Equations 17, which have been obtained from this and the work at Caltech, are included in Table V.

Perhaps the most striking conclusion from Table V is that the P-wave contributions to $\sigma(\gamma^0)$ and $\sigma(\gamma^+)$ appear to have a similar angular dependence

TABLE VI

THE ANGULAR DISTRIBUTION FOR THE REACTION $\gamma+p\rightarrow\pi^0+p$*

γ-ray energy	220 to 280 Mev	280 to 330 Mev
A_0	9 ± 1	18 ± 1
A_1	-2.5 ± 1	2.3 ± 1
A_2	-7.5 ± 2	-15 ± 3

* The coefficients A_0, A_1, and A_2 are those of Equation 31. This is based on preliminary MIT data.† The units are 10^{-30} cm.²/steradian.

† We are much indebted to Dr. Osborne for several discussions of this work, which is still quite preliminary. See reference (26).

and show a ratio of approximately 2:1 in strength. This is in agreement with the simple "resonance" theory given in the first part, *The total cross sections*, of this section. We proceed now with a more precise development of this theory.

A quantitative discussion of the angular distribution for photoproduction may conveniently be given in terms of a multipole expansion of the amplitudes for γ-ray absorption (25, 26). Because of the pseudoscalar parity of the pion, if the meson is emitted into an S-state, the transition must

be electric dipole with matrix element E_1. If the meson is emitted into a P-state with $j=1/2$, then the transition must be magnetic dipole with matrix element $M_1(1/2)$. A P-state with $j=3/2$ may be either magnetic dipole with matrix element $M_1(3/2)$ or electric quadrupole with matrix element E_2. Since an arbitrary combination of these may occur, we can write the scattering amplitude T for photoproduction in the concise form (20) (in the barycentric system):

$$\begin{aligned} T = {} & iE_1\boldsymbol{\sigma}\cdot\hat{\boldsymbol{\varepsilon}} - M_1(1/2)[\boldsymbol{\kappa}\times\hat{\boldsymbol{\varepsilon}}\cdot\boldsymbol{q} - i\boldsymbol{\sigma}\cdot(\boldsymbol{\kappa}\times\hat{\boldsymbol{\varepsilon}})\times\boldsymbol{q}]\kappa^{-1}q^{-1} \\ & - M_1(3/2)[2\boldsymbol{\kappa}\times\hat{\boldsymbol{\varepsilon}}\cdot\boldsymbol{q} + i\boldsymbol{\sigma}\cdot(\boldsymbol{\kappa}\times\hat{\boldsymbol{\varepsilon}})\times\boldsymbol{q}]\kappa^{-1}q^{-1} \\ & + iE_2 1/2[\sigma\cdot\boldsymbol{\kappa}\hat{\boldsymbol{\varepsilon}}\cdot\boldsymbol{q} + \boldsymbol{\sigma}\cdot\hat{\boldsymbol{\varepsilon}}\boldsymbol{\kappa}\cdot\boldsymbol{q}]\kappa^{-1}q^{-1}. \end{aligned} \qquad 26.$$

Here $\boldsymbol{\sigma}$ is the nucleon spin, $\boldsymbol{\kappa}$ is the photon momentum and $\hat{\boldsymbol{\varepsilon}}$ is its polarization vector, and $\boldsymbol{q}$ is the momentum of the meson. As mentioned above, there are four photoproduction processes, so we have actually four T's to be designated by

$$T^+,\ T^-,\ T^0,\ T(\pi 0).$$

Also, of course, there will be four sets of each of the multipole moments: E_1^+, E_1^-, etc.

The differential cross section σ is obtained in the usual manner by averaging $|T|^2$ over spin and polarization states:

$$\begin{aligned} \sigma = W\{ & |E_1|^2 + |M_1(1/2)|^2 + |M_1(3/2)|^2 1/2[5 - 3\cos^2\theta] \\ & + |E_2|^2 1/8[1 + \cos^2\theta] \\ & - 2\,Re\,[E_1^*(M_1(3/2) - M_1(1/2)) - 1/2E_2]\cos\theta \\ & - 1/2\,Re\,[E_2^*(M_1(3/2) - M_1(1/2))][3\cos^2\theta - 1] \\ & - Re\,[M_1^*(3/2)M_1(1/2)][3\cos^2\theta - 1]\}. \end{aligned}$$

In this equation θ is the angle between $\boldsymbol{\kappa}$ and $\boldsymbol{q}$ (all quantities referred to the barycentric system, as stated above). "Re (. . .)" means the "real part of (. . .)"; W is the statistical weighting factor, which is approximately

$$W = (2\pi)^4 \frac{\eta\omega}{\left[1+\frac{\kappa}{Mc}\right]^2}, \qquad 28.$$

where $\omega = [1+\eta^2]^{1/2}$ and M is the nucleonic mass.

We have, of course, four cross sections, $\sigma(\gamma^+)$, $\sigma(\gamma^-)$, etc. of the form of Equation 27. This means that there are 16 multipole amplitudes. When use is made of charge independence (7), then this number is reduced to 12 independent multipole amplitudes. Although these are complex quantities, this complexity is rather trivial. Indeed, in an appropriate representation the complex phases of the multipole amplitudes can be explicitly calculated in terms of the six phase shifts α (see SCATTERING OF PIONS BY NUCLEONS) characterizing the pion scattering.[11] This leaves us with twelve

[11] This fact has been noted independently by K. Aizu, by E. Fermi (Unpublished data), and by K. Watson (27a).

"real" parameters to describe the four photo cross sections. These arguments as well as the explicit form of the amplitudes are given in the Appendix.

The coefficients A_0, A_1, and A_2 of Equation 15 can be expressed in terms of the multipole amplitudes by means of Equation 27. We do this in a form suggested by Fermi (27). Let us define

$$\begin{aligned} X &\equiv 3/2M_1(3/2) + 1/4E_2 \\ Y &\equiv 1/2[M_1(3/2) - 1/2E_2] + M_1(1/2) \\ K &\equiv [M_1(3/2) - 1/2E_2] - M_1(1/2). \end{aligned} \tag{29.}$$

Then

$$\begin{aligned} A_0 &= W[|E_1|^2 + |X|^2 + |Y|^2] \\ A_2 &= W[|K|^2 - |X|^2 - |Y|^2] \\ A_1 &= -W\{2\,Re\,[E_1^*K]\}. \end{aligned} \tag{30.}$$

From the expressions given in the Appendix for the multipole matrix elements, we see that these are all "real" for energies sufficiently near threshold that the scattering phase shifts are small [say $E_\gamma < 250$ Mev for $\sigma(\gamma^+)$]. This is the energy range for which we have assumed that Equations 17 remain valid. For these energies, then E_1, X, Y, and K are "real" and are expected to have a simple energy dependence. We obtain, then immediately from Equations 30 a useful relation due to Fermi (27) between the g's of Equations 17:

$$g_1^2 = 4g_{0S}[g_{0P} - g_2]. \tag{31.}$$

Since the four g's can in principle each be determined experimentally, Equation 31 presents a test of the present model of photoproduction. It is satisfied to within the experimental errors by the values given in Table V for $\sigma(\gamma^+)$.

The small value of g_1^+ in Table V shows that $\sigma(\gamma^+)$ varies approximately as

$$\sin^2\theta$$

by Equation 31. We can determine directly from g_{0S}^+ the strength of the electric dipole term near threshold. This is

$$\sqrt{\omega}\,E_1^+ = \sqrt{\frac{\eta}{\nu}}\,3.3(10)^{-15}\text{ cm}. \tag{32.}$$

The smallness of g_1^+ makes it impossible to fit the threshold cross sections with a single P-wave multipole term, in contrast to the Brueckner-Watson hypothesis (20). The data may be fitted, however, with any two of the three terms, $M_1(3/2)$, $M_1(1/2)$, or E_2, nonvanishing. There is no reason to suppose that all three are not present.

Because of the smallness of E_1^0 near threshold for $\sigma(\gamma^0)$, the relation 31 is not expected to be valid for any appreciable energy interval for π^0-cross sections. Here a more elaborate analysis is required (see footnote 11).

To summarize our arguments for $\sigma(\gamma^+)$ and $\sigma(\gamma^0)$ near threshold, we find

an appreciable electric dipole term only for the former. The P-wave contributions to both cross sections appear to vary with angle roughly as $\sin^2\theta$. The 2:1 ratio of P-waves implied by the "resonance theory" seems to hold fairly well.

Let us now investigate the experimental data in the resonance region. Since the resonant ($I=3/2$, $j=3/2$, $l=1$) state can contribute only to $M_1(3/2)$ and E_2, we can expect these terms to be predominant. The expected enhancement of these two terms in the resonance region does not, of course, imply that the other multipole terms will be absent. However, if the resonance theory is valid, we should be able to neglect the remaining terms in a first approximation. Then, from the form given in the Appendix for the multipole moments, we can write (near the resonance energy)

$$\sqrt{W}\, M_1(3/2) = e^{i\alpha_3} \sin\alpha_{33} \left[\frac{\nu^{1/2}}{\eta^{3/2}}\right] \mu_1$$

$$\sqrt{W}\, E_2 = e^{i\alpha_{33}} \sin\alpha_{33} \left[\frac{\nu^{1/2}}{\eta^{3/2}}\right] \epsilon_2. \qquad 33.$$

Here μ_1 and ϵ_2 are real constant amplitudes. The complex factors $e^{i\alpha_{33}}$ appear for the reasons given in the Appendix. The factor $\sin\alpha_{33}$ represents a generalization of the energy dependence of Equation 21. Its use was discussed in reference (23).[12]

For the study of $\sigma(\gamma^+)$, Figure 9 shows that E_1^+ is also of importance. From the form given in the Appendix for E_1^+ and E_1^0 and also from the observation that E_1^0 seems to be very small at the energetic threshold, we shall set [in the notation of the Appendix]

$$2E_1^{(3)} = 1/2[E_1^{(1)} - 2\delta E_1^{(1)}]. \qquad 34.$$

This assures us that $E_1^0=0$ at threshold, which seems to be a reasonable approximation. Using Equation 34, we can write E_1^+ as

$$\sqrt{W}\, E_1^+ = \sqrt{\frac{\eta}{\nu}}\, \frac{\epsilon_1}{3} [e^{i\alpha_3} + 2e^{i\alpha_1}]. \qquad 35.$$

Here ϵ_1 has been defined by

$$\sqrt{2W}\, E_1^{(3)} = \sqrt{\frac{3}{\nu}}\, \epsilon_1.$$

We shall further suppose that ϵ_1 may be taken as a constant for $E_\gamma < 300$ Mev (which of course may not be correct).

Equations 30 may now be written as [using Equations 33 and 35]

[12] Equation 33 puts the resonance theory on a considerably sounder basis than did Equation 21, but are equivalent to this equation if α_{33} is of the form implied by Equation 10. For instance the more sophisticated theories of Sachs (29) and of Chew (see the section on MESON THEORY) will both relate the photoproduction to the scattering in the resonance region by equations 33.

$$A_1^+ = -2/3 \frac{\sin \alpha_{33}}{\eta} \epsilon_1 [\mu_1 - 1/2\epsilon_2][\cos(\alpha_{33} - \alpha_3) + 2\cos(\alpha_{33} - \alpha_1)]$$

$$A_2^+ = -\frac{\sin^2 \alpha_{33}}{4} \left[\frac{\nu}{\eta^3}\right] \{[3\mu_1 + 1/2\epsilon_2]^2 - 3[\mu_1 - 1/2\epsilon_2]^2\}$$

$$A_0^+(P) = \frac{\sin^2 \alpha_{33}}{4} \left[\frac{\nu}{\eta^3}\right] \{[3\mu_1 + 1/2\epsilon_2]^2 + [\mu_1 - 1/2\epsilon_2]^2\}. \quad 36.$$

From Equation 32 we obtain

$$\epsilon_1 = 3.3(10)^{-15} \text{ cm.} \quad 37.$$

From the data of Figure 9 we can determine the three A's and thus at any given energy Equations 36 represent three equations to determine two parameters: μ_1 and ϵ_2. It is evident from Figure 8 that the energy dependence of the A's may agree only roughly with that calculated from Equations 36.[13]

The first point of interest is that A_1^+ should change sign when $[\cos(\alpha_{33}-\alpha_3)+2\cos(\alpha_{33}-\alpha_1)]=0$. Using the phase shifts obtained from Table IV, we find that this factor vanishes at $E_\gamma = 335$ Mev. The experimental value of A_1, as obtained from Figure 9, vanishes at $E_\gamma \cong 325$ Mev. The agreement is evidently much better than the present experimental accuracy warrants. We may also use the slope of A_1^+ as it passes through zero to determine $(\mu_1 - 1/2\epsilon_2)$, since ϵ_1 is known. We obtain

$$\mu_1 - 1/2\epsilon_2 = 1.6(10)^{-15} \text{ cm.}, \quad 38.$$

although one must be cautious in view of the limited accuracy of the preliminary experiments quoted (19). We may now determine μ_1 and ϵ_2 by using either A_2^+ or $A_0^+(P)$. This leads to

$$\mu_1 = 2.5(10)^{-15} \text{ cm.}$$
$$\epsilon_2 = 1.8(10)^{-15} \text{ cm.} \quad 39.$$

Fortunately each of the two independent determinations leads to a value agreeing to within better than 10 per cent of those given by Equation 39. This seems to be a reassuring consistency check on our model (although perhaps not as impressive as its prediction of the vanishing of A_1^+ at $E_\gamma = 335$ Mev).

An important test of the resonance model is its prediction that

$$A_2^0/A_2^+ = \frac{A_0^0}{A_0^+(P)} = 2.$$

These relations do seem to be satisfied to within the experimental error (although the experimental ratio may be as large as 2.5). We also note [from Figure 9 and Table VI] that

[13] It has been pointed out to us by Professors G. Chew and G. Bernardini that by giving up the energy dependence of α_{33} implied by Equation 10 and using instead that of Table IV, one can fit better both the scattering and photoproduction (using Equations 36).

$$\frac{A_0^+(P)}{A_2^+} \cong 1.35, \quad \frac{A_0^0}{A_2^0} \cong 1.3. \tag{40.}$$

These are evidently subject to considerable experimental uncertainties ($\cong$25 per cent). If there were no electric quadrupole contribution (20), this ratio should be $5/3 \cong 1.67$ in both cases. These ratios, as well as Equations 38 and 39 do suggest that there is an electric quadrupole contribution.

Having once determined the multipole amplitudes in the "resonance region" for P_γ^+ the theory predicts uniquely the coefficient A_1^0 as well as A_0^0 and A_2^0 for P_γ^0. In the notation of Equations [see the Appendix and footnote 11]:

$$A_0^0 \cong A_0^0(P) = 1/2A_0^+(P)$$
$$A_2^0 = 1/2A_2^+$$
$$A_1^0 = -4/3 \frac{\sin \alpha_{33}}{\eta} \epsilon_1[\mu_1 - 1/2\epsilon_2][\cos(\alpha_{33} - \alpha_3) - \cos(\alpha_{33} - \alpha_1)]. \tag{41.}$$

When more detailed experimental information is available, these equations will provide a critical test of the "resonance model."

Before attacking the more complicated phenomena of nucleonic production of mesons, we may summarize our conclusions from the scattering and photoproduction. The three postulates of the section on SOME PHYSICAL CONCEPTS APPLYING TO PIONS [i.e., (*a*) the finite range of interaction; (*b*) the hypothesis of charge independence; (*c*) the resonance hypothesis] have provided a rather successful and reasonably complete framework for describing the present evidence for meson phenomena at "low energies." This seems to imply a certain inherent simplicity in the phenomena and lessens the burden to be met by a more basic and detailed theory.

π-MESON PRODUCTION IN NUCLEON-NUCLEON COLLISIONS[14]

We shall consider in this section the emission and absorption of pions by a system of two nucleons. The emission process can be studied experimentally by observing pions produced in the bombardment of hydrogen with neutrons or protons (or in an equivalent experiment using polyethylene-carbon difference). Absorption of pions can be studied by means of the reactions $\pi^+ + D \rightarrow 2P$ and $\pi^- + D \rightarrow 2N$.

According to the hypothesis of charge independence, the isotopic spin I of two nucleons may undergo, during the emission of a pion, one of three changes:

$I = 1 \rightarrow I = 0$, total cross section denoted by σ_{10}
$I = 0 \rightarrow I = 1$, total cross section denoted by σ_{01}
$I = 1 \rightarrow I = 1$, total cross section denoted by σ_{11}.

[14] This section overlaps considerably in content a paper by A. H. Rosenfeld to be published in the *Physical Review*. His paper and this article were written at the same time with frequent consultation between him and the authors. We wish to thank Dr. Rosenfeld for many stimulating discussions.

The process $I=0\rightarrow I=0$ is forbidden since the emitted pion carries away unit isotopic spin.

Since the deuteron has $I=0$, only the first process listed above can lead to deuteron formation. Accordingly we write $\sigma_{10}=\sigma_{10'}+\sigma_{10''}$, where $\sigma_{10'}$ refers to deuteron formation ("bound" reaction) and $\sigma_{10''}$ to the formation of two free nucleons with $I=0$ ("unbound" reaction).

The total cross sections for the various observable reactions involving meson production may be expressed in terms of $\sigma_{10'}$, $\sigma_{10''}$, σ_{01}, and σ_{11} as follows:

$$\begin{aligned}
&P+P\rightarrow\pi^{+}+D && \sigma=\sigma_{10'}\\
&P+P\rightarrow\pi^{+}+N+P && \sigma=\sigma_{10''}+\sigma_{11}\\
&P+P\rightarrow\pi^{0}+P+P && \sigma=\sigma_{11}\\
&N+P\rightarrow\pi^{0}+D && \sigma=1/2\sigma_{10'}\\
&N+P\rightarrow\pi^{0}+N+P && \sigma=1/2\sigma_{10''}+1/2\sigma_{01}\\
&N+P\rightarrow\pi^{+}+N+N && \sigma=1/2\sigma_{11}+1/2\sigma_{01}\\
&N+P\rightarrow\pi^{-}+P+P && \sigma=1/2\sigma_{11}+1/2\sigma_{01}.
\end{aligned} \qquad 42.$$

The factor 1/2 occurs in the N-P cross sections because the N-P system has equal probabilities of having $I=1$ and $I=0$, while the P-P system always has $I=1$.

The two observable absorption reactions may be expressed in terms of $\sigma_{10'}$ by means of the principle of detailed balancing:

$$\begin{aligned}
&\pi^{+}+D\rightarrow P+P\\
&\pi^{-}+D\rightarrow N+N
\end{aligned} \qquad \sigma=\sigma_{10'}\cdot 2/3\,\frac{\hat{p}^2}{\mu^2c^2}\,\frac{1}{\eta^2}. \qquad 43.$$

Here μ is the pion mass, c the velocity of light, $\hat{p}$ the final momentum of each neutron in the center-of-mass system, and η the pion momentum in the center-of-mass system in units of μc.

All the relations based on charge independence are subject to correction on account of Coulomb forces, the mass difference between neutron and proton, the mass difference between charged and neutral pion, and other minor charge-dependent effects, apart from any gross failure of the principle of charge independence.

We shall restrict our discussion of meson production to a region of bombarding energy ($<$450 Mev) in which η is always <1. In the same energy interval the internal energy E of the residual two-nucleon system is always $<\mu c^2(\sqrt{2}-1)=57$ Mev and tends to be much lower because of a preference for high pion momenta, as we shall see; let us say $E<25$ Mev for the most part. Now we may imagine the phenomenon of meson production to take place at a characteristic distance R from the center of collision, and R is certainly of the order of magnitude of $\hbar/\mu c$. In the energy region we are considering the product of R by either final neutron momentum or final meson momentum is thus $\lesssim\hbar$. We may safely suppose, then, that the meson will be emitted in an S- or a P-state with respect to the two nucleons and that the two final nucleons will be in an S- or a P-state relative to each other. In

the case of the nucleons the strong attractive force in the S-state (as contrasted with the relatively weak forces in the P-state at low energies) will strongly favor $l=0$ as well as enhancing the preference for low values of E. In the case of the meson, experiment reveals that the P-state is preferred (except very close to threshold), which indicates that the coupling responsible for meson production is primarily an interaction of the nucleon spin with the meson momentum, as in pseudoscalar meson theory.

In the absorption experiments, the internal angular momentum of the initial two nucleon system is always that of the deuteron, which is preponderantly $^3S_1$ with a small ($\sim$4 per cent) admixture of $^3D_1$. Again we shall be concerned only with energies for which $\eta<1$ and so the principal contribution to the process will come from S- and P-state mesons.

Let us consider first the best-known reaction, which is the one involving the formation (or disintegration) of a deuteron. The cross section for meson production with deuteron formation is the one we have designated by $\sigma_{10'}$. In this process, if the meson is emitted in an S-state, the total angular momentum of the final state is merely that of the deuteron, $J=1$. The parity in the final state is negative for a pseudoscalar meson. In the initial state of the two nucleons, then, we must have $I=1$, $J=1$, and negative parity. According to the Pauli principle a two-nucleon wave function symmetric in isotopic spin ($I=1$) and antisymmetric in space (negative parity) must be symmetric in spin (triplet). Thus the only possible initial configuration is $^3P_1$.

If the meson is emitted in a P-state, the total angular momentum of the final state may be $J=0$, 1, or 2, and the parity is positive. The initial state, with $I=1$ and positive parity, must be singlet and so the only possible initial configurations are $^3S_0$ and $^3D_2$.

At low energies, then, there are three possibilities as far as angular momentum is concerned:

(a') $\qquad 2N(^3P_1) \rightarrow D(^3S_1) +$ meson in S-state.

(b') $\qquad 2N(^1D_2) \rightarrow D(^3S_1) +$ meson in P-state.

(c') $\qquad 2N(^1S_0) \rightarrow D(^3S_1) +$ meson in P-state.

We will denote by δ_0 the ratio of the complex amplitude for process (c') to that for process (b'), the subscript referring to the fact that $J=0$, for (c'). Similarly we will denote by δ_1 the ratio of the amplitude of (a') to that of (b'). These ratios of complex amplitudes are related to the conventional S-matrix elements u_0, u_1, u_2 for $J=0$, $J=1$, and $J=2$ respectively, by the formulae

$$\delta_0 = -\frac{u_0}{\sqrt{5}\,u_2}$$

$$\delta_1 = -i\sqrt{3/5}\,\frac{u_1}{u_2}. \qquad 44.$$

Process (a') cannot interfere with the other two in the angular distribution or in the total cross section since (a') involves an initial triplet state and (b') and (c') an initial singlet state. We may therefore discuss S-wave and P-wave production of mesons separately.

The S-wave reaction must be characterized by an isotropic angular distribution and should have a cross section (near threshold) proportional to the meson momentum. At low energies, then, we may write

$$4\pi \frac{d\sigma_{10'}}{d\Omega} (S\text{-wave}) = \alpha\eta \tag{45.}$$

where α is independent of angle and energy. A value for the constant α has been determined by Brueckner, Serber, & Watson (3), using experimental data and one theoretical calculation. Let us follow their argument in detail.

Panofsky, Aamodt & Hadley (2) have measured the branching ratio between the two processes $\pi^- + D \to 2N$ and $\pi^- + D \to 2N + \gamma$ following the capture of negative pions in deuterium. The pion is presumably absorbed from an S-orbit around the deuteron. Panofsky's ratio is thus about equal to the ratio of the corresponding cross sections for the absorption of slow pions. Using his value of 7/3 we have

$$\sigma(\pi^- + D \to 2N) = 7/3\sigma(\pi^- + D \to 2N + \gamma) \tag{46.}$$

for slow pions. If we use (43) and the fact that for slow mesons $p^2 = \mu c^2 M$, where M is the nucleon mass, we have

$$\sigma_{10'} = \sigma(P + P \to \pi^+ + D) = 3/2\eta^2\mu/M\sigma(\pi^- + D \to 2N). \tag{47.}$$

Now Brueckner, Serber & Watson have estimated by calculation that

$$\sigma(\pi^- + D \to 2N + \gamma) = 2/3\sigma(\pi^- + P \to N + \gamma). \tag{48.}$$

From detailed balancing we have the further relation

$$\sigma(\pi^- + P \to N + \gamma) = \frac{2}{\eta^2}\sigma(\gamma + N \to \pi^- + P). \tag{49.}$$

The ratio of π^-- production to π^+-production in the photopion effect on deuterium is quoted (22) as 1.4, which indicates that

$$\sigma(\gamma + N \to \pi^- + P) = 1.4\sigma(\gamma + P \to \pi^+ + N). \tag{50.}$$

Combining 46, 47, 48, 49, and 50, we obtain

$$\sigma_{10'} = 14/3(1.4\mu/M)\sigma(\gamma + P \to \pi^+ + N) \approx \sigma(\gamma + P \to \pi^+ + N). \tag{51.}$$

Using Bernardini's value (16) of η (0.14 millibarn) for $\sigma(\gamma + P \to \pi^+ + N)$ near threshold and attaching a probable error to cover the various uncertainties in the steps 46 to 50, we come up with something like

$$\sigma_{10'}(S\text{-wave}) = \eta(.14 \pm .05) \text{ millibarn} \tag{52.}$$

or

$$\alpha = .14 \pm .05 \text{ millibarn.} \tag{53.}$$

Unlike the S-wave, the P-wave contribution to $\sigma_{10'}$ should be characterized by an η^3-dependence near threshold. The angular distribution is not unique, however, but depends on the complex number δ_0, the ratio of the amplitude of process c') to that of process b'). It turns out that the angular distribution of the P-wave cross section is of the form $X+\cos^2\theta$, where X is given by the equation

$$X = \left[\left|\frac{2-\sqrt{2}\,\delta_0}{1+\sqrt{2}\,\delta_0}\right|^2 - 1\right]^{-1}. \qquad 54.$$

Near threshold, we have then for the dependence of the P-wave cross section on energy and angle the formula

$$4\pi \frac{d\sigma_{10'}}{d\Omega}(P\text{-wave}) = \beta\eta^3 \frac{X+\cos^2\theta}{X+1/3}. \qquad 55.$$

Taking S- and P-waves together, we obtain for the total cross section

$$\sigma_{10'} = \alpha\eta + \beta\eta^3 \qquad 56.$$

and for the angular distribution $A+\cos^2\theta$, where

$$A = X + \frac{(X+1/3)}{\eta^2}\frac{\alpha}{\beta}. \qquad 57.$$

Now at a finite energy above threshold the parameters α, β, and X may all become functions of η. However, it is theoretically reasonable that as long as the meson wave length is larger than the critical distance R for meson production, *i.e.*, $\eta<1$, these parameters should vary slowly. We shall try to interpret the experimental data on the assumption that they are constant in the energy range we are considering (Equation 9).

We may then determine β and X by comparing the cross section and angular distribution formulae 56 and 57 with experiment at a single energy. Let us use the data of Crawford & Stevenson (28) (see Table VII), who quote, for $\eta=.58$, the values

$$\sigma_{\text{total}} = .269 \pm .026 \text{ millibarn}$$

and

$$A = .29 \pm .08.$$

If we take $\alpha=.14$ millibarn as in (53) we then find

$$\beta = 1.0 \text{ millibarn} \qquad 58.$$

and

$$X = .1. \qquad 59.$$

We may now compare our three-parameter semi-empirical formula

$$4\pi \frac{d\sigma}{d\Omega}\left\{.14\eta + 1.0\eta^3\frac{(.1+\cos^2\theta)}{(.1+1/3)}\right\} \text{ millibarn} \qquad 60.$$

with all the available experimental results in the reactions $P+P\rightarrow\pi^{+}+D$ and $\pi^{+}+D\rightarrow P+P$. Such a comparison is given in Table VII. It should be noted that cross sections for pion absorption have been converted to equivalent cross sections for the inverse process. Similarly the energies have been converted to equivalent proton bombarding energies.

TABLE VII

EXPERIMENTAL DATA ON NUCLEONIC MESON PRODUCTION

Reaction observed	Proton bombarding energy (Mev)	η	Measured value of $\sigma_{10'}$ (mb.)	Calculated value of $\sigma_{10'}$ (mb.)	Measured value of A	Calculated value of A	Reference
$P+P\rightarrow\pi^{+}+D$	311	.39	$.100\pm.013$	.11		.49	(*a*); (*b*)
	315	.42	$.133\pm.016$	.13		.44	(*a*); (*b*)
	321	.46	$.168\pm.018$	.16		.38	(*a*); (*b*)
	324	.48	$.178\pm.016$	.17	$.28\pm.07$	.36	(*a*); (*b*)
	330	.52	$.228\pm.017$	.21		.32	(*a*); (*b*)
	332	.54	$.245\pm.013$	.23	$.32\pm.05$	.31	(*b*)
	336	.56	$.264\pm.019$	.25		.29	(*a*); (*b*)
	338	.58	$.269\pm.026$	.28	$.29\pm.08$	.28	(*b*)
	340	.59	$.18\pm.06$	.29	$.11\pm.06$	.27	(*c*)
$\pi^{+}+D\rightarrow P+P$	341	.59	$.284\pm.050$	.29		.27	(*d*)
	346	.62	$.22\pm.02$	.33	$.19\pm.09$	.26	(*e*)
	382	.82	$.66\pm.07$	.67	$.26\pm.14$	.19	(*e*)
	413	.96	$.97\pm.10$	1.02	$.18\pm.15$	.17	(*e*)
$P+P\rightarrow\pi^{+}+D$	437	1.05	$1.15\pm.13$	1.30	$.20\pm.02$	.15	(*f*)

References:

(*a*): Schulz, A. G., *U. S. Atomic Energy Commission Document UCRL-1756* (1952).

(*b*): Crawford, F. S., and Stevenson, M. L., *U. S. Atomic Energy Commission Document UCRL-2187–2188* (1953).

(*c*): Cartwright, W. F., Richman, C., Whitehead, M. N., and Wilcox, H. A., *Phys. Rev.*, **91**, 677 (1953).

(*d*): Clark, D. L., Roberts, A., and Wilson, R., *Phys. Rev.*, **83**, 649 (1951).

(*e*): Durbin, R., Loar, H., and Steinberger, J., *Phys. Rev.*, **84**, 581 (1951).

(*f*): Fields, T. H., Fox, J. G., Kane, J. A., Stallwood, R. A., and Sutton, R. B., *Bull. Am. Phys.*, **29** (4) (1954).

The results of Cartwright *et al.* [Table VII, reference (*c*)] and of Durbin *et al.* [Table VII, reference (*e*)] at about 340 Mev are the only data in serious disagreement with the semi-empirical formula and are presumably to be thought of as superseded by the results of Crawford & Stevenson.

There are two experimental results on the reaction $N+P\rightarrow\pi^{0}+D$, which,

according to the hypothesis of charge independence, should be absolutely identical with the process $P+P\rightarrow\pi^{+}+D$ except for a factor of 1/2 in the absolute cross section (as in Equation 42). Hildebrand (29) gives an angular distribution of $.21\pm.06+\cos^{2}\theta$ at $\eta=.96$ and Schluter (30) a total cross section of $.6\pm.2$ millibarn in the range $.85<\eta<1.05$. Comparison with equation 60 shows that the charge independence is not violated insofar as the experimental error permits any conclusion.

The determination of the p-wave angular distribution parameter X does not fix the value of the complex number δ_0, the ratio of $J=0$ and $J=2$ contributions to the production of mesons in p-states. Rather δ_0 is restricted to lying on a circle in the complex plane. In fact,

$$\delta_0 = -\frac{1}{\sqrt{2}}(1+3X)+\frac{3}{\sqrt{2}}X(X+1)e^{i\omega_0} \qquad 61.$$

For $X=.1$ we have

$$\delta_0 = -.92+.70e^{i\omega_0} \qquad 62.$$

The value of the phase angle cannot be discovered by means of experiments such as we have discussed. However, it may be found by measuring the polarization of the deuterons in the reaction $P+P\rightarrow\pi^{+}+D$ or the asymmetry in the angular distribution of the reaction $\pi^{+}+D\rightarrow P+P$ when the target deuterons are polarized. In the case of $P+P\rightarrow\pi^{+}+D$, the deuterons associated with the P-wave part of the cross section are polarized perpendicular to the plane of scattering with the degree of polarization P_p given by Watson & Richman (31):

$$P_p = \frac{2\sqrt{X(X+1)}\sin\theta\cos\theta}{X+\cos^{2}\theta}\,\frac{\sin\omega_0}{1+2X-2\sqrt{X(X+1)}\cos\omega_0} \qquad 63.$$

where $-1\leqq P_p\leqq 1$. The deuterons associated with the S-wave part of the cross section are not polarized perpendicular to the plane of scattering.

We have not yet discussed the relative phase of the amplitudes for S-wave and P-wave meson production. The complex parameter δ_1 gives the ratio of the S-wave amplitude ($J=1$) to the amplitude for P-wave mesons with $J=2$. The absolute magnitude of δ_1 is determined by the relation

$$\frac{|\delta_1|^2}{1+|\delta_0|^2}=\frac{\alpha}{\beta\eta^2}, \qquad 64.$$

but the phase of δ_1 has not yet entered our work. It may be found by measuring the angular distribution of the reaction $P+P\rightarrow\pi^{+}+D$ using polarized protons or by measuring the polarization of the protons in the reaction $\pi^{+}+D\rightarrow P+P$. (The former experiment is certainly the easier one.) If the incoming proton beam (travelling in the Z-direction) is characterized by a degree of polarization P_1 in the $+X$-direction then the angular distribution of mesons and deuterons is given by (32).

$$\frac{d\sigma_{10'}}{d\Omega}\propto A+\cos^{2}\theta+P_1QA\sin\theta\sin\phi \qquad 65.$$

where

$$Q = \frac{1}{\sqrt{2}} \frac{2b}{1+b^2} \sin(\psi - \tau_1) \tag{66.}$$

if we put

$$\delta_1 = |\delta_1| e^{i\tau_1}, \tag{67.}$$

$$b = \frac{|\delta_0 + \sqrt{1/2}|}{|\delta_1|}, \tag{68.}$$

and

$$\psi = \arg(\delta_0 + \sqrt{1/2}). \tag{69.}$$

So far we have adopted the point of view that quantities do not vary appreciably with energy unless they have to. With such an attitude we would expect that, while $|\delta_1|$ will be inversely proportional to η as in Equation 64, the phase τ_1 should be roughly constant for $\eta \leqq 1$. Then the parameter of asymmetry Q will reach its maximum value of $\sqrt{2}/2 \sin(\psi - \tau_1)$ when

$$|\delta_1| = |\delta_0 + \sqrt{1/2}| \tag{70.}$$

or, using Equation 64, when

$$\eta = \eta_c \equiv \sqrt{\frac{\alpha}{\beta}} \frac{\sqrt{1 + |\delta_0|^2}}{|\delta_0 + \sqrt{1/2}|}. \tag{71.}$$

The energy dependence of the asymmetry becomes, with the use of Equations 64, 66, and 71,

$$Q/Q_{\max} = \frac{2\eta\eta_c}{\eta^2 + \eta_c^2}. \tag{72.}$$

The energy of maximum asymmetry corresponds to $\eta_c \approx .77$ no matter what value the phase ω_0 takes. (We put $\alpha/\beta = .14$ as in (60) and use (62) for δ_0.) The maximum value of $|Q|$ may range from 0 to .71 depending on the phase $\psi - \tau_1$. If this phase happens to be propitious for asymmetry, then the reaction using polarized protons may provide a valuable check on the proportion of S-wave as well as contribute to the determination of the phases.[15]

The phases are of considerable importance since they are closely related to the scattering phase shifts of the proton-proton system. We have put

$$\delta_1 = |\delta_1| e^{i\tau_1}. \tag{67.}$$

Let us, in the same way, write

$$\delta_0 = |\delta_0| e^{i\tau_0}, \tag{73.}$$

Then it can be shown that near the threshold for pion production τ_1 and τ_0

[15] A preliminary result of Marshall, Marshall & de Carvalho (a personal communication) indicates very little asymmetry ($Q = 4 \pm 6$ per cent) around $\eta = 1$; the phase $\psi - \tau_1$ must be very small, and no check on the proportion of S-wave can be made in this way.

can be expressed in terms of the P-P scattering phase shifts $\alpha(^1S_0)$, $\alpha(^1D_2)$, and $\alpha(^3P_1)$ by the relations (where n and n' are integers)

$$\tau_0 = \alpha(^1S_0) - \alpha(^1D_2) + n\pi. \qquad 74$$

and

$$\tau_1 = \alpha(^3P_1) - \alpha(^1D_2) + (n' + 1/2)\pi. \qquad 75.$$

The arguments leading to Equations 74 and 75 are similar to those used in the appendix to determine the phases of photopion matrix elements in terms of pion-nucleon scattering phase shifts. Equations 74 and 75 begin to fail at energies for which there is appreciable elastic or inelastic scattering of pions by deuterons. If the character of such scattering is understood, then Equations 74 and 75 can be corrected accordingly.

Let us now turn from meson production with deuteron formation to the corresponding reaction in which the two final nucleons are left unbound; in the notation of Equation 42, we pass from $\sigma_{10'}$ to $\sigma_{10''}$. Again the final nucleons have $I=0$ and zero relative orbital angular momentum; they are thus in a $^3S_1$ state like the deuteron. As in the deuteron reaction, there are three possible processes as far as angular momentum is concerned:

(a'') $\quad 2N(^3P_1) \rightarrow 2N(^3S_1) +$ meson in s-state.

(b'') $\quad 2N(^1D_2) \rightarrow 2N(^3S_1) +$ meson in p-state.

(c'') $\quad 2N(^1S_0) \rightarrow 2N(^3S_1) +$ meson in p-state.

We may suppose, in accordance with the point of view we have adopted, that the basic matrix element for each of these processes does not, for a fixed meson momentum, vary very rapidly with the energy of the residual nucleons and may be taken to be roughly constant over the energy range we are considering. In the same spirit, we should say that the matrix element for (a'') should be the same as that for (a') at the same meson momentum, etc. Then we may deduce, from our semi-empirical formula for $\sigma_{10'}$, both the value of $\sigma_{10''}$ and the energy spectrum of the mesons produced in the "unbound" reaction. The only factors we need take into account are the density of final states and the effect of nucleon-nucleon binding in the final states.

Let the bombarding energy be such that a total kinetic energy T_0 is available in the center-of-mass system after the reaction. Of this, an amount $T=\mu c^2(\sqrt{1+\eta^2}-1)$ is taken by the meson and $E=T_0-T$ by the internal motion of the two-nucleon system (neglecting its recoil). The differential cross section for the "unbound" reaction should be given by (23).

$$d\sigma_{10''} = (\alpha\eta + \beta\eta^3)\,\frac{\rho_E dE}{1}\,\frac{|\psi(R)|^2}{|\psi_D(R)|^2} \qquad 76.$$

where $\alpha\eta+\beta\eta^3$ is, of course, the cross section for production of mesons of the same momentum η associated with deuteron formation; $\rho_E dE/1$ is the ratio of the numbers of final states in the "unbound" and "bound" reactions; and $|\psi(R)|^2/|\psi_D(R)|^2$ is the ratio of the squares of the final two-nucleon wavefunctions at the critical distance for meson production. This last factor ex-

presses the relative effect in the "unbound" and "bound" reactions of the enhancement of the meson production cross sections by the attractive nucleon-nucleon forces in the final state. If we adopt a simple zero-range model for the nuclear force in the ${}^3S_1$ state, with a scattering length a related to the deuteron binding energy B by the equation

$$B = \hbar^2/Ma^2, \tag{77.}$$

and if we take $R \approx 0$, then we obtain

$$\left| \frac{\psi(R)}{\psi_D(R)} \right|^2 = \frac{2\pi a \hbar^2}{M(B+E)V} \tag{78.}$$

where V is a normalizing volume. The density of states is given, of course, by

$$\rho_E = \frac{V}{(2\pi\hbar)^3} 2\pi M^{3/2} E^{1/2}. \tag{79.}$$

We have then (23),

$$\frac{d\sigma_{10}''}{dE} = (\alpha\eta + \beta\eta^3) \frac{1}{2\pi} \left(\frac{E}{B}\right)^{\frac{1}{2}} \frac{1}{E+B} \tag{80.}$$

while the cross section for deuteron formation at the same bombarding energy is

$$\sigma_{10}' = \alpha\eta_D + \beta\eta_D^3 \tag{81.}$$

with η_D denoting the momentum in units of μc of the meson accompanying the deuteron.

Integration of the meson spectrum (Equation 80) with respect to energy and use of Equation 81 yields a predicted value of the ratio

$$\sigma_{10}''/\sigma_{10} = \frac{\sigma_{10}''}{\sigma_{10}' + \sigma_{10}''},$$

which is tabulated as a function of nuclear bombarding energy in Table VIII.

In order to find experimental values of the meson spectrum and the "continuum fraction" $\sigma_{10}''/\sigma_{10}$, it is necessary to examine the reactions $P+P \rightarrow \pi^+ + N + P$ or $N+P \rightarrow \pi^0 + N + P$ and to allow for the fact that the cross section for the former is $\sigma_{10}+\sigma_{11}$ and for the latter $\sigma_{10}''/2+\sigma_{01}/2$ rather than just σ_{10}'' and $\sigma_{10}''/2$ respectively. Fortunately both σ_{11} and σ_{01} are small in our energy region (see below); in Table VIII the experimental ratios need never be corrected by more than 10 per cent on this account. In those cases in which the quantity measured is σ_{10} rather than the "continuum fraction," the fraction is computed using the semi-empirical formula 60 for σ_{10}'. The agreement between measured and predicted ratios is fair, but the predicted values appear to be uniformly low, insofar as the large experimental errors permit any conclusion.

Those experiments which throw light on the continuum meson spectrum predicted in 72 have had, so far, insufficiently good resolution to make comparison with the theory worthwhile. They do not appear, at least, to be in

TABLE VIII

THE "CONTINUUM FRACTION"

Quantity measured	Value of ratio* $\sigma_{10}''/\sigma_{10}$	Predicted ratio*	Bombarding energy in Mev	Reference
$\sigma_{10}''/\sigma_{10}(P+P)$	35 ± 10	20	341	Cartwright, W. F., (Private communication to A. H. Rosenfeld)
$\sigma_{10}''/\sigma_{10}(P+P)$	45 ± 10	20	341	Peterson, V., Iloff, E., and Sherman, D., *Phys. Rev.*, **84**, 372 (1951)
$\sigma_{10}(P+P)$	40 ± 30	21	345	Passman, S., Block, M. M., and Havens, W. W., Jr., *Phys. Rev.*, **88**, 1239 (1952)
$\sigma_{10}(P+P)$	40 ± 30	28	365	Passman, S., Block, M. M., and Havens, W. W., Jr., *Phys. Rev.*, **88**, 1239 (1952)
$\sigma_{10}(P+P)$	55 ± 30	29	381	Passman, S., Block, M. M., and Havens, W. W., Jr., *Phys. Rev.*, **88**, 1239 (1952)
$\sigma_{10}''/\sigma_{10}(N+P)$	60 ± 15	32	400	Hildebrand, R. H., and Rosenfeld, A. H., Personal communication.
$\sigma_{10}(P+P)$	73 ± 40	36	440	Rosenfeld, A. H., Personal communication

* Ratio shown in per cent.

obvious contradiction. However, the existing experimental evidence on the continuum reaction does not rule out the possibility that the nucleons are left in a P-state in an appreciable fraction of the meson production events, at least near the high end of the energy range we are considering. The strongest of these processes would presumably be those in which the meson is emitted in a P-state:

$$\begin{aligned} 2N(^3P_0) &\rightarrow 2N(^1P_1) + \text{meson in } P\text{-state.} \\ 2N(^3P_1) &\rightarrow 2N(^1P_1) + \text{meson in } P\text{-state.} \\ 2N(^3P_2) &\rightarrow 2N(^1P_1) + \text{meson in } P\text{-state.} \\ 2N(^3F_2) &\rightarrow 2N(^1P_1) + \text{meson in } P\text{-state.} \end{aligned} \qquad 82.$$

For such reactions the cross section per unit energy would be proportional to $\eta^3 E^{3/2}$ rather than the expression 80, provided we ignore the effect of nuclear forces in the final state. (The nature of nuclear forces in the P-state is not well understood, but they are probably relatively weak.) On the same assumption the total excitation function for reactions 82 should be proportional to $\eta_{\max}{}^8$, where $\eta_{\max}$ is the maximum value of η for a given bombarding energy.

So far we have examined only the process $I=1\rightarrow I=0$. Let us take up next the process $I=1\rightarrow I=1$, which constitutes the whole of the reaction $P+P\rightarrow P+P+\pi^0$. In the process we have studied up to now the dominant

situation is one in which the meson is emitted in a P-state and the nucleons are left in an S-state. Such a situation is forbidden in the present process, $I=1\rightarrow I=1$. If the nucleons are left in an S-state, it is a singlet S-state. For the meson to be emitted in a P-state, the total angular momentum must be 1 and the parity of the system even. The only initial states of even parity are $^1S_0$, $^1D_2$, $^1G_4$, etc., none of which has angular momentum 1.

The only allowed situation in which the final nucleons are in an S-state is given by

$$(d) \qquad 2N(^3P_0) \rightarrow 2N(^1S_0) + \text{meson in } S\text{-state}.$$

Process (d) is characterized, of course, by an isotropic angular distribution. Near threshold the cross section per unit energy must be of the form

$$\frac{d\sigma_{11}(\text{process } d)}{dE} = \text{const.}\ \eta \frac{E^{1/2}}{E+B'} \qquad 83.$$

as in the s-state part of formula 80, with the binding energy B of the deuteron replaced by the energy B' of the virtual $^1S_0$ state of two neutrons. Since B' is very small ($\approx$60 Kev) we shall drop it. Then the total cross section near threshold is of the form

$$\sigma_{11}(\text{process } d) = \text{const.}\ \eta_{\max}{}^2. \qquad 84.$$

As in the case of σ_{10}'', we must not disregard the possibility that the nucleons are left in a P-state. This is particularly true of σ_{11} since the process which is dominant in σ_{10}'' (the production of mesons in P-states with the nucleons left in an S-state) is entirely absent in σ_{11}. If the final nucleons are in a P-state and the meson is emitted in a P-state, we have a list of possible processes analogous to 82:

$$\begin{aligned}
&2N(^3P_0) \rightarrow 2N(^3P_1) + \text{meson in } P\text{-state}.\\
&2N(^3P_1) \rightarrow 2N(^3P_0) + \text{meson in } P\text{-state}.\\
&2N(^3P_1) \rightarrow 2N(^3P_1) + \text{meson in } P\text{-state}.\\
&2N(^3P_1) \rightarrow 2N(^3P_2) + \text{meson in } P\text{-state}.\\
&2N(^3P_2) \rightarrow 2N(^3P_1) + \text{meson in } P\text{-state}.\\
&2N(^3P_2) \rightarrow 2N(^3P_2) + \text{meson in } P\text{-state}.\\
&2N(^3F_2) \rightarrow 2N(^3P_1) + \text{meson in } P\text{-state}.\\
&2N(^3F_2) \rightarrow 2N(^3P_2) + \text{meson in } P\text{-state}.\\
&2N(^3F_3) \rightarrow 2N(^3P_2) + \text{meson in } P\text{-state}.
\end{aligned} \qquad 85.$$

For these processes, as for those in Equation 28, we should expect a cross section per unit energy proportional to $\eta^3 E^{3/2}$ and a total cross section proportional to $\eta_{\max}{}^8$. Whereas in the case of σ_{10}'' the $\eta_{\max}{}^8$ term in the total cross section has not been detected experimentally with any certainty (it is presumably masked by the dominant reaction), there is strong experimental evidence for this term in σ_{11}. The reaction $P+P\rightarrow\pi^0+P+P$ has been investigated by Mather & Martinelli (33) at 341 Mev ($\eta_{\max}=.66$) and by Marshall & Marshall (34) at 430 Mev ($\eta=1.11$). The reported values for the

total cross section are $.010 \pm .003$ *mb.* and $.45 \pm .15$ *mb.* respectively. These results are consistent with a pure η_{max}^{8} law of the form

$$\sigma_{11} = (.2mb)\eta_{max}^{8}. \tag{86.}$$

In 86, we have completely ignored process (*d*), in which the nucleons are left in an *S*-state and the cross section varies as η_{max}. That process (*d*) is probably not absent, we shall see below. It should be important in the total cross section only at low energies, however, where the cross section is very small and measurement difficult.

We come now to the reaction $I=0 \rightarrow I=1$. In this reaction, if the nucleons are to be left in an *S*-state, the only possible processes are

(*e*) $2N(^3S_1) \rightarrow 2N(^1S_0) +$ meson in *P*-state, and

(*f*) $2N(^3D_1) \rightarrow 2N(^1S_0) +$ meson in *P*-state.

For these we should expect, near threshold, a cross section per unit energy of the form

$$\frac{d\sigma_{01}(\text{processes } e \text{ and } f)}{dE} = \text{const. } \eta^3 \frac{E^{1/2}}{E + B'}. \tag{87.}$$

As in 83, we may drop B'; we obtain in this case a total cross section obeying the law

$$\sigma_{01}(\text{processes } e \text{ and } f) = \gamma\eta_{max}^{4}. \tag{88.}$$

If the final nucleons are in a *P*-state and the meson emitted in a *P*-state, the possibilities are:

$$\begin{aligned} &2N(^1P_1) \rightarrow 2N(^3P_0) + \text{meson in } P\text{-state.} \\ &2N(^1P_1) \rightarrow 2N(^3P_1) + \text{meson in } P\text{-state.} \\ &2N(^1P_1) \rightarrow 2N(^3P_2) + \text{meson in } P\text{-state.} \\ &2N(^1F_3) \rightarrow 2N(^3P_2) + \text{meson in } P\text{-state.} \end{aligned} \tag{89.}$$

For these, we should expect, as usual, a total cross section varying like η_{max}^{8}.

Unfortunately, experimental evidence on σ_{01} is available only at a single energy. It can be seen from Equation 42 that σ_{01} is always observed experimentally in conjunction with either σ_{10}'' or σ_{11}. In fact,

$$\sigma(N + P \rightarrow \pi^+ + N + N) = \sigma(N + P \rightarrow \pi^- + P + P) = 1/2\sigma_{11} + 1/2\sigma_{01}. \tag{90.}$$

and

$$\sigma(N + P \rightarrow \pi^0 + N + P) = 1/2\sigma_{10}'' + 1/2\sigma_{01}. \tag{91.}$$

A total cross section for $N+P \rightarrow \pi^+ + N + N$ or $N+P \rightarrow \pi^- + P + P$ at around 405 Mev ($\eta = .915$) is reported by Yodh (35) who finds $.22 \pm .07$ *mb.* (See also 36.) If we now estimate σ_{11} at this energy by means of an interpolation formula like 86, and then use 90 to find σ_{01}, we obtain a very rough value of .3 *mb.* for σ_{01} at $\eta = .915$. Despite the enormous probable error to be attached to this value of σ_{01}, its smallness in comparison to the value of σ_{10}'' at the same energy ($\gtrsim 1$ *mb.*) is certainly significant.

Since we have no information concerning σ_{01} at other energies, we cannot check whether processes e and f effectively dominate the processes in 89. Let us tentatively assume, however, that the final nucleons are left primarily in S-states in which case we have for the constant in Equation 88

$$\gamma \approx 0.5mb. \qquad 92.$$

It should be noted that the relations 90 and 91 apply to total cross sections. In the case of 91, no interference is possible between the two isotopic spin processes under the hypothesis of charge independence, and so a similar formula obtains for the differential cross sections. Moreover, there is no forward-backward asymmetry in the angular distribution. (In a given isotopic spin state, the neutron and proton behave like indistinguishable particles.) In the reaction described by 90, however, interference between the two processes is possible and can lead to forward-backward asymmetry.

The angular distribution of the reaction $N+P \to \pi^- + P + P$ has been investigated by Yodh (35) and by Wright & Schluter (36), and forward-backward asymmetry has been discovered. If the reaction $I=0 \to I=1$ does leave the final nucleons mainly in S-states, then the reaction $I=1 \to I=1$ must also do so at least part of the time in order to produce such interference. Thus the process (d) above probably occurs with appreciable strength. It is difficult, however, on the basis of existing experimental evidence, to say anything quantitative.

Let us now review the principal features of the experimental data, interpreted in the manner we have described. It appears that low energy meson production phenomena have the following properties:

Nucleons left in S-states:

$I = 1 \to I = 0$: Meson production in P-states large, in S-states small. P-wave angular distribution is $\approx .1 + \cos^2 \theta$.

$I = 0 \to I = 1$: Meson production in P-states, small, in S-states forbidden.

$I = 1 \to I = 1$: Meson production in P-states forbidden, in S-states small.

Nucleons left in P-states:

Need be invoked only in case $I=1 \to I=1$. Not well understood.

In particular there are at present four important experimentally determined quantities that must be predicted by a theory that is to transcend the simple theoretical picture we have used:

(A) The ratio of S-wave to P-wave meson production in the reaction $I=1 \to I=0$.

$$\alpha/\beta \cong 1/7. \text{ (See Equations 45, 53, 55, and 58.)}$$

(B) The P-wave angular distribution parameter in the reaction $I=1 \to I=0$.

$$X \cong .1. \text{ (See Equations 55 and 59.)}$$

(C) The ratio of P-wave meson production in the reaction $I=0 \to I=1$ to that in the reaction $I=1 \to I=0$.

$\sigma_{01}/\sigma_{10}'' \lesssim .3$ (See discussion preceding Equation 92.)

(*D*) The absolute cross section for meson production.

$\beta \cong 1mb$. (See Equations 55 and 58.)

If we try to predict these quantities on the basis of some version of pseudoscalar meson theory, we see that the fourth one is related directly to the coupling constant and thus to the details of the theory (37). The other three also involve to some extent the details of the theory, but we can nevertheless obtain some understanding of their magnitudes in a fairly simple manner.

With regard to (*A*), it has been observed in the introduction that pseudoscalar mesons should interact with nucleons strongly in *P*-states, while the *S*-state interaction is in the nature of a recoil correction. Near the threshold for meson production, the basic matrix element for the emission of a pseudoscalar meson in a *P*-state is proportional to $\boldsymbol{\sigma}\cdot\boldsymbol{k}$, where $\boldsymbol{\sigma}$ is the spin of the emitting nucleon and $\boldsymbol{k}=\mu\boldsymbol{v}$ is the meson momentum. If we now insert a correction for the motion of the nucleon, we must replace $\boldsymbol{v}$ by $\boldsymbol{v}-\langle\boldsymbol{v}\rangle_n$, where $\langle\boldsymbol{v}\rangle_n$ is the average of the initial and final velocities of the emitting nucleon. (The principle of invariance under Galilean coordinate transformations requires that matrix elements depend on relative and not absolute velocities.) Now the final nucleon velocity is close to zero, while the initial one $\boldsymbol{v}_0$ (in the center-of-mass system) satisfies

$$M\boldsymbol{v}_0^2 \cong \mu c^2 \qquad 93.$$

since the kinetic energy of the colliding nucleons is transformed into meson rest energy. Thus recoil corrections add to the term $\boldsymbol{\sigma}\cdot\boldsymbol{k}$ (representing *P*-wave meson production) a term $-\boldsymbol{\sigma}(\mu\boldsymbol{v}_0/2)$ representing *S*-wave meson production and the ratio of intensities is of the order of $\mu^2v_0^2/4k^2=(\mu/4M)(1/\eta^2)$, which should correspond roughly to $\alpha/\beta\eta^2$. We see, then, the α/β should be of the order of μ/M. This conclusion is borne out by detailed meson theories.

With regard to (*B*) and (*C*), an explanation of the smallness of $\sigma_{01}/\sigma_{10}''$ and the closeness of X to 1/3 (it could have, in principle, any value between 0 and ∞!) has been offered by Aitken *et al.* (37). They make use of the strong pion-nucleon attraction in the (3/2, 3/2) state, which has been discussed in earlier sections. The basic idea is that if in the final state of a meson production process the pion and one of the nucleons can form a (3/2, 3/2) state the strong attractive forces enhance the matrix element for the process involved. (In a similar way, we have seen that the nucleon-nucleon forces serve to enhance those reactions in which the final nucleons are left in an *S*-state.)

Now there are four processes which contribute to *P*-wave meson production (with the nucleons left in a continuum *S*-state); we have labeled them as b'', c'', e and f. Of these, b'' and c'' contribute to σ_{10}'', while e and f contribute to σ_{01}. Processes e and f cannot be enhanced by the (3/2, 3/2) effect since the total isotopic spin of the system in these cases is 0, while a nucleon and a pion in an $I=3/2$ state plus another nucleon can have $I=1$ or 2 only.

Process c'' is not enhanced either, provided that the two nucleons are close together when the meson is produced, compared to the wave-length of the meson. (We have used this assumption before in assigning low angular momentum values to the outgoing particles.) The $J=0$ state then cannot result in the formation of a pion and nucleon in a $J=3/2$ state plus another nucleon in an S-state. The same argument applies to process c', which results in deuteron formation.

In the case of process b'' and b', enhancement occurs, and so we can understand that $\sigma_{01} \ll \sigma_{10}''$ and that the angular distribution of the $I=1 \rightarrow I=0$ process is close to the form characteristic of b'' or b' alone, i.e., $1/3+\cos^2\theta$. Note that if we accept this explanation of the angular distribution, the phase angle ω_0 in (62) must be close to 0°. Aitken *et al.* (37) have formed this argument more quantitatively, using detailed meson theory.

Meson Theory[16]

Meson theory, since the original proposal of Yukawa, has been constructed by analogy with quantum electrodynamics. Just as the primary process in electrodynamics is the virtual emission or absorption of a single photon by an electron, so in meson theory it is the virtual emission or absorption of a single pion by a nucleon. The "bare" nucleon (uncoupled to the pion field) is supposed to be described, like the electron, by Dirac's equation. The pseudoscalar pion field operator $\phi(\boldsymbol{x}, t)$ is analogous to the vector (spin 1) field operators $A_\mu(\boldsymbol{x}, t)$ representing the quantized potentials of the electromagnetic field. As $A_\mu(\boldsymbol{x}, t)$ is coupled to the vector Dirac operator γ_μ for the electron, so $\phi(\boldsymbol{x}, t)$ may be coupled to the pseudoscalar Dirac operator γ_5 for the nucleon (PS or pseudoscalar coupling) or else the gradient of ϕ, $\partial\phi/\partial x_\mu$ $(\boldsymbol{x}, t)$, may be coupled to the pseudovector Dirac operator $\gamma_5\gamma_\mu$ for the nucleon (PV or pseudovector coupling). No simple coupling of the pion field other than these two has been suggested. (It should be noted that to describe the three charge states of the pion, a three-component field ϕ_i is required, the three components forming a vector in the space of isotopic spin. In order to fulfill the requirements of charge independence, a "symmetrical" theory is used (5) in which the components ϕ_i are coupled to the components τ_i of the nucleon isotopic spin.)

For each of the two couplings a fully relativistic theory of pion-nucleon interactions can be set up and studied by the perturbation method, *i.e.*, expansion of observable quantities in powers of the coupling constant $g^2/4\pi\hbar c$ (for PS) or $f^2/4\pi\hbar c$ (for PV) for the interaction. As in quantum electrodynamics, the coefficients in such an expansion turn out to be infinite (after the lowest power of the coupling constant). In electrodynamics these infinities disappear when the results are re-expressed in terms of the observed mass and charge of the electron (the so-called mass and charge renormalization). The

[16] In this section we shall usually put $\hbar=c=1$.

same is found to be true in the PS theory of pions (38).[17] In the PV theory, however, infinities remain and the relativistic theory must be modified if finite results are to be obtained. A suitable modification is the introduction of a finite radius a for the bare nucleon, of the order of the nucleon Compton wavelength $\hbar/Mc$. All integrals over virtual pion momenta are then cut off at a momentum of $\hbar/a$ or an energy of $\omega_{\max}=\sqrt{\mu^2c^2+\hbar^2/a^2}$.

When the cut-off PV theory is employed for calculations, it is usual to introduce the static approximation, that is, to treat nucleons as fixed and ignore all or most effects of nucleon recoil. This approximation is not absolutely necessary, since in principle a relativistically invariant cut-off can be used and the effects of nucleon motion in the PV theory retained. However, it is usually felt that, since a cut-off must be used, recoil is probably badly treated anyway and might just as well be left out.

The static, cut-off PV theory has been treated in weak and strong coupling by several authors [for references to earlier work see (39); for recent work see (40)]. It has been found that while very weak and very strong coupling are both incompatible with experimental data on pion phenomena, the cases of moderately weak and moderately strong coupling both present features which are strongly suggestive of the experimental situation, particularly the presence of strong attractive forces between pions and nucleons in the (3/2, 3/2) state. The case of moderately weak coupling has recently been studied in great detail by Chew (40) and the results of calculation compared with experiment (41).[18] He finds that with a coupling constant $f^2/4\pi\hbar c=.058$ and a cut-off energy $\omega_{\max}=.84\ mc^2$ it is possible to obtain rough quantitative agreement with experimental data on pion scattering and the photopion effect at meson energies <250 Mev and the anomalous magnetic moments of neutron and proton, all phenomena involving a single nucleon. We shall refer to his approach as the Chew theory; let us examine it in some detail.

The Hamiltonian of the Chew theory is of the form

$$H = H_\pi + \frac{f}{\mu}\sum_i \tau_i\sigma\cdot\int \rho(x)\nabla\phi_i(x)d^3x + M. \qquad 94.$$

Here H_π is the field Hamiltonian of the pion and $\rho(x)$ is the function describing the nucleon as a source with finite extension; ρ is roughly characterized by the cut-off energy ω_c and the condition

$$\int \rho(x)d^3x = 1. \qquad 95.$$

The nucleon is placed at the origin.

This Hamiltonian need not be thought of as an approximation to that of the relativistic PV theory. If we wish to construct a charge-symmetric

[17] In the case of PS meson theory, it is in fact necessary to introduce and renormalize one more parameter, describing the scattering of mesons by mesons. (See 47.)

[18] We wish to thank Professor Chew for sending us many papers in advance of publication.

theory of the interaction of pseudoscalar mesons with a stationary nucleon, and if the interaction is to be linear in the meson field so that only a single meson is created or destroyed in an elementary act, we are led almost uniquely to 94.

If interaction with the photon field is to be introduced, then additional terms must be included in the Hamiltonian:

$$H_{\text{add.}} = H_{ph} - \int \mathbf{j}\cdot\mathbf{A}d^3x + \frac{fe}{\mu}\int d^3x\rho(\mathbf{x})\boldsymbol{\vartheta}\cdot\mathbf{A}(\phi_1\tau_2 - \phi_2\tau_1). \qquad 96.$$

Here the first term is the field Hamiltonian of the photon field; the second is the interaction of the meson current with the electromagnetic potential; the third is a term describing direct photomeson production; it arises from the requirement of gauge invariance. We have omitted all Coulomb interactions, the interaction of the Dirac magnetic moment of the proton with the photon field, and terms required by gauge-invariance inside the nucleon.

It is convenient to determine the coupling constant from experimental data on the photo-pion effect near threshold. In the Chew theory, this effect arises at low energies entirely from the third term in 96; moreover, it charge renormalization is performed in the conventional way, then the formula obtained by lowest-order perturbation theory is exact:

$$\sigma(\gamma^{\pm}) = 8\pi\left(\frac{e^2}{4\pi\hbar c}\right)\left(\frac{f^2}{4\pi\hbar c}\right)\left(\frac{\hbar}{\mu c}\right)^2\frac{\eta}{\nu} \qquad (\eta \ll 1). \qquad 97.$$

Here η and ν are, as in the section on PHOTOPRODUCTION OF π-MESONS FROM NUCLEONS, the momenta of meson and photon respectively in units of μc. Comparison with the experimental results of Bernardini & Goldwasser (16) gives for the coupling constant the value $f^2/4\pi\hbar c = .038$. Chew points out, however, that it is possible to correct formula 97 for certain kinematic effects of nucleon motion that are not included in the Chew theory itself. The resulting formula is

$$\sigma(\gamma^{\pm}) = 8\pi\left(\frac{e^2}{4\pi\hbar c}\right)\left(\frac{f^2}{4\pi\hbar c}\right)\left(\frac{\hbar}{\mu c}\right)^2\frac{\eta}{\nu}\left(1 \mp \frac{\omega}{2Mc^2}\right)^2\left(1 + \frac{\nu\mu}{M}\right)^{-1}\left(1 + \frac{\omega}{Mc^2}\right)^{-1}$$
$$(\eta \ll 1). \qquad 98.$$

where ω is the pion energy $\mu c^2\sqrt{1+\eta^2}$. If formula 98 rather than 97 is compared with the data of Bernardini & Goldwasser the coupling constant turns out to be $.058 \pm .015$. Equation 98 predicts for $\sigma(\gamma^-)/\sigma(\gamma^+)$ near threshold a value 1.3 in good agreement with the experimental value quoted in Equation 20.

Using the value we have just found for the coupling constant, Chew (40, 41) and others have calculated the p-wave phase shifts for pion-nucleon scattering. (It should be noticed that the Chew theory predicts no scattering in any states other than P-states. This is a rather serious difficulty, especially since it seems impossible to interpret the observed S-scattering as a recoil

effect; we have, in fact, at present no theoretical understanding of the S-wave in pion-nucleon scattering.)

In the P-wave phase shift calculations, it is found that perturbation theory is inadequate, especially for the (3/2, 3/2) state. Although the coupling is moderately weak and second and fourth order perturbation theory suffice more or less for calculating the "effective potential" in pion-nucleon scattering, this "potential" is not in itself weak enough in all states to be treated in Born approximation. The word "potential" is placed in quotation marks because the actual operator calculated is not a static potential $V(r)$ but something rather highly momentum- and energy-dependent. It was Tamm (42) and Dancoff (43) who first suggested that in problems such as these it would be better to calculate the nonstatic "potential" by perturba-

TABLE IX

P-WAVE PION-NUCLEON PHASE SHIFTS AS CALCULATED BY CHEW

E_{lab} (Mev)	η	α_{33}	$\alpha_{31}=\alpha_{13}$	α_{11}
38	.67	3.7°		
57	.83	8.0°	−1.0°	− 2.3°
78	.98	14.7°		
99	1.12	24.9°	−2.0°	− 4.3°
122	1.25	39.4°		
144	1.38	56.9°	−3.3°	− 6.4°
167	1.50	73.2°		
190	1.62	85.8°	−4.8°	− 8.4°
215	1.73	94.6°		
240	1.85	99.5°	−6.3°	−10.3°

tion theory and then calculate the scattering phases exactly than to expand the phase shifts directly in powers of the coupling constant. The method is now referred to as the Tamm-Dancoff or T-D method. It is not applicable when the coupling strength is so large that even the "potential" cannot be treated correctly by perturbation theory.

Using a slight modification of the T-D method and solving for the phase shifts by numerical methods, Chew (40), Gammel (44), and Salzman & Snyder (45) have found, with $\omega_{max}\cong.84\ mc^2$, values of the phase shifts that are in satisfactory agreement with the present experimental evidence. Chew's phase shifts are listed in Table IX. It is seen that the scattering in the (3/2, 3/2) state is attractive and "resonant"; in the other states it is repulsive and quite weak. It would presumably be unreasonable to compare the static cut-off theory with experiment at energies much greater than those listed, since recoil effects and the detailed nature of the cut-off should begin to enter the picture.

We may now return to the photopion effect and inquire what the Chew theory predicts for energies at which formula 98 no longer applies. Unfortu-

nately the relevant calculations are not yet in fully satisfactory shape; moreover, a static theory is necessarily ambiguous with regard to the treatment of the Dirac magnetic moment of the proton. Chew (41) reports, however, that preliminary calculations seem to agree fairly well with experimental data in the "resonance" region. Certainly the fact that the (3/2, 3/2) resonance occurs in the theory will cause to be applicable the kind of analysis we have used in the section on PHOTOPRODUCTION OF π-MESONS FROM NUCLEONS.

The meson-current contribution to the proton and neutron magnetic moments (necessarily equal and opposite in the two cases) has been calculated in perturbation approximation by Chew and collaborators (41). The result, with the same parameters as above, is ± 1.15 nuclear Bohr magnetons in second order and ± 1.48 when fourth order corrections are added. The experimental values of the anomalous moments are, of course, $+1.79$ and -1.91 for proton and neutron respectively.

In addition to Chew's program of investigation of one-nucleon problems, the static PV theory has been applied to the two-nucleon problem, *i.e.*, the meson theory of nuclear forces. The second- and fourth-order static potentials between a pair of nucleons have been calculated by Taketani *et al.* (46), Feynman & Lopes (47), Brueckner & Watson (48), and others. These potentials are highly singular at the origin and a boundary condition at small distances must be introduced if the Schrödinger equation is to be solved. The usual choice is the vanishing of the two-nucleon wave function at a separation of around $1/2\hbar/\mu c$ [the so-called hard core, discussed originally by Jastrow (49)]. With such an assumption and a coupling constant not substantially different from Chew's, it has been found that all the experimental parameters relating to the low energy two-body problem can be predicted with fair accuracy. Moreover it has lately been shown by Taketani *et al.* (50) and by Brueckner (51) that the qualitative features of nucleon-nucleon scattering up to 90 Mev can be well understood in terms of the same potential. It is important to show, of course, that higher order effects do not spoil the agreement with experiment. Present indications (48, 50) are that sixth and higher order potentials, while very strong, are also of very short range, and may not be of great importance outside the "core." The same may be true of effects due to the "new particles."

Let us now turn from the static cut-off PV theory to the fully relativistic PS theory, which gives finite results without a cut-off. The behavior of the PS theory is not so well understood as that of the other theory we have been discussing. It is quite certain that if the coupling constant is so small that straight perturbation theory is applicable, then the PS theory disagrees with observation. Also, no strong coupling approximation has ever been found that remotely resembles the experimental situation. Various approximations have been suggested for which validity is claimed in the range of intermediate coupling strength. It is at present doubtful, however, whether any of these

really gives an accurate picture of the predictions of the PS theory. As to the agreement of these approximations with experimental data, it is probably fair to say that they agree with experiment just insofar as they resemble the static cut-off theory of Chew. It may indeed be true that the Chew theory is a fair approximation to the PS theory with intermediate coupling strength, but a demonstration of that proposition has yet to be given.

The coupling constant that must be used in the PS theory if it is to agree with experiment can be determined by a method very similar to that employed above for the Chew theory, i.e., comparison with the photopion effect near threshold. Lowest-order perturbation theory gives for the PS theory Equation 98 with $f^2/4\pi\hbar c$ replaced by $(\mu/2M)^2g^2/4\pi\hbar c$, where $g^2/4\pi\hbar c$ is the PS coupling constant. Now in PS theory this formula is not correct to all orders as Equation 97 is in the Chew theory. However, Kroll & Ruderman (52) have shown that it is correct to all orders except for terms of the order of μ/M; they present arguments, too, to show that such terms are indeed small.[19] If we determine $g^2/4\pi\hbar c$ in this way, we find a value of about 10. It is clear why perturbation theory is not altogether satisfactory for calculating other processes!

In order to gain some insight into the structure of the PS theory, we may apply it to the method of Foldy & Wouthuysen (53). They eliminate from the Hamiltonian by a succession of canonical transformations the odd Dirac matrices (those anticommuting with β) in successive approximations in $1/M$. The original PS Hamiltonian, which we write for simplicity in the "one-particle" form, is

$$\mathrm{H_{PS}} = \mathrm{H}_\pi + \boldsymbol{\alpha}\cdot\boldsymbol{p} + \beta M + ig\beta\gamma_5\sum_i \tau_i\phi_i(\boldsymbol{x}), \qquad 99.$$

where $\boldsymbol{x}$ and $\boldsymbol{p}$ are the coordinate and momentum respectively of the nucleon. After transformation, to first order in $1/M$, we have

$$\mathrm{H_{PS}}' = \mathrm{H}_\pi + \frac{g}{2M}\boldsymbol{\sigma}\cdot\boldsymbol{\Delta}\sum_i \tau_i\phi_i(\boldsymbol{x}) + M + \frac{g^2}{2M}\sum_i \phi_i^2(\boldsymbol{x}) + \frac{p^2}{2M}\cdot \qquad 100.$$

If we compare 100 with Equation 94 for the Chew theory, putting $f = g\mu/2M$, we see that the first three terms in 100 correspond exactly to the Chew Hamiltonian, although the cut-off is not present. However, the recoil kinetic energy term $p^2/2M$ provides a cut-off of much the same kind after renormalization. The chief difference lies in the term

$$\frac{g^2}{2M}\sum_i \phi_i^2(\boldsymbol{x}),$$

which corresponds to the interaction of S-wave mesons with the nucleon, through scattering and through creation and destruction of pairs of mesons.

[19] Note that the correctness of the perturbation theory result as $(\mu/M)\to 0$ depends on the conventional choice of charge renormalization procedure.

Further, the recoil term couples the S-wave and P-wave mesons to some extent. At first sight, it would seem that Equation 100 must be an improvement over 94, since it gives similar results for P-wave mesons but predicts in addition some S-wave scattering, the lack of which was a flaw in the Chew theory. If we calculate the S-wave scattering using formula 100, though, we find it in disagreement with experiment. First of all, perturbation theory gives a very strong S-wave scattering which is totally at variance with experience. A refined treatment by Wentzel (54) shows that this effect is very strongly damped by higher order processes; the magnitude of the S-wave scattering is then similar to that observed. However, the isotopic spin and energy dependence of the S-scattering are still in contradiction with experiment. The success of 100 is not significantly different from that of the Chew theory.

However, 100 represents only an approximation to the PS theory. One may hope, therefore, that a correct treatment of the full PS Hamiltonian will give at least as good agreement with the known properties of pions in P-states and, in addition, explain such effects as the weak, isotopic spin-dependent S-wave scattering. A research project has been undertaken at Cornell by Bethe, Dyson and others (55) to determine whether this is in fact the case. They make use of the Tamm-Dancoff method, which is unfortunately not of proved validity in the case of PS theory with a coupling constant of 10. Calculations are in progress of cross sections for meson scattering and photomeson production and preliminary reports of the work seem encouraging as regards agreement with experiments on P-wave pions.

If the full PS theory is to prove correct, one other feature of the approximate Hamiltonian 100 must be preserved; that is the damping of S-wave scattering. Some indication that this may occur in the relativistic PS theory has been provided by a very rough calculation of Brueckner, Gell-Mann & Goldberger (56).

Bethe (55) has expressed confidence that the PS theory will turn out to give a correct description of pion phenomena at moderately low energies. He attaches great significance to the fact that the PS theory is the only known relativistically invariant theory of pseudoscalar mesons that gives finite results after renormalization without a cut-off. Chew (41) is inclined, on the other hand, to believe that attempts to refine the static cut-off PV theory must be more ambitious than the use of the PS theory, and must ultimately involve a description of the "new unstable particles." It is indeed difficult to believe that such a description is possible within the framework of any existing theory.

The authors would like to express their appreciation to Professors G. Bernardini, G. F. Chew, E. Fermi, and R. G. Sachs, and Dr. A. H. Rosenfeld for enlightening conversations and suggestions and for supplying material in advance of publication. Also they would like to acknowledge the great value to them in preparing this review of the 1954 Rochester Conference on High Energy Physics.

APPENDIX:

CALCULATION OF THE COMPLEX PHASES OF THE MATRIX ELEMENTS FOR PHOTOPRODUCTION

We indicate briefly the method employed in references of footnote 11 for determining the phases in Equations 19 and 20. Consider the transition between eigenstates of a Hamiltonian H_0 induced by an interaction V. Then the integral equation satisfied by the reaction matrix K is*

$$K = V + V\frac{1}{E - H_0}K, \qquad \text{A-1.}$$

where E is the energy of the system. If V and H_0 are invariant under the Wigner time reversal operator $\boldsymbol{K}$, then so is K; i.e.

$$\boldsymbol{K}K\boldsymbol{K}^{-1} = K. \qquad \text{A-2.}$$

The integral equation relating K to the scattering amplitude T is*

$$T = K + iKT, \qquad \text{A-3.}$$

where all quantities are here restricted to the energy shell (in contrast to those of Equation A-1). Let us denote the eigenfunctions of H_0 by

$$\phi_{rj}{}^{m}$$

where r denotes the channel parameter (i.e., the types of states into which the scattering may lead) and j is the total angular momentum with z-component m. (There will in general be other eigenvariables which we shall ignore for the sake of brevity.) We may expand K in terms of the ϕ's:

$$K = \sum_{r,r'}\sum_{m}(r/K/r')\phi_{rj}{}^{m}\phi_{r'j}{}^{*m}. \qquad \text{A-4.}$$

Here $(r/K/r')$ is a function only of energy and r and r'. If we choose the most common representation, then

$$\boldsymbol{K}\phi_{rj}{}^{m} = (i)^{2m}\phi_{rj}{}^{-m} \qquad \text{A-5.}$$

and (since $\boldsymbol{K}$ involves complex conjugation)

$$\boldsymbol{K}K\boldsymbol{K}^{-1} = \sum_{r,r'}\sum_{m}(r/K/r')^{*}(i)^{2m}(-i)^{2m}\phi_{rj}{}^{-m}\phi_{r'p}{}^{*-m}. \qquad \text{A-6.}$$

Making use of Equation A-2 we see that

$$(r/K/r')^{*} = (r/K/r') \equiv K_0. \qquad \text{A-7.}$$

Thus the submatrix $(r/K/r')$ is real and symmetric (since it is hermitean), a result which depends upon choosing the ϕ's to satisfy equation A-5.

* See, for instance, M. Gell-Mann & M. L. Goldberger, *Phys. Rev.*, **91**, 398 (1953) for the general theory of scattering processes.

To illustrate the implications of equation A-7 let us consider meson-nucleon scattering for a pure (j, l) state and photoproduction to the same state of the meson and nucleon. Then

$$K_0 = \begin{pmatrix} 0 & \gamma \\ \gamma & \tan\delta \end{pmatrix} \begin{matrix} (\gamma\text{-ray-nucleon state}) \\ (\text{pion-nucleon state}), \end{matrix} \qquad \text{A-8.}$$

where δ is the scattering phase shift and γ is the strength of the coupling to the γ-ray channel. We consider γ to be small (since it involves an electromagnetic interaction) and neglect the γ-γ scattering by a nucleon. (This is the reason that the element in the upper left hand corner of K_0 is zero.)

Returning to Equation A-3, we expand T in the form of Equation A-4, letting

$$T_0 \equiv (r/T/r').$$

In terms of T_0 and K_0, Equation A-3 is

$$T_0 \equiv K_0 + iK_0T_0,$$

or

$$T_0 = (1 - iK_0)^{-1}K_0. \qquad \text{A-9.}$$

The matrix products are easily evaluated and we find

$$T_0 = \begin{pmatrix} 0 & e^{i\delta}\gamma\cos\delta \\ e^{i\delta}\gamma\cos\delta & e^{i\delta}\sin\delta \end{pmatrix}. \qquad \text{A-10.}$$

Here the off diagonal matrix elements represent a single multipole matrix element for photoproduction. Since δ and γ are real, this has the form

$e^{i\delta}$ times a real quantity.

This result has a number of implications for photoproduction. These have been derived in detail (see footnote 11, page 241). We quote them here. The multipole expressions of Equations 26 are expressed in terms of the amplitude for transitions to pure I-states. Then (here the α's are the pion-nucleon scattering phase shifts evaluated at the energy of pion and nucleon in the final state)

$$\begin{aligned}
E_1^+ &= e^{i\alpha_3}\sqrt{2}\,E_1^{(3)} + e^{i\alpha_1}\frac{1}{\sqrt{2}}\left[E_1^{(1)} - 2\delta E_1^{(1)}\right] \\
E_1^0 &= e^{i\alpha_3}2E_1^{(3)} - e^{i\alpha_1}1/2\left[E_1^{(1)} - 2\delta E_1^{(1)}\right] \\
M_1(1/2)^+ &= e^{i\alpha_{31}}\sqrt{2}\,M_1(1/2)^{(3)} + e^{i\alpha_{11}}\frac{1}{\sqrt{2}}\left[M_1(1/2)^{(1)} - 2\delta M_1(1/2)^{(1)}\right] \\
M_1(1/2)^0 &= e^{i\alpha_{31}}2M_1(1/2)^{(3)} - e^{i\alpha_{11}}1/2\left[M_1(1/2)^{(1)} - 2\delta M_1(1/2)^{(1)}\right] \\
M_1(3/2)^+ &= e^{i\alpha_{33}}\sqrt{2}\,M_1(3/2)^{(3)} + e^{i\alpha_{13}}\frac{1}{\sqrt{2}}\left[M_1(3/2)^{(1)} - 2\delta M_1(3/2)^{(1)}\right] \\
M_1(3/2)^0 &= e^{i\alpha_{33}}2M_1(3/2)^{(3)} - e^{i\alpha_{13}}1/2\left[M_1(3/2)^{(1)} - 2\delta M_1(3/2)^{(1)}\right] \\
E_2^+ &= e^{i\alpha_{33}}\sqrt{2}\,E_2^{(3)} + e^{i\alpha_{13}}\frac{1}{\sqrt{2}}\left[E_2^{(1)} - 2\delta E_2^{(1)}\right] \\
E_2^0 &= e^{i\alpha_{33}}2E_2^{(3)} - e^{i\alpha_{13}}1/2\left[E_2^{(1)} - 2\delta E_2^{(1)}\right].
\end{aligned} \qquad \text{A-11.}$$

The 12 quantities $E_1^{(3)}$, $M_1(1/2)^1$, $\delta E_2^{(1)}$, etc. represent transition amplitudes to pure I-states of the final pion-nucleon system. The superscript is just twice the value of this I-spin. The primary significance of these equations is that the 12 quantities $E_1^{(3)}$, etc., are real functions of the γ-ray energy only.

We obtain the multipole amplitudes for P_γ^- from those for P_γ^+ and for $P_{(\gamma no)}$ from those for P_γ^- in Equations A-11 by simply changing the sign of $\delta E_1^{(1)}$, $\delta M_1(1/2)^{(1)}$, $\delta M_1(3/2)^{(1)}$ and $\delta E_2^{(1)}$. Thus the 16 complex multipole amplitudes are expressed in terms of 12 real quantities. For further details see footnote 11, p. 241.

Only $E_2^{(3)}$ and $M_1(3/2)^{(3)}$ contribute to the "resonant state." For $E_\gamma \cong 320$ Mev, these are expected to have the form (23)

$$M_1(3/2)^{(3)} \text{ and } E_2^{(3)} = \frac{\sin \alpha_{33}}{\eta^2} \text{ times a real constant,}$$

as written in Equation 33.

LITERATURE CITED

1. Dilworth, C., Occhialini, G. P. S., and Scarsi, L., *Ann. Rev. Nuclear Sci.*, **4**, 271-314 (1954)
2. Panofsky, W., Aamodt, L., and Hadley, J., *Phys. Rev.*, **81**, 565 (1951)
3. Brueckner, K., Serber, R., and Watson, K., *Phys. Rev.*, **81**, 575 (1951)
4. Breit, G., and Feenberg, E., *Phys. Rev.*, **50**, 850 (1936)
5. Kemmer, N., *Proc. Cambridge Phil. Soc.*, **34**, 354 (1938)
6. Heitler, W., *Proc. Roy. Irish Acad.*, **51**, 33 (1946)
7. Watson, K., *Phys. Rev.*, **85**, 852 (1952); Watson, K., and Brueckner, K., *Phys. Rev.*, **83**, 1 (1951)
8. Brueckner, K. A., *Phys. Rev.*, **86**, 206 (1952)
9. Crussard, J., *Proc. Conf. on High Energy Physics* (Rochester, New York, 1954)
10. Ashkin, J., *Proc. Conf. on High Energy Physics* (Rochester, New York, 1954)
11. de Hoffmann, F., Metropolis, N., Alei, E., and Bethe, H. A., *Phys. Rev.* (To be published)
12. Anderson, H., Fermi, E., Martin, R., and Nagle, D., *Phys. Rev.*, **91**, 155 (1953); Fermi, E., and Metropolis, N. (Unpublished data); Martin, R. L., *Bull. Am. Phys. Soc.*, **29**, Abstr. KA2 (1954); Bethe, H., and Glicksman, M., *Proc. Conf. High Energy Physics* (Rochester, New York, 1954)
13. Silverman, A., and Stearns, M., *Phys. Rev.*, **88**, 1225 (1952)
14. Goldschmidt-Clermont, Y., Osborne, L. S., and Scott, M. B., *Phys. Rev.*, **89**, 329 (1953)
15. Walker, R., Oakley, D., and Tollestrup, A., *Phys. Rev.*, **89**, 1301 (1953)
16. Bernardini, G., and Goldwasser, E. L., *Phys. Rev.*, **94**, 729 (1954)
17. Tollestrup, A., Keck, J., and Worlock, R., *Phys. Rev.*, **92**, 1090 (A) (1953); and (Personal communication, January 4, 1954)
18. Walker, R., Teasdale, J., Peterson, V., and Vette, J., *Phys. Rev.*, **92**, 1090 (1953); and (Personal communication, January, 1954)
19. Bacher, R. F., Keck, J., Peterson, V., Teasdale, J., Tollestrup, A., Walker, R., and Worlock, R., *Phys. Rev.*, **92**, 1090 (1953)
20. Brueckner, K. A., and Watson, K. M., *Phys. Rev.*, **86**, 923 (1952)

21. Feld, B. T., *Phys. Rev.*, **89,** 330 (1943)
22. Sands, M., Teasdale, J., and Walker, R., *Phys. Rev.*, **95,** 592 (1954)
23. Watson, K., *Phys. Rev.*, **88,** 1163 (1952)
24. Sachs, R. G., *Phys. Rev.* (To be published)
24a. Oakley, D., and Walker, R. D., *Phys. Rev.* (To be published)
25. Bernardini, G., and Goldwasser, E. (Personal communication)
26. Osborne, L. S., Goldschmidt-Clermont, Y., and Scott, M. (Unpublished data)
27. Fermi, E. (Personal communication, April, 1954)
27a. Watson, K., *Phys. Rev.*, **95,** 228 (1954)
28. Crawford, F. S., and Stevenson, M. L., *U. S. Atomic Energy Commission Document, UCRL-2187-88* (1953)
29. Hildebrand, R. H., *Phys. Rev.*, **89,** 1090 (1953)
30. Schluter, R. A., *Bull. Am. Phys. Soc.*, **29,** (4) (1954)
31. Watson, K. M., and Richman, C., *Phys. Rev.*, **83,** 1257 (1951)
32. Marshak, R. E., and Messiah, A. M. L., *Nuovo cimento*, **11,** 337 (1954)
33. Mather, J. W., and Martinelli, E. A., *Phys. Rev.*, **92,** 780 (1953)
34. Marshall, J., and Marshall, L., *Phys. Rev.*, **88,** 632 (1952)
35. Yodh, G. B. (Personal communication)
36. Wright, C., and Schluter, R. A., *Bull. Am. Phys. Soc.*, **29,** (4) (1954); and (Personal communication, May, 1954)
37. Aitken, A. L., Mahmoud, H. M., Henley, E. M., Ruderman, M. A., and Watson, K. M., *Phys. Rev.*, **93,** 1349 (1954)
38. Ward, J. C., *Phys. Rev.*, **84,** 897 (1951)
39. Pauli, W., *Meson Theory of Nuclear Forces* (Interscience Publishers, New York, N. Y., 69 pp., 1946)
40. Chew, G. F., *Phys. Rev.*, **89,** 591 (1953); Blair, J. S., and Chew, G. F., *Phys. Rev.*, **90,** 1065 (1953)
41. Chew, G. F., *Phys. Rev.*, **95,** 285 (1954)
42. Tamm, I., *J. Phys. U.S.S.R.*, **9,** 449 (1945)
43. Dancoff, S., *Phys. Rev.*, **78,** 382 (1950)
44. Gammel, J., *Phys. Rev.*, **95,** 209 (1954)
45. Salzman, F., and Snyder, J., *Phys. Rev.*, **95,** 286 (1954)
46. Taketani, M., *et al.*, *Progr. Theoret. Phys.* (*Japan*), **6,** 581 (1951); Taketani, M., *et al.*, *Progr. Theoret. Phys.* (*Japan*), **7,** 45 (1952)
47. Feynman, R. P., and Leite Lopes, J., *Notas de Fisica*, No. 2 (1954)
48. Brueckner, K. A., and Watson, K. M., *Phys. Rev.*, **92,** 1023 (1953)
49. Jastrow, R., *Phys. Rev.*, **81,** 165 (1951)
50. Fujii, S., Iwadare, J., Otsuki, S., Taketani, M., Tani, S., and Watari, W., *Progr. Theoret. Phys.* (*Japan*), **11,** 11 (1954)
51. Brueckner, K. A. (Personal communication, May, 1954)
52. Kroll, N., and Ruderman, M., *Phys. Rev.*, **93,** 233 (1954)
53. Foldy, L. L., and Wouthuysen, S. A., *Phys. Rev.*, **78,** 29 (1950); Dyson, F. J., *Phys. Rev.*, **73,** 929 (1948)
54. Wentzel, G., *Phys. Rev.*, **86,** 802 (1952)
55. Dyson, F. J., Schweber, S. S., and Visscher, W. M., *Phys. Rev.*, **90,** 372 (1953); Ross, M., *Phys. Rev.*, **92,** 454 (1954); Bethe, H. A., and de Hoffmann, F., *Meson Physics*, N.P. (1954)
56. Brueckner, K. A., Gell-Mann, M., and Goldberger, M., *Phys. Rev.*, **90,** 476 (1953)

HEAVY MESONS[1,2]

By C. Dilworth, G. P. S. Occhialini, and L. Scarsi
Department of Physics, University of Milan, Milan, Italy
and
Department of Physics, University of Brussels, Brussels, Belgium

"And small fleas have smaller ones
And so ad infinitum?"

The present knowledge of heavy mesons is limited to a considerable extent by a lack of coherence in the observation and measurements. There now exists a goodly number of events of the less infrequent type, and yet the information available on them is not such as to permit a unique classification.

The root of the trouble lies in the complexity of the problem as well as in the diversity of apparatus employed (Wilson chamber with and without magnetic field, multiplate chamber, photographic emulsion), in its inherent imperfections, in the limited precision with which certain measurements can be made, and in the paucity of knowledge of certain constants and relations indispensable to the interpretation of these measurements.

We will therefore devote the first section of this article to a critical survey of the experimental framework in which must be considered the results assembled in later sections.

The Experimental Background

The Photographic Emulsion.—The imperfections of this detector of particles are being surmounted with such rapidity that it is perhaps idle to dwell too long on them. The lack of sensitivity which in 1946 limited the study of unstable particles to those whose decay product is of low velocity (e.g., the π-meson) was remedied by 1948 with the introduction of emulsions sensitive to minimum ionisation. The immediate result was the discovery of the τ-meson decay. The elaboration of the technique of processing improved so fundamentally the qualities of the instrument, that what was in 1945 hardly more than a two-dimensional indicator of events, became by 1950 a precision instrument. More recently, the introduction of the technique of stripped emulsions has increased twentyfold and more the available thickness of the emulsion, and so has given the instrument a true third dimension.

It is thus conceivable that what we describe here as the present limitations, by the time this article appears in print, will already be eliminated. We must, however, take both these and past defects into serious consideration if we are to evaluate the significance of the data which have accumulated up to now. It is convenient to consider in turn each type of measurement which

[1] The survey of literature pertaining to this review was completed in July, 1954.
[2] For abbreviations used see Code at the end of the chapter.

may be necessary in order to determine the nature of a particle and of its mode of decay.

Measurement of scattering.—A concise survey and bibliography of the theory and methods of measurement of scattering can be found in articles by Goldschmidt-Clermont (1) and by Voyvodic (2). We would like to summarise here the sources of possible error in these measurements.

The most widely adopted method involves the measurement of the sagitta of a track (3, 4). The fundamental relation by which the product, momentum-velocity ($p\beta$), of a particle is related to the mean value $\overline{D}$ of the second differences of the y coordinates of a track aligned roughly parallel to the x axis is

$$\overline{D} = (K/p\beta)t^{3/2} \qquad 1.$$

where t is the cell length in units of 100 microns. The scattering "constant" K in this relation is a slowly varying function of t and β. Its absolute value can be calculated knowing the constitution of the emulsion. There are several different methods (2) but they all give values of K which agree to within 3 per cent.

In early measurements, K was taken as a constant, hence its misleading name. As required precision has increased many attempts have been made to check the theoretical value and the variation of K by careful calibration on particles of known mass and energy. The results are shown in Voyvodic's article (see Figure 17 on page 273) in which the experimental points appear to be scattered with a spread of about 8 per cent with respect to the theoretical curve (based on the Williams-Molière theory). As Voyvodic points out, even in two experiments in which measurements are made on the same particles of the same energy from the same synchrocyclotron, the values obtained by two different groups (5, 6) differ by 15 per cent, whereas the error on each measurement is only 3.5 per cent.

The reason for these discrepancies can lie in the different techniques employed. It is difficult to decide if they arise from systematic differences or from wider fluctuations than are represented by the error quoted. The problem is important. If it is because of systematic differences, then each worker can calibrate his own method, and his results, based on his calibration, will be correct within the limits of the error he gives. If on the other hand, it is attributable to fluctuations, then, for lack of more precise determinations, the theoretical value of K should be taken with an error of 8 per cent.

The chief sources of such fluctuations and systematic errors are the following:

(*a*) Smoothing introduced by the reading of the position of the baricentre of several grains at the centre of the cell, rather than that of a single central grain. If the length of the subcell so formed is less than one-fifth of the cell, this effect is negligible (7). A systematic use of too long a subcell will introduce a systematic error, while a lack of care in keeping the subcell constant will cause fluctuations.

(*b*) Cutoff of the large angles. The technique of cutoff, and the point in the distribution at which it is applied, influence the mean value of the angle of scattering obtained. Even using the same classical cutoff at four times the arithmetic mean, two different criteria for its application on the same group of proton tracks led to a difference of 7 per cent between the two mean values found (5). Thus, the results obtained by groups using different cutoff techniques may not be immediately comparable. On small statistics, the arbitrariness of most cutoffs employed at present leads to fluctuations of the mean.

(*c*) Spurious scattering or noise attributable to inaccuracies in measurement, nonlinearity in the stage movement, and dispersal of the grains around the track. There are several ways of correcting for, or eliminating, this factor. The danger here lies in overconfidence in the elimination of the noise. It is sometimes forgotten that the correction made is itself subject to a fluctuation. In a desire to reduce the statistical error, the cell of measurement is kept as short as possible, with the result that the correction is as large as the true effect. This, in some cases, is correct according to statistical analysis; but in practice, in dealing with a quantity whose mean value depends on the state of the observer, etc., it is dangerous.

(*d*) Distortion of the tracks introduced by the deformation of the emulsion during processing can be a very important source of error. It tends to increase the value of the scattering observed. On the other hand, if the correction applied is too rigorous, the result is a smoothing of the tracks. Practically all the present methods of control and correction are based on the assumption that the distortion introduces a slow and continuous curvature in the track. They cannot take into account irregular distortion nor local distortion resulting from specks of dirt or small inhomogeneities in the emulsion. Moreover, they have been established and proved on emulsions with glass supports. It is doubtful if they are completely efficacious when applied to stripped emulsions. These latter are subject to new types of deformation when they are rolled on the glass support for processing.

Of the errors discussed here, a part (the presence of noise and distortion, and an inadequate cutoff) lead to an overestimate of the scattering of a track and hence to an underestimate of the energy and mass of the particle. Smoothing, a too stringent cutoff, and over-correction for noise or distortion will tend to decrease the scattering and lead to an overestimate of mass and energy. The differences of technique between laboratories, and the fluctuations present in excess of those admitted, lead to such a spread in a spectrum of mass or energy that it is often difficult to discriminate between particles of similar mass or energy solely on the basis of scattering measurements.

Ionisation.—The measurement of ionisation has the advantage and disadvantage of being a purely relative measurement. The disadvantage lies in the fact that a serious calibration must be made for every measurement. The advantage comes from the fact that when the calibration is well done, there is no uncertainty resulting from unknown constants or relations.

A consideration of the numerous sources of fluctuation in grain density in a single plate shows that a calibration designed to allow discrimination between tracks of grain density differing by as little as 10 per cent is no light matter. For a given point in the plate (x, y, z) and a given relative ionisation I/I_0 where I_0 is the minimum ionisation, the relative grain density N/N_0 will be a function of the type:

$$N/N_0 = f(x)g(y)h(z)\phi(I/I_0).$$

The calibration must be sufficiently precise as to allow a definition of these four functions to within 2 per cent (3000 grains for every point on the curve).

Very often in the literature, calibration is said to be made on tracks in the "vicinity" of the track to be measured, without a definition of what is meant by "vicinity." It should mean that zone of the plate in which the grain density can be considered to be constant. It has already been suggested at Varenna (8) that such zones should be explicitly defined in every case; without this guarantee we are obliged to treat with caution results based on measurements of small differences in grain density.

Range.—The measurement of range is generally the most accurate measurement possible in photographic emulsions and has recently regained importance with the use of stacks of stripped emulsions in which a much larger fraction of the tracks can be brought to rest than was possible even in the thickest plates.

The energy of the particle can be deduced from the range-energy relation obtained for protons by Vigneron (9): $E = KR^{0.568}$ for protons up to 100 Mev. Above this energy an extrapolation can be based on the point obtained at 342.5 Mev., range 92.68 g/cm.^{2} at an emulsion density of 3.815(10).

Although the measurement of a length in the emulsion can be made accurate to within 1 μ, there are several factors which increase the error on the range. These factors are

(*a*) Variation of stopping power with humidity: The stopping power of an emulsion depends on the amount of water it contains. If the humidity at the time of exposure is unknown, the stopping power should be checked by measurement of the range of μ-mesons from the π-μ decay.

(*b*) Uncertainty in the factor of shrinkage: There is about 10 per cent uncertainty in the nominal thickness of the emulsion. This fact can introduce a tangible error on the range of tracks which do not lie completely in the plane of the plate. It is therefore necessary to derive from the known thickness after processing, the original thickness by an extensive calibration on tracks of known length.

(*c*) Straggling: This is well known (11, 12) and small for long tracks.

(*d*) Scattering and distortion: Errors are also introduced by the multiple scattering and by the elongation or contraction of the tracks in the deformed emulsion.

Measurement of angle.—The measurement of the angles between two

tracks involves a measurement in the plane of the plate, and a measurement perpendicular to it, i.e., the dip of each track. The former determination can be made accurate to within 1′, the latter will have the precision depending on the accuracy of the z micrometer (most of them now read to within 1μ) and on the uncertainty in the shrinkage factor noted in the discussion of range. Both values will be influenced by distortion. If the distortion, considered as the displacement of the upper planes of the emulsion with respect to the lower, be expressed by

$$S_{(z)} = S_0 + \left(\frac{dS}{dx}\right) \cdot z + \left(\frac{d^2S}{dx^2}\right) \frac{z^2}{2} + \cdots ,$$

the third term is the one encountered in scattering measurements and can be determined from observations on the curvature of steeply dipping tracks. The second term, the linear displacement of the upper layers with respect to the lower, is much more difficult to estimate. The measurement of the angle between two tracks is one of the few cases in which this type of distortion is important. In most of the values given this effect has been ignored.

This survey of the sources of error and the various modes of correction shows us that we can expect systematic differences from laboratory to laboratory in which the techniques are different. In addition, overconfidence in the corrections made, can lead to an underestimate of the error on the measurement. Collective action, such as that represented by the Recommendations of the Varenna Summer School (8), designed to encourage a certain uniformity in techniques and a more thorough representation of the errors, may correct this. In the meantime, it is as well to consider all results based on measurements in photographic emulsions to carry a higher fluctuation than is apparent in the published limits of error.

Wilson Chamber.—The technique of the Wilson chamber, apart from the original discovery of the V-particles, has contributed an important part of the data available at present on heavy mesons (13). This is particularly true for the neutral V-particles. Like the photographic emulsion, the cloud chamber has certain features which affect the quality of the information which can be obtained from it.

The chamber must be controlled by counters which select expansions in such a way that the efficiency of observation of the desired events should be greatest. It is possible that this can introduce a bias in the type of event selected. Whatever the system of control, the frequency of the events studied is low at mountain altitude and, on the other hand, the operation of Wilson chambers at high altitude is a costly and difficult undertaking.

While in general the Wilson chamber is most adapted to the study of decay in flight, as compared with the photographic emulsion, whose more important feature is the possibility it affords of the examination of the decay or interaction at rest of short-lived particles, the multiplate chamber is used with advantage for this latter problem, with, however, the limitation that

the details of the decay or interactions are hidden within the material in which the particle stops.

The technique of measurement with cloud chambers requires a long apprenticeship, and to a certain extent depends on the particular instrument employed. The determination of curvature of the tracks in the magnetic field is generally made with precision as good as or better than that of the multiple scattering in the photographic emulsion. The principal factors which limit it are associated with peculiarities of the individual chamber (e.g., Coulomb scattering, migration of ions before the photography of the track, movement of the body of the gas at the moment of expansion, and thermal convective movements). Given the diversity of functioning from chamber to chamber and in the same chamber from one time to another, it is difficult to judge the precision of any single measurement.

The ionisation and the scattering of tracks in the Wilson chamber cannot be measured with a precision approaching that obtained in photographic plates. Even measurements of range can be inaccurate because of the impossibility of determining the origin of a particle or of the point at which it comes to rest if this point lies within a dense absorber.

On the other hand, the cloud chamber has certain advantages over the photographic plate, for instance, in the possibility of recognising association in time between events and in the study of cascade events (successive interaction, presence, and multiplication of the photonic component). In general, a cloud chamber possesses those advantages which arise from the possibility of observing events occurring within 1/10 sec. in a volume up to 1 m.[3]

To obtain the maximum possible information (sign, momentum, mean life, multiplicity of production, association with other events, etc.) it is convenient to use a telescope arrangement of two chambers, one with magnetic field, the other a multiplate chamber. (See the description of the P.E.P. double chamber in the section on *V*- and *S*-events).

Nomenclature

This article summarizes a part of the known evidence on particles whose mass lies between that of the π-meson and that of the proton. The following nomenclature has been used:

τ: a particle of mass 966 m_e decaying into 3 π-mesons.

K_L: a particle of mass between that of proton and π-meson decaying into a light meson and neutral particle(s).

K_π: *K*-particle decaying into a π-meson and neutral particle(s).

K_μ: A *K*-particle decaying into a μ-meson and one very light neutral particle.

κ: a *K*-particle decaying into a μ-meson and two neutral particles.

K_e: a *K*-particle decaying into an electron and neutral particle(s).

${}_\sigma K$: a *K*-particle stopping and giving rise to a nuclear interaction.

${}_\rho K$: A *K*-particle stopping and giving rise to no visible secondary products.

Here we have kept to the present standard nomenclature (14) on V- and Y-particles, for example,

V_2^0: a neutral heavy meson giving rise to two light secondaries, and

θ^0: that V_2^0 identified as giving 2π-mesons with a Q of 214 ± 5 Mev.

Where evidence on a particle is more complete, sign and mass being known as well as the nature of the decay products, we can include all this information in the symbolism

e. g.
$$\binom{\nu}{\gamma}^{920} K_{\mu}^{+}$$

to describe the K_μ where the left subfix describes the neutral decay products.

In this article we have profited freely from the excellent treatment by Leprince-Ringuet of the evidence up to and including the Bagnères Conference (June, 1953) on heavy unstable particles in Volume 3 of this *Review* (15).

The Tau-Meson

$\tau^{\pm} \rightarrow \pi^{+} + \pi^{-} + \pi^{\pm}$.—The τ-meson decay into three charged π-mesons is one of the events about which information is the most complete. This is attributable to the fact that this event is easily recognisable, since it is the decay of a charged particle into three charged secondaries; the energies of the secondaries are such that it is frequently possible to determine their mass and energy with good precision; in stripped emulsions they often stop in the stack. Further, there are no neutral particles to allow for, and the product particles are all the same (π's). (This is true at least up to the date of writing.)

The first τ-decay observed in photographic emulsion by Brown *et al.* (16) was already remarkably clear. Later observations (15) confirmed the first tentative assumption about the mass of the τ-meson and established that the τ-meson actually decays into three π-mesons. The validity of this decay scheme was strongly supported by the statistical analysis of Amaldi *et al.* (17) Since then, the use of stacks of stripped emulsions has made possible the direct confirmation (18). In stacks of stripped emulsions, 51 secondary particles have been followed to their end in the emulsion, and, of these, 33 give the π-μ-decay; 16 give a σ-star, and only 2 end without giving rise to a secondary effect.

All the eight "complete" τ-meson decays observed (events in which all three secondaries end in the emulsion) are positive (18). In addition, the fact that among the secondaries the ratio of the positive (π- μ decays) to negative (σ-stars) is 1.8 indicates that at least 80 per cent of τ-mesons observed to decay at rest in the photographic emulsion are positive (18). If some of them were negative, we might expect a disturbance of the coplanarity, caused by the τ-meson's being captured into a Bohr orbit round the nucleus before decaying. This is not observed.

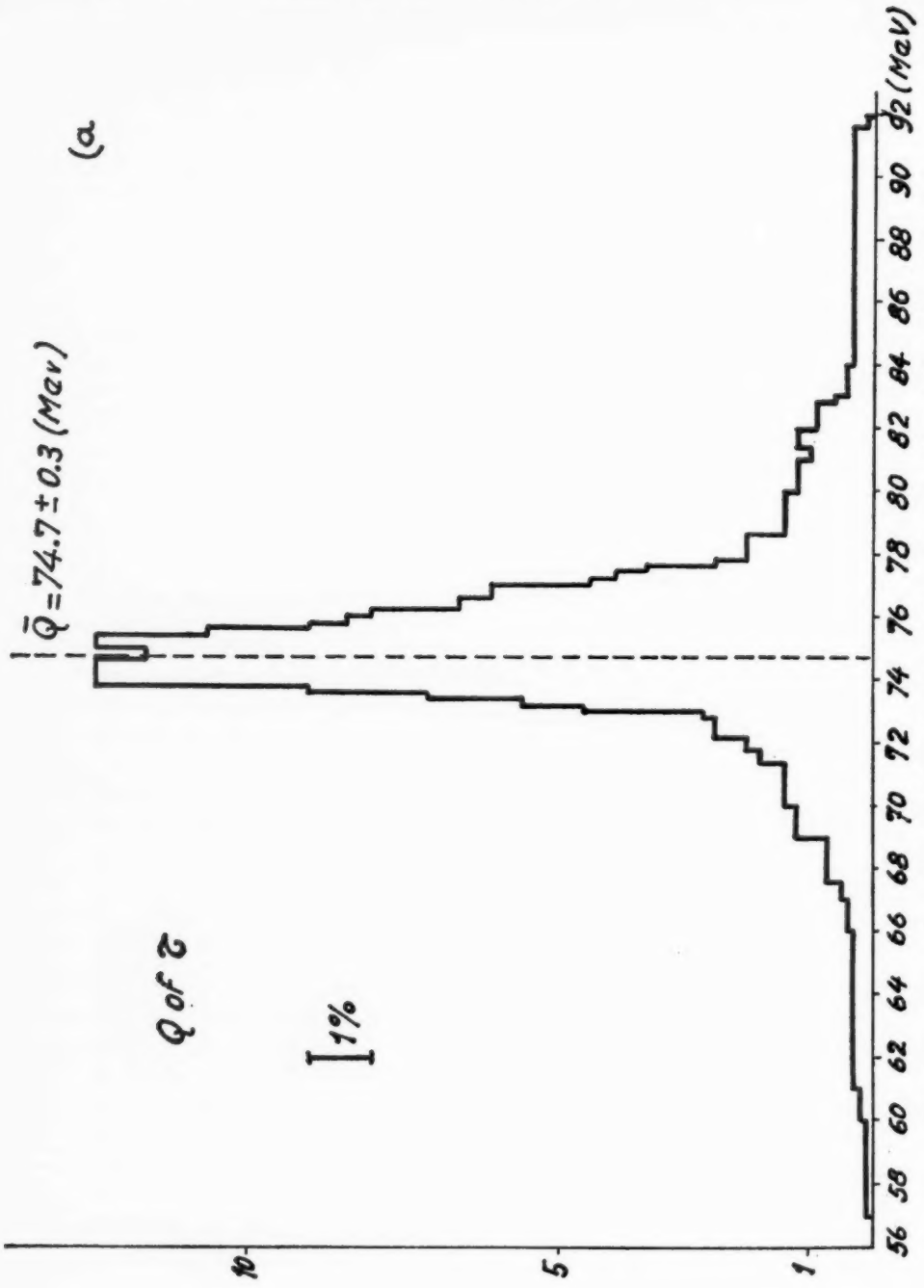

FIG. 1. Tau-mesons in nuclear emulsions. Section (a) above. Sections (b) and (c) on following pages.

FIG. 1. Tau-mesons in nuclear emulsions. Section (a) above. Sections (b) and (c) on following pages.

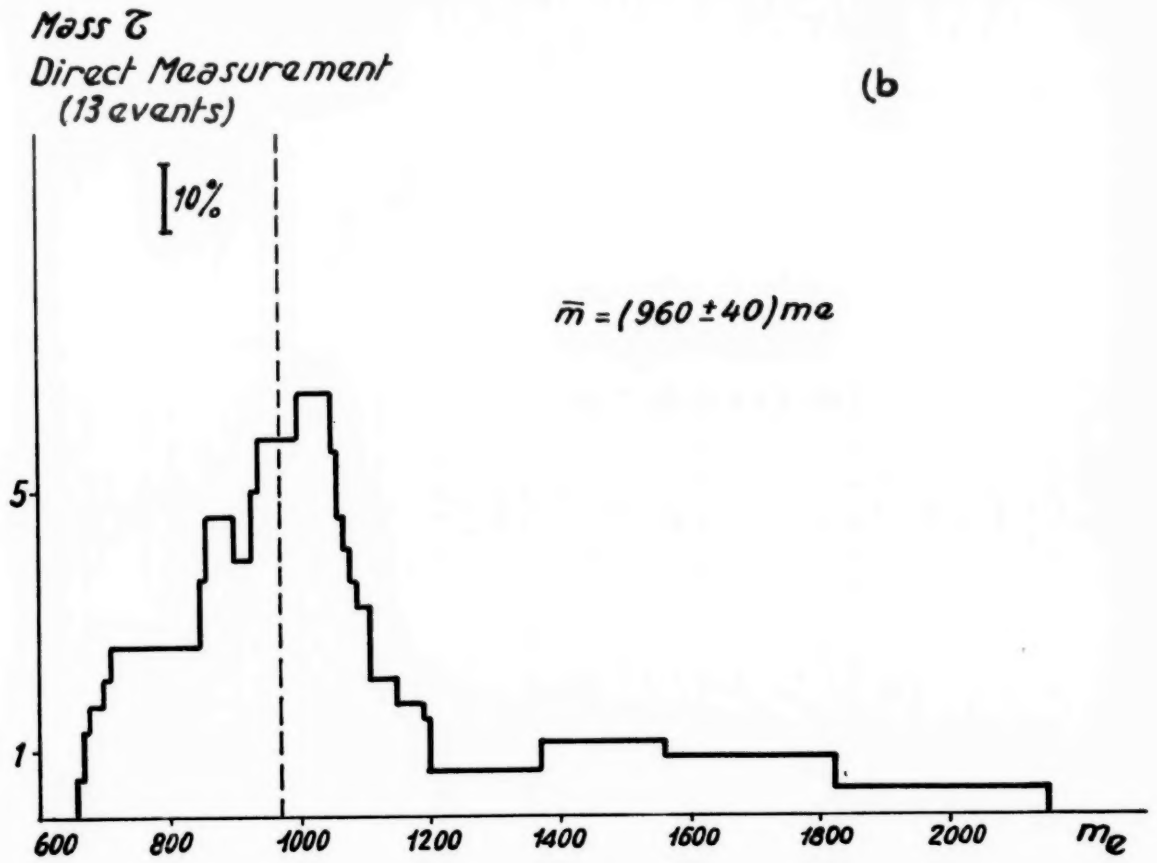

FIG. 1b.

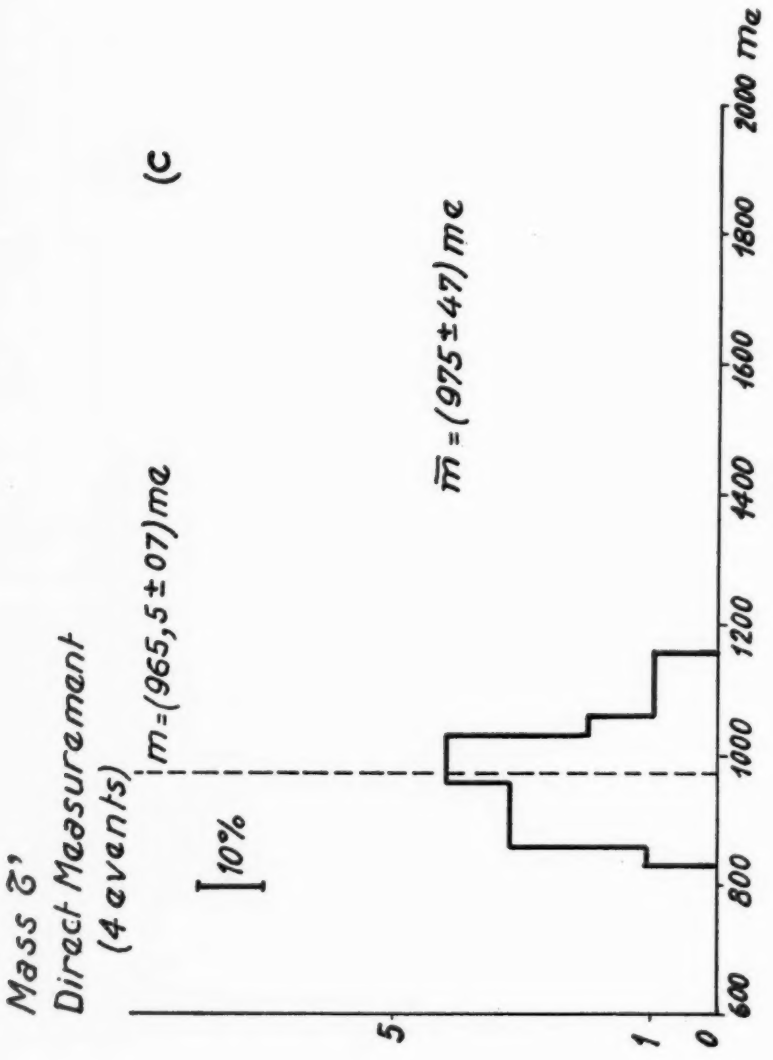
Mass 2'
Direct Measurement
(4 events)
m=(965,5±07)me
10%
(c
m̄ = (975±47) me
5
1
0
600
800
1000
1200
1400
1600
1800
2000 me

FIG. 1c.

Observations in Wilson chambers show a positive excess (eleven positive and four negative) among τ-mesons decaying in flight, but clearly the statistics are very small. The question of what may happen to the negative τ when captured by the nucleus is treated later.

In the emulsions the mass of the τ-meson can be obtained generally with much greater precision from the determination of the Q value of the decay than from direct measurement either by range-ionisation or by range-scattering. In exceptional cases in which the track is several cm. long and the plane containing the secondary tracks is at a large angle to the plane of the emulsion this may not be true, but in the majority of events, the Q value can be determined to within at least 5 per cent, while such a precision by direct mass measurement requires a track length of 10 cm. in favorable conditions. Most often experimenters give both values, and their results are shown in Figure 1 (a, b). The best value of the Q is 74.7 ± 0.3 Mev and of the mass is $965.5 \pm 0.7\ m_e$.

The limitations on the accuracy of the Q value arise from (*a*) the error on the secondary momenta and (*b*) the error in the determination of the angles between the tracks. The momenta of the secondaries are generally determined either from their scattering or ionisation or from the range when they stop in the emulsion. In the first case the errors are those of simple scattering ionisation measurements, and, since the maximum energy available is 54.4 Mev, good precision can be obtained. Track lengths of the order of 1 cm. will give an error of less than 7 per cent. In the second case the precision is generally higher but is still subject to the errors previously noted in this article. The errors involved the measurement of the angles between the tracks. The departure from coplanarity of the order of 2° is completely explained by these instrumental errors.

In the τ-meson decays observed in the photographic emulsion, the primary particle is always at the end of its range. Calculation of the total moderation time made at the Padova Congress (18) on all of the τ-mesons observed up to that time gave for the lifetime $> 8.10^{-9}$ sec. Observations in Wilson chamber (18) give a value of the order of that of the K_μ i.e., $2.8\ 10^{-8}$ sec., and it seems certain, therefore, that $\tau_\tau > 10^{-8}$ sec.

The first observations, made in plates exposed under diverse conditions, led to little conclusive evidence concerning the frequency and mode of production of this type of meson. Now there is a much greater uniformity of exposure, many laboratories unite to expose their plates in a single set of balloon flights, and the technique of stacks of stripped emulsions make it possible to follow back the primary particle in many cases to its point of origin in a star. Thus, of 24 τ-mesons found in stacks of stripped emulsions, 20 have been found to come from stars.

These data refer necessarily to τ-mesons produced with rather low energy. Mass spectra of particles of high energy produced in high-energy showers and which do not end in the stack show the existence of particles of mass of the order of 1000 m_e, but this class will include all the K-particles.

$\tau \rightarrow \pi^{\pm} + \pi^0 + \pi^0$.—An alternative mode of decay, into one charged and two neutral π-mesons, was suggested by Pais (19) on the basis of charge independence. Such an event would appear in the photographic emulsion as a K-particle decaying into a single slow π-meson ($E < 57$ Mev). Among K_π-particles observed, seven have been found to have an energy less than 57 Mev; of these, six are positive and one negative. The mean mass of the primaries is 975 ± 47 m_e as compared with the value 960 ± 40 m_e of the τ-mass by direct measurement (Table VI; Fig. 1c).

It is tempting to attribute these events, at least those which are positive,[3] to the Pais mode of decay of the τ-meson. However, as will be seen later, it is not as yet possible to prove definitely that they form a group separate from the other K_π-particles.

Nature of the tau-meson.—Dalitz (20) has shown that, if charge independence is valid, and if an isotopic spin 1 can be significantly attributed to the τ-meson, then the branching ratio, $R = (\tau \rightarrow \pi^+ + \pi^- + \pi^{\pm})/(\tau' \rightarrow \pi^{\pm} + \pi^0 + \pi^0)$, must lie between 1 and 4. Although, as we have seen, we cannot be certain of the identity of the examples of possible τ' so far available, it seems to us constructive to assume here that the six positive events are τ'. We can then go on to examine the consequences of their existence and compare the available experimental information with the fuller analyses of Dalitz and Fabri. The ratio (number of τ)/(number of τ') is 36/6. A part of these six τ'-events were found by following back π-mesons which stop in the emulsion. There are three possibilities of finding a τ against one possibility of finding a τ' in this method of research. Taking into account also the fact that the τ' is less easily recognisable than the τ, we can place $3 < R < 6$.

The fact that all the τ-events so far observed conserve a good coplanarity indicate that electromagnetic interaction does not sensibly disturb the decay scheme. A further consequence of the charge independence is that there should exist a neutral tau-meson (19). An obvious way for it to decay would be $\tau^0 \rightarrow \pi^+ + \pi^- + \pi^0$. This decay would be observed most easily in the Wilson chamber and would appear as a V_2^0 event with 2π secondaries and Q value less than about 80 Mev. (It is not possible to fix exactly this limit a priori since the mass of the τ^0 may not be equal to that of the $\tau^{\pm}$.) Certain of the anomalous V_2^0 events reported by various laboratories (21) have Q values which are consistent with their being τ^0 decays.

More detailed theoretical analyses of the τ-meson have been made on the existing mesonic theories by Dalitz (22) and Fabri (23). The conclusions of Dalitz are summarised in Table I. We consider first states with spin 0 or 1. Among these we can neglect the case (*b*), spin 0 parity even, (scalar meson) in which the decay $\tau \rightarrow 3\pi$ is forbidden. In state (*c*) the ratio $n_{l-}/n_{l+} = 1/10$, where n_{l-} is the number of events in which the slowest of the three π's

[3] The event in which a negative π is emitted may be interpreted as a $K\sigma$, i.e., a heavy meson stopping, interacting, and giving rise to a π-meson with no visible evaporation.

TABLE I

POSSIBLE MODES OF DECAY OF THE TAU-MESON*

State		Decay scheme		Branching ratio	n_{l-}/n_{l+}
Spin	Parity	Allowed	Forbidden	R	
(a) J=0	odd (PS)	$\tau\to3\pi$	$\tau\to2\pi$	~4	1/2
(b) J=0	even (S)	$\tau\to2\pi$	$\tau\to3\pi$		
(c) J=1	even (PV)	$\tau\to3\pi$ $\tau\to\pi+\gamma$		?	1/10
(d) J=1	odd (V)	$\tau\to3\pi$ $\tau\to\pi+\gamma$ $\tau\to2\pi$		1	?
(e) J≧2	$\neq(-1)^J$	$\tau\to3\pi$ $\tau\to\pi+\gamma$	$\tau\to2\pi$	?	?
(f) J≧2	$(-1)^J$	$\tau\to3\pi$ $\tau\to\pi+\gamma$ $\tau\to2\pi$		?	?

In all cases $\tau\to\mu+\nu+\gamma$
$\tau\to\mu+\nu$

Experimental data

R (Branching ratio τ/τ' $3<R<6$.
Sign ratio of the slowest of the three π-secondaries $n_{l-}/n_{l+}=7/15$.
* [Dalitz (22)].

secondaries is negative, and n_{l+} is the number in which the slowest is positive; the experimental ratio is $n_{l-}/n_{l+}=7/15$. In state (*d*) the branching ratio R is predicted as equal to 1. Even considering the experimental bias it is difficult to reconcile this with the above value. To state (*a*), that of the pseudoscalar τ-meson, are assigned the values $R\sim4$, and $n_{l-}/n_{l+}=1/2$, which are not inconsistent with the experimental data. Also the total energy spectrum of the secondaries (Fig. 2a) and the energy spectrum of the odd π (the negative π in the decay $\tau\to\pi^+\pi^-\pi^+$ and the charged π in the $\tau'\to\pi^\pm+\pi^0+\pi^0$ decay) are not inconsistent with the pseudoscalar hypothesis (Fig. 2b).

On the other hand, the long lifetime of the τ can be explained by consideration of conservation of momentum, supposing that total spin should be 1, 3, or higher (24). Dalitz does not analyse in detail states of high spin. Fabri (23) shows that the distribution of the three possibilities, $E_3<E_1, E_2$; $E_1<E_3<E_2$; and $E_3>E_1, E_2$, where E_3 is the energy of the odd π, and E_2 and E_1 are the energies of the like π's, can be used also to determine the spin and parity of the τ. The available statistics are small, and the practically uniform distribution obtained (Table II) agrees equally well with a state of spin 3 and odd parity (*f*), and a state of spin 0 and odd parity (*a*).

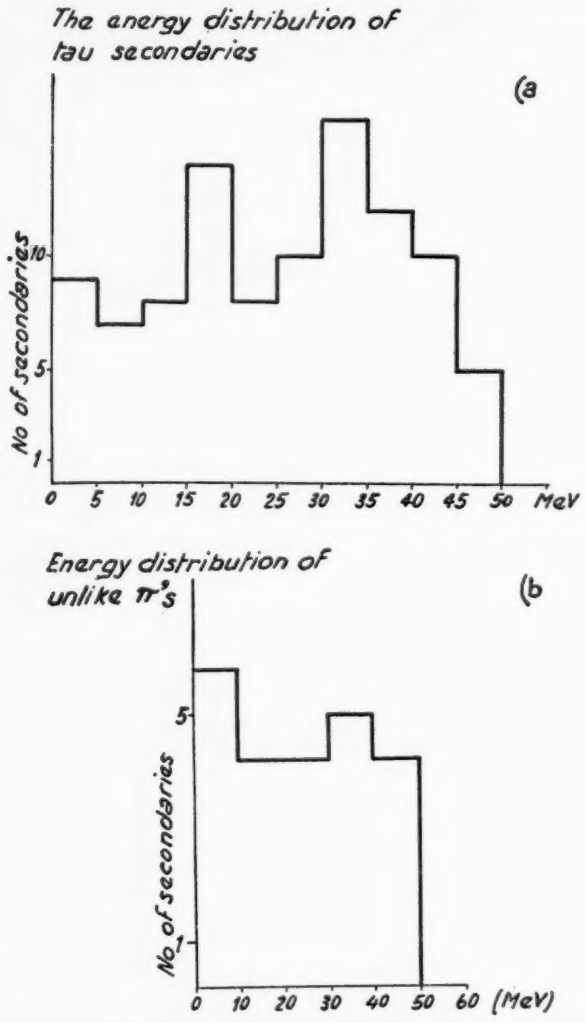

FIG. 2. Tau-mesons in nuclear emulsions.

Thus we are left with the choice of the pseudoscalar τ, if low spin states are considered, or with the possibility of a spin 3(f) as a means of explaining the long life. (The present state of theory leaves open the possibility of alternative explanations of the long lifetime of the heavy mesons).

Depending on the choice of these two possibilities is the attribution to the τ-meson of a mode of decay, $\tau \rightarrow \pi + \gamma$. This is forbidden for spin 0 odd parity (a), but admitted for spin 3 odd parity (f). Space and energy random

TABLE II

SPIN AND PARITY OF τ'S AS DETERMINED FROM ENERGY DISTRIBUTION OF SECONDARIES

Class	$E_3<E_1, E_2$	$E_1<E_3<E_2$	$E_3>E_1, E_2$
No. of events*	7	8	7

χ^2 TEST FOR SPIN AND PARITY DETERMINATION

Spin and parity	69 per cent probability		31 per cent probability	
	χ^2	ρ	χ^2	ρ
(0−)	10^{-1}	$1-\epsilon$	10^{-1}	$1-\epsilon$
(1+)	6.3	0.04	9	0.01
(1−)	4.18	0.12	6.3	0.04
(2+)	3.5	0.18	2.9	0.24
(3−)	0.24	$1-\epsilon$	0.96	0.61

* One event, included in the second class, has a 69 per cent probability of belonging to this class and a 31 per cent probability of belonging to the first class.

distribution of the secondaries seems to exclude strong meson-meson interaction.

THE NEUTRAL *V*-MESONS

Two forked tracks observed by Rochester & Butler (25) in a Wilson chamber were interpreted by them as representing the respective decay of a neutral and a charged particle of mass considerably greater than that of the π-mesons. Later work (26) confirmed the existence of these particles, which were classified into two groups: (*a*) V_1^0 and $V_1^{\pm}$ (now known as Y^0 and $Y^{\pm}$), particles of mass greater than that of the proton. These events we shall not discuss here as they enter rather into the category of supernucleons or excited states of nucleons than that of heavy mesons; (*b*) V_2^0 and $V_2^{\pm}$ particles of mass less than that of the proton. The V_2^0 are further subdivided into the group V_4^0 or θ^0, the most numerous and the most sure, and other more or less speculative groups which we can call tentatively V_3^0 and τ^0, and maybe more.

The V_2^0, in common with practically all neutral particles are more easily studied in the Wilson chamber than in the photographic emulsion (see page 276). Most of the experimental results obtained come from the former instrument.

The group V_4^0 or θ^0 was proposed as a neutral particle decaying into two light-charged mesons only (28). Among those events in which the origin of

the neutral particle could be determined, coplanarity was respected within the experimental errors (27). A good estimate of Q value of the decay scheme can be made by analysis of the observed momenta p_+ and p_- and the angle ψ between the tracks in a sufficient number of events. This analysis is most easily made in terms of two parameters: p_t = the momentum transverse to the line of flight of the θ^0, and therefore invariant under the Lorentz transformation, and

$$\alpha = \frac{p_+^2 - p_-^2}{p^2} \quad \text{where} \quad p = p_+ + p_-.$$

The conservation of momentum and energy lead to the expression $[1/2 \cdot M\beta(\alpha - \alpha^*)]^2 - p_t^2 = p^{*2}$ where $\alpha^* = (m_+^2 - m_-^2)M^2$ (m_+ = mass of positive secondary; m_- = mass of negative secondary; M = mass of primary), and p^* is the momentum of either secondary in the centre of mass system.

Thompson *et al.* (28), working on high-energy events, can assume $\beta \sim 1$ and make the plot p_t versus α, which is an ellipse centred around the point $\alpha = \alpha^*$. Their analysis shows a group of points fitting an ellipse centred on $\alpha = 0 (m_+ = m_-)$ and consistent with the decay scheme:

$$\theta^0 \rightarrow \pi^+ + \pi^- + Q; \qquad Q = (214 \pm 5) \text{ Mev} \qquad 1.$$

They are also consistent with the scheme:

$$\theta^0 \rightarrow \pi + \mu + Q; \qquad Q = (230 \pm 5) \text{ Mev} \qquad 2.$$

However, work in multiplate chambers (29) shows that the greater part of the secondaries of these events are nuclear interacting, and therefore we can assume with a certain confidence that the two secondaries are π-mesons, and decay scheme 1 describes the θ^0-meson.

Armenteros *et al.* (30) of the Manchester group had at their disposal lower energy events for which β varies between 0.5 and 1.0. They could not, therefore, apply a type of analysis such as that of the Indiana group. They proceeded in two steps. First, from a histogram of the p_t values, they were able to conclude that the decay was consistent with a two-body decay with a value p about 200 Mev/c. Then, assuming the particular decay scheme, $\theta^0 \rightarrow \pi^+ + \pi^- + Q$, they calculated the corresponding curve of α versus p_t, and found most of their points grouped well around the curve with $Q = (211 \pm 20)$ Mev. Table III gives the Q values published by various groups. They are all consistent with that given by Thompson *et al.* (28) which is generally accepted as the best value $Q = 214 \pm 5$ Mev.

Also in Table III are given the mean lifetimes calculated for the θ^0. They are obtained from the mean path length between the assumed point of origin and the observed point of decay. Geometrical corrections are applied to take into account the path of the particles before they enter and after they leave the chamber, care being taken to allow for the experimental bias against events occurring in unfavourable regions of the chamber, and therefore not suitable for analysis. The values generally accepted as most reliable are:

$$\tau_{\text{Manchester}} = (0.7^{+0.8}_{-0.2})10^{-10} \text{ sec.}$$

$$\tau_{\text{M.I.T.}}{}^{2} = (0.9^{+1.6}_{-0.3})10^{-10} \text{ sec.}$$

In experiments on the Brookhaven cosmotron, with a primary beam of 1.5 Bev negative π-mesons (31), there have been found two cases of $\wedge^0+\theta^0$, two of $\Lambda^0+\begin{cases}\theta^0\\ 2\pi^0,\end{cases}$ one of Λ^-+K^+, and one of $\Lambda^-+?$. The cross section for production of these events is 1 mbarn against a total collision cross section for $\pi-p$ of 34 mbarn.

TABLE III

DATA ON THE θ^0 PARTICLE

Group	Q value	Lifetime
Go. (33)	—	$(2.3^{+2.1}_{-0.7})10^{-10}$ sec.
In. (28)	(214 ± 5) Mev	—
Mn. (30)(34)(37)	(211 ± 20) Mev	$(0.7^{+0.3}_{-0.2})10^{-10}$ sec.
Mn. (38)	—	$(1.2^{+0.8}_{-0.3})10^{-10}$ sec.
M.I.T. (35)	(210 ± 35) Mev	$(0.9^{+1.6}_{-0.3})10^{-10}$ sec.
Pas. (39)	—	$(1.6\pm0.5)10^{-10}$ sec.
Pr. (36)	210	—

Having hypothesized the existence of the particle $\theta^0\rightarrow\pi^++\pi^-+214$ Mev with mass $966\pm10\ m_e$, we may ask if there does not exist a charged counterpart. Let us call this $\theta^\pm$. We would expect it to decay as $\theta^\pm\rightarrow\pi^\pm+\pi^0+Q$, where Q could be of the order of 220 Mev. This would be observed in the Wilson chamber as a two-body decay of $V^\pm\rightarrow\pi^\pm+?$ where $p_\pi{}^*\sim200$ Mev/c, or in the photographic emulsion as $K_\pi\rightarrow\pi^++?$ where $p\beta_\pi\sim170$ Mev/c. Particles have been observed which are consistent with this scheme, though their identification with $\theta^\pm$ is not immediate because of the existence of other S and K particles. This will be discussed in a later section of this article.

Apart from these rather well-classified events, a number of events have been reported, which when analysed on the basis of a decay into two π's, give Q values inconsistent with the 214 Mev. Two possibilities have been suggested to account for these events: (*a*) If coplanarity is not satisfied $\tau^0\rightarrow\pi^++\pi^-+\pi^0+80$ Mev can account for Q values less than 80 Mev (see previous section). (*b*) $V_3{}^0\rightarrow\tau^\pm+\pi^\mp+60$ Mev has been suggested by Leighton

(see 32). The Q value found by analysis of such a particle on the assumption that it is a θ^0, will depend on the velocity of the primary. Some of the anomalous Q values are consistent with this scheme (21).

Observations in Wilson Chamber of the Decay at Rest and in Flight of the Charged Heavy Mesons (S and V Events)

The first example of a large-angle deflection of a track of a particle heavier than the π-meson, which did not seem to be caused by a scattering of the particle, was observed by Rochester & Butler (25) in a cloud chamber operated at sea level. An analysis of this event led them to interpret it as the decay in flight of a heavy unstable particle. Since then, cloud chambers operated largely at mountain altitudes have confirmed this view and made it possible to divide these V events into three classes: that in which the primary has a mass of the order of 1000 m_e and decays into a light meson and one or more light neutral particles; that in which the primary is heavier than the proton and decays into a nucleon and a light meson; and a third group of the so-called cascade events in which one of the decay products of the charged V is a neutral V-particle.

The second group, that of the hyperons, does not lie within the scope of this article; neither does the third. In fact, the observed cases can up to now be readily explained as decays into neutral hyperons, following the scheme (40, 41)

$$Y \rightarrow \Lambda^0 + \pi + Q.$$

It is too early to establish that this is the only type of cascade event, but so far there is no evidence for other kinds.

Together with the particles decaying in flight, there exists a group of particles, discovered in 1951 by the M.I.T. group, which have mass greater than that of the π-meson and were observed to decay at rest in the multiplate chamber; these are called S-particles. Hyperons decaying at rest are certainly present among them, but the greater part of the S-particles have mass less than that of the proton.

The characteristics of the cloud chambers used by five representative groups working on V and S particles are given in Table IV, drawn up on the model of that of Rochester & Butler (42).

In Table V are summarized the data obtained by the various groups. The apparent contradictions are a result of the diversity of the characteristics of the apparatus employed, i.e., size, altitude, plate sets, and triggering. In addition, each group has its individual method of analysis of its results based on the particular data available from their experiments. We shall give the line of argument followed by each of them and the conclusions they reach. We shall discuss first the results obtained in multiplate chambers on S-particles.

S-particles.—M.I.T.'s Annis *et al.* (43) defined as S-particles those particles observed in the Wilson chamber to decay at rest with the emission of a

TABLE IV

CLOUD CHAMBER DATA

Group	Location and altitude (m.)	Chamber dimensions (cm.)	Metal plates in chamber	Magnetic field (Gauss)	Maximum detectable momentum (ev/c)
Manchester	Pic du Midi, France, 2867	Diameter 28; illuminated depth 7	2 cm. Pb or 1.5 cm. W-Cu alloy	7500	10^{10} on 10 cm.
Manchester	Jungfraujoch, Switzerland, 3460	54×54; illuminated depth 8	2.5 cm. Pb	6000	4×10^{9} on 25 cm.
Caltech[3]	Pasadena, 220 Mt. Wilson, 1750 California	Two chambers each 33×19 high; illuminated depth 12; used one above other	2.5 cm. Pb between chambers	5000	2.5×10^{9} for long tracks
M.I.T.	Echo Lake, Colorado, 3000	50×50; illuminated depth 15	11 plates of Pb each 0.6 cm. thick, or brass plates 1.2 cm. thick	—	—
P.E.P.[3]	Pic du Midi, France, 2867	Two chambers, used one above other:			
		(I) 64×68 high; illuminated depth 30	—	2600	1.5×10^{10} ev. on 50 cm.
		(II) 68×64 high; illuminated depth 40	8 plates of Pb each 0.7 cm. thick and 6 plates of C each 1.5 cm. thick alternated, or 15 plates of Cu each 1 cm. thick	—	—

secondary heavier than an electron and of energy greater than 100 Mev. This definition in itself indicates a certain bias in the observations, in that in many experiments all particles giving rise to secondaries of energy less than this are discarded from the statistics in the event that they might be either π- or μ-meson decays.

The M.I.T. group (44), using the single multiplate chamber, gives the mean mass of their S-particles, determined by scattering range measurements as $(1200^{+270}_{-200})\ m_e$. They point out, however, that given the low precision obtainable on individual measurements by this method, it is possible that a few of their S-particles can be hyperons. This should be kept in mind in considering the data obtained by them. The information on the 48 S-particles observed by them to date (45) is given in ideogram I (Fig. 3). From these data they conclude that the charged secondaries observed in their chamber can be any one of the following:

(a) All π-mesons with a unique value of range $\sim$102 gm./cm.^{2} of Pb (momentum $p=266$ Mev/c; $p\beta=250$ Mev/c). The mass of the primary particle should be about 1110 m_e if the neutral particle is of zero mass. The short ranges observed (1-5-14-17 in ideogram I) could be explained as

TABLE V

DATA ON $V^{\pm}$- AND S-PARTICLES

Group	$n.V^{\pm}$	$n.V^{+}$	$n.V^{-}$	$n.S^{\pm}$	$n.S^{+}$	$n.S^{-}$	Mass m_e	Life-time (sec.)	Suggested mode of decay
Manchester Pic du Midi	40	5	14	—	—	—	950 to 1100	—	$V^{\pm}\rightarrow L^{\pm}+n^0+n^0$ $V^{\pm}\rightarrow L^{\pm}+?$
Manchester Jungfraujoch	—	29	13	—	—	—	900 to 1100 (one case with mass 1000 m_e)	$>10^{-9}$	$V^{\pm}\rightarrow L^{\pm}+n^0+n^0$
Caltech[2]	103								
Upper chamber	—	14	28	—	—	—	1000	$5\times10^{-10}<\tau<2\times10^{-8}$	$V^{\pm}\rightarrow L^{\pm}+n^0+n^0$
Lower chamber	—	29	14	—	—	—	—	$10^{-11}<\tau<3\times10^{-10}$	$V^{+}\rightarrow P+\pi^0$ $V\rightarrow\pi+N$
M.I.T.	6	—	—	48	—	—	1200^{+270}_{-200}	$>10^{-9}$	$S^{\pm}\rightarrow L^{\pm}+\pi^0$ $S^{\pm}\rightarrow\mu^{\pm}+\gamma+\nu$ $S^{\pm}\rightarrow\mu^{\pm}+n^0$
P.E.P.[3]									
Upper chamber	—	66	40	—	—	—	—	$\sim2\times10^{9}$	$V^{\pm}\rightarrow L^{\pm}+n^0+n^0$
Lower chamber	2	1	—	34	25	—	914 ± 20	$\sim2.8\times10^{-8}$	$S^{+}\rightarrow\mu^{+}+\nu$

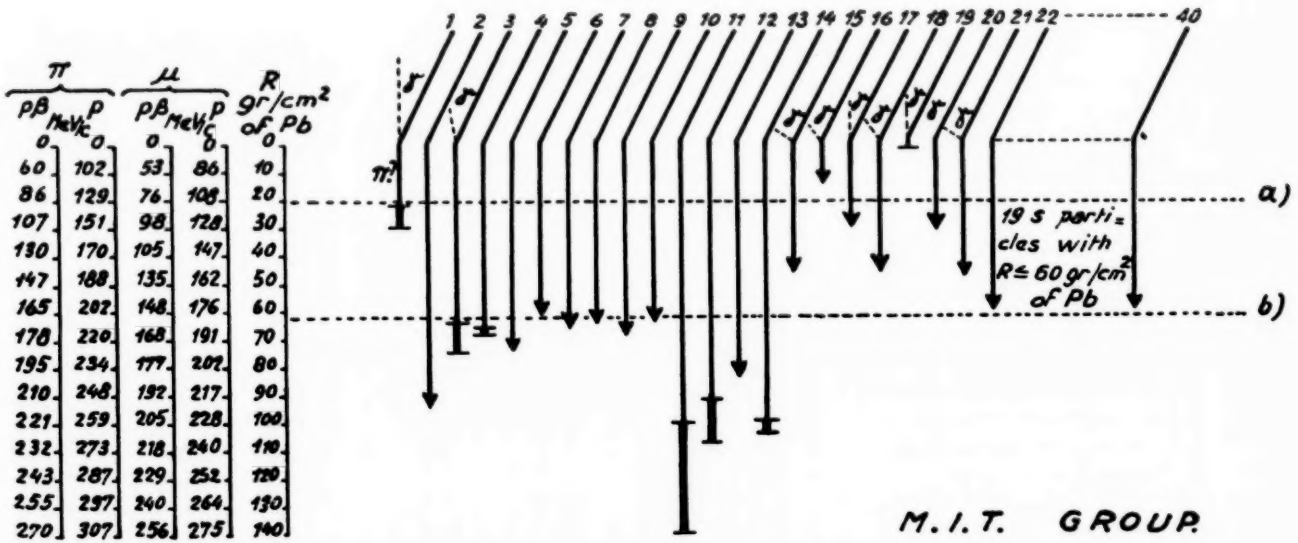

pβ MeV/c (π)	p (π)	pβ MeV/c (μ)	p (μ)	R gr/cm² of Pb
0	0	0	0	
60	102	53	86	10
86	129	76	108	20
107	151	98	128	30
130	170	105	147	40
147	188	135	162	50
165	202	148	176	60
178	220	168	191	70
195	234	177	202	80
210	248	192	217	90
221	259	205	228	100
232	273	218	240	110
243	287	229	252	120
255	297	240	264	130
270	307	256	275	140

FIG. 3. (Ideogram I). Ideogram for cloud chamber work (M.I.T.)

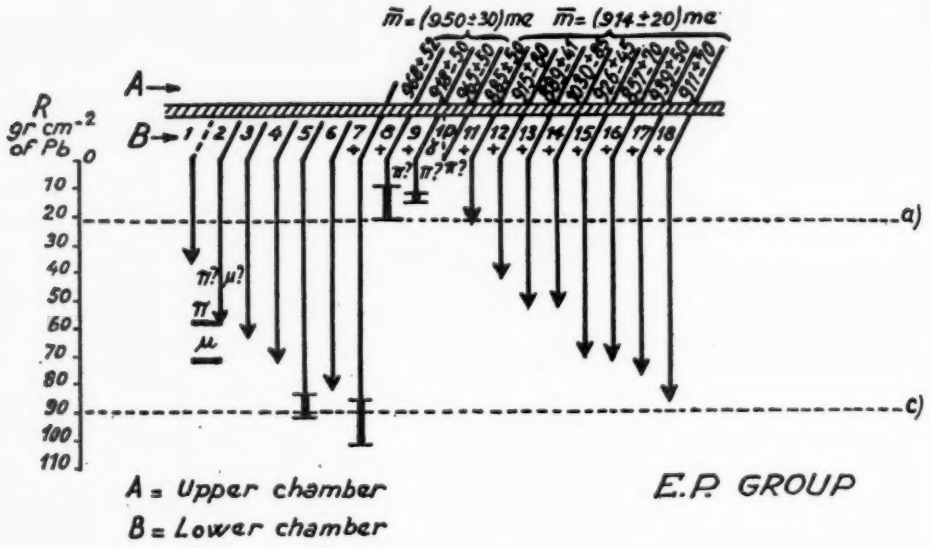

FIG. 3. (Ideogram II). Ideogram for cloud chamber work (P.E.P.)
a) Limiting Range of π secondaries from τ'decay
b) Range of π secondaries from postulated $^{969}{}_{\pi^0}K_\pi$
c) Limiting Range of μ secondaries from $^{914}\binom{\nu}{\gamma}K_\mu^+$

resulting from nuclear interactions of the secondary in the metal plate, the products of the interactions being stopped inside the plate.

(*b*) Two groups of monochromatic π- and μ-mesons emitted respectively in two-body decays. If the μ-meson is that which gives the ranges observed in (36-38-39), the mass of its corresponding primary particle is 969 m_e.

(*c*) All μ-mesons emitted in a three-body decay with a spectrum strongly peaked at the high energy end.

Analysing the ranges of those secondaries which do not stop in the chamber, the most probable range of the secondaries, considered as π-mesons, is given as about 115 gm./cm.^{2} Pb, and, considered as μ-mesons, about 101 gm./cm.^{2} Pb. The corresponding momenta can be read on the ideogram.

The electronic showers which constitute the evidence for the neutral products of the *S*-disintegration lie in the direction opposed to that of the charged secondary. Their deviation from collinearity and their frequency of observation lead M.I.T. to the following alternative conclusions:

(*a*) The electronic showers are produced by photons emitted directly in a three-body decay of the *S*-particles. The possibility that the γ-rays be a monochromatic decay product of the *S* is excluded on the basis of the angular distribution of the electronic showers.

(*b*) The electronic shower is the tertiary produced by the decay of a

monochromatic π^0-meson. This second hypothesis cannot account for all the observed S-decays. The observed frequency is too low, taking into consideration the energy and direction of the γ-rays.

Should a unique mass and mode of decay of the S-particles be required, M.I.T. results are not inconsistent with the scheme:

$$^{969}S \rightarrow \mu + \gamma + \nu.$$

The double chamber of the Ecole Polytechnique group allows the determination of the mass and the sign of particles which traverse the upper chamber and stop in the lower (46) (lifetime greater than 5×10^{-9} sec., greater than in the M.I.T. chamber). Their results are summarized in ideogram II (Fig. 3), and their conclusions can be outlined as follows:

(*a*) All the S-particles whose sign is measurable were found to be positive.

(*b*) Events No. 10 through 21 whose decay product is of short range can be attributed to τ contamination.

(*c*) The masses of the remaining S-particles are consistent with a unique value of 914 ± 20 em, to be compared with the mass postulated by the M.I.T. group to explain their results.

(*d*) Seven of the secondaries of this group have range greater than that compatible with the momentum of a π-meson emitted in the decay of a particle of this mass. This leads to the postulation of a heavy meson

$$^{914}K_\mu \rightarrow \mu + \text{neutral particle or particles.}$$

(*e*) Apart from two particles whose primary mass in unknown and which have secondaries of momentum of the order 220 Mev/c (if they are μ-mesons), no momentum superior to this value has been established.

(*f*) The analysis of the observed ranges leads to the attribution of either a two-body decay to the K_μ or a three-body decay with a strong grouping of the momentum of the charged particle around the upper limit.

The grouping of the secondary momenta around 220 Mev/c is supported if we add two V-particle secondaries of the Indiana group (47).

(*g*) Among those S-particles which are not observed in the upper chamber, there are those whose secondaries have a range consistent with a line at 90 gm./cm.^{2} Pb and two of longer range.

There seem to be discrepancies between the M.I.T. and P.E.P.^{2} results. These may be explained partly on difference in interpretation (e.g., M.I.T. suggests that short range secondaries might be attributed to inelastic scattering of π-mesons, whereas P.E.P. considers them to be the products of τ-decay), partly on the different lifetimes selected, and partly (γ-rays) to the difference of the multiplate sets.

V-particles.—A comprehensive account of the situation of V-particles up to and including the Conference of Bagnères de Bigorre (June, 1953) is contained in the article by Leprince-Ringuet (15). Since then little has been added to our knowledge of these particles. The position is complicated by the necessary selection made in order to exclude π-μ and μ-e decays and hyper-

ons. Greater caution is used to scrutinise every event giving a π-meson secondary in the doubt that it might be a Y-decay.

The Manchester and Caltech[2] groups both confirm the evidence for the existence among the V-particles of at least one particle undergoing a three-body decay. The mass of these particles is of the order of 1000 m_e, but there is some evidence, the clearest examples of which are the high momentum secondaries of the Manchester group (48) and Caltech group (49), for mass values of the order of 1200 em.

Nature of the V-secondaries.—Information on the nature of the charged V-secondaries comes from the P.E.P. double cloud chamber experiment. When a $V^{\pm}$ is observed to decay in the upper chamber and the secondary passes into the lower, the nature of the secondary can, in some cases, be determined. They find, among 13 V^- secondaries which cross the lower chamber, 8 which show nuclear interactions and are therefore considered to be π-mesons. One of these comes from the cascade decay $V^- \rightarrow \pi^- + \Lambda^0$, but they do not assert that all the π-secondaries are so produced. Among eight V^+ secondaries measured, they identify two μ-mesons by mass measurement and one π-meson by the fact that it shows nuclear interaction. This latter has low velocity in the center of mass system, and they assume it to come from a τ'-decay. On the nature of the neutral secondary particles, the only information comes from one event of the Princeton group (50). A very unlikely combination of probabilities has produced a Wilson chamber photograph in which a charged particle seems to decay into five secondaries. Analysis of the momenta and ionisation of the five secondaries leads to the conclusion that this event represents the decay in flight of a heavy meson into a light charged meson and a neutral π-meson decaying in two γ-rays. If the interpretation is correct, assuming the charged secondary to be a π^0-meson, the decay scheme $\theta^+ \rightarrow \pi^+ + \pi^0 + (213_{-10}^{+15})$ Mev can be compared with $\theta^0 \rightarrow \pi^+ + \pi^- + (214 \pm 5)$ Mev of the θ^0.

Charge symmetry in V's.—The evidence on the charge symmetry of the V's seems to be related to the lifetimes of the respective component types of particles. P.E.P. (51) has made an analysis of the charge ratios obtained by various groups as a function of the time of flight in their respective chambers and conclude that there are present two types of particles, one of long life ($>5\times10^{-9}$) sec. which is predominantly positive (K_μ), and a shorter-lived particle ($10^{-10} < \tau < 5\times10^{-9}$) sec., having charge symmetry and identified by them with the κ of O'Ceallaigh (see section on HEAVY MESONS IN PHOTOGRAPHIC EMULSION). On the other hand, the Manchester group states that the positive excess observed by its members can be attributed solely to statistical fluctuations. York *et al.* (49) add to the two groups of P.E.P. (51) a further group of even shorter life ($10^{-11} < \rho < 10^{-10}$) sec. which is again mainly positive. However, they believe that this third group might be largely composed of hyperons.

Relative frequencies in V- and S-particles.—Since it seems likely that the V and S are particles of the same type, a comparison of their observed fre-

quencies on the basis of their respective lifetimes can give an indication of their frequency of production. The P.E.P. group has made an analysis of the relative number of V- and S-particles in their two chambers, supposing the existence of two types of particle: the K_μ and the κ. When this analysis was made, the evidence of the Princeton group was not yet available. Their conclusions are these (51):

(*a*) The lifetime of the τ- and K_μ-particles is of the order of 2.8×10^{-8} sec.

(*b*) The lifetime of a shorter-lived κ-particle undergoing a three-body decay, assumed to account for the greater part of the events decaying in the upper chamber and of V-particles in general, is of the order of 2.4×10^{-9} sec.

(*c*) The relative frequencies of these two groups of particles are given as

(1) at production $K_\mu/\kappa\sim1.7$

(2) to be observed in multiplate chambers $K_\mu/\kappa\sim4.5$

(3) to be observed in photographic emulsions $K_\mu/\kappa\sim3.5$.

It is difficult to reconcile the relative frequencies given by them with either the M.I.T. or the photographic plate results. As we shall see in the next section, however imprecise the photographic plate information may be, it does not leave any place for a 3.5 to 1 ratio of K_μ/κ unless the range-scattering and ionisation-scattering methods of mass determination are hopelessly wrong (see page 272).

It is, however, possible that it is not only the observed time of flight which determines the relative frequency of these particles, but also their mode of production. The continuously sensitive photographic plate flying at high altitudes might register different types of particles from those seen in the earth-bound, selective Wilson chamber.

Heavy Mesons in the Photographic Emulsion (K-Particles)

During an intensive investigation of the decay spectrum of μ-mesons, O'Ceallaigh (52) found two anomalous decays. In one event, Br 1, a slow particle came to rest in the emulsion and decayed to a fast secondary of ionisation close to the minimum. Measurements of scattering on the secondary particle showed it to have a $p\beta$ of (235 ± 35) Mev/c well over the limit for the decay electron of the μ-meson. The measured mass of the primary particle was (1260 ± 260) m_e, intermediate between the π-meson and the proton. In the second event, Br 2, the μ-meson, whose secondary was being measured, was followed back for 5.67 mm., and its origin was found at the end of the range of a particle of mass (1125 ± 230) m_e. O'Ceallaigh concluded that these two events represented the decay of particles intermediate between the π-meson and the proton, and called them κ-particles. Assuming the two particles to be the same, the different energy of the secondaries suggested a three-body decay.

Since then 116 examples of K-particles decaying at rest have been observed. The relevant data are collected in Table VI. One might expect out of this wealth of results obtained all by the same instrument clear cut informa-

TABLE VI (PART 1)

DATA ON K-MESONS

Event	Primary: Parent star	Primary: Total range, mm.	Primary: Time of flight T 10^{-9} sec.	Primary: Mass in m_e		Secondary: Length, mm.	Secondary: g^*	Secondary: $p\beta$ Mev/c	Secondary: Mass m_e
				$g-R$	$\alpha-R$				
Bk_1	?	9.0	0.1068	—	850±200	—	steep		—
Bo_1*	20+5n	13.7	0.1462	950±100	955±140	—	—	226±20	—
Bo_2*	14+2n	11.3	0.1232	1120±100	980±155	—	.96± .12	—	—
Bo_3*	?	5.4	0.0744	1115±100	1025± 95	—	1	—	—
Bo_4*	1+2n	32.0	0.2618	980±100	740± 85	—	.93 ± .07	—	—
Bo_5*	8+2α	13.3	0.1386	865±100	1005±170	—	—	—	—
Br_1	?	4.1	0.0622	1380±180	1260±260	2.2	.97 ± .04	235±35	$\mu(\pi-e)$
Br_2	?	5.67	0.0782	1125±150	1125±230	1.1	—	11.8	μ
Br_3	?	0.53	0.0138	—	1000 to 2000	5.9	.96 ± .026	144±12	$\mu(e)$
Br_4	?	2.1	0.0368	—	1370±320	0.17	1	—	—
Br_5	?	1.54	0.0286	950±200	1220±400	8.9	1.705± .083	66±11	$\mu(\pi)$
Br_6	?	2.55	0.0442	1050±200	1036±280	0.1	1	—	—
Br_7	?	0.38	0.0114	—	1000	2.5	1.09 ± .05	170±29	$\pi(\mu)$
Br_8	?	2.55	0.0418	900±200	1460±320	7.65	1.14 ± .025	187±17	π
Br^9	?	0.63	0.0168	—	1000	19.5	1.094± .016	162± 9	π
Br_{10}	?	1.38	0.0286	—	1100±330	0.275	1	—	—
Br_{11}	?	0.54	0.0153	—	1300	0.1	1	—	—
Br_{12}	?	13.2	0.1386	—	1210±150	0.15	1	—	—
Br_{13}	?	0.96	0.0224	—	1080±450	0.2	1	—	—
Br_{14}	?	3.44	0.0536	—	925±190	0.5	1.02± .10	120±44	$\mu(e, \pi)$
Br_{15}	?	9.56	0.1152	—	1100±170	4.1	1.028± .031	184±30	$\pi(\mu, e)$
Br_{16}	?	1.7	0.0314	—	1000	2.8	1.030± .045	153±24	$\mu(\pi)$
Br_{17}	?	4.31	0.0644	—	1200±230	6.5	1.15 ± .03	172±17	π
Br_{18}	?	1.85	0.0342	—	1500	4.0	1	315±70	$\mu(\pi, e)$
Br_{19}	?	1.02	0.0224	—	1000 to 2000	0.8	1	125±35	$\mu(\pi, e)$
Br_{20}	?	6.675	0.0858	—	990±150	0.18	1	—	—
Br_{21}	1+0n	0.35	0.0105	—	—	18.0	0.93	205± 5	μ
Br_{22}*	1+0p	28.0	0.2384	780± 90	780± 90	6.0	1.09 ± .04	170±20	280±20
Br_{23}*	19±3n	7.56	0.0930	990±150	—	3.0	—	—	—
Br_{24}*	10+0p	8.56	0.1034	1200±200	1400±200	54.0	1.2 to 1	119± 9	203± 8
Br_{25}*	24+3p	3.77	0.0580	1000±250	1150±250	0.5 per plate	—	—	—
Br_{26}*	19+24	42.1	0.3170	990± 55	1100±150	—	∼1	>100	—
Br_{27}	?	∼8	0.1000	—	—	—	—	—	—
Br_{28}	?	∼8	0.1000	—	—	—	—	—	—
Br_{29}	?	∼1.3	0.1386	—	1000	—	—	—	—
Br_{30}*	?	40.0	0.3064	—	—	Energy 50–60 Mev estimated from change in grain density			—
Br_{31}*	13+3p	19.09	0.1814	900±200	—	—	∼1	145±25	—
Br_{32}*	27+3p	19.18	0.1814	1050±150	—	—	—	—	—
Br_{33}*	7+5p	4.03	0.0602	850±200	—	—	∼1	112±20	—
Br_{34}*	23+13p	—	—	—	—	—	steep	—	—
Br_{35}*	15+5p	48.36	0.3064	910±200	—	—	—	—	—
Br_{36}*	—	—	—	—	—	—	—	—	—
Br_{37}*	4+1n	∼8	0.1000	—	720±200	Provisional results		67	poss. e
Br_{38}*	11+4p	18.81	0.1746	1200±200	—	—	—	—	—
Br_{39}*	?	23.0	0.2012	900±200	—	—	—	—	—
Br_{40}*	—	—	—	—	—	—	—	—	—
Br_{41}*	19+3n	39.0	0.2954	∼950	—	—	—	—	—
$GeMi_1$	?	2.0	0.3690	—	1270±290	3.44	0.94± .03	150±27	—

TABLE VI (PART 1)—*Continued*

Primary						Secondary			
Event	Parent star	Total range, mm.	Time of flight T 10^{-9} sec.	Mass in m_e		Length, mm.	β^*	$p\beta$ Mev/c	Mass m_e
				$\beta-R$	$\alpha-R$				
GeMi$_3$	$30+8\alpha$	5.26	0.0744	1050± 140	1030± 165	0.45	1.15± .1	—	—
GeMi$_2$	$36+6p$	1.88	0.0342	1170± 270	1540± 380	2.08	1.14± . 03	108± 18	190± 32
GeMi$_4$	?	1.47	0.0286	—	1360± 340	2.5	1.06 ± .04	200± 33	300± 50
GeMi$_5$	?	0.64	0.0168	—	1000	—	—	—	—
GeMi$_6$	?	3.4	0.0536	980± 290	1010± 200	—	—	—	—
GeMi$_7$	?	12.57	0.1350	—	1100± 165	0.6	1	—	—
GeMi$_8$*	$4+0n$	5.69	0.0782	—	1380± 270	—	short	—	—
GeMi$_9$*	$7+0p$	19.24	0.1814	—	1015± 160	51.0	1.12± .012	135± 7	—
GeMi$_{10}$*	?	18.5	0.1746	—	1025± 200	40.0	0.97 ± .012	150± 10	—
GeMi$_{11}$*	$10+7p$	18.33	0.1746	—	900± 125	53.0	0.97 ± .13	190± 15	—
GeMi$_{12}$*	$4+2p$	15.85	0.1534	—	850± 120	60.0	1.21 ± .025	146± 10	—
GeMi$_{13}$*	$16+0p$	9.4	0.1068	—	870± 165	—	steep	—	—
Bx$_1$	?	3.0	0.0490	—	800± 160	—	—	—	—
Bx$_2$	?	2.0	0.0368	—	750± 170	—	—	—	—
Bx$_3$	?	1.4	0.0286	—	985± 255	—	—	—	—
Bx$_4$	?	20.0	0.1880	—	1100± 110	5.0	1.09	200± 30	—
It$_1$	?	5.0	0.0704	—	1020± 140	0.2	1.12± .11	—	—
It$_2$	?	0.52	0.0138	—	—	4.7	1.07± .03	172± 26	280± 50
It$_3$	?	0.12	0.0051	—	—	2.5	2.75 ± .08	24.5± 2.5	191± 30
It$_4$	?	11.3	0.1232	1080± 150	1000^{+260}_{-190}	0.13	1	—	—
It$_5$	?	10.4	0.1152	1030± 250	1190± 400	0.34	1.15± .4	—	—
It$_6$	?	1.7	0.0314	—	1000	0.25	1.56 ± .14	—	—
It$_7$	?	0.44	0.0122	—	—	0.64	1.1 ± .1	111± 35	190± 60
Ko$_1$*	?	1.4	0.0286	—	1680^{+760}_{-520}	21.0	0.93 ± .02	190± 20	—
Ko$_2$*	?	0.3	0.0097	—	—	—	—	—	—
Ko$_3$*	$12+2p$	3.0	0.0490	1110± 160†	1100± 300	64.0	0.96 ± .015	223± 22	poss. π
Ko$_4$*	$11+12p$	30.0	0.2502	—	970± 210	58.0	1.02 ± .02	167± 8	prob. π
Ko$_5$*	$6+1p$	5.3	0.0744	1000± 40	880± 160	—	steep	—	—
Ko$_7$*	$16+2n$	44.0	0.3276	—	1630± 160	34.0	—	—	—
Ko$_8$*	$23+9p$	15.0	0.1534	—	—	—	steep	—	—
O$_1$	$16+3p$	14.0	0.1462	—	1090± 180	2.5	1.05 ± .03	126± 21	200± 20
Mn$_1$	?	3.28	0.0512	—	1030± 300	9.1	1.010± .05	124± 12	—
Pd$_1$*	$20+7n$	42.5	0.3170	964± 60	—	21.0	—	160± 10	275± 33
Pd$_2$*	$15+1p$	19.14	0.1814	975± 200	961± 122	40.0	—	110± 15	—
Pd$_3$*	$4+1p$	19.31	0.1814	1006± 100	920± 330	37.5	—	70± 16	—
Pd$_5$*	$14+11p$	17.24	0.1676	850± 100	865± 290	44.4	—	52± 20	—
Pd$_7$*	$5+1p$	36.5	0.2844	943± 60	948± 100	24.0	—	159± 9	276± 30
Pd$_8$*	$15+7\alpha$	26.93	0.2262	1180± 140	895± 225	—	—	190± 15	175± 50
Pd$_9$*	$17+2p$	12.0	0.1310	1060± 100	1420± 360	21.0	—	153± 36	—
Pd$_{10}$*	$10+5p$	25.2	0.2262	1100± 160	—	10.0	—	67± 15	—
Pep$_1$	?	1.3	0.0256	1150± 300	970± 300	20.0	0.97 ± .03	197± 13	μ
Pep$_3$	$13+18p$	4.95	0.0700	900± 75	860± 105	0.16	0.85 ± .2	—	—
Pep$_2$	$9+2p$	6.04	0.0820	1015± 85	1090± 130	few grains		—	—
Pep$_4$	$6+1p$	9.0	0.1068	910± 70	890± 90	0.85	1.0 ± .1	—	—
Pep$_5$	?	1.52	0.0290	800± 250	1070± 220	0.2	1	—	—
Pep$_6$	?	1.4	0.0286	960± 220	825± 180	3.4	0.975± .05	290± 60	—
Pep$_8$*	$28+6p$	9.5	0.1068	980± 150 862± 60†	920± 155	—	1	—	—

TABLE VI (PART 1)—*Continued*

Primary						Secondary			
Event	Parent star	Total range, mm.	Time of flight T 10^{-9} sec.	Mass in m_e		Length, mm.	g^*	$p\beta$ Mev/c	Mass m_e
				$g-R$	$\alpha-R$				
Pep_9*	2+0p	2.05	0.0368	950±250	1210±390	—	1	—	—
Pep_{10}*	11+2n	8.7	0.1034	990±150 920± 60†	1100±200	—	1	—	—
Pep_{11}*	29+11p	2.7	0.0442	950±140	1083±294	—	1	—	—
Pep_{12}*	13+5p	37.4	0.2954	960±130	805±180	—	1	—	—
Pep_{13}*	?	19.3	0.1880	880± 80† 960±130 1240± 90†	1420±310	7.18	1.03 ±.03	200±20	—
Pep_{14}*	?	9.63	0.1152	1300±175 1050± 90‡	934±165	23.205	E=33.3 Mev		μ
Pep_{15}*	21+0p	4.66	0.0684	—	1005±320	—	1	—	—
Pep_{16}*	8+2p	27.8	0.2384	—	1075±190	—	0.96± .09	—	—
Pep_{17}*	3+6p	14.0	0.1462	steep	steep	49.0	1.05 ±.02	180±10	—
Pep_{18}*	?	10.3	0.1152	—	1195±260	—	1	—	—
Pep_{19}*	4+0n	0.585	0.0153	—	—	—	1.14 ±.11	—	—
Pep_{20}*	?	18.0	0.1746	steep	steep	—	1	—	—
Pep_{21}*	?	40.0	0.3064	—	1120±160	20.0	0.98 ±.02	194±34	—
Pep_{22}*	7+0n	29.5	0.2384	—	1230±240	5.0	1.16 ±.15	195±30	—
Pep_{24}*	19+1p	18.4	0.1814	—	1060+200	—	—	—	—
Rc_1*	16+0n	7.54	0.0930	—	660±210	—	steep	—	—
Rc_2*	25+15HN	23.8	0.2138	—	1020±300	—	steep	—	—
Rc_3*	8+0n	49.5	0.3582	—	850±125	—	1.02 ±.06	steep	—
Rc_4*	6+3p	3.6	0.0558	—	1060±260	—	steep	—	—
Rc_5*	?	31.8	0.2618	—	950±220	—	—	—	—
Rc_6*	9+4α	40.0	0.3064	—	1030±160	—	steep	—	—
Rc_7*	?	20.2	0.1880	980±130	—	14.6	E=28 Mev		μ
Ro_3*	?	24.6	0.2138	935± 40	—	29.0	1.24 ±.07	—	—
Ro_2*	14+6n	20.2	0.1880	860± 35 980± 60 950± 50	1020^{+150}_{-120}	18.0	1.07 ±.06	230±30	—
Ro_4*	6+0p	35.7	0.2844	1000± 40 980±330	720+120 90	4.83	E=13.6±.3 Mev		μ

* Stripped emulsions.
† Measured by photometric method.
‡ Grain count.

tion on the masses of the primaries and on the nature of the decay schemes. That the first hope is in vain is shown by histograms (Figs. 4, 5) which contain all the measurements of mass of heavy mesons by the method of ionisation-range. Figure 4 is a straight histogram, Figure 5 a weighted histogram, constructed on a modification of the constant area method, in which each value is represented by a rectangle of base equal to one standard deviation on either side of the mean and of height proportional to the reciprocal of the percentage error. This method has been used in order to avoid bias against the high values of mass introduced in the constant area method.

It should be borne in mind that this graph refers to particles which decay at rest with a visible charged secondary. In Figure 5 the positions of the K_μ

TABLE VI (PART 2)

DATA ON K PARTICLES DECAYING INTO π-MESON STOPPING IN THE EMULSION

Event	Primary particle				Secondary particle			
	Range, mm.	Mass (em) $(g-R)$	Mass (em) $(\alpha-R)$	Parent star	Range, mm.	Energy Mev	Sign	$p\beta$ Mev/c
It1	0.32	—	—	—	—	4.3	+	8.2
Mi1	6.83	—	—	17+7p	—	41.5	+	72.0
Pd1	—	—	966±100	8+3n	0.9	6.0	+	11.5
Pep1	6.8	930±100	—	21+1p	9.7	22.7	+	41.5
Rc1	16.0	940±100	975±170	—	—	14.7±.26	+	28.0
Rc3	13.8	995±100	1550±300	2+0p or 2+1n	—	15.2±.37	+	28.0
Ro1	12.1	1020± 65	1040+240 −180	16+8n	—	38.5	—	68.0

and the charged counterpart of the θ^0 are indicated. The greater part of the measured masses lie between 850 and 1200 m_e. Between these limits there is place for several different particles; outside them there is little space. The weighted mean of the mass values is 985 ± 14 m_e.

The scattering-range method applied to 83 of the events leads to an average mass of 1050 ± 20 m_e. That scattering-range measurements give a higher mass than that found by ionisation-range is a feature of all the means

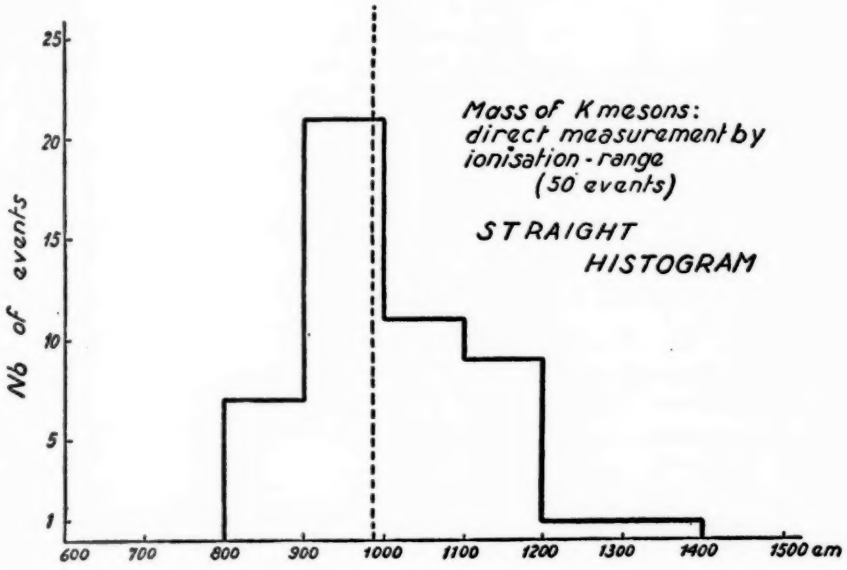

FIG. 4. K-Meson in nuclear emulsions (Straight histogram).

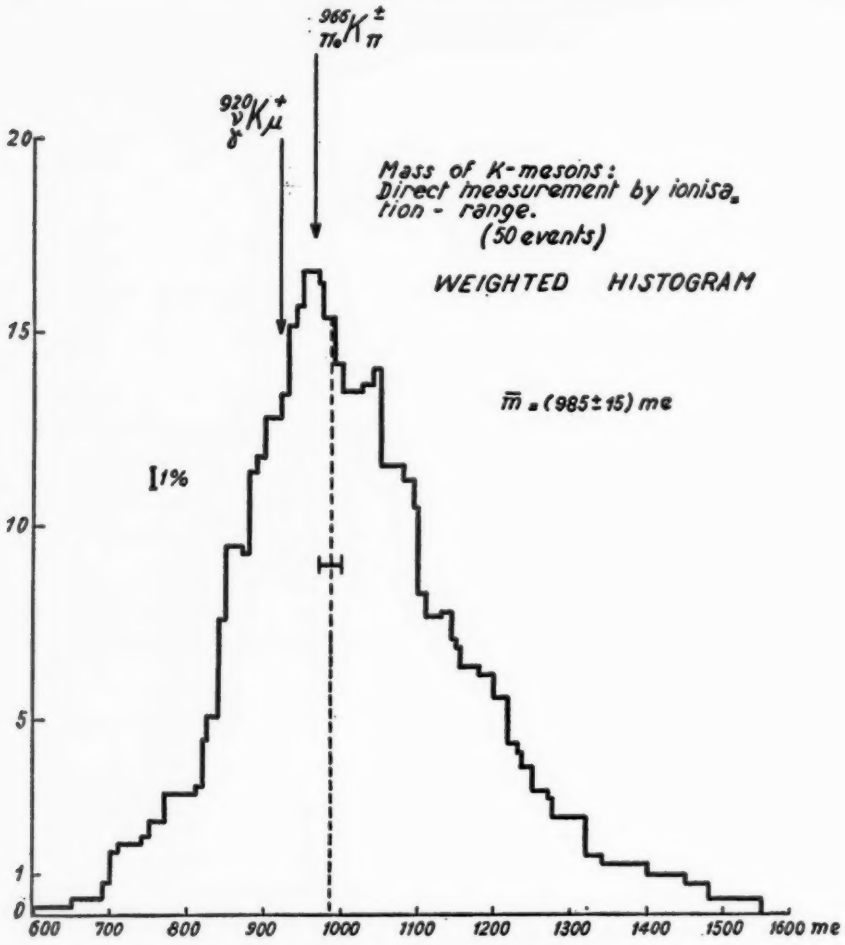

FIG. 5. *K*-Meson in nuclear emulsions (Weighted histogram).

made here. The ionisation-range values have been chosen to represent the data for two reasons:

(*a*) While recently some of the groups have calibrated their scattering measurements on known particles, a considerable part of these data are based on a scattering "constant" whose value is not well established (see section on EXPERIMENTAL BACKGROUND). The reverse is true for the ionisation measurements; most, although not all of these results, are based on internal calibration by each group.

(*b*) The spread on a histogram giving the frequency of the mass values from scattering range is enhanced by the difference in routine in the

various laboratories and by a high mass tail attributable to the asymmetry in error arising from the fact that the quantity measured, the angle of scattering, is inversely proportional to a power of the mass.

Since it is not possible to discriminate between the particles by direct mass measurement on the primaries, we might hope for significantly different modes of decay to give us, on the secondaries, the information we need. This hope is in part realised.

The information on the secondaries is based on the measurement of range, of scattering which gives the value of $p\beta$, and on a combination of scattering and energy loss as evaluated by grain- or blob-counting, which should in principle give the mass of the particle. It must be clear that the very nature of the ionisation-scattering curve limits the possibility of identification of the particles to certain well-defined regions of $p\beta$. In the opinion of the authors, in view of the complete absence of distortion and unevenness of development, it is easy to distinguish between a π- and μ-meson only if the $p\beta$ is less than 150 Mev/c; for values of $p\beta$ lying between 150 and 200 the distinction is difficult and dangerous; above 200 Mev/c it is practically impossible.

In absence of other information one cannot exclude the possibility that the particle is an electron if ionisation of the track is less than 1.1 times minimum ($p\beta \sim 125$ for μ; ~ 170 for π). This must be kept in mind in considering Figure 6, in which is given the information on the 54 secondaries which were suitable for measurement. The figure can be divided into four regions of $p\beta$: (*a*) $p\beta$ less than 80 Mev/c. In this region both π- and μ-mesons have been identified; (*b*) $p\beta$ lying between 80 and 140 Mev/c. In this region μ-secondaries have been identified, but no π-meson; (*c*) $140 < p\beta < 200$ Mev/c identified μ- and π-mesons; (*d*) $p\beta$ greater than 200 Mev/c. Identification no longer possible. The greater part of the secondaries have $p\beta$ less than 240 Mev/c. Two values, with a large experimental error lie above.

We shall first consider the secondaries on the basis of their identification as μ or π and see to what extent their decay scheme can be precisely defined.

K-particles decaying into a μ-meson and two neutral secondaries (the κ-meson).—A glance at the four regions of $p\beta$ defined above shows that μ-mesons are found in all regions of $p\beta$ in which their identification is possible. This leads to the supposition of a continuous spectrum from a three-body decay, as proposed by Menon & O'Ceallaigh (53). They called this particle the κ-meson, writing, $\kappa \rightarrow \mu + ? + ?$. The mean mass of the 8 measurable primaries of these 12 μ-secondaries is $M = (1060 \pm 35)\ m_e$ by ionisation-range, $(1110 \pm 84)\ m_e$ by scattering-range. The high precision which appears on the mean of the ionisation-range measurements is perhaps illusory, since it is based almost entirely on two precise but rather different values: Pep 14 $(1180 \pm 60)\ m_e$; and Ro 4 $(980 \pm 30)\ m_e$. These two primaries decay to a slow and therefore completely identified μ-meson.

Taking the value of the mean mass by ionisation range, the maximum $p\beta$ which the μ-meson from the decay of the κ can have, supposing the two

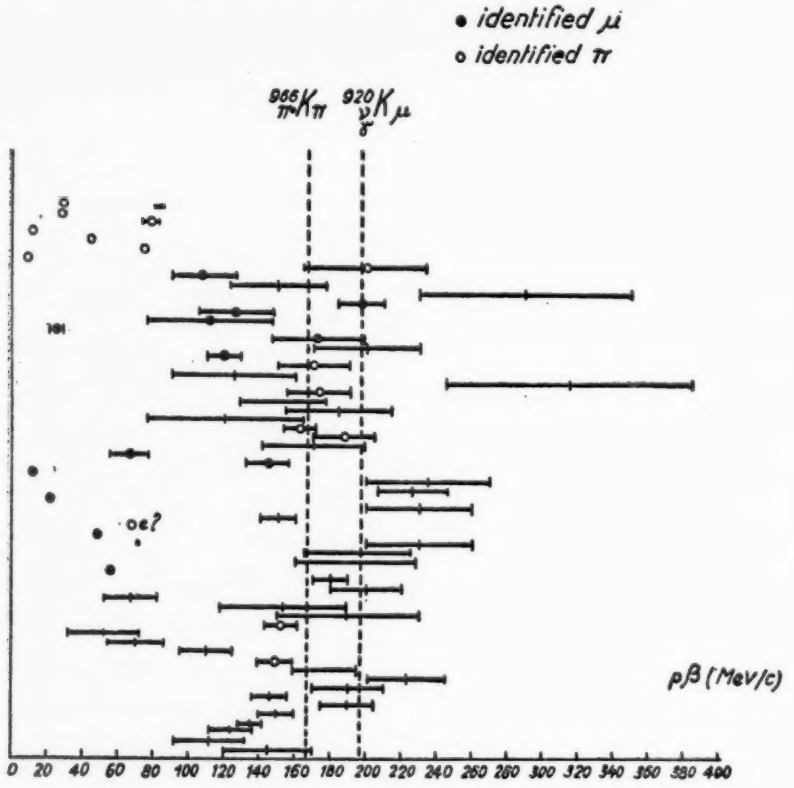

FIG. 6. Distribution in $p\beta$ of secondaries of K-particles.

neutral particles to be of zero mass, is (240 ± 10) Mev/c. The two particles which seem to lie above this limit, but not outside the error, might be associated with the Manchester event [see (48)] as giving an indication of a K-particle of even higher mass, or as arising from an alternative mode of decay in which the charged secondary is an electron, of which one possible example has been given by Menon at the Padova Congress (54).

K-particles giving charged π-secondaries (the K_π).—In the analysis of Figure 6 it appeared that π-mesons have been found in two groups, one at the low values of $p\beta$, and the other at the higher end of the discriminatory region. For greater clarity, these points are plotted separately in Figure 7. We shall deal first with the slower π's which are a by-product of the stripped emulsions whose increased path made it possible to identify them by their being brought to rest and giving the classical $\pi \rightarrow \mu \rightarrow e$ decay or a σ star. Of these events, six are positive; the negative particle Ro_1*, is discussed in the section on K-capture. Since all the secondaries of this group have energy less than

46 Mev ($p\beta$ less than 80 Mev/c) and there is a gap in the $p\beta$-distribution from 80 to 140 Mev/c, it is tempting to assume that the slow mesons arise from a type of particle different from that from which the group of fast π's arises. It has been seen in the section, the TAU MESON, that they might be attributed to the Pais-Dalitz alternative mode of decay of the τ-meson. This simple explanation rests however on a set of statistics which is not yet very solid. It is not easy, in fact, to explain why before 1954 no slow π had been detected, and it is possible, now that the problem is clear, that more particles will be found in the near future to fill the gap.

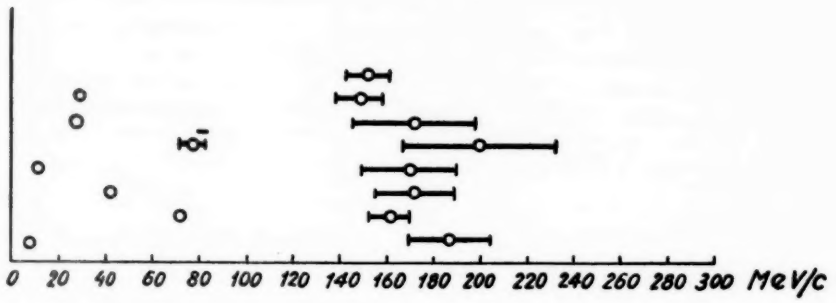

FIG. 7. Distribution in $p\beta$ of K secondaries indicated as π-mesons.

With this reserve let us examine the second group. This contains the evidence for the Menon & O'Ceallaigh χ-meson (53). They have been identified by measurements of mass on secondaries long enough to give good precision for ionisation and scattering measurements, but in a region of velocity in which discrimination is difficult. They are, in fact, at the limit of the possibilities of the method, so that, even if the spectrum extends above 200 Mev/c, it is not possible to see it. For this reason it is also difficult to assess the importance of this group. One of the points for example, the GeMi$_4$, lies on the edge of the impossible region, and its attribution to a π-meson is evidently questionable. It is, therefore, the absence of points below a $p\beta$ of 140 Mev/c which leads to the consideration of this group as representing a line spectrum, arising from a decay scheme such as that proposed by Menon & O'Ceallaigh, $\chi \rightarrow \pi +$?. The mean value of $p\beta$ of this group is (162 ± 5) Mev/c, so that, if it is a two-body decay and the neutral particle is of zero mass, the mass of the primary particle should be $M = (870 \pm 15)\ m_e$. If, on the other hand, the neutral particle were a π^0-meson, the mass of the χ should be $(950 \pm 15)\ m_e$. The measured masses of the primaries of the 8 π-secondaries give as a weighted mean:

$$m_{K_\pi} = (955 \pm 44) m_e \quad \text{I.R. (ionisation-range)}$$
$$(995 \pm 65) m_e \quad \text{S.R. (scattering-range)}$$

It is obviously tempting to associate this particle with the charged counterpart of the θ^0 (see pages 285–88 and 293–94), with decay scheme

$$\theta^+ \rightarrow \pi^\pm + \pi^0,$$

and mass probably close to that of the θ^0. In Table VII are assembled the data of M.I.T., Princeton, and the emulsion work, which might be considered as evidence for the above decay scheme. Although taken together they seem to give some indication of the existence of such a particle, no one of them is sufficient in itself to prove it, and their combined evidence is

TABLE VII

POSSIBLE EVIDENCE FOR A PARTICLE $\theta^\pm \rightarrow \pi^\pm + \pi^0$

Group	Mass of primary (m_θ)	Nature of the charged secondary	Momentum of the charged secondary (Mev/c)	Nature of the neutral secondary	Momentum of the neutral secondary (Mev/c)	Q (Mev) for scheme $\theta^\pm \rightarrow \pi^\pm + \pi^\circ + Q$
M.I.T. (45)	1200^{+270}_{-200}	π or μ	1 event at $p=130$–150 1 event at $p=205$–230 7 unknown	π° or $\gamma+?$	$\sim$200 if π° continuous if $\gamma+?$	$\sim$200
Princeton (50)	?	π^+ or μ^+	—	π°	—	231^{+15}_{-10}
Plates	(955 ± 44)	π	$p=200 \pm 5$	?	—	210 ± 7

purely circumstantial and subject in each point to an alternative interpretation.

In particular we recall the point raised above in connection with the energy distribution of the π-secondaries in the emulsion work. If, instead of taking the division into two groups on its face value, we consider that all the π-mesons are the decay product of the same particle, then the decay of the K_π is a three-body decay, such as $\kappa_\pi \rightarrow \pi + ? + ?$.

Relative frequency of μ and π among the K secondaries.—Apart from the uncertainty in the validity of the identification of some of the particles noted above, the velocity limit for the discrimination of π- from μ-mesons imposed by the nature of the ionisation-scattering curve makes it difficult to obtain from the mass measurements on the fast secondaries an estimate of the relative numbers of π- and μ-mesons among them. To do so it would be necessary to know the nature of the decay spectra of the particles, and this we are far from being able to determine.

Some information is given by the total interaction length. To date, $\sim$94 cm. of secondary track have been followed, and no interaction has been observed in flight. Since the interaction length for π-mesons in the photo-

graphic emulsion is ~25 cm., this seems to indicate a prevalence of μ-mesons among the K-secondaries.

The high momentum region and comparison with the Wilson Chamber.—The presence of a considerable number of μ-meson secondaries among those with high values of $p\beta$, though impossible to prove directly (the identification in E.P.$_1$ of a μ-meson of $p\beta = 197$ Mev/c. is as doubtful as that of GeMi$_4$ already noted), is likely following the argument of the last paragraph. The question is whether these secondaries represent only the high energy tail of the continuously-spread spectrum of the κ-meson, or are also the decay products of a particle, such as the $K\mu$ of the P.E.P. group, which gives either a line or a highly-peaked spectrum with a sharp maximum in the region of $p\beta + 200$ Mev/c. Comparison with the multiplate chanber evidence to date (55) indicates a much smaller proportion of secondaries of S-events in the interval between 80 and 150 Mev/c. (20 to 60 gm./cm^2 Pb) than among the K-particles. While statistics are yet small this seems to indicate that the proportion of κ-particles in multiplate chambers is considerably smaller than that of the $K\mu$, and consequently if there is only one $K\mu$ it should account for all the long-range S-secondaries, i.e., that its mass should be higher than 914 m_e, nearer to that of the τ-meson. It seems also that the ration $\kappa/K\mu$ is considerably higher in the photographic emulsions than in the multiplate chamber sample; this might be accounted for on the basis of different lifetimes. The lifetime of the $K\mu$ should be greater than that of the χ and considerably greater than that of the κ, while all three must be contained within the rather close limits of 10^{-9} to 3×10^{-8} sec. If the decay into an electron exists, an unknown fraction of the secondaries could arise from this phenomenon.

Sign ratio[4].—Of the greater part of the K-particles which decay in the emulsion, the sign is unknown. Only those which decay into a slow π-meson which presents at the end of its range its visiting card in the shape of a π-μ-e decay, or of a σ star, can be assigned a definite sign. The fact that the four slow μ-mesons observed to date all give the electron decay does not have a great significance. Only with much improved statistics could the ratio of μ-e to ρ among the μ secondaries give an estimate of the sign ratio of the κ's. In fact even when a ρ secondary is observed such as that of the Brussels group (56) there is considerable doubt as to its identification as either π or μ.

A number of nuclear interactions were observed to be produced at rest by particles of mass in order of 1000 m_e. These σK particles can be defined as negative, not forgetting that some decaying K particles may also be negative. There is strong experimental bias against the finding of the σK, which readily disguise themselves as either normal σ or evaporation stars, and therefore relative frequencies of $\sigma K/K$ based on normal scanning are not reliable. Experiments in which all grey tracks emitted from stars are

[4] The work of the P.E.P. group has shown that charge symmetry does not hold for all heavy mesons.

followed to their end of their range (57) should give the answer; so far in the Bristol experiments 10 K-particles were observed to decay at rest, one in flight, and none to give a nuclear interaction. It seems possible that either the K-particles in general are weakly interacting and only one or two types are strongly interacting, or that there is a strong positive excess among the greater part of the K-particles. In this connection we recall the positive excess found for the $K\mu$ and possibly also for the τ meson.

If most of the K-particles are produced in equal numbers of positive and negative and are weakly interacting, then one might expect to find a certain number of ρK, i.e., K-particles stopping and giving rise to no visible secondary. There is some theoretical basis (58) for expecting a higher proportion of decays than captures among particles such as the κ-meson if this is a Fermion than among the μ-meson, which is known to decay in 70 per cent of the cases in which it stops in the emulsion (59). The discrimination of the ρK from the proton would be very difficult, being based entirely on direct mass determination. The Lund group has reported three examples (60).

K particles which interact at the end of their range. σK.—In Table VIII are given the data on the 16 events in which a primary particle of measured mass about 1000 m_e stops in the emulsion and gives rise to a star. Other events have been published, but only those are given here for which there is direct proof of the identity of the primary particle. Since there are so few σK, any additional evidence would be welcome, and a re-examination of the old events to squeeze out the necessary information might be worthwhile.

It might be considered that the negative K of Rome (Ro_1*) should be added to the above Table as the limiting case in which the visible evaporation is zero. As we have seen above, the strong positive excess observed among the K_μ makes it unlikely that these particles contribute to any considerable extent to the category of σK. The sign ratio of the κ and other possible K-particles is unknown, and these might or might not contribute. The Bombay group (61) has proposed that, on the rather shaky statistics so far available, the contribution of negative τ-mesons could be sufficient to account for the total number of σK observed to date.

A prong frequency histogram for the σK events shows a marked absence of one-prong σK stars. This may well be a purely experimental effect since, given that the majority of the prongs are of low energy, a one-prong σK star could often seem to be a single scattering at the end of a track, indistinguishable by eye from that of a proton; and consequently it might not be measured.

Among the few σK events observed up to now, three general classes can be distinguished: A very small evaporation star is accompanied by (*a*) a π-meson; (*b*) a charged hyperon; (*c*) no charged unstable particle. In general the energy of the evaporation is very small, and this gives rise to the suspicion that in class (*c*) either high energy neutrons or unstable neutral particles (*e.g.*, π^0 or λ^0) are emitted.

TABLE VIII

Nuclear Interactions Produced by K-Particles at Rest (σK) in Photographic Emulsions

Primary						Star particles	
Event	Parent star	Total range, mm.	Time of flight $T \cdot 10^{-9}$ sec.	Mass in m_e		Nature	Energy Mev
				$g-R$	$\alpha-R$		
Bo$_1$*†	$14+2n$	0.3	0.0097	—	1000^{+720}_{-400}	Proton Proton π meson	1.0 0.5 28.1 ± 0.1
Bo$_2$*	$4+6n$	25.0	0.2138	975 ± 100	1015 ± 120	Proton Proton Proton Proton or Deuteron Proton	7.8 2.1 4.1 > 17.0 >180.0
Bo$_4$*	?	29.26	0.2400	1320 ± 100	850 ± 95	Proton Proton	8.1 9.0
Bo$_5$*	?	1.2	0.0256	—	540^{+290}_{-170}	Proton Proton	6.5 120.0
GeMi$_1$*	$10+2n$	10.64	0.1160	—	1170 ± 230	Very slow particle Y decaying in flight	
GeMi$_2$*	$7+4p$	41.0	0.3064	—	970 ± 90	Proton Proton Slow electron	6.7 18.3
Bh$_1$	?	3.6	0.0558	1050 ± 150	1200 ± 300	Triton or α particle π meson? Slow electron	
Ko$_1$*	$11+4p$	21.0	0.1950	880 ± 250	880 ± 250	2 short black tracks 1 track at minimum	
Lu$_1$*	$2+1n$ or $2+0p$	1.82	0.0342	985 ± 70 (photo-electric)	—	Proton Probable π meson 4 grains	22.0
Mn$_1$†	?	1.62	0.0314	1000 ± 150	1900 ± 500	π meson Proton	54.0 15.0
Mn$_2$	?	1.56	0.0300	1060 ± 150	1260 ± 400	Proton Proton Proton	>1.0 >1.0 7.5
Pd$_1$*	$6+1p$	11.1	0.1232	—	1070 ± 160	Proton Proton π meson recoil	42.0 17.0 37.0
Pd$_2$*	$9+1n$	47.0	0.3380	—	985 ± 150	Proton Proton	13.0 11.0
Pd$_3$*	$5+1n$	7.5	0.0930	—	987 ± 120	Proton α Proton Proton	7.0 7.0 90.0 45.0
Ps$_1$*†	?	16.1	0.1606	—	1745 ± 100	π^+ meson (gives μ decay) electron track at 1 to 1.5 min.	27.0 2.0
Ta$_1$*	$4+4\alpha$	34.0	—	—	1310 ± 245	5 black tracks	

* Stripped emulsions.
† Could also be Y particle interactions.

Friedlander & Harris (62) in a first and fruitless search for these events (fruitless in part because they were constrained to search for them in single plates in which recognition is difficult) calculated the type of interaction they expected to find. They considered two possible modes of interaction: (*a*) interaction of the heavy meson with two nucleons; (*b*) interaction of the heavy meson with one nucleon. In the first case they expected to find interactions similar to the normal σ star, together with a certain probability for the ejection of one or more π-mesons. In the second, there should be formed only an evaporation star of mean energy of the order of 90 Mev. The experimental data are as yet too scarce to allow an estimate of the relative frequencies of these two modes of interaction. That the situation is in fact more complicated than this is shown by the event $GeMi_1$ in which a charged hyperon of about 60 Mev energy is emitted. This event might be associated with the Wilson chamber evidence of Butler (63) of an unidentified negative particle which stops in a lead plate and seems to be the point of origin of a neutral V-particle observed close by in the gas, and with four cases reported by M.I.T. (64) of heavy mesons interacting in the metal plates of the chamber. In one case, only an electron shower is observed to come from the point of stopping of the particle; in three other cases a Y^0 is emitted, with energy 31 ± 3, 30 ± 8, and 59 ± 15 Mev. respectively. In the first of the three, an L-meson is also observed with an energy of between 81 and 106 Mev. DeStaebler points out (64) that these events can be explained on the basis of interactions of the type:

$$K^- + N \rightarrow \lambda^0 + \pi^-$$
$$K^- + P \rightarrow \lambda^0 + \pi^0$$

While the expected energies of emission are $E \sim 28$ Mev. and $E \sim 150$ Mev., interaction of the π within the nucleus or motion of nucleons in the nucleus may cause the observed energies to be rather different. The Genova-Milan event might represent the result of an interaction of the type

$$K^- + P \rightarrow \lambda^+ + \pi^-.$$

Production of K mesons.—There is not yet a consistent body of evidence on the mode of production of K-particles. In the Brookhaven experiments (31) one case of the production of a charged K (Bk 1) and a negative hyperon has been observed. Taken together with the other cases in which the corresponding neutral particles (Y^0 and K^0) are produced, this indicates a production process of the type

$$\pi + \text{ nucleon} \rightarrow \text{hyperon} + K\text{-meson}.$$

The Bombay and Bristol groups have each reported cases of the presence in one star of both a K-meson and a hyperon, consistent with the above process (65).

A study of the mass spectrum of particles emitted in cosmic ray stars has been undertaken by the Bristol school and has led to conclusions which differ according to the velocity range of the particles being examined. One group

TABLE IX

POSSIBLE PARTICLES NEAR 1000 Em

Particle	Observed decay products	Evidence*		Mass m_e	Lifetime (10^{-9} sec.)	Possible attribution
		Plate	W.C.C.			
$\tau^{965.5}{}_0K_3$	3π	XXX	XX	965.5 ± 0.7	~ 28	$\tau^{\pm} \to \pi^+ + \pi^- + \pi^{\pm}$
$\theta^{966}{}_0K_{2\pi^0}$	2π	X	XXX	966 ± 10	0.10	$\theta^0 \to \pi^+ + \pi^-$
$\tau'^{975}{}_{2\pi}K_{\pi}$	π($E<57$ Mev)	XX	X	975 ± 44	> 1	$\tau^{\pm} \to \pi^{\pm} + \pi^0 + \pi^0$
$\chi^{955}{}_{?}K_{\pi}$	π monoenergetic	XX	—	955 ± 44	> 1	$\theta^{\pm} \to \pi^{\pm} + \pi^0$
$\kappa^{1060}{}_{?,?}K_{\mu}$	μ continuous	XXX	XX	1060 ± 35	~ 2	$\kappa \to \mu + \nu + \gamma$ or $\to \mu + \nu + \nu$
$K_{\mu}{}^{914}{}_{\nu}K_{\mu}{}^{+}$	μ monoenergetic	—	XX (P.E.P.)	914 ± 20	~ 28	$\kappa_{\mu} \to \mu + \nu$
$\pi^0 K_L$	$L+\gamma$-rays from π^0	—	XX (PRI)	—	—	$\theta^{\pm} \to \pi^{\pm} + \pi^0$
	$L+\gamma$-ray from monoenergetic π^0		XX (M.I.T.)	—	—	
$\gamma,?K_L$	$L+\gamma$-ray continuous			—	—	$\kappa \to \mu + \nu + \gamma$
$?,?K_e$	Electron	XX	—	—	—	$\kappa \to e + \nu + \nu$
$^{1200}K_l$	Light secondary of high momentum	X	XX	—	—	^{1450}K or K_e
^{1650}K	No decay yet observed	X	—	~ 1450		

* XXX=strong evidence; XX=good evidence; X=just evidence.

(57), following to the end of their range tracks which when emitted are "grey," has found, between the proton and π-meson groups, ten K-particles of mass of the order of 1000 m_e (see p. 306). Another team (66), continuing with greater accuracy the work which was reported at Bagnères to give evidence for K-particles of mass of the order of 1200 m_e, now finds two groups of intermediate particles, one at 1000 m_e, and the other at 1450 m_e. These results, obtained by scattering-ionisation measurements on 'shower' particles (ionisation less than twice the minimum) are still subject to caution because of the poor statistics and to the inherent uncertainties of the scattering-ionisation method. It is to be expected that these results will become definite when it will be possible to follow to the end of their range also these high velocity particles.

Conclusion

Since 1949, the family of K-mesons which started with the τ's, grew up with the contribution of the κ's and χ's and the possibility of the Bristol 1250 mass particles. At the Bagnères de Bigorre meeting, a gallant attempt was made to reduce these particles to one, the τ-meson with its manifold possibilities of decay. One year afterwards, as stated conservatively by the Manchester Jungfraujoch group, "the subject is if anything growing in complexity" (48).

After the Padova meeting, an estimate of the possible particles is that given in Table IX.

Code

Bk.	Brookhaven National Laboratory, Brookhaven, New York, U.S.A.
Bo.	Tata Institute of Fundamental Research, Bombay, India
Br.	H. H. Wills Physical Laboratory, University of Bristol, England
Ge.	Istituto di Fisica dell'Universitá, Genoa, Italy
Mi.	Istituto Scienze Fisiche dell'Universitá, Sezione di Milano dell'I.N.F.N., Milan, Italy
Bx.	Laboratoire de Physique Nucléaire de l'Université Libre, Brussels, Belgium
It.	Cornell University, Ithaca, New York, U.S.A.
Ko.	Physical Institute of University, Copenhagen, Denmark
O.	Physical Institute of University, Oslo, Norway
Mn.	Physical Institute of University, Manchester, England
P.E.P.	Laboratoire de Physique de l'Ecole Polytechnique, Paris, France
P.S.	Laboratoire de Physique de la Sorbonne, Paris, France
Pd.	Istituto di Fisica dell'Universitá, Sezione di Padova dell'I.N.F.N., Padua, Italy
Rc.	University of Rochester, Rochester, New York, U.S.A.
Ro.	Istituto di Fisica dell'Universitá, Sexione di Roma dell'I.N.F.N., Rome, Italy

Lu. Physical Laboratories, Lund, Sweden
M.I.T. Massachusetts Institute of Technology, Cambridge, Massachusetts, U.S.A.
Caltech. California Institute of Technology, Pasadena, California, U.S.A.
In. Indiana University, Bloomington, Indiana, U.S.A.
Go. Max Planck Institut für Physik, Göttingen, Germany
Ta. Israel, A.E.C., Tel Aviv, Israel

We wish to thank, for their valuable advice during the writing of this article, C. Peyrou, G. D. Rochester, B. Rossi, and B. F. Touschek.

LITERATURE CITED

1. Goldschmidt-Clermont, Y., *Ann. Rev. Nuclear Sci.*, **3,** 141 (1953)
2. Voyvodic, L., *Progress in Cosmic Ray Physics*, **2,** Chap. 5 (North Holland Publishing Co., Amsterdam, Holland, 322 pp., 1954)
3. Fowler, P. H., *Phil. Mag.*, **41,** 169 (1950)
4. Menon, M. G. K., O'Ceallaigh, C., and Rochat, O., *Phil. Mag.*, **42,** 932 (1951)
5. Gottstein, K., Menon, M. G. K., Mulvey, J. H., O'Ceallaigh, C., and Rochat, O., *Phil. Mag.*, **42,** 708 (1951); Gottstein, K., and Mulvey, J. H., *Phil. Mag.*, **42,** 1089 (1951)
6. Berger, M., *Phys. Rev.*, **88,** 59 (1951)
7. Menon, M. G. K., O'Ceallaigh, C., and Rochat, O., *Phil. Mag.*, **42,** 932 (1951)
8. Report of the Varenna Summer School, *Nuovo cimento*, **11,** Suppl. *2*, 228 (1954)
9. Vigneron, L., *J. Phys. radium*, **14,** 145 (1953)
10. Heinz, O., *Phys. Rev.*, **94,** 1728 (1954)
11. Beiser, A., *Rev. Mod. Phys.*, **24,** 273 (1952)
12. Fry, W. F., and White, G. R., *Phys. Rev.*, **90,** 207 (1953)
13. Wilson, J. G., *Progress in Cosmic Ray Physics*, **2,** Chap. 2 (North Holland Publishing Co., Amsterdam, Holland, 1954)
14. Amaldi, E., Anderson, C. D., Blackett, P. M. S., Fretter, W. B., Leprince-Ringuet, L., Peters, B., Powell, C. F., Rochester, C. D., Rossi, B., and Thompson, B. W., *Nuovo cimento*, **11,** 213 (1954)
15. Leprince-Ringuet, L., *Ann. Rev. Nuclear Sci.*, **3,** 39 (1953)
16. Brown, R. H., Camerini, U., Fowler, P. H., Muirhead, H., Powell, C. F., and Ritson, D. M., *Nature*, **163,** 82 (1949)
17. Amaldi, E., Baroni, G., Castagnoli, C., Cortini, G., and Manfredini, A., *Nuovo cimento*, **10,** 937 (1953)
18. *Report of the Tau Commission of the Padova Meeting* (Padua, Italy; April, 1954) *Nuovo cimento* (To be published)
19. Pais, A., *Phys. Rev.*, **86,** 663 (1953)
20. Dalitz, R. H., *Proc. Phys. Soc.* (*London*), [A]**66,** 710 (1953)
21. Atsbury, J. P., *Report of Padova Meeting* (Padua, Italy, April, 1954) (To be published in *Nuovo cimento*); *Report on Congress on Cosmic Ray Physics* (Bagnères-de-Bigorre, France, 1953)
22. Dalitz, R. H., *Phil. Mag.*, **44,** 1068 (1953); *Report on Congress on Cosmic Ray Physics* (Bagnères-de-Bigorre, France, 1953)
23. Fabri, E., *Nuovo cimento*, **11,** 479 (1954)
24. Fabri, E., and Touschek, B. F., *Nuovo cimento*, **11,** 96 (1954)
25. Rochester, G. D., and Butler, C. C., *Nature*, **160,** 855 (1947)
26. Armenteros, R., Barker, K. H., Butler, C. C., and Cachon, A., *Phil. Mag.*, **42,** 1113 (1951)
27. Barker, K. H., *Report on Congress on Cosmic Ray Physics* (Bagneres-de-Bigorre, France, 1953)
28. Thompson, R. W., Burwell, J. R., Cohn, H. O., Hugget, R. W., Karzmark, C. J., and Kim, Y. B., *Report at Rochester Conference* (Rochester, New York, January, 1954)
29. Gregory, B. P., and Reynolds, G. T., *Report on Congress on Cosmic Ray Physics*, p. 35 (Bagneres-de-Bigorre, France, 1953)
30. Armenteros, R., Barker, K. H., Butler, C. C., Coates, and Sowerby, *Report*

on Congress on Cosmic Ray Physics, p. 35 (Bagnéres-de-Bigorre, France, 1953)
31. Fowler, W. B., Shutt, R. P., Thorndike, A. M., and Whittemore, W. L., *Phys. Rev.*, **93,** 861 (1954)
32. Leighton, R. B., *Report on Congress on Cosmic Ray Physics* (Bagnéres de Bigorre, France, 1953)
33. Deutschmann, M., *Report on Congress on Cosmic Ray Physics*, p. 48 (Bagnéres-de-Bigorre, France, 1953)
34. Barker, K. H., *Proc. Roy. Soc.* (*London*), [A]**221,** 328 (1954)
35. Bridge, H., and Rossi, B., *Report on Congress on Cosmic Ray Physics*, p. 26 (Bagnéres-de-Bigorre, France, 1953)
36. Reynolds, G. T., *Report on Congress on Cosmic Ray Physics*, p. 42 (Bagnéres-de-Bigorre, France, 1953)
37. Page, D. I. (Personal communication, May, 1954)
38. Gayther, D. B., *Phil. Mag.*, **45,** 570 (1954)
39. Alford, K. L., and Leighton, R. B., *Phys. Rev.*, **90,** 627 (1953)
40. Armenteros, R., Barker, K. H., Butler, C. C., Cachon, A., and York, C. M., *Phil. mag.* **43,** 597 (1952)
41. Cowan, W. E., *Phys. Rev.*, **94,** 16 (1954)
42. Rochester, G. D., and Butler, C. C., *Repts. Progr. in Phys.*, **16,** 364 (1953)
43. Annis, M., Bridge, H., Courant, H., Olbert, S., and Rossi B., *Nuovo cimento* **9,** 624 (1952)
44. Rossi, B., and Bridge, H., *Report on Congress on Cosmic Ray Physics*, p. 107 (Bagnéres-de-Bigorre, France, 1953)
45. Bridge, H., Courant, H., Dayton, B., DeStaebler, H. C., Jr., Rossi, B., Safford, R., and Willard, D. (Personal communication, July, 1954); and *Nuovo cimento*, **12,** 81 (1954)
46. Gregory, B., Lagarrigue, A., Leprince-Ringuet, L., Muller, F., and Peyrou, C., *Nuovo cimento*, **11,** 292 (1954)
47. Thompson, R. W., Burwell, J. R., Cohn, H. O., Rugget, R. W., Karzmark, C. J., and Kim, Y. B., *Report at Rochester Conference* (Rochester, New York, January, 1954)
48. Buchanam, J. S., Cooper, W. A., Millar, D. D., and Newth, J. A. (Personal communication, May, 1954)
49. York, C. M., Leighton, R. B., and Bjørnerud, E. K., *Phys. Rev.*, **95,** 1591 (1954)
50. Hodson, A. L., Baillouw, J., Arnold, W. H., Harris, D. R., Rau, R. R., Reynolds, G. T., and Treiman, S. B. (Private communication)
51. Armenteros, R., Gregory B., Lagarrigue A., Leprince-Ringuet L., Muller, F., and Peyrou, C., *Report on Padova Meeting* (Padua, Italy, April, 1954); *Nuovo cimento* (to be published).
52. O'Ceallaigh, C., *Phil. Mag.*, **42,** 1032 (1951)
53. Menon, M. G. K., and O'Ceallaigh, C., *Proc. Roy. Soc.* (*London*), **221,** 292 (1954)
53a. Davidson, J. P., *Phys. Rev.*, **91,** 1020 (1953)
54. Menon, M. G. K., *Report on Padova Meeting* (Padua, Italy, Avril, 1954); *Nuovo cimento* (To be published)
55. Dilworth, C., and Remi, B., *Report on the Varenne Summer School, 1954* (To be published in *Nuovo cimento*)
56. Hirschberg, D., and Hirschberg, L., *Nuovo cimento*, **12,** 296 (1954)

57. Dananayake, C., Francois, P. E., Fujimoto, Y., Iredale, P., Waddington, C. Y., and Yasin, M., Report on Padova *Meeting* (Padua, Italy, Avril, 1954); *Nuovo cimento* (To be published)
58. Dellaporta, N., *Nuovo cimento*, **11**, 82 (1954)
59. Bonetti, A., and Tomasini, G., *Nuovo cimento*, **8**, 693 (1951)
60. Friesen, S. von, Kristiansson, K., and Alinder, E., *Report on Padova Congres* (Padua, Italy, Avril, 1954); *Nuovo cimento* (To be published)
61. Lal, D., Pal, Y., and Peters, B., *Proc. Indian Acad. Sci.*, **38**, 398 (1953)
62. Friedlander, M. W., Harris, G. G., and Menon, M. G. K., *Proc. Roy. Soc.* (*London*), **221**, 394 (1954)
63. Butler, C. C., *Report on Rochester Conference* (Rochester, New York, January, 1954)
64. DeStaebler, H. C., Jr. (Private communication, July, 1954)
65. *Report of the K commission of the Padova Meeting* (Padua, Italy, April, 1954 (To be published)
66. Fowler, P. H., and Perkins, D. H., *Report on Padova Congres* (Padova, Italy, Avril, 1954); *Nuovo cimento* (To be published)

PENETRATION OF HEAVY CHARGED PARTICLES IN MATTER[1]

By Edwin A. Uehling

Department of Physics, University of Washington, Seattle, Washington

Introduction

All charged particles in their passage through matter lose energy as a consequence of excitation and ionization of the atoms and molecules of the medium through which they pass. At high and low energies additional processes come into play, and in the appropriate energy ranges some of these processes will affect profoundly the behavior of the penetrating particle. The nature of these various processes and their influence on the penetration phenomena are similar for all charged particles.

Nevertheless, we find it convenient to distinguish between two types: electrons and positrons on the one hand, and all charged particles heavier than electrons on the other. One reason for this distinction is that as soon as we go beyond the mere study of energy loss, light particles behave essentially differently than heavy particles. This is in part a consequence of the very different fractional energy transfers which are possible in a single collision in these two cases. It is a consequence also of important differences in behavior between one type of particle and another in close collisions which show up rather weakly in the energy loss problem but which may be of fundamental significance in various associated phenomena.

We restrict ourselves in this discussion to the heavy particles. This restriction should not imply that recent advances in the field of heavy particles are of greater significance than corresponding advances in the case of light particles. However, it does imply that important advances have been made, and that some of the more significant of these advances are conveniently discussed from the point of view of the heavy particles.

We will not necessarily find it advisable to omit all further references to light particles. In particular, some penetration phenomena do not depend sensitively on those types of collisions for which the differences between one kind of charged particle and another are important. With certain restrictions this is the case for the most probable energy loss of a high velocity particle in a thin foil. It is the case also for the effects attributable to polarization of the medium. In treating phenomena of this kind we will occasionally draw upon experimental data involving light particles in order to supplement the available data on heavy particles.

The most recent summaries of the penetration phenomena involving heavy particles are contained in an article by Taylor (1), a chapter by Bethe & Ashkin (2) in the recent book on Experimental Nuclear Physics, and an

[1] The survey of literature pertaining to this review was concluded in April, 1954.

article by Allison & Warshaw (3). The article of Taylor summarizes the status of range-energy relations as it was in 1952; the chapter by Bethe and Ashkin is a comprehensive treatment of the penetration of several types of radiation through matter; the article of Allison and Warshaw brings together nearly all of the recent data on stopping power, particularly in the low-energy region, and on charge exchange and some other low-energy phenomena.[2]

One of the principal by-products of the study of penetration phenomena is the acquisition of range-energy and stopping power data which are useful in numerous fields of investigation. We will not be primarily concerned with the over-all data in this article. Good tabulations which include all but the most recent information are now available in several places. Thus, most of the available range-energy information is contained in the chapter of Bethe & Ashkin (2) and in a compilation of Aron, Hoffman & Williams (4). In addition, stopping power information will be found in the calculated tables of Aron (5) and in the article of Allison & Warshaw (3). The experimental and theoretical bases for the tables and curves presented are adequately described in these sources. It will be sufficient here to describe the kind of data available. The range-energy information summarized in Bethe & Ashkin (2) is for α-particles in air (0 to 15 Mev), protons in air, Al, Cu, Ag, and Pb (0 to 10^4 Mev), and protons in H_2 and glycerol tristearate (based on calculations for energies up to several Mev). The summary of range-energy information contained in Aron, Hoffman & Williams (4) is for protons in a large variety of light and heavy elements, and covers the energy range up to 10^3 Mev. Low-energy stopping power data are summarized in Allison & Warshaw (3). These data cover the energy range from 20 or 50 kev to 1.0 or 2.0 Mev. Most of it relates to protons: in the gases H_2, O_2, N_2, and air; in the metals Be, Al, Cu, Ag, Au, and Ni; in the noble gases He, Ne, A, Kr, and Xe; and in such inorganic and organic gases as NH_3, H_2O, NO, CO_2, N_2O, CCl_4, CH_4, C_2H_2, C_2H_4, and C_6H_6. In addition, there are stopping power data for: protons in mica and D_2O ice; for α-particles in Au; and for He, N, and Ne ions in H_2, Ne, A, and air. The high-energy stopping power data given in the tables of Aron (5) are for protons of 1 to 10^4 Mev in H_2, He, Li, Be, C, Al, A, Cu, Ag, and Pb. The tables are based on calculations using appropriately adjusted values of the mean excitation potential and a correction for inner shell electrons according to methods which were available at that time.

We make no attempt in this article to cover the whole field of penetration phenomena even insofar as the heavy particles are concerned. Instead, we treat only a few special topics in which there appears to have been the greatest interest within the last year or two. In doing this we will perhaps omit a

[2] An additional recent summary related to some of the topics discussed in this article, but with emphasis on light particles and gamma rays, is given in Corson, D. R., and Hanson, A. O., "Extranuclear Interactions of Electrons and Gamma Rays," *Ann. Rev. Nuclear Sci.*, **3**, 67–92 (1953).

number of topics of considerable importance. We will rely heavily on the readily available sources of discussion in order to avoid undue repetition. References to such sources will always be given, but no attempt will be made to provide a bibliography which is in itself complete. The summary articles already mentioned provide such bibliographies.

The Theory of Energy Loss

There has been some confusion in the literature with regard to the appropriate formulae for energy loss for the various types of charged particles. In order to clarify this situation, we will review the arguments on the basis of which the energy loss expressions are derived.

It is convenient to divide the possible energy transfers to an atomic electron in a single collision into two classes: those for which the actual energy transfer Q is less than some quantity η, and those for which the transfer is greater than η. One imposes the following conditions on η: (*a*) η must be large compared with the binding energies of electrons in the atom; and (*b*) η must be sufficiently small that for energy transfers of order η and less, the effective collision parameter is large compared with atomic dimensions and consequently the charged particle can be represented as a point particle. For particles of sufficiently high velocity it is possible to find a value of η which satisfies both of these conditions. Its value is of the order 10^4 to 10^5 ev.

The average energy losses for the two kinds of collisions are now considered separately. For the distant collisions corresponding to $Q<\eta$ the energy loss is obtained by summing over all the excitation probabilities of the atom. The formula for the energy loss per cm. in this type of collision as derived by Bethe (6) is

$$\left(-\frac{dE}{dx}\right)_{Q<\eta} = \frac{2\pi n(ze^2)^2}{m\beta^2c^2}\left[\ln\frac{2m\beta^2c^2\eta}{(1-\beta^2)I^2} - \beta^2\right] \qquad 1.$$

where ze is the charge of the penetrating particle, $\beta=v/c$, n is the number of electrons per cm.^{3} in the medium, m is the electron mass and I is the mean excitation potential of the medium. Because of the stipulated condition on η, this expression is valid for charged particles of all types including electrons and positrons.

The expressions for the energy loss in close collisions corresponding to $Q>\eta$ depend on the type of particle. Since, however, η is large compared with the binding energies of the electrons, the energy loss contributed by collisions of this kind may be calculated from the differential cross sections for the transfer of energy Q in dQ to essentially free electrons. The cross sections for energy transfer by heavy particles of mass M to free electrons have been calculated by Bhabha (7) for spin 0 and spin $\frac{1}{2}$ particles, by Massey & Corben (8) for spin $\frac{1}{2}$ and spin 1 particles, and by Oppenheimer, Snyder & Serber (9) for spin 1 particles. The results are

$$\text{for spin 0, } d\sigma = \left[\frac{2\pi(ze^2)^2}{m\beta^2c^2}\frac{dQ}{Q^2}\right]\left[1-\beta^2\frac{Q}{Q_{\max}}\right] \qquad 2.$$

$$\text{for spin } \tfrac{1}{2},\ d\sigma = \left[\frac{2\pi(ze^2)^2}{m\beta^2c^2}\,\frac{dQ}{Q^2}\right]\left[1-\beta^2\frac{Q}{Q_{\max}}+\frac{Q^2}{2E^2}\right] \qquad 3.$$

$$\text{for spin } 1,\ d\sigma = \left[\frac{2\pi(ze^2)^2}{m\beta^2c^2}\,\frac{dQ}{Q^2}\right]\left[\left(1-\beta^2\frac{Q}{Q_{\max}}\right)\left(1+\frac{Q}{3Q_c}\right)+\frac{Q^2}{3E^2}\left(1+\frac{Q}{2Q_c}\right)\right] \qquad 4.$$

where $E=E_k+Mc^2$ is the total energy of the particle, $Q_{\max}$ is the maximum possible energy transfer to an electron in a single collision and $Q_c=M^2c^2/m$.

The conservation laws yield (7)

$$Q_{\max} = Mc^2\,\frac{(E/Mc^2)^2-1}{(M/2m)+(m/2M)+(E/Mc^2)}.$$

Consequently, if we restrict our considerations to heavy particles of energies $E_k \ll M^2c^2/2m$ (10^{10} ev for mesons) we can write

$$Q_{\max} = \frac{2mv^2}{1-\beta^2}. \qquad 5.$$

Then also $Q_{\max}/E \ll 1$, $Q/Q_c \ll 1$ and the differential cross section for all heavy particles reduces to equation 2 for spin 0 particles. It is interesting to observe that radiative corrections are probably already important in a region of energy which may be somewhat lower than that in which a distinction between the various heavy particle types becomes important. Jankus (10) has shown that for energies below 100 Mc^2, radiative corrections to energy loss are unimportant and, in fact, the radiative loss attributable to the emission of radiation and to virtual photons is only of the order of 1 per cent of the ionization loss at $E \sim 100\,Mc^2$. Consequently, for heavy particles up to energies of order 100 Mc^2 we can neglect both the distinction between particles and the effects of radiation insofar as energy losses are concerned.

We now obtain the energy loss per cm. of path length for heavy particles resulting from energy transfers for which $Q>\eta$ by using equation 2 for the differential cross section and integrating over the possible energy transfers.

$$\left(-\frac{dE}{dx}\right)_{Q>\eta} = n\int^{Q_{\max}} Q\,d\sigma = \frac{2\pi n(ze^2)^2}{m\beta^2c^2}\int_\eta^{Q_{\max}}\frac{dQ}{Q}\left(1-\beta^2\frac{Q}{Q_{\max}}\right)$$
$$= \frac{2\pi n(ze^2)^2}{m\beta^2c^2}\left[\ln\frac{Q_{\max}}{\eta}-\beta^2\right]. \qquad 6.$$

The total average energy loss for heavy particles is the sum of equations 1 and 6, i.e. the contributions from distant and close collisions respectively:

$$\left(-\frac{dE}{dx}\right) = \frac{2\pi n(ze^2)^2}{m\beta^2c^2}\left[\ln\frac{2m\beta^2c^2Q_{\max}}{(1-\beta^2)I^2}-2\beta^2\right]. \qquad 7.$$

Introducing equation 5 we obtain the desired relation valid for all heavy particles

$$\left(-\frac{dE}{dx}\right) = \frac{4\pi n(ze^2)^2}{m\beta^2c^2}\left[\ln\frac{2m\beta^2c^2}{(1-\beta^2)I}-\beta^2\right]. \qquad 8.$$

It is interesting to observe that the relativistic term $[-\ln(1-\beta^2)-\beta^2]$ comes

from both the close and distant collisions with equal contributions from each.

Though we will have little occasion in this article to use the corresponding expressions for electrons and positrons we will digress briefly in order to include them along with the heavy particle expressions. The differential cross sections for the transfer of energy Q in dQ to a free electron by an electron was calculated by Møller (11), and the corresponding expression for the transfer of energy from a positron was calculated by Bhabha (12). These expressions are:

$$d\sigma = \frac{2\pi e^4}{m\beta^2c^2}\frac{dQ}{Q^2}\left[1+\left(\frac{Q}{E_k-Q}\right)^2+\left(\frac{\gamma-1}{\gamma}\right)^2\left(\frac{Q}{E_k}\right)^2-\frac{2\gamma-1}{\gamma^2}\left(\frac{Q}{E_k-Q}\right)\right] \quad 9.$$

(for electrons)

$$d\sigma = \frac{2\pi e^4}{m\beta^2c^2}\frac{dQ}{Q^2}\left[1-\frac{\gamma^2-1}{\gamma^2}\frac{Q}{E_k}+\frac{1}{2}\left(\frac{\gamma-1}{\gamma}\right)^2\left(\frac{Q}{E_k}\right)^2\right.$$
$$-\left(\frac{\gamma-1}{\gamma+1}\right)\left(\frac{Q}{E_k}\right)\left\{\frac{\gamma+2}{\gamma}-2\frac{\gamma^2-1}{\gamma^2}\left(\frac{Q}{E_k}\right)+\left(\frac{\gamma-1}{\gamma}\right)^2\left(\frac{Q}{E_k}\right)^2\right\}$$
$$\left.+\left(\frac{\gamma-1}{\gamma+1}\right)^2\left(\frac{Q}{E_k}\right)^2\left\{\frac{1}{2}+\frac{1}{\gamma}+\frac{3}{2\gamma^2}-\left(\frac{\gamma-1}{\gamma}\right)^2\frac{Q}{E_k}\left(1-\frac{Q}{E_k}\right)\right\}\right] \quad 10.$$

(for positrons)

where $E_k = mc^2(\gamma-1)$ is the kinetic energy of the electron or positron and $\gamma = (1-\beta^2)^{-\frac{1}{2}}$.

As before, we calculate the energy loss per cm. of path length resulting from collisions for which the energy transfer is greater than η. Thus:

$$\left(-\frac{dE}{dx}\right)_{Q>\eta} = n\int_\eta^{Q_{\max}} Q\,d\sigma$$

where $Q_{\max} = E_k$ for positrons and $E_k/2$ for electrons, since in the case of electrons the outgoing particle of higher energy is defined to be the primary one. The result is

$$\left(-\frac{dE}{dx}\right)_{Q>\eta} = \frac{2\pi ne^4}{m\beta^2c^2}\left[\ln\frac{E_k}{4\eta}+1-\frac{2\gamma-1}{\gamma^2}\ln 2+\frac{1}{8}\left(\frac{\gamma-1}{\gamma}\right)^2\right] \quad \text{(for electrons)} \quad 11.$$

$$= \frac{2\pi ne^4}{m\beta^2c^2}\left[\ln\frac{E_k}{\eta}-\frac{\beta^2}{12}\left\{11+\frac{14}{\gamma+1}+\frac{10}{(\gamma+1)^2}+\frac{4}{(\gamma+1)^3}\right\}\right] \quad 12.$$

(for positrons).

These equations and the corresponding electron-positron differences are discussed by Rohrlick & Carlson (13).

We now add the contributions for $Q>\eta$ of equations 11 and 12 to the contributions for $Q<\eta$ given by equation 1. In doing so we substitute in equation 1

$$\frac{m\beta^2c^2}{1-\beta^2} = mc^2(\gamma^2-1) = E_k(\gamma+1)$$

and of course $z = \pm 1$. Thus we obtain

$$\left(-\frac{dE}{dx}\right)=\frac{2\pi ne^4}{m\beta^2c^2}\left[\ln\frac{E_k^2(\gamma+1)}{2I^2}+(1-\beta^2)-\frac{2\gamma-1}{\gamma^2}\ln 2+\frac{1}{8}\left(\frac{\gamma-1}{\gamma}\right)^2\right] \quad 13.$$

(for electrons)

$$=\frac{2\pi ne^4}{m\beta^2c^2}\left[\ln\frac{2E_k^2(\gamma+1)}{I^2}-\frac{\beta^2}{12}\left\{23+\frac{14}{\gamma+1}+\frac{10}{(\gamma+1)^2}+\frac{4}{(\gamma+1)^3}\right\}\right] \quad 14.$$

(for positrons).

Equations 8, 13, and 14 are the final expressions for the average rate of energy loss for heavy particles (providing $E_k/Mc^2 < M/2m$), electrons and positrons respectively. For particles of the same relativistic velocity, the average energy loss by heavy particles will exceed that of electrons and positrons by a fractional amount of order $\ln\gamma/\ln(\gamma^2mc^2/I)^2$. This may amount to as much as 10 per cent in a medium of heavy atoms when $\gamma\sim 10$. If these formulas are written in terms of the maximum energy transferable, and if the conditions of an experiment are such that only energy transfers below a fixed amount are measured, then the differences between the energy losses of light and heavy particles at relativistic energies are insignificant. Furthermore, the formula for electrons is nearly identical with the expression derived by Bloch (14) in the limit of $ze^2/\hbar v \ll 1$. The latter expression has frequently been used by various authors as a basis for energy loss calculations.

We will conclude this section by anticipating some results of later sections in order to obtain expressions for energy loss which are appropriate to certain experimental conditions. We consider first the form of the energy loss expression which is to be used when the conditions of measurement are such that single energy transfers greater than a fixed quantity T are disregarded.

This is the case when the energy loss is measured by droplet counting in a cloud chamber, by grain counting in an emulsion, or by pulse height measurements in a scintillation counter of finite size. Under these circumstances large energy transfers will be disregarded by the omission of the ion count along δ-ray tracks, by failure to note the escape of high-energy electrons from the grains along the track of the primary particle in an emulsion, or by failure of a crystal to stop completely all of the high-energy electrons which are produced. Such measurements evaluate the sum of all energy transfers for which $Q < T$ where T may be of the order of 2 to 10 kev in cloud chamber and emulsion experiments, and it may be of the order of several million electron volts in crystal experiments. The correct expression for average energy loss is then obtained by the substitution of T for $Q_{\max}$. We should distinguish two cases. If T is small compared with the appropriate dividing line between close and distant collisions, all collisions relevant to the experiment belong to the class of distant collisions and the substitution of T for $Q_{\max}$ should be made in equation 1. From now on we will measure all ranges in units of gm./cm.^{2} rather than in cm. Consequently, dividing equation 1 by ρ, the density of the medium, and substituting T_1 for η, we obtain the average energy loss formula

$$\left(-\frac{1}{\rho}\frac{dE}{dx}\right)_{Q<T_1} = \frac{2\pi n(ze^2)^2}{\rho mv^2}\left[\ln\frac{2mv^2T_1}{(1-\beta^2)I^2} - \beta^2\right] \qquad 15.$$

where we use the symbol T_1 to designate that the maximum energy transfers are small compared with the separation energy η between close and distant collisions. For measurements of energy loss in a crystal, the relevant energy transfers may be very much larger. Denoting the maximum energy transfer measured in this case by the symbol T_2 we obtain by substitution of T_2 for $Q_{\max}$ in equation 7 the result

$$\left(-\frac{1}{\rho}\frac{dE}{dx}\right)_{Q<T_2} = \frac{2\pi n(ze^2)^2}{\rho mv^2}\left[\ln\frac{2mv^2T_2}{(1-\beta^2)I^2} - 2\beta^2\right]. \qquad 16.$$

Equation 15 is valid for all particle types; equation 16 is strictly valid only for heavy particles.

In some experiments the average energy loss is not easily measured. It is often more convenient to measure an energy loss distribution, and from the distribution the most probable loss or the median loss. We will describe energy loss distributions in a later section, but will give here some results which bear on the measurement of most probable losses. The problem of determining the most probable loss was considered by Williams (15) and later by Landau (16). The most probable loss and the width of the energy loss distribution can be specified in terms of a single parameter ξ given by

$$\xi = \frac{2\pi n(ze^2)^2}{\rho mv^2}t \qquad 17.$$

where t is the thickness of the medium (in gm. cm.$^{-2}$) through which the primary particle passes. The physical meaning of this parameter is that it is just that single collision energy loss which the particle experiences once on the average in its passage through the medium of thickness t. Energy losses large compared to ξ are too rare to affect either the value of the most probable loss or the shape of the distribution. Energy losses small compared to ξ affect the most probable loss but are too small to cause appreciable departures from a Gaussian distribution. Energy losses of order ξ affect both the shape of the distribution and the most probable loss. For values of ξ which are sufficiently small, the most probable loss turns out to be given by equation 15 provided we replace T_1 by ξ and add a term equal to 0.373 ξ. We will denote the most probable loss by Δ_{mp}. One then has the result

$$\Delta_{mp} = \xi\left[\ln\frac{2mv^2\xi}{(1-\beta^2)I^2} - \beta^2 + 0.373\right] \qquad 18.$$

where the term 0.373 ξ represents the contribution to the most probable loss from energy transfers of order ξ.

In a later section we will discuss the way in which energy losses are modified by polarization of the medium. The effect of polarization is to reduce the energy loss by an amount which depends on the properties of the medium and on the velocity of the particle. In the notation of Sternheimer (17) we

will denote the reduction in energy loss in the appropriate units by the symbol δ. The description and calculation of δ will be discussed later.

We will conclude this discussion by collecting the various formulas for the energy losses under typical conditions and with inclusion of the quantity δ which represents the polarization or density correction.

From equation 8 the average energy loss per gm. cm.$^{-2}$ by a heavy particle with momentum p is

$$\left(-\frac{1}{\rho}\frac{dE}{dx}\right) = \frac{4\pi n(ze^2)^2}{\rho mv^2}\left[\ln\frac{2mv^2}{(1-\beta^2)I} - \beta^2 - \frac{\delta}{2}\right]$$
$$= \frac{4\pi n(ze^2)^2}{\rho mv^2}\left[\ln\frac{2mc^2}{I} + 2\ln\frac{p}{Mc} - \beta^2 - \frac{\delta}{2}\right]. \qquad 19.$$

From equation 15 the average energy loss by a light or heavy particle resulting from energy transfers less than T_1 (where T_1 is small compared to the energy transfer η separating close and distant collisions) is

$$\left(-\frac{1}{\rho}\frac{dE}{dx}\right)_{Q<T_1} = \frac{2\pi n(ze^2)^2}{\rho mv^2}\left[\ln\frac{2mv^2T_1}{(1-\beta^2)I^2} - \beta^2 - \delta\right]$$
$$= \frac{2\pi n(ze^2)^2}{\rho mv^2}\left[\ln\frac{2mc^2T_1}{I^2} + 2\ln\left(\frac{p}{Mc}\right) - \beta^2 - \delta\right]. \qquad 20.$$

If energy transfers up to some value $T_2 > \eta$ are to be considered, we should, according to equation 16, substitute $2\beta^2$ for β^2 in equation 20.

From equation 18 the most probable energy loss in a medium of thickness t is

$$\Delta_{mp} = \xi\left[\ln\frac{2mv^2\xi}{(1-\beta^2)I^2} - \beta^2 + 0.373 - \delta\right]$$
$$= \xi\left[\ln\frac{2mc^2\xi}{I^2} + 2\ln\left(\frac{p}{Mc}\right) - \beta^2 + 0.373 - \delta\right] \qquad 21.$$

where

$$\xi = \frac{2\pi n(ze^2)^2}{\rho mv^2}t.$$

Binding Energy Corrections

The average energy loss at nonrelativistic velocities may be written simply as

$$\left(-\frac{dE}{dx}\right) = \frac{4\pi(ze^2)^2}{mv^2}NB \qquad 22.$$

where

$$B = Z\ln\frac{2mv^2}{I}$$

N is the number of atoms per cm.^{3} of atomic number Z ($NZ = n$, the density of electrons in the previous expressions), and B is the so-called stopping number.

The derivation of this expression is based on an approximation (independent of Born approximation) which is used only to simplify the calculations. The condition is $v \gg v_{el}$ where v is the velocity of the penetrating particle and v_{el} is the velocity of electrons. The simplified expression for the energy loss is valid only if v is large compared with the largest electronic velocity in the atom $v_{el} = Ze^2/\hbar$. Then all electrons contribute equally to the energy loss. As the particle velocity is reduced, the contributions to energy loss of the K electrons begins to fall off, and with further reductions in velocity the contributions of L and higher shell electrons begin to fall off in succession.

In order to preserve the meaning of I, the mean excitation potential, as a velocity independent parameter depending, in fact, only on the properties of the medium, it is necessary to evaluate the corrections which must be applied to the simplified formulas in order to take care of the reduced contributions of those electrons with velocity of the order of or greater than the velocity of the penetrating particle. The evaluation of the corrections has been the subject of a long investigation by Bethe and his students. The following discussion will be based largely on the paper of Walske (18) in which, also, the earlier references will be found.

The corrections are determined by evaluating the energy loss over again and performing the calculation for each electronic shell separately. The stopping number B_i is calculated for the ith shell and the total stopping number B to be used in equation 22 is $B = \sum_i B_i$. The procedures for calculating B_i are discussed in (18) and the earlier papers. We will discuss the results.

It is convenient to define certain parameters in terms of which the correction terms may be expressed. In Walske's notation (18), with a few minor changes, we define the following:

Z_i^* the effective value of Z in the ith shell. (For the K shell $Z_K^* = Z - 0.3$ approximately.)

n_i the principal quantum number in the ith shell.

η_i the energy of the incident particle in units of $MZ_i^{*2}Ry/m$, where $Ry = me^4/2\hbar^2$ is the Rydberg unit.

θ_i the observed ionization potential of the ith shell in units of $(Z_i^*)^2 Ry/n_i^2$.

$\lambda_i(\theta_i)$ the mean excitation potential I_i of the electrons in the ith shell in units of $(Z_i^*)^2 Ry/n_i^2$.

The parameter η_i may also be defined as the ratio of the incident particle velocity to the velocity of electrons in the ith shell:

$$\eta_i = \frac{m}{M}\left(\frac{E}{(Z_i^*)^2 Ry}\right) = \frac{mv^2}{2(Z_i^*)^2 Ry} = \left(\frac{v}{v_0 Z_i^*}\right)^2$$

where $v_0 = e^2/\hbar$.

The stopping number of electrons in the ith shell is now expressed in terms of η_i and other parameters as

$$B_i(\theta_i,\eta_i) = S_i(\theta_i) \ln \frac{4n_i^2\eta_i}{\lambda_i(\theta_i)} - C_i(\theta_i,\eta_i) \qquad 23.$$

where

$$S_i(\theta_i) = \tfrac{1}{2}N_i(1 + f_i(\theta_i)) \qquad 24.$$

N_i is the number of electrons in the ith shell and $f_i(\theta_i)$ is the oscillator strength for all optical transitions per i-shell electron into the continuous spectrum and to the unoccupied discrete levels.

The quantities which must be calculated by numerical integration or asymptotic methods in this expression are $f_i(\theta_i)$, $\lambda_i(\theta_i)$ and $C_i(\theta_i\eta_i)$. θ_i is given by observed data when available and η_i is a known parameter.

If we introduce the previously defined parameters η_i and λ_i and sum over all shells, we obtain

$$B = \sum_i B_i(\theta_i n_i) = \sum_i [S_i(\theta_i) \ln (2mv^2/I_i) - C_i(\theta_i\eta_i)].$$

It has been shown that $\sum_i S_i(\theta_i) = Z$. Consequently we can write

$$B = Z \ln (2mv^2/I) - \sum_i C_i(\theta_i\eta_i) \qquad 24.$$

where

$$Z \ln I = \sum_i S_i(\theta_i) \ln I_i = \sum_i S_i(\theta_i) \ln \left[\frac{(Z_i^*)^2\lambda_i(\theta_i)Ry}{n_i^2}\right]. \qquad 25.$$

From equation 25 we observe that it has been possible to define I as a velocity independent parameter.

Equation 24 expresses the desired result by expressing the stopping number B in the original form but with the addition of correction terms contributed by each of the electronic shells. This result is useful if numerical values of $C_i(\theta_i\eta_i)$ can be given for the various atomic species as a function of the particle energy η_i.

We consider the K shell for which the corrections per electron are, of course, the largest. Numerical values of $C_K(\theta_K\eta_K)$ have been calculated. In order to give these results we refer again to equation 23 and with B_K in the form

$$B_K(\theta_K\eta_K) = S_K(\theta_K) \ln \eta_K + T_K(\theta_K) - C_K(\theta_K\eta_K). \qquad 26.$$

The available information for calculation of the stopping number B_K, or alternatively the correction C_K, for K shell electrons is contained in Tables I to IV and Figures 1 and 2. Table I taken from Bethe & Ashkin (2) gives values of θ_K for typical elements. Figures 1 and 2 give values of C_K and B_K

TABLE I

EFFECTIVE VALUES OF θ_K, OSCILLATOR STRENGTH, AND λ_K

	Air	Si	Ca	Zn	Mo	Nd	W	U
Z	7.22	14	20	30	42	60	74	92
θ_K	0.665	0.724	0.761	0.797	0.828	0.858	0.869	0.880
f_K	0.90	0.77	0.70	0.65	0.61	0.57	0.56	0.54
λ_K	0.967	0.944	0.937	0.929	0.926	0.923	0.922	0.921

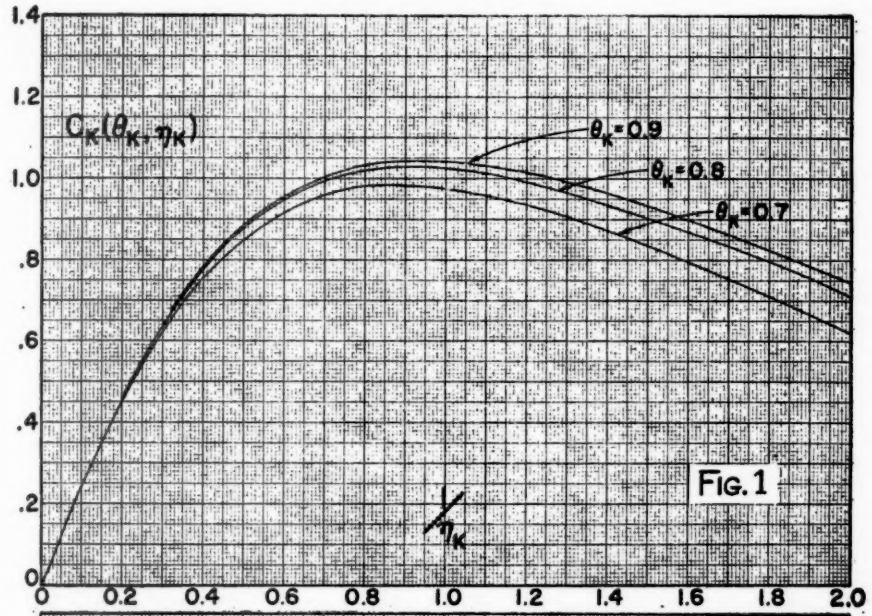

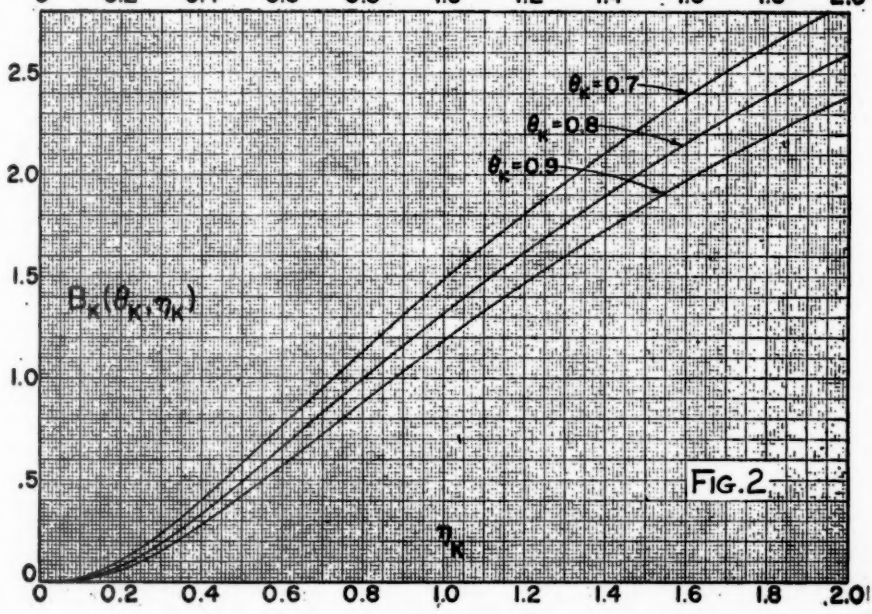

FIG. 1. K shell electron correction C_K to the stopping number B of equation 24.
FIG. 2. Stopping number B_K for K shell electrons.

TABLE II

VALUES OF $S_K(\theta_K)$ AND $T_K(\theta_K)$ IN EQUATION 26

θ_K	$S_K(\theta_K)$	$T_K(\theta_K)$
0.7	1.8133	2.4603
0.75	1.7223	2.4044
0.8	1.6457	2.3462
0.85	1.5807	2.2868
0.9	1.5250	2.2273

TABLE III

VALUES OF U_K, V_K, AND W_K IN THE ASYMPTOTIC FORM OF $C_K(\theta_K)$

θ_K	U_K	V_K	W_K
0.7	2.0662	7.3246	−45.0 Approximately for all θ_K
0.75	2.0999	7.3194	
0.8	2.1196	7.3191	
0.85	2.1290	7.3218	
0.9	2.1309	7.3263	

TABLE IV

STOPPING NUMBER $B_K(\theta_K\eta_K)$ FOR K ELECTRONS

η_K	$\theta_K=0.7$	$\theta_K=0.8$	$\theta_K=0.9$
1.5	2.249	2.031	1.857
1.75	2.573	2.337	2.142
2.0	2.851	2.595	2.385
2.5	3.366	3.077	2.841
3.5	4.122	3.782	3.508
5.0	4.931	4.537	4.221
10.0	6.406	5.900	5.496

respectively over limited ranges of variation of η_K and for three values of θ_K equal to 0.7, 0.8, and 0.9. Tables II to IV provide additional information. We will illustrate the use of the tables and curves by considering the calculation of the correction term $C_K(\theta_K\eta_K)$ for a particular atom. We first decide on the value of θ_K by referring to Table I or by using other available data. Then we proceed as follows:

(*a*) For values of η_K lying between 0.5 and 10 or 20 we use Figure 1 for a direct determination of $C_K(\eta_K)$.

(*b*) For values of η_K somewhat less than 2 we can make an indirect determination of $C_K(\eta_K)$ by using Figure 2 for $B_K(\eta_K)$, equation 26 and the values of S_K and T_K in equation 26 obtained from Table II.

(*c*) For values of η_K from 10 or 20 to larger values Table III gives the values of U_K, V_K and W_K in the expression

$$C_K = \frac{U_K}{\eta_K} + \frac{V_K}{\eta_K^2} + \frac{W_K}{\eta_K^3}.$$

(*d*) For values of η_K from 1.5 to 10 we can use Table IV for B_K, Table II for S_K and T_K, and equation 26 for an indirect evaluation of $C_K(\eta_K)$.

Corrections for L-shell electrons have also been considered by Walske (19). These calculations are much more difficult than the K-shell calculations, and small calculated values of θ_L and large values of f_L imply that the use of hydrogenic wave functions is not very good. The use of Hartree functions would give better results, but the calculation would be very laborious. Walske shows that the range effects as a result of binding do not necessarily decrease for the higher shells. For example, he estimates that for a 300 Mev proton in Pb there is an 0.18 per cent change in range attributable to K-shell binding effects and a 0.43 per cent change in range attributable to L-shell binding effects. The over-all binding effect would be of the order of 1 per cent which reflects itself in an apparent variation in I of the order of 10 per cent.

It is not apparent that all binding effects in heavy atoms will be successfully calculated by these methods. For heavy atoms a calculation based on a statistical model of the atom, or based on an approach to the stopping power problem which considers not the individual electrons but the electrons of the atom as a whole would be fruitful. A start in this direction seems to have been made by Lindhard & Scharff (20). We will have occasion to refer to this paper in another connection.

Determination of Mean Excitation Potentials

An important area of concentration within recent years has been the attempt to measure the mean excitation potential I. This quantity is difficult to determine on purely theoretical grounds. Attempts to evaluate it on semi-theoretical grounds, which have proved to be reasonably successful, will be discussed later in connection with the density effect. We will consider here the experimental data leading to an empirical determination.

There are many reasons for interest in this quantity. It is the central parameter appearing in the stopping power and range-energy expressions on the basis of which extrapolations from one set of measurements in terms of energy and experimental conditions to another set is possible. It is a parameter whose numerical value depends on well-defined but somewhat complex properties of the atom about which some theoretical predictions, as for example the Z dependence, can be made, and it is of importance to determine whether or not these predictions are verified. From the point of view of energy loss theory it is a parameter, which is in principle velocity

independent, and considerable interest centers about the question of whether in fact this is the case when all precautions in connection with the application of binding energy corrections have been applied.

For these reasons many experimentalists have attempted to obtain stopping power and range data of the required accuracy on charged particles of various energies in a large variety of media. The stated objective demands the utmost precision in the measurements. The precision measurement of particle energy and the energy loss or particle range are only the first of several requirements which must be met. Reference to equation 22 shows that a fractional error or variation in the measured stopping power $\delta\Delta/\Delta$ is connected with a fractional variation in the mean excitation potential by the relation

$$\frac{\delta I}{I} = -\frac{\delta\Delta}{\Delta}\ln\frac{2mv^2}{I}.$$

Since the logarithmic factor usually has a value of 5 to 10, an error of 1 per cent in the measurements is equivalent to an error of 5 to 10 per cent in I.

Among the many recent measurements which have been performed and which have the determination of I for various media as a primary objective one may mention the following. All involve the use of protons as the primary particle, and all make measurements in a variety of media from the lightest to the heaviest elements and in gases, metals, other solids, and a few liquids. Total range measurements have been made by Mather & Segrè at 340 Mev (21), Bloembergen & Van Heerden at 35 to 120 Mev (22), Hubbard & MacKenzie at 18 Mev (23), and Simmons at 10 Mev (24). In the latter measurements proton energies are determined by the measurements of ranges in emulsions. Stopping power measurements have been made by Bakker & Segrè at 340 Mev (25), Sachs & Richardson at 18 Mev (26), and Thompson at 270 Mev (27). The measurements of Bakker and Segrè are relative to Al, those of Thompson are relative to Cu, and those of Sachs and Richardson are absolute. The latter were among the first of the absolute measurements using protons. Thompson's measurements for the determination of I were part of a program in which a primary objective was the study of the chemical effect; i.e., a determination of the small deviations between the stopping power of a compound and the sum of the stopping powers of the various elements which enter into the compound. Such deviations are, of course, a consequence of the change in I resulting from increased binding of the outer electrons in the formation of the molecule.

The interpretation of these and other measurements has in many cases been given by the authors themselves, and a synthesis of some of the results has been given by Bethe & Ashkin (2), Allison & Warshaw (3), and Bogaardt & Koudijs (28). Some of the data, as for example, the data at 300 Mev, are at sufficiently high energy that binding energy corrections are often negligible, except that even at this high energy, binding effects begin to be important for Fe and are quite important for Pb.

In order to determine I for various materials from the data obtained in relative measurements one uses an accepted value of I for the standard substance. Thus, Bethe (2) interprets the data of Bakker & Segrè using Wilson's value of I for Al (150 ev) and making the K-shell binding energy corrections for all elements heavier than Al. It is satisfying to find that these measurements then yield a value of I for Be (60.4 ev) which agrees within experimental error with the previous determination for this element in the careful measurements of Madsen and Venkateswarlu (64 ± 5 ev). In a somewhat different procedure, the measurements of Simmons in Al make use of the range-energy relations of Rotblatt (29) for emulsion and Smith's range tables for conversion between emulsion and Al. He finds Smith's ranges to be 0.8 per cent too low and obtains a value for I in Al equal to 155 ± 3 ev.

The absolute measurements have not been fully analyzed. The data of Mather and Segrè which depend on measurements of Cerenkov radiation for energy determination are of high accuracy both in range and energy. However, these are total range data and binding effects are difficult to take into account. Neglecting the binding effects Bethe evaluates I for the various elements and in general obtains higher values of I for the heavy elements than are given by the data of Bakker & Segré. It is doubtful, however, that more than about half of this discrepancy can be attributed to binding. Since these measurements are of very high accuracy one might expect them to yield the most accurate determinations of I when binding effects are eventually taken into account.

More striking results become apparent when the data obtained at somewhat lower energies are used. Two of the absolute range determinations are the measurements of Bloembergen and van Heerden at about 100 Mev and those of Hubbard and MacKenzie at 18 Mev. These measurements employ similar techniques and are of comparable high accuracy. Bloembergen and van Heerden determine I by comparing their measured ranges with the calculated data of Aron, Hoffman & Williams (4) which were in turn based on the assumption of $I = 11.5Z$ ev in the case of heavy elements in agreement with Wilson's value for I in Al of 150 ev. They find that their experimental ranges do not agree with the theoretical ranges unless in the latter I for Al is adjusted upward to 161 ± 5 ev. Similarly, in Cu and Pb the values of I required by their experiments are about 30 per cent higher than the values obtained by Bakker and Segrè. However, binding energy corrections have not been taken into account. A somewhat similar result is found in the lower energy measurements of Hubbard and MacKenzie. The value of I for Al now turns out to be 167 ev which is more than 10 per cent higher than the value given by Mather and Segrè. Perhaps, half of this discrepancy can be attributed to the L-shell binding correction which is important at the energy of 18 Mev.

The first of the thin foil measurements are those of Sachs and Richardson, at 18 Mev. Their result for I in Al, as corrected in their second paper, is $I = 168$ ev, in good agreement with the result of Hubbard and MacKenzie

at the same energy. K-shell binding corrections have been applied. Considering all of these data together one has the beginnings of a composite picture of the values of I for a single substance obtained at different energies. There is an unmistakable trend toward increasing values of I with decreasing energy. The magnitude of this trend is greater than the experimental errors. The application of binding energy corrections decreases the magnitude of the variation somewhat, but it is not clear that a systematic application of these corrections will reduce it to zero. It is apparent that a continuing program of experimental investigation and interpretation is required.

Another approach to the interpretative problem may be in the point of view expressed by Lindhard & Scharff (20). It is argued that the Bethe-Bloch theory of energy loss rests more heavily on the properties of the individual electrons than is actually required. All atomic electrons make comparable contributions to this loss. Since in a statistical distribution a large fraction of the electrons can be regarded as having the properties of the distribution, and only a few of the electrons corresponding to the number which are on the fringes of the distribution fail to be adequately described, the statistical method appears to be ideally suited to the discussion of energy loss by heavy atoms. Such a theory would fail only to the extent that the few electrons which are responsible for specific atomic properties and others which are very tightly bound and consequently lie outside of the main distribution make appreciable contributions to the energy loss.

Considering then only the large fraction of electrons which are adequately described by a statistical model, one concludes that the various media in which energy loss occurs can be distinguished by a single scale factor appropriate to the distribution. In the case of the Thomas-Fermi atom the scale factor is the atomic unit of time which is proportional to Z^{-1}. Thus, atomic frequencies are proportional to Z. Only one other frequency enters into the argument of the logarithm in the energy loss expression

$$-\frac{dE}{dx}=\frac{4\pi n(ze^2)^2}{mv^2}\ln\frac{2mv^2}{I}$$

and that is the frequency $\omega_{\max}=2mv^2/\hbar$ corresponding to the maximum transfer of energy to an atomic electron. Consequently, this argument can depend only on the ratio of $\omega_{\max}$ to atomic frequencies which are in turn scaled by a factor Z. Thus, the variable in the argument of the logarithm must be $\zeta\equiv v^2/Zv_0^2$ where $v_0=e^2/\hbar$ is introduced for dimensional reasons.

The Bethe-Bloch theory of energy loss, derived by disregarding the effects of binding, leads to the logarithmic functional dependence on this variable. The consequences of binding can be only the alteration of this functional dependence. Thus, Lindhard and Scharff write

$$-\frac{dE}{dx}=\frac{4\pi n(ze^2)^2}{mv^2}L(\zeta)$$

where $L(\zeta)$ is $\ln\zeta$ for large ζ. This conclusion suggests an examination of all

data (low and high-energy particles and atoms of all Z) by plotting on a single graph the measured values of

$$\frac{mv^2}{4\pi n(ze^2)^2}\left(-\frac{dE}{dx}\right)+\ln(1-\beta^2)+\beta^2$$

as a function of ζ, where relativistic factors are again introduced. If the argument is correct, one would expect all data to lie on a smooth curve with only minor fluctuations away from this curve resulting from the contribution of the small fraction of electrons not adequately described by statistical methods. This is actually the case. A curve obtained in this manner and including all the available data from Be to U and for heavy particle energies from a few hundred kev to 300 Mev is given by Allison & Warshaw (3). A single smooth curve representing the functional dependence of $L(\zeta)$ is obtained and as expected the fluctuations around this curve are indeed minor.

For $\zeta>100$ the function $L(\zeta)$ is logarithmic and the Bethe-Bloch theory of energy loss without binding energy corrections is obtained. Then in this region $a\zeta=2mv^2/I$ where a is a constant determined by the experimental data. One obtains the interesting result that $I=I_0Z$ where $I_0=10.2$ ev, a value slightly higher than obtained from the data of Bakker and Segrè alone.

For $\zeta<100$ the function $L(\zeta)$ drops rather rapidly to values less than $\ln(a\zeta)$ and over a range of ζ from about 20 to 2 it remains below $\ln(a\zeta)$ by an approximately constant amount. With further reduction in ζ the difference between $L(\zeta)$ and $\ln(a\zeta)$ decreases, and at $\zeta\sim0.5$ the numerical values of the two functions are again equal. For $\zeta<0.5$, $L(\zeta)$ is larger than $\ln(a\zeta)$ which is now decreasing rapidly to zero before taking on negative values. This is precisely the behavior one would expect. The dip below the values of $\ln(a\zeta)$, and the crossing of the curves at $\zeta=0.5$ are consistent with the observations of Reynolds *et al.* (30) and especially Kahn (31) which have been interpreted in terms of the variation of I with energy at low energies. The measurements of Kahn, taken together with those of Warshaw on protons in metals from about 100 kev to 1.3 Mev and interpreted in terms of the Bethe-Bloch theory with binding energy corrections for the K-shell, display the pronounced maximum in I associated with the dip of $L(\zeta)$ below $\ln(a\zeta)$ and the crossing of the curves at still lower energies.

Other recent low-energy data which have been transferred to the Lindhard-Scharff curve are those of Madsen (0.2 to 2 Mev) (32) and Chilton, Cooper & Harris (0.4—1.0 Mev) (33). All of these data, and the high-energy data of Bakker & Segrè (25), Mather & Segrè (21), Sachs & Richardson (26), Bloembergen & Van Heerden (22), and Thompson (27), are well described by it.

The Polarization Effect

At high velocities of the penetrating particle, cooperative effects among the atoms of the medium become important unless the density of the medium

is very low. This effect has been discussed by Bohr (34) in considerable detail, and a quantitative theory was first developed by Fermi (35).

The medium is polarized by the field of the charged particle. When the velocity exceeds a critical value which is determined by the dielectric properties of the medium, ionization and energy losses are reduced. The magnitude of the reduction depends in a fairly complicated way on the dispersive properties of the medium, and the over-all ionization or energy loss depends critically on the techniques of observation.

Polarization effects have been observed with protons, π- and μ-mesons, and probably the heavier mesons, as well as with electrons and positrons. The effects are independent of the nature of the particle, and in the case of the heavy particles there are no complications which are attributable to radiative effects.

An important consequence of the measurements, and of the impetus which the observations have given to theoretical interpretation, is the fact that attention has been focussed upon the dispersive properties of the medium. This has resulted in a reexamination of the dispersion laws and of the various kinds of data which are available for the determination of the constants which enter into these laws. The attempt to reconcile the observations on ionization and energy loss with the theory has provided a new mechanism for study and possible verification of data from other sources on transition frequencies and line widths of the atomic systems comprising a condensed system. These are also the quantities on which the mean excitation potential depends. Thus, a study of polarization effects is also a study of mean excitation potentials, and an understanding of these effects is of some importance in the interpretation of the potentials.

The subject under consideration has an extensive history. We will mention only a few of the major points. Fermi (35), Bohr (34), Schoenberg (36), Huybrechts & Schoenberg (37), and Messel & Ritson (38) examined the connection between the polarization effect and the Cerenkov radiation, and showed that for a medium consisting of one dispersion oscillator and with no absorption the relativistic rise in the ionization loss should escape as Cerenkov radiation. Wick (39), Halpern & Hall (40), and Sternheimer (17) developed the theory using a more general type of dispersion law and considered some of the consequences of absorption. Budini (41) and Sternheimer (42) investigated quantitatively the questions of escape of Cerenkov radiation from a AgBr grain in an emulsion and from the vicinity of an ionization track in a cloud chamber with the result that, in the case of the AgBr grain, the escape of radiation is negligible and, in the case of a cloud chamber track, the energy escape is not more than approximately one-third of the total relativistic rise with polarization effects taken into account. In a recent paper, Sternheimer (43) investigates some of the consequences of the polarization effect insofar as the interpretation of mean ionization potentials in condensed media and measured at low-energy is concerned.

The Fermi theory of energy loss is a condensed medium is a calculation

of the energy transmitted through the surface of a circular cylinder which has the path of the moving particle as its axis. The energy radiated per second divided by the velocity of the particle gives the energy loss per cm. of path through the cylinder. The result is

$$W_b = \frac{2e^2b}{\pi v^2} Re \int_0^\infty \left[\frac{1}{\epsilon(\omega)} - \beta^2\right] i\omega k^* K_1(k^*b) K_0(kb) d\omega \qquad 27.$$

where the radius of the cylinder is taken as b, v is the velocity of the particle, $\epsilon(\omega)$ is the Fourier component at frequency ω of the dielectric constant, Re denotes "real part of," K_0 and K_1 are the modified Bessel functions of second kind, and k is the square root with real part $\geqq 0$ of

$$k^2 = \frac{\omega^2}{c^2}\left[\frac{1}{\beta^2} - \epsilon\right].$$

We will discuss some of the consequences of the Fermi theory omitting all calculations.

The density correction.—We can choose b to be of order of atomic dimensions without violating the conditions for validity of a classical calculation. Thus, we can set $|k|b \ll 1$ and write

$$K_0(kb) \sim \frac{1}{2} \ln \frac{4}{3.17k^2b^2}$$

$$K_1(k^*b) \sim \frac{1}{k^*b}.$$

The integral in this limit of small $|k|b$ has been evaluated with $\epsilon(\omega)$ expressed as a sum over many dispersion frequencies and with inclusion of damping by Halpern & Hall (40), Sternheimer (17), and others. The result for W_b is then compared with the analogous classical calculation made by Bohr in which polarization effects were disregarded. We will denote the energy loss per cm. as calculated by Bohr W_{b0}. One finds $W_{b0} > W_b$ and the difference of these quantities is to be regarded as the reduction in energy loss which is a consequence of polarization. This difference does not depend on b, and since no polarization effects can come from distances which are closer to the particle than atomic dimensions this difference represents the total polarization correction. We express it in the form

$$\Delta = W_{b0} - W_b = \frac{2\pi ne^4}{mv^2}\delta \qquad 28.$$

Δ includes the effect of the dispersion frequencies and the damping. Before subtracting it from the energy loss expressions which do not take account of polarization but do include the effects of close and distant collisions, Sternheimer sets the damping constants equal to zero on the assumption that the measured mean excitation potentials which appear in the energy loss formulas already include the effects of damping. With neglect of damping Sternheimer's expression for δ in equation 28 is

$$\delta = \sum_i f_i \ln \frac{l_i^2 + l^2}{\nu_i^2} - l^2(1 - \beta^2) \qquad 29.$$

where the frequencies ν_i are measured in units of the plasma frequency $(ne^2/\pi m)^{1/2}$, n is the density of electrons in the medium, f_i is the oscillator strength at frequency ν_i, $l_i = \sqrt{\nu_i^2 + f_i}$ and l is determined as a solution of the equation

$$\frac{1}{\beta^2} - 1 = \sum_i \frac{f_i}{\nu_i^2 + l^2}. \qquad 30.$$

The density correction as given by equations 28 and 29 is included in equations 19, 20 and 21, and δ of these equations is given by equation 29.

Onset of the density correction.—For $\beta < 1$ and decreasing, l as determined by equation 30 decreases until it attains the value 0. At this point $\beta = \beta_0$ with β_0 given by

$$\frac{1}{\beta_0^2} = 1 + \sum_i \frac{f_i}{\nu_i^2} = \epsilon$$

where ϵ is the static dielectric constant. Thus, ionization loss will follow the uncorrected relativisitic ionization curve as the velocity increases until β reaches the value β_0. For condensed media this may occur near the relativistic minimum of the ionization curve. For rare media, such as gases, the break from the uncorrected curve will occur at considerably higher velocities. For $\beta \leqq \beta_0$, $l = 0$ and we have

$$\delta = \sum_i f_i \ln \frac{l_i^2}{\nu_i^2} = \sum_i f_i \ln \left(1 + \frac{f_i}{\nu_i^2}\right)$$

Thus, for a single dispersion oscillator we have Fermi's low-energy result

$$\delta = \ln \left(1 + \frac{1}{\nu_1^2}\right) = \ln \epsilon$$

where ϵ is the static dielectric constant.

The measured mean excitation potential.—The result of the previous paragraph shows that the density correction does not vanish at low energies. However, the measurements of I are customarily made by employing energy loss formulas in which no correction term appears. Consider, for example the average energy loss as given by equation 19 which we will now denote by $\bar{\Delta}$ and which at nonrelativistic velocities we write as

$$\bar{\Delta} = \frac{4\pi n(ze^2)^2}{\rho m v^2}\left[\ln \frac{2mv^2}{I} - \frac{\delta}{2}\right].$$

The mean excitation potential I in this expression has a definite meaning in terms of the transition frequencies and damping of the medium. However, this is not the I which is generally measured since the term $\delta/2$ is disregarded when stopping power data are interpreted in terms of a measured mean excitation potential. Denote the latter by I_{exp}. Taking $l = 0$ in equation 29 for

δ (since the measurements are being made at low-energy) we obtain the relation

$$I_{\text{exp}} = I\prod_i \left(1+\frac{f_i}{\nu_i^2}\right)^{f_i/2}.$$

Thus, the I_{exp} as measured in experiments of the Bakker-Segrè type is larger than the I as determined from the observed spectral lines of the isolated atoms, not only because of a possible shift in some of these frequencies due to condensation, but by a factor $\Pi_i(1+f_i/\nu_i^2)^{f_i/2}$ resulting from polarization. For the case of a single dispersion frequency this factor is $(1+1/\nu_1^2)^{1/2}=\sqrt{\epsilon}$ where ϵ is the static dielectric constant. This result has been indicated previously by Goldwasser, Mills & Hanson (44) in their article on energy loss distributions of electrons. Sternheimer (43) has evaluated this factor from his data on f_i and ν_i for the various elements. Writing

$$I = I_{\text{exp}}e^{-D/2}$$

he obtains $D\sim 0.05$ for heavy elements to $D\sim 0.34$ for Li.

Since δ represents the full density correction based on I as determined in the noncondensed medium, equation 19 becomes after substitution for I_{exp},

$$\overline{\Delta} = \frac{4\pi n(ze^2)^2}{\rho mv^2}\left[\ln\frac{2mv^2}{(1-\beta^2)I_{\text{exp}}} - \beta^2 - \frac{1}{2}\delta'\right] \qquad 31.$$

where

$$\delta' = \sum_i f_i \ln\left(1+\frac{l^2}{l_i^2}\right) - l^2(1-\beta^2). \qquad 32.$$

In this form the density correction vanishes at low velocities when $l=0$.

Thus, in equations 19, 20, and 21 one uses δ or δ' depending on the meaning to be assigned to I.

The high-energy plateau.—Consider the case of energy transfers $Q<T_1$. Then from equation 20 we write for the average rate of energy loss

$$\overline{\Delta}_{Q<T_1} = \frac{2\pi ne^4}{\rho mv^2}\left[\ln\frac{2mv^2T_1}{(1-\beta^2)I_{\text{exp}}^2} - \beta^2 - \delta'\right]$$

where we have set $z=1$ and have used I_{exp} and δ'. At high-energies with $\beta\sim 1$, equation 30 yields

$$l^2 \cong \frac{1}{1-\beta^2}$$

so that

$$\delta' \cong -1 - \ln(1-\beta^2) - \sum_i f_i \ln l_i^2.$$

Remembering that ν_i is in units of $(ne^2/\pi m)^{1/2}$ we have

$$I_{\text{exp}} = \left(\frac{ne^2}{\pi m}\right)^{1/2} h\prod_i (l_i)^{f_i}$$

in which we use the frequencies l_i instead of ν_i since the low-energy polarization effect is included. Then

$$\sum_i f_i \ln l_i^2 = 2 \ln \prod_i (l_i)^{f_i} = \ln I_{\exp}^2 + \ln \frac{m}{4\pi n e^2 \hbar^2}$$

$$\delta' = -1 - \ln (1-\beta^2) - \ln I_{\exp}^2 - \ln \frac{m}{4\pi n e^2 \hbar^2}$$

and consequently

$$\bar{\Delta}_{Q<T_1} = \frac{2\pi n e^4}{\rho m c^2} \ln \frac{m^2 c^2 T_1}{2\pi n e^2 \hbar^2} \tag{33.}$$

where in the final result we have set $\beta = 1$. The existence of a plateau is a consequence of the fact that a term $-\ln(1-\beta^2)$ attributable to the relativistic change in the coulomb field extension and appearing in the ionization loss expression is cancelled by a similar term in the density correction. Another term $-\ln(1-\beta^2)$ in the ionization loss expression which is present when all energy transfers are permitted was removed by the substitution of T_1 for $2mv^2/(1-\beta^2)$. Consequently, the average energy loss with all possible energy transfers considered does not saturate, but the rate of rise with increasing energy is smaller than it would be in the case of no density correction. Except for universal constants the value of $\bar{\Delta}_{Q<T_1}$, in the plateau depends only on the density of the medium and on the maximum energy transfer considered.

In order to obtain the fractional rise above minimum ionization we need the expression for $\bar{\Delta}_{Q<T_1}$ at the minimum. The minimum occurs at $E \cong 4Mc^2$ or $\beta^2 \cong 15/16$. Thus at the minimum

$$\bar{\Delta}_{Q<T_1} = \frac{16}{15} \frac{2\pi n e^4}{\rho m c^2} \left[\ln \frac{2mc^2 T_1}{I_{\exp}^2} + 1.77 \right]. \tag{34.}$$

Denoting the ratio of $\bar{\Delta}_{Q<T_1}$ in the plateau to the value of this quantity at the minimum by $R_{Q<T_1}$ one has

$$R_{Q<T_1} = \frac{15}{16} \frac{\ln (m^2 c^2 T_1 / 2\pi n e^2 \hbar^2)}{\ln (2mc^2 T_1 / I_{\exp}^2) + 1.77}. \tag{35.}$$

We can also write down the expression for this ratio in the case of most probable energy loss by noting that, according to equations 20 and 21, Δ_{mp} follows from $\bar{\Delta}_{Q<T_1}$ by substitution of ξ for T_1 in the logarithm and adding a numerical term 0.373. Denoting the ratio of plateau to minimum ionizations in the case of the most probable loss by R_{mp} we have

$$R_{mp} = \frac{15}{16} \frac{\ln (m^2 c^2 \xi / 2\pi n e^2 \hbar^2) + 0.37}{\ln (2mc^2 \xi / I_{\exp}^2) + 2.14} \tag{36.}$$

Equations 35 and 36 will be used in connection with the discussion of experiments.

The escape of Cerenkov radiation.—The concept of most probable energy loss is in a different category from the other losses considered. It is the maxi-

mum in a distribution of energy losses, whereas, the others are average losses. This is the case even though we put a maximum on the single collision energy loss considered, as for example, by restricting Q to values less than T_1. Such restrictions are intended to conform to the conditions of a particular experiment in which energy transfers of greater value are either not counted, or the electron receiving the transfer of energy in question escapes from the region of observation and the energy loss is not measured.

We must now consider another form of energy loss which may not be measured, and if so, should be subtracted from the energy loss expressions before comparisons with experiments are made. This is the possible escape of Cerenkov radiation, generated, let us say, in the region of a cloud chamber track but not reabsorbed in the immediate vicinity of this track. Such radiation will be absorbed elsewhere, but will not be counted as a part of the total loss.

This problem has been studied by Budini (41) and Sternheimer (42). One is here concerned with the total energy passing through the walls of a cylinder of radius b surrounding the track of the particle. In this case b is very much larger than atomic dimensions and, in fact, has a value of the order of 0.1 cm. in the case of cloud chamber tracks and 0.15 μ in the case of emulsion grains. The condition $|k|b \gg 1$ is fulfilled for a large fraction of the spectrum. Using the development

$$K_0(kb) \cong \sqrt{\frac{\pi}{2kb}}\, e^{-kb}$$

$$K_1(k^*b) \cong \sqrt{\frac{\pi}{2k^*b}}\, e^{-k^*b}$$

equation 27 for W_b becomes

$$W_b = \frac{e^2}{v^2} Re \int_0^\infty \left[\frac{1}{\epsilon(\omega)} - \beta^2\right] i\omega \sqrt{\frac{k^*}{k}}\, e^{-(k+k^*)b} d\omega.$$

We may observe, incidentally, that this expression immediately gives the formula of Frank and Tamm for the Cerenkov radiation at infinity if we make the unrealistic assumption that the medium has no absorption. In this case ϵ is real and k^2 is real and negative if β is large enough and frequency ranges exist for which $\beta^2 > 1/\epsilon(\omega)$. Then k is pure imaginary and the energy loss W_b is independent of b (with $|k|b \gg 1$ however). The Frank and Tamm result follows

$$W_b = \frac{e^2}{v^2} \int_{\beta\sqrt{(\epsilon)}\omega > 1} \left[\beta^2 - \frac{1}{\epsilon(\omega)}\right] \omega d\omega.$$

We are interested, however, in the escape of Cerenkov radiation under the actual conditions of damping which prevail. Using the available data on the dispersion frequenceis and damping constants in AgBr and in some gases, Sternheimer finds that the loss to Cerenkov radiation in an emulsion is .0022

Mev/gm. cm.$^{-2}$ which is small compared to the relativistic rise of 0.12 Mev/gm. cm.$^{-2}$, and may be neglected in the evaluation of experiments. The situation is not quite so favorable for cloud chamber tracks, but the escaping Cerenkov radiation loss is still a small fraction, of the order of one-third or less, of the total relativistic rise.

A somewhat different point of view in which primary ionization and excitation, energy absorption, and kinetic energy of primary electrons are calculated separately is taken by Allen (45). The grain density is assumed to be proportional to the number of electrons released in the grains.

Experiments on emulsions. —A considerable quantity of data has been accumulated on the grain count along the track of a relativistic particle in an emulsion. References to this data are given in the few recent papers which will be cited here. All of the experiments agree in the sense that a high-energy plateau of ionization exists, that the rise from the ionization minimum lies somewhere between 8 and 14 per cent, and that the saturation occurs at a value of E/Mc^2 which is greater than 20 and may be somewhat greater than 100. There is no over-all detectable difference between the behavior of the various types of particles: electrons, muons, pions, and protons.

The earlier data suggests the lower values of the relativistic rise and the lower energies for saturation. The data of Morrish, Daniel *et al.*, Pickup & Voyvodic, Michaelis & Violet, and Powell[3] all suggest a relativistic rise not exceeding 10 per cent and a saturation at about $E/Mc^2 \sim 20$.

There is, however, more recent data suggesting that the magnitude of the rise is greater than 10 per cent and may be as large as 14 per cent, and that the saturation may not occur before $E/Mc^2 \sim 100$ or greater. The measurements of Fleming & Lord (46) provide data of unusually good statistics on one electron energy and four pion energies. The pion energies are at the ionization minimum and below and confirm the rapid ionization decrease in the approach to the minimum. The electron point lies at $E/Mc^2 = 67$. This data, together with the earlier data, suggests a relativistic rise of 10 to 11 per cent and a saturation at about 100 Mc^2. The slower rise to saturation is suggested also by the measurements of Shapiro & Stiller (47) on electrons, pions, and protons covering an energy range from the ionization minimum to $E \sim 2{,}000\ Mc^2$. Energies are measured by scattering, and a considerable quantity of data on each of the three types of particles is obtained in the energy ranges for which the energy of each can be accurately measured. The results indicate a relativistic rise of 14 per cent and a saturation at $E \sim 100\ Mc^2$ or greater.

The theory predicts the slow rise to saturation and is consequently in better agreement with the data of Stiller and Shapiro than with the earlier data. Using equation 35 we calculate readily the prediction with respect to the magnitude of the rise. For this purpose we use $I = 376$ ev. for AgBr and take $T_1 = 2$ kev. Expressing all energies in Mev, we have

[3] References to these and other data are given as references in (46) and (47).

$$\ln [2mc^2(10^6 \text{ ev})/I^2] = 15.8$$

$$\ln (T_1/10^6 \text{ ev}) = -6.2$$

$$\ln [m^2c^2(10^6 \text{ ev})/2\pi ne^2\hbar^2] = 19.9$$

This gives $R_{Q<T_1} = 1.127$, or a rise of about 13 per cent in good agreement with the measurements of Stiller and Shapiro. If we use $T_1 = 10$ kev we obtain $R_{Q<T_1} = 1.103$.

Experiments with crystal and liquid scintillators.—Recent experimental work on the measurement of energy loss distributions of μ-mesons includes the work of Bowen & Roser (48) with anthracene, Hudson & Hofstadter (49) with NaI, and Baskin & Winckler (50) with xylene. The range of energies covered in each experiment is from the ionization minimum at about 300 Mev and lower to about 2000 Mev. The anthracene and NaI (Tl) crystals used had dimensions of about 3 and 5 cm. respectively, and the corresponding energy losses in the region above minimum ionization were of the order of 6 and 26 Mev respectively. The xylene solution was used as a liquid scintillator with a path length for the μ-meson of about 5 cm. and an energy loss of about 8 Mev. Thus, all energy loses are small compared with the incident energy, and as will be described in the next section, the conditions for an asymmetric energy loss distribution prevail.

From the histograms of the energy loss distribution measurements, one can draw conclusions with respect to the value of the most probable loss and the median loss. One does not easily measure the average energy loss. The data of the Hudson and Hofstadter experiment were treated in a different way than those of the others because measurements on selected energy groups were not made. In order to interpret the data, it was necessary to calculate the most probable energy loss for various energies in the range of measurement, superimpose an appropriate distribution at each energy, and fold this with the known cosmic ray spectrum. The result was a theoretical distribution which could be compared with the experimental distribution. The theoretical distribution was calculated with and without density corrections, and consequently conclusions with respect to the density correction were possible.

The results of all three experiments are in agreement on the point that density corrections are required. In the more direct measurements of Bowen and Roser and of Baskin and Winckler there is no detectable rise in ionization between the minimum and an energy of over 2000 Mev. In each case a rise of more than 2 or 3 per cent could have been detected. In the case of the experiment of Hudson and Hofstadter, the authors calculate a rise of about 11 per cent, but the comparison of theory and experiment is not sensitive to the precise value of the rise.

We may illustrate the differences between media of various kinds, with respect to the magnitude of the relativistic rise, by considering the most probable energy loss and using equation 36 to calculate it for the two cases of NaI and xylene as used in these experiments. In the experiment of Hudson and Hofstadter on NaI, the mean excitation potential is $I = 375$ ev, the den-

sity is $\rho = 3.8$ gm./cm.^{3}, and the path length is $t = 5.5$ cm. $= 21$ gm./cm.^{2}. From the tables of Sternheimer, $2\pi ne^4/mc^2\rho = 0.0653$ Mev./gm. cm.$^{-2}$, and consequently $\xi = 1.35/\beta^2$ Mev. Expressing all energies in Mev, ln $[2mc^2(10^6 \text{ ev.})/I^2] = 7.9$, ln $\xi = 0.3$ and ln $[m^2c^2/2\pi ne^2\hbar^2] = 12.6$. Then from equation 36, $R_{mp} = 1.21$, a rise of 21 per cent. The comparison with xylene is striking. For this material $I = 58$ ev. and $\rho = 0.88$ gm./cm.^{3} The path length in the experiment was $t = 5$ cm. $= 4.4$ gm. cm.$^{-2}$. Using $2\pi ne^4/mc^2\rho = 0.0821$ Mev/gm. cm.$^{-2}$, one obtains $\xi = 0.36/\beta^2$ Mev, ln $\xi = -1.0$, ln $[2mc^2(10^6 \text{ ev})/I^2] = 19.5$ and ln $[m^2c^2/2\pi ne^2\hbar^2] = 21.6$. Making the substitutions into equation 36, one finds that there is no relativistic rise. The reason for the difference in these two cases is the relatively high value of the ionization at the minimum, in the case of xylene, as a result of the low mean excitation potential which more than offsets the lower value of ξ in this experiment. The ionization in the plateau is about the same in these two cases because the ratio of electron densities is about the same as the ratio of values of the parameter ξ.

Experiments in gases.—The saturation in the ionization as observed by droplet counting in cloud chamber tracks has been observed by Gosh, Jones & Wilson (51) for μ-mesons in O_2, and by Carter & Whittemore (52) for μ-mesons in He. At atmospheric pressure the saturation sets in at $p/Mc \sim 100$ (10^4 Mev). Sternheimer (42) makes a detailed calculation in the case of O_2 including the effect of escaping Cerenkov radiation and obtains good agreement with the experimental observations of Gosh, Jones and Wilson. In the case of He he shows that the escaping Cerenkov radiation is not negligible, and allowance must be made for this loss of energy before making a comparison with ionization measurements.

Measurements of energy loss of μ-mesons in gases have been made by Kupperian & Palmatier (53) using proportional counters for mesons of 160 Mev to over 1800 Mev divided into four groups. They observe a relativistic rise after demonstrating that a failure to observe this rise in some experiments of this kind is a consequence of the effects of locally generated showers and counter-wall generated secondary electrons. The measurements are primarily concerned with the determination of energy loss distributions.

It may be noted that in the case of gases the onset of the density correction for μ-mesons does not occur below about $p/Mc \sim 100$. This is in an energy region where E is of the order and greater than $Mc^2(M/2m)$ for mesons and consequently Q_{max} in equation 5 should be written as $E - (M^2c^2/2m)$ from the conservation laws and used in place of $2mv^2/(1-\beta^2)$ to obtain the equation for the average energy loss. The consequence of this replacement is to reduce the rate of rise of ionization loss in the high-energy region both before and after correcting for the density effect. In the high-energy region the density effect reduces the slope of the average energy loss curve to one-third of its uncorrected value.

Energy Loss Distributions

The various straggling phenomena have been discussed by Bethe & Ashkin (2), Allison & Warshaw (3), and others. We will consider only the

energy loss distribution which is attained by a beam of high velocity particles after passing through a small thickness of stopping medium such that only a small fraction of the incident energy is lost. This problem was first solved on the basis of the continuity equation for the distribution function by Landau (16). Landau's solution was further refined by Blunck & Leisegang (54) and then was solved more generally by Symon (55).

A parameter of primary importance in describing the distribution of energy losses is

$$G = \xi/Q_{\max} \qquad 37.$$

where ξ is defined by equation 17. This parameter is generally very large for heavy particles and small for electrons and positrons. If we use equation 17 for ξ and note that the quantity $2\pi ne^4/mc^2\rho$ has a numerical value of order 0.1 Mev/gm. cm.$^{-2}$ for all media (0.06 in a medium of heavy atoms to 0.15 in a medium of light atoms), we have

$$G = \frac{0.1}{Q_{\max}}\left(\frac{c}{v}\right)^2 t$$

where Q_{max} is in Mev and t in gm. cm.$^{-2}$ Since $Q_{max} = 2\ mv^2/(1-\beta^2) \cong 4mE/M$ for nonrelativistic heavy particles, we find that, for t of order 1 mg./cm.^{2}, $G \gg 1$ for protons if their energy is less than 100 Mev and $G \gg 1$ for mesons if their energy is less than 10 Mev. In the case of electrons for which $Q_{max} = \frac{1}{2}E$ it is difficult to find experimental conditions for which $G > 1$, and, in fact, the usual condition is $G \ll 1$.

Now one shows easily that the integral equation which expresses the continuity of the distribution function $f(E_0,E,t)dE$, where E_0 is the incident energy and t is the thickness of the stopping medium, reduces to a simple differential equation with a Gaussian function as its solution when $G \gg 1$. The maximum in the distribution is precisely at the value of E obtained from E_0 by subtracting the average energy loss, and the width is given by $W = (\xi\ Q_{max})^{1/2}$. Consequently, for protons and mesons of sufficiently low energy the distribution is Gaussian.

However, the condition $G < 1$ is experimentally important even for the heavy particles. The problem was solved by Landau for the case of $G < 0.05$. He obtained the result which we have incorporated into equations 18 and 21 insofar as the most probable energy loss is concerned. In addition he obtained the distribution function.

The case $G < 0.05$ does not fit all of the interesting experimental situations. In order to obtain more generally applicable solutions Symon considered the problem again. He solved the problem numerically considering separately the problem of thin absorbers, for which the average energy E after passing through the absorber is $\geqq 0.9\ E_0$, and thick absorbers for which $\bar{E} \leqq 0.9\ E_0$. Symon's solution for thin absorbers and the curves which are needed in order to obtain the distribution in any given case are given in the book of Rossi (56). In order to obtain the distribution function one must determine the numerical value of two parameters corresponding to the value of G appropriate to the experiment. One of these parameters is used to select

the particular distribution that is required and the other defines the energy scale. The graphical solutions cover the range of G from $G=0.01$ to $G=10.0$. Landau's special solution is modified in one other respect. The numerical term 0.373 which appears in equations 18 and 21 is correct only for value of $G<0.2$ for small velocities and $G<0.05$ for high velocities. For larger values of G this number decreases and, in fact, becomes negative. We now observe that the value of the numerical term which we used in the description of the Hudson-Hofstadter experiment and the Baskin-Winckler experiment, namely 0.373 is correct. At minimum ionization $Q_{max}=2mc^2/(1-\beta^2)=30mc^2$ $=15$ Mev. Since in the NaI and xylene experiments we found $\xi=1.35$ Mev and 0.36 Mev respectively, the values of $G=\xi/Q_{max}$ is 0.09 for the μ-mesons in NaI and 0.02 in xylene. Above minimum ionization G is still smaller since Q_{max} increases from 15 Mev to about 400 Mev for μ-mesons of 2000 Mev.

Data on energy loss distributions for heavy particles in the range where departures from Gaussian distributions are to be expected are apparently rather meagre. Igo, Clark & Eisberg (57), using a proportional counter with pulse height discrimination, measured the frequency distribution in pulse heights with 31.5 Mev protons. The measured distribution is asymmetric and compares favorably with the Landau distribution as calculated from Symon's curves. The distribution measurements of Kupperian and Palmatier (53) also involve proportional counters. The μ-meson energies are divided into four groups with mean energies of about 300, 600, 1300, and >1800 Mev. The distributions in each case are of the Landau type. The somewhat greater width of the experimental distribution is attributed to experimental conditions. Landau distributions are involved but not measured in the μ-meson experiments of Hudson & Hofstadter (49) and Baskin & Winckler (50).

Energy Loss and Ionization

Ionization by radiations of all kinds has been a subject of intensive investigation for many years. A few years ago Jesse, Forstat & Sadauskis (58) initiated a program of careful measurements which, in 1950, led to a considerable clarification of a subject which had become highly confused. Their program was the determination of w, the ratio of energy loss by a charged particle to the total ionization in a gas which is produced by it. In their 1950 paper they provided unambiguous evidence that w has an appreciable variation with energy of the particle in air but that in argon there is no variation within 0.5 per cent. These results had immediate quantitative implications with respect to the validity of range-energy relations which were in use at that time.

The measurements also had other implications. The factors responsible for the wide variation in the numerical values of w as obtained by different experimenters were discovered. In particular, the effect of minute quantities of impurities was established. They have found that the addition of 0.13 per cent A to He alters the measured value of w in He from 41.3 ev per ion pair

to 29.7 ev per ion pair after which there is no further rapid change in w as A is added. Similar results are obtained when A is added to Ne.

The cause of the sensitivity of the measured values of w to the presence of impurities in the case of certain gases whereas there is no such sensitivity in the case of others has been established. It is attributed to the discharge of metastable states in the atoms of the principal gas which occurs on collision with atoms of the contaminant. The discharge of metastable states results in the possible production of additional ions. This effect can occur whenever the ionization potential of the contaminant is lower than the excitation energy of the metastable state in the principal gas.

The factors involved in the precise measurement of w are numerous and Jesse *et al.* have concentrated on the study of one type of charged particle, namely the α-particle and a few gas types. The results obtained using carefully purified samples of the five noble gases and air, CO_2, H_2, O_2, N_2, and several hydrocarbons are given in a recent paper of Jesse & Sadauskis (59) in which also a comparison is made with the results of similar measurements by Sharpe (60), Valentine & Curran (61), and Haeberli, Huber & Baldinger (62). Jesse's value of 42.7 ev /ion pair for He is much larger than the value of order 31 obtained by the other experimenters, but it is lower than a recently reported value of 46 by Bortner & Hurst (63). His value of 36.8 ev/ion pair for Ne is considerably larger than previously reported results in the literature. Similar measurements are now in progress using β- instead of α-particles.

Measurements of w as a function of concentration when A is mixed with known quantities of CH_4, C_2H_5OH and C_6H_6 have been made by Bertolini, Bettoni & Bisi (64) using Po α-particles. The experimental results are interpreted by plotting w for the mixture as a function of a parameter depending on the known stopping powers of the various gases. Departures from linearity are used as a means of detecting the interaction of excited atoms in the two kinds of gas. Such interactions are found.

A different kind of measurement is that of Frost & Nielsen (65). They measure specific probable ionization by electrons in a cloud chamber. They interpret the results by using the theoretical energy loss formula for transfers less than a value appropriate to the largest ion cluster which is counted. The number of ion pairs/cm. is counted and a value of w is determined for air, H_2, He, and A. A primary objective of this experiment is the measurement of probable ionization in the region where the ionization varies rapidly, since little information in this region has been available previously. The results are in excellent agreement, except in the case of He, with the energy loss curves when values of w are used which are not very different from the values obtained by Jesse and others. The values of specific ionization at the ionization minimum are compared with measurements of Sen Gupta (66) and Hazen (67). There are unresolved discrepancies in the results of the various measurements.

The Problem of Electron Capture and Loss

The most important low-energy process affecting the penetration phenomena is the capture and loss of electrons. According to general principles discussed by Bohr (68), these processes are of dominating importance when the particle has a velocity whose magnitude is of the order of the velocity of atomic electrons. This occurs for protons at an energy of about 25 kev, and consequently the capture and loss processes are important only near the end of the range. On the other hand, the heavy fission fragments, which are initially highly ionized, have velocities comparable with electronic velocities throughout a large fraction of their range.

The experimental data has been summarized by Allison & Warshaw (3) where also a full discussion of measurements of the charge exchange phenomena is given. The techniques for measurement of equilibrium ratios of the various charge states and of measuring the capture and loss cross sections separately have been refined considerably within recent years by Allison and others. The result is that a considerable quantity of reliable data is now available as a check against the results of the much more frustrating problem of attempting to construct adequate theories of the phenomena in question.

One approach to the theoretical problem is the method of perturbed stationary states valid on the low-energy side of the maximum in the capture probability. The theory of this method is discussed in the book of Mott & Massey (69). A further attempt to refine these methods and to discover their implications has been initiated by Bates, Massey & Stewart (70). Recent applications of the method have been made by Garstang (71), who has extended the early calculations of Massey and Smith by calculating the capture cross section into the $2S$ rather than the $1S$ state of a H atom for the case of protons in He, and Dalgarno & Yadov (72) who have performed the resonance calculation for protons in H_2. Garstang finds that the method used does not have validity at the energy where the $2S$ cross section has its maximum but he is able to estimate that the contribution of this state is small compared to that of the $1S$ state.

The relation of the method of impact parameters to the method of perturbed stationary states has been discussed by Bates, Massey & Stewart (70), and the method has been further developed by Kohn (73) for protons in H_2. Jackson (74) has applied the method of impact parameters to the calculation of the resonance exchange of electrons between He ions and He atoms. He calculates the capture cross section in the energy range from 200 ev to 100 kev (where $v \sim v_0$) and finds good agreement with the experimental data of Hasted (75) and Snitzer (76). The calculated cross sections fail to agree with the measurements of Keene (77) in the energy range of 4 to 40 kev but the latter results also fail to join smoothly to the cross section curves as obtained by Hasted.

The Born approximation calculation of capture cross sections by Brinkman and Kramers (78) has recently been extended with excellent results by Bates & Dalgarno (79), Schiff (80), and Jackson & Schiff (81). The extension

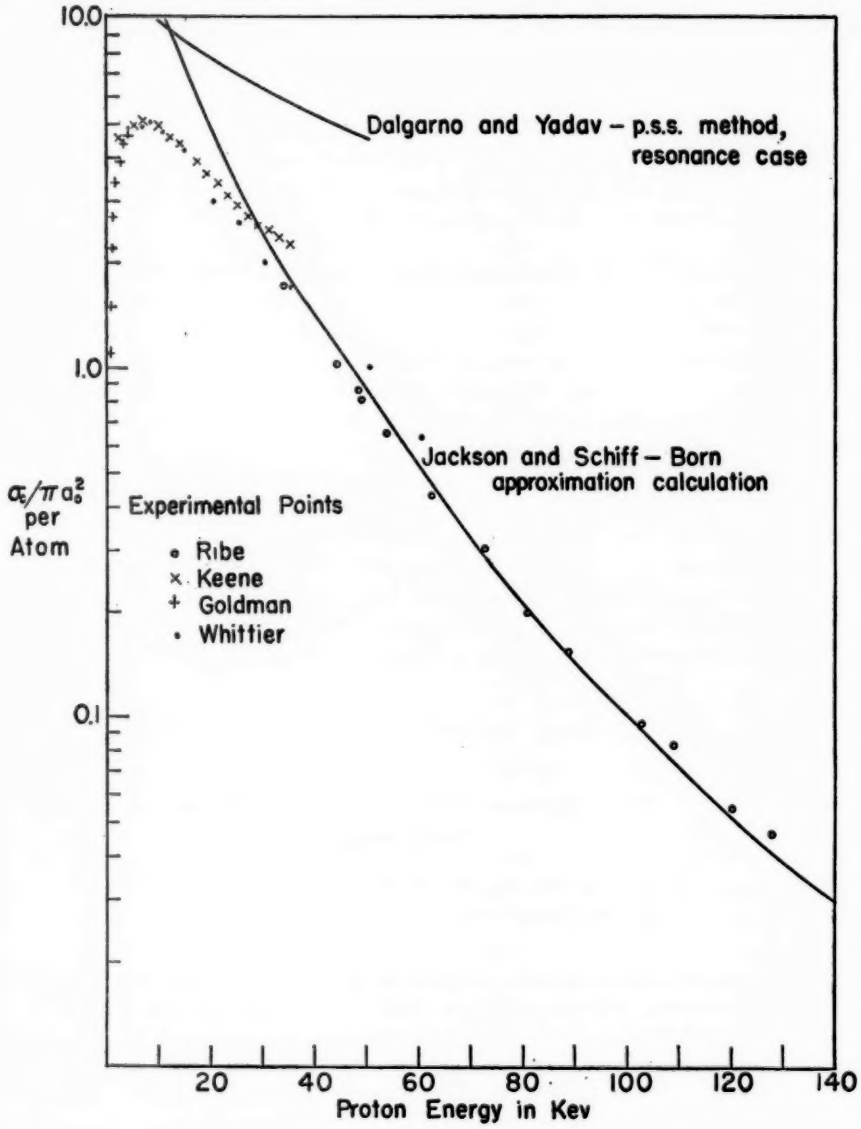

FIG. 3. Cross section for electron capture by protons in hydrogen as a function of energy.

consists of the inclusion of the heavy particle interaction together with the electron-heavy particle interaction. Calculated cross sections for the case of protons in H_2 are in excellent agreement with the measurements of Keene

(77), Ribe (82), and Whittier (83) at all energies down to 25 kev ($v \sim v_0$) where the Born approximation method might not be expected to be valid. The Brinkman-Kramers result is about a factor 5 too large throughout the energy range where capture processes are of importance. The improved results are a consequence of interference in the contributions to the wave amplitude which are important at small impact parameters. A summary of the experimental and theoretical information on the cross sections for protons in H_2, and He ions in He, is given in Figures 3 and 4.

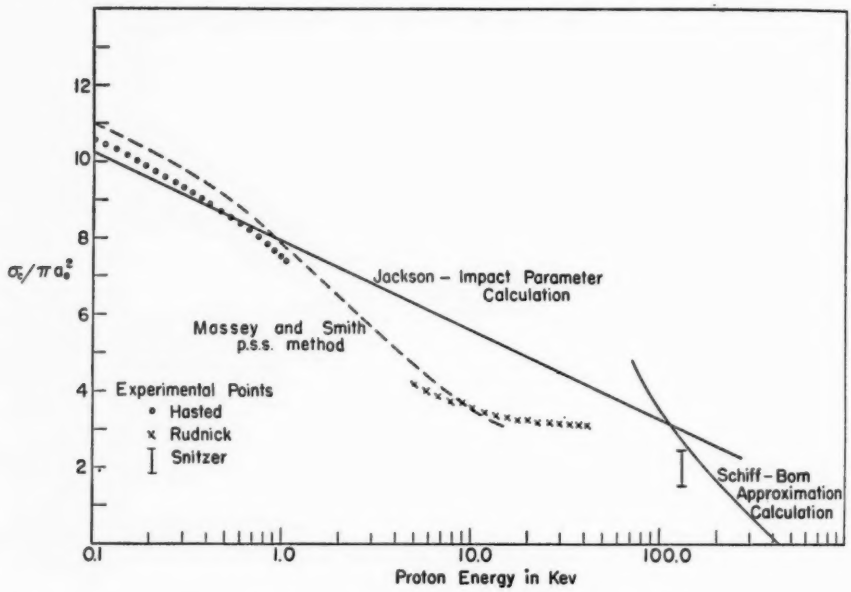

FIG. 4. Cross section for electron capture by singly charged He ions in He as a function of energy.

The calculation of capture cross sections by fission fragments can be treated by entirely different methods. Bell (84) shows that it is a good approximation to treat both the capture and the loss cross sections by classical methods in this case. He calculates these cross sections and determines the effective charge of the fission fragment as a function of its velocity and of the medium through which the particle passes. His results are in good agreement with the experiments except for the case of fission fragments in H_2 and He.

Experimental data on the effects of capture and loss on ions of mass intermediate between protons and fission fragments has been obtained by Barkas (85). Barkas has studied the range correction for electron pickup of Li^8 and B^8 nuclei of low velocities in emulsions. By a comparison of the ranges of these nuclei with those of helium and hydrogen isotopes of the same velocity

he is able to obtain an empirical range-energy relation for the low velocity light nuclei.

We will conclude this section with a remark concerning the constant of Blackett and Lees and a recent experiment that bears upon it. The well-known relation which connects the ranges of α-particles and protons in the same medium is

$$R_H(E) = 1.0072\ R_\alpha(3.971\ E) - C$$

where C is a constant if E is sufficiently high. C differs from zero because the effects of electron capture and loss together with the effects of binding are different for two different particles. There has been one measurement of this constant. This was by Blackett and Lees who obtained the value 0.20 cm. for ranges in air. This number has been used to establish the range-energy relations for protons in air from the α-particle relations.

A recent experiment of Cook, Jones & Jorgensen (86) provides data obtained under identical conditions on the ranges of protons and α-particles. The measurements cover the energy region of 4 kev to 250 kev. In this region the quantity C is not expected to be a constant. However, it is interesting to observe that a smooth dependence on velocity is found, and that the value of the constant decreases with decreasing velocity in about the way one would expect if its value at 300 kev for protons is the value assigned by Blackett and Lees. From the data obtained and for air at atmospheric pressure, C has the value 0.13 cm. at a proton energy of 100 kev and decreases to 0.02 at an energy of 6.7 kev.

Very Low-Energy Region

There are other processes in addition to those of capture and loss which are of importance when the energy of the particle has decreased to a few electron volts. For example, a particle of kinetic energy lower than the lowest electronic excitation potential will lose energy by excitation of oscillational modes of a lattice or of the individual molecules. In a recent paper, Frohlich & Platzman (87) consider the energy loss resulting from the interaction between the charged particle and the permanent electric dipole moments of molecules in a dipolar medium. They make applications to the passage of electrons through water and ice.

In the case of heavy media, statistical theories will describe over-all features of the energy loss. Warshaw (88) has compared the results of his measurements on low-energy protons with the theoretical expression for energy loss derived by Fermi & Teller (89). The latter should account for the energy loss by a heavy particle from zero energy to several kilovolts. Warshaw's measurements join smoothly to the Fermi-Teller curve at low energies and after passing through the maximum in stopping power they join smoothly to the Bethe-Bloch curve.

LITERATURE CITED

1. Taylor, A. E., *Repts. Progr. in Phys.*, **15,** 49 (1952)
2. Bethe, H., and Ashkin, J., *Experimental Nuclear Physics*, Chap. 2 (Segrè, E., Ed., John Wiley and Sons, Inc., New York, N. Y., 789 pp., 1953)
3. Allison, S. K., and Warshaw, S. D., *Rev. Mod. Phys.*, **25,** 779 (1953)
4. Aron, W. A., Hoffman, B. G., and Williams, F. C., *Report AECU-663* (1949); *University of California Radiation Laboratory Report, UCRL-121* (1949)
5. Aron, W. A., *The Passage of Charged Particles Through Matter* (Doctoral thesis, University of California, Berkely, Calif., 1951; *University of California Radiation Laboratory Report UCRL-1325* (1951)
6. Bethe, H. A., *Handbuch der Physik*, **24/1,** 2nd ed., p. 273 (Julius Springer, Berlin, Germany, 853 pp., 1933)
7. Bhabha, H. J., *Proc. Roy. Soc.* (*London*), [A]**164,** 257 (1938)
8. Massey, H. J., and Corben, H. C., *Proc. Cambridge Phil. Soc.*, **35,** 463 (1939)
9. Oppenheimer, J. R., Snyder, H., and Serber, R., *Phys. Rev.*, **57,** 75 (1940)
10. Jankus, V. Z., *Phys. Rev.*, **90,** 4 (1953)
11. Møller, C., *Ann. Physik*, **14,** 531 (1932)
12. Bhabha, H. J., *Proc. Roy. Soc.* (*London*) [A]**154,** 195 (1936)
13. Rohrlich, F., and Carlson, B. C., *Phys. Rev.*, **93,** 38 (1954)
14. Bloch, F., *Z. Physik*, **81,** 363 (1933)
15. Williams, E. J., *Proc. Roy. Soc.* (*London*) [A]**125,** 420 (1929)
16. Landau, L., *J. Phys.* (*U.S.S.R.*), **8,** 201 (1944)
17. Sternheimer, R. M., *Phys. Rev.*, **88,** 851 (1952)
18. Walske, M. C., *Phys. Rev.*, **88,** 1283 (1952)
19. Walske, M. C., *The Stopping Power of K and L Shell Electrons* (Doctoral thesis, Cornell University, Ithaca, New York, 1951)
20. Lindhard, J., and Scharff, M., *Kgl. Danske Videnskab. Selskab. Mat. fys. Medd.*, **27,** 15 (1953)
21. Mather, R., and Segrè, E., *Phys. Rev.*, **84,** 191 (1951)
22. Bloembergen, N., and Van Heerden, P. J., *Phys. Rev.*, **83,** 561 (1951)
23. Hubbard, E. L., and MacKenzie, K. R., *Phys. Rev.*, **85,** 107 (1952)
24. Simmons, D. H., *Proc. Phys. Soc.* (*London*), [A]**65,** 454 (1952)
25. Bakker, C. J., and Segrè, E., *Phys. Rev.*, **81,** 489 (1951)
26. Sachs, D. C., and Richardson, J. R., *Phys. Rev.*, **83,** 834 (1951); **89,** 1163 (1953)
27. Thompson, T., *University of California Radiation Laboratory Report, UCRL-1910* (1952)
28. Bogaardt, M., and Koudijs, B., *Physica*, **17,** 703 (1951)
29. Rotblatt, J., *Nature*, **167,** 550 (1951)
30. Reynolds, H. K., Dunbar, D. N. F., Wenzel, W. A., and Whaling, W., *Phys. Rev.*, **92,** 742 (1953)
31. Kahn, D., *Phys. Rev.*, **90,** 503 (1952)
32. Madsen, C. B., *Kgl. Danske Videnskab. Selskab, Mat. fys. Medd.*, **27,** 13 (1953)
33. Chilton, A. B., Cooper, J. N., and Harris, J. C., *Phys. Rev.*, **93,** 413 (1954)
34. Bohr, A., *Kgl. Danske Videnskab. Selskab, Mat. fys. Medd.*, **24,** No. 19 (1948)
35. Fermi, E., *Phys. Rev.*, **57,** 485 (1940)
36. Schoenberg, M., *Nuovo Cimento*, **8,** 159 (1951); **9,** 372 (1952)
37. Huybrechts, M., and Schoenberg, M., *Nuovo cimento*, **9,** 764 (1952)
38. Messel, H., and Ritson, D., *Phil. Mag.*, **41,** 1129 (1950)
39. Wick, G. C., *Nuovo cimento*, **1,** 302 (1943)

40. Halpern, O., and Hall, H., *Phys. Rev.*, **73,** 477 (1948)
41. Budini, P., *Nuovo cimento*, **10,** 236 (1953)
42. Sternheimer, R. M., *Phys. Rev.*, **91,** 256 (1953)
43. Sternheimer, R. M., *Phys. Rev.*, **93,** 351 (1954)
44. Goldwasser, E. L., Mills, F. E., and Hanson, A. O., *Phys. Rev.*, **88,** 1137 (1952)
45. Allen, J. R., *Phys. Rev.*, **93,** 353 (1954)
46. Fleming, J. R., and Lord, J. J., *Phys. Rev.*, **92,** 511 (1953)
47. Stiller, B., and Shapiro, M. M., *Phys. Rev.*, **92,** 735 (1953)
48. Bowen, T., and Roser, F. X., *Phys. Rev.*, **85,** 992 (1952)
49. Hudson, A., and Hofstadter, R., *Phys. Rev.*, **88,** 589 (1952)
50. Baskin, R., and Winckler, J. R., *Phys. Rev.*, **92,** 464 (1953)
51. Gosh, S. K., Jones, G. M. D. B., and Wilson, J. G., *Proc. Phys. Soc.* (*London*), [A]**65,** 68 (1952)
52. Carter, R. S., and Whittemore, W. L., *Phys. Rev.*, **87,** 494 (1952)
53. Kupperian, J. E., Jr., and Palmatier, E. D., *Phys. Rev.*, **91,** 1186 (1953)
54. Blunck, O., and Leisegang, S., *Z. Physik*, **128,** 500 (1950)
55. Symon, K. R. (Doctoral thesis, Harvard University, Cambridge, Mass., 1948)
56. Rossi, B., *High Energy Particles* (Prentice-Hall, Inc., New York, N. Y., 569 pp., 1952)
57. Igo, G. J., Clark, D. D., and Eisberg, R. M., *Phys. Rev.*, **89,** 879 (1953)
58. Jesse, W. P., Forstat, H., and Sadauskis, J., *Phys. Rev.*, **77,** 782 (1950)
59. Jesse, W. P., and Sadauskis, J., *Phys. Rev.*, **90,** 1120 (1953)
60. Sharpe, J., *Proc. Phys. Soc.* (*London*), [A]**65,** 859 (1952)
61. Valentine, J. M., and Curran, S. C., *Phil. Mag.*, **43,** 964 (1952)
62. Haeberli, W., Huber, P., and Baldinger, E., *Helv. Phys. Acta*, **25,** 467 (1952), **26,** 145 (1953)
63. Bortner, T. E., and Hurst, G. S., *Phys. Rev.*, **90,** 160 (1953)
64. Bertolini, G., Bettoni, M, and Bisi, A., *Phys. Rev.*, **92,** 1586 (1953)
65. Frost, R. H., and Nielsen, C. E., *Phys. Rev.*, **91,** 864 (1953)
66. Sen Gupta, R. L., *Proc. Natl. Inst. Sci. India*, **9,** 295 (1943)
67. Hazen, W. E., *Phys. Rev.*, **65,** 259 (1944); **67,** 269 (1945)
68. Bohr, N., *Kgl. Danske Videnskab. Selsckab. Mat. fys. Madd.*, **18,** No. 8 (1948)
69. Mott, N. F., and Massey, H. S. W., *The Theory of Atomic Collisions*, 2nd ed. (Clarendon Press, Oxford, England, 388 pp., 1949)
70. Bates, D. R., Massey, H. S. W., and Stewart, A. L., *Proc. Roy. Soc.* (*London*), [A]**216,** 437 (1953)
71. Garstang, R. H., *Phys. Rev.*, **87,** 529 (1952)
72. Dalgarno, A., and Yadov, H. N., *Proc. Phys. Soc.* (*London*), [A]**66,** 173 (1953)
73. Kohn, W., *Phys. Rev.*, **90,** 383 A (1953)
74. Jackson, J. D., *Can. J. Phys.*, **32,** 60 (1954)
75. [4]Hasted, J. B., *Proc. Roy Soc.* (*London*), [A]**205,** 421 (1951)
76. Snitzer, E., *Phys. Rev.*, **89,** 1237 (1953)
77. Keene, J. P., *Phil Mag.*, **40,** 369 (1949)
78. Brinkman, H. C., and Kramers, H. A., *Proc. Acad. Sci. Amsterdam*, **33,** 973 (1930)
79. Bates, D. R., and Dalgarno, A., *Proc. Phys. Soc.* (*London*), [A]**65,** 919 (1952)

[4] See also *Proc. Roy. Soc.* (*London*), [A]**212,** 235 (1952) for further data on charge exchange involving various atomic and molecular ions in A, Kr, Xe, and H_2O.

80. Schiff, H., *Electron Capture Cross Sections* (Doctoral thesis, McGill University, Montreal, Canada, 1953)
81. Jackson, J. D., and Schiff, H., *Phys. Rev.*, **89**, 359 (1953)
82. Ribe, F., *Phys. Rev.*, **83**, 1217 (1951)
83. Whittier, A. C., *Can. J. Phys.*, **32**, 275 (1954)
84. Bell, G. I., *Phys. Rev.*, **90**, 548 (1953)
85. Barkas, W. H., *Phys. Rev.*, **89**, 1019 (1953)
86. Cook, C. J., Jones, E., Jr., and Jorgensen, T., Jr., *Phys. Rev.*, **91**, 1417 (1953)
87. Frohlich, H., and Platzman, R. L., *Phys. Rev.*, **92**, 1152 (1953)
88. Warshaw, S. D., *Phys. Rev.*, **76**, 1759 (1949)
89. Fermi, E., and Teller, E., *Phys. Rev.*, **72**, 399 (1947)

BIOCHEMICAL EFFECTS OF RADIATION[1]

By Kenneth P. DuBois and Donald F. Petersen

United States Air Force Radiation Laboratory, University of Chicago, Chicago, Illinois

During the last decade a tremendous amount of research has been done on the biological effects of ionizing radiations. Numerous approaches to the problem of the mechanism of action of high-energy radiations have been explored including studies on crystalline chemical compounds, solutions or suspensions of biologically important materials and intact microorganisms, invertebrates, plants and animals. All of these approaches have contributed to our present knowledge of the biological actions of ionizing radiations. Stimulating theories have been advanced as a result of numerous investigations, but thus far conclusive supportive evidence is lacking for all current explanations of radiation injury.

The gross aspects of the radiation syndrome have already received sufficient study to permit description of the sequence of events in animals and microorganisms injured by toxic doses of ionizing radiations. The general physiological effects and certain specific aspects of the actions of ionizing radiations on living cells have recently been reviewed by Warren (1), Dobson & Lawrence (2), and Patt (3, 4). Rapid progress has also been made in the elucidation of changes in gross cellular structure produced by ionizing radiations. The histopathology of radiation damage has been described in detail (5, 6). The cytological (7) and genetic (8, 9) effects of ionizing radiations have also received special consideration in recent review articles.

As the accumulation of knowledge regarding the action of ionizing radiations on organ systems and intact cells has progressed, more extensive interest has been manifested in the biochemical mechanisms which may be involved in the production of the injurious effects of radiation. The underlying cause of the morphological and functional changes in tissues injured by ionizing radiations has thus become a problem of major interest. The numerous contributions to the search for an explanation of radiation injury to cells in terms of biochemical lesions were recently reviewed by Ord & Stocken (10). Several phases of biochemistry have been considered worthy of investigation in connection with the mode of action of ionizing radiations. The possibility that disturbances in enzyme systems alter the functional activity and subsequently the morphology of irradiated cells has received the attention of numerous investigators. Although the actions of high-energy radiations on enzyme systems require a great deal of additional study, sufficient research has been done to permit a general discussion of the extent to which enzyme action is interrupted in cells injured by ionizing radiations. The present review deals primarily with the actions of ionizing radiations on enzyme

[1] The survey of literature pertaining to this review was concluded in March, 1954

systems. It does not attempt to cover the entire field of the biochemical effects of radiations nor to enumerate and discuss all of the publications on the actions of ionizing radiations on enzyme systems, but rather to present a general survey of the present status of knowledge of the extent of alteration of enzyme reactions by high-energy radiations. It is anticipated that the particular areas of enzymology which have been studied sufficiently with respect to radiation damage, as well as those areas which have been given insufficient attention, will be recognizable from this type of presentation of the subject under discussion.

Primary Mode of Action

Ionizing radiations are assumed to affect biological compounds either by direct action or by production of substances in the medium which act indirectly (11). No experimental means is at hand for distinguishing these two kinds of mechanism in any actual functioning biological system. There is also some considerable doubt that concepts such as "ionization" and "excitation," clearly defined for chemical processes in the gas phase, have a precise experimental meaning in the condensed liquid phase. A recent discussion of these matters is available and should be consulted (12).

From the standpoint of defining radiation damage in terms of biochemical defects in cellular metabolism one may suppose that chemical alteration of critical biochemical compounds results from both the direct alteration of these compounds and the interaction of radiation products of water and other compounds with critical cell components. The labile products must react soon after their formation with important cellular compounds. Primary biochemical changes should, therefore, occur immediately after irradiation. From the practical standpoint of investigating the nature of the biochemical lesion in irradiated tissues, the differences in the time of occurrence of the primary biochemical changes caused by the direct or indirect action of ionizing radiations would not be appreciably different. The time of occurrence of the primary alterations in cellular constituents by the direct and indirect actions would be considered to be essentially the same from the standpoint of the biologist studying intact animals. This viewpoint may be contrasted with the more precise interpretations resulting from *in vitro* chemical and physical measurements where very small differences in time relationships have fundamental significance. The above considerations are important in connection with the search for biochemical changes in irradiated tissues. They are equally important when considering the problem of treatment of radiation injury. The idea that toxic intermediates react rapidly with cell constituents necessarily implies that successful treatment of radiation injury requires (*a*) reversal of a biochemical change produced by the toxic intermediate products, or (*b*) the replacement or substitution of the damaged cellular constituents, unless intervention with therapeutic agents could be accomplished immediately after exposure to radiation. In line with this

concept of rapid biochemical injury by the intermediate products produced by high-energy radiations in tissues, it follows that only the prior or simultaneous administration of drugs can be expected to prevent the initial formation of toxic intermediates produced by ionizing radiations or to react with these toxicants and thus spare cellular constituents from chemical alteration.

The extent to which the chemical constituents within living cells are altered by exposure to ionizing radiations is apparently dependent upon a number of factors. The inherent susceptibility of a particular cell type is a factor of major importance. Interpretation of differences in susceptibility of cells in terms of biochemistry is not yet possible on the basis of existing information. However, several possible explanations for the difference in the actions of ionizing radiations on various cells and tissues seem worthy of mention. Thus, sensitive cells might contain essential biochemical constituents not found in radioresistant cells, and a greater susceptibility of these compounds to chemical alteration by ionizing radiations could profoundly affect the metabolism of the cells in which they are located. This possibility emphasizes the importance of conducting biochemical studies on the known radiosensitive tissues or cells rather than using resistant cells or organisms. Investigations on the influence of high-energy radiations on metabolic pathways which are common to both radioresistant and radiosensitive cells would not seem to be a profitable line of approach to the problem of elucidating the mechanism of radiation damage especially when radioresistant tissues are used for the experimentation.

Specific intermediary metabolites, biocatalysts, and other essential cellular constituents should have the same inherent susceptibility to the products of the ionization of water or to the direct action of high-energy radiations regardless of the particular tissue in which they are located. Studies on metabolic reactions of radiosensitive tissues, which are not part of metabolic pathways common to all tissues, would appear to be a profitable approach to the problem of the biochemistry of radiation damage. However, toxic products capable of activating or inhibiting general metabolic pathways might be formed locally in radiosensitive tissues to form a secondary product capable of interfering with normal metabolic reactions. This type of biochemical action could result in alteration of metabolic pathways common to both radiosensitive and radioresistant tissues. The dose of radiation to which cells are exposed is another important factor determining the amount and type of damage to biochemical systems. In animal experimentation, important changes in metabolic reactions should appear with doses below the lethal level since toxic chemicals, whose mechanism of action is known, exert measurable effects on specific metabolic reactions at doses far below the lethal level. In connection with the relationship between dosage of high-energy radiations and biochemical effects, it is difficult to visualize applicability of findings made on unicellular organisms with high dosages in attempting to explain the biochemical mechanism of action of ionizing

radiations on more susceptible mammalian species. Nevertheless, findings made on any biological material may provide important suggestions for research on mammalian species.

The accumulation of general information on the biochemical effects of radiation during recent years has provided a background for future research. It should be possible henceforth to direct more careful attention to systematic investigations of the effects of high-energy radiations on metabolic reactions of radiosensitive tissues in their normal environment, using moderate dosages of the injurious radiations.

Effects on Biological Compounds in Vitro

The influence of high-energy radiations on chemical compounds *in vitro* has been the subject of numerous studies. In aqueous solutions, changes in chemical compounds are mainly attributable to the indirect action in which the solvent molecules undergo ionization or excitation and react with the solute molecules (11). *In vitro* studies thus provide an indication of the relative susceptibility of various compounds to alteration by the products of ionization of water. A number of the early studies involved measurements of the decomposition of solutions of simple organic compounds by ionizing radiations (14, 23, 24). One of the valuable contributions resulting from these measurements (25) was the observation that the addition of various substances to aqueous solutions of a compound protected the solute under investigation from decomposition by irradiation. This finding is noteworthy in a consideration of biochemical effects of radiation because a similar situation in which a number of solutes are irradiated simultaneously must necessarily exist in the intact cell.

Following studies on the action of ionizing radiations on simple organic compounds in solution, Dale (17) undertook an investigation of the actions of ionizing radiations on enzymes *in vitro*. Several crystalline or partially purified enzymes were shown (17, 26) to be inactivated in dilute solution including carboxypeptidase, polyphenol oxidase, and D-amino acid oxidase. Detailed studies (27, 28, 29) on these enzyme inactivations were then conducted in which protection against the loss of catalytic activity by the addition of a variety of substances was noted. The results of these studies contributed important information on the actions of ionizing radiations on catalytically active proteins. However, the fact that the particular enzymes employed for these studies were radiation sensitive *in vitro* must not be interpreted as evidence that the same enzymes would be affected in intact cells. The protective effect obtained by the addition of specific substrates and other unrelated compounds to solutions of crystalline enzymes is indicative of the competition between compounds in solution for the products of ionization.

The known oxidizing ability of the products of ionization of water led Barron and associates (30) to consider the possibility that sulfhydryl enzymes would be inactivated by irradiation through conversion of their sulfhydryl groups to the inactive disulfide forms. This idea was tested using solutions

of crystalline or partially purified enzymes whose catalytic activity was known to depend on sulfhydryl groups. These enzymes included hexokinase, succinic dehydrogenase, phosphoglyceraldehyde dehydrogenase, and adenosine triphosphatase. Only 13 per cent inhibition of hexokinase activity was obtained with 1000 r, whereas 75 per cent inhibition of succinic dehydrogenase was obtained with 5000 r. Phosphoglyceraldehyde dehydrogenase was markedly inhibited by doses of x-ray below 500 r, and inhibition of adenosine triphosphatase activity was reported to occur with doses as low as 1 r to 10 r when aged myosin preparations were used as the source of enzyme. Several nonsulfhydryl enzymes were included in this study for comparison. Doses of x-ray as high as 5000 r produced no inhibition of lactic dehydrogenase, cytochrome oxidase, and catalase. Catalase had been shown by previous investigators (31) to be relatively insensitive to ionizing radiations. The activity of trypsin was 25 per cent inhibited and ribonuclease exhibited 26 to 60 per cent inhibition after 5000 r (30). Reversal of the inhibition of sulfhydryl enzymes by glutathione clearly demonstrated that the loss of activity was attributable to oxidation of the sulfhydryl groups of the enzyme molecules. The results of these studies thus demonstrated the inherent susceptibility of sulfhydryl enzymes to the injurious actions of ionizing radiations. However, it is noteworthy that high doses were necessary to inactivate some of the enzymes even though they were purified and, therefore, more sensitive than would be expected in their normal environment in the presence of compounds capable of competing for the ionization products of water. Even the use of crystalline or purified enzymes does not permit a precise measurement of the relative susceptibilty of enzymes to irradiation unless the enzyme preparations contain the same amounts and types of contaminating impurities and other conditions including the absolute quantity of enzyme are carefully controlled.

Barron & Dickman (32) studied the effects of α-, β- and γ-rays on phosphoglyceraldehyde dehydrogenase and urease. The inhibition of phosphoglyceraldehyde dehydrogenase produced by α-rays was not reversed by glutathione. Inhibition of urease by γ-rays was also noted but reversal with glutathione was not obtained. However, by the addition of p-chloromercuribenzoate, a sulfhydryl inhibitor, to the urease solution, reactivation of the enzyme by glutathione was achieved after irradiation. This was interpreted (32) as protection by p-chloromercuribenzoate of the sulfhydryl groups against oxidation by γ-rays.

Some additional reports on crystalline, partially purified and impure enzyme preparations have appeared in literature. Byers, Tytell & Logan (33) found that soft x-rays had no inhibitory effect on a crude preparation of hyaluronidase but marked inhibition of the enzyme in purified form could be produced by the same dose of radiation. Other investigators (34) have reported inactivation of crude preparations of this enzyme with extremely high doses of x-ray. Forssberg (35) partially inactivated crystalline catalase in solution with 12,400 r, but other studies with lower doses (30, 31) indicated

no inhibitory effect on this enzyme *in vitro*. Bier & Nord (36) modified the conditions under which crystalline catalase preparations were irradiated, and found that the solutions were more sensitive at acid than at alkaline pH values and that frozen solutions were less sensitive than liquid preparations.

The experiments mentioned above give an indication of the types of results which are obtained by irradiation of enzyme systems *in vitro*. Factors such as the purity of the enzyme, the concentration of the enzyme in solution, and the nature of the impurities markedly affect the amount of alteration of enzyme activity by ionizing radiations. The results of *in vitro* studies thus provide an indication of the inherent susceptibility of various enzymes to the direct and indirect actions of ionizing radiations, and thereby give some evidence of changes which could take place in intact cells. However, the increasing realization of the limitations of *in vitro* studies on the actions of high-energy radiations on biocatalysts, as a method of finding the mechanism of radiation injury in living cells, has forced investigators to turn their attention to the more difficult task of examining the actions of radiations on enzyme systems *in vivo*. Relatively little research on inactivation of enzyme systems by ionizing radiations *in vitro* is being conducted at the present time.

Effects on Carbohydrate Metabolism

The important role of intermediary carbohydrate metabolism as a source of energy for the functional activity of tissues is now well established. Systematic investigations of the mechanism of action of new toxicants generally includes an examination of their effects on the reactions involved in carbohydrate metabolism. Current interest in the possible actions of ionizing radiations on enzymes involved in carbohydrate utilization thus follows the the pattern established for the investigation of the mechanism of action of physiologically active chemical compounds. Many investigators have turned their attention toward a search for disturbances in carbohydrate metabolism as a causative factor in the production of radiation damage. Investigations are being conducted at the cellular level and on intact animals. Although research on this phase of metabolism has not yet provided an acceptable explanation for radiation damage, the information obtained to date represents valuable contributions to the ultimate understanding of the mode of action of ionizing radiations. Various approaches to the study of the actions of high-energy radiations on enzyme systems have been used. The early work consisted primarily of the irradiation of solutions of enzymes *in vitro*. Most of the more recent studies have been carried out on irradiated cells or animals.

As a result of *in vitro* studies on irradiated sulfhydryl enzymes, Barron (30, 32) postulated that these enzymes constituted the most sensitive biochemical compounds in cells. He conducted (37) an investigation on tissue slices from irradiated animals to test this hypothesis, using whole body x-irradiation in doses of 100 r to 900 r. Most of the substrates employed

were those which require sulfhydryl enzymes for oxidation. Spleen, liver, kidney, thymus, adrenals, testis, and submaxillary glands were studied. It was concluded that the oxidation of substrates requiring sulfhydryl enzymes including succinate, D-amino acids, pyruvate, and glutamate was inhibited by the doses of x-ray employed, with pyruvate oxidation being the most susceptible to inhibition. The wide variability in individual values makes it difficult to ascertain the real significance of the changes. The indication from these experiments, that radioresistant tissues such as kidney exhibit inhibition of oxidative reactions which surpass quantitatively the effects observed in radiosensitive tissues, suggests that these biochemical effects are unrelated to tissue damage by x-ray. Subsequent studies by Doull & DuBois (38) indicated that doses of 2000 r of γ-radiation exerted no effect on the endogenous respiration, or on the oxidation of malate and succinate, by liver and kidney slices from mice. Ballin & Doull (39) recently conducted detailed measurements on the respiration of kidney, liver, heart, and brain slices taken from rats at intervals from 4 to 48 hr. after 10,000 r and 20,000 r of x-ray. They found that the oxidation of glucose, succinate, and pyruvate by these tissues was not significantly altered during the survival time after 10,000 r and 20,000 r of whole body x-irradiation. The ability of rat kidney, liver, heart, and brain slices to oxidize oxalacetate, citrate, α-ketoglutarate, glutamate, fumarate, and malate was unaffected at 24 hr. after 20,000 r of whole body x-irradiation. Kunkel & Phillips (40) reported a small transitory increase in the endogenous respiration of liver homogenates from x-irradiated rats. Most observations to date support the conclusion that the enzymes and cofactors involved in the oxidation of several intermediates of the carbohydrate cycle are insensitive to ionizing radiations. The results of some of the studies (38, 39) indicate rather conclusively that the sulfhydryl enzymes of several tissues are not oxidized even by extremely high doses of x-ray nor are the enzymes irreversibly denatured by these high doses of radiation. Sullivan & DuBois (41) have shown that slices of spleens and thymus glands of rats exhibit a reversible decrease in endogenous respiration after 400 r of whole body x-irradiation. A decrease in the endogenous respiration and the succinic dehydrogenase activity of bone marrow of hens has been noted after 300 r of x-ray (42). These data indicate that some enzyme systems in radiosensitive tissues are inhibited by x-irradiation, but there is no direct evidence at hand at the present time to implicate sulfhydryl enzymes in this decrease in endogenous respiration. Sufficient indication of a change in intermediary metabolism of hematopoietic tissues of irradiated animals has been obtained to warrant continuation of the search for the specific enzyme systems involved.

In an attempt to obtain further information concerning the extent to which carbohydrate metabolism is influenced by x-ray in the intact animal, DuBois, Cochran & Doull (43) measured citric acid synthesis in several tissues of irradiated animals. This particular investigation involved the use of the technique of sequential blocking of metabolic pathways described by

Potter (44). This is based on the finding of Buffa & Peters (45, 46) that fluoroacetate causes an accumulation of citric acid in tissues (47, 48, 49) attributable to inhibition of the oxidation of citric acid. This inhibitory action of fluoroacetate is accomplished by prior conversion of fluoroacetate to fluorocitrate which inhibits aconitase and thus causes an accumulation of citric acid in the tissues. When a second toxicant such as ionizing radiation is administered to fluoroacetate-treated animals, a difference in citrate accumulation will occur if the second toxic agent interferes with the operation of the citric acid cycle. The application of this technique to irradiated rats (43) indicated that 800 r of x-ray exerted a marked inhibitory effect on citrate synthesis in spleen and thymus glands. After this dosage of x-ray, inhibition of citrate synthesis was also observed in ileum, pancreas, testis, and skeletal muscle. Additional experiments, in which the dose of x-ray was varied, indicated a relationship between dosage of x-ray and amount of inhibition in the spleen and thymus glands in the range of 100 r to 400 r. After sublethal doses the change in citrate synthesis was reversible, and the values approached normal within two to three weeks after irradiation. These studies indicated that x-ray produces a disturbance in the carbohydrate metabolism of radiosensitive tissues, although the exact cause of the change in citric acid formation as measured by the fluoroacetate technique could be far removed from the tricarboxylic acid cycle itself.

In contrast to other tissues in which x-ray either produced no effect or inhibited citrate synthesis, the livers of irradiated male rats exhibited an increase in citric acid formation. The livers of normal male rats are unable to accumulate citrate to any appreciable extent following fluoroacetate treatment (50, 51), although the liver is capable of producing large quantities of citrate *in vitro* (50). The alteration in citrate synthesis in the liver persisted for a period of several weeks after irradiation, in contrast to the reversible effect of sublethal doses of x-ray on citrate synthesis in the hematopoietic tissues of irradiated animals (43). The long duration of the alteration in the metabolism of the liver indicated that this effect was not involved as a causative factor in the lethality of acutely toxic doses of x-ray.

During the course of studies on the influence of x-irradiation on citrate synthesis in the liver, it was found (43) that the livers of normal female rats could accumulate citric acid after fluoroacetate treatment, thus resembling those of irradiated males. This observation suggested that citrate synthesis in the liver might be under regulatory influence by steroid hormones. Some information concerning this possibility was obtained (52) by studies on citrate formation in the livers of rats after castration or treatment with estradiol or testosterone, The results of these tests indicated that male rats acquired the ability to accumulate citrate in the liver after castration. Testosterone depressed citrate formation, and estradiol exerted no direct effect but antagonized the actions of androgens on this metabolic reaction in the liver *in vivo*. These results do not prove, but support the idea, that the alteration in the metabolic pattern in the livers of x-irradiated male rats (43) may be at-

tributable to a release of the liver from the regulatory action of androgens.

Ord & Stocken (53) have recently conducted similar studies on citrate accumulation in the livers of irradiated and castrated male rats and have confirmed the findings of other investigators (43, 52). The less pronounced changes found by these investigators are undoubtedly attributable, at least in part, to the use of suboptimum conditions with respect to dosage of fluoroacetate and time of sacrifice of the animals. Under the experimental conditions employed (53), small changes appear to be of different significance than in the case where the sequential blocking technique as originally described (44) is employed. It is worthy of emphasis that the change in citrate accumulation produced by starvation is opposite in direction to that produced by x-irradiation. The nutritional state of the animals will obviously alter the ability of tissues to accumulate citric acid, and studies on the influence of external factors on this process necessarily require caution unless the change produced by the toxicant is opposite in direction to that produced by secondary factors such as starvation.

The nitrogen mustards, ethyl *bis*(2-chlorethyl)amine and methyl *bis*(2-chlorethyl)amine, produce effects (54) on citrate synthesis *in vivo* which resemble the changes produced by x-irradiation (43). Thus, a decreased citrate synthesis is observed in spleen and thymus glands, but x-irradiation is considerably more effective than the nitrogen mustards in depressing citrate formation in the hematopoietic tissues. However, the alteration in the metabolic pattern of the liver is more pronounced and more consistent with the nitrogen mustards than with x-ray. This similarity is interesting in view of the small number of biochemical effects which have thus far been found common to both radiomimetic chemical agents and ionizing radiations.

A variety of experiments involving measurements of some aspect of carbohydrate metabolism in intact irradiated animals has been performed. Barron *et al.* (55) reported a decrease in absorption of glucose by rat intestine within a few hours after sublethal doses of x-ray. Lourau & Lartigue (56) demonstrated a decrease in the rate of absorption of glucose from the intestine of guinea pigs, but this change was observed almost two weeks after 500 r of x-ray. Goodman *et al.* (57) have demonstrated that absorption availability of the small intestine is markedly reduced by a delay in gastric emptying time following x-irradiation. Maximum reduction occurred in 48 hr. and persisted for about 21 days after the administration of 450 r of total body x-irradiation. Thus, from the standpoint of time, the decreased absorption availability roughly parallels the observed decrease in glucose absorption. However, more definitive information is needed to indicate whether the apparent decreased glucose absorption is a specific effect or secondary to structural damage to the intestine or to some other non-specific cause.

Glycogen synthesis in the livers of irradiated animals has been the subject of a considerable number of studies. In this respect, an interesting observation was the finding (58, 59) that liver glycogen increased in the early postradiation period after sublethal and lethal doses of x-ray. The cause of

this glycogen deposition is as yet unknown. Other investigators (60) have found that the liver glycogen of mice is reduced after repeated exposure to 300 r to 450 r, and a reduction of liver glycogen also occurs in several other species (61) after lethal x-irradiation.

Lethal doses of x-irradiation have been found to reduce glycogenolysis (62) and to cause blood sugar tolerance curves to remain elevated for longer than normal periods of time. Blair (63) found hyperglycemia in rabbits after 2000 r. This rise in blood sugar could be counteracted by insulin. Lourau & Lartigue (64) observed that the hyperglycemia produced by fasting of guinea pigs was aggravated by irradiation. The maximal effect was observed in two to three weeks after 500 r. Diminished glucose tolerance was observed at about two weeks after this dose of x-ray. Glycogen deposition (65) from ingested glucose fell to a minimum at 15 to 20 days after irradiation. There was no apparent correlation between the maximum glucose intolerance and the liver glycogen levels. No impairment of glycogen synthesis was observed but animals were unable to retain glycogen in the liver to the normal extent after irradiation. More recent studies (66) have indicated that higher doses of 1000 r and 2000 r of x-ray administered to fasting mice and guinea pigs cause enhanced gluconeogenesis and an increase in liver glycogen. The effect was most pronounced after 2000 r, and 500 r was without immediate effect. Retarded glycogenolysis in rat liver following 1000 r of x-ray has also been reported by Denson *et al.* (67).

A number of investigators have measured the oxygen consumption and carbon dioxide output of irradiated animals. In general, the changes found are not striking, considering the doses of radiation employed and the fact that many of the measurements were made at time intervals after radiation when they could be secondary effects. In the early work on this subject massive doses of total body irradiation were employed, and a shock-like syndrome was described (68, 69) in which oxygen consumption decreased with a concomitant elevation of the respiratory quotient. Kirschner *et al.* (70) reported that rats given doses sufficient to cause death in three to five days exhibited an increase of 35 per cent in oxygen consumption in 24 hr. after irradiation. In animals given doses producing death in about ten days a sustained increase in oxygen consumption of about 58 per cent occurred, and this was believed to be a true metabolic change. Doses far below the lethal dose (54 r) also caused a slight increase in oxygen consumption. Smith *et al.* (71) were unable to confirm these findings when they employed experimental animals which were fed *ad libitum*, but they did observe an increase in the metabolism of fasted male rats after doses of 800 r. Further studies by Smith *et al.* (72) revealed that LD_{30} doses of x-ray did not alter the oxygen consumption of guinea pigs fasted 4 to 24 hr. prior to measurement, when compared with litter mate controls. In view of these contradictory data, Mole (73) has recently undertaken a reexamination of the effects of radiation on basal oxygen consumption in rats, employing an improved technique for the estimation of oxygen utilization. The results of this study indicate that

no increase, and perhaps a slight decrease, in oxygen consumption occurs during the three-day period of maximum weight loss after doses of 300 r to 1000 r of x-ray. However, from the fourth day until death (6 to 14 days) after 800 r oxygen consumption increases to a maximum of 35 per cent above the control value and similar but smaller changes are also noted after 600 r. Hasegawa, Taubman & Landahl (74) find no change in oxygen consumption and only a slight decrease in CO_2 production during the survival time or during an 18 to 20 day period following 700 r and 850 r of x-ray. Hevesy & Forssberg (75) report that the amount of CO_2 resulting from the metabolism of uniformly labelled glucose is depressed within 10 min. after 2000 r, and the amount of C^{14} appearing in the liver is increased as compared with normal animals. In mice a reduction in expired CO_2 and a decrease in the incorporation of C^{14} into desoxyribose nucleotides is also observed (75).

Several investigators have considered the possibility that an increased metabolism after x-irradiation might be attributable to involvement of the thyroid gland (76, 77, 78) although the administration of desiccated thyroid to irradiated mice causes no increase in the basal oxygen consumption above that seen in thyroid-treated control animals (79). Reports have appeared which indicate that an increased iodine uptake occurs in the thyroid glands of irradiated animals. Increased thyroid activity usually occurs soon and persists for a relatively short period of time after rather high doses of radiation. It has been suggested (80) that the effect on the thyroid gland may be attributable to a stimulation of the production of the thyrotropic hormone by the pituitary gland after sublethal doses, and to a depressant effect on the production of this hormone after lethal doses of radiation. Korson & Botkin (81) have demonstrated depletion of basophilic granules in the pituitary and these structures are the proposed source of thyrotropic hormone. Mole & Batt (82) observed an irreversible reduction of iodine uptake by thyroid tissue in acutely irradiated rats. Thus, these studies support the hypothesis (80) that changes in thyroid function in irradiated animals are controlled by factors outside the thyroid gland and that the observed thyroid effects of radiation are secondary in nature.

A considerable number of studies have been performed on the influence of radiation on unicellular organisms. It is generally necessary to use extremely high doses of radiation to produce changes in lower forms as compared with mammals, and the metabolic pathways necessarily differ considerably from those in mammals. It is usually not possible to extrapolate biochemical changes found in microorganisms to higher forms, but suggestive evidence of possible value in studying the biochemical changes in mammalian tissues may be derived from such studies. Barron *et al.* (83, 84) found that high doses of radiation decreased the respiration of sea urchin sperm. Lower doses of radiation stimulated their respiration (85). Exposure of *Escherichia coli* to 60,000 r of x-ray has been shown (86) to produce a latent inhibition of oxygen consumption. Tahmisian (87) and Tahmisian & Adamson (88, 89) have conducted extensive studies on the influence of radiation on the metabolism

of grasshopper eggs. They noted that the oxidation of hydroquinone by the eggs in the diapause stage was decreased immediately after irradiation but was increased at eight days after irradiation. This increase was noted after doses as high as 200,000 r. The initial decrease in respiration was not accompanied by oxidation of sulfhydryl groups. Inhibition of CO_2 production has been observed (90) with diluted yeast suspensions after high doses of x-ray.

A sufficient number of experiments have indicated changes in the carbohydrate metabolism of intact animals, whole cell preparations, and crystalline enzymes exposed to ionizing radiations to warrant further investigation of this aspect of the biochemistry of radiation damage. Systematic examination of individual enzyme systems irradiated in the presence of other normal cellular constituents seems desirable, from the standpoint of obtaining more definitive information on the extent to which alteration in enzyme activity is involved in the injurious actions of ionizing radiations. Enzyme assays on tissues taken from irradiated animals provide a means of estimating the extent to which alteration of enzyme activity is involved in the injurious actions of ionizing radiations. In this connection, the dosage level of radiation employed and the time at which the assays are performed after irradiation are important factors to be considered. It is also important to ascertain whether the particular alteration in enzyme activity occurs after administration of sublethal as well as lethal doses of the toxicant. In general, poisons which produce their physiologic effects by interference with a particular enzyme system cause measurable changes in enzyme activity at doses far below the lethal dose. Ascertaining whether an enzyme change in the tissues of irradiated animals occurs after sublethal doses is thus a logical sequence to studies employing lethal doses.

Thus far, relatively few investigations involving assays of individual enzymes have been conducted on tissues of irradiated animals, and most of these have utilized lethal doses of x-ray. However, several significant findings have been made using this approach to the study of the mechanism of radiation damage. DuBois *et al.* (91) found that the succinic dehydrogenase activity of liver, kidney and testis of mice was unaffected immediately after and at seven days after 2000 r of whole body γ-radiation. LeMay (92) measured the succinic dehydrogenase activity and cytochrome oxidase activity of kidney homogenates of rats sacrificed within 2 hr. after 400 r or 800 r of x-ray. No inhibition of these enzymes was noted. Thomson *et al.* (93) exposed rats to 800 r of γ-radiation, and sacrificed the animals at intervals from 3 to 96 hr. for succinic dehydrogenase, malic dehydrogenase, and cytochrome oxidase assays on the thymus glands. They found negligible changes in the activity of these enzymes. Ashwell & Hickman (94) measured the succinic dehydrogenase and cytochrome oxidase activities of the spleens of mice sacrificed at various intervals from 24 hr. to 17 days after irradiation. No significant change in the activity of these enzymes was observed. Fischer *et al.* (95) measured the succinic dehydrogenase, cytochrome oxidase, and lactic de-

hydrogenase activities of kidney, liver, and spleen of rats given 800 r of x-ray. They reported that no change in any of the enzymes occurred except in the case of succinic dehydrogenase of the spleen which exhibited a small decrease. Pretreatment with cysteine prevented this decrease in enzyme activity.

Thus far, many of the studies on the influence of ionizing radiations on individual enzymes *in vivo* have involved measurements of succinic dehydrogenase activity. Interest in the actions of ionizing radiations on this enzyme *in vivo* was stimulated by the findings of Barron *et al.* (30) who observed inhibition when succinic dehydrogenase was irradiated *in vitro*. At the present time, specific evidence indicating inhibition of sulfhydryl enzymes or other biocatalysts involved in the oxidative phase of carbohydrate metabolism *in vivo* is lacking. However, evidence obtained by studies on intact animals (43) and tissue slices (41) have demonstrated that intermediary carbohydrate metabolism is altered in radiosensitive tissues *in vivo*. Studies on individual enzymes which are directly involved in carbohydrate metabolism and ancillary reactions should, therefore, be continued.

Phosphorus Metabolism

The important role of organic phosphate esters in the normal metabolic processes in the tissues of mammals and lower forms has stimulated the interest of a number of investigators in determining whether ionizing radiations influence the synthesis or hydrolysis of phosphate esters. Research on this subject has involved measurements of the actions of high-energy radiations on phosphatases *in vitro*, chemical measurements of the concentrations of phosphorylated compounds in the tissues of irradiated animals, and measurements of the influence of radiation on phosphorylating enzymes and phosphatases *in vivo*. The results of several of these studies have indicated that ionizing radiations produce disturbances in phosphorus metabolism.

The influence of ionizing radiations on phosphatases has received considerable attention. In 1939 Iwatsuru & Nanjo (96) reported an increase in the serum alkaline phosphatase activity of x-irradiated rabbits. Other investigators have subsequently reported variations in the alkaline phosphatase of the serum of several species which appear to depend upon the particular species, the magnitude of the dose of radiation, and the type of radiation. Reinhart (97) found that the alkaline phosphatase of the serum of rats, rabbits, and dogs decreased during the first four days after low doses of neutron irradiation and returned to normal by the seventh day. Larger doses of neutron irradiation caused three to six-fold increases in the phosphatase activity of the serum of dogs. Prosser (98) described an increase in the plasma phosphatase activity of dogs following acute total body x-irradiation. A transitory increase in serum phosphatase during the first 24 hr. followed by a decrease has been observed (99, 100) in rats after 400 r to 600 r of x-ray. Other investigators have noted a decrease in rat serum alkaline

phosphatase after the administration of radium chloride (101) and large local doses of x-ray (102).

Norris & Cohn (101) found that an internal α-emitter, radium chloride, significantly reduces the alkaline phosphatase activity of bone as early as three hours after 10 to 100 rep/hr. Serum alkaline phosphatase levels were also depressed, suggesting that at least part of the serum phosphatase was derived from the radiosensitive elements of bone. *In vitro* exposure of serum and bone homogenates to doses as high as 10,000 r did not alter the alkaline phosphatase activity, indicating that radiation injures the phosphatase forming elements of bone rather than exerting a direct effect on the enzyme. Evidence has been accumulated (103, 104) indicating that osteoblasts function as the source of bone phosphatases and these cells are relatively sensitive to radiation (102). The failure of Ra to depress phosphatase activity beyond a certain limit regardless of the dose of Ra administered (101) and in spite of the preferential uptake of Ra salts in bone (105) has been interpreted as indicating that radiation affects some of the alkaline phosphatases of bone and has no effect on others.

Measurements of the phosphatase activity of the soft tissues have demonstrated that ionizing radiations produce an increase in enzyme activity in some tissues and exert no influence on alkaline phosphatases of other tissues. DuBois *et al.* (106) found no change in the adenosinetriphosphatase activity of the kidney, liver, and testis of mice either immediately after or at seven days after 2000 r of whole body γ-radiation. The conversion of hexose diphosphate to phosphoglyceric acid by liver and kidney homogenates of mice was inhibited less than 20 per cent after 2000 r of γ-radiation *in vivo*. This finding indicated that phosphoglyceraldehyde dehydrogenase is not sensitive to radiation *in vivo* in contrast to its high susceptibility to inactivation when solutions of the crystalline enzyme are irradiated *in vitro* (30). This experiment also indicated that the other enzymes of liver and kidney which function in the conversion of hexose diphosphate to phosphoglyceric acid are unaffected *in vivo* by high doses of radiation. Further studies (107), in which measurements of the alkaline phosphatase activity of the spleen and thymus glands were included, demonstrated that 800 r of x-ray produced marked increases in the ability of these tissues of mice and rats to hydrolyze phosphate esters within 24 hr. after irradiation. The phosphate esters employed for this study were 5-adenylic acid and β-glycerophosphate. Ludewig & Chanutin (100) also observed that the alkaline phosphatase activity of rat spleen and thymus glands increased after whole body irradiation, while the activity of liver and kidney was unaffected by 500 r of x-ray. Arvy *et al.* (108) measured the alkaline phosphatase activity of spleen, intestine, and kidney tissue of mice after 2000 r of whole body x-irradiation using the histochemical technique of Gomori (109). An increased activity in spleen and an apparent decrease in the activity of kidney and intestinal villi was observed. Although 500 r of x-ray produces no increase in the alkaline phosphatase activity of liver (100, 110), Petrakis and associates (111) report that slightly

higher doses of x-ray cause some increase in liver phosphatase activity. Rév *et al.* (112) demonstrated a marked increase in the alkaline phosphatase activity of rat liver and bronchial epithelium after 2000 r and 4000 r of x-ray. Extensive desquamation prevented ascertaining whether radiation altered the phosphatase activity of the intestine. However, Ross & Ely (113) have reported an increase in the phosphatase activity of rat intestine after lethal exposure to neutrons, and Doyle (114) has observed an increase in the concentration of alkaline phosphatase in the epithelium of rabbit appendix, but the total activity was diminished as a result of sloughing of the mucosa after 500 r of x-ray. An example of the resistance of the phosphatases of some tissues toward ionizing radiations is evident in the case of mouse brain which exhibits (115) no alteration in ability to hydrolyze 5-adenylic acid after 30,000 r of whole body x-irradiation.

Following these observations, more detailed studies were conducted on the phosphatase activity of tissues of irradiated animals. The earlier experiments indicated that the alteration in activity of this group of enzymes was confined to radiosensitive tissues. A survey (116) of the effects of 800 r of x-ray on several tissues of rats, mice, and hibernating and nonhibernating ground squirrels demonstrated that, of the several tissues studied, only spleen and thymus glands showed appreciable changes in phosphatase activity. Two to three-fold increases were observed in these tissues. These observations were followed by detailed studies (117, 118) in which the influence of various sublethal and lethal doses of x-irradiation on the 5-nucleotidase and adenosine triphosphatase activities of the spleen and thymus glands of rats and mice were measured. DuBois & Petersen (118) noted that the increased ability to hydrolyze these phosphate esters as measured by specific assay procedures (119, 120) was detectable as early as 3 hr. after x-ray and reached a maximum within 72 hr. The alteration in enzyme activity was reversible with the rate of reversal depending upon the dose of x-ray. Within the dose range of 25 r to 400 r, the amount of increase in the adenosinetriphosphatase activity of the spleens and thymus glands of rats was directly related to the dose of x-ray administered. Doses in excess of 400 r did not evoke additional increases in the adenosinetriphosphatase activity of the hematopoietic tissues. A similar relationship between dose and nucleotidase activity was observed when doses of 100 r to 400 r were administered. Ashwell & Hickman (121) have also observed an increase in the adenosinetriphosphatase activity of spleens of mice. These investigators employed a lethal dose (640 r) and pooled the results of assays conducted on tissues taken from one to eleven days after irradiation. The relationship between dosage and magnitude of the effect and the reversibility after sublethal doses was thus not apparent in these studies. Attempts (121) have been made to determine which structure within the spleen contains the increased phosphatase activity. It was not possible (121), on the basis of fractionation of the spleen, to account for the increased enzyme activity on the basis of destruction of an enzymatically inactive cell fraction which would tend to cause an apparent increase in the enzyme

activity of the whole organ. Thomson *et al.* (93) observed no increase in the adenosinetriphosphatase activity of the thymus glands of rats during the first four days after 800 r of x-ray. Fischer *et al.* (95) reported that there was no increase in the adenosinetriphosphatase activity of the spleens of rats after 800 r of x-ray when the activity was expressed on the basis of dry weight of the tissue. However, other studies (118) have indicated that the dry weight change is insufficient to account for the marked increase in phosphatase activity of hematopoietic tissues. The exact cause of the increase in phosphatase activity of hematopoietic tissues of irradiated animals remains to be determined. This subject seems worthy of further investigation because the increase in enzyme activity is restricted to radiosensitive tissues, can be detected after sublethal doses and is closely associated in time, with acute radiation damage. A relationship may exist between the change in phosphatase activity and the decreased ability of hematopoietic tissues to esterify phosphorus (122, 123), synthesize citric acid (43), and to synthesize desoxyribose nucleotides (124).

The influence of high-energy radiations on the synthesis of phosphate esters has been studied by several investigators. Thomson *et al.* (93) measured the phosphorylation of creatine by thymus homogenates from rats receiving 800 r of x-ray and found a decrease in phosphate esterification which was not accounted for entirely on the basis of accelerated phosphatase activity. Potter & Bethell (122) reported that mitochondria prepared from spleens of rats given 800 r of x-ray exhibit a reduced capacity to carry out oxidative phosphorylation which was detectable as early as one hour after irradiation. Other investigators have observed (94, 123) a decreased phosphorylation by mouse spleen homogenates and mitochondria after 640 r of x-ray. Hickman & Ashwell (125) found a decrease in anaerobic glycolysis by homogenates of the spleens of mice which appeared to be attributable to destruction of adenine nucleotide phosphate acceptor in irradiated spleen. Florsheim *et al.* (126, 127) studied oxidative phosphorylation in mouse brain and liver after massive doses of x-ray (20,000 r) and concluded that radiation does not impair the uptake of P_{32} by either of these tissues. In view of the importance of the phosphorylation process in the normal metabolism of cells, the changes which have been observed in oxidative phosphorylation in hematopoietic tissues of irradiated animals may be of considerable significance in the biochemical mechanism of radiation damage. However, thus far, lethal doses of radiation have been employed in all of the reported studies and caution must be exerted in the interpretation of the results until data are obtained on tissues taken from animals receiving sublethal doses of radiation. More attention should also be given to the possible influence of accelerated phosphatase activity on the levels of phosphate esters in phosphorylation experiments.

Chemical analyses of the concentrations of various organic phosphorus-containing compounds have been conducted by many investigators. The majority of these measurements have been concerned with nucleic acid phos-

phorus. It is not intended that this communication include a resume of the vast amount of research on the effects of radiation on nucleic acids, but mention of some of the findings may serve to illustrate the possibility that the changes in phosphatase activity and phosphorylation produced by radiation might have some direct bearing on the alteration in nucleic acid metabolism produced by radiation.

Decreases in the rate of incorporation of phosphorus into nucleic acids has been observed by many workers under a variety of conditions. An inhibition of the incorporation of radioactive phosphorus into desoxyribonucleic acid has been observed in tumors (128, 129, 130), intestine (131), liver and muscle (132), kidney, lung, and spleen (133). A reduction in the rate of incorporation of phosphorus into desoxyribonucleic acid of rat thymus gland has been considered by Harrington & Lavik (134) as the cause of the radiosensitivity of this tissue. Rapid initial decreases in the nucleic acid phosphorus of bone marrow and spleen have been observed (135) which were reversible in about 50 days after sublethal doses of x-ray, and proliferating cells exhibited a shift from desoxyribonucleic acid to ribonucleic acid (136). Nucleic acid changes occur in some tissues which do not exhibit changes in phosphatase activity, and the time relationships with respect to onset and duration of the effects on phosphatases and nucleic acid metabolism do not correlate closely enough to be related as cause and effect. However, the increased hydrolysis of phosphate esters may be a contributing factor toward the alteration of nucleic acid metabolism in some tissues. Measurements of the adenosine nucleotide levels of the hematopoietic tissues of irradiated animals have shown (137) that lethal and sublethal doses of x-ray cause a reduction in the adenosinetriphosphate levels in these tissues. This reduction may be explainable on the basis of the increased adenosinetriphosphatase activity of these tissues after irradiation (118).

Effects on Fat and Protein Metabolism

Some evidence has been obtained which indicates a disturbance in fat metabolism in the tissues of irradiated animals. Fatty change in the livers of rats (138 to 143) and mice (144, 145, 146) have been observed after high doses of radiation. Ellinger has stated (141) that doses in the range of the LD_{70} are required for induction of these changes. After sublethal doses of radiation changes in the fat content of the liver fail to occur (147, 148). In addition to studies on the total lipid content of tissues, investigations of the effects of radiation on several lipid fractions have been conducted. A decrease in the blood cholesteral has been observed (149) in irradiated mice. On the other hand, Kohn (150) has reported a sustained elevation of the serum cholesterol levels of guinea pigs after 200 r of x-ray. Buchanan *et al.* (148) found that doses of 500 r did not alter urinary choline excretion, and that 650 r did not cause appreciable changes in plasma choline levels in irradiated rats. However, high doses (2000 r) caused an elevation of the plasma choline of fasted animals. Radiation-induced lipemia (151) associated with

increased phospholipid (152) and lipoprotein (153) has been reported. Other forms of injury also caused increased serum lipid levels. Thus, Chanutin & Gjessing (154) have reported elevated serum lipid levels after partial hepatectomy, thermal injury, and administration of β-chlorethylamines. Reduction of serum lipase activity has also been observed in irradiated rats (155), rabbits, (156) and human patients receiving local radiation therapy (157).

Enhanced incorporation of P_{32} into liver phospholipids (158) and increased lipogenesis (159) have been observed after irradiation. The latter effect, which was slight after doses of 200 r and maximal after 2500 r, was demonstrable in rat liver slices but could not be detected in mouse liver. A similar study (160) was conducted in which the capacity of bone marrow from irradiated rabbits to incorporate labeled acetate into fatty acids indicated an immediate acceleration of the synthesis of saturated fatty acids. This was followed by a decrease after about one week. There was an opposite effect on the synthesis of unsaturated fatty acids during the same time interval. Bacq & associates (161) found that the livers of irradiated rats increased in fat content if the animals were fed a high fat diet. Starved rats showed (161) a slower decline in body fat than starved controls apparently because of decreased utilization or accelerated fat synthesis.

Sensitivity of mice to lethal doses of x-ray has been reported to increase when they are fed a diet deficient in essential fatty acids (162, 163). Incorporation of essential fatty acids in the diet afforded some protection (163, 164, 165). However, genetically obese mice and mice made obese by injection of goldthioglucose (166) exhibited no resistance toward radiation (167).

Most of the data available at the present time indicate that high doses of radiation are required to produce alterations in fat metabolism and it, therefore, appears that changes in fat metabolism are not of primary importance in radiation lethality. However, the lack of systematic studies at the enzymatic level renders the dismissal of possible radiation effects on fat metabolism unjustified at the present time.

The nitrogen metabolism of irradiated animals has received considerable attention. The endogenous nitrogen excretion has been shown (168) to increase in rats after 400 r of x-ray. Irradiated rats exhibit (169) a greater negative nitrogen balance than controls. Increases in the blood uric acid (170, 171) and blood urea (169, 171) have been found after lethal doses of radiation. Urea excretion (172) has also been shown to increase after irradiation. The influence of alterations in the nutritional state of animals with respect to protein has received some attention. Protein depletion and low protein diets increase sensitivity to radiation (173, 174, 175).

The influence of radiation on some of the enzymes involved in various phases of nitrogen metabolism has been studied. Feinstein & Ballin (176) found that whole body x-irradiation increased the carboxypeptidase activity of liver, kidney, and intestine. These investigators (177) demonstrated the presence of a naturally occurring carboxypeptidase inhibitor in tissues and obtained evidence (176) that the destruction of this inhibitor by x-irradiation

caused the observed increase in enzyme activity at least in the case of kidney. Tonhazy, White & Umbreit (178) found no effect by x-irradiation on the transaminase activity of liver or heart *in vivo* when the glutamate-aspartate system was studied. High doses of x-ray (1500 r) have been reported (179) to increase the activity of the glutamate-alanine transamination system in the liver of rats and to decrease the activity of this enzyme system in the duodenum. Rauch & Stenstrom (180) irradiated the pancreas of dogs locally and found that the production of trypsin, lipase, and amylase was reduced beginning at about 12 hr. after irradiation. It seems probable that additional research on the actions of ionizing radiations on nitrogen metabolism would yield interesting results since there exists sufficient information at the present time to indicate some influence by radiation on this phase of cellular biochemistry. However, it is not clear from the available information whether these effects are secondary to other biochemical lesions.

Effects on Other Enzymes

Most of the investigations on the influence of radiation on enzyme systems have been conducted on biocatalysts involved in the oxidative or glycolytic phase of carbohydrate metabolism, phosphorus metabolism, nucleic acid synthesis, and to a lesser extent on fat and protein metabolism. The influence of radiation on enzymes not directly involved in these processes has received some attention.

Measurements of the cholinesterase activity of the tissues have been made by several investigators. In 1936 Kwiatkowski (181) reported some inactivation of a pseudocholinesterase preparation of rabbit serum by low doses of x-ray. Barnard (182) noted a decrease in the blood cholinesterase levels of patients receiving roentgen therapy and suggested this effect as an explanation for the cholinergic symptoms of radiation sickness. Baglioni & Piemonte (183) have reported a slight increase in the cholinesterase activity of rat skin after doses of x-ray ranging from 25 r to 300 r. Conard (184) also measured cholinesterase levels during a study of the factors which might be responsible for the increased tone and motility of the intestine (185) after irradiation. It was found that the cholinesterase activity of the intestine showed a significant depression at 15 to 20 hr. after 500 r of x-ray, reached nearly 60 per cent depression by the fourth day and then recovered slowly to normal values during the following three weeks. However, correlation of the enzyme changes with intestinal motility was not apparent. Burn, Kordik & Mole (186) measured the cholinesterase activity of the intestine of rats after 1000 r of x-ray and found a diminution in the amount of pseudocholinesterase to about half the normal value at 48 hr. after x-ray. In contrast to these *in vivo* effects, the administration of doses of x-ray as high as 3000 r to intestine homogenates causes no inactivation of cholinesterase (187).

The idea of Sawyer & Everett (188) that pseudocholinesterase is synthesized in the liver led Burn *et al.* (186) to conclude that the effect of radiation on cholinesterase might be primarily attributable to an action by x-ray on

the liver. A more extensive study of the cholinesterase activity of the tissues of irradiated rats has been conducted by Doull (189), who observed that doses as high as 1200 r of x-ray exerted no effect on the cholinesterase activity of brain, heart, skeletal muscle, or submaxillary gland. The pseudocholinesterase activity of the intestine of rats was significantly decreased by doses exceeding 100 r of x-ray. The cholinesterase activity of the liver of female rats was decreased, but no effect was noted in the liver of male rats. The results of these experiments did not support the idea (186) that the decrease in cholinesterase activity of the intestine was an indirect effect resulting from an action by x-ray on the liver. Doull (189) also found an increase in the cholinesterase activity of the spleens of irradiated animals which occurred after sublethal and lethal doses of x-ray. Partial fractionation of the spleen (190) indicated that the increase in enzyme activity could not be entirely accounted for on the basis of destruction of cellular constituents containing low cholinesterase activity with a consequent apparent increase in activity of the whole tissue. The cause of the increase in cholinesterase activity of the spleen is a problem worthy of further study.

Feinstein *et al.* (191) found that 800 r of x-ray caused a decrease in the liver catalase of mice. The onset of this decrease occurred about 24 hr. after irradiation. Ludewig & Chanutin (110) were unable to find any change in the catalase activity of the livers of rats after 500 r of x-ray .Since relatively high doses of x-ray apparently do not produce consistent decreases in the activity of this enzyme in various species, it is difficult to attach significance to changes in catalase activity of tissues in connection with the mechanism of acute radiation damage at the present time. Thomson & Mikuta (192) have observed an increase in the tryptophan peroxidase-oxidase system of the livers of irradiated rats. The increase did not occur in adrenalectomized animals and was, therefore, considered as an indirect effect of x-ray. An increase in the xanthine oxidase activity of rat liver has been observed (155) after 600 r of x-ray, but this change was not evident until the fifth day after radiation. Choline oxidase activity of rat liver was not affected by 200 r to 600 r of x-ray *in vivo* (40, 155).

Summary

Although research on the biochemical effects of ionizing radiations has yielded a vast amount of information, no satisfactory explanation of the exact mechanism by which tissue damage is inflicted has yet been obtained. Research on the biochemical mechanism of radiation damage has been underway for a relatively short period of time. A considerable amount of research done on this subject during recent years was necessarily exploratory in nature. Many approaches to the problem of the mechanism of radiation damage to cells have been employed. A large number of the earlier studies dealt with *in vitro* systems. The information obtained from such studies has been valuable in indicating the chemical linkages and groups which are the most susceptible to alteration by ionizing radiations. However, attempts to apply

in vitro findings with ionizing radiations to intact cells have been generally disappointing. Biologists have, therefore, turned their attention to the more difficult task of attempting to define radiation damage in terms of interference with biochemical systems, through research on irradiated animals and microorganisms.

Many experiments have been performed on the gross aspects of carbohydrate, fat, and protein metabolism in irradiated animals. Changes in all of these phases of metabolism have been reported. However, the conditions under which experiments on intact animals have been done vary widely with respect to species, dose of radiation, and the time after exposure at which the measurements were made. In many cases the metabolic changes observed may be secondary to more important changes. This is especially likely when lethal doses are employed and when the measurements are made at time intervals approaching the end of the survival period. Findings made under these circumstances should be followed by additional measurements made with lower doses of radiation and at short time intervals after irradiation.

The search for the mechanism of action of ionizing radiations at the cellular and subcellular levels has proceeded along several different lines. Studies on tissue slices have provided a considerable amount of information on the actions of ionizing radiations on intermediary metabolism. More definitive information is now being obtained by studying isolated individual reactions in tissues taken from irradiated animals. The role which interference with enzyme reactions may play in acute radiation damage can be ascertained by systematic investigations in which due consideration is given to the dose of radiation, time of onset of the changes in enzyme activity, and the selectivity of the effects with respect to their occurrence in radiosensitive tissues. An enzyme alteration of primary importance in acute radiation damage should be detectable soon after radiation. Experience with other poisons has generally indicated that the important biochemical changes can be detected after sublethal doses. Therefore, it seems proper to assume that enzyme changes of importance in radiation damage should also be detectable after sublethal doses. Furthermore, the changes in a particular enzyme system in radiosensitive tissues should be more prominent than those in radioresistant tissues. At the present time it is not possible to ascribe radiation damage to interference with specific enzyme systems, but it is anticipated that future research based on knowledge accumulated in recent years will determine the extent to which enzyme alteration is involved as a primary factor in radiation injury.

LITERATURE CITED

1. Warren, S., *Ann. Rev. Physiol.*, **7**, 61 (1945)
2. Dobson, R. L., and Lawrence, J. H., *Ann. Rev. Physiol.*, **10**, 479 (1948)
3. Patt, H. M., *Physiol. Revs.*, **33**, 35 (1953)
4. Patt, H. M., *Ann. Rev. Nuclear Sci.*, **1**, 495 (1952)

5. Bloom, W., *Histopathology of Irradiation from External and Internal Sources* (McGraw-Hill Publishing Company, New York 18, N. Y., 808 pp., 1948)
6. Furth, J., and Upton, A. C., *Ann. Rev. Nuclear Sci.*, **3**, 303 (1953)
7. Sparrow, A. H., *Ann. N. Y. Acad. Sci.*, **51**, 1508 (1951)
8. Catcheside, D. G., *Ann. Rev. Physiol.*, **12**, 47 (1950)
9. Kimball, R. F., *Ann. Rev. Nuclear Sci.*, **1**, 479 (1952)
10. Ord, M. G., and Stocken, L. A., *Physiol. Revs.*, **3**, 356 (1953)
11. Lea, D. E., *Actions of Radiations on Living Cells* (The Macmillan Company, New York 11, N. Y., 402 pp., 1947)
12. *Physical and Chemical Aspects of Basic Mechanisms in Radiobiology*, Nuclear Science Series, No. 305 (National Research Council, Washington, D. C., 245 pp., 1953)
14. Fricke, H., *Cold Spring Harbor Symposia Quant. Biol.*, **2**, 241 (1934)
17. Dale, W. M., *Biochem. J.*, **34**, 1367 (1940)
22. Allsop, C. B., *Trans. Faraday Soc.*, **40**, 79 (1944)
23. Fricke, H., *Cold Spring Harbor Symposia Quant. Biol.*, **3**, 55 (1935)
24. Fricke, H., and Hart, E. J., *J. Chem. Phys.*, **2**, 824 (1934)
25. Fricke, H., Hart, E. J., and Smith, H. P., *J. Chem. Phys.*, **4**, 418 (1938)
26. Dale, W. M., *Biochem. J.*, **36**, 80 (1942)
27. Dale, W. M., *J. Physiol.*, **102**, 50 (1943)
28. Dale, W. M., *Brit. J. Radiol.*, **16**, 171 (1943)
29. Dale, W. M., Meredith, W. J., and Tweedie, M. C. K., *Nature*, **151**, 281 (1943)
30. Barron, E. S. G., Dickman, S., Muntz, J. A., and Singer, T. P., *J. Gen. Physiol.*, **32**, 537 (1949)
31. Tytell, A. A., and Kersten, H., *Proc. Soc. Exptl. Biol. Med.*, **48**, 521 (1941)
32. Barron, E. S. G., and Dickman, S., *J. Gen. Physiol.*, **32**, 595 (1949)
33. Byers, S. O., Tytell, A. A., and Logan, M. A., *Arch. Biochem.*, **22**, 66 (1949)
34. Schoenberg, M. D., Brooks, R. E., Hall, J. J., and Schneiderman, H., *Arch. Biochem.*, **30**, 333 (1951)
35. Forssberg, A., *Nature*, **159**, 308 (1947)
36. Bier, M., and Nord, F. F., *Arch. Biochem. and Biophys.*, **31**, 335 (1951)
37. Barron, E. S. G., *U. S. Atomic Energy Commission Document, CH-3654* (1946)
38. Doull, J., and DuBois, K. P., *Univ. of Chicago Toxicity Lab. Quarterly Progress Report No. 3*, p. 46 (1949)
39. Ballin, J. C., and Doull, J., *U. S. Air Force Radiation Lab. Quarterly Progress Report No. 10*, p. 44 (1954)
40. Kunkel, H. O., and Phillips, P. H., *Arch. Biochem. and Biophys.*, **37**, 366 (1952)
41. Sullivan, M. F., and DuBois, K. P., *U. S. Air Force Radiation Lab. Quarterly Progress Report No. 10*, 35 (1954)
42. Dinning, J. S., Meschan, I., Keith, G. K., and Day, P. L., *Proc. Soc. Exptl. Biol. Med.*, **74**, 776 (1950)
43. DuBois, K. P., Cochran, K. W., and Doull, J., *Proc. Soc. Exptl. Biol. Med.*, **76**, 422 (1951)
44. Potter, V. R., *Proc. Soc. Exptl. Biol. Med.*, **76**, 41 (1951)
45. Buffa, P., and Peters, R. A., *Nature*, **163**, 914 (1949)
46. Buffa, P., and Peters, R. A., *J. Physiol.*, (*London*), **110**, 488 (1950)
47. Liebecq, C., and Peters, R. A., *Biochim. et Biophys. Acta*, **3**, 215 (1949)
48. Elliott, W. B., and Kalnitsky, G., *Federation Proc.*, **9**, 168 (1950)
49. Potter, V. R., and Busch, H., *Federation Proc.*, **9**, 215 (1950)
50. Potter, V. R., and Busch, H., *Cancer Research*, **10**, 353 (1950)

51. Potter, V. R., Busch, H., and Bothwell, J., *Proc. Soc. Exptl. Biol. Med.*, **76,** 38 (1951)
52. DuBois, K. P., Cochran, K. W., and Zerwic, M. M., *Proc. Soc. Exptl. Biol. Med.*, **78,** 452 (1951)
53. Ord, M. G., and Stocken, L. A., *Proc. Soc. Exptl. Biol. Med.*, **83,** 695 (1953)
54. DuBois, K. P., Deroin, J., and Cochran, K. W., *Proc. Soc. Exptl. Biol. Med.*, **81,** 230 (1952)
55. Barron, E. S. G., Wolkowitz, W., and Muntz, J. A., *U. S. Atomic Energy Commission Document, MDDC Rept. 1241* (1947)
56. Lourau, M., and Lartigue, O., *Arch. sci. physiol.*, **5,** 83 (1951)
57. Goodman, R. D., Lewis, A. E., and Schuck, E. A., *Am. J. Physiol.*, **169,** 242 (1952)
58. North, N., and Nims, L. F., *Federation Proc.*, **8,** 432 (1950)
59. Ross, M. H., and Ely, J. O., *J. Cellular Comp. Physiol.*, **37,** 163 (1951)
60. Koch, R., and Bohlander, A., *Nuclear Sci. Abstr.*, **6,** 1383 (1952)
61. Levy, B., and Rugh, R., *Proc. Soc. Exptl. Biol. Med.*, **82,** 223 (1953)
62. McKee, R. W., *Federation Proc.*, **11,** 256 (1952)
63. Blair, H. A., *Nuclear Sci. Abstr.*, **6,** 4699 (1952)
64. Lourau, M., and Lartigue, O., *Arch. sci. physiol.*, **4,** 197 (1950)
65. Lourau, M., and Lartigue, O., *J. physiol. (Paris)*, **43,** 593 (1951)
66. Lourau, M., *Compt. rend. acad. sci.*, **236,** 422 (1953)
67. Denson, J. R., Gray, E. J., Gray, J. L., Tew, J. T., and Jensen, H., *Proc. Soc. Exptl. Biol. Med.*, **82,** 707 (1953)
68. Jugenburg, A., *Acta Radiol.*, **11,** 168 (1928)
69. Reding, R., *Cancer (Brussels)*, **12,** 9 (1935)
70. Kirschner, L. B., Prosser, C. L., and Quastler, H., *Proc. Soc. Exptl. Biol. Med.*, **71,** 463 (1949)
71. Smith, D. E., Tyree, E. B., Patt, H. M., and Jackson, E., *Proc. Soc. Exptl. Biol. Med.*, **78,** 774 (1951)
72. Smith, F., Buddington, W. G., and Grenan, M. M., *Proc. Soc. Exptl. Biol. Med.*, **81,** 140 (1952)
73. Mole, R. H., *Quart. J. Exptl. Physiol.*, **38,** 69 (1953)
74. Hasegawa, A., Taubman, J., and Landahl, H. D., *U. S. Air Force Radiation Lab. Quarterly Progress Report No. 10*, p. 87 (1954)
75. Hevesy, G., and Forssberg, A., *Nature*, **168,** 692 (1951)
76. Evans, T. C., Clarke, G., and Sobel, E., *Anat. Record*, **99,** 577 (1947)
77. Hursh, F. B., Van Valkenburg, P. A., and Mohney, J. B., *Radiology*, **57,** 411 (1951)
78. Botkin, A. L., Praytor, E. H., Austing, M. E., and Jensen, H., *Endocrinology*, **50,** 550 (1952)
79. Smith, W. W., and Smith, F., *Am. J. Physiol.*, **165,** 651 (1951)
80. Betz, H., *Compt. rend. soc. biol.*, **146,** 315 (1952)
81. Korson, R., and Botkin, A. L., *Nuclear Sci. Abstr.*, **7,** 6329 (1953)
82. Mole, R. H., and Batt, O. D., *Proc. Roy. Soc. Med.*, **46,** 250 (1953)
83. Barron, E. S. G., Flood, V., and Gasvoda, B., *Biol. Bull.*, **97,** 51 (1949)
84. Barron, E. S. G., Gasvoda, B., and Flood, V., *Biol. Bull.*, **97,** 44 (1949)
85. Barron, E. S. G., and Seki, L., *J. Gen. Physiol.*, **35,** 865 (1952)
86. Billen, D., Stapleton, G. E., and Hollaender, A., *Nuclear Sci. Abstr.*, **6,** 1079 (1952)
87. Tahmisian, T. N., *J. Exptl. Zool.*, **112,** 449 (1949)

88. Tahmisian, T. N., and Adamson, D. M., *J. Exptl. Zool.*, **115,** 379 (1950)
89. Tahmisian, T. N., and Adamson, D. M., *Anat. Record*, **108,** 516 (1950)
90. Sherman, F. G., and Chase, H. B., *J. Cellular Comp. Physiol.*, **34,** 207 (1949)
91. DuBois, K. P., Cochran, K. W., Mazur, M., and Doull, J., *Univ. of Chicago Toxicity Lab. Quarterly Progress Report No. 1*, p. 6 (1949)
92. LeMay, M., *Proc. Soc. Exptl. Biol. Med.*, **77,** 337 (1951)
93. Thomson, J. F., Tourtellotte, W. W., and Carttar, M. S., *Proc. Soc. Exptl. Biol. Med.*, **80,** 268 (1952)
94. Ashwell, G., and Hickman, J., *Proc. Soc. Exptl. Biol. Med.*, **80,** 407 (1952)
95. Fischer, M. A., Coulter, E. P., and Costello, M. J., *Proc. Soc. Exptl. Biol. Med.*, **83,** 266 (1953)
96. Iwatsuru, R., and Nanjo, K., *Biochem. Z.*, **300,** 429 (1939)
97. Reinhart, F. E., *Neutron Effects on Animals* (Williams & Wilkins Publishing Co., Baltimore 2, Md., 198 pp., 1947)
98. Prosser, C. L., *Radiology*, **49,** 299 (1947)
99. Ludewig, S., *Federation Proc.*, **9,** 198 (1950)
100. Ludewig, S., and Chanutin, A., *Am. J. Physiol.*, **163,** 648 (1950)
101. Norris, W. P., and Cohn, S. H., *J. Biol. Chem.*, **196,** 255 (1952)
102. Cohn, S. H., and Gong, J. K., *Am. J. Physiol.*, **173,** 115 (1953)
103. Gould, B. S., and Schwachman, H., *Am. J. Physiol.*, **135,** 485 (1942)
104. Franseen, C. C., and McLean, R., *Am. J. Cancer*, **24,** 299 (1935)
105. Norris, W. P., and Kisieleski, W. E., *Cold Spring Harbor Symposia Quant. Biol.*, **13,** 164 (1948)
106. DuBois, K. P., Cochran, K. W., Mazur, M., and Doull, J., *Univ. of Chicago Toxicity Lab. Quarterly Progress Report No. 1*, p. 8 (1949)
107. DuBois, K. P., Mazur, M., and Cochran, K. W., *Univ. of Chicago Toxicity Lab. Quarterly Progress Report No. 6*, p. 79 (1950)
108. Arvy, L., Boiffard, J. A., and Gabe, M., *Compt. rend. soc. biol.*, **143,** 223 (1949)
109. Gomori, G., *J. Cellular Comp. Physiol.*, **17,** 71 (1941)
110. Ludewig, S., and Chanutin, A., *Arch. Biochem.*, **29,** 441 (1950)
111. Petrakis, N. L., Ashler, F. M., and Ferkel, R. L., *Naval Radiological Defense Laboratory Report AD-126(B)* (1949)
112. Rév, K., Rév, L., and Vorteresz, V., *Acta Morphol. (Budapest)*, **1,** 467 (1951)
113. Ross, M. H., and Ely, J. O., *Am. J. Roentgenol. Radium Therapy*, **62,** 723 (1949)
114. Doyle, W. L., *Am. J. Anat.*, **87,** 79 (1950)
115. Petersen, D. F., Cotter, G. J., and DuBois, K. P., *U. S. Air Force Radiation Lab. Quarterly Progress Report No. 9*, p. 28 (1953)
116. Petersen, D. F., and DuBois, K. P., *J. Pharmacol. Exptl. Therap.*, **106,** 410 (1952)
117. Petersen, D. F., Deroin, J., and DuBois, K. P., *Federation Proc.*, **12,** 356 (1953)
118. DuBois, K. P., and Petersen, D. F., *Am. J. Physiol.*, **176,** 282 (1954)
119. DuBois, K. P., and Potter, V. R., *J. Biol. Chem.*, **150,** 185 (1943)
120. Cochran, K. W., Zerwic, M. M., and DuBois, K. P., *J. Pharmacol. Exptl. Therap.*, **102,** 165 (1951)
121. Ashwell, G., and Hickman, J., *J. Biol. Chem.*, **201,** 651 (1953)
122. Potter, R. L., and Bethell, F. H., *Federation Proc.*, **11,** 270 (1952)
123. Maxwell, E., and Ashwell, G., *Arch. Biochem. and Biophys.*, **43,** 389 (1953)
124. Carter, C. E., *Federation Proc.*, **8,** 351 (1949)
125. Hickman, J., and Ashwell, G., *Federation Proc.*, **12,** 66 (1953)

126. Florsheim, W. H., Doernbach, C., and Morton, M. E., *Proc. Soc. Exptl. Biol. Med.*, **81**, 121 (1952)
127. Florsheim, W. H., and Morton, M. E., *Am. J. Physiol.*, **176**, 15 (1954)
128. Marshak, A. J., *J. Gen. Physiol.*, **25**, 275 (1941)
129. Holmes, B. E., *Brit. J. Radiol.*, **20**, 450 (1947)
130. Holmes, B. E., *Brit. J. Radiol.*, **22**, 487 (1949)
131. Ely, J. O., and Ross, M. H., *Cancer Research*, **8**, 285 (1948)
132. Kelly, L. S., and Jones, H. B., *Proc. Soc. Exptl. Biol. Med.*, **74**, 493 (1950)
133. Kelly, L. S., and Payne, A. H., *Federation Proc.*, **12**, 76 (1953)
134. Harrington, H., and Lavik, E. S., *Federation Proc.*, **12**, 214 (1953)
135. Lutwak-Mann, C., *Biochem. J.* (*London*), **49**, 300 (1951)
136. Nicola, M., *Experientia*, **6**, 432 (1950)
137. Uyeki, E., *Federation Proc.*, **13**, 413 (1954)
138. Pohle, E., and Bunting, C. H., *Acta Radiol.*, **13**, 117 (1932)
139. Leblond, C. P., van Thoai, N., and Segal, G., *Compt. rend. soc. biol.*, **130**, 1557 (1939)
140. Leblond, C. P., and Segal, G., *Am. J. Roentgenol. Radium Therapy*, **47**, 302 (1942)
141. Ellinger, F., *Radiology*, **44**, 241 (1945)
142. Ellinger, F., *Science*, **104**, 502 (1946)
143. Chevallier, A., Burg, C., and Spehler, H., *Compt. rend. soc. biol.*, **147**, 497 (1953)
144. Ellinger, F., *Proc. Soc. Exptl. Biol. Med.*, **64**, 31 (1947)
145. Ellinger, F., *Radiology*, **50**, 234 (1948)
146. Smith, W. W., Highman, B., Mitchell, J. R., and Blount, H. C., Jr., *Proc. Soc. Exptl. Biol. Med.*, **71**, 498 (1949)
147. Coniglio, G., Darby, W. J., Wilkerson, M. C., Stewart, R., Stockell, A., and Hudson, G. W., *Am. J. Physiol.*, **172**, 86 (1953)
148. Buchanan, D. J., Darby, W. J., Bridgeforth, E. B., Hudson, G. W., and Efner, J. A., *Am. J. Physiol.*, **174**, 336 (1953)
149. Low-Beer, A., *Strahlentherapie*, **46**, 469 (1933)
150. Kohn, H. I., *Am. J. Physiol.*, **162**, 703 (1950)
151. Rosenthal, R. L., *Science*, **110**, 43 (1949)
152. Entenman, C., Neve, R. A., and Olmstead, C. A., *Federation Proc.*, **12**, 40 (1953)
153. Hewitt, J. E., Hayes, T. L., Gofman, J. W., Jones, H. B., and Pierce, F. T., *U. S. Atomic Energy Commission Document UCRL-1549* (1952)
154. Chanutin, A., and Gjessing, E. C., *J. Biol. Chem.*, **178**, 1 (1949)
155. Roth, J. S., Eichel, H. J., Wase, A., Alper, C., and Boyd, M. J., *Arch. Biochem. and Biophys.*, **44**, 95 (1953)
156. Del Buono, G., *Boll. soc. ital. biol. sper.*, **27**, 290 (1951)
157. Goldstein, M. J., and Neworaschkin, J. P., *Stahlentherapie*, **36**, 736 (1930)
158. Entenman, C., and Weinman, E. O., *Federation Proc.*, **11**, 44 (1952)
159. Lerner, S. R., Warner, W. L., and Entenman, C., *Federation Proc.*, **12**, 85 (1953)
160. Altman, K. I., Richmond, J. E., and Salomon, K., *Biochim. et Biophys. Acta*, **7**, 460 (1951)
161. Bacq, Z. M., Burg, C., Chevallier, A., and Heusghem, J., *J. physiol.* (*Paris*), **43**, 640 (1951)
162. Decker, A. B., and Mead, J. F., *Nuclear Sci. Abstr.*, **4**, 5565 (1950)

163. Cheng, A. L. S., Kryder, G. D., Bergquist, L., and Deuel, H. J., *J. Nutrition*, **48,** 161 (1952)
164. Deuel, H. J., Cheng, A. L. S., Kryder, G. D., and Bingemann, M. E., *Science*, **117,** 254 (1953)
165. Cheng, A. L. S., and Deuel, H. J., *Federation Proc.*, **12,** 410 (1953)
166. Brecher, G., and Waxler, S. H., *Proc. Soc. Exptl. Biol. Med.*, **70,** 489 (1949)
167. Smith, W. W., Chapman, W. H., and Alderman, I. M., *Am. J. Physiol.*, **169,** 511 (1952)
168. Gros, C., and Mandel, P., *Compt. rend.*, **231,** 631 (1950)
169. Gustafson, G. E., and Koletsky, S., *Am. J. Physiol.*, **171,** 319 (1952)
170. Stearner, S. P., Brues, A. M., and Christian, E. J. B., *Nuclear Sci. Abstr.*, **5,** 1723 (1951)
171. Cornatzer, W. E., Engelstad, O., and Davison, J. P., *Federation Proc.*, **12,** 192 (1953)
172. Brues, A. M., *Nuclear Sci. Abstr.*, **7,** 7 (1953)
173. Jennings, F. L., *Proc. Soc. Exptl. Biol. Med.*, **72,** 487 (1949)
174. Smith, W. W., Ackerman, I. B., and Alderman, I. M., *Am. J. Physiol.*, **169,** 491 (1952)
175. Schlesinger, M. J., *U. S. Atomic Energy Commission Document UR-279* (1953)
176. Feinstein, R. N., and Ballin, J. C., *Proc. Soc. Exptl. Biol. Med.*, **83,** 6 (1953)
177. Feinstein, R. N., and Ballin, J. C., *Proc. Soc. Exptl. Biol. Med.*, **83,** 10 (1953)
178. Tonhazy, N. E., White, N. G., and Umbreit, W. W., *Arch. Biochem.*, **28,** 36 (1950)
179. Brin, M., *Federation Proc.*, **11,** 190 (1952)
180. Rauch, R. F., and Stenstrom, K. W., *Gastroenterology*, **20,** 595 (1952)
181. Kwiatkowski, H., *Fermentforschung*, **15,** 138 (1936)
182. Barnard, R. D., *Med. Record*, **161,** 350 (1948)
183. Baglioni, T., and Piemonte, A., *Boll. soc. ital. biol. sper.*, **23,** 372 (1947)
184. Conard, R. A., *Am. J. Physiol.*, **170,** 418 (1952)
185. Conard, R. A., *Am. J. Physiol.*, **165,** 375 (1951)
186. Burn, J. H., Kordik, P., and Mole, R. H., *Brit. J. Pharmacol.*, **7,** 58 (1952)
187. Augustinsson, K., *Acta physiol. Scand.*, **15,** Suppl. 52, 1–85 (1948)
188. Sawyer, C. H., and Everett, J. W., *Am. J. Physiol.*, **148,** 675 (1947)
189. Doull, J., *J. Pharmacol. Exptl. Therap.*, **110,** 14 (1954)
190. Doull, J., and Cummings, O. K., *U. S. Air Force Radiation Lab. Quarterly Progress Report No. 10*, p. 59 (1954)
191. Feinstein, R. N., Butler, C. L., and Hendley, D. D., *Science*, **111,** 149 (1950)
192. Thomson, J. F., and Mikuta, E. T., *Proc. Soc. Exptl. Biol. Med.*, **85,** 29 (1954)

VERTEBRATE RADIOBIOLOGY (LETHAL ACTIONS AND ASSOCIATED EFFECTS)[1]

By John F. Thomson

Division of Biological and Medical Research, Argonne National Laboratory, Lemont, Illinois

Although the lethal actions of ionizing radiations on vertebrates have not heretofore been discussed under such a specific title in the *Annual Review of Nuclear Science*, various aspects of the subject have been recently surveyed by several authors (1 to 6). In addition, some 2100 abstracts of papers in radiobiology prior to 1952 have recently been assembled in convenient form (7). Hence, primary emphasis has been placed here on recent work concerned with radiation toxicology, modification of lethal effects, and mechanisms of lethal action.

Radiation Toxicity

Total-body x- and γ-radiation.—Reasonably complete information has been obtained on the LD_{50} (the amount of radiation required to kill 50 per cent of an animal population in a given time, generally 30 days) of single-exposure x-radiation for most common small animal species, with the exception of cats. Table I shows representative LD_{50} data. The 30-day LD_{50} for

TABLE I

LD_{50} of Single Dose X-Radiation For Several Animal Species

Species	LD_{50}(r)*	References and Comments
Guinea pig	250	(9); range 200 r (10) to 400 r (11)
Dog	315	Walker foxhounds, 2000 kvp (12)
Swine	350–400	Bilateral exposure, 2000 kvp (13)
Mouse	540–630	Range for six strains (14)
Monkey	~600	(15, 16)
Rat	665	Typical value (17); varies with strain
Ground squirrel†	700	(18)
Leopard frog	700	6-week mortality (19); 30-day value 780 r
Chicken	600–800	Adults (20); young more sensitive, show marked dose rate effects (21)
Rabbit	790	NL #1 strain (14)
Hamster	~800	2000 kvp (22)
Box turtle	~1000	4-month mortality (23)

* 100–250 kv., doses measured in air, 30-day observation period unless otherwise specified.

† *Citellus tridecemlineatus*; commonly but erroneously called the gopher.

[1] The survey of literature pertaining to this review was concluded in February, 1954.

man has been estimated as 400 ±100 r of 250 kvp. X-radiation [McLean *et al.* (8)]. Spear (6) suggests 500 r for man exposed to total-body γ-radiation.

Several recent studies on acute radiation mortality have employed γ-emitters, used either as single or multiple point sources. Rust *et al.*, using multiple Ta^{182} and Co^{60} sources of external γ-radiation (24), observed a 30-day LD_{50} for burros of 651 r at dose rates of 18 to 23 r/hr. (25, 26). Repeated exposures of nine burros to 400 r/day (Co^{60}) for ten days resulted in the deaths of all animals within one day after termination of exposure; one burro died after only four days of exposure (27). Thomson & Tourtellotte (28) estimated the 30-day LD_{50} for mice exposed to γ-radiation from a Co^{60} point source to be about 800 r for dose rates above 240 r/hr. Clark *et al.* (29) have found a somewhat higher value, 920 r, at a dose rate of 600 r/hr. Thus, the relative biological effectiveness (RBE) of Co^{60} γ-radiation in comparison with 200 kv. x-rays at similar dose rates is about 0.65 to 0.75 on the basis of mouse mortality.

Problems such as the effects of fractionated doses and variation in dose rate, although basically important in roentgen therapy in man and the object of considerable study with unicellular organisms, viruses, and *in vitro* systems, have not received as much attention in connection with mortality studies in higher animals.

Rajewsky *et al.* (30) have studied the survival of mice after x-irradiation at doses ranging from 250 to 160,000 r; from their data, as well as from similar data presented by Bonet-Maury & Patti (31), it is apparent that the decrease in life span is a function of both the total dose and the dose rate. At 190,000 r/min., half of the mice died during a 50 sec. exposure (30), as nearly an "instantaneous" death as can probably be produced by ionizing radiation.

The effect of varying dose rate on mouse mortality was studied by Thomson & Tourtellotte (28), who showed that for intensities between 37 and 2530 r/hr. (Co^{60} source) the increase in LD_{50} with decreasing intensity resembled a first-order process with a half-recovery, or half-accommodation, time of 25 hr.; but that at lower dose rates (< 6r/hr.) this simple treatment broke down. Tyree *et al.* (32) showed in preliminary tests that the survival of rats exposed to 900 r of 250 kv. x-radiation varied from 0 to 75 per cent over an intensity range of 34 to 5 r/min., the lethal efficiency dropping most abruptly in the range of 10 r/min. This phenomenon differs quantitatively from that obtaining with γ-irradiation in mice. The significance of these experiments is doubtful; it should be pointed out that the slope of the probit-dose curve decreases with decreasing dose rate (28), so that survival at a single dose does not permit an accurate description of dose rate effects on mortality unless the slope is known.

Thomson *et al.* (33) studied the lethal effects of exposure of rats, mice and guinea pigs to continuous γ-irradiation at rates varying from 15 to 140 r/day, and noted that for a given survival time the daily γ-ray doses delivered in the course of 24 hr. and the daily x-ray doses delivered in a few

minutes differed by a factor considerably greater than would be expected on the basis of specific ionization alone. Further, they showed that this factor (after correction for the specific ionization effect) was approximately the ratio between the single dose LD_{50} for mice exposed in 24 hr. and that for mice exposed in 3 hr. or less, i.e., about 1.5. In addition to this short-time dose attenuation, there is manifestly a long-time recovery factor, estimated from limited continuous exposures to be about 4, 8, and 11 per cent of the accumulated dose per day for guinea pigs, rats, and mice, respectively (33). These empirical factors are unsatisfactory at dose rates below 70 r/day of Co^{60} radiation.

The time factor in radiobiology has been discussed at some length by Kepp & Müller (34), who have emphasized the relationships between ion density and dose-rate dependence, and the difficulties in separating physical from biological time factors. It might be interesting to apply to higher animals the ultrafractionation technique subsequently used by these investigators and their associates for irradiating insect eggs and bacteria (35 to 37), whereby the intensity of the radiation is kept constant but by means of a rapidly rotating shield the radiation becomes an interrupted rather than a continuous beam. By altering both the size of the shield and the speed of its rotation, one could vary the time required to deliver a given dose of radiation while maintaining constant intensity during the actual exposure, in contrast to the usual time-intensity studies wherein both factors must be varied.

Partial-body irradiation.—Exposure of rats to a collimated 190 Mev deuteron beam has been described by Bond *et al.* (38 to 40). On the basis of mortality from local irradiation, the RBE was unity compared with local 250 kv. x-rays. Austin *et al.* (41), using the graying of mouse hair as an indicator, found no differences in effectiveness between 150 kvp. x-radiation and 17 Mev electrons. Court Brown & Mahler (42) studied sickness in man after local irradiation of the spine with integral doses ranging from 2.87 to 5.18 Mg. r. They noted that the time of onset of radiation sickness was significantly correlated negatively with both body weight and surface area, but not with total dose. Most of the recent experiments on partial-body x-irradiation of animals have been concerned with studies on physiologic mechanisms or protective effects, and are discussed elsewhere in this review.

Neutron irradiation.—Vogel *et al.* (43) have described an apparatus permitting the exposure of animals to either fast neutrons or Co^{60} γ-rays, or to both simultaneously in varying proportions. The evaluation of the RBE of neutrons in terms of x- or γ-radiation is complicated by the fact that for many criteria, such as mortality of animals, the response to neutrons is independent of dose rate while that to x- or γ-radiation is not. Bonet-Maury & Patti have shown that the shapes of the survival-time:dose curves are markedly different for neutrons and x- or γ-rays (31).

In terms of mouse (29) or chicken (44) mortality, the RBE is about 4 in comparison with γ-radiation delivered in the course of 3 hr., but rises to about 6 when the exposure time for LD_{50} is 24 hr. (45). The RBE of fast neu-

trons versus γ-radiation is about 20 on the basis of incidence of cataracts in exposed mice (46). These workers have noted with mixed neutron and γ-radiation a synergistic rather than a simple additive effect, the potentiation becoming maximal when the γ component of the radiation represented one-third or less of the total rep administered (47). The reasons for this departure from simple additivity are not known. Storer & Harris, on the other hand, did not observe this potentiation with animals exposed simultaneously to x-rays and thermal neutrons (48). The Los Alamos group reported values for thermal neutron RBE's of 1.70 for lethal effects (49), 1.7 for mitotic inhibition (50), 1.25 for loss in spleen and thymus weight (51), and 15 for production of lens opacities (52).[2]

Patt *et al.* (54) obtained protection with cysteine against fast neutrons, but found it less effective than against γ-rays; pointing out the inverse relationships between ionization density and both cysteine protection and the oxygen effect, these authors interpreted their observations in terms of the spatial distributions and subsequent reactions of free radicals formed in water. Storer *et al.* noted that glutathione and *p*-aminopropiophenone, both of which were effective prophylactically against x-radiation, failed to protect against thermal neutron-irradiated mice (55), despite the rather high γ component of the exposure. It is reported that, in contrast to x- or γ-radiation, fast neutrons are more lethal to males than to females [Neary *et al.* (56)].

The effects of neutrons and x- or γ-rays on the lens have recently been studied by several investigators. The great susceptibility of mice to cataracts has been shown by Upton *et al.* (57), who reported for x-radiation a threshold dose of 15 r; after 45 r the incidence of cataracts approached 100 per cent. Dogs are much more resistant, to judge from the work of Moses *et al.* (58), who failed to observe cataracts in dogs exposed to 60 to 150 N of fast neutrons (6 to 8 Mev.). Doses of 810 to 900 N produced cataracts within two years in 60 to 75 per cent of the eyes exposed; 1500 N resulted in complete necrosis of the globe, orbit, and surrounding structures in less than three months. In rabbits, 33 to 100 N resulted in cataract formation within two to five months; weekly exposures to 3.1 N for 17 to 27 weeks did not, however, produce any abnormalities of the lens (58), an indication of a fairly efficient recovery process.

In humans exposed to 100 or 200 kv. x-radiation, the threshold dose is about 600 r, with a latent period of one to ten years after exposure (59). Fillmore found 78 Hiroshima patients with presumably radiation-induced cataracts five years after exposure; the cataracts represented the only late effects attributable to irradiation (60).

Little work has been done on the mechanisms of cataract formation. That the effect is primarily a local one, attributable to direct exposure of the

[2] These investigators have published a detailed account of the dosimetry problems encountered in their thermal neutron exposures (53); the results of their biological studies were scheduled to be published in a subsequent issue of *Nucleonics*, not yet available at the time of conclusion of this review.

lens, has been shown by the shielding experiments of Upton *et al.* (57) and Alter & Leinfelder (61). Zeller (62) reported that the lens contains little catalase; this observation would presumably be of significance only if H_2O_2 were formed in appreciable quantity in the lens as a result of ionizing radiation, and if there were a correlation between tissue radiosensitivity and catalase content. Permutt & Johnson (63) believe that x-rays and slow neutrons depolymerize the protein-polysaccharide components of the lens. Pirie *et al.* (64) found that x-radiation produced a decrease in glutathione reductase and a concomitant decrease in reduced glutathione in the lens; ultimately the total protein sulfhydryl concentration was diminished. Further work by these authors [cited by Gray (65)] has revealed that other sulfhydryl enzymes also decrease in concentration during the course of development of opacity, but are not immediately altered; hence it appears that inhibition of synthesis of new enzymes, rather than inactivation of those present at the time of irradiation, is of primary importance.

Internal radiation.—Stokinger (66) has discussed various mechanisms which regulate the distribution of an element in the animal body, and has pointed out how the size of the administered dose may affect tissue distribution of (*a*) those elements which exist as colloidal cations subject to phagocytosis by the reticulo-endothelial system; and (*b*) those, such as I and Fe, the distribution of which is governed at least in part by the activity of organ-specific biochemical systems, i.e., thyroxin and hemoglobin synthesis. These factors should be borne in mind in the interpretation of data on toxicity of many radioactive elements. That P^{32} is distributed independently of the dose administered was shown by Bhattacharya *et al.* (67), who noted no differences in relative concentrations of P^{32} in rat tissues over a 15-fold range of dosage.

Finkel *et al.* (68) have presented information on the toxicity, distribution, and retention of Po^{210} in mice; the 30 day LD_{50} for single intravenous injection was 30 to 40 μc/kg. Although the liver contained the largest amount of polonium, the spleen showed the highest concentration per unit weight tissue. Blair (69) has estimated that in comparison with x-radiation, the α-radiation from Po^{210} has an RBE of 3 for acute effects and 60 for chronic effects. On the basis of chronic toxicity, Po is five times as toxic as radium according to Blair (69), three times according to Finkel (70). Finkel (70) has further assigned effectiveness ratios, at the near-tolerance level, of seven, two, and one to Pu^{239}, U^{232}, and U^{233} respectively, in comparison with Ra.

The distribution and toxicity of At^{211} have been studied by Hamilton *et al.* (71). At^{211} is highly toxic to the thyroid, in which organ it is localized, although to a lesser extent than is I. The maximum amount given to rats, 150 μc, killed one animal out of four; the corresponding dose was estimated to be 135 rep (neglecting the amount taken up by the thyroid and assuming otherwise homogeneous distribution). The hematologic picture at this dose resembled that produced by 600 r of 200 kv. x-rays; hence an RBE of 4 to 5 can be inferred, although the precision of this figure may be no better than

±2. For thyrotoxic effect, the RBE was about 20 to 25, compared with x-rays.

Recent studies with I^{131} have emphasized its effect on the ovaries as well as on the thyroid (72). Rugh (73) has produced complete and permanent sterilization in suckling female mice (but not in males) by feeding I^{131} to the mother; the maximum amount received via the milk was 30 μc. In adult rats, irregularities in the estrus cycle were produced by as little as 20 μc. [Tillotson *et al.* (74)]; doses above 1000 μc. per mouse produced temporary anestrus. However, as judged by the production of normal offspring, complete recovery occurred, even after 2000 μc. The greater sensitivity of the ovaries of immature animals to I^{131} parallels the results of total-body x-radiation studies on mortality (75).

Cancericidal potentialities of Ga^{72} and of Au^{198} have prompted extensive studies of these isotopes. Brucer *et al.* (76) have summarized the radiochemical, toxicological, and clinical properties of Ga^{72}. Although most of the acute toxic effects of Ga^{72} can be attributed to the toxicity of the stable isotope, repeated intravenous administration of 1 to 7 mc./kg. twice a week produced a leucopenia not obtained by equivalent amounts of stable Ga (77). Further, although both stable and radioactive Ga produced gastrointestinal effects, these manifestations appeared sooner with the latter. A striking species difference in mortality was noted between dogs and rats, the former being at least twelve times as sensitive to Ga as the latter (78).

Clinical applications of Au^{198} have been discussed by Meyers *et al.* (79) and Andrews *et al.* (80). Meneely *et al.* (81) have followed body distribution, pathologic effects, and survival in dogs given Au^{198} transbronchially. Hahn *et al.* (82) found that repeated bleeding of dogs renders them sensitive to the production of ascites and liver cirrhosis after hepatic doses of 15,000 to 30,000 rep of β-radiation from Au^{198} injected intravenously in two doses four to six weeks apart. Liver doses of as much as 80,000 rep were normally tolerated by healthy adult dogs. The splenotoxic action of Au^{198} in mice is borne out by the studies of Friedell *et al.* (83). Splenectomy increased the toxicity of P^{32} and Sr^{89}, but not of Au^{198}. The mortality produced by simultaneous administration of both Au^{198} and P^{32} was also not affected by splenectomy, since Au^{198} effectively eliminates the spleen as a potential protective mechanism. Harel (84) reported liver damage with histologic indications of cancer, following intraperitoneal injection of Au^{198}.

Pinson *et al.* (85) have studied the percutaneous absorption of tritium water, both liquid and vapor, and have concluded that absorption through the total skin surface (ignoring the effects of clothing) would be nearly equal to the absorption via the lungs. Using the depression of incorporation of Fe^{59} into erythrocytes as an index, Furchner *et al.* have shown that the β-radiation from tritium oxide is 1.59 times as effective as Co^{60} γ-radiation (86).

Intragastric irradiation by a number of β-emitters has been described by

Littman *et al.* (87). Doses above 5000 rep to the wall of the stomach were found to be lethal. Although they used small numbers of animals, these investigators noted that gastrectomy following exposure could prevent death, an indication that mortality from intragastric β-irradiation is largely attributable to effects secondary to local radiation trauma. Smaller doses of intragastric β-radiation diminished gastric acidity (88).

Attempts to detoxify radioactive substances deposited internally have not been especially rewarding. Hamilton & Scott (89) concluded that the Ca salt of ethylenediamine tetraacetic acid (EDTA; Versene) offered negligible advantage in the treatment of chronic plutonium poisoning. Cohn & Gong (90) similarly found no effect of EDTA on removal of Sr^{89} deposited in the skeleton. Favorable effects have been reported in the removal by EDTA of La^{190} [Hart & Laszlo (91)] and of Y^{90} [Cohn *et al.* (92)] from rats; however, in both instances the decontaminating agent was given very soon after administration of the radioisotope. Hackett (93) reported that repeated injections of zirconium citrate had little effect on tissue distribution of plutonium when administration was begun 32 days after plutonium injection; in confirmation of previous work, she observed that immediate initiation of treatment led to a marked decrease in deposition of plutonium in bone with an elevated concentration in soft tissues. 2,3-Demercaptopropanol (BAL) was found to have no effect on distribution or excretion of plutonium [Kawin & Copp (94)]. In general, it would seem that the use of complexing agents such as EDTA or BAL offers little hope of removing radioactive substances already deposited in the skeleton, although immediate treatment after contamination may be beneficial (89, 95). In any case, the possibility must be considered that attempts to alter the distribution of a toxic metal may result in an increased toxicity by facilitating a redistribution from a relatively insensitive locus to a more susceptible one; such a phenomenon was recognized some years ago in the use of dithiols to detoxify Pb (96) and Cd (97).

Attention is directed to methods of surveying human subjects for residual radioactivity by the use of high pressure ionization chambers (98) and liquid (99) or crystal (100) scintillation detectors.

Factors Modifying Toxicity

Trauma and stress.—Cassen & Kistler (101) found that pulmonary edema in rats resulting from experimental blast injury was enhanced by prior x-irradiation. Alpen & Sheline (102) showed that sublethal x-ray doses increased mortality in rats previously scalded by immersion in hot water, and that the area of burned skin necessary to cause death was smaller in x-irradiated animals than in controls. Parr *et al.* (103) have also observed a potentiation of x-ray lethality by thermal burns.

On the other hand, major surgery in dogs (resection of the ileum) did not noticeably increase mortality after x-irradiation [Gustafson & Cebul (104)]. In contrast to previous claims by Allen *et al.* (105), Miller *et al.* (106) have

reported that irradiated dogs are no more susceptible to transfusion than are normal animals, provided reasonable caution is taken to insure compatibility.

The work of Kimeldorf and his associates have shown that violent exercise increased the susceptibility of rats to lethal effects of x-radiation (107); conversely, x-ray exposure decreased the resistance of rats to fatigue (108). Further, a decrease in volitional activity occurred immediately after exposure to doses of 200 to 1000 r (109). At high doses, there was steady decrease until death; at lower doses there was a return to normal activity within five days. Intermediate doses produced a biphasic effect, with a second depression in activity occurring about three weeks after exposure.

Diet.—The increased survival of chronically irradiated rats fed supplements of either methyl linoleate or cottonseed oil has been discussed by Deuel *et al.* (110, 111). Cottonseed oil did not alter acute effects (110). Paris & Vevasseur (112) stated that a diet of fodder beets, turnips, spinach, carrots, or green cabbage increased radiosensitivity of rabbits, whereas red beets, lettuce, or red cabbage increased their resistance to x-rays. Duplan (113) had previously reported that guinea pigs given carrot supplements prior to irradiation were more radiosensitive than others given cabbage (color not specified). Smith (114) was unable to improve the survival of x-irradiated rats by force feeding various diets. Schlesinger (115) observed that the mortality in rats receiving 250 r one week after an initial exposure to 400 r was increased when the animals were placed on a protein-free diet after the first exposure.

Endocrines.—The action of radiation on the endocrines and the influence of endocrine secretions on the development of the radiation syndrome continue to be investigated, with considerable emphasis on the adrenals. Langendorff & Lorenz (116) have demonstrated a response of the adrenal cortex even after local irradiation of the hypophysis, testes, or thigh of rats. Palazzi (117) found that the alkaline phosphatase of the gut was decreased by x-rays to a greater extent in adrenalectomized rats than in normals. According to Betz (118), adrenalectomy increased hematopoietic regeneration after 500 r (but not 800 r), provided the adrenals were removed through the back of the animal rather than through the more traumatizing ventral approach. Thomson & Mikuta (119) noted a two-fold increase in tryptophan peroxidase of rat liver within four hours after exposure to 1000 r x-radiation; the fact that this increase could be entirely prevented by prior adrenalectomy but not hypophysectomy casts some doubt on the universal application of the general adaptation syndrome in interpretation of radiation pathology (38, 120, 121).[3]

[3] Betz (120) has proposed that the lesions produced by radiation are relatively immaterial insofar as their contribution to the death of the animal is concerned. According to Betz, death is due to the disturbance of the general adaptation syndrome; such a conclusion is tantamount to saying that the animal dies, not because

Hochman & Bloch-Frankenthal (122) confirmed that the ascorbic acid of rat adrenals was rapidly depleted after irradiation; their observation that the extent of the depletion was not dose-dependent is consistent with current views on the "permissive" role of the hormones of the adrenal cortex in response to various stresses (123). Decreases in tissue ascorbic acid were also reported by Oster *et al.* (124), who claimed that, in addition to endocrine mediation, direct destruction of ascorbic acid by x-irradiation occurred in one strain of rats. Oster *et al.* did not, however, present evidence of a dose dependence, which would be expected if direct radiation destruction were involved.

Except for the gonads, the endocrines themselves are generally considered radioresistant. Rugh *et al.* (125) gave massive doses of x-radiation to hamsters without producing especially dramatic histologic effects in the endocrine tissues. Korson & Botkin (126), on the other hand, reported histologic changes in the rat pituitary which they attributed to decreased thyrotropic and increased adrenocorticotropic function. However, Allen *et al.* (127) found that more than 20,000 r was required to alter thyrotropic function in tadpoles; and Sommers (128) concluded from his experiments with parabiotic rats that the gonadotropic, adrenocorticotropic, somatotropic, and thyrotropic activities of the hypophysis were unaffected or slightly stimulated, provided the adrenals were intact. Similarly, Westman (129) reported that local irradiation of the pituitary (2,000 r) produced little or no interference with sexual development in young rats. The observations on human subjects by Hecht *et al.* (130), that irradiation of the pituitary-midbrain area altered the permeability of the cutaneous vascular bed, are of doubtful significance as far as pituitary activity is concerned.

Some recent experiments have raised a question about the radiosensitivity of the thyroid. In contrast to most previous investigators [see Furth & Upton (4)], Tusques *et al.* have detected histologic changes in the thyroids of rats exposed to 600 r (131). Landau *et al.* (132) reported that local x-irradiation of the thyroid after administration of I^{131} led to a decreased discharge of I from the gland. Monroe *et al.* (133), although they demonstrated an increased uptake of both protein-bound and thyroxin iodine one day after exposure of rats to 500 r of x-rays (but not at 7 or 37 days after irradiation), failed to observe histologic changes at any time. They concluded that the thyroid response was referable to pituitary effects, and that the extent of the response was dependent on the nature, amount, and possibly the rate, of exposure. Mole & Batt (134) reported a decreased uptake of I by the rat thyroid three days after irradiation (600 to 1000 r) concomitant

---

radiation produces irreparable cellular damage, but because he cannot adapt himself to live in the presence of the damage wrought by exposure. It is sufficient to point out that postirradiation administration of agents such as the adrenocortical steroids, which are considered to improve the capacity for adaptation, have been abysmally unsuccessful in averting death in irradiated animals.

with a 25 per cent elevation in the metabolic rate (135); they feel that the former phenomenon is attributable to effects of radiation on neither the thyroid nor the pituitary, but on the abdomen (136).

Most of the endocrine hormones have previously been found to be valueless or even harmful when administered to animals before or after irradiation (1, 5). Somatotropic hormone (STH), however, was reported by Lacassagne & Tuchman-Duplessis (137) to prevent radiation mortality in rats when given in six daily doses of 1 mg. (near the lethal range) either before or after x-irradiation; in guinea pigs, only a prophylactic action was observed. On the other hand, Gordon *et al.* (138) found not only a lack of curative action of STH in rats maintained on 0.6 mg./day after exposure, but also an apparent antagonism by STH of the beneficial effects of streptomycin. Betz (139) found STH to be of no value in promoting hematopoietic regeneration in normal rats exposed to 800 r; in adrenalectomized rats maintained on cortisone, STH stimulated hematopoiesis. A pituitary preparation known as Gonadophysin, containing both follicle-stimulating and luteinizing hormones, accentuated testicular atrophy and inhibited regeneration when administered to irradiated male rats (140).

Postirradiation infection.—In 1950 Miller *et al.* showed that penetration of the blood stream by bacteria normally confined to the intestinal tract was an important postirradiation sequel (141), and that administration of antibiotics, notably streptomycin, was often effective in preventing death of irradiated mice (142). This field has by now attracted the attention of many investigators approaching the problem of postirradiation infection from various aspects. Current papers describe an increased sensitivity to bacteria (143, 144), toxins (145), and viruses (146); altered immunologic responses (147 to 151); impairment of phagocytic function (152, 153) [but see (154)]; and a decreased bactericidal action of serum (155) in irradiated animals.

Recent work on antibiotic prophylaxis and therapy has been reported by Smith *et al.* (143, 156, 157), Coulter & Miller (158), Furth *et al.* (159), and Gustafson & Koletsky (160), with varying degrees of success. Enhancement of the efficacy of antibiotics in irradiated mice has been shown by Marston *et al.* (161) with extracts of spleens of immature animals, and by Genaud & Meot (162) with serum from anemic horses which reputedly contains a hematopoiesis-stimulating hormone.

Prophylaxis and therapy.—Considerable attention has been devoted to the protective action of β-mercaptoethylamine (163 to 165), referred to hereafter as cysteamine (166). Although on a molar basis it is more effective than cysteine, it is also more toxic (165), so that the therapeutic indices would appear to be similar. Bacq *et al.* (163) suggested that cysteamine acts primarily through the liver, a view supported by Kaplan & Lyon (167), solely because they were unable to protect mice from genetic effects of irradiation by cysteamine. Patt, however, feels that the evidence on which Bacq *et al.* based their suggestion is inconclusive (5). As yet there seem to be no decisive, unequivocal data to convince one that the differences between cys-

teamine and cysteine are other than quantitative, referable to differences in distribution and in rates of absorption and destruction. Whether the protective effects of cysteine and cysteamine are additive or not is not established: Straube & Patt (165) presented clear-cut data to show a simple additive effect, while Salerno & Friedell (168) stated no additivity existed in either toxic or protective effects. The evidence (169) that x-radiation destroys coenzyme A (CoA) *in vivo*, and that the administration of cysteamine before radiation results in increased CoA concentration in the liver, seems tenuous indeed.[4] An indication that at least one acetyl transfer mechanism is not affected by radiation is the lack of impairment in the capacity of rats to acetylate p-aminobenzoic acid or sulfanilamide at any time during the first 72 hr. after exposure to 1000 r (171). CoA protected mice when given prior to exposure (172); the preparations used were highly toxic, however.

Enhancement of the beneficial effects of liver shielding by cysteamine given after irradiation has been claimed by Maisin *et al.* (173, 174). Straube & Patt (165) failed to confirm this curative action of cysteamine. However, some subsequent communications by the Louvain group (175, 176) indicated the importance of starving the animals 48 hr. before exposure, a condition not mentioned in their earlier papers. Whether the fact that Straube and Patt fed their animals *ad libitum* was responsible for their inability to confirm this work is not known. A combination of cysteamine and thymic extracts given to guinea pigs after irradiation has been reported curative by Gros (177).

Recent studies on the therapeutic effects of tissue extracts include those of Hilfinger *et al.* (178) who were able to protect rabbits by injection, three days after exposure, of not only a homologous bone marrow emulsion but the supernatant fraction of the emulsion as well.[5] Cole *et al.* (179), on the other hand, found that the most active fraction of splenic extracts was the most easily sedimentable portion; although their active preparation contained cell nuclei plus a few intact cells, the fact that they used a suspending medium containing an electrolyte suggests strongly that the nuclei were contaminated with appreciable quantities of agglutinated cytoplasmic particulates. Nevertheless, the loss of protective capacity of their preparation after incubation with desoxyribonuclease (180) seemingly established the significance of the nuclear components. This group has reported that, like spleen shielding, bone marrow injections are less effective in rats than in mice (181). Kelly & Jones have noted, with mashes of embryonic tissue, marginal protective effects which they attribute to a stimulation of DNA metabolism (182). Several recent papers have been concerned with the effects of tissue extracts primarily on hematopoietic regeneration (183 to 185).

[4] Although cysteamine is a component of CoA, recent work indicates that cysteamine cannot replace cysteine or cystine in the biosynthesis of this substance (170).

[5] There is an unfortunate ambiguity in this paper because of a curious omission of any mention of early deaths in the treated groups of rabbits prior to initiation of treatment.

Newer studies on the protective effects of partial body shielding include those of Swift *et al.* (186) on alternate shielding of two sections of an animal in successive exposures. Protection was obtained whether the spleen alone was shielded during the first exposure and the remainder of the animal except for the spleen protected during the second, or vice versa. Van Lancker has observed improved hematopoietic regeneration in rats with shielded femurs (184), livers (187), and spleens (185).

Parabiosis, a protective technique akin to both shielding and administration of tissue extracts, has been studied by Finerty *et al.* (188 to 190), who have shown that adrenalectomy, hypophysectomy, or splenectomy of the nonirradiated partner does not detract from the protective effect. Further, although their best results were obtained when the animals were joined within a few hours after exposure, some protection was still furnished even when the union was deferred for as long as four days after irradiation.

Cole & Ellis showed that sodium nitrite, protective in mice but not in rats, acted additively with cysteine but not with ethanol in protection against x-irradiation, a finding implying identical loci of action for ethanol and sodium nitrite (191). Mefferd *et al.* (192) reported that a bacterial pyrogen with the proprietary name of "Piromen" was beneficial to mice when given prior to x-irradiation, but deleterious after exposure. Other compounds reported to have protective effects are methacholine and carbaminoyl choline (193), succinonitrile (194), malonitrile (*sic*) (31),[6] cobalt (196), and "coal gas" (31), the beneficial component of which is probably carbon monoxide.

Generally, most experiments on protection have been limited to an assessment based on reduction of mortality over a 30-day period after exposure. Bennett *et al.* (197) have presented data on the long-term survival of rats protected from acute lethality by anoxia; they recorded a marked decrease in life expectancy, with an increase in frequency of deaths due to pneumonia. More observations of this type would be desirable.

A number of candidates for prophylaxis or therapy have been described as useless or even deleterious in counteracting radiation effects, i.e., polyvinylpyridone (198), citrovorum factor (199), oxypolygelatin (200), allylthiourea (201), tocopherols (202), miscellaneous autonomic drugs (203 to 205), catalase, propylthiouracil, chlorol, guanidine, and several proprietary remedies with various pharmacologic properties (31).

The demonstration that temperature- and oxygen-dependent changes occur in nucleic acids (206), unsaturated fats (207), and proteolytic enzymes (208, 209) after irradiation of these substances *in vitro* suggests that there exists a possibility of successfully averting these delayed effects. However,

[6] It seems likely that Bonet-Maury & Patti meant malononitrile $CH_2(CN)_2$ which had been previously found to be effective by Bacq & Herve (195), rather than malonitrile ($NC \cdot CH_2 \cdot CHOH \cdot CN$), a compound which so far as can be ascertained has never been employed in any biological experiments.

aside from antibiotics to control postirradiation infection, tissue extracts to promote hematopoietic regeneration, and assorted pharmacologic agents (generally valueless per se in preventing mortality) to provide symptomatic palliation, nothing especially promising has been unearthed for successful treatment, after exposure, of radiation damage in higher animals. The use of protective agents prior to irradiation has been more fruitful in decreasing radiation mortality; however, at least for the present, total-body shielding is the only protective measure which this reviewer would trust implicitly for himself.

Studies on the Mechanisms of Lethal Action

The physico-chemical events following irradiation of biological material have recently been summarized by Gray (65). Under aerobic conditions, radicals are formed which, although potential reducing agents, interact with dissolved oxygen to become oxidizing agents. These free radicals may diffuse from their point of origin along the ionization track to critical biological loci, or, as seems probable in the case of the highly reactive OH and HO_2 radicals, may generate less reactive but longer lived radicals which can produce chemical changes of biological significance at some distance from their point of origin. Direct inactivation of critical cellular components, although less probable, is not to be ignored; however, our knowledge of such events is lacking.

Of the events between the primary ionization and the manifestation of physiologic changes in an irradiated animal our knowledge is almost negligible. Mole (136), who has perhaps overstated his case somewhat, has argued for this reason that total-body x-irradiation is more nearly medicine, rather than radiobiology, and that at least for the present our understanding of the lethal actions of ionizing radiation in higher animals is not helped and is possibly hindered by what he calls "radiobiology," i.e., studies on *in vitro* systems, viruses, unicellular organisms, etc.

The great diversity of symptoms of radiation injury described in different species, or even in the same species under different conditions of irradiation, complicates tremendously our understanding of basic mechanisms. For example, the mammalian kidney is generally considered radioresistant; local exposure to 2000 r or more produces only marginal alterations in function (210). In young birds, however, local irradiation of the kidney with 1000 r results in profound morphologic and functional deterioration, with death from renal failure ensuing in a matter of hours (211). To becloud the picture still further, death from renal failure does not occur in adult birds, or in young birds exposed at low dose rates (21). Rajewsky *et al.* (30) showed that after exposure of mice to doses greater than 50,000 r (fatal in 24 hr. or less) the animals became hyperirritable, finally going into tonic and clonic convulsions. This behavior is in contrast to the terminal apathetic state of animals exposed to 1200 to 12,000 r (death in three to four days). Additional evidence of central nervous system (CNS) involvement after high doses,

not noted in the 30-day LD_{50} range, was reported by Andrews & Brace (212) in guinea pigs receiving 25,000 r in eight hours. These authors suggest on the basis of shielding experiments that the CNS effects are indirect or "abscopal" (136). Alterations in the weight and hematologic responses of rats given total-body or partial-body x-irradiation or internal β- or γ-irradiation were described by Lamerton *et al.* (213, 214). Smith & Tyree (215) similarly reported that the weight loss and reduced food intake in irradiated rats varied with different patterns of partial-body shielding. Whether a single radiosensitive protoplasmic constituent can be so altered to initiate a chain of successive metabolic imbalances, conditioned in turn by physiologic mechanisms peculiar to the species and the mode of radiation to produce characteristic and differentiated syndromes, is a point which has thus far successfully eluded experimentation.

The hypothesis of production by radiation of specific toxic substances (different from endocrine and neurohumoral compounds) responsible for deleterious effects has generally been in disfavor in recent years (216); however, Court Brown & Mahler (42) have suggested, without direct evidence, that radiation sickness in man is attributable to such a diffusible factor. Lavik *et al.* (217) have shown that survival of lethally irradiated dogs is not enhanced by diverting the circulating blood through an artificial kidney (*in vivo* dialysis); this observation, of course, does not rule out the presence of a nondialyzable toxin.

Nucleic acids.—An effect of ionizing radiations on desoxyribonucleic acid (DNA) has long been favored because of association of this macromolecule with genic material, its rapid disappearance *in vivo* in radiosensitive organs, and its susceptibility to depolymerization by radiation *in vitro*. Recently Epstein (218) calculated that for small viruses the nucleic acid volume is nearly identical with the target volume. However, despite the excellent studies on depolymerization and degradation of DNA *in vitro* by ionizing radiations (206, 219 to 222), it is felt that the applicability of such experiments to an understanding of *in vivo* effects is not readily apparent. On the other hand, these and other experiments, such as the observations on depolymerization of polymethyl methacrylate (223 to 225) and the polymerization of acrylonitrile (226) by radiation, are of interest in the field of radiation chemistry, and may possibly serve to test chemical protective agents.

It seems more likely that impaired DNA synthesis is of more significance than an accelerated destruction. In a recent review of biochemical effects of radiation, Ord & Stocken (3) concluded that disturbances in energy metabolism are of considerable importance as underlying causes for the complex manifestations of radiation damage in biological systems. It seems necessary to point out here that impairment of energy utilization, such as decreased esterification of inorganic phosphate with resultant interference with synthetic properties contingent on high-energy phosphate bonds, should be expected to be manifested in a generalized breakdown of anabolism; this is

not entirely the case in tissues of irradiated animals. On the basis of P^{32} incorporation, DNA synthesis has generally been found to be much more susceptible to interference by radiation than ribonucleic acid (RNA) synthesis (227 to 230). In rabbit bone marrow (231) and in mouse liver (232) decreased concentrations of both DNA and RNA have been observed. In the former case, however, the decrease in RNA could be attributed to the selective elimination of myeloid elements containing high concentrations of RNA. The alteration in distribution of cell types after irradiation also complicates the interpretation of results obtained on the rate of incorporation of P^{32} into nucleic acids of rat bone marrow and spleen (230).

Gros *et al.* (233) were able to prevent the decrease in DNA and RNA of irradiated rat spleen by pretreatment with cysteamine. Parr *et al.* (234) have made similar observations with cysteine and the intestinal mucosa. These observations seem referable to the general protective action of these compounds (2).

Other metabolic effects.—Mole (135) has reexamined the effect of x-irradiation on the basal metabolic rate of rats, and reported no change during the first three days. On the fourth day, a 25 to 35 per cent increase was noted in rats receiving >800 r; a much smaller increase was seen after <600 r. The increase with higher doses took place despite impairment of thyroid function (134).

Brace (235) showed that development of radiation damage in marmots is greatly delayed in hibernation. These results confirm earlier data on amphibia [see (2)]. Doull & DuBois (18) have made similar observations with ground squirrels: although in hibernation the survival time after irradiation is greatly increased, the ultimate survival is not altered. These authors also observed that ground squirrels irradiated at room temperature did not hibernate when returned to a 5°C. environment.

Although the liver is considered to be radioresistant from a histologic standpoint, numerous metabolic aberrancies associated with liver dysfunction have been noted, particularly in connection with carbohydrate and fat metabolism. Further, the beneficial effects of shielding this organ during irradiation suggest a greater role of the liver in the development of injury and the repair of radiation damage than has hitherto generally been considered. Both Nims & Sutton (236) and Schwarz *et al.* (237) have described in irradiated animals an initial rapid decrease in liver glycogen, followed by a secondary increase. Denson *et al.* (238) interpreted this latter effect as an apparent retardation of glycogenolysis; at a time when glycogen stores of fasted control rats were nearly depleted, the liver of fasted irradiated rats contained 2 per cent glycogen. Lourau (239) obtained in mice and guinea pigs results similar to those of Denson *et al.*, but proposed an accelerated gluconeogenesis rather than retarded glycogenolysis to account for the effects. Increased gluconeogenesis would be expected in view of the endocrine response elicited by radiation, and indeed has been suggested by Nims & Sutton (236) to explain this increase in liver glycogen. However, the observa-

tion by Denson *et al.* (238) that adrenalectomy did not prevent this abnormal glycogen storage seemingly casts doubt on this interpretation. On the other hand, Nims & Sutton (236) reported that hypophysectomy, which induces adrenal atrophy, did prevent the secondary increase in liver glycogen. Thus, the effect of moderate x-ray exposure on mammalian liver glycogen is not definitely settled. Massive doses (10^5 r) rapidly depleted the glycogen stores of both mammalian and amphibian liver (240).

Denson *et al.* (238) also described changes in inorganic and acid labile phosphates of rat liver, the most striking effect being a premortal increase in labile phosphate [of which ATP (adenosinetriphosphate) is an important constituent], the inorganic phosphate remaining at control levels. It is regrettable that specific analyses for ATP have not been performed; an unequivocal demonstration of an increase in ATP in the tissues of moribund irradiated animals would be indeed surprising.

In comparison with pair-fed control rats, the absorption of fat and the hepatic storage of lipids, including vitamin A, were not altered during a 28-day postirradiation period (500 to 650 r), according to Coniglio *et al.* (241). However, repeated exposure of rats to 50 r/day for an average of 46 days resulted in an elevated fat concentration in the liver, demonstrable both histologically and chemically [Chevallier *et al.* (242)]; higher daily doses were less effective, possibly because the survival of the animal was too short for the change to develop. Buchanan *et al.* (17) found a high concentration in plasma of phospholipids, presumably attributable to cytolysis of leucocytes, 48 hr. after irradiation; otherwise, no effects of irradiation on choline metabolism were observed. Cornatzer *et al.* (243) reported that supralethal doses of x-rays (500 r) produced an increase in total blood cholesterol and a decrease in per cent esterified cholesterol in dogs; they found in addition an elevated uric acid level and a decrease in the albumin:globulin (A/G) ratio. Westphal *et al.* (244) noted that the A/G ratio of rat plasma was unchanged. However, there was a decrease in the γ-globulin fraction, with concomitant increases in the α- and β-globulins.

Bowers *et al.* (245) noted an increase of Na^+ and Cl^- with a concomitant decrease in K^+ in the gut, but not in the liver or skeletal muscles, of irradiated animals [see also Denson *et al.* (238)]. How these changes are related to other metabolic disturbances is not established; it is worthwhile to record that Goodman & Vogel (246) observed no significant changes in serum K or Na of irradiated rabbits except occasionally as a terminal event.

More extensive reviews on the biochemical effects of irradiation have been written by Ord & Stocken (3) and DuBois (247).

Conclusions

When one considers that the mechanisms by which ionizing radiations produce death in unicellular organisms are as yet poorly understood, it is not surprising that there are confusion and contradiction in regard to the lethal effects of radiation in the tremendously more complex vertebrate

species, which consist of tissues with different functions and with widely differing capacities for adaptation to radiation-induced environmental changes, and which possess a bewildering multiplicity of compensatory and regulatory processes of metabolic, humoral, neural, circulatory, and possibly psychic nature.

Although there has been no abatement in recent months in the volume of experimental work in vertebrate radiobiology, a majority of the publications, howsoever competent the investigators and valid the data, seem to deal with reiteration, extension, or refinement of previously established concepts. The number of recent papers which indicate new approaches to the solutions of problems in vertebrate radiobiology has been disappointingly small.

LITERATURE CITED

1. Patt, H. M., *Ann. Rev. Nuclear Sci.*, **1**, 495–523 (1952)
2. Patt, H. M., *Physiol. Revs.*, **33**, 35–76 (1953)
3. Ord, M. G., and Stocken, L. A., *Physiol. Revs.*, **33**, 356–86 (1953)
4. Furth, J., and Upton, A. C., *Ann. Rev. Nuclear Sci.*, **3**, 303–38 (1953)
5. Patt, H. M., *Ann. Rev. Physiol.*, **16**, 51–80 (1954)
6. Spear, F. G., *Radiations and Living Cells* (Chapman and Hall, Ltd., London, England, 222 pp., 1953)
7. [7] Stephens, S. V., and Boche, R. D., *U. S. Atomic Energy Commission Document, ANL-5111* (1953)
8. McLean, F. C., Rust, J. H., and Budy, A. M., *Military Surgeon*, **112**, 174–82 (1953)
9. Dauer, M., and Coon, J. M., *Proc. Soc. Exptl. Biol. Med.*, **79**, 702–7 (1952)
10. Piguory, L., and Nizza, P., *Compt. rend.*, **234**, 370–72 (1952)
11. Lorenz, E., Congdon, C., and Uphoff, D., *Radiology*, **58**, 863–77 (1952)
12. Gleiser, C. A., *Am. J. Vet. Research*, **14**, 287–97 (1953)
13. Tullis, J. L., Chambers, F. W., Morgan, J. E., and Zeller, J. H., *Am. J. Roentgenol. Radium Therapy Nuclear Med.*, **67**, 620–28 (1952)
14. Grahn, D. (Personal communication, January, 1954)
15. Eldred, E., and Eldred, B., *Blood*, **8**, 262–69 (1953)
16. Eldred, E., and Trowbridge, W. V., *Radiology*, **62**, 65–73 (1954)
17. Buchanan, D. J., Darby, W. J., Bridgforth, E. B., Hudson, G. W., and Efner, J. A., *Am. J. Physiol.*, **174**, 335–40 (1953)
18. Doull, J., and DuBois, K. P., *Proc. Soc. Exptl. Biol. Med.*, **84**, 367–70 (1953)
19. Stearner, S. P., *J. Exptl. Zool.*, **115**, 251–62 (1950)
20. Jacquez, J. A., and Karnofsky, D. A., *Am. J. Roentgenol. Radium Therapy*, **64**, 289–97 (1950)
21. Stearner, S. P., *Am. J. Roentgenol. Radium Therapy*, **65**, 265–71 (1951)
22. Rugh, R., Levy, B., and Sapadin, L., *J. Morphol.*, **91**, 237–68 (1952)
23. Altland, P. D., Highman, B., and Wood, B., *J. Exptl. Zool.*, **118**, 4–14 (1951)
24. Wilding, J. L., Simons, C. S., and Rust, J. H., *Nucleonics*, **10**(5), 36–40 (1952)
25. Rust, J. H., Wilding, J. L., Trum, B. F., Simons, C. S., Kimball, A. W., Jr., and Comar, C. L., *Radiology*, **60**, 579–82 (1953)

[7] Information concerning the availability of this document may be obtained from the Office of Technical Service, Department of Commerce, Washington 25, D. C.

26. Trum, B. F., *Military Surgeon*, **112**, 333–41 (1953)
27. Trum, B. F., Haley, T. J., Bassin, M., Heglin, J., and Rust, J. H., *Am. J. Physiol.*, **174**, 57–60 (1953)
28. Thomson, J. F., and Tourtellotte, W. W., *Am. J. Roentgenol. Radium Therapy Nuclear Med.*, **69**, 826–29 (1953)
29.[7] Clark, J. W., Vogel, H. H., Jr., and Jordan, D. L., *U. S. Atomic Energy Commission Document, ANL-4948* (1953)
30. Rajewsky, B., Heuse, O., and Aurand, K., *Z. Naturforsch.*, **8b**, 157–59 (1953)
31. Bonet-Maury, P., and Patti, F., *Brit. J. Radiol.*, **27**, 72–76 (1954)
32. Tyree, E. B., Nickson, J. J., Bane, H. N., and Schulz, R. J., *Radiation Research*, **1**, 232–33 (1954)
33. Thomson, J. F., Tourtellotte, W. W., Carttar, M. S., Cox, R. S., Jr., and Wilson, J. E., *Am. J. Roentgenol. Radium Therapy Nuclear Med.*, **69**, 830–38 (1953)
34. Kepp, R. K., and Müller, K., *Strahlentherapie*, **88**, 139–49 (1952)
35. Müller, K., and Hase, H., *Strahlentherapie*, **92**, 33–38 (1953)
36. Dieckman, C., *Strahlentherapie*, **92**, 39–42 (1953)
37. Dieckman, C., Hoffman, D., Kepp, R. K., and Müller, K., *Strahlentherapie*, **92**, 43–47 (1953)
38. Bond, V. P., Swift, M. N., Taketa, S. T., Welch, G. P., and Tobias, C. A., *Am. J. Physiol.*, **174**, 259–63 (1953)
39. Tobias, C. A., Anger, H. O., and Lawrence, J. H., *Am. J. Roentgenol. Radium Therapy Nuclear Med.*, **67**, 1–27 (1952)
40.[7] Swift, M. N., Bond, V. P., Taketa, S. T., Anger, H. O., and Sayeg, J. A., *U. S. Naval Radiological Defense Laboratory Document, USNRDL-365* (1952); *Am. J. Roentgenol. Radium Therapy Nuclear Med.* (In press)
41. Austin, M. K., Laughlin, J. S., and Quastler, H., *Brit. J. Radiol.*, **26**, 152–53 (1953)
42. Court Brown, W. M., and Mahler, R. F., *Science*, **118**, 651–52 (1953)
43. Vogel, H. H., Jr., Blomgren, R. A., and Bohlin, N. J. G., *Nucleonics*, **11**(3), 29–31 (1953)
44.[7] Stearner, S. P., and Vogel, H. H., Jr., *U. S. Atomic Energy Commission Document, ANL-5129* (1953)
45.[7] Vogel, H. H., Jr., Clark, J. W., and Jordan, D. L., *U. S. Atomic Energy Commission Document, ANL-5086* (1953)
46. Vogel, H. H., Jr., Clark, J. W., and Jordan, D. L., *Anat. Record*, **117**, 529–30 (1953)
47.[7] Vogel, H. H., Jr., Clark, J. W., Jordan, D. L., Bink, N., and Story, V. M., *U. S. Atomic Energy Commission Document, ANL-5200* (1954)
48.[7] Storer, J. B., and Harris, P. S., *U. S. Atomic Energy Commission Document, LA-1502* (1952)
49.[7] Brennan, J. T., Harris, P. S., Carter, R. E., and Langham, W. H., *U. S. Atomic Energy Commission Document, LA-1408* (1952)
50.[7] Storer, J. B., *U. S. Atomic Energy Commission Document, LA-1400* (1952)
51.[7] Harris, P. S., and Brennan, J. T., *U. S. Atomic Energy Commission Document, LA-1410* (1952)
52.[7] Storer, J. B., and Harris, P. S., *U. S. Atomic Energy Commission Document, LA-1455* (1952)
53. Brennan, J. T., Harris, P. S., Carter, R. E., and Langham, W. H., *Nucleonics*, **12**(2), 48–56 (1954)

54. Patt, H. M., Clark, J. W., and Vogel, H. H., Jr., *Proc. Soc. Exptl. Biol. Med.*, **84,** 189–93 (1953)
55.[7] Storer, J. B., Ellinwood, L. E., Langham, W. H., and Sanders, P., *U. S. Atomic Energy Commission Document, LA-1527* (1953)
56. Neary, G. J., Munsun, R. J., and Mole, R. H., *Nature*, **171,** 256 (1953)
57. Upton, A. C., Christenberry, K. W., and Furth, J., *Arch. Ophthalmol. (Chicago)*, **49,** 164–67 (1953)
58.[7] Moses, C., Linn, J. G., Jr., and Allen, A. J., *U. S. Atomic Energy Commission Document, AECU-2527* (1953)
59. Cogan, D. G., and Dreisler, K. K., *Arch. Ophthalmol. (Chicago)*, **50,** 30–34 (1953)
60.[7] Fillmore, P. G., *U. S. Atomic Energy Commission Document, NP-4560* (1953)
61. Alter, A. J., and Leinfelder, P. J., *Arch. Ophthalmol. (Chicago)*, **49,** 257–60 (1953)
62. Zeller, E. A., *Am. J. Ophthalmol.*, **36,** 51–53 (1953)
63. Permutt, S., and Johnson, F. B., *Arch. Pathol.*, **55,** 20–30 (1953)
64. Pirie, A., van Heyningen, R., and Boag, J. W., *Biochem. J. (London)*, **54,** 682–88 (1953)
65. Gray, L. H., *Brit. J. Radiol.*, **26,** 609–18 (1953)
66. Stokinger, H. E., *Nucleonics*, **11**(4), 24–27 (1953)
67. Bhattacharya, K. L., Chakraborty, K. P., Bose, A., and Das Gupta, N. N., *Science*, **118,** 651–52 (1953)
68. Finkel, M. P., Norris, W. P., Kisieleski, W. E., and Hirsch, G. M., *Am. J. Roentgenol. Radium Therapy Nuclear Med.*, **70,** 477–85 (1953)
69.[7] Blair, H. A., *U. S. Atomic Energy Commission Document, UR-274* (1953)
70. Finkel, M. P., *Proc. Soc. Exptl. Biol. Med.*, **83,** 494–98 (1953)
71. Hamilton, J. G., Asling, C. W., Garrison, W. M., and Scott, K. G., *Univ. Calif. (Berkeley) Publ. Pharmacol.*, **2,** 283–324 (1953)
72. Rugh, R., *J. Exptl. Zool.*, **122,** 151–68 (1953)
73. Rugh, R., *Proc. Soc. Exptl. Biol. Med.*, **83,** 762–64 (1953)
74. Tillotson, F. W., Rose, R. G., and Warren, S., *Am. J. Roentgenol. Radium Therapy Nuclear Med.*, **70,** 599–604 (1953)
75. Casarett, G. W., *Arch. Pathol.*, **55,** 393–402 (1953)
76. Brucer, M., Andrews, G. A., and Bruner, H. D., *Radiology*, **61,** 534–36 (1953)
77. Perkinson, J. D., Jr., and Ingols, R. S., *Radiology*, **61,** 545–50 (1953)
78. Bruner, H. D., Cooper, B. M., and Rehbock, D. J., *Radiology*, **61,** 550–55 (1953)
79. Meyers, W. G., Colmery, B. H., Jr., and McLellan, W. M., *Am. J. Roentgenol. Radium Therapy Nuclear Med.*, **70,** 258–73 (1953)
80. Andrews, G. A., Root, S. W., Kniseley, R. M., and Kerman, H. D., *Radiology*, **61,** 903–15 (1953)
81. Meneely, G. R., Auerbach, S. H., Woodcock, C. C., Kory, R. C., and Hahn, P. F., *Am. J. Med. Sci.*, **225,** 172–77 (1953)
82. Hahn, P. F., Carothers, E. L., and Brummit, H., *Am. J. Physiol.*, **175,** 162–66 (1953)
83.[7] Friedell, H. L., Salerno, P. R., and Rosenberg, S. A., *U. S. Atomic Energy Commission Document, NYO-4020* (1953)
84. Harel, J., *Bull. assoc. franc. étude cancer*, **40,** 68–77 (1953)
85.[7] Pinson, E. A., Anderson, E. C., and Lotz, V., *U. S. Atomic Energy Commission Document, AECU-2571* (1953)

86.[7] Furchner, J., Storer, J., and Lotz, V., *U. S. Atomic Energy Commission Document, LA-1544* (1953)
87. Littman, A., Fox, B. W., Schoolman, H. M., and Ivy, A. C., *Am. J. Physiol.*, **174,** 347–51 (1953)
88. Fox, B. W., Littman, A., Grossman, M. I., and Ivy, A. C., *Gastroenterology*, **24,** 517–34 (1953)
89. Hamilton, J. G., and Scott, K. G., *Proc. Soc. Exptl. Biol. Med.*, **83,** 494–98 (1953)
90. Cohn, S. H., and Gong, J. K., *Proc. Soc. Exptl. Biol. Med.*, **83,** 550–54 (1953)
91. Hart, H., and Laszlo, D., *Science*, **118,** 24–25 (1953)
92. Cohn, S. H., Gong, J. K., and Fishler, M. C., *Nucleonics*, 11(1) 56–61 (1953)
93. Hackett, P. L., *Proc. Soc. Exptl. Biol. Med.*, **83,** 710–13 (1953)
94. Kawin, B., and Copp, D. H., *Proc. Soc. Exptl. Biol. Med.*, **84,** 702–4 (1953)
95. Hursh, J. B., *Proc. Soc. Exptl. Biol. Med.*, **79,** 210–12 (1952)
96. Braun, H. A., Lusky, L. M., and Calvery, H. O., *J. Pharmacol. Exptl. Therap.*, **87** (suppl.), 119–25 (1946)
97. Tepperman, H. M., *J. Pharmacol. Exptl. Therap.*, **89,** 343–49 (1947)
98. Burch, P. R. J., and Spiers, F. W., *Nature*, **172,** 519–21 (1953)
99. Reines, F., Schuck, R. L., Cowan, C. L., Jr., Harrison, F. B., Anderson, E. C., and Hayes, F. N., *Nature*, **172,** 521–23 (1953)
100. Marinelli, L. D., Norris, W. P., Gustafson, P. F., and Speckman, T. W., *Radiology*, **61,** 903–15 (1953)
101.[7] Cassen, B., and Kistler, K., *U. S. Atomic Energy Commission Document, UCLA-266* (1953)
102.[7] Alpen, E. L., and Sheline, G. E., *U. S. Naval Radiological Defense Laboratory Document, USNRDL-402* (1953)
103.[7] Parr, W. H., Daggs, V. M., O'Neill, T. A., and Bush, S. G., *Army Medical Research Laboratory Document, AMRL-94* (1952)
104. Gustafson, G. E., and Cebul, F. A., *Surg. Gynecol. Obstet.*, **98,** 49–54 (1954)
105. Allen, J. G., Basinger, C., Landy, J. J., Sanderson, M. H., and Enerson, D. M., *Science*, **115,** 523–26 (1953)
106. Miller, R. W., Cotton, W. K., and Swisher, S. N., *Science*, **118,** 111–12 (1953)
107.[7] Kimeldorf, D. J., Jones, D. C., and Castanera, T. J., *U. S. Naval Radiological Defense Laboratory Document, USNRDL-390* (1953)
108. Kimeldorf, D. J., Jones, D. C., and Castanera, T. J., *Am. J. Physiol.*, **174,** 341–46 (1953)
109.[7] Jones, D. C., Kimeldorf, D. J., Rubadeau, D. O., Osborn, G. K., and Castanera, T. J., *U. S. Naval Radiological Defense Laboratory Document, USNRDL-400* (1953)
110. Cheng, A. L. S., Kryder, G. D., Bergquist, L., and Deuel, H. J., Jr., *J. Nutrition*, **48,** 161–82 (1952)
111. Deuel, H. J., Jr., Cheng, A. L. S., Kryder, G. D., and Bingemann, M. E., *Science*, **117,** 254–55 (1953)
112. Paris, R., and Vevasseur, J., *Thérapie*, **8,** 57–61 (1953)
113. Duplan, J. F., *Compt. rend.*, **236,** 424–26 (1952)
114. Smith, D. E. (Personal communication, October, 1953)
115.[7] Schlesinger, M. J., Jr., *U. S. Atomic Energy Commission Document, UR-279* (1953)
116. Langendorff, H., and Lorenz, W., *Strahlentherapie*, **88,** 177–89 (1952)
117. Palazzi, D., *Arch. E. Maragliano patol. e clin.*, **7,** 821–36 (1952)

118. Betz, H., *Compt. rend. soc. biol.*, **147**, 168–70 (1953)
119. Thomson, J. F., and Mikuta, E. T., *Proc. Soc. Exptl. Biol. Med.*, **85**, 29–32 (1954)
120. Betz, H., *J. belge radiol.*, **25**, 380–92 (1952)
121. Court Brown, W. M., *Brit. Med. J.*, **I**, 802–5 (1953)
122. Hochman, A., and Bloch-Frankenthal, L., *Brit. J. Radiol.*, **26**, 599–600 (1953)
123. Ingle, D. J., *Recent Progr. Hormone Research*, **6**, 151–94 (1952)
124. Oster, H. L., Kretchmar, A. L., and Bethell, F. H., *Proc. Soc. Exptl. Biol. Med.*, **84**, 470–73 (1953)
125. Rugh, R., Levy, B., and Sapadin, L., *J. Cellular Comp. Physiol.*, **41**, 359–86 (1953)
126. Korson, R., and Botkin, A. L., *Endocrinology*, **54**, 225–26 (1954)
127. Allen, B. M., Schjeide, O. A., Piccirillo, R. T., and Kowitz, G., *J. Exptl. Zool.*, **124**, 131–45 (1953)
128. Sommers, S. C., *J. Lab. Clin. Med.*, **42**, 396–407 (1953)
129. Westman, A., *Acta Obstet. Gynecol. Scand.*, **32**, 108–19 (1953)
130. Hecht, H., Neumayr, A., and Thurnher, B., *Strahlentherapie*, **91**, 261–69 (1953)
131. Tusques, J., Berger, M., and Moret, R., *Compt. rend. soc. biol.*, **147**, 337–39 (1953)
132. Landau, P., Leschi, J., and Tubiana, M., *Compt. rend.*, **236**, 240–42 (1953)
133. Monroe, R. A., Rust, J. H., and Trum, B. F., *Science*, **119**, 65–66 (1954)
134. Mole, R. H., and Batt, O. D., *Proc. Roy. Soc. Med.*, **46**, 250 (1953)
135. Mole, R. H., *Quart. J. Exptl. Physiol.*, **38**, 69–74 (1953)
136. Mole, R. H., *Brit. J. Radiol.*, **26**, 234–41 (1953)
137. Lacassagne, A., and Tuchman-Duplessis, H., *Compt. rend.*, **236**, 440–43 (1953)
138. Gordon, L. E., Miller, C. P., and Hahne, H. J., *Proc. Soc. Exptl. Biol. Med.*, **83**, 85–88 (1953)
139. Betz, H., *Compt. rend. soc. biol.*, **147**, 171–73 (1953)
140. Storer, J. B., and Sanders, P., *Proc. Soc. Exptl. Biol. Med.*, **83**, 259–62 (1953)
141. Miller, C. P., Hammond, C. W., and Tompkins, M., *Science*, 540–41 (1950)
142. Miller, C. P., Hammond, C. W., and Tompkins, M., *Science*, **111**, 719–20 (1950)
143. Marston, R. Q., Gonshery, L., Alderman, I. M., and Smith, W. W., *Am. J. Physiol.*, **172**, 365–71 (1953)
144. Shechmeister, I. L., Paulissen, L. J., and Fishman, M., *Proc. Soc. Exptl. Biol. Med.*, **83**, 205–9 (1953)
145.[7] Silverman, M. S., Chin, P. H., Greenman, V., and Young, J. C., *U. S. Naval Radiological Defense Laboratory Report, USNDRL-389* (1953)
146. Cheever, F. S., *J. Immunol.*, **71**, 431–35 (1953)
147.[7] Fulton, J. D., and Mitchell, R. B., *U. S. Atomic Energy Commission Document, NP-4279* (1953)
148. Hale, W. M., and Stoner, R. D., *Yale J. Biol. and Med.*, **25**, 326–33 (1953)
149.[7] Stoner, R. D., and Hale, W. M., *U. S. Atomic Energy Commission Document, BNL-1401* (1953)
150. Maurer, P. H., Dixon, F. J., and Talmage, D. W., *Proc. Soc. Exptl. Biol. Med.*, **83**, 163–66 (1953)
151. Stevens, K. M., Gray, I., and Schwartz, M. C., *Am. J. Physiol.*, **175**, 141–46 (1953)
152. Gabrielli, E. R., and Auskaps, A. A., *Yale J. Biol. and Med.*, **26**, 159–69 (1953)
153. Taplin, G. V., Finnegan, C., Noyes, P., and Sprague, G., *Am. J. Roentgenol. Radium Therapy Nuclear Med.*, **71**, 294–305 (1954)

154. Esplin, D. W., Marcus, S., and Donaldson, D. M., *J. Immunol.*, **70,** 454–60 (1953)
155. Marcus, S., and Donaldson, D. M., *Proc. Soc. Exptl. Biol. Med.*, **83,** 184–87 (1953)
156. Gonshery, L., Marston, R. Q., and Smith, W. W., *Am. J. Physiol.*, **172,** 359–64 (1953)
157. Smith, W. W., Smith, F., Ruth, H. J., Canter, H. Y., and Grenan, M. M., *Am. J. Physiol.*, **172,** 351–58 (1953)
158.[7] Coulter, M. P., and Miller, R. W., *U. S. Atomic Energy Commission Document, UR-276* (1953)
159. Furth, F. W., Coulter, M. P., Miller, R. W., Howland, J. W., and Swisher, S., *J. Lab. Clin. Med.*, **41,** 918–28 (1953)
160. Gustafson, G. E., and Koletsky, S., *Proc. Soc. Exptl. Biol. Med.*, **84,** 266–69 (1953)
161. Marston, R. Q., Ruth, H. J., and Smith, W. W., *Proc. Soc. Exptl. Biol. Med.*, **83,** 289–91 (1953)
162. Genaud, P. E., and Meot, R., *Compt. rend.*, **236,** 2004–6 (1953)
163. Bacq, Z. M., Dechamps, G., Fischer, P., Herve, A., LeBihan, H., LeComte, J., Pirotte, M., and Rayet, P., *Science*, **117,** 633–36 (1953)
164. Rugh, R., and Wang, S. C., *Proc. Soc. Exptl. Biol. Med.*, **83,** 411–14 (1953)
165. Straube, R. L., and Patt, H. M., *Proc. Soc. Exptl. Biol. Med.*, **84,** 702–4 (1953)
166. Bacq, Z. M., Baddiley, J., Eldjarn, L., Lipmann, F., and Lynen, F., *Science*, **119,** 163–64 (1954)
167. Kaplan, W. D., and Lyon, M. F., *Science*, **118,** 777–78 (1953)
168. Salerno, P. R., and Friedell, H. L., *Radiation Research*, **1,** 228 (1954)
169. Bacq, Z. M., and Herve, A., *Bull. acad. roy. de méd. Belg.*, [VI]**17,** 13–58 (1952)
170. Pierpoint, W. S., and Hughes, D. E., *Biochem. J.* (*London*), **56,** 130–35 (1954)
171.[7] Thomson, J. F., and Mikuta, E. T., *U. S. Atomic Energy Commission Document, ANL-4932* (1952)
172. Bacq, Z. M., and Herve, A., *Arch. intern. physiol.*, **61,** 434–36 (1953)
173. Maisin, J., Mandart, M., Lambert, G., and Maisin, H., *Compt. rend. soc. biol.*, **147,** 362–64 (1953)
174. Maisin, J., Lambert, G., Mandart, M., and Maisin, H., *Nature*, **171,** 971 (1953)
175. Maisin, J., van Lancker, J., Dunjic, A., Lambert, G., and Passeau, L., *Compt. rend. soc. biol.*, **147,** 1517–20 (1953)
176. Maisin, J., Dunjic, A., van Lancker, J., Lambert, G., and Passeau, L., *Compt. rend. soc. biol.*, **147,** 1520–22 (1953)
177. Gros, C. M., and Comsa, J., *Compt. rend.*, **236,** 1611–13 (1953)
178. Hilfinger, M. F., Jr., Ferguson, J. H., and Riemenschneider, P. A., *J. Lab. Clin. Med.*, **42,** 570–80 (1953)
179. Cole, L. J., Fishler, M. C., and Bond, V. P., *Proc. Natl. Acad. Sci.*, **39,** 759–72 (1953)
180. Cole, L. J., and Ellis, M. E., *Radiation Research*, **1,** 128–29 (1954)
181.[7] Fishler, M. C., Cole, L. J., Bond, V. P., and Milne, W. L., *U. S. Naval Radiological Defense Laboratory Document, USNRDL-410* (1953)
182. Kelly, L. S., and Jones, H. B., *Am. J. Physiol.*, **172,** 575–78 (1953)
183. Brown, M. B., Kaplan, H. S., Weymouth, P. P., and Paull, J., *Science*, **117,** 693–95 (1953)
184. Van Lancker, J., *Compt. rend. soc. biol.*, **147,** 1513–15 (1953)

185. Van Lancker, J., *Compt. rend. soc. biol.*, **147,** 1523–25 (1953)
186.[7] Swift, M. N., Taketa, S. T., and Bond, V. P., *Radiation Research*, **1,** 241–52 (1954)
187. Van Lancker, J., *Compt. rend. soc. biol.*, **147,** 1515–17 (1953)
188. Finerty, J. C., Binhammer, R. T., and Schneider, M., *Science*, **118,** 654–55 (1953)
189. Schneider, M., Wybourn, R. C., Binhammer, R. T., and Finerty, J. C., *Radiology*, **62,** 234–40 (1954)
190. Binhammer, R. T., Schneider, M., and Finerty, J. C., *Am. J. Physiol.*, **175,** 440–42 (1953)
191. Cole, L. J., and Ellis, M. E., *Am. J. Physiol.*, **175,** 429–36 (1953)
192. Mefferd, R. B., Jr., Henkel, D. T., and Loefer, J. B., *Proc. Soc. Exptl. Biol. Med.*, **83,** 54–56 (1953)
193. Burnett, W. T., Jr., Burke, A. W., Jr., and Upton, A. C., *Am. J. Physiol.*, **174,** 254–58 (1953)
194. Mazzanti, L., and Franchi, M., *Arch. ital. sci. farmacol.*, **2,** 261–62 (1952)
195. Bacq, Z. M., and Herve, A., *Brit. J. Radiol.*, **24,** 617–21 (1951)
196. Parr, W. H., O'Neill, T., and Krebs, A., *Science*, **117,** 155–56 (1953)
197. Bennett, L. R., Chastain, S. M., Flint, J. S., Hansen, R. A., and Lewis, A. E., *Radiology*, **61,** 411–19 (1953)
198. Rugh, R., Suess, J., and Scudder, J., *Nucleonics*, **11**(8), 52–54 (1953)
199. Buchanan, D. J., Pearson, W. N., Amarasingham, C., Hudson, G. W., and Darby, W. J., *Am. J. Physiol.*, **175,** 437–39 (1953)
200.[7] Detrick, L. E., Debley, V., and Haley, T. J., *U. S. Atomic Energy Commission Document, UCLA-265* (1953)
201. Feinstein, R. N., and Cotter, G. J., *Science*, **118,** 552 (1953)
202.[7] Haley, T. J., McCulloh, E. F., and McCormick, W. G., *U. S. Atomic Energy Commission Document, UCLA-271* (1953)
203. Haley, T. J., and Rhodes, B. M., *Science*, **117,** 139–40 (1953)
204. Detrick, L. E., Rhodes, B., Debley, V., and Haley, T. J., *J. Am. Pharm. Assoc., Sci. Ed.*, **42,** 296–300 (1953)
205. Haley, T. J., Heglin, J., and McCulloh, E., *Radiation Research*, **1,** 176–79 (1954)
206. Conway, B. E., *Brit. J. Radiol.*, **27,** 42–47 (1954)
207. Hannan, R. S., and Shepherd, H. J., *Brit. J. Radiol.*, **27,** 36–42 (1954)
208. Anderson, R. S., *Brit. J. Radiol.*, **27,** 56–61 (1954)
209. McDonald, M. R., *Brit. J. Radiol.*, **27,** 62–63 (1954)
210. Mendelsohn, M. L., and Caceres, E., *Am. J. Physiol.*, **173,** 351–54 (1953)
211. Stearner, S. P., Christian, E. J. B., and Brues, A. M., *Radiation Research*, **1,** 270–81 (1954)
212. Andrews, H. L., and Brace, K. C., *Am. J. Physiol.*, **175,** 138–40 (1953)
213. Lamerton, L. F., Elson, L. A., and Christensen, W. R., *Brit. J. Radiol.*, **26,** 510–18 (1953)
214. Lamerton, L. F., Elson, L. A., and Harriss, E. B., *Brit. J. Radiol.*, **26,** 568–76 (1953)
215. Smith, D. E., and Tyree, E. B., *Am. J. Physiol.* (In press)
216. Lawrence, J. S., Valentine, W. N., and Dowdy, A. H., *Blood*, **3,** 593–611 (1950)
217. Lavik, P. S., Leonards, J. R., Buckaloo, G. W., Heisler, C., and Friedell, H. L., *Proc. Soc. Exptl. Biol. Med.*, **83,** 618–20 (1953)

218. Epstein, H. T., *Nature*, **171**, 394–95 (1953)
219. Koenig, V. L., and Perrings, J. D., *Arch. Biochem. Biophys.*, **44**, 443–54 (1953)
220. Smith, C. L., *Arch. Biochem. Biophys.*, **46**, 12–17 (1953)
221. Daniels, M., Scholes, G., and Weiss, J., *Nature*, **171**, 1153–54 (1953)
222. Scholes, G., and Weiss, J., *Biochem. J.*, (*London*), **56**, 65–72 (1953)
223. Alexander, P., and Fox, M., *Nature*, **170**, 1022–23 (1952)
224. Alexander, P., *Brit. J. Radiol.*, **26**, 413–16 (1953)
225. Charlesby, A., and Ross, M., *Nature*, **171**, 1153 (1953)
226. Prevot-Bernas, A., *J. chim. phys.*, **50**, 445–46 (1953)
227. Payne, A. H., Kelly, L. S., and Entenman, C., *Proc. Soc. Exptl. Biol. Med.*, **81**, 698–701 (1952)
228. Vermund, H., Barnum, C. P., Huseby, R. A., and Stenstrom, K. W., *Cancer Research*, **13**, 633–39 (1953)
229. Thomson, J. F., Carttar, M. S., and Tourtellotte, W. W., *Radiation Research*, **1**, 165–75 (1954)
230.[7] Rambach, W. A., Cooper, J. A. D., and Alt, H. L., *U.S.A.F. School of Aviation Medicine*, Proj. No. 21-3501-0001, Report No. 1 (1953)
231. Thomson, J. F., Tourtellotte, W. W., Carttar, M. S., and Storer, J. B., *Arch. Biochem. Biophys.*, **42**, 185–96 (1953)
232. Paigen, K., and Kaufmann, B. N., *J. Cellular Comp. Physiol.*, **42**, 163–78 (1953)
233. Gros, C., Mandel, P., and Rodesch, J., *Compt. rend.*, **236**, 2010–12 (1953)
234.[7] Parr, W. H., Puckett, N., Ransom, R., Spradling, S., and Krebs, A., *Army Medical Research Laboratory Document, AMRL-102* (1952)
235. Brace, K. C., *Science*, **116**, 570–71 (1952)
236. Nims, L. F., and Sutton, E., *Am. J. Physiol.*, **177**, 51–54 (1954)
237. Schwarz, H. P., Riggs, H. E., Glick, C., McGrath, J., Childs, R., Bew, E., Jr., and Stone, F., *Proc. Soc. Exptl. Biol. Med.*, **85**, 96–100 (1954)
238. Denson, J. R., Gray, E. J., Gray, J. L., Herbert, F. J., Tew, J. T., and Jensen, H., *Proc. Soc. Exptl. Biol. Med.*, **82**, 707–11 (1953)
239. Lourau, M., *Compt. rend.*, **236**, 442–44 (1953)
240. Levy, B., and Rugh, R., *Proc. Soc. Exptl. Biol. Med.*, **82**, 223–25 (1953)
241. Coniglio, J. C., Darby, W. J., Wilkerson, M. C., Stewart, R., Stockell, A., and Hudson, G. W., *Am. J. Physiol.*, **172**, 86–92 (1953)
242. Chevallier, A., Burg, C., and Spehler, H., *Compt. rend. soc. biol.*, **147**, 497–500 (1953)
243. Cornatzer, W. E., Engelstad, O., and Davidson, J. P., *Am. J. Physiol.*, **175**, 153–56 (1953)
244. Westphal, U., Priest, S. G., Stets, J. F., and Selden, G. L., *Am. J. Physiol.*, **175**, 424–28 (1953)
245. Bowers, J. Z., Davenport, V., Christensen, N., and Goodner, C. J., *Radiology*, **61**, 97–101 (1953)
246. Goodman, R. D., and Vogel, M., *Am. J. Physiol.*, **175**, 29–32 (1953)
247. DuBois, K. P., *Ann. Rev. Nuclear Sci.*, **4**, 351–76 (1954)

RADIOACTIVITY IN GEOLOGY AND COSMOLOGY[1,2]

By Truman P. Kohman and Nobufusa Saito[3]

Department of Chemistry, Carnegie Institute of Technology, Pittsburgh, Pennsylvania

The study of natural radioactivity has experienced a substantial revival in recent years. One reason is the general increase in importance and popularity of all aspects of nuclear science, with this branch partaking of its share. The practical importance as raw materials for nuclear energy of uranium and thorium, which are the parents of most of the known natural radionuclides, has stimulated a study of the properties and occurrences of the latter. It has also been realized that natural radioactivity is a phenomenon of considerably greater variety and more general incidence than had been believed previously (339, 340, 379).

The well established and newly discovered geological ramifications of the occurrence of radioactivity in nature have induced considerable numbers of earth scientists to employ nuclear tools in their studies. The natural occurrence of radionuclides with lifetimes from less than a minute to billions of years provides information on phenomena ranging from micrometeorology to cosmic history. On the other hand, nuclear scientists have continued to find nature a valuable laboratory associate, with the foresight to start experiments for them many millions of years ago and the ability to accelerate bombarding particles to energies far beyond their own capabilities.

Nuclear geochemistry was reviewed by Fleischer & Rabbitt in Volume 1 of *Annual Review of Nuclear Science* (198), that review covering mainly papers published in 1950. The present review is concerned chiefly with material published from early 1951 to early 1954, but with references to some earlier work which is pertinent to recent developments. The number of publications in this area is increasing rapidly each year. The preparation under the editorship of Faul of a symposium-type volume on *Nuclear Geology* (190), whose publication is expected in 1954, may mark the recognition of a separate branch of science of that name. Several other books in or related to this field are rumored to be in preparation.

NATURAL RADIONUCLIDES

A recently published *Glossary of Terms in Nuclear Science and Technology* (424) gives a classification of naturally-occuring radionuclides as follows: primary: unstable nuclides having lifetimes sufficiently long to have pre-

[1] The preparation of this paper has been assisted by the United States Atomic Energy Commission through its support of nuclear chemistry research at Carnegie Institute of Technology.

[2] The following abbreviations are used in this chapter: dis. (disintegration); m.y. (million years); B.P. (before present).

[3] Visiting Research Chemist. Present address: Department of Chemistry, Faculty of Science, University of Tokyo, Tokyo, Japan.

vented complete decay of the original supply present at the hypothetical origin of the elements; secondary: short-lived nuclides which are disintegration products of primary natural radionuclides; induced: short-lived nuclides present in nature as a result of current or recent production by nuclear reactions; extinct: unstable nuclides having lifetimes sufficiently short to have resulted in complete decay since the presumed origin of the elements, yet sufficiently long for their persistence into early geologic times to have produced effects in nature which can be identified at the present time. This terminology will be used in this review.

Much new information has been accumulated on the nuclear properties of the well-known primary and secondary natural radionuclides. Here we will consider only those half lives which are of importance for geology and cosmology.

Uranium.—A summary of measurements pertaining to the abundances and disintegration rates of the naturally-occurring uranium isotopes has been given by Fleming, Ghiorso & Cunningham (200), who conclude that on the basis of all work to date the best values are the following:

S = Specific activity of natural uranium	$25{,}020 \pm 50$ α/sec./gm.
$T(238)$ = Half-life of U^{238}	$(4.51 \pm 0.01) \times 10^9$ yr.
$T(235)$ = Half-life of U^{235}	$(7.13 \pm 0.14) \times 10^8$ yr.
r = Isotope ratio $N(238)/N(235)$	138.0 ± 1.0
$R = N(235)\lambda(235)/N(238)\lambda(238)$	0.046 ± 0.001

From the above half lives can be calculated:

$\lambda(238)$ = Disintegration constant of U^{238}	$(1.537 \pm 0.003) \times 10^{-10}$ yr.$^{-1}$
$\lambda(235)$ = Disintegration constant of U^{235}	$(9.72 \pm 0.19) \times 10^{-10}$ yr.$^{-1}$

It is of considerable interest that the values of R and $T(235)$ obtained from alpha counting studies are identical with those obtained some time ago by Nier from a study of radiogenic lead isotope ratios (427). In 1942 Wickman suggested that some radiogenic Pb^{206} might be lost from uranium minerals as a result of escape of radon (577), and extensive use was made of this idea in calculating ages of such minerals, particularly by Holmes (273, 274, 275, 277, 278). Holmes' method is to postulate a fractional radon loss which would make the Pb^{206}/U^{238} and Pb^{207}/Pb^{206} ages coincide with the Pb^{207}/U^{235} age. Thus his geologic time scale (273) is directly proportional to $T(235)$. The assumption of frequent occurrence of radon losses implies the need for a downward correction of Nier's value of R and an increase in $T(235)$. At about the same time certain nuclear physical measurements (107, 328) indicated a value of $T(235)$ considerably greater than Nier's. On the other hand, counting results of Sayag (500) have provided additional confirmation of $R = 0.046$, and Fleming's results seem to settle the matter. The apparent correctness of Nier's original determination of R would seem to imply that radon loss is probably not very important in uranium minerals. However, there is still an uncertainty of $\sim$2 per cent in $T(235)$, $\sim$1 per cent in r, and probably 3 or 4 per cent in Nier's determination of R, leaving open the possibility of an average loss of several per cent of the radon in uranium

minerals. Evidence that this may indeed be the case is cited under LEAD METHODS of geologic time measurement. More precise determinations of $T(235)$ and r are presumably possible with available techniques and are much to be desired. Ingerson (295) mentions plans of the United States Geological Survey to determine r from a variety of natural sources.

Thorium.—The currently accepted values of the disintegration constants of Th^{232}, $\lambda(232) = 4.99 \times 10^{-11}$ yr.$^{-1}$ and $T(232) = 1.39 \times 10^{10}$ yr. (348), have stood for 16 years, unchallenged by modern techniques. There has been reported, though not published, a measurement of the half-life ratio $T(232)/T(238) = 2.75$ (108), from which a value of $T(232) = 1.24 \times 10^{10}$ yr. can be calculated; however, the authors claim only a low accuracy for the ratio. A precise redetermination of $T(232)$ is needed to help put the Pb^{208}/Th^{232} method of age determination on a sound basis.

Potassium.—An extensive literature has grown on the natural radioactivity of K^{40}. That through 1950 has been summarized by Birch (70), and the nuclear data through late 1953 by Endt & Kluyver (179). The latter give the following as weighted averages of all measurements:

$S(\beta)$ = Specific negatron activity	27.6 β/sec./gm.
$S(\gamma)$ = Specific gamma activity	3.4 γ/sec./gm.

Assuming from experimental evidence that virtually all of the electron-capture transitions go to the excited state of A^{40} [which is supported by theoretical considerations (414)], and, utilizing 0.0119 ± 0.0001 per cent for the isotopic abundance of K^{40} (430) [although there is a more recent determination giving 0.0118 ± 0.0001 per cent (475)], they derive:

$\lambda(\beta)$ = Negatron emission disintegration constant	4.72×10^{-10} yr.$^{-1}$
$\lambda(\epsilon)$ = Electron-capture disintegration constant	5.7×10^{-11} yr.$^{-1}$
$\lambda(\epsilon)/\lambda(\beta) = S(\gamma)/S(\beta)$ = Branching ratio	0.12_3
$\lambda = \lambda(\beta) + \lambda(\epsilon)$ = Total disintegration constant	5.29×10^{-10} yr.$^{-1}$
T = Half-life	1.31×10^{9} yr.

These values are quite close to those determined by Sawyer & Wiedenbeck (498), which are preferred by Birch, and to those selected by Burch (94) as best.

Inghram and co-workers have measured the radiogenic A^{40}/Ca^{40} ratio in a sylvite and calculated an ϵ/β^- branching ratio of 0.126 ± 0.005; this they regard as a lower limit because of the possibility of argon loss (297). Investigators at Toronto have determined the potassium and radiogenic argon contents of potassium feldspars of supposedly known ages and calculated K^{40} branching ratios therefrom. Their initial results, ~0.06 (418, 489), were found to involve incomplete argon recovery (506, 572). Their more recent values, ~0.09 (506), may still be low because of estimation of ages by the Pb^{207}/Pb^{206} method, which usually gives too high results (LEAD METHODS). Wasserburg & Hayden (572) believe that their measurements on a single specimen are not inconsistent, considering the uncertainties, with a branching ratio as high as 0.13 (we calculate 0.10_4 using their Pb^{207}/U^{235} age). Subsequent indications, however, are that, if argon loss is unimportant, a

branching ratio of 0.08 would be required to bring the argon ages into agreement with their assumed lead ages (573). This method of determining disintegration constants is not as accurate as those based on radiation measurements. The comparison suggests that feldspars may lose some of their radiogenic argon. For minerals having complete argon retentivity, the value of $\lambda(\epsilon)$ is still not known with sufficient accuracy for precise argon age determination.

Rubidium.—Recent determinations of the half-life of Rb^{87} began with that of Eklund (177), who obtained $(5.8 \pm 1.0) \times 10^{10}$ yr. with a screen-wall Geiger counter calibrated against α- and UX_1 β-radiations from uranium; neglect of differential backscattering of α- and β-radiations should make this a lower limit. Haxel, Houtermans & Kemmerich (251, 329) observed coincidences between radiations from opposite sides of a thin layer of RbCl, concluded that each β-particle was accompanied by a highly converted γ-transition, and gave $(6.0 \pm 0.6) \times 10^{10}$ yr. for the half-life. Haxel & Houtermans (252) using a double Geiger counter as a 4π detector obtained $(6.9 \pm 0.7) \times 10^{10}$ yr. However, Kalkstein (320) and Curran, Dixon & Wilson (127, 128) could find no evidence for radiations other than a single β-spectrum, and attributed the coincidences observed by Haxel *et al.* to backscattering. Curran's group, using a large proportional counter containing RbCl spread on aluminum, extrapolating the beta spectrum below 10 kev and, applying small backscattering and self-absorption corrections, derived a half-life of $(6.15 \pm 0.3) \times 10^{10}$ yr. Charpak & Suzor (106) believed Curran *et al.* to have underestimated the backscattering correction, and revised their value to $(7.6 \pm 0.4) \times 10^{10}$ yr. Bähnisch, Huster & Walcher (52) found that coincidences observed in double Geiger counters (251, 252, 329) were attributable to light emitted in the counter discharge as well as to backscattering, and they were able to eliminate all coincidences by using a thin but light-tight sample support and lining the tubes with organic foils. Their single-counter rate for very thin RbCl samples corresponded to a half-life of 4.8×10^{10} yr., which they regarded as a lower limit because of the possibility of slight backscattering from the support. However, they did not believe this effect could be sufficient to make their results consistent with a half-life as large as 6×10^{10} yr., and they suggested that Curran *et al.* had greatly underestimated self-absorption resulting from possible unevenness of their sample. On the other hand, MacGregor & Wiedenbeck (394), using a double Geiger counter, obtained a half-life similar to that of Haxel *et al.* [$(6.37 \pm 0.3) \times 10^{10}$ yr. when recalculated using the latest measurements of the isotopic abundance of Rb^{87}, 27.85 ±0.06 per cent (431)]. Recently, they have repeated this determination with enriched Rb^{87}, obtaining $(6.2 \pm 0.3) \times 10^{10}$ yr. (395). Confirmation of a high value has been supplied by Lewis (378) who reported $(5.9 \pm 0.3) \times 10^{10}$ yr. from an investigation with a scintillation spectrometer with rubidium incorporated into a NaI(Tl) crystal. However, this result involved an extrapolation from 13 kev and the assumption of 100 per cent efficiency for this and higher energies. Flinta & Eklund (206) also reported a high

value $(6.1 \pm 0.2) \times 10^{10}$ yr., but obtained an indication of a high abundance of low energy electrons.

Evidence presented under the STRONTIUM METHOD of geochronometry indicates that ages determined by the strontium method and calculated with a half-life of $\sim 6 \times 10^{10}$ yr. seem consistently higher than those determined by methods based on α-decay (344). Since the calculated ages are proportional to the half-life assumed, these apparent discrepancies might be reconciled if the Rb^{87} half-life were actually somewhat smaller than the above value. This suggests the approximate correctness of the results of Bähnisch *et al.* The spectrum found by Curran *et al.* and roughly confirmed by Lewis exhibits a rapid rise in the number of particles per unit energy interval as the energy approaches zero, which indicates the possibility of considerable self-absorption in Curran's measurements. In addition, the extrapolation to zero energy could well have been made too conservatively both by Curran and by Lewis. An alternate possibility has been suggested by Kohman (345): that the observed emission of free β-particles might be augmented by the unobserved process of "bound beta disintegration," involving creation of the electron in an atomic orbital of the disintegrating atom and the carrying away of virtually all of the disintegration energy by the neutrino. This process has been postulated to account for certain experimental results in the disintegration of $Ra^{228}(MsTh_1)$ and $Pb^{210}(RaD)$, and considered theoretically by Daudel *et al.* (144 to 147), Sherk (510), Ivanenko & Lebedev (301), and Fabre de la Ripelle (183). Although the calculations disagree as to the quantitative importance of the process, they agree that it should be relatively more important for heavy elements and low transition energies. The calculations made to date pertain only to allowed transitions, whereas the process might be of considerably greater importance in highly forbidden cases like Rb^{87} (third-forbidden). Further work, both experimental and theoretical, is urgently needed on the half-life of Rb^{87}. In this connection should be mentioned the suggested possibility of a secular variation of the relative rates of β- and α-disintegrations (284), based on a more general premise of variability of physical "constants" (318).

Other primary natural radionuclides.—New information has appeared on the radioactive properties of Sm^{147} (173, 474, 535), Lu^{176} (39, 41, 170, 336, 501), La^{138} (420, 471, 503), and Re^{187} (129, 228). Very recently, Curran, McNair & Dixon (131, 171) have reported inability to detect the natural radioactivity reported in rhenium (423, 534). Since the new measurements were made with a proportional counter and the older ones with a Geiger counter, the results might be reconciled if Re^{187} emits radiations of energy less than 1 kev, the lower limit of the proportional counter measurements. Natural alpha activity has been reported in Bi^{209} by two groups (187, 477) but denied by a third (265). An alpha activity has been found in tungsten and assigned to a very rare isotope such as W^{178} (470), but the uncertainty in the energy measurement would permit an alternative assignment to W^{180} (340, 345). Alpha activity has also been found in Nd^{144} (570). Unsuccessful

searches have been made for natural radioactivity in Ca^{48} (317, 503), V^{50} (109, 259, 503, 505, 524, 531), Zr^{96} (503), Cd^{113} (503), In^{113} (259), Sb^{123} (503), Te^{123} (259, 503), and Nd^{150} (128, 171, 419). An indication of natural activity in molybdenum (211) could not be substantiated (503); radiogenic Te^{100} from a possibly unstable Mo^{100} (339) cannot account for certain astronomical observations of technetium (289, 406, 407, 408, 412). Direct searches for double-beta disintegration in several elements have given negative or dubious results (63, 195, 211, 216, 321, 376, 400, 401, 402, 586). An excess of Xe^{130} in old tellurium minerals has been observed and attributed to double-beta disintegration of Te^{130} (255, 298); however, Te^{130} is probably unstable against ordinary beta disintegration to I^{130}, and this process might equally well account for the radiogenic Xe^{130} (345).

It seems probable now that no new primary natural radionuclides of geological utility will be discovered. However, Arnold (41) believes that Lu^{176} is sufficiently short-lived to be of such value, considering the chemical difference and low isotopic abundance of its daughter. Libby (388) has pointed out that if the Re^{187} radiations are much softer than had been supposed previously its half-life would also be considerably shorter, and it too may be useful geochemically. Saito *et al.* (493) have been unable to detect excess Ba^{138} in old rare earth minerals, indicating probable lack of usefulness of La^{138} for geological purposes.

Secondary natural radionuclides.—The half-lives of Ra^{226} and Th^{230} are involved in age determinations by the radium-ionium method. The most recent value for radium, 1622 ± 13 yr. (341), is in sufficient agreement with many earlier determinations for geological applications, although its accuracy has been been questioned (335, 442, 445). The results of a new determination by Paneth (442) have not yet appeared. The value $(8.0 \pm 0.3) \times 10^4$ yr. (294) for ionium is adequate for geological purposes. The radiolead method of geochronometry requires use of the half-lives of Pb^{210} and its descendants. No determinations of the half-life of Pb^{210} (RaD) seem to have been published since the adoption of the value 22 yr. in 1931 (126), although a value of 25 yr. has been quoted in an unpublished report (569). A precise determination is needed. For Bi^{210} (RaE), recent values include 5.02 ± 0.02 (62) and 4.989 ± 0.013 days (389). Recent values for Po^{210} (RaF) are 138.3 ± 0.1 (60), 138.39 ± 0.14 (236) and 138.374 ± 0.032 days (132).

Induced natural radionuclides.—The half-life of H^3 (tritium) has been reported as 10.7 ± 2.0 yr. (238), 12.1 ± 0.5 yr. (435), 12.46 ± 0.1 yr. (310, 311), and 12.41 ± 0.2 yr. (316), agreement being satisfactory.

In the case of C^{14}, a great many more measurements have been made, and the spread is considerable. Libby has reviewed all of the data as of September, 1951, in his book *Radiocarbon Dating* (382), and selects as the most probable half-life 5568 ± 30 yr., a weighted mean of three selected values from measurements of the specific activity by mass spectrometry and gas counting. This mean has been adopted universally for radiocarbon age calculations. Only two measurements have been published subsequently, 5370

± 200 yr. by Manov & Curtiss (396) and 5900 ± 250 yr. by Caswell *et al.* (102a). Manov & Curtiss consider that on the basis of all the evidence the most probable value is 5400 ± 200 yr. Libby stresses the importance of applying entirely different techniques for further determinations and mentions the possibility of utilizing careful measurements of historically dated samples; this, however, presumes a constancy of the specific activity of atmospheric carbon which has not yet been proven.

OCCURRENCE AND DISTRIBUTION OF RADIONUCLIDES IN NATURE

Uranium and Thorium

The economic importance of uranium and thorium has continued to stimulate extensive investigations of the terrestrial occurrence and distribution of these elements. Because of their geochemical similarities, and because their presence is often indicated by their radioactivity in a way which does not distinguish between them, it is convenient to discuss the two elements together here. A general review has been given by Davidson (149). The extensive program of the Geochemistry and Petrology Branch of the U. S. Geological Survey on the geochemistry of uranium, and on related analytical techniques and some of the results obtained, are described by Ingerson (295). The terrestrial (199) and cosmic (451, 556, 557) abundances of these elements have been tabulated and discussed. Several chapters of *Nuclear Geology* (190) deal with subjects of this section.

Igneous rocks.—The gross concentration of uranium has been determined in igneous rocks of many types and from many localities (22, 45, 53, 54, 61, 163, 164, 165, 178, 182, 208, 264, 295, 296, 465, 485, 519, 538, 562, 576). The value for a given rock type varies from one sample to another, but the averages are comparable to the earlier values of Evans & Goodman (181). Less attention has been paid to the thorium content of igneous rocks (163, 164, 165, 465). A mass-spectrometric isotope dilution analysis technique using ionium as the diluent and capable of high precision was developed by Tilton *et al.* (547).

Several interesting phenomena relating to the distribution of radioactivity within a given igneous complex have been observed. In six of nine intrusive rock bodies in three areas of Canada, radioelements are concentrated towards the outer margin of the batholith (296). In some igneous rocks the radioactivity is closely associated with lamprophyric accumulations or dikes (178, 209). In Colorado, bostonites containing up to 20 times as much uranium as the average granite were found. In this rock body, pitchblende-bearing veins are associated with bostonite dikes low in uranium (295).

The development of the nuclear emulsion technique has greatly extended knowledge of the distribution of radioelements within rocks. In igneous rocks, the radioactivity is concentrated in the so-called accessory minerals, including zircon, allanite, sphene, uraninite, thorite, apatite, monazite, epidote,

and some unidentified inclusions. Quartz, feldspar, hornblende, pyroxene, magnetite, and some micas contribute little to the total radioactivity even though they may account for most of the mass of a rock (61, 254, 264, 519, 538, 576). These observations confirm and extend the earlier findings of Piggot (468), Keevil & Larsen (325, 326, 327, 372), and Kimura and his collaborators (331, 332, 491). The qualitative and semi-quantitative nuclear emulsion results have been supplemented by precise analyses by Tilton *et al.*, employing U^{235} and Th^{230} in mass spectrometric isotope dilution analyses (16, 262, 545, 547), and by the U. S. Geological Survey group (295). Zircon generally has the highest uranium content, of the order of 0.1 per cent. A thorium content of 0.54 per cent was observed in sphene from Essonville granite (547). The minerals from granitic rocks have higher uranium contents than the same species from more basic rocks. According to Picciotto (465) the extreme concentration of radioactivity in accessory minerals or occlusions mentioned above is found only in acidic rocks such as granite, whereas in basic rocks the radioelements are distributed rather homogeneously. In Etna lava, radioactivity was mainly found in the groundmass, but not in the phenocryst (538).

Sedimentary rocks.—The distribution of uranium in sedimentary rocks is also quite variable (89, 238a, 319, 392, 421, 432, 495, 575). Some have considerably higher contents than the average values for sediments: silty quartzite in Arizona contains up to 0.22 per cent uranium (319), while algal limestones contain up to 0.15 per cent (392).

Among studies of phosphorites (74, 150, 162, 246, 393, 467, 488, 544), the most extensive has been that of Davidson & Atkin. They find up to 0.12 per cent uranium in materials from Florida and South Carolina, and up to 0.09 per cent in those from the British Isles. Some fossil bones contain up to 0.44 per cent uranium. These workers consider that adsorption plays an important role in the acquisition of uranium by phosphorite as well as fossil bones (150).

Studies of the distribution of uranium in carbonaceous and related rocks are of interest from the viewpoint of the possibility of formation of organic complexes of uranium. In the black shale in Montana, uranium was found to be fixed in the fine clay fraction, but not in the black organic matter (89). In coal, it is contained in an organic-uranium complex, rather than in association with minerals (295).

In recently-deposited deep sea sediments the uranium content is from 1.5 to 2.5 p.p.m. of dried clay (257). The thorium content is $\sim$5 p.p.m. on the same basis, so the Th/U ratio is slightly lower than but similar to its average value for continental rocks (466). Gross β,γ-activity has been measured in Chesapeake Bay bottom sediments (306).

Economic occurrences.—The literature on surveys and reconnaissances for radioactive deposits and on specific occurrences is too extensive for more than brief mention here. Preparation of a comprehensive "Bibliography and Index of Literature on Uranium and Thorium and Radioactive Occurrences

in the United States" has been undertaken by Cooper. Part 1 (117) covers Arizona, Nevada, and New Mexico, part 2 (118) California, Idaho, Montana, Washington, and Wyoming, and part 3 (119) Colorado and Utah. The scope of this compilation will eventually be expanded to cover the entire world and will be published in several volumes. *Nuclear Science Abstracts* is an excellent key to the publications and parapublications of this nature. Many of them are also abstracted by Marble in the *Report of the Committee on the Measurement of Geologic Time* (397, 398, 399).

Mineralogy.—Mineralogical and chemical studies were made on many radioactive minerals from different localities. The following new mineral discoveries were announced: Huttonite ($ThSiO_4$) from New Zealand (438), sabugalite [$HAl(UO_2)_4(PO_4)_4 \cdot 16H_2O$] from Portugal (215), novacekite [$Mg(UO_2)_2(AsO_4)_2 \cdot nH_2O$] from Germany (215), and cheralite [(Th, RE, Ca, U)(P, Si)O_4](RE = Ce, La, Pr, Nd, etc.) from India (83). For more extensive information *Mineralogical Abstracts* and the bibliographic sources mentioned in the preceding paragraph may be consulted.

Hydrosphere.—The uranium content of mineral spring waters in Japan was determined by Nakanishi (421). Results varied from <0.002 μg./l. (Schuzenji Hot Springs) to 0.95 μg./l. (Shinarima Hot Springs). Its distribution in sinter deposits is variable. Stalagmites from Austrian mineral springs were reported to contain from 1 to 1000 p.p.m. of uranium (502), whereas sinter deposits from mineral springs in Japan were quite low, values ranging from 0.004 to 0.05 p.p.m. (both extremes for Masutomi Mineral Springs) (421). The uranium content of brine from the oil field of southern Kansas was reported to be 0.16 μg./l., and of the associated deposits from traces to 50 p.p.m. (239).

North America river waters were analyzed to contain 0.016 to 0.040 μg./l. uranium (481). Great Salt Lake water contains about 5 μg./l. (520). Average values of the uranium content of sea water were reported as 2.82 μg./l. for deep northwestern Pacific waters (422), 0.62 μg./l. for open waters of the Northwest Atlantic (481), and 2.49 μg./l. for Pacific Ocean coastal waters (520). The precise and sensitive procedure developed by Stewart & Bentley for assaying natural waters for uranium, based on neutron-induced fission counting of an organic solvent extract from samples of a few ml. or less in volume (520), justifies hope for the rapid accumulation of new data and renders premature discussion of the differences of the above results with each other and with previous results.

Meteorites.—The concentrations of uranium and thorium in meteoritic materials are so low that especially sensitive analytical methods must be used. Dalton and co-workers have developed several such methods for use with iron meteorites: alpha counting of radon and thoron from chemically concentrated radium (133); fluorimetric estimation of chemically isolated uranium (133, 135); counting of thorium C+C′ alpha particles in thorium B separated from chemically isolated thorium (133, 135). The use of U^{233} tracer increases the accuracy of the uranium assay (135). Patterson *et al.*

(451) have employed mass-spectrometric isotope dilution analysis using enriched U^{235} as the diluent (262, 545).

Patterson *et al.* found close to 10^{-8} parts by weight of uranium in two stony meteorites (451). In iron meteorites, Paneth and the Durham group found uranium ranging from $\sim10^{-9}$ to $\sim10^{-8}$ and thorium from $\sim10^{-9}$ to $\sim10^{-7}$ (133, 134, 135, 443). In a single specimen of troilite from an iron meteorite, Patterson *et al.* found 9×10^{-9} uranium (451). In a metal-bearing chondrite Chackett *et al.* found nearly the same uranium concentration, $\sim10^{-7}$, in both metal and silicate phases, whereas the thorium content was about the same in the metal phase but about four times as high in the silicate (103, 105).

Except for the work of Arrol *et al.* (44) and Davis (153), the earlier determinations of uranium in meteorites are definitely too high.

Potassium and Rubidium

Ahrens and his collaborators have made many spectrochemical analyses of potassium and rubidium in igneous rocks and silicate meteorites (10, 11, 280). A remarkable geochemical coherence of these two elements was observed, the K/Rb weight ratio being $\sim$90 in crustal rocks and $\sim$100 in chondrites and tektites. Average values for various materials are:

granite	3.55 per cent K	0.052 per cent Rb
basalt, gabbro, diabase	0.9 per cent K	0.01 per cent Rb
crustal rocks average	2.7 per cent K	0.035 per cent Rb
ultramafic rocks	0.001 per cent K	<0.0002 per cent Rb
chondrites	0.09 per cent K	0.0009 per cent Rb
tektites	1.77 per cent K	0.018 per cent Rb

In some pegmatitic minerals and other "small volume residuals" rubidium is enriched relative to potassium; in lepidolite the K/Rb weight ratio averages 6 and may be as low as 3 (10).

For chondrites the average potassium content is only about half the formerly accepted value (10), while for ultramafic rocks, mainly dunite and serpentinite, the average is lower by a factor of $\sim$30 than the results of previous wet chemical analyses, probably because of contamination of reagents by potassium (280). The geophysical significance of these findings is discussed under RADIOGENIC TERRESTRIAL HEAT.

Hée & Jarovoy have investigated the applicability of the autoradiographic technique to potassium-containing materials, but find that the resolution is inadequate for determining the distribution of potassium in rocks (258).

Secondary Natural Radionuclides

Rona & Urry have found $\sim3\times10^{-14}$ gm./l. of radium in North American river waters, the radium/uranium ratio being about four times its equilibrium value. In sea water the radium content varies from 0.7 to 5.8×10^{-14} gm./l. and averages 3.1×10^{-14} gm./l., but the activity ratio averages only

about 0.16. This ratio is very close to the reciprocal of its average value for freshly deposited ocean sediments, 6.4. For waters of intermediate salinities, the ratios fall on a smooth curve connecting the values for river water and ocean water of full salinity (481). Saito has found that radium has a much smaller tendency to form radiocolloids in river and sea water than does thorium (492).

No measurements of the ionium content of river or ocean waters have been made, but calculations of Rona & Urry (481) and of Holland & Kulp (267) indicate that the ionium/uranium activity ratio is only a small fraction of unity. The latter authors have given a particularly detailed discussion of the transport and deposition of uranium, ionium, and radium in rivers, oceans, and ocean sediments, and emphasize the paucity of experimental data.

Studies of the radium and ionium content of ocean sediments are discussed under the RADIUM-IONIUM METHOD of age determination. Holland & Kulp (268) present evidence that base exchange equilibria are responsible for the selective removal of radium and ionium from the sea by sediments. The radium content of varved clay in Seattle was studied by Sanderman & Utterback (495), who found an annual periodicity with a higher radium content in the winter layers than in the neighboring summer layers. The radium is probably in transient equilibrium with the ionium present in these deposits.

The radioactivity of natural waters, especially that attributable to radium isotopes and their descendents, has been reviewed by Love (391). A determination of radium (mass number unspecified) in rain water has been reported (136). Additional studies of radium isotopes in mineral spring sinter deposits were made (304, 410, 411, 487). Activities as high as 1.0×10^{-9} curie of Ra^{224} and 6×10^{-10} curie of Ra^{226} per gm. of sulfurous sinter from Tamagawa Hot Springs, Japan, were found (411). Ra^{224} and Ra^{226} were observed in United States oil field brines and associated deposits (239, 370). The latter contain from 0.007 to 0.05 p.p.m. of Ra^{226}, which is far in excess of the amount which would be in equilibrium with the uranium present (239). This is similar to the situation found for Japanese mineral springs (366, 421).

Studies have continued on the distribution of radon and thoron and their decay products in the atmosphere (76, 136, 138, 155, 219, 249, 299, 305, 374, 433, 434, 551, 581, 582) and hydrosphere (36, 46, 47, 48, 69, 79, 368, 369, 370, 436, 437, 483, 507, 508, 509, 549, 550, 553, 554). These studies generally confirmed the lack of equilibrium between radon and its decay products in the hydrosphere emphasized by Kimura and co-workers (333, 366, 367, 588). The existence of Pb^{210} in rain water was first reported in 1952 (76).

Minami and his collaborators have determined Pb^{210} and Po^{210} in the sulfurous sinter and hokutolite [$(Pb, Ba)SO_4$] in Tamagawa Hot Springs, in Japan, finding up to 5×10^{-10} curie of each nuclide per gm. of solid. In the freshly deposited sulfurous sinter these nuclides are not in equilibrium with Ra^{226}, whereas in rather old hokutolite equilibrium is almost obtained. The

possibility of determining ages and rates of formation of sinter deposits by utilizing this relation was suggested (411).

Iwasaki *et al.* (303) and Kamada (322) have measured radon and thoron in gases from volcanic fumaroles in Japan, and have reported concentrations up to and exceeding 10^{-7} curie/l. for each. These concentrations are much greater than the few previous measurements (367, 504) and are considered almost unbelievably high (370). Faul and others have measured the radon content of helium-containing gases from 1200 gas wells in the Texas Panhandle region, finding from $<10^{-12}$ to 7×10^{-10} curie/l. Variation of the radon content with flow rate indicates that the radon may originate in the immediate vicinity of the bore in most wells (189, 189a, 189b).

The first observation of radioactive spontaneous fission products has been reported by Kuroda & Edwards. Sr^{90} was observed in Great Bear Lake pitchblende and uranium metal, and Sr^{89} and Sr^{90} in a uranium salt. In all cases a part of the activity could definitely be attributed to spontaneous fission, though neutron absorption also contributed to the fissions (370, 371).

Artificial Radionuclides

Artificial radioactivity produced by nuclear explosions was detected in air, dust, rain, snow and surface waters throughout the world. The level of this activity relative to that from natural radioelements was sometimes considerable, and disturbing amounts of contamination and high background counting rates were observed in many places after test explosions (1, 2, 3, 136, 176, 184, 220 to 227, 253, 405, 482, 496, 542,).

Induced Natural Radionuclides

Carbon 14.—The production and distribution of natural radiocarbon on earth has been reviewed by Anderson in Volume 2 of *Annual Review of Nuclear Science* (28). The results of Libby, Anderson & Arnold (25, 380) indicate that the specific C^{14} activity of the carbon of contemporary wood is constant to within 2 per cent throughout the world and equal to[2] 15.3 ± 0.5 dis./min./gm. For recent shell they found 16.5 ± 0.5 dis./min./gm., the fractionation factor of 1.09 ± 0.03 being unexpectedly large. Kulp *et al.* found a shell to wood ratio of 1.11 ± 0.02 (350). However, Blau *et al.* (75) found that in a much wider selection of shells the majority had the same specific activity as wood, and Suess (533) has obtained similar results. Surface sea water carbonate seems to have the same activity as contemporary shell, but deep sea waters are distinctly lower (352). The carbonate of hard-water lakes and streams, and the organic and inorganic materials derived therefrom, have reduced specific activity because of the presence of inactive carbon derived from limestone (159). Independent measurements of the absolute number of C^{14} disintegrations per minute per gram of contemporary plant carbon are 14.5–14.8 (172), 12.9 ± 0.2 (256), and 15.2 (40). Anderson estimates the average specific activity of the "exchange reservoir" to be 16.6 ± 0.6 dis./min./gm. Theoretical values based on cosmic ray neutron intensities and geo-

chemical estimates of the exchangeable carbon are 18.8 ± 5 (25), 13.5 to 18 (463), and 19 ± 4 (28).

The agreement between radiocarbon and historical ages back to about 5000 years ago (37) indicates that the specific C^{14}-activity of atmospheric carbon has been fairly constant for the past few half-lives (382). The claim that the cosmic ray intensity has been constant to within 10 per cent for 20,000 years (37) appears extravagant, however; such high constancy is actually implied only for about two half-lives, or roughly during post-glacial time. Kulp & Volchok (358) have compared C^{14} and ionium ages of layers of deep sea cores, and from the agreement they conclude that the C^{14}-concentration and, hence, the cosmic ray flux has not varied by more than from 10 to 20 per cent over the last 35,000 years, or well back into the ice age. However, there were only a few samples, none over 25,000 years old, and all had considerable measurement uncertainty, and so this conclusion must also be accepted with reservation pending additional evidence. Ionium ages are quite sensitive to the original ionium concentration in the sediments, and it is known that climatic differences, such as those between glacial and interglacial times, result in differences in the character of marine deposits. A 5 per cent change in ionium content corresponds to a change in the apparent age of 6000 years, which in turn would correspond to a change of a factor of two in the natural radiocarbon specific activity. Although the reservoir of exchangeable carbon dioxide has probably not changed appreciably for much of the past (486), Martin (400) believes, from a study of the He^3 and He^4 contents of meteorites, that the average cosmic ray flux during geologic time has been several times as high as the present value.

An indication of a small decrease in the C^{14}-concentration of the atmosphere in recent decades has been obtained by Suess (532, 533). This could be attributable to the introduction into the atmosphere of large amounts of inactive CO_2, resulting from the combustion of coal and petroleum. The natural carbon of the atmosphere seems to have been diluted about 3 per cent up to 1950.

Tritium.—The concentration of tritium in natural hydrogen is much more variable. Faltings & Harteck (185) examined the molecular hydrogen component of the atmosphere, finding about one tritium atom in this chemical form per 10 $cm.^3$ of air, or about one T atom per 10^{14} H atoms; this has been confirmed by Suess working with Libby (531a). Grosse *et al.* (244) have found the T/H ratio of Norwegian fresh water to be about 10^{-18}, from which it follows that tritium is enriched in the H_2 by a factor of $\sim 10^4$ over the H_2O in the atmosphere (250). Grosse, with another group (245), has obtained several values of T/H for atmospheric H_2 averaging $(1.66 \pm 0.10) \times 10^{-14}$, while Kaufman & Libby (324) have made numerous measurements of this ratio in natural waters, finding values ranging from 0.5 to 66×10^{-18}. Extreme variations are found in rain waters, even for a single locality, but the average for a given region, as represented by rivers and agricultural products, is more nearly constant; for central North America

and continental Europe this is $\sim 4 \times 10^{-18}$. Fireman & Schwarzer (197) have found T/H ratios as high as 800×10^{-18} in rain water, whereas glacial water contained $< 0.5 \times 10^{-18}$ T/H. Inshore ocean surface waters have been found to contain substantial concentrations of tritium (197, 324), but the oceans as a whole are virtually unsampled.

Fireman (196) has calculated the rate of tritium production by cosmic rays, obtaining 0.4 to 0.9 T atoms per second per cm.^{2} of the earth's surface. About one-fourth of this is produced by the N^{14} (n, t) C^{12} reaction, and the remainder by ejection of tritons in cosmic ray "stars"; other processes contribute negligiblibly. On the other hand, Kaufman & Libby (324) estimate from their measurements a production rate of only 0.12 atom/sec./cm.^{2} The average T/H in the oceans should be 1 or 2×10^{-20} according to Fireman but only $\sim 4 \times 10^{-21}$ according to the data of Kaufman & Libby. Grosse *et al.* (245) have elaborated on the explanation of Faltings & Harteck (185) for the large differential between atmospheric hydrogen and rain water. A general discussion is given by Libby (387).

Beryllium 7.—Arnold has recently discovered Be^7 (half-life 45 days) in rain water, presumably carried down from the upper atmosphere, where it is produced by cosmic ray spallation reactions (42).

Induced activities in radioactive minerals.—Quantitative studies have been made of the natural occurrence of plutonium in uranium minerals (377, 458). The occurrence of the $(4n+1)$ radioactive series in nature was established by the isolation of Np^{237} and some of its decay products from Belgian Congo pitchblende (459). Kuroda & Edwards have observed a radioactive fission product, Sr^{90}, in Great Bear Lake pitchblende at a level of $(1.3 \pm 0.1) \times 10^{-14}$ curie per gm. U. This is slightly but significantly greater than the amount expected from spontaneous fission, and suggests that ~ 27 per cent of the activity comes from neutron-induced fission (270, 371).

Extinct Natural Radionuclides

No definite evidence for the occurrence of an extinct natural radionuclide as defined above has yet been found. It has been pointed out (342, 346, 347) that the half life would have to be between $\sim 3 \times 10^7$ yr. and $\sim 3 \times 10^8$ yr.; thus, in the gap between U^{236} (2.4×10^7 yr.) and U^{235} (7.1×10^8 yr.). Sm^{146} has recently been identified and its half-life given as $\sim 5 \times 10^7$ yr. (174), but, even if its half-life is in the right range, the fact that it and its decay product are both rare earth nuclides would probably make detection of natural effects difficult. A supposition that part of the Xe^{129} in the earth's atmosphere is of radiogenic origin, resulting from the decay of residual I^{129} after the formation of the earth (323), has been held unsubstantiated (530). Earlier indications of an excess of Xe^{129} caused by decay of I^{129} in old minerals (298) were not substantiated by subsequent measurements (255). Rosenblatt has discussed conceivable consequences of a primeval endowment of U^{236} (484), but quantitative calculations show that its lifetime is too short for the effects imagined. Invocation of now-extinct radioactive parents of zirconium

or hafnium to account for geochemical variations in their abundance ratio (116) is preposterous.

RADIOACTIVITY AND GEOLOGIC TIME

The annual *Reports of the Committee on the Measurement of Geologic Time*, prepared by Marble (397, 398, 399), are the most extensive sources of information on the applications of radioactivity to this problem and on many related matters. In addition to abstracts of conventional publications, reports of many types are abstracted, and summaries of recent work are given by Marble and others. Zeuner's *Dating the Past* (592) discusses radioactive methods briefly. Recent general reviews have been written by Boganik (80), Picciotto (464), López de Azcona (390), Starik (518), and Curran (130). Burling (97) emphasizes the basic physical principles and Ubisch (552) describes the mass spectrometric aspects, while Moore (413) and Wilson (584) discuss the correlation of mineral ages with geologic events and times. The useful age methods are reviewed by respective authorities, with presentation of new data in some cases, in *Nuclear Geology* (190).

Rodgers (480) has considered and recalculated all available age data from the Appalachian region, most ages being chemical ages for uranium and thorium minerals without benefit of atomic weights or isotope analyses. By considering together a number of related determinations, it was possible to select those which were probably most reliable. Groupings of ages suggest major orogenies about 800, 600, 350 and 260 m.y. ago.[2] Similar discussions have been given by Cahen for Katanga, Belgian Congo (98, 99, 101) by Bose for India (81), by Jolliffe for the Great Bear Lake area of Canada (315), and by Cooke for South Africa (115a).

Lead Methods

Chemical method.—Mineral ages calculated from chemical analyses for uranium, thorium and lead continue to be reported (49, 81, 100, 207, 263, 334, 455, 456, 536, 537, 587). In all cases these are probably upper limits because of the possible presence of common lead. Although in the past corrections have often been made on the basis of atomic weight determinations of the lead, this refinement has not been applied in any of the recent work, and, in fact, is hardly justifiable any more in view of the development of mass spectrometric isotope analysis.

Wasserstein (574) has found that the cube-edge of uraninite as determined by x-ray diffraction decreases progressively with age by about 0.0025 to 0.0041 Å per 100 m.y., and has proposed this as a method of geochronometry. Since the cell dimension change is caused by the replacement of uranium by lead, this is evidently to be regarded as an alternative chemical method, with the possible advantage that common lead may be excluded from the original uraninite lattice and hence may not interfere.

Uranium lead isotopic methods.—It is now generally considered that reliable lead ages can be obtained only through mass spectrometric determina-

tion of the isotopic composition of the lead, and this is becoming standard practice in most current age determinations.

Collins and co-workers (110, 111, 112, 114, 115, 188) have utilized mainly Pb^{207}/Pb^{206} ratios without chemical analyses for uranium and lead, and they claim that this age index is more reliable than the Pb^{206}/U^{238} and Pb^{207}/U^{235} indices since, as was first pointed out by Nier (428) this ratio is least affected by loss of some uranium or lead during the lifetime of the mineral. From numerous measurements on Canadian uraninites and pitchblendes, they conclude that uraninites generally correctly date their host rocks but pitchblendes may be of any age up to that of the rocks. Wilson (584) has discussed the results and their use in dating the orogenic activity in the geologic provinces of the Canadian Shield. Ehrenberg (175) has also reported several Pb^{207}/Pb^{206} ages.

Kulp and collaborators (361, 364) have made both chemical and lead isotopic analyses of a number of uranium minerals and have come to the conclusion that the Pb^{207}/U^{235} and Pb^{206}/Pb^{210} (see below) ages are most reliable over the greatest range of geologic time. The Pb^{206}/U^{238} age supersedes the Pb^{207}/U^{235} age in precision for young minerals, though it is often several per cent low because of radon loss. The Pb^{207}/Pb^{206} age is quite unreliable; because of its high sensitivity to radon loss, it is almost always too large.

The discordant conclusions of Collins *et al.* and Kulp *et al.* on the reliability of the Pb^{207}/Pb^{206} age index may be attributed in part to a difference in the age range of chief interest. For ages of a few hundred million years or less the isotope ratio changes very slowly with age, and Kulp's conclusion is certainly correct. Where alterations, radon loss, or mass spectrometric errors are appreciable, the resulting age calculation has no meaning at all, as shown by the work of Stieff *et al.* (522) referred to below. On the other hand, for very old minerals the ratio is a more rapidly varying function of age, and should be a more reliable indicator. Holmes gives it preference for a series of minerals over 2000 m.y. old (279). More work is needed to establish the reliability of Pb^{207}/Pb^{206} ages, especially in the range from 1000 to 2000 m.y. At present, no uranium mineral can be considered reliably dated without both chemical and isotopic analyses.

Kulp's group has made laboratory studies of the leakage of radon from uranium minerals by the emanation technique (57, 58, 364). Samarskites emanate to an extent less than 0.1 per cent, uraninites and pitchblendes leak from 0.1 to 1 per cent, and secondary minerals such as carnotites may leak as much as 20 per cent. Emanating power increases with increasing temperature and with decreasing particle size. Although the average radon leakage throughout the history of a mineral may have been different from the laboratory result, application of a correction based on the latter often brings the Pb^{206}/U^{238} and Pb^{207}/Pb^{206} ages close to the Pb^{207}/U^{235} age, which is unaffected by emanation.

The variability of the isotopic composition of common lead leads to uncertainty in the common lead correction, which affects particularly the

Pb^{207}/Pb^{206} age. Kulp's group finds that all common lead samples from a given region have nearly the same constitution, which considerably reduces the uncertainty in the common lead corrections (59). According to Kulp, if all refinements and corrections are made, lead age determinations with 2 per cent uncertainty in the range from 50 to 3000 m.y. are a practical possibility for the near future (364).

In the United States the publication of age determinations of uranium-containing minerals utilizing both chemical and isotopic analyses is becoming frequent (263, 330, 521, 522, 523). Some of the latest measurements of the Toronto group involve chemical as well as isotopic analyses (115). The first such publication in France has been made by Demay (166), with mention of additional results to be published by Chervais & Roth. Holmes has published several such determinations in Great Britain (279).

Secondary and sedimentary radioactive minerals have generally been avoided in age studies, but Stieff, Stern & Milkey (522) have undertaken an extensive study of Colorado Plateau uranium ores, mainly carnotites. The carnotite Pb^{206}/U^{238} ages are mostly in the neighborhood of 70 m.y., corresponding to the ages of some uraninites of the same district, but the Pb^{207}/Pb^{206} ages fluctuate enormously. This is attributed in part to sensitivity to mass spectrometric errors and to radon loss but mainly to uncertainty in the common lead corrections; the "common" lead seems to be largely "radiogenic" in many cases. If the 70 m.y. age of these deposits is correct, they must have been formed in the sediments considerably later than had been deduced from field evidence only.

Thorium lead isotopic method.—Pb^{208}/Th^{232} ages are not as frequently used as are those based on uranium and its end products. Most thorium minerals have enough uranium to provide independent age calculations for comparison. It is well known that the thorium lead ages are usually lower than the best estimate by the uranium lead method, often considerably so (16, 273, 274, 277).

Kulp *et al.* mention unpublished measurements on minerals high in both uranium and thorium which give good agreement in calculated ages, though they find anomalies when either uranium or thorium is low. They consider the Pb^{208}/Th^{232} ratio usable for minerals high in thorium (364). However, of three monazites analyzed recently, two, which happen to be those with the highest thorium contents, gave thorium lead ages considerably below the values selected by Holmes as most probable (279).

Tilton *et al.* have observed low thorium lead ages in zircon and other highly radioactive accessory minerals separated from granites (16, 546). They propose that preferential loss of Pb^{208} occurs from metamict areas of minerals containing a high enrichment of thorium (546). This hypothesis is supported by an acid leaching experiment on a granitic sphene separate, which resulted in decidedly greater removal of Pb^{208} than of Pb^{206}, and by measurements indicating transfer of lead between mineral constituents in a granite rock (16).

This explanation is not obviously applicable to high-thorium minerals. Present efforts in this area are directed towards an understanding of the discrepancies, which will be necessary before any thorium lead age measurements can be considered reliable.

Radiolead method.—Houtermans (286) has proposed an age method for uranium and thorium minerals based on the fact that the rate of production of a lead isotope can be indicated by any member of the disintegration series from the parent down to the immediate precursor, assuming secular equilibrium. Pb^{210} (RaD) is a particularly suitable indicator of the Pb^{206} production rate because its isotopy with the latter preserves their ratio during chemical separation, which need not be quantitative. The absolute specific RaD activity must be determined radiochemically, either through the Bi^{210} (RaE) betas (63, 64, 65, 286, 494, 494a), or the Po^{210} alphas (362). The method has the advantage of reducing the errors resulting from radon leakage and weathering. If the radon leakage has been the same for the entire lifetime of a mineral as for the last few decades, the radiolead method should give its correct age. Recent leaching of uranium from the mineral should not affect the radiolead age as much as the chemical age, because ionium can support RaD for awhile.

Houtermans and collaborators have applied this method as a modification of the chemical method, for which it must be assumed that thorium and common lead are absent. For Shinkolobe (Belgian Congo) pitchblendes good agreement was obtained between this and the ordinary chemical method employing lead and uranium analyses (63, 64, 65, 286).

Kulp *et al.* have used the radiolead method in conjunction with mass spectrometric determination of the radiogenic Pb^{206} content, thus obtaining Pb^{206}/Pb^{210} ages. For a number of samples ranging from 60 to 1400 m.y. old the Pb^{206}/Pb^{210} ages agreed with the "best" isotopic lead ages within several per cent, from which it was concluded that uranium leaching and radon loss have been negligible (362). Since the two effects could be compensatory, since the errors amounted to 3 to 10 per cent, and since the RaD counter was standardized with lead from (unspecified) uranium minerals of "known" age, these conclusions are uncertain. Later work by Kulp's group, in which an independent standardization of the RaD assay was made, has shown discrepancies between Pb^{206}/U^{238} and Pb^{206}/Pb^{210} ages indicating that radon losses of several per cent are frequent (365). Measurements on a large number of carnotite leads by Saito and others have indicated severe departures from secular equilibrium between U^{238} and Pb^{210} in such minerals (494a).

Kulp states that the Pb^{206}/Pb^{210} ages aften agree more closely with the Pb^{207}/U^{235} ages than do the Pb^{206}/U^{238} ages (365). Because of frequent failures of the various age methods to agree, it is probable that the radiolead method will have its greatest usefulness in conjunction with the other methods rather than independently of them.

Houtermans (286) suggests that the same method could be applied to thorium-containing minerals, but with greater difficulty because of the short

half-life (10.6 hr.) of the radiolead involved, Pb^{212} (ThB). No applications have been reported.

Application to common types of rocks.—It has long been realized that dating methods applicable to common rock types would be more useful than those requiring uncommon minerals. Many years ago Taylor (540) applied the chemical lead method to concentrates of accessory zircon from granite, but because of the unknown content of common lead the ages were only approximate upper limits. Miholic (409) has attempted to calculate ages of igneous rocks from gross chemical analyses, but overlooked the necessity, recently reemphasized by Burling (97), of a geochemical separation or fractionation to define each event being dated.

Wickman (578) has pointed out that the common lead difficulty can be overcome by taking advantage of differences in the U/Pb and U/Th ratios in the various mineral phases of igneous rocks at the time of their segregation. Brown and his collaborators (86, 262, 450, 545, 547a) have made chemical and isotopic analyses of several mineral separates from a Precambrian granite from Ontario, which show that the separations may be even more favorable than was visualized by Wickman. Perthite is relatively high in lead and low in uranium, whereas in zircon, sphene, and apatite the reverse is true. The Pb^{207}/U^{235} age derived from the zircon-perthite combination, 1050 m.y., and the Pb^{207}/Pb^{206} age from the sphene-perthite combination, 1070 m.y., agree within the accuracy of the measurements. There is a suggestion, however, that transport of elements between mineral phases in the granite has occurred (547a).

Larsen, Keevil & Harrison (373) have meanwhile applied the chemical method to accessory minerals isolated from igneous rocks, using alpha activity measurements and an average U/Th ratio to estimate the rate of Pb generation. Zircon, allanite, sphene, and monazite have high radioactivity and presumably low common lead, zircon being the most satisfactory. Fair agreement with stratigraphic ages was obtained on Paleozoic and older rocks, but excessive ages resulted from younger rocks, probably because of the relatively greater importance of common lead. An application to rocks of unknown age has been made (425).

These results are hopeful, but accurate chemical and isotopic analyses apparently will be necessary for accurate dating of rocks. The procedures are tedious and difficult, although facilitated by isotope dilution techniques (262). Investigations of the applicability of the method to sedimenatry rocks, as also suggested by Wickman (579), are much to be desired.

Common lead methods.—Nier long ago observed that variations in the isotopic composition of common lead could be attributed to gradual contamination of primeval lead (dispersed in the earth's crust) by Pb^{206}, Pb^{207}, and Pb^{208} produced by uranium and thorium (also so dispersed), with the composition frozen in a given sample at the time of its concentration into a mineral (427). Variations in the U/Pb and Th/Pb ratios cause regional differences in the isotopic composition of lead at a given time in geologic his-

tory, though Holmes (270) pointed out that the ratios Pb^{206}/Pb^{204}, Pb^{207}/Pb^{204}, and Pb^{208}/Pb^{204} vary roughly monotonically with stratigraphic mineral age. There are two approaches to the estimation of the age of a lead mineral from its isotopic composition: (*a*) to disregard regional geochemical variations and to consider the isotope ratios as universal age indices, though subject to errors because of those variations; and (*b*) to recognize the regional variations and attempt to deduce not only the age but also the U/Pb and Th/Pb ratios of the source rocks or magmas of each mineral.

The first approach has been advocated by McCrady (403), who considered $(Pb^{206}+Pb^{207})/Pb^{204}$ as a universal function of time in the earth's crust and established the relation by assigning ages to the extreme samples then known, 100 m.y. for Joplin, Missouri, galena and 2780 m.y. for Ivigtut, Greenland galena. It has been pointed out, however (137), that the leads from these two localities are both unusual, and consequently the resulting ages for other minerals show little correlation with their stratigraphically assigned ages. McCrady makes the important and not always recognized point that the lead in a mineral may be older as likely as younger than the enclosing rocks, but the discrepancies are too large and systematic for his ages to be acceptable. A refinement was introduced by Russell *et al.* (18, 490), who used average curves of Pb^{206}/Pb^{204}, Pb^{207}/Pb^{204}, and Pb^{208}/Pb^{204} versus time derived from statistical analysis of a large number of independently dated lead minerals (20, 114). They expected the older lead samples to fit the theoretical curves more closely than the younger ones, and derived Pb^{206}/Pb^{204}, Pb^{208}/Pb^{204} and mean ages ranging from 1830 to 2860 m.y. for a considerable number of lead minerals. Wickman (579) has suggested that this method might be applied to certain minerals constituents of marine sediments which have high Pb/Th or Pb/U ratios, on the assumption that oceanic Pb might actually be a good average sample of contemporaneous crustal lead. Patterson and colleagues (88, 452) have undertaken work along these lines.

The second approach involves the assumption that at a certain time all crustal regions had the same lead isotopic composition though different U/Pb ratios, so that subsequently the radiogenic isotopes were added at different rates. The ratio (radiogenic Pb^{207})/(radiogenic Pb^{206}) provides an indication of the time of removal of the lead from contact with uranium. This dating possibility was mentioned by Bullard & Stanley (91) but was considered by Collins *et al.* (114) to be unreliable. It has been applied by Damon (137), Houtermans (287), and Geiss (229). Damon used Holmes' values (271) for the age of the crust and for the original Pb^{206}/Pb^{204} and Pb^{207}/Pb^{204} ratios to derive ages of a number of samples analyzed by Nier (427, 429) and Collins *et al.* (113, 114). Houtermans and Geiss used the isotopic composition of meteoritic Pb (451) and a derived age of the earth of 4460 m.y., and calculated ages for samples analyzed by Geiss and previous investigators (75, 114, 229, 427, 429, 564). According to the discussion given below under MEGASCOPIC HISTORY OF THE EARTH, this is not a logical basis, the proper

one being that derived by a Holmes-Houtermans type of analysis from independently dated Pb minerals. Thus Damon's ages should be more nearly correct than Houtermans' and would be improved by the use of the recent set of parameters of Collins *et al.* (112, 114) in place of the older Holmes' set. For old samples Damon's ages should be somewhat low and Houtermans' considerably high.

An interesting comparison of the two approaches is provided by the exceptional Ivigtut galena. Allen *et al.* derive by the first method 1830 m.y. Damon derives by the second method 550 m.y. The age assigned by Holmes on stratigraphic evidence is 600 m.y. If this lead was derived from source rocks or magna of exceptionally low U/Pb (137), a large error would result by the first approach. However, the two calculations were based on different samples analyzed in different laboratories.

Helium Method

Terrestrial rocks and minerals.—Hurley (292) has pointed out that past helium age measurements indicate low and variable helium retentivities. Part of this had been shown to be ascribable to concentration of uranium and thorium along grain boundaries and other planes of weakness, from which helium can readily escape; acid treatments to remove such radioelements generally improved the helium ages (291). In continuing work, Hurley has found that the rate of escape of helium from the interior of mineral crystals is a function of the radiation damage of the crystals. Escape of helium from zircon and sphene appears negligible when the alpha bombardment has been low, and increases progressively with integrated flux. The escape rate is approximately directly proportional to the extent of previous irradiation. Thus the helium content goes through a maximum and approaches zero again when the lattice has suffered a bombardment of $\sim 10^{16}\alpha$/mg. After determining the proportionality factors with zircons and sphenes of known ages, Hurley was able to derive corrections for helium loss and thus calculate ages for minerals of unknown antiquity. He also showed that the method could be applied to accessory zircons isolated from granites. Although some apparent discrepancies were observed, the general agreement with known or possible ages justifies considerable hope for salvaging the helium method (292).

Pellas (457) has given theoretical support for this mechanism of escape of helium from zircon. A study of helium loss from monazite as a function of temperature and of gas pressure and composition has been made by von Erichsen (180).

Carr & Kulp (102) have used the helium method to determine the age of a basalt boulder from the lower slopes of the Mid-Atlantic Ridge. The result, 30 ± 15 m.y., confirms Tertiary volcanic activity on the ocean floor.

Gentner *et al.* have measured U, Th, and He contents of Lower Oligocene sylvites of the Rhine Valley deposits. The apparent helium age is about 10 m.y., but dependence of the helium content on crystal size indicated dif-

fusion loss of helium. A calculation to allow for this loss, under the assumption of a higher temperature in the past in order to achieve agreement between the corrected helium and argon ages, yielded 25 ±4 m.y. as the age of the deposits (232). Loss of radiogenic gases may have been influenced by crystal damage by the K^{40} β- and γ-radiations. Thomson & Wardle (543) have observed that at least some rocksalts contain more helium than can be accounted for by their uranium and thorium contents, and that freshly grown rocksalt crystals incorporate significant amounts of helium from air-saturated water.

Meteorites.—The extensive program of helium and radioelement assay of meteorites and calculations of their ages by Paneth and his collaborators (44, 445) has been resumed (446). A few years ago it was pointed out that cosmic ray bombardment might be responsible for a considerable quantity of the helium in meteorites. Although Paneth at first believed the effect to be unimportant (103, 441), he and his collaborators have examined the isotopic composition of meteoritic helium with the idea that a contribution by cosmic rays should reveal itself by the presence of He^3, which cannot be produced radiogenically. Theoretical expectations were that the He^3/He^4 ratio in cosmogenic helium should be about 0.3 (375) or 0.4 (511). In five iron meteorites He^3/He^4 ratios of 0.178 to 0.315 were found, the lower value being for a moderately low-helium meteorite [Bethany (Harvard), 0.36×10^{-6} cm.^{3}/gm.] and the higher value being for a high-helium meteorite [Mount Ayliff, 36.8×10^{-6} cm.^{3}/gm.] (443, 444). Evidently, at least in the high-helium meteorites, a majority of the helium is cosmogenic, and substantial downward revision of some of the helium ages is required. An assumption that the cosmogenic helium of the Bethany (Harvard) meteorite has the same composition as that of Mount Ayliff allows a calculation of the radiogenic helium of the latter; its corrected age is about 75 m.y., compared to ~200 m.y. on the previous basis of calculation. Whereas helium ages ranging up to ~7000 m.y. (Mount Ayliff) had formerly been calculated (44), a period of ~1000 m.y. now seems sufficient to account for all observed helium contents (443).

A considerable number of new determinations of the concentrations in iron meteorites of uranium and thorium (133, 134, 135) and of helium (105, 134, 447) have been published. For many of the specimens the isotopic composition of the helium has been determined (134, 447). Studies of the helium content and He^3/He^4 ratio as a function of depth in the fallen mass showed no appreciable depth effect for small or irregular meteorites, but for a large and nearly spherical meteorite a definite effect was observed. Both the content and the ratio rise for the first few centimeters and then fall (447). The maximum is attributable to the effect of the cosmic ray secondaries, including π-mesons; considerably more of the helium is produced by the secondaries than by the primaries (400).

More reliable age calculations can now be made for iron meteorites. A group of meteorites having low helium contents and He^3/He^4 values <0.26 have maximum radiogenic helium ages of 100–300 m.y., but some of them

must be at least 100 m.y. old (134). Several meteorites having very low helium contents were found to have normal radioelement contents, and must therefore be very young; some have maximum helium ages of ~1 m.y. or less (134, 443).

Theoretical discussions of the production of helium in meteorites by cosmic rays have been given by Singer (511, 512, 513, 514) and by Martin (400). Both estimate the rate of this process, and use it to calculate ages for helium-rich meteorites. Martin feels that some meteorites give excessive ages on the assumption of a constant cosmic ray intensity and postulates that the mean value during the past ~100 m.y. has been several times as great as its present value. This conclusion, which is supported by certain ideas on the origin of cosmic rays, is important in connection with the foundations of the radiocarbon dating method.

Methods Based on Potassium 40

Argon method.—In most of the current work mass spectrometric determination of the A^{40}/A^{36} ratio is made in order to permit correction for non-radiogenic argon.

Argon age determinations of potassium chloride in the Lower Oligocene salt deposits in the Upper Rhine Valley (Buggengen) and Alsace have been made by Gentner and co-workers. The early measurements (440, 517) gave an age of 20 m.y., which was regarded as a minimum because of indications of diffusion loss of argon. From a study of the argon content in relation to the size of crystals (230, 231) it was later concluded that the most probable age of these deposits is 21 ± 3 m.y., provided their temperature has remained essentially constant. Recently, these workers (232) have made helium and alpha activity measurements on the same minerals. From a consideration of both argon and helium contents in relation to crystal size, they concluded that a higher temperature prevailed in the past and that the most probable age is 25 ± 4 m.y. They consider their results to indicate that the absolute ages of younger Tertiary formations have been overestimated previously.

Several laboratories are engaged in the application of the argon age method to silicate minerals. Fritze & Strassmann obtained an argon age of 1880 m.y. for microcline from Varutrask, Sweden (213). Gerling *et al.* have determined ages of several amazonites, nordmarkites, lepidolites, and microlines by this method (235). Gentner and co-workers have begun applications of the method to potassium feldspars, their first result agreeing with the stratigraphically estimated age (233).

Because of the ubiquitous geochemical nature of potassium and the fact that newly crystallized minerals should be rather free of argon, dating methods based on K^{40} offer great promise. Many geologists expect the argon method ultimately to be the most important method of geochronometry, since it is applicable directly to igneous rocks. However, it is not yet beyond the testing stage. The work of the Toronto (418, 489, 506) and Chicago (572, 573) groups mentioned in the section on NATURAL RADIONUCLIDES sug-

gests that argon loss may be appreciable even in silicates. The decay constants of K^{40} are not yet known with sufficient precision. All minerals tested contain some common argon, and it is not proper to assume, as has been done hitherto, that the common argon incorporated into the crystallizing mineral had the same A^{40} content as present-day atmospheric argon. Boato and collaborators have found substantial enrichments of A^{40} in the argon from Italian fumaroles and suffioni, the A^{40}/A^{36} ratios ranging up to twice that in the atmosphere (77, 78). Deep underground argon might have even higher proportions of A^{40}. Studies of the content and isotopic composition of argon in potassium-poor minerals would yield information of considerable value in this connection.

Gerling & Pavlova have determined argon ages of two chondrite meteorites. Both yielded ages close to 3000 m.y. (234). This result is of considerable interest in the light of the younger helium ages for most iron meteorites, and it is hoped that further results will be forthcoming.

Suess and others have made a study of the gases of tektites, among which they found only small amounts of argon, none of which was conclusively of radiogenic origin. Upper limits of 73, 10 and 32 m.y. were obtained for two Philippinites and an Australite (528). It seems probable to Suess that the ages of the tektites may be practically equal to the ages of the including terrestrial strata, which supports his view that they are meteorites derived from molten fragments of comets (529).

Calcium method.—The first observation of radiogenic Ca^{40} in a potassium mineral was that of Inghram *et al.* in Stassfurt sylvite, whose geological age was given as 10^8 years. The calcium present was about 70 per cent radiogenic Ca^{40}, which constituted 2.84 p.p.m. of the sample (297). Although the potassium content was not given, an assumption that the material was pure KCl permits a calculation of its age; the result, 95 m.y., is in agreement with the above estimate. This suggests the feasibility of the calcium method of geochronometry for essentially calcium-free potassium minerals.

Ahrens (8) has considered the feasibility of the calcium method for rocks. Most silicate minerals contain too high a Ca/K ratio, but lepidolite and possibly late-pegmatite muscovite are believed to be suitable. In these, the radiogenic Ca^{40} content of the calcium should be from 1 to 30 per cent, and the method should be useful for pre-Cambrian rocks.

Strontium Method

Until 1950, except for the pioneering work of Hahn and collaborators, all strontium age determinations were based on chemical analyses only. Ahrens used spectrochemical anlalysis (7) to determine Sr/Rb ratios and calculate ages of a large number of lepidolites (4, 6, 9). Reasons were given for supposing most of the strontium in this mineral to be of radiogenic origin, so the upper age limits thus obtained are presumed close to the actual ages in most cases. Venkatasubramanian (563) has applied the chemical strontium method to phlogopites. Miholic (409) made similar age calculations from

gross Sr and Rb analyses of igneous rocks but failed to show that common strontium was absent in the types of rocks analyzed.

Beginning in 1950, mass spectrometry has been applied to the determination of strontium ages, both for the evaluation of radiogenic Sr^{87} in the strontium (5, 9, 13, 154, 260, 548) and for isotope dilution assay of Rb and Sr contents of the minerals (15, 154, 548). This makes it possible to apply the method to more common types of minerals, such as biotite, in which the content of common strontium is appreciable. The high sensitivity of the isotope dilution technique permits the use of as little as 10 mg. of lepidolite and 100 mg. of biotite (548). These developments are significant because biotite is a nearly ubiquitous constituent of igneous rocks, whereas lepidolite is found almost exclusively in rarer pegmatites.

A complication to the determination of radiogenic Sr^{87} in the presence of common strontium is the variability of the isotopic composition of the element in nature, reported by Aldrich *et al.* The Sr^{86}/Sr^{88} ratio varies through a range of about 5 per cent (13, 14). Although changes in Sr^{87}/Sr^{88} or Sr^{87}/Sr^{86} as a result of geochemical processes would be expected to be only half as great as the change in Sr^{86}/Sr^{88}, there are additional variations in the Sr^{87} due to its radiogenic origin (13, 14, 260). The Sr^{87}/Sr^{88} ratio in celestite and feldspar, which have low Rb/Sr ratios, shows variations through a range which is also about 5 per cent. Furthermore, these variations are not well correlated with geologic age, in contrast to earlier expectations (571, 579). The evidence seems to indicate considerable variations in the Sr/Rb ratio in the source materials of the strontium (260). Thus the error or uncertainty in the amount or radiogenic Sr^{87} is considerable when the majority of the strontium is nonradiogenic, as in biotites.

Herzog *et al.* feel that the strontium method for biotites shows considerable promise but that more work is necessary to determine its limits of usefulness. Some pholgopite and muscovite samples showed excess Sr^{87}, and these minerals are also worthy of further investigation (260). However, at present the method is applicable mainly to lepidolites, and because of the slowness of the $Rb^{87} \rightarrow Sr^{87}$ transition, it gives useful information only for relatively old minerals. Nevertheless, according to Ahrens, it may ultimately become the most reliable method for dating early pre-Cambrian geology.

It is noteworthy that the strontium method has given the greatest mineral ages obtained so far (9). Davis & Aldrich reported 3160 ± 100 m.y. for a lepidolite from Bikita Quarry, S. Rhodesia and 3360 ± 100 m.y. for one from Winnipeg River, S. E. Manitoba (154). The former date agrees with Ahren's chemical strontium age of 2950 ± 300 m.y. (6). Tomlinson & Das Gupta derived an age of 3230 m.y. for a biotite from Sickle Lake, N. E. Saskatchewan (548). Aldrich *et al.* have obtained a number of very great lepidolite strontium ages, including one of 3570 ± 300 m.y. from the western United States (16) and two of $\sim$3800 m.y. from South Africa (16, 426). If correct, these dates imply an age for the earth's crust greater than has been considered seriously hitherto.

However, where comparisons with ages determined by alpha decay methods are possible, the strontium ages appear consistently larger. Bikita and other Southern Rhodesia pegmatites have given monazite lead ages of about 2640 m.y. (279). The orogenic belt passing through S. E. Manitoba has been dated at about 2200 m.y. by lead (274) and helium (290) methods. The strontium age of 2000 ± 20 m.y. for a Black Hills, S. D., lepidolite (154) exceeds the lead ages of around 1500 m.y. for the region (151, 269, 590), although younger strontium ages have also been obtained in the region (4, 548). Tomlinson & Das Gupta mention that their strontium age of 570 m.y. for biotite from Mt. Monadnock, N. H., is high relative to related lead ages (480). They furthermore state that a uraninite intimately associated with their Saskatchewan biotite was dated at only 1900 m.y. from the Pb^{207}/Pb^{206} ratio by the Toronto group; other uranium minerals in this area do not exceed 1850 m.y. in age (115). Holmes feels that there is a systematic error leading to abnormally high strontium ages (279). Persistent preferential loss of rubidium would of course explain the discrepancies (16), but acid leaching experiments make this seem unlikely (548). It has been pointed out in the section on NATURAL RADIONUCLIDES that the value of the Rb^{87} half-life used in all these calculations, $\sim 6 \times 10^{10}$ yr., may be too large and that the strontium age method cannot be considered reliable until the half-life is known with greater certainty (344).

Radiation Damage Methods

Several methods have been suggested for utilizing the effects of energetic radiations on natural crystals as a measure of the time to which they have been exposed to these radiations. Kulp and collaborators have proposed differential thermal analysis of partly metamict minerals as a measure of the radiation damage (266), and have carried out a series of measurements on several types of minerals (356). Specific alpha activities were also measured, and it was found that for zircons and samarskites the ratio of the area under the exothermic peak of the thermal curve to the alpha activity increases with the independently determined geologic age. However, exceptions occur, and nonuniformity of the crystalline material gives difficulties, requiring more work to develop a useful age method.

Daniels and co-workers have studied radiation-induced thermoluminescence in natural materials as an age index (140, 141, 142, 448, 449, 497, 589, 590). Most of the work so far has been on limestones and fluorites, whose alpha activities were also measured. In addition to the light emitted on the initial heating of a mineral, that emitted after reactivation by x- or γ-rays can also be measured. The method can be calibrated with minerals of known age, or by artificial α-particle bombardment. However, the area under the glow-curve peak depends not only on age and alpha activity, but also on activating and quenching impurities, crystal imperfections, and opacity, and in order to determine ages more knowledge of the effects of these other factors is necessary. In an extension of this work, Saunders has found

that light absorption by natural fluorites is a function of, *inter alia*, age (497).

Apparently the most quantitative index of radiation damage in minerals is the change in the unit crystal cell dimension of partially metamict zircons, which has been the object of a study of Hurley & Fairbairn (293). For a great many specimens, including both pegmatite zircon crystals and accessory zircon from granitic rocks, the x-ray diffraction angle from the 112 plane was found to be a fairly definite function of the product of specific alpha activity and geologic age. Apparently the rate of annealing of metamict zircon is negligible at temperatures slightly below its crystallization temperature, in contrast to many other minerals, which anneal rapidly at ordinary surface rock temperatures. The method is not applicable to the strongly radioactive minerals which exhibit metamictization because of the complete loss of crystal structure; for zircons it is generally limited to specimens of activity less than 500 α/hr./mg. A review of the metamict state by Pabst (439) is pertinent here.

Radium-Ionium Method

Pettersson has recently reviewed the early work on the radium, ionium and uranium content of sea water and the ocean floor, and described current work centered at the Oceanographic Institute in Göteborg (462). The measurements of the radium content versus depth in bottom cores do not bear out the expectation of a gradual change corresponding to rise of radium to transient equilibrium with ionium followed by decay of ionium to secular equilibrium with uranium. Instead, the radium concentration varies quite irregularly with depth down to at least 50 cm. in cores from the slowly deposited Central Pacific floor (349) and down to several meters in more rapidly deposited Atlantic Ocean sediments (67). Apparently, vertical migration of radium takes place extensively, and estimates of sedimentation rates from radium analyses are unreliable. Thus, from the growth of radium in the Atlantic sediments, a deposition rate of 2 to 3 cm./1000 yr. was calculated, whereas from the decay of ionium in the same sediments a rate of 2 to 3 mm./1000 yr. was derived. In an attempt to get around these difficulties, Pettersson has proposed a calculation of the ionium precipitation rate to the ocean floor, so that from the ionium content of the recently deposited matter its deposition rate can be inferred (461).

Recently, direct determinations of ionium have been made in Pacific cores, and it was shown that radium is not in equilibrium with ionium even at depths exceeding 30 cm. (300). The ionium concentration, however, does seem to decrease gradually with depth, thorium evidently being much less mobile than radium. From the decay with depth of the directly measured ionium, a sedimentation rate of $\sim$1 mm./1000 yr. was calculated for the Central Pacific Ocean (462).

These results are to some extent contradictory to the experience of Urry, who has found smooth radium-depth curves of the simple theoretical type in a number of cores. In other cores the radium content varied with sediment

type, but by plotting separately the measurements for a given sediment type fairly smooth curves were again obtained (560). Picciotto & Wilgain suggest use of the ionium/thorium ratio as an age index as a possible way of eliminating difficulties resulting from variable precipitation and sedimentation rates (446).

Hough (282) has recently correlated Urry's (560) Ra-Io age measurements on two long southeastern Pacific cores with their stratigraphy, which according to his interpretations provides a definite record of climatic conditions. He was thus able to date the post-glacial thermal maximum at 6000 yr. ago, six substages of the Wisconsin glacial stage at 11,000, 15,000, 26,000, 37,800, 51,000, and 64,000 yr. ago, and three Illinois substages at 274,000, 310,000, and 330,000 yr. By extrapolation, four Kansan substages could be approximately dated from ~700,000 to ~900,000 yr. ago, where the record ended. In earlier work Hough had obtained an extrapolated age for a cold zone in an Antarctic core, probably correlative with the Nebraskan glacial period, of ~900,000 yr. (281). Good correlations were found between the ages of cold-water zones in cores from the southeastern Pacific, the North Atlantic, and the Antarctic, indicating that major climatic fluctuations were approximately contemporaneous throughout the world (282). If Urry's measurements and Hough's interpretations are correct, they give us the best quantitative picture of Pleistocene chronology yet available.

Volchok & Kulp have undertaken similar studies (566, 567, 568). They find that, whereas cores from the Atlantic are heterogeneous and show an irregular radium versus depth relationship, an unusually homogeneous core from the Caribbean showed a smooth depth curve with a rapid rise followed by a slow decline, in accord with simple theory. Pertinent discussions have been given by Holland & Kulp (267, 268). Studies of correlations between ionium and radiocarbon ages of ocean sediments (358) have been mentioned above. The total alpha activity of sediments cannot be correlated with their age (357).

Backus *et al.* have found that major fluctuations in radium deposition in Gulf of Mexico sediments are correlated with fluctuations in manganese concentration, while the fluctuations in uranium content are smaller and uncorrelated. A sedimentation rate of 18 cm./1000 yr. was computed. It is indicated that the results are to be used to date *Foraminifera* population profiles (51). Zeuner has reviewed past attempts to link continental glaciology with submarine chronology in this manner (592). To date, no definite success along this line has been achieved.

Von Buttlar and Houtermans have determined the growth rate of manganese nodules from the decay of radium towards the interior, this element being preferentially deposited with MnO_2. They obtained 0.6 mm./1000 yr. (97a). Menard believes the deposition of MnO_2 is generally intermittent, with the long-term rate being much lower than that given by the radioactivity measurements (405a).

Some years ago Urry noted variations in the radium content of layers in the varved clay at Hartford, and attempted an age calculation (559). Koczy

claims that the measurements are not sufficiently reliable for age determination, and he was unable to verify Urry's calculation (338). Sanderman and Utterback have now made similar measurements on varved clay at Seattle, and, although seasonal and other variations were observed, the results were considered to offer no evidence of departure from equilibrium at the time of deposition (495). However, in both cases the deposits were many radium half-lives old, so the radium contents reflect the ionium contents. Since the spans of a few centuries covered by the varves studied are very short relative to the ionium half-life, such measurements could not possibly reveal departures from equilibrium. To do this would require uranium analyses, and probably direct ionium analyses as well. Furthermore, the calculation of an ionium age would require a knowledge of the ionium-uranium ratio in freshly deposited clay of the same type, and this may be impossible to determine.

Radiocarbon Method

Fleischer & Rabbit (198) reported that no age determinations by the C^{14} method were published in 1950, though several laboratories were working on the method. This work has now borne much fruit. The greatest number of radiocarbon dates has so far been determined by Libby and collaborators at the University of Chicago (38, 43, 381, 382, 283, 385), although extensive measurements have also been made by Kulp and collaborators at Columbia University (350, 352). Laboratories at Yale University (75), the University of Michigan (242), and Copenhagen (29) have begun to publish substantial results, and a few dates have appeared from California Institute of Technology (172), Poland (415, 416), and New Zealand (192, 540a). Radiocarbon dating laboratories are in preparation as follows: Universities of Saskatchewan (32), Manitoba (33), Pennsylvania, California, Colorado, and Texas (31), Carnegie Institute of Technology (169), Los Alamos Scientific Laboratory (212, 256), United States Geological Survey (532, 533), Magnolia Petroleum Company (95), Germany (186), The Netherlands (167, 168), England (55, 125), and Norway (240). Undoubtedly there are still others, and will be many more.

A number of laboratories have adopted the solid-carbon counting technique of Libby (26, 382), sometimes without modification. This method is capable of determining times back to about 25,000 yr. ago. Kulp has found that a mercury shield between the radiocarbon and cosmic-ray guard counters reduces the background from about 5 to about 2 counts per min., extending the limit to about 30,000 yr. (353, 354). Automatic sample-background alternating devices have been added (124, 191), and a double-counter modification permits simultaneous measurement of sample and background (27, 29). The screen of the screen-wall counter was found unnecessary with a metal or carbon cathode (124). The low efficiency ($\sim$5 per cent) and low sensitivity (6 to 8 counts/min. for contemporary carbon) of the Libby technique has led to many attempts to find a more efficient and sensitive method of measurement of natural radiocarbon.

These include use of a sensitive ionization chamber in a deep underground

location (172), a Geiger counter containing CO_2+CS_2 (417), and proportional counters filled with ethane (186), carbon dioxide (167, 168, 212), methane (95, 169), and acetylene (55, 125, 533). Although Anderson & Levy conclude that for small counters at moderate pressure solid-sample counting is superior to gas counting (27), the reverse is true for large counters and pressures of one or more atmospheres. Suess has obtained a contemporary carbon rate of 10 counts/min. over a background of 2 counts/min., permitting dating to about 38,000 yr. (533). Crathorn has obtained over 34 counts/min. for the contemporary carbon excess in a larger gas counter (125), and it seems likely that counting rates of several hundred per min. can be obtained by this method if appropriate effort is exerted, allowing dating back to about 60,000 yr.

Scintillation counting is also being applied to natural radiocarbon measurement (33, 34, 40, 50, 256), the sample carbon being incorporated into a solvent or solute of a liquid scintillator. Arnold has obtained contemporary carbon counting rates of over 50 per min. and feels this can be raised several-fold, enabling dating back to about 45,000 yr. The high sensitivity of the method is offset in part, particularly for old samples, by the high backgrounds (26 counts/min. in Arnold's apparatus), which should not be as effectively reduced by anticoincidence techniques as in the case of gas counters. Also, the efficiencies attained so far are somewhat lower. Nevertheless, Kulp believes that liquid scintillation counting will make dating feasible back to 100,000 yr. ago (355, 359, 360).

A possibility largely unexplored for extending the range of radiocarbon dating is isotopic enrichment of the carbon with respect to C^{14}. This was employed by Anderson *et al.* in the initial detection of natural C^{14} (23, 24). By thermal diffusion of methane an enrichment by a factor of 260 was obtained. This technique has not yet been applied to dating, although Libby has announced plans to do so (380). Since each factor of 2 extends the limit of dating by one half-life, the above factor of 260 would extend the limit by 45,000 years. A difficulty is that very large samples would be required.

To aid Libby in the development and testing of the method, a Committee on Radioactive Carbon 14 was established by the American Anthropological Association and the Geological Society of America in 1948–49. This committee set up a program of nine archeological and two geological projects, with an invited specialist in charge of each. The reports of the archeological projects were assembled by Johnson and published as a Memoir of the Society for American Archeology (312). The geological results were reported in brief papers by Flint (201) and Deevey (156) in the same Memoir and elsewhere (202), and in an exhaustive joint paper (203). The entire program was assessed by Johnson (314) in a concluding chapter in Libby's book *Radiocarbon Dating* (382). Several general review papers on the method and its results have appeared (123, 158, 204, 240, 355, 358, 386, 478, 479), including several emphasizing the geological aspects (73, 243, 248, 359) and innumerable semi-technical and popular articles.

Several tests of the bases of the radiocarbon dating method have been made. The question of constancy of the specific activity of carbon throughout the world today and in the past has under discussed under OCCURRENCE AND DISTRIBUTION OF RADIONUCLIDES IN NATURE. Although constancy sufficient for dating back to several thousand years with a precision of a few hundred years seems to have been demonstrated, more careful testing will be needed for more accurate dating. If the industrial carbon dilution effect found by Suess (532, 533) is substantiated, it would necessitate an additive correction of some 200 yr. to all old ages based on contemporary carbon.

More important at present are the difficulties in insuring that the carbon derived from a sample is not contaminated with "older" or "younger" carbon. Datability of various materials, techniques of preparation of samples, and possibilities of errors have been discussed by Libby (382) and others (30, 35, 56, 121, 157, 159, 203, 210, 237, 313, 472a, 533, 591).

Radiocarbon dating is perhaps of greatest value to archeology and anthropology, but a number of important geological applications have also been made, and its geologic importance will increase as its range is extended. Flint & Deevey (203) state that most of Libby's early radiocarbon dates of geologic samples fall into the same order as that given by their stratigraphic positions. In view of the possibility of error both in age measurement and in stratigraphy, no alarm is occasioned by those that do not. The method is becoming accepted as basically sound and capable of giving at least reliable relative ages. With present sensitivity, it covers all of post-glacial time and the last part of the Wisconsin ice age. It should ultimately be capable of dating the entire Wisconsin glaciation.

The most important of the early geological results is a general shortening of late- and post-glacial time. The Two Creeks warm interval between the last two (Cary and Mankato) sub-ages of the Wisconsin ice age in North America has been consistently dated at about 11,400 yr. ago (38), placing the Mankato maximum at about 11,000 B.P.[2] (203). A previous estimate for the latter had been 25,000 B.P. Closely similar ages have been obtained for the similar Alleröd horizon in several localities in Europe, the average age being 10,800 yr. (38, 203, 237). Confirmation has come from a series of datings in Copenhagen, which yield about 12,000 B.P. for beginning of the Alleröd warm interval, 10,800 B.P. for its close, and about 10,300 B.P. for the resumption of the warm conditions responsible for the final retreat of the ice from Scandinavia (29, 302). Evidently, major climatic changes are synchronous on two continents and presumably throughout the northern hemisphere and possibly throughout the world.

The last date mentioned above corresponds closely with that estimated previously by G. DeGeer and others on the basis of varve counting, although the varve chronology contains a gap and an extrapolation of unknown duration. All doubt that the varves are annual deposits has been dispelled (237). The results are regarded by E. DeGeer (160, 161) as completely confirming

her husband's varve chronology. This conclusion is accepted as far as the Scandinavian chronology for the past 10,000 yr. is concerned (156, 214), but DeGeer's transatlantic correlations have been criticized by Antevs (35). Antevs also criticizes the radiocarbon dates, claiming that his North American varve chronology indicates that the Mankato maximum occurred at least 19,000 years ago, and that the radiocarbon dating of 11,000 B.P. must be incorrect. Nevertheless, sufficient Two Creeks and Alleröd samples have been dated to prove that the two periods were contemporaneous, regardless of the absolute accuracy of the C^{14} time scale. Since Antevs places the Two Creeks interval several thousand years earlier than the Alleröd, his chronology, which also involves a transatlantic correlation, cannot be completely correct.

Deevey (156, 157, 203) and the Danish workers (29, 302) are employing radiocarbon dating to establish fixed points on the relative time scale derived from analysis of fossil pollen in peat, lake mud, etc. The two methods will thereby strengthen each other. Deevey thus finds that in its northward advance the pine-dominated "Boreal" climate zone included West Virginia about 9000 yr. ago, Connecticut and southern Minnesota 8000 yr. ago, northern Minnesota 7000 yr. ago, and Maine 6000 yr. ago. The post-glacial thermal maximum in climate has not been precisely fixed, but associated dates range from 3000 to 6000 yr. ago (203).

Kulp has dated various positions of the sea level as it rose with the melting of the glaciers. A weathered surface 273 feet below the present level is older than 30,000 yr. A drowned forest in Bermuda 80 ft. deep is about 11,000 yr. old. The level −73 feet was attained 9000 yr. ago, −25 feet 3000 yr. ago (352, 359, 360). Kulp has also determined the apparent ages of deep ocean masses, finding some to be about 1700 yr. old, and suggesting that ocean circulation is much slower than had been generally supposed.

In conjunction with Kulp, Smith (515, 516) has shown that hydrocarbon-like substances present in fairly recent marine sediments contain measurable amounts of radiocarbon (apparent ages about 12,000 yr. in specimens examined), indicating that petroleum formation does not require unusual conditions or very long times.

These examples illustrate the enormous potentialities of the radiocarbon method for dating late pleistocene and recent geologic events, not only directly but through calibration of relative chronologies, particularly after expected increases in precision and range and checking of the absolute accuracy of the radiocarbon scale. Radiocarbon dates are already being quoted, discussed, and used extensively in papers on geological subjects (19, 205, 472).

Tritium Method

Possible applications of natural tritium to age determinations have been discussed by Libby (324, 384, 387). Datable materials include agricultural products, stored water, natural rain water, snow, and ice. Kaufman & Libby

demonstrated that the tritium content of wine from a given area decays as expected with the time since manufacture (324). Fireman & Schwarzer were unable to detect tritium in glacial water ($T/H < 5 \times 10^{-19}$) (197); this suggests a hold-up of many years between precipitation and melting.

For measurement of the tritium in a natural water sample, Kaufman & Libby enrich the heavy hydrogen isotopes by electrolytic reduction of the volume by a factor of $\sim 10^3$ or $\sim 10^4$. So little of the tritium goes into the gas that when the protium content is reduced by a factor of the above order of magnitude the tritium content is reduced by a factor of only about two. The tritium enrichment is calculated from a measurement of the deuterium enrichment in each sample. Gaseous hydrogen from the residual water is counted in an anticoincidence-shielded Geiger counter of about a liter volume, several counts per min. usually being obtained (324). Fireman & Schwarzer introduce the hydrogen from 14 ml. of water into a 100 pounds per sq. in. continuously sensitive diffusion cloud chamber, and count the tritium beta tracks visually. Most natural waters give of the order of one track per min. without enrichment, but moderate electrolytic enrichment (by factor of $\sim$10 to 40) is sometimes employed (197). This method is not as precise or (with the enrichments employed) as sensitive as the Geiger counter method.

As a result of the variability of the tritium content of fresh natural waters, which was discussed under OCCURRENCE AND DISTRIBUTION OF RADIONUCLIDES IN NATURE, determination of ages by tritium assay will be more complicated and less accurate than in the case of radiocarbon dating. The shortness of the H^3 half-life limits the method to about a century, anything older than that appearing indefinitely old.

In addition to dating, natural tritium should have many other applications in hydrology and meteorology. These include distinction between juvenile and meteoric ground waters, investigation of vertical mixing of air masses, and identification of the sources of moisture in air masses (384).

Extinct Natural Radioactivity Method

Applications of extinct natural radioactivity to obtaining information of cosmological importance are discussed below under Age of the Elements and the Universe. Kohman has described a possible method by which this phenomenon, if it occurs and is discovered, can be put to use to provide an accurate geochronometry for the early history of the earth. In a mineral which once contained a now-extinct nuclide, the ratio of the radiogenic product to a stable or long-lived isotope of the parent should be an exponential function of the time of mineralization. If the "cosmic decay curve" of the nuclide could be established, a measurement of that ratio would give the time of mineralization. Since this method would be increasingly accurate with increasing age, it would complement existing methods based on primary natural radioactivity, whose accuracy decreases with increasing age (342, 347).

RADIOGENIC TERRESTRIAL HEAT

General reviews on the earth's internal constitution and thermal history with reference to natural radioactiviy and to radiogenic heat have been given by Gutenberg (247), Urey (555, 558), and Jeffreys (309), and a more recent review by Birch (72) is concerned primarily with the radiogenic heat itself. This subject is intimately associated with other aspects of geophysics, and the interested reader will find the U. S. Geological Survey's *Geophysical Abstracts* an excellent key to the current literature on this and related subjects.

Radioactive sources of heat in the earth.—The principal sources of radiogenic heat are the U^{238}, U^{235}, and Th^{232} families, and K^{40}. According to Birch (72), current nuclear data, with allowance for energy loss by neutrinos, lead to specific heat production rates of 0.73 cal./gm./yr. for natural uranium and 0.20 cal./gm./yr. for thorium, when each radioactive series is in secular equilibrium. These values have changed but little in two decades. In the case of potassium, revisions of the nuclear data have caused the estimated heat production rate to fluctuate considerably until recently. Alburger (12) has calculated that the average beta particle energy for the third-forbidden K^{40} transition is 0.605 ± 0.010 Mev if the maximum energy is 1.34 ± 0.02 Mev. Using the decay constants of Sawyer & Wiedenbeck (498), he obtained 27 ± 1 μcal./gm./yr. for the specific heat production rate of natural potassium; with more recent disintegration data (179), this becomes 26 ± 1 μcal./gm./yr.

Although the corresponding figure for rubidium, 36 μcal./gm./yr. (72), exceeds that of potassium, the fact that rubidium is only ~1 per cent as abundant as potassium and parallels the latter in its distribution makes it unimportant as an earth heater. Samarium produces about 300 μcal./gm./yr., but is not many times as abundant as uranium and thorium, like which it is distributed, so it too is geothermally unimportant. All other natural radionuclides present on earth today are insignificant in this respect. It is shown below that the possibility of important early contributions to the earth's heat by additional shorter-lived nuclides is small.

Cormack (120) has recently revived the idea that neutrinos from the sun may contribute to heat generation within the earth (66, 122, 499). Although it has been shown that neutrino capture in inverse β-processes cannot liberate significant amounts of heat (499), Cormack calculates that a neutrino magnetic moment between 10^{-6} and 10^{-5} Bohr magneton would allow energetic neutrinos to escape from the sun and leave some energy in the earth through interactions with electrons. The maximum possible effect, ~0.02 μcal./gm./yr., is greater than the radiogenic heat production rate in iron meteorites and might exceed the radiogenic sources in parts of the earth. However, there is experimental (122, 193) and theoretical (288) evidence against an interaction of this order of magnitude, and the liberation of $\sim 10^4$ electron volts per sec. per gm. of terrestrial matter in the form of ionizing electrons could readily be detected by present techniques.

The possibility, occasionally suggested, of storage of substantial amounts of radioactive energy in crystals by atomic dislocations, to be released suddenly in the form of heat, has been shown by Hurley & Fairbairn to be nonexistent (293).

Quantities and distribution of radioelements in the earth.—The accumulation of analytical results is gradually improving our picture of the content of uranium, thorium, and potassium, and the heat production in important types of terrestrial and meteoritic matter. Nevertheless, the large variations observed in otherwise similar materials make a selection of preferred or average values difficult. Accordingly, the best that can be done is to give representative or typical values, as in Table I, which is taken with some

TABLE I

CONCENTRATION OF RADIOELEMENTS AND SPECIFIC HEAT PRODUCTION RATES IN IGNEOUS ROCKS AND METEORITES

Rock Type	Granitic	Intermediate	Basaltic	Ultramafic	Stony Meteorites	Iron Meteorites
p.p.m. U	4[a]	2[a]	0.6[a]	0.05[c]	0.02[d]	0.004[e]
p.p.m. Th	15[b]	7[b]	2[b]	0.2[b]	0.07[b]	0.015[f]
per cent K	3.5[g]	2[a]	0.9[g]	0.001[h]	0.09[g]	—
q(U)	3	1.5	0.4	0.04	0.015	0.003
q(Th)	3	1.5	0.4	0.04	0.015	0.003
q(K)	0.9	0.5	0.3	0.0003	0.023	—
q	7	3.5	1.1	0.08	0.05	0.006

[a] From compilation of Birch (72), using $U/Ra = 3.0 \times 10^6$.

[b] Derived from figures on uranium under assumption that thorium and uranium contribute equally to heat ($Th/U \approx 3.7$) (72).

[c] From data of Davis (152). Birch (72) selects a considerably lower value.

[d] From data of Davis (153) and Patterson *et al.* (451).

[e] From data of Davis (153) and Dalton *et al.* (133, 134, 135).

[f] From data of Dalton *et al.* (133, 134, 135).

[g] Ahrens, Pinson and Kearns (10).

[h] Holyk and Ahrens (280).

modifications from Birch's summary (72). Here q is the total specific heat production rate of the material in μcal./gm./yr., and q(U), q(Th), and q(K) are the contributions by the individual radioelements indicated.

Most discussions of the distribution of radioactive heat sources within the earth (72, 247, 309) start with the assumption that the proportion of radioelements in the earth as a whole is the same as in a suitable mixture of stony and iron meteorites. That there has been a concentration of uranium

and thorium in the continental rocks, to such an extent that a thickness of 20 to 40 km. of such rocks would suffice to account for the entire flow of heat to the surface in continental areas, has long been known (247, 309), but the actual distribution of radioelements in the interior of the earth has been a matter of widely varying speculation. Several recent findings have contributed to a better, though still incomplete, understanding of this distribution.

From the mean value of the potassium content of chondrites indicated by previous analyses, ~0.21 per cent (84), it had appeared that K^{40} might supply a major part of the earth's total heat. However, Birch, in a detailed discussion of the radiogenic heat of potassium (70), stated that there is an indication that the mean potassium content of the earth ought not to exceed about 0.1 per cent. The new lower average value for chondrites, ~0.09 per cent, found by Ahrens *et al.* (10) brings the meteorite hypothesis into line with Birch's suggestion, and in combination with the recent estimates of the uranium and thorium contents of chondrites indicates that the radiogenic heat contribution of K^{40} is probably not much, if any, greater than that of U+Th.

An alternate way of estimating the earth's K^{40} content is to assume that the mantle, which is generally believed to be ultramafic, has the same potassium concentration as surface ultramafic rocks (70). The previously accepted value for this, ~0.03 per cent, leads to a total quantity of potassium in the mantle about equal to that in the crust. Though this would not detectably affect the surface heat flux, it might have an appreciable influence on the temperatures deep within the earth. According to the new lower K content of ultramafics, ~10 p.p.m., found by Holyk & Ahrens (280), the K^{40} heat in such a mantle should be insignificant relative to that of the U and Th present there. But Holyk & Ahrens have noted that the assumptions that the average K content of the earth's silicates is the same as that in chondrites and that the K content of the mantle is the same as that of surface ultramafic rocks are mutually inconsistent. Since the mass of the crust is ~1 per cent of that of the mantle, the assumptions would require a concentration of ~9 per cent K in crustal rocks. Since only ~2 per cent is found, an alternative hypothesis is that only ~25 per cent of the initial chondrite-like material has differentiated into crustal and ultramafic rocks, the remainder being present in the mantle with its original K content (280). Thus the K^{40} heat contribution, which is relatively minor in the crust, may be anywhere from insignificant to substantial in the mantle.

Until recently, the only measurements of the flux of heat to the earth's surface were in continental areas. Nearly all of the reliable results are in the neighborhood of 1.2 μcal./cm.^{2}/sec. (72, 93). Besides the fact that these measurements do not represent an adequate sampling of continental areas, the absence of measurements from the oceanic areas, representing three-fourths of the earth's surface, prevented obtaining an average and integral for the earth as a whole. However, there was little doubt that the production

and flow of heat beneath the oceans was smaller than beneath land because of the absence of granitic material (247). The first indication that this might not be the case came from unexpectedly high thermal gradients found in the ocean floor by the Swedish Deep Sea Expedition of 1947–48 (460). Subsequent heat flow determinations in the Pacific by Revelle & Maxwell, averaging 1.2 μcal./cm.^{2}/sec. (476), and in the Atlantic by Bullard, averaging 1.0 μcal./cm.^{2}/sec. (93), indicate that there is no substantial difference in the heat flux in oceanic and continental areas. Although reservations concerning possible systematic errors have been expressed by Birch (72), Bullard believes that this conclusion is valid (93). He suggests that the total quantity of radioelements beneath unit area of the earth's surface is everywhere about the same, at least to a depth of a few hundred km. (92). However, even under the oceans there must be a concentration into the upper layers, since in the absence of convective heat transport the interior would melt, and convection would result in a differential between continents and oceans. Since neither the thin sedimentary and basaltic layers comprising the crust beneath the ocean floor nor a mantle of ultramafic rocks could supply more than a small part of the oceanic heat flow, this upward concentration of radioelements must extend into the mantle (93, 476).

This idea is in accord with the above-mentioned calculations of Holyk & Ahrens on the K content of the mantle. The average U and Th contents of chondrites are not sufficiently well known to permit a similar calculation for these elements, but Birch believes that (because the crust may contain less granite than generally assumed) the average radioactivity of the crust may be lower, and of the subcrust higher, than is usually supposed (72).

Information about the materials and temperatures of the earth's interior obtained by seismic and other geophysical methods can be used to derive information about the distribution of radioactivity within the earth. Birch (71) believes that the mantle contains a transitional layer between the depths of 200 to 900 km., within which there is a change in chemical composition or phase or both. In and above this but below the crust there seems to be a concentration of aluminum, calcium, and alkalis in mineral assemblages similar to eclogite. This region would have the proper composition and could develop the necessary temperatures to supply the copious supply of basaltic magma needed for petrogenesis (71), particularly if the electropositive elements uranium and thorium, like potassium, were concentrated in the eclogite-like phase.

Urey (555, 558) gives reasons for believing that Mars has a relatively uniform composition, indicating that it was not completely molten when formed or at any subsequent time. Because of its smaller size and possibly higher thermal conductivity, more effective conductive loss of radiogenic heat should cause plutonic activity to be less important than on earth. However, McLaughlin cites evidence for volcanism on Mars (404).

Temporal variations of radiogenic heat.—As difficult as is the interpretation of the evidence bearing on the thermal state of the earth on a steady-

state basis, it is complicated still further by variations in the intensity of the heat sources as well as by the slowness of heat transfer in such a massive body. Unless convection in the solid silicate mantle occurs fairly rapidly, heat transfer is so slow that steady-state conditions may not have been attained in the time since the earth's formation. Thus, the present state may reflect to some extent the initial state. If, as is indicated below, the earth's age is closer to 5000 m.y. than to 3000 m.y., the working out of the present state and recent history of the earth's interior may be simplified for two reasons: (*a*) more time has been available for approach to a steady-state condition, and (*b*) the radiogenic heat early in the earth's history was greater, so that influences of its original state may have been more completely wiped out.

Now that the disintegration constants of K^{40} are known reasonably well, knowledge of the heat generated by the four principal contributors at any time in the past depends only on a knowledge of the amounts and distribution of uranium, thorium, and potassium. Although many writers have considered qualitatively the effects of the greater vigor of these radioelements in their youth, the only quantitative applications of radioactive decay to earth models have been those of Urry (561) and Urey (555, 558). Each considered consequences of several sets of postulates. Urry assumed that the earth is now cooling from a once-molten state and derived a minimum age of ~6000 m.y. for an initially cold earth. Urey, on the other hand, assumed an age of 3000 m.y. and an initial temperature of ~1200° K. in all of his calculations, and deduced consequences of several initial states. In all of his models the temperatures deep within the earth are still increasing at the present time. The considerations of Jung (318a) were limited to the outer parts of the earth.

Most recent discussions of the earth's thermal history (247, 309) assume that the earth was once largely molten and is at present cooling, the cooling being greatly retarded by radioactivity. Arguments for this are the layered structure and chemical differentiation of the earth and the molten state of the outer core and the consequently necessary high temperatures (in the neighborhood of 4000° or 5000°K.) in the deep interior. Urey's conclusion that the earth is still heating up depends on the relatively young age assumed. A greater age would increase not only the time but also the intensity of heating. This is particularly important for K^{40}, which was the dominant radioactive heater (among those known now) in the earth's earliest stages. Birch calculates that potassium alone would have sufficed to bring a cold mantle containing 0.06 per cent K to the molten state in about 2000 m.y. prior to 3300 m.y. ago. Allowance for a higher initial temperature and for other radioelements would shorten this estimate (70). The relatively long requirement of 3000 or 4000 m.y. estimated by Urry results from an assumed 0.04 per cent K for the part of the earth outside of the core, which is considerably below the K content of chondrites. Thus it seems that if the

earth is close to 5000 m.y. old, and was made of material similar to meteorites, it almost certainly passed through a state of large-scale melting.

Dauvillier has discussed evidences of greater volcanic activity in the past, attributing the decrease to diminution of the intensity of radiogenic heat (148).

It is frequently suggested that relatively short-lived and now-extinct radionuclides may have been present in the original earth and made additional contributions to its heat. The most specific of such suggestions is that of Rosenblatt, who considers that U^{236}, whose half-life is 24 m.y., might have been present in substantial quantities in the young earth and promptly melted it (484). However, if U^{236} and U^{238} were equally abundant originally, the heat generation by the former would have decayed to equality with that from the latter in only 100 m.y. Considering the importance of K^{40} in those early times, U^{236} could not have been significant as a heat source after the first 100 m.y. of the universe. Although there is no direct evidence to the contrary, the theoretical speculations of Gamow (217, 218) make it seem unlikely that planetary bodies could have been formed earlier than a few hundred m.y. after the presumed nucleogenic event. Even if Sm^{146} should have a lifetime as long as 50 m.y., it is at best a border-line case because of its low primordial abundance. To be thermally important an unknown nuclide would have to have a half-life fairly close to 100 m.y. and probably be isotopic with one of the lighter and more abundant elements. These requirements make the probability rather small, but there are some still unknown nuclides which are possibilities. For example, if Fe^{60} has a half-life of 10^8 years and originally comprised 1 per cent of iron, it would have had an enormous effect for over 1000 m.y. after nucleogenesis. A more detailed discussion is given elsewhere (347).

RADIOACTIVITY AND COSMIC HISTORY

Megascopic History of the Earth

Inferences from common lead isotopes.—In 1946 Holmes (270, 271, 276) and Houtermans (283, 285) independently published graphical methods of calculating, from the isotopic composition of common lead samples of known ages, a time since all lead had the same isotopic composition and began changing as a result of the addition of Pb^{206}, Pb^{207}, and Pb^{208} in different proportions. Holmes called this time the "age of the earth," Houtermans, the "age of uranium." Subsequent treatments by different methods were given by Jeffreys (307, 308) and Bullard & Stanley (91), the latter using a least-squares analytical method. The results of the analyses based on the data available before 1952 (427, 429) are: Holmes, 3350 m.y.; Houtermans, 2900 m.y.; Jeffreys, $\leqq$4000 m.y.; Bullard & Stanley, 3290 m.y. New isotopic analyses of common leads have now become available (18, 113, 114, 175, 229, 363, 490, 522, 564). Collins *et al.*, using their own data in addition to

Nier's, repeated the Bullard-Stanley calculation and obtained 3500 ± 200 m.y. for what they call the "age of the earth's crust" (113, 114).

Some confusion about the exact meaning of the age so calculated exists. It should be clear that it represents the time since, as a result of geochemical (or cosmochemical) fractionations, the ratio (dispersed U)/ (dispersed Pb) began to have different values in different parts of the matter of (or later to become) the earth's heterogeneous crust. Houtermans felt that these fractionations might have occurred either during the formation of uranium (and the other elements), or during the formation of the earth's crust, and at first he inclined to the former view (285). Later, he favored the latter view, but considered the two as limiting cases (287), implying that the age so calculated should be a maximum age for the earth's crust. Holmes (272) states that the age determined refers to the time when the granitic layer separated from the average earth material during the consolidation of the globe, and is not appreciably different from the age of the earth. Jeffreys refers to the "age of the crust." Burling (96) calls it the age of the sial crust, or the time since melting and layering of the earth. Bullard & Stanley, and Collins *et al.* state that the physical and chemical processes of solidification produced differences in the amounts of lead, uranium, and thorium from place to place, justifying the identification of this time with the age of the earth's crust.

Current geological thought seems to be that the sialic material of the continents was formed and extruded above the surface of the earth gradually over long periods of time (90, 583, 584, 585). The variations in the U/Pb ratio in different regions probably date from the formation of the continental masses. The lead minerals seem to be derived mainly from sources having U/Pb ratios characteristic of granitic rocks (137, 229, 270, 285), and these sources presumably are the continental masses. Therefore, there should be no unique time such as that postulated by Holmes, Houtermans, and their followers. The time so calculated probably represents some sort of average age of the continental masses, and should therefore be a minimum for the age of the earth's crust, which may have existed for some time in a relatively undifferentiated state prior to the formation of the continents.

McCrady (403) has discussed the use of lead isotope ratios in estimating the age of the earth, but since he disregarded the regional variability of the U/Pb ratio he was unable to come to any conclusions. Damon (139) has proposed a model for the formation of lead minerals based on the continuous creation of the earth's crust. The model as first formulated did not account for the extent of variability of lead isotope ratios actually observed in lead minerals; this is evidently because Damon too neglected regional variations in the U/Pb ratio, although he had considered them in an earlier paper (137). Although he did not attempt to calculate times associated with the formation of the crust, his approach if suitably amplified may ultimately enable that to be done.

Alpher & Herman (20) have considered the variations in isotope ratios of common leads of a given age as random fluctuations about a mean, and have

used a least squares analysis to calculate the mean value of Pb^{206}/Pb^{204}, Pb^{207}/Pb^{204}, and Pb^{208}/Pb^{204} as functions of time. Using Nier's data (427, 429), they found that the Pb^{206}/Pb^{204} ratio extrapolated to zero at 5300 m.y. ago, giving an upper limit to the age of the earth's crust. McCrady (403) derived similar curves by a different method and found that the Pb^{207}/Pb^{204} curve extrapolated to zero at 5070 m.y. ago. Collins *et al.* (113, 114) repeated the Alpher-Herman calculation using their own data in addition and found that the Pb^{207}/Pb^{204} curve extrapolated to zero at 5500 m.y. ago. Although, as Alpher & Herman (20) and Vinogradov *et al.* (564) pointed out, such curves have no significance for times prior to the existence of the earth's crust, McCrady and Collins *et al.*, call their result "the maximal possible age of matter" and "the maximum age of the elements," respectively; this, of course, is incorrect. In fact, this time may only be an upper limit to the age of the present continental masses, since if in their formation the U/Pb ratio increased, the earth's crust as a whole could be older.

Voitkevich (565) has calculated an age of 5000 m.y. on the assumption that all of the Pb^{206} and Pb^{207} in the present earth's crust is radiogenic, and seem to regard this as a maximum possible age of the earth. Such a calculation had been made before by Koczy (337), who regarded his result (5330 m.y.) as an upper limit to the age of terrestrial matter. Both interpretations are erroneous, since if actually a smaller fraction of the present Pb^{206} than of Pb^{207} is radiogenic, the calculation would give too low a value for the time of their radiogenesis.

Inferences from meteoritic data.—As a culmination of long efforts, Patterson and collaborators (451) have succeeded in determining the isotopic composition of lead in an iron meteorite, finding $Pb^{204}:Pb^{206}:Pb^{207}:Pb^{208} = 1:9.4:10.3:29.2$. Because of the low cosmic and meteoritic U/Pb and Th/Pb ratios, such lead is probably primordial (285, 451, 545). Relative to Pb^{204} the other isotopes are considerably lower than in any lead found on earth or calculated as "primordial" with respect to the earth's crust by the Holmes-Houtermans' method, thus confirming the great antiquity of at least some meteorites. By subtracting the primordial Pb^{206} and Pb^{207} values from those of contemporary terrestrial leads, Patterson *et al.* derived Pb^{207}/Pb^{206} ages for the earth's crust of 4500 m.y. (453, 454). The same calculation was made independently by Houtermans, who obtained 4500 ± 300 m.y., referring to this as the "age of the earth" (287). But since the strong enrichment of U relative to Pb in the present earth's crust may not have been established until some time after the formation of planetary bodies, this age is probably best regarded as a minimum age of the solar system. Houtermans (287) and Geiss (229), however, apparently feel that this age should be the same as that corresponding to the beginning of the divergence of common terrestrial leads, since they use the same symbol (w) for each age.

Festa & Santangelo (194) have proposed a method for determining the age of the earth based on a comparison of the Ca^{40} contents of meteoritic and terrestrial calcium. Since the K/Ca ratio is different in chondrites and the

earth's crust, the method is valid in principle. But their computation involves the assumption (not stated) that meteoritic calcium has the same Ca^{40} content as that on earth. This has never been measured. As Birch (70) points out, the resulting age should have been zero under this assumption. Moreover, they used incorrect K^{40} disintegration constants, so their result (3160 $\pm$600 m.y.) has no significance. However, it suggests the desirability of a careful mass spectrometric examination of meteoritic calcium. Because of the large abundance of Ca^{40}, its variations may be too small to detect.

Helium and argon age determinations on meteorites have been reviewed under RADIOACTIVITY AND GEOLOGIC TIME. Herzog & Pinson have undertaken an investigation of the isotopic composition of meteoritic strontium. Here the possibilities for age determinations seem to be better than in the case of calcium (261).

Inferences from argon 40 in the earth's atmosphere.—It has been agreed for some time that most of the argon of the earth's atmosphere is radiogenic A^{40} produced by the decay of K^{40} within the earth (87). Early attempts at quantitative interpretations were hindered by inadequate knowledge of the electron-capture disintegration rate. Following clarification of the latter, it was recognized by Tatel (539) and by Poole & Delaney (469) that the earth's crust alone contains insufficient K^{40} to have generated all of the atmospheric A^{40} in the last $\sim$3000 m.y. and that consequently the bulk must have escaped from considerable depths in the earth. The contrary conclusion of Chackett (104) is based on his assumption of a mean potassium content of 2.6 per cent to a depth of 40 km. over the whole surface of the earth, giving an improbably large amount of potassium in the crust.

Kulp and Birch have postulated the gradual growth of the argon component of the atmosphere through geologic time, paralleling the growth of the oceans and continents. Kulp (351) showed that the atmospheric argon amounts to 14 per cent of all the A^{40} generated in a mantle containing 0.18 per cent K (a then accepted average for chondrites) in the past 3300 m.y., that being the fraction which has escaped. (This fraction would be doubled if the newer mean K content of chondrites were used.) Comparing the amount of water in the oceans and crustal rocks with that originally in a mantle having the same H_2O content as chondrites, 0.54 per cent, leads to the conclusion that about 9 per cent of the water has escaped. The slightly higher fraction for argon as compared to water is regarded as supporting Rubey's ideas on the continual discharge of H_2O and CO_2 into the hydrosphere and atmosphere from the lithosphere (486).

Birch (70) assumes that the potassium in the earth's crust has been introduced there from the interior at a uniform rate over the past 3300 m.y., in such a manner that the argon previously generated by the ejected potassium escapes into the atmosphere at the same time. The calculated A content of the atmosphere agrees well with observation, but in obtaining this result Birch assumed a world-wide average crustal thickness of 33 km. and K content of 2.6 per cent, or nearly as much crustal potassium as did Chackett.

If the actual amount is lower, an additional source of argon or a longer time would have to be invoked.

Rankama (473) has taken a different approach, postulating that weathering of igneous rocks releases to the atmosphere the A^{40} generated by their potassium. In this way he obtains 6500 kg./cm.^{2}, corresponding to a thickness of 22 km., for the total quantity of igneous rock weathered during the geologic history of the earth, taken as 3500 m.y. This is much higher than estimates based on other considerations (580). Boato *et al.* (77, 78) have demonstrated that there are other means for radiogenic argon to escape into the atmosphere.

All of these calculations are based on the assumption that argon could not be retained by the earth prior to 3000 or 3500 m.y. ago. This now seems somewhat low for the age of the earth. If it is older, a relatively short early period would have sufficed to produce most of the present atmospheric argon, particularly if degassing was moderate (70, 484a, 539, 555). In fact, if the earth is as old as 4500 or 5000 m.y., contains close to 0.1 per cent K in its silicates, and passed through a molten state, the amount of atmospheric argon is embarrassingly small, unless the temperature has been sufficiently high to allow much of the argon to escape from the atmosphere.

Brown (87) believes that Venus and Mars probably have argon atmospheres similar to the earth's, with A^{40} possibly the major atmospheric constituent of Mars.

Suggested history of the earth.—Most of the above-mentioned observations pertaining to radioactivity and the megascopic history of the earth can be fitted into a unified picture. This can be described with reference to Figure 1, which shows how the isotopic composition of lead would have varied in various terrestrial and meteoritic materials at different times in the past. In this much-simplified model, events that undoubtedly took place over considerable spans of time are pictured as instantaneous.

It is assumed that the major vertical segregation of the earth's materials, establishing the core, mantle, and crust, took place at the same time that the meteorites were formed, in which case the age 4500 m.y. calculated from meteoritic lead refers to this event. At this time the crust was rather uniform, although its U/Pb (as well as Th/Pb) ratio was considerably greater than the original cosmic ratio. The age 3500 m.y. derived from analysis of common leads refers to a later event in which regional differences in the U/Pb ratio were established. These lateral segregations may also have been accompanied by vertical segregations within the upper lithosphere, and may represent the formation of the continental masses.

This picture is consistent with the hypotheses of Wilson (583, 584, 585), according to which the continents have been and are expanding by a process of differentiation in which radioelements are concentrated upwards, of Bucher (90), according to which the continents were formed by alterations of an initial basaltic crust, which still remains in the deep oceanic regions, and of Bullard (92) according to which when the earth solidified most of the

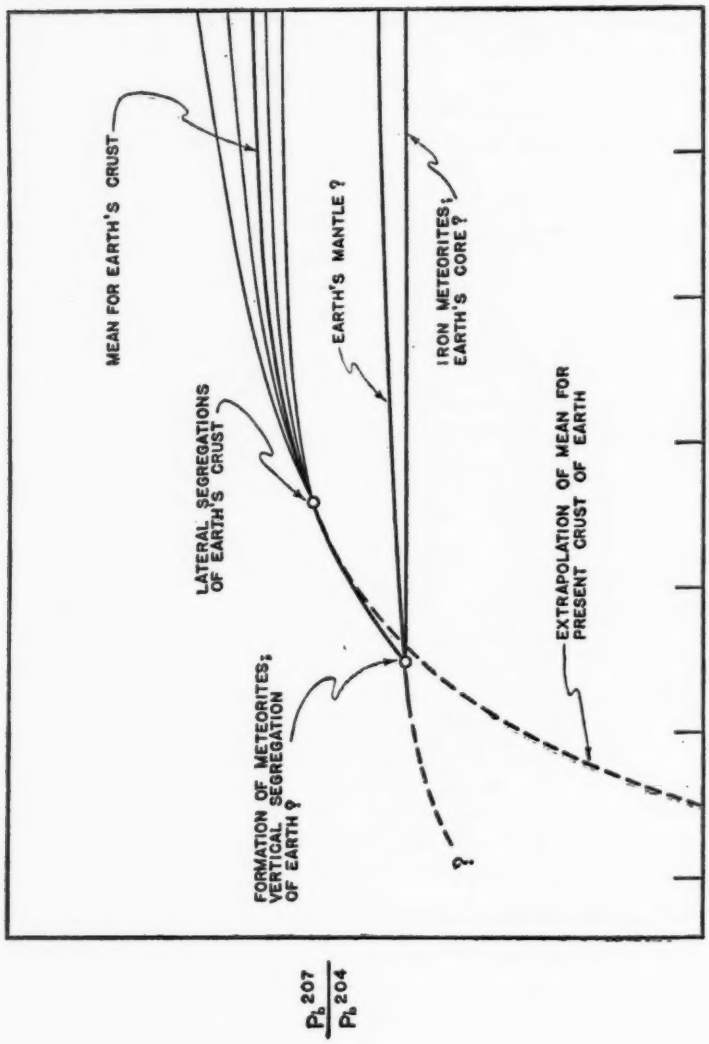

FIG. 1.—Schematic representation of variation of lead isotope ratios in various earth materials according to an idealized model.

radioactivity was concentrated in the upper ~150 km. of the mantle, with a subsequent further concentration into the top 10 to 20 km. under the continents.

Since the orogenies in the Canadian and Rhodesian shields dated by radioactive minerals apparently go back only to ~2500 m.y. ago (115, 279), they may not represent the original formation of the continental masses as has been supposed. On the other hand, since the 3500 m.y. age represents only some instant during a process of some duration, this picture would permit the possibility that the lepidolite ages approaching 4000 m.y. discussed under the STRONTIUM METHOD are actually correct.

Going back further in time, if the earth originated as a cold and undifferentiated body some time before being heated sufficiently for stratification, the time spent in that condition would have to be added to 4500 m.y. to arrive at the total age of the earth and meteorites.

AGE OF THE ELEMENTS AND THE UNIVERSE

A recent survey of astronomical evidence bearing on the age of the universe has been given by ter Haar (541). Those methods based on stellar and galactic dynamics and evolution give only approximate values, which may refer to events later than the birth of the universe. The current ideas on the origin of the elements, which were reviewed by Alpher & Herman in Volume 2 of *Annual Review of Nuclear Science* (21), indicate that there was an event of large-scale nucleogenesis, which should have initiated an expansion of the universe such as is apparently observed in the red-shifts of the spectra of distant galaxies. Estimates of the time during which this expansion has been taking place, which may be called the "age of the universe," are now undergoing revision (82, 241, 525). Radioactivity provides several possibilities for determining what might be called the "age of the elements," which according to the above-mentioned view should be the same as the "age of the universe."

Burling (96) has listed and criticized several previous computations purporting to give the age of the elements, and has shown that most of them give only upper limits for chemical separations which occurred some time after the elements were in existence. Presumably no fractionations of the elements accompanied their formation, so the only possibilities from a study of decay products are upper limits or very rough estimates based on cosmic abundances of parent and daughter combinations, as was attempted by Suess (527). The approximate nature of cosmic abundance information and primordial abundance assumptions make such age calculations no more than order-of-magnitude estimates.

Another type of estimate is possible from consideration of the decay of relatively short-lived primary natural radionuclides which have stable or longer-lived isotopes. The dependence on cosmic abundance is eliminated, but not that on primordial isotopic abundance estimates. Only U^{235} and K^{40} have decayed sufficiently in cosmic time to yield results by this method.

Brown (85) gives as an upper limit 10×10^9 yr. Suess' estimate based on 1 per cent primordial isotopic abundance of K^{40} (526) becomes 8.4×10^9 yr. with the modern half life. Wefelmeier is quoted by Houtermans (285) as giving 7.4×10^9 yr. as the limit from the assumption that originally U^{238}/U^{235} was at least 0.3. Houtermans now considers that U^{235} was never more abundant than U^{238}, whence the maximum age of the elements is 6.0×10^9 yr. (287). Since every factor of two in the uncertainty of the primordial abundance ratio gives an uncertainty of one half life in the time of decay, the discovery of a shorter-lived primary natural radionuclide would lead to a closer estimation of the age of the elements.

The discovery of an extinct natural radioactivity would open the way for an even better estimate. The steepness of the "cosmic decay curve" of a nuclide with a half life of $\sim10^8$ yr. would make the determination of its time of formation relatively insensitive to error in the estimate of its primordial isotopic abundance (347). Brown was the first to recognize this possibility, suggesting meteorites as the products of early chemical fractionations in which the decay product of an extinct nuclide might be found (85). Katcoff and co-workers have attempted an application to the earth as a whole. From the assumption that some atmospheric Xe^{129} is attributable to decay of terrestrial I^{129} following loss of noble gases by the nascent earth, they calculated a time of 270 m.y. for the interval between the formation of the elements and the formation of the earth; adding this to Holmes's figure for the "age of the earth," they derived an age of 3600 m.y. for the age of the elements (323). However, Suess & Brown claimed that evidence for abnormality of atmospheric xenon is lacking, and that only a lower limit of 400 m.y. for the interval in question can be inferred (530). Kohman has suggested that terrestrial minerals might also be of use for this purpose. Although none may have been formed as early as the meteorites, they represent more complete and varied chemical separations of elements (346, 347).

Completely independent and fairly precise estimates of the "age of the universe" and of the "age of the elements" would be highly desirable, in order to determine whether or not they are indeed identical. Current astronomical research should provide the first of these desiderata, and, in view of the possibility that one or more extinct natural radionuclides may exist, the obtaining of the other may not be out of the question.

LITERATURE CITED

1. Abribat, M., Pinoir, R., Pouradier, J., and Venet, A. M., *Compt. rend.*, **234**, 1161–63 (1952)
2. Abribat, M., Pouradier, J., and Venet, A. M., *Compt. rend.*, **235**, 157–59 (1952)
3. Abribat, M., and Pouradier, J., *Compt. rend.*, **237**, 1233–35 (1953)
4. Ahrens, L., *Bull. Geol. Soc. Amer.*, **60**, 217–66 (1949)
5. Ahrens, L. H., and Gorfinkle, L. G., *Nature*, **166**, 149 (1950)
6. Ahrens, L. H., and Macgregor, A. M., *Science*, **114**, 64–65 (1951)
7. Ahrens, L. H., and Gorfinkle, L. G., *Am. J. Sci.*, **249**, 451–56 (1951)
8. Ahrens, L. H., *Geochim. et Cosmochim. Acta*, **1**, 312–16 (1951)

9. Ahrens, L. H., *Trans. Am. Geophys. Union*, **33**, 193–95 (1952)
10. Ahrens, L. H., Pinson, W. H., and Kearns, M. M., *Geochim. et Cosmochim. Acta*, **2**, 229–42 (1952)
11. Ahrens, L. H., *Appl. Spectroscopy*, **6**(5), 11–13 (1952)
12. Alburger, D. E., *Phys. Rev.*, **81**, 888 (1951)
13. Aldrich, L. T., Herzog, L. F., Holyk, W. K., Whiting, F. B., and Ahrens, L. H., *Phys. Rev.*, **89**, 631–32 (1953)
14. Aldrich, L. T., Herzog, L. F., Doak, J. B., and Davis, G. L., *Trans. Am. Geophys. Union*, **34**, 457–60 (1953)
15. Aldrich, L. T., Doak, J. B., Davis, G. L., *Am. J. Sci.*, **251**, 377–87 (1953)
16. Aldrich, L. T., Davis, G. L., Nicolaysen, L. O., and Tilton, G. R., *Carnegie Inst. Wash. Yearbook No. 52*, 78–84, 110–16 (1953)
18. Allan, D. W., Farquhar, R. M., and Russell, R. D., *Science*, **118**, 486–88 (1953)
19. Allison, I. S., *Am. J. Sci.*, **250**, 907–9 (1952)
20. Alpher, R. A., and Herman, R. C., *Phys. Rev.*, **84**, 1111–14 (1951)
21. Alpher, R. A., and Herman, R. C., *Ann. Rev. Nuclear Sci.*, **2**, 1–40 (1953)
22. Amstutz, G. C., *Schweiz. mineralog. petrog. Mitt.*, **31**, 588 (1951)
23. Anderson, E. C., Libby, W. F., Weinhouse, S., Reid, A. F., Kirschenbaum, A. D., and Grosse, A. V., *Science*, **105**, 576–77 (1947)
24. Anderson, E. C., Libby, W. F., Weinhouse, S., Reid, A. F., Kirschenbaum, A. D., and Grosse, A. V., *Phys. Rev.*, **72**, 931–36 (1947)
25. Anderson, E. C., and Libby, W. F., *Phys. Rev.*, **81**, 64–69 (1951)
26. Anderson, E. C., Arnold, J. R., Libby, W. F., *Rev. Sci. Instruments*, **22**, 225–32 (1951)
27. Anderson, E. C., and Levi, H., *Kgl. Danske Videnskab. Selskab. Mat. fys. Medd.*, **27**(6), 22 pp. (1952)
28. Anderson, E. C., *Ann. Rev. Nuclear Sci.*, **2**, 63–78 (1953)
29. Anderson, E. C., Levi, H., and Tauber, H., *Science*, **118**, 6–9 (1953)
30. Anon., *Nature*, **168**, 725–26 (1951)
31. Anon., *Am. Antiquity*, **18**, 89–90 (1952)
32. Anon., *Nucleonics*, **11**(7) 71 (1953)
33. Anon., *Science*, **119**, 116 (1954)
34. Anon., *Chem. Eng. News*, **32**, 2872 (1954)
35. Antevs, E., *J. Geol.*, **61**, 195–230 (1953)
36. Arndt, R. H., and Kuroda, P. K., *Econ. Geol.*, **48**, 551–67 (1953)
37. Arnold, J. R., and Libby, W. F., *Science*, **110**, 678–80 (1949)
38. Arnold, J. R., and Libby, W. F., *Science*, **113**, 111–20 (1951)
39. Arnold, J. R., and Sugihara, T., *Phys. Rev.*, **90**, 332 (1953)
40. Arnold, J. R., *Science*, **119**, 155–57 (1954)
41. Arnold, J. R., *Phys. Rev.*, **93**, 743–45 (1954)
42. Arnold, J. R. (Personal communication, 1954)
43. Arrhenius, G., Kjellberg, G., and Libby, W. F., *Tellus*, **3**, 222–29 (1951)
44. Arrol, W. J., Jacobi, R. B., and Paneth, F. A., *Nature*, **149**, 235–38 (1942)
45. Asayama, T., *Mem. Fac. Ind. Arts Kyoto Tech. Univ., Sci. and Technol.*, **2B**, 53–69 (1953)
46. Ashizawa, T., *Repts. Balneol. Lab., Okayama Univ.*, **4**, 4–5 (1951)
47. Ashizawa, T., *Repts. Balneol. Lab., Okayama Univ.*, **4**, 5–7 (1951)
48. Ashizawa, T., *Repts. Balneol. Lab., Okayama Univ.*, **6**, 12–14 (1952)
49. Aswathanarayana, U., *Proc. Indian Acad. Sci.*, [A]**38**, 84–92, 226–32 (1953)

50. Audric, D. N., and Long, J. V. P., *Nature*, **173**, 992–93 (1954)
51. Backus, M. M., Hurley, P. M., and Stetson, H. C., *Bull. Geol. Soc. Amer.*, **64**, 1391A (1953)
52. Bähnisch, I., Huster, E., and Walcher, W., *Naturwissenschaften*, **39**, 379–80 (1952)
53. Barbera, L., Curatolo, M., Indovina Addario, M. M., and Santangelo, M., *Ann. geofis. (Rome)*, **5**, 603–11 (1952)
54. Barbera, L., Curatolo, M., Indovina Addario, M. M., Palumbo, D., and Santangelo, M., *Ann. geofis. (Rome)*, **6**, 161–72 (1953)
55. Barker, H., *Nature*, **172**, 631–32 (1953)
56. Bartlett, H. H., *Science*, **114**, 55–56 (1951)
57. Bate, G. L., Giletti, B. J., and Kulp, J. L., *Bull. Geol. Soc. Amer.*, **63**, 1233A (1952)
58. Bate, G. L., Giletti, B. J., and Kulp, J. L., *Am. Mineralogist*, **38**, 329A (1953)
59. Bate, G. L., and Eckelmann, W. R., *Bull. Geol. Soc. Amer.*, **64**, 1393A (1953)
60. Beamer, W. H., and Easton, W. C., *J. Chem. Phys.*, **17**, 1298–1300 (1949)
61. Beer, K. E., *Geol. Survey Gt. Brit. and Museum, Atomic Energy Div., Report No. 123*, 5 pp. (1952)
62. Begemann, F., and Houtermans, F. G., *Z. Naturforsch.*, **7a**, 143–44 (1952)
63. Begemann, F., Buttlar, H. v., Houtermans, F. G , Isaac, N., and Picciotto, E., *Bull. centre phys. nucléaire univ. libre Bruxelles, No. 37*, 36 pp. (1952)
64. Begemann, F., Buttlar, H. v., Houtermans, F. G., Isaac, N., and Picciotto, E., *Bull. soc. belge géol. paléontol. et hydrol.*, **61**, 223–26 (1952)
65. Begemann, F., Buttlar, H. v., Houtermans, F. G., Isaac, N., and Picciotto, E., *Geochem. et Cosmochim. Acta*, **4**, 21–35 (1953)
66. Benfield, A. E., *Phys. Rev.*, **74**, 621 (1948)
67. Bernert, T., *Wien. Ber.*, IIa, **160**, 99–111 (1951)
68. Berthelot, A., Chaminade, R., Levi, C., and Papineau, L., *Compt. rend.*, **236**, 1769–71 (1953)
69. Binggeli, E., and Haenny, C., *Bull. soc. vaudoise sci. nat.*, **65**, 253–64 (1952)
70. Birch, F., *J. Geophys. Research*, **56**, 107–26 (1951)
71. Birch, F., *J. Geophys. Research*, **57**, 227–86 (1952)
72. Birch, F., in *Nuclear Geology* (Faul, H., Ed., John Wiley and Sons, New York, N. Y., In press, 1954)
73. Bitterli, P., *Bull. ver. schweiz. Petroleum-geol. u. Ing.*, **20**, 61–64 (1953)
74. Bizard, C., *Compt. rend.*, **236**, 1587–89 (1953)
75. Blau, H., Deevey, E. S., Jr., and Gross, M. S., *Science*, **118**, 1–6 (1953)
76. Blifford, I. H., Lockhart, L. B., Jr., and Rosenstock, H. B., *J. Geophys. Research*, **57**, 499–509 (1952)
77. Boato, G., Careri, G., Nencini, G., and Santangelo, M., *Ann. geofis. (Rome)*, **4**, 111–12 (1951)
78. Boato, G., Careri, G., and Santangelo, M., *Il Nuovo Cimento*, **9**, 1–6 (1952)
79. Boever, A., *Rev. tech. luxembourg.*, **44**, 99–101 (1952)
80. Boganik, N. S., *Izvestia Akad. Nauk S.S.S.R., Geol. Ser., No. 4*, 57–70 (1951)
81. Bose, R., *Bhu-Vidya*, **13**, 33–43 (1951)
82. Bowen, I. S., *Carnegie Inst. Washington Yearbook No. 52*, 3–37 (1953)
83. Bowie, S. H. U., and Horne, E. T., *Mineralog. Mag.*, **30**, 93–99 (1953)
84. Brown, H., and Patterson, C., *J. Geol.*, **55**, 405–11 (1947)
85. Brown, H., *Phys. Rev.*, **72**, 348 (1947)

86. Brown, H., Inghram, M. G., Larsen, E. S., Jr., Patterson, C., and Tilton, G., *Bull. Geol. Soc. Amer.*, **62**, 1426A (1951)
87. Brown, H., in *The Atmospheres of the Earth and Planets*, Revised ed., 258–66 (Kupier, G. P., Ed., Univ. Chicago Press, Chicago, Ill., 434 pp., 1952)
88. Brown, H. (Personal communication, 1954)
89. Brown, J. H., Jr., and Keller, W. D., *Science*, **116**, 632–33 (1952)
90. Bucher, W. H., *Trans. Am. Geophys. Union*, **31**, 495–507 (1950)
91. Bullard, E. C., and Stanley, J. P., *Veröffentl. Finn. Geodätischen Inst., No. 36*, 33–40 (1949)
92. Bullard, E. C., *Nature*, **170**, 200 (1952)
93. Bullard, E., C., *Proc. Roy. Soc.* (*London*), [A]**222**, 408–29 (1954)
94. Burch, P. R., *Nature*, **172**, 361–62 (1953)
95. Burke, W. H., Jr., and Meinschein, W. G., *Phys. Rev.*, **93**, 915A (1954)
96. Burling, R. L., *Phys. Rev.*, **84**, 839–40 (1951)
97. Burling, R. L., *Nucleonics*, **10**(5), 30–5 (1952)
97a. Buttlar, H. v., and Houtermans, F. G., *Naturwissenschaften*, **37**, 400–1 (1950)
98. Cahen, L., *Bull. soc. belge géol. paléontol. hydrol.*, **60**, 80–87 (1951)
99. Cahen, L., *Bull. soc. belge géol. paléontol. hydrol.*, **60**, 88–97 (1951)
100. Cahen, L., and Jacobs, T., *Bull. soc. belge géol. paléontol. hydrol.*, **60**, 97 (1951)
101. Cahen, L., *Bull. soc. belge géol. paléontol. hydrol.*, **60**, 97–112 (1951)
102. Carr, D. R., and Kulp, J. L., *Bull. Geol. Soc. Amer.*, **64**, 253–54 (1953)
102a. Caswell, R. S., Brabant, J. M., and Schwebel, A., *J. Research Natl. Bur. Standards* (*U.S.*), **53**, 27–28 (1954)
103. Chackett, K. F., Golden, J., Mercer, E. R., Paneth, F. A., Reasbeck, P., Hey, M. H., and Smith, W. C., *Geochim. et Cosmochim. Acta*, **1**, 3–14 (1950)
104. Chackett, K. F., *Phys. Rev.*, **81**, 1057 (1951)
105. Chackett, K. F., Reasbeck, P., and Wilson, E. J., *Geochim. et Cosmochim. Acta*, **3**, 261–71 (1953)
106. Charpak, G., and Suzor, F., *Compt. rend.*, **233**, 1356–57 (1951)
107. Clark, F. L., Spencer-Palmer, H. J., and Woodward, R. N., *Brit. Atomic Energy Document, BR-522* (1944)
108. Clark, F. L., Spencer-Palmer, H. J., and Woodward, R. N., *Brit. Atomic Energy Document, BR-584* (1945)
109. Cohen, S. G., and Bauminger, R., *Bull. Research Council Israel*, **2**, 195 (1952)
110. Collins, C. B., Freeman, J. R., and Wilson, J. T., *Phys. Rev.*, **82**, 966–67 (1951)
111. Collins, C. B., and Freeman, J. R., *Trans. Roy. Soc. Canada*, [IV]**45**, 23–30 (1951)
112. Collins, C. B., Lang, A. H., Robinson, S. C., and Farquhar, R. M., *Proc. Geol. Assoc. Canada*, **63**, 15–41 (1952)
113. Collins, C. B., Farquhar, R. M., and Russell, R. D., *Phys. Rev.*, **88**, 1275–76 (1952)
114. Collins, C. B., Russell, R. D., and Farquhar, R. M., *Can. J. Phys.*, **31**, 402–18 (1953)
115. Collins, C. B., Farquhar, R. M., and Russell, R. D., *Bull. Geol. Soc. Amer.*, **65**, 1–21 (1954)
115a. Cooke, H. B. S., *S. African J. Sci.*, **50**, 123–33 (1953)
116. Cooley, R. A., Martin, A. V., Feldman, C., and Gillespie, J., *Geochem. et Cosmochim. Acta*, **3**, 30–33 (1953)
117. Cooper, M., *Bull. Geol. Soc. Amer.*, **64**, 197–234 (1953)

118. Cooper, M., *Bull. Geol. Soc. Amer.*, **64**, 1103–72 (1953)
119. Cooper, M., *Bull. Geol. Soc. Amer.*, **65**, 467–589 (1954)
120. Cormack, A. M., *Phys. Rev.*, **95**, 580–81 (1954)
121. Craig, H., *J. Geol.*, **62**, 115–49 (1954)
122. Crane, H. R., *Revs. Modern Phys.*, **20**, 278–95 (1948)
123. Crane, H. R., *Nucleonics*, **9**(6), 16–23 (1951)
124. Crane, H. R., and McDaniel, E. W., *Science*, **116**, 342–47 (1952)
125. Crathorn, A. R., *Nature*, **172**, 632–33 (1953)
126. Curie, M., Debierne, A., Eve, A. S. Geiger, H., Hahn, O., Lind, S. C., Meyers, S., Rutherford, E., and Schweidler, E., *Revs. Modern Phys.*, **3**, 427–45 (1931)
127. Curran, S. C., Dixon, D., and Wilson, H. W., *Phys. Rev.*, **84**, 151–52 (1951)
128. Curran, S. C., Dixon, D., and Wilson, H. W., *Phil. Mag.*, (7)**43**, 82–92 (1952)
129. Curran, S. C., *Physica*, **18**, 1161–70 (1952)
130. Curran, S. C., *Quart. Rev. Chem. Soc.* (*London*), **7**, 1–18 (1953)
131. Curran, S. C., McNair, A., and Dixon, D., reported in *European Scientific Notes* (*U. S. Office of Naval Research, London Office*), **8**, 30–31 (1954)
132. Curtis, M. L., *Phys. Rev.*, **92**, 1489 (1953)
133. Dalton, J. C., Golden, J., Martin, G. R., Mercer, E. R., and Thomson, S. J., *Geochim. et Cosmochim. Acta*, **3**, 272–87 (1953)
134. Dalton, J. C., Paneth, F. A., Reasbeck, P., Thomson, S. J., and Mayne, K. I., *Nature*, **172**, 1168–69 (1953)
135. Dalton, J. C., and Thomson, S. J., *Geochim. et Cosmochim. Acta*, **5**, 74–80 (1954)
136. Damon, P. E., and Kuroda, P. K., *Nucleonics*, **11**(12), 59 (1953)
137. Damon, P. E., *Trans. Am. Geophys. Union*, **34**, 906–14 (1953)
138. Damon, P. E., and Kuroda, P. K., *Trans. Am. Geophys. Union*, **35**, 208–16 (1954)
139. Damon, P. E., *Trans. Am. Geophys. Union*, **35**, 631–35 (1954)
140. Daniels, F., Boyd, C. A., and Saunders, D. F., *Science*, **109**, 440A (1949)
141. Daniels, F., and Saunders, D. F., *Science*, **111**, 462A (1950)
142. Daniels, F., Boyd, C. A., and Saunders, D. F., *Science*, **117**, 343–49 (1953)
143. Danilevich, S. I., *Izvest. Akad. Nauk. S.S.S.R., Ser. Geofiz., 1952* (1), 3–11 (1952)
144. Daudel, R., Benoist, P., Jacques, R., and Jean, M., *Compt. rend.*, **224**, 1427–29 (1947)
145. Daudel, R., Jean, M., and Lecoin, M., *Compt. rend.*, **225**, 290–92 (1947)
146. Daudel, R., Jean, M., and Lecoin, M., *J. phys. rad.*, (8)**8**, 238–43 (1947)
147. Daudel, R., Jacques, R., Jean, M., Ratier, J., and Benoist, P., *J. phys. rad.*, (8) **8**, 257–62 (1947)
148. Dauvillier, A., *Compt. rend.*, **237**, 1202–3 (1953)
149. Davidson, C. F., *Mining Mag.*, **85**, 329–40 (1951)
150. Davidson, C. F., and Atkin, D., *Geol. Survey Gt. Brit. and Museum, Atomic Energy Div., Report No. 124*, 16 pp. (1952)
151. Davis, C. W., *Am. J. Sci.*, (5)**11**, 201–17 (1926)
152. Davis, G. L., *Am. J. Sci.*, **245**, 677–93 (1947)
153. Davis, G. L., *Am. J. Sci.*, **248**, 107–11 (1950)
154. Davis, G. L., and Aldrich, L. T., *Bull. Geol. Soc. Amer.*, **64**, 379–80 (1953)
155. Dawson, K. B., *Brit. J. Cancer*, **6**, 22–31 (1952)
156. Deevey, E. S., Jr., *Mem. Soc. Am. Archaeol. No. 8, Am. Antiquity*, **17**, (1) Pt. 2, 56–57 (1951)
157. Deevey, E. S., Jr., and Potzger, J. E., *Am. J. Sci.*, **249**, 473–511 (1951)

158. Deevey, E. S., Jr., *Am. Scientist*, **186**(2), 24–28 (1952)
159. Deevey, E. S., Jr., Gross, M. S., Hutchinson, G. E., and Kraybill, H. L., *Proc. Natl. Acad. Sci. U. S.*, **40**, 285–88 (1954)
160. DeGeer, E. H., *Geol. Fören. i Stockholm Förh.*, **73**, 517–18 (1951)
161. DeGeer, E. H., *Geol. Fören. i Stockholm Förh.*, **73**, 557–70 (1951)
162. Delaney, C. F. G., Matthews, C. M. E., and Poole, J. H. J., *Sci. Proc. Roy. Dublin Soc.*, **26**, 165–72 (1953)
163. Demay, A., *Compt. rend.*, **232**, 639 (1951)
164. Demay, A., *Compt. rend.*, **232**, 338–40 (1951)
165. Demay, A., Lepape, A., and Geslin, M., *Compt. rend.*, **232**, 1950–52 (1951)
166. Demay, A., *Compt. rend.*, **237**, 48–50 (1953)
167. de Vries, H., and Barendsen, G. W., *Physica*, **18**, 652 (1952)
168. de Vries, H., and Barendsen, G. W., *Physica*, **19**, 987–1003 (1953)
169. Diethorn, W. S., Simanton, J. R., and Kohman, T. P. (Unpublished work, 1954)
170. Dixon, D., McNair, A., and Curran, S. C., *Phil. Mag.*, (7)**45**, 683–94 (1954)
171. Dixon, D., and McNair, A. (Unpublished data, 1954)
172. Douglas, D. L., *Gen. Elec. Rev.*, **55**(5), 16–20 (1952)
173. Dunlavey, D. C., and Seaborg, G. T., *Phys. Rev.*, **87**, 165–66 (1952)
174. Dunlavey, D. C., and Seaborg, G. T., *Phys. Rev.*, **92**, 206 (1953)
175. Ehrenberg, H. F., *Z. Physik.*, **134**, 317–33 (1953)
176. Eisenbud, M., and Harley, J. H., *Science*, **117**, 141–47 (1953)
177. Eklund, S., *Ark. Mat. Astron. Fysik*, **33A**(14), 79 pp. (1946)
178. Emmons, R. C., Reynolds, C. D., and Saunders, D. F., *Mem. Geol. Soc., Amer. No. 52*, 89–99 (1953)
179. Endt, P. M., and Kluyver, J. C., *Revs. Modern Phys.*, **26**, 95–166 (1954)
180. Erichsen, L. von., *Neues Jahrb. Mineral.*, 25–33 (1951)
181. Evans, R. D., and Goodman, C., *Bull. Geol. Soc. Amer.*, **52**, 459–90 (1941)
182. Exner, C., and Pohl, E., *Jahrb. geol. Bundesanstalt (Austria)* (1949–51), **94**(2) 1–57 (1951)
183. Fabre de la Ripelle, M., *Compt. rend.*, **232**, 1655–57 (1951)
184. Fafarman, A., and Shamos, M. H., *Nucleonics*, **11**(6), 80–81 (1953)
185. Faltings, V., and Harteck, P., *Z. Naturforsch.*, **5a**, 438–39 (1950)
186. Faltings, V., *Naturwissenschaften*, **39**, 378–79 (1952)
187. Faraggi, H., and Berthelot, A., *Compt. rend.*, **232**, 2093–95 (1951)
188. Farquhar, R. M., Palmer, G. H., and Aitken, K. L., *Nature*, **172**, 860 (1953)
189. Faul, H., Gott, G. B., Manger, G. E., Mytton, J. W., and Pierce, A. P., *Bull. Geol. Soc. Amer.*, **64**, 1420A (1953)
189a. Faul, H., Gott, G. B., Manger, G. E., Mytton, J. W., and Sakakura, A. Y., *U. S. Geol. Survey Rept., TEM-533*, 17 pp. (1953)
189b. Faul H., Gott, G. B., Manger, G. E., Mytton, J. W., and Sakakura, A. Y., *Proceedings of Conference on Nuclear Processes in Geologic Settings*, 50–51 (Williams Bay, Wisconsin, September, 1953) (Published 1954)
190. Faul, H., Ed., *Nuclear Geology* (John Wiley and Sons, New York, N. Y.) (In press, 1954)
191. Fergusson, G. J., *New Zealand J. Sci. Technol.*, [B]**35**, 90–108 (1953)
192. Fergusson, G. J., and Rafter, T. A., *New Zealand J. Sci. Technol.*, [B]**35**, 127–28 (1953)
193. Fermi, E., *Nuclear Physics*, 85 (Univ. of Chicago Press, Chicago, Ill., Revised ed., 246 pp., 1950)

194. Festa, C., and Santangelo, M., *Ann. geofis.* (*Rome*), **3**, 251–61 (1950)
195. Fireman, E. L., and Schwarzer, D., *Phys. Rev.*, **86**, 451–53 (1952)
196. Fireman, E. L., *Phys. Rev.*, **91**, 922–26 (1953)
197. Fireman, E. L., and Schwarzer, D., *Phys. Rev.*, **94**, 385–88 (1954)
198. Fleischer, M., and Rabbitt, J. C., *Ann. Rev. Nuclear Sci.*, **1**, 465–78 (1952)
199. Fleischer, M., *U. S. Geol. Surv. Circ.*, **285**, 7 pp. (1953)
200. Fleming, E. H., Jr., Ghiorso, A., and Cunningham, B. B., *Phys. Rev.*, **88**, 642–52 (1952)
201. Flint, R. F., *Mem. Soc. Am. Archaeol. No. 8, Am. Antiquity*, **17**(1), *Pt.* 2, 54–55 (1951)
202. Flint, R. F., *Nature*, **167**, 833–36 (1951)
203. Flint, R. F., and Deevey, E. S., Jr., *Am. J. Sci.*, **249**, 257–300 (1951)
204. Flint, R. F., *Natural History*, **60**, 200–6 (1951)
205. Flint, R. F., *Bull. Geol. Soc. Amer.*, **64**, 897–919 (1953)
206. Flinta, J., and Eklund, E., *Ark. Fys.*, **7**, 401–11 (1954)
207. Florencio, W., *Mineração e Metalurgia*, **15**, 191–96 (1951)
208. Florencio, W., *Anais acad. brasil. cienc.*, **24**, 249–59 (1952)
209. Foldvari, A., *Acta Geol. Acad. Sci. Hung.*, **1**, 37–48 (1952)
210. Franke, H. W., *Naturwissenschaften*, **38**, 527–28 (1951)
211. Fremlin, J. H., and Walters, M. C., *Proc. Phys. Soc.* (*London*), [A]**65**, 911–15 (1952)
212. Freedman, A. J., and Anderson, E. C., *Nucleonics*, **10**(8), 57–59 (1952)
213. Fritze, K., and Strassmann, F., *Naturwissenschaften*, **39**, 522–23 (1952)
214. Fromm, E., *Geol. Fören. Stockholm Förh.*, **75**, 403 (1953)
215. Frondel, C., *Am. Mineral.*, **36**, 671–79 (1951)
216. Fulbright, H. W., *Physica*, **18**, 1026–31 (1952)
217. Gamow, G., *Am. Scientist*, **39**, 393–406 (1951)
218. Gamow, G., *Dan. Mat. Fys. Medd.*, **27**(10), 15 pp. (1953)
219. Garrigue, H., *Compt. rend.*, **232**, 722–24 (1951)
220. Garrigue, H., *Compt. rend.*, **232**, 827–29 (1951)
221. Garrigue, H., *Compt. rend.*, **232**, 1003–4 (1951)
222. Garrigue, H., *Compt. rend.*, **233**, 860–62 (1951)
223. Garrigue, H., *Compt. rend.*, **233**, 1447–48 (1951)
224. Garrigue, H., *Compt. rend.*, **235**, 1498–99 (1952)
225. Garrigue, H., *Compt. rend.*, **236**, 2309–11 (1953)
226. Garrigue, H., *Compt. rend.*, **237**, 802–3 (1953)
227. Garrigue, H., *Compt. rend.*, **237**, 1232–33 (1953)
228. Gauthé, B., and Blum, J. M., *Compt. rend.*, **236**, 1255–56 (1953)
229. Geiss, J., *Z. Naturforsch.*, **9a**, 218–27 (1954)
230. Gentner, W., Präg, R., and Smits, F., *Z. Naturforsch.*, **8a**, 216–17 (1953)
231. Gentner, W., Präg, R., and Smits, F., *Geochim. et Cosmochim. Acta*, **4**, 11–20 (1953)
232. Gentner, W., Goebel, K., and Präg, R., *Geochim. et Cosmochim, Acta*, **5**, 124–33 (1954)
233. Gentner, W., Jensen, F., and Mehnert, K. R., *Z. Naturforsch.*, **9a**, 176 (1954)
234. Gerling, E. K., and Pavlova, T. G., *Doklady Akad. Nauk S.S.S.R.*, **77**, 85–86 (1951)
235. Gerling, E. K., Ermolin, G. M., Baranovskaya, N. V., and Titov, N. E., *Doklady Akad. Nauk S.S.S.R.*, **86**, 593–96 (1952)

236. Ginnings, D. C., Ball, A. F., and Nier, D. T., *J. Research Natl. Bur. Standards (U. S.)*, **50**, 75–79 (1953)
237. Godwin, H., *Am. J. Sci.*, **249**, 301–7 (1951)
238. Goldblatt, M., Robinson, E. S., and Spence, R. W., *Phys. Rev.*, **72**, 973 (1947)
238a. Gott, G. B., Wyant, D. G., and Beroni, E. P., *U. S. Geol. Surv. Circ.*, **220**, 31–35 (1952)
239. Gott, G. B., and Hill, J. W., *U. S. Geol. Surv. Bull., 988-E*, 69–122 (1953)
240. Grande, P., *Fra Fysik. Verden*, **15**(1), 19–28 (1953)
241. Gray, G. W., *Sci. American*, **188**(6), 56–66 (1953)
242. Griffin, J. B., in *Archeology of Eastern United States*, 365–70 (Griffin, J. B., Ed., Univ. Chicago Press, Chicago, Ill., 392 pp., 1952)
243. Gross, H., *Eiszeitalter u. Gegenwart*, **2**, 68–92 (1952)
244. Grosse, A. V., Johnston, W. M., Wolfgang, R. L., and Libby, W. F., *Science*, **113**, 1–2 (1951)
245. Grosse, A. V., Kirshenbaum, A. D., Kulp, J. L., and Broecker, W. S., *Phys. Rev.*, **93**, 250–51 (1954)
246. Guntz, A. A., *Compt. rend.*, **234**, 868–70 (1952)
247. Gutenberg, B., Chapters VII, IX, and XVI, in *Internal Constitution of the Earth* (Gutenberg, B., Ed., Dover Publications, Inc., New York, N. Y., 2nd ed., 439 pp., 1951)
248. Halicki, B., *Wiadomości Muzeum Ziemi*, **6**, 291–97 (1952)
249. Harley, J. H., *Nucleonics*, **11**(7), 12–15 (1953)
250. Harteck, P., and Faltings, V., *Nature*, **166**, 1109 (1950)
251. Haxel, O., Houtermans, F. G., and Kemmerich, M., *Phys. Rev.*, **74**, 1886–87 (1948)
252. Haxel, O., and Houtermans, F. G., *Z. Physik.*, **124**, 705–13 (1948)
253. Haxel, O., and Schumann, G., *Naturwissenschaften*, **40**, 458–59 (1953)
254. Hayase, K., *Kagaku*, **21**, 543–44 (1951)
255. Hayden, R. J., and Inghram, M. G., *Natl. Bur. Standards Circ.*, **522**, 189–92 (1953)
256. Hayes, F. N., Williams, D. L., and Rogers, B., *Phys. Rev.*, **92**, 512–13 (1953)
257. Hecht, F., priv. comm. to Picciotto, E., and Wilgain, S., *Nature*, **173**, 632–33 (1954)
258. Hée, A., and Jarovoy, M., *Ann. géophys.*, **9**, 153–58 (1953)
259. Heintze, J., and Haxel, O., reported in *European Scientific Notes* (*U. S. Office of Naval Research, London Office*), **8**, 110–11 (1954)
260. Herzog, L. F., Aldrich, L. T., Holyk, W. K., Whiting, F. B., and Ahrens, L. H., *Trans. Am. Geophys. Union*, **34**, 461–70 (1953)
261. Herzog, L. F., and Pinson, W. H., in *U. S. Atomic Energy Commission Document, NYO-3934-II* (1954)
262. Hess, D. C., Brown, H., Inghram, M. G., Patterson, C., and Tilton, G., *Natl. Bur. Standards Circ.*, **522**, 183–87 (1953)
263. Hewett, D. F., and Glass, J. J., *Am. Mineral.*, **38**, 1040–50 (1953)
264. Hieke-Merlin, O., *Rend. soc. mineralog. ital.*, **8**, 129–30 (1952)
265. Hincks, E. P., and Millar, C. H., *Proc. Roy. Soc. Can.*, (3)**46**, 143A (1952)
266. Holland, H. D., and Kulp, J. L., *Science*, **111**, 312 (1950)
267. Holland, H. D., and Kulp, J. L., *Geochim. et Cosmochim. Acta*, **5**, 197–213 (1954)
268. Holland, H. D., and Kulp, J. L., *Geochim. et Cosmochim. Acta*, **5**, 214–24 (1954)
269. Holmes, A., *Bull. Natl. Research Council (U. S.)*, **80**, 334–38 (1931)

270. Holmes, A., *Nature*, **157**, 680–84 (1946)
271. Holmes, A., *Nature*, **159**, 127–28 (1947)
272. Holmes, A., *Geol. Mag.*, **84**, 123–26 (1947)
273. Holmes, A., *Trans. Geol. Soc. Glasgow*, **21**, 117–52 (1947)
274. Holmes, A., *Trans. Geol. Soc. Edinburgh*, **14**, 176–94 (1948)
275. Holmes, A., Smales, A. A., Leland, W. T., and Nier, A. O., *Geol. Mag.*, **86**, 288–302 (1949)
276. Holmes, A., *Nature*, **163**, 453–56 (1949)
277. Holmes, A., Leland, W. T., and Nier, A. O., *Am. J. Sci.*, **248**, 81–94 (1950)
278. Holmes, A., Leland, W. T., and Nier, A. O., *Am. Mineral.*, **35**, 19–28 (1950)
279. Holmes, A., *Nature*, **173**, 612–14 (1954)
280. Holyk, W., and Ahrens, L. H., *Geochim. et Cosmochim. Acta*, **4**, 241–50 (1953)
281. Hough, J. L., *J. Geol.*, **58**, 254–60 (1950)
282. Hough, J. L., *J. Geol.*, **61**, 252–62 (1953)
283. Houtermans, F. G., *Naturwissenschaften*, **33**, 185–86, 219 (1946)
284. Houtermans, F. G., and Jordan, P., *Z. Naturforsch.*, **1**, 125–30 (1946)
285. Houtermans, F. G., *Z. Naturforsch.*, **2a**, 322–28 (1947)
286. Houtermans, F. G., *Sitzber. heidelberg. Akad. Wiss. Math.-naturw. Kl., No. 2*, 123–36 (1951)
287. Houtermans, F. G., *Nuovo cimento*, **10**, 1623–33 (1953)
288. Houtermans, F. G., and Thirring, W., *Helv. Phys. Acta*, **27**, 81–88 (1954)
289. Hubenet, H., de Jager, C., Zwaan, C., *Mém. soc. roy. sci. Liège*, **14**, 471 (1954)
290. Hurley, P. M., *Science*, **110**, 49–50 (1949)
291. Hurley, P. M., *Bull. Geol. Soc. Amer.*, **61**, 1–7 (1950)
292. Hurley, P. M., *Trans. Am. Geophys. Union*, **33**, 174–83 (1952)
293. Hurley, P. M., and Fairbairn, H. W., *Bull. Geol. Soc. Amer.*, **64**, 659–73 (1953)
294. Hyde, E. K., *Natl. Nuclear Energy Ser., IV-14B*, 1435–38 (1949)
295. Ingerson, E., *Geochim. et Cosmochim. Acta*, **5**, 20–39 (1954)
296. Inghram, W. N., and Keevil, N. B., *Bull. Geol. Soc. Amer.*, **62**, 131–48 (1951)
297. Inghram, M. G., Brown, H., Patterson, C., and Hess, D. C., *Phys. Rev.*, **80**, 916–17 (1950)
298. Inghram, M. G., and Reynolds, J. H., *Phys. Rev.*, **78**, 822–23 (1950)
299. Israel, H., in *Compendium of Meteorology*, 155–61 (Malone, T. F., Ed., Am. Meteorol. Soc., Boston, Mass., 1334 pp., 1951)
300. Issac, N., and Picciotto, E., *Nature*, **171**, 742–43 (1953)
301. Ivanenko, D. D., and Lebedev, V., *Zhur. Eksptl. i Teort. Fiz.*, **20**, 91–92 (1950)
302. Iverson, J., *Science*, **118**, 9–11 (1953)
303. Iwasaki, I., Ishimori, T., and Hataye, I., *J. Chem. Soc. Japan, Pure Chem. Sect.*, **72**, 736–39 (1951)
304. Iwasaki, I., and Matsuda, F., *J. Chem. Soc. Japan, Pure Chem. Sect.*, **72**, 94–97 (1951)
305. Jacoe, P. W., *Arch. Ind. Hyg. Occupational Med.*, **8**, 118–24 (1953)
306. Jaffe, G., and Hughes, J. H., *Trans. Am. Geophys. Union*, **34**, 539–42 (1953)
307. Jeffreys, H., *Nature*, **162**, 822–23 (1948)
308. Jeffreys, H., *Nature*, **164**, 1046–47 (1949)
309. Jeffreys, H., *The Earth*, 3rd ed, Chap. 10 (Cambridge Univ. Press, Cambridge, England, 392 pp., 1952)
310. Jenks, G. H., Ghormley, J. A., and Sweeton, F. H., *Phys. Rev.*, **75**, 701–2 (1949)
311. Jenks, G. H., Sweeton, F. H., and Ghormley, J. A., *Phys. Rev.*, **80**, 990–95 (1950)

312. Johnson, F., Ed., *Radiocarbon Dating* (*Mem. Soc. Am. Archaeol. No. 8*, Suppl. to *Am. Antiquity*, **17**, *No. 1, Pt. 2*, 65 pp., 1951)
313. Johnson, F., Rainey, F., Collier, D., and Flint, R. F., *Mems. Soc. Am. Archaeol. No. 8, Am. Antiquity*, **17**, *No. 1, Pt. 2*, 58–62 (1951)
314. Johnson, F., in *Radiocarbon Dating*, 97–111 (W. F. Libby, Univ. Chicago Press, Chicago, Ill., 124 pp., 1952)
315. Jolliffe, A. W., *Intern. Geol. Congr., Rept. 18th Sess. Gt. Brit. 1948, Pt. 13*, 141–49 (1952)
316. Jones, W. M., *Phys. Rev.*, **83**, 537–39 (1951)
317. Jones, J. W., and Kohman, T. P., *Phys. Rev.*, **85**, 941 (1952)
318. Jordan, P., *Phys. Z.*, **45**, 183–90 (1944)
318a. Jung, K., *Geofis. pura e appl.*, **17**, 1–2 (1950)
319. Kaiser, E. P., *U. S. Geol. Survey Circ.*, **137**, 1–10 (1951)
320. Kalkstein, M. I., *Double Beta Decay and Other Natural Radioactive Processes.* (Doctoral thesis, Univ. of Chicago, Chicago, Ill., 1950)
321. Kalkstein, M. I., and Libby, W. F., *Phys. Rev.*, **85**, 368–69 (1952)
322. Kamada, M., *Sci. Rep. Kagoshima Univ. (Japan)*, **1**, 1, 11, 21 (1952)
323. Katcoff, S., Schaeffer, O. A., and Hastings, J. M., *Phys. Rev.*, **82**, 688–90 (1951)
324. Kaufman, S., and Libby, W. F., *Phys. Rev.*, **93**, 1337–44 (1954)
325. Keevil, N. B., *Am. J. Sci.*, **236**, 406–16 (1938)
326. Keevil, N. B., *Am. J. Sci.*, **240**, 13–21 (1942)
327. Keevil, N. B., Larsen, E. S., and Wank, F. J., *Am. J. Sci.*, **242**, 345–53 (1944)
328. Keinberger, C. A., *Phys. Rev.*, **76**, 1561–63 (1949)
329. Kemmerich, M., *Z. Physik*, **126**, 399–409 (1949)
330. Kerr, P. F., and Kulp, J. L., *Science*, **115**, 86–88 (1952)
331. Kimura, K., and Kuroda, P. K., *J. Chem. Soc. Japan*, **63**, 688–90 (1942)
332. Kimura, K., and Saito, N., *J. Chem. Soc. Japan*, **64**, 107–11 (1943)
333. Kimura, K., Kuroda, K., and Yokoyama, Y., *J. Chem. Soc. Japan, Pure Chem. Sect.*, **69**, 34 (1948)
334. Kimura, M., and Nagashima, K., *J. Chem. Soc. Japan, Pure Chem. Sect.*, **72**, 53–54 (1951)
335. Kirby, H. W., *Anal. Chem.*, **25**, 1238–41 (1953)
336. Klinkenberg, F. A., *Physica*, **17**, 715–16 (1951)
337. Koczy, F. F., *Nature*, **151**, 24 (1943)
338. Koczy, F. F., *Geochim. et Cosmochim. Acta*, **1**, 73–85 (1951)
339. Kohman, T. P., *Phys. Rev.*, **73**, 16–21 (1948)
340. Kohman, T. P., *Phys. Rev.*, **76**, 448–49 (1949)
341. Kohman, T. P., Ames, D. P., and Sedlet, J., *Natl. Nuclear Energy Ser.*, IV-14B, 1675–99 (1949)
342. Kohman, T. P., *Science*, **119**, 851–52 (1954)
344. Kohman, T. P., *Proceedings of Conference on Nuclear Processes in Geologic Settings*, 10–13 (Williams Bay, Wisconsin, September, 1953) (1954)
345. Kohman, T. P., *Proceedings of Conference on Nuclear Processes in Geologic Settings*, 14–16 (Williams Bay, Wisconsin, September, 1953) (1954)
346. Kohman, T. P., *Proceedings on Conference on Nuclear Processes in Geologic Settings*, 18–20 (Williams Bay, Wisconsin, September, 1953) (1954)
347. Kohman, T. P., *Ann. N. Y. Acad. Sci.* (Accepted for publication in 1954)
348. Kovarik, A. F., and Adams, N. I., Jr., *Phys. Rev.*, **54**, 413–21 (1938)
349. Kröll, V. S., *Nature*, **171**, 742 (1953)
350. Kulp, J. L., Feely, H. W., and Tryon, L. E., *Science*, **114**, 565–68 (1951)

351. Kulp, J. L., *Bull. Geol. Soc. Amer.*, **62,** 326–29 (1951)
352. Kulp, J. L., Tryon, L. E., Eckelman, W. R., and Snell, W. A., *Science*, **116,** 409–14 (1952)
353. Kulp, J. L., and Tryon, L. E., *Rev. Sci. Instruments*, **23,** 296–97 (1952)
354. Kulp, J. L., Tryon, L. E., and Feely, H. W., *Trans. Am. Geophys. Union*, **33,** 183–92 (1952)
355. Kulp, J. L., *Sci. Monthly*, **65,** 259–67 (1952)
356. Kulp, J. L., Volchok, H. L., and Holland, H. D., *Am. Mineral*, **37,** 709–18 (1952)
357. Kulp, J. L., Volchok, H. L., Holland, H. D., and Ericson, D. B., *J. Marine Research*, **11,** 19–28 (1952)
358. Kulp, J. L., and Volchok, H. L., *Phys. Rev.*, **90,** 713–14 (1953)
359. Kulp, J. L., *Atomics*, **4,** 96–98 (1953)
360. Kulp, J. L., *J. Chem. Education*, **30,** 432–35 (1953)
361. Kulp, J. L., Eckelmann, W. R., Owen, H. R., and Bate, G. L., *U. S. Atomic Energy Commission Document, NYO-6199*, 17 pp. (1953)
362. Kulp, J. L., Broecker, W. S., and Eckelmann, W. R., *Nucleonics*, **11**(8), 19–21 (1953)
363. Kulp, J. L., Owen, H. R., Eckelmann, W. R., and Bate, G. L., *U. S. Atomic Energy Commission Document, NYO-6197*, 13 pp. (1953)
364. Kulp, J. L., Bate, G. L., and Boecker, W. S., *Am. J. Sci.*, **252,** 345–65 (1954)
365. Kulp, J. L. (Personal communication, 1954)
366. Kuroda, P. K., and Yokoyama, Y., *Chemical Researches, Inorg. Chem.*, **3,** 29–68 (1948)
367. Kuroda, P. K., and Yokoyama, Y., *Bull. Chem. Soc. Japan*, **21,** 52–58 (1948)
368. Kuroda, P. K., and Yokoyama, Y., *Anal. Chem.*, **25,** 832–35 (1953)
369. Kuroda, P. K., Damon, P. E., and Hyde, H. I., *Am. J. Sci.*, **252,** 76–86 (1954)
370. Kuroda, P. K., and Edwards, R. R., in *Annual Progress Report to U. S. Atomic Energy Commission Contract AT(40-1)-1313 Univ. Arkansas* (1954)
371. Kuroda, P. K., and Edwards, R. R. (Paper *Q26* presented at Am. Chem. Soc. Meeting, Kansas City, Mo., March, 1954)
372. Larsen, E. S., and Keevil, N. B., *Am. J. Sci.*, **240,** 204–215 (1942)
373. Larsen, E. S., Jr., Keevil, N. B., and Harrison, H. C., *Bull. Geol. Soc. Amer.*, **63,** 1045–52 (1952)
374. Lecolazet, R., and Hée, A., *Ann. géophys.*, **8,** 320–22 (1952)
375. Le Couteur, K. J. (Personal communication to Paneth, F. A., Reasbeck, P., and Mayne, K. I.); *Geochim. et Cosmochim. Acta*, **2,** 300–3 (1952); *Nature*, **172,** 200–1 (1953)
376. Levine, C. A., Ghiorso, A., and Seaborg, G. T., *Phys. Rev.*, **77,** 296 (1950)
377. Levine, C. A., and Seaborg, G. T., *J. Am. Chem. Soc.*, **73,** 3278–83 (1951)
378. Lewis, G. M., *Phil. Mag.*, (7)**43,** 1070–74 (1952)
379. Libby, W. F., *Phys. Rev.*, **69,** 671–72 (1946)
380. Libby, W. F., Anderson, E. C., and Arnold, J. R., *Science*, **109,** 227–28 (1949)
381. Libby, W. F., *Science*, **114,** 291–96 (1951)
382. Libby, W. F., *Radiocarbon Dating* (Univ. Chicago Press, Chicago, Ill., 124 pp., 1952)
383. Libby, W. F., *Science*, **116,** 673–81 (1952)
384. Libby, W. F., *Proc. Natl. Acad. Sci. U. S.*, **39,** 245–47 (1953)
385. Libby, W. F., *Science*, **119,** 135–140 (1954)
386. Libby, W. F., *Endeavor*, **13,** 5–16 (1954)

387. Libby, W. F., *Sci. American*, **190**(4), 38–42 (1954)
388. Libby, W. F. (Personal communication, 1954)
389. Lockett, E. E., and Thomas, R. H., *Nucleonics*, **11**(3), 14–17 (1953)
390. López de Azcona, J. M., *Bol. inst. geol. y minero España*, **63**, 257–559 (1951)
391. Love, S. K., *Ind. Eng. Chem.*, **43**, 1541–44 (1951)
392. Love, J. D., *U. S. Geol. Survey Circ.*, **278**, 10 pp. (1953)
393. Lowell, W. R., *U. S. Geol. Survey Bull., 982A*, 55 pp. (1952)
394. MacGregor, M. H., and Wiedenbeck, M. L., *Phys. Rev.*, **86**, 420–21 (1952)
395. MacGregor, M. H., and Wiedenbeck, M. L., *Phys. Rev.*, **94**, 138–40 (1954)
396. Manov, G. G., and Curtiss, L. F., *J. Research Natl. Bur. Standards (U. S)*, **46**, 328–33 (1951)
397. Marble, J. P., *Report of the Committee on the Measurement of Geologic Time, 1950–51* (National Research Council, Washington, D. C., Publication 212, 140 pp., 1952)
398. Marble, J. P., *Report of the Committee on the Measurement of Geologic Time, 1951–52* (National Research Council, Washington, D. C., Publication 245, 151 pp., 1953)
399. Marble, J. P., *Report of the Committee on the Measurement of Geologic Time, 1952–53* (National Research Council, Washington, D. C., Publication 319, 187 pp., 1954)
400. Martin, G. R., *Geochim. et Cosmochim. Acta*, **3**, 288–309 (1953)
401. McCarthy, J. A., *Phys. Rev.*, **90**, 853–57 (1953)
402. McCarthy, J. A. (Personal communication, 1953)
403. McCrady, E., *Trans. Am. Geophys. Union*, **33**, 156–70 (1952)
404. McLaughlin, D. B., *Bull. Geol. Soc. Amer.*, **65**, 715–17 (1954)
405. Meinke, W. W., *Science*, **113**, 545–46 (1951)
405a. Menard, H. W., *Bull. Geol. Soc. Amer.*, **64**, 1279–94 (1953)
406. Merrill, P. W., *Astrophys. J.*, **116**, 21–26 (1952)
407. Merrill, P. W., *J. Roy. Astr. Soc. Canada*, **46**, 181–90 (1952)
408. Merrill, P. W., *Science*, **115**, 484A (1952)
409. Milholić, S., *J. Chem. Soc.*, 3402–5 (1950)
410. Minami, E., Saito, N., and Yamagata, N., *Research Reports Tamagawa Hot Springs*, **3**, 1 (1952)
411. Minami, E., Saito, N., and Ishimori, I., *Research Reports Tamagawa Hot Springs*, **3**, 3 (1952)
412. Moore, C. E., *Science*, **114**, 59–61 (1951)
413. Moore, R. C., *Trans. Am. Geophys. Union*, **33**, 150–56 (1952)
414. Morrison, P., *Phys. Rev.*, **82**, 209–11 (1951)
415. Mościcki, W., *Wiadomości Muzeum Ziemi*, **6**, 298–312 (1952)
416. Mościcki, W., *Acta Geol. Polon.*, **3**, 187–89 (1953)
417. Mościcki, W., *Acta Phys. Polon.*, **12**, 238–40 (1953)
418. Mousuf, A. K., *Phys. Rev.*, **88**, 150–51 (1952)
419. Mulholland, G. I., and Kohman, T. P., *Phys. Rev.*, **85**, 144–45 (1952)
420. Mulholland, G. I., and Kohman, T. P., *Phys. Rev.*, **87**, 681–82 (1952)
421. Nakanishi, M., *Bull. Chem. Soc. Japan*, **24**, 33–36 (1951)
422. Nakanishi, M., *Bull. Chem. Soc. Japan*, **24**, 36–38 (1951)
423. Naldrett, S. N., and Libby, W. F., *Phys. Rev.*, **73**, 487–93, 929 (1948)
424. National Research Council (U. S.), *Glossary of Terms in Nuclear Science and Technology*, Section I. Physics (1953) (American Society of Mechanical Engineers, New York, N. Y., in 9 sections, 1950–53)

425. Neuerburg, G. J., and Gottfried, D., *Bull. Geol. Soc. Amer.*, **65**, 465 (1954)
426. Nicolaysen, L. O., Aldrich, L. T., and Doak, J. B., *Trans. Am. Geophys. Union*, **34**, 342A (1953)
427. Nier, A. O., *J. Am. Chem. Soc.*, **60**, 1571–76 (1938)
428. Nier, A. O., *Phys. Rev.*, **55**, 153–63 (1939)
429. Nier, A. O., Thompson, R. W., and Murphey, B. F., *Phys. Rev.*, **60**, 112–16 (1941)
430. Nier, A. O., *Phys. Rev.*, **77**, 789–93 (1950)
431. Nier, A. O., *Phys. Rev.*, **79**, 450–54 (1950)
432. Norin, R., *Geol. Fören. Stockholm Förh.*, **73**, 406–8 (1951)
433. Norinder, H., Siksna, R., and Metnieks, A., *Geol. Fören. Stockholm Förh.*, **74**, 450–54 (1952)
434. Norinder, H., Metnieks, A., and Siksna, R., *Arkiv Geofysik*, **1**, 571–59 (1952)
435. Novick, A., *Phys. Rev.*, **72**, 972 (1947)
436. Okabe, I. S., and Nishio, J., *J. Chem. Soc. Japan, Pure Chem. Sect.*, **74**, 923–25 (1953)
437. Oshima, Y., *Repts. Balneol. Lab., Okayama Univ. (Japan)*, **4**, 13–14 (1951)
438. Pabst, A., and Hutton, C. O., *Am. Mineral.*, **36**, 60–69 (1951)
439. Pabst, A., *Am. Mineral.*, **37**, 137–57 (1952)
440. Pahl, M., Hiby, J., Smits, F., and Gentner, W., *Z. Naturforsch.*, **5a**, 404–5 (1950)
441. Paneth, F. A., *Nature*, **165**, 454 (1950)
442. Paneth, F. A., *J. chim. phys.*, **48**, 163–67 (1951)
443. Paneth, F. A., Reasbeck, P., and Mayne, K. I., *Geochim. et Cosmochim. Acta*, **2**, 300–3 (1952)
444. Paneth, F. A., *Nature*, **170**, 729 (1952)
445. Paneth, F. A., *Endeavor*, **12**, 5–17 (1953)
446. Paneth, F. A., *Geochim. et Cosmochim. Acta*, **3**, 257–60 (1953)
447. Paneth, F. A., Reasbeck, P., and Mayne, K. I., *Nature*, **172**, 200–1 (1953)
448. Parks, J. M., Jr., and Saunders, D. F., *Bull. Geol. Soc. Am.*, **62**, 1468A (1951)
449. Parks, J. M., Jr., and Saunders, D. F., *Am. Mineral.*, **37**, 297A (1952)
450. Patterson, C., *U. S. Atomic Energy Commission Document*, AECD-3180, 31 pp. (1951)
451. Patterson, C., Brown, H., Tilton, G., and Inghram, M., *Phys. Rev.*, **92**, 1234–35 (1953)
452. Patterson, C. C., Goldberg, E. D., and Inghram, M. G., *Bull. Geol. Soc. Amer.*, **64**, 1387–88 (1953)
453. Patterson, C., Tilton, G., and Inghram, M. G., *Bull. Geol. Soc. Amer.*, **64**, 1461A (1953); *Chem. Eng. News*, **31**, 4874 (1953)
454. Patterson, C., *Proceedings of Conference on Nuclear Processes in Geologic Settings*, 36–40 (Williams Bay, Wisconsin, September, 1953) (1954)
455. Peixoto, F., and Guimaraes, D., *Anais. acad. brasil. cienc.*, **24**, 315–27 (1952)
456. Peixoto, F., and Guimaraes, D., *Escola engenharia, Univ. Minas Gerais, Inst. pesquisas radioactivas, Publ. No. 1*, 1–35 (1953)
457. Pellas, P., *Compt. rend.*, **235**, 1134–36 (1952)
458. Peppard, D. F., Studier, M. H., Gergel, M. V., Mason, G. W., Sullivan, J. C., and Mech, J. F., *J. Am. Chem. Soc.*, **73**, 2529–31 (1951)
459. Peppard, D. F., Mason, G. W., Gray, P. R., and Mech, J. F., *J. Am. Chem. Soc* **74**, 6081–84 (1952)

460. Pettersson, H., *Nature*, **164**, 468–70 (1949)
461. Pettersson, H., *Nature*, **167**, 942 (1951)
462. Pettersson, H., *Am. Scientist*, **41**, 245–55 (1953)
463. Pfotzer, G., *Z. Naturforsch.*, **7a**, 145–49 (1952)
464. Picciotto, E. E., *Bull. soc. belge géol. paléontol. hydrol.*, **59**, 102–35 (1951)
465. Picciotto, E. E., *Bull. soc. belge géol. paléontol. hydrol.*, **59**, 170–98 (1951)
466. Picciotto, E., and Wilgain, S., *Nature*, **173**, 632–33 (1954)
467. Piénkowski, S., *Bull. acad. polon. sci., Classe III*, **1**, 39–41 (1953)
468. Piggot, C. S., *J. Am. Chem. Soc.*, **50**, 2910–16 (1928)
469. Poole, J. H. J., and Delaney, C. F. G., *Nature*, **167**, 680–81 (1951)
470. Porschen, W., and Riezler, W., *Z. Naturforsch.*, **8a**, 502 (1953)
471. Pringle, R. W., Standil, S., Taylor, H. W., and Fryer, G., *Phys. Rev.*, **84**, 1066–67 (1951)
472. Quimby, G. I., *Am. Antiquity*, **19**, 317–31 (1954)
472a. Rafter, T. A., *New Zealand J. Sci. Technol.*, [B]**35**, 64–89 (1953)
473. Rankama, K., *Geochim. et Cosmochim. Acta*, **5**, 81–84 (1954)
474. Rasmussen, J. O., Jr., Thompson, S. G., and Ghiorso, A., *Phys. Rev.*, **89**, 33–48 (1953)
475. Reuterswärd, C., *Arkiv. Fysik.*, **4**, 203–5 (1952)
476. Revelle, R., and Maxwell, A. E., *Nature*, **170**, 199–200 (1952)
477. Riezler, W., and Porschen, W., *Z. Naturforsch*, **7a**, 634–35 (1952)
478. Roberts, F. H. H., Jr., *Trans. Am. Geophys. Union*, **33**, 170–74 (1952)
479. Roberts, F. H. H., Jr., *Ann. Rept. Smithsonian Inst. 1951*, 335–50 (1952)
480. Rodgers, J., *Am. J. Sci.*, **250**, 411–27 (1952)
481. Rona, E., and Urry, W. D., *Am. J. Sci.*, **250**, 241–62 (1952)
482. Rose, D. C., and Katzman, J., *Can. J. Phys.*, **30**, 111–16 (1952)
483. Rosenblatt, D. B., and Lindeman, H., *Science*, **116**, 689–90 (1952)
484. Rosenblatt, D. B., *Phys. Rev.*, **91**, 1474–75 (1953)
484a. Rostagni, A., *Geofis. pura e appl.*, **18**, 128–31 (1950)
485. Rothé, J. P., and Peterschmitt, É., *Compt. rend.*, **234**, 1610–12 (1952)
486. Rubey, W. W., *Bull. Geol. Soc. Amer.*, **62**, 1111–48 (1951)
487. Rüling, J., Scheminzky, F., *Tschermaks mineralog. petrog. Mitt.*, **2**, 283–89 (1951)
488. Runnels, R. T., Schleicher, J. A., and Van Nortwick, H. S., *State Geol. Survey, Kansas, Bull. No. 102*, 93–104 (1953)
489. Russell, R. D., Shillibeer, H. A., Farquhar, R. M., and Mousuf, A. K., *Phys. Rev.*, **91**, 1223–24 (1953)
490. Russell, R. D., Farquhar, R. M., Cumming, G. L., and Wilson, J. T., *Trans. Am. Geophys. Union*, **35**, 301–9 (1954)
491. Saito, N., *J. Chem. Soc. Japan*, **64**, 1–6, 209–13, 1150–53 (1943)
492. Saito, N., *Intern. Congr. Hydrol., Brussel Assembly, August, 1951* (In press)
493. Saito, N., Kohman, T. P., Hayden, R. J., and Inghram, M. G. (Unpublished data, 1954)
494. Saito, N., Kohman, T. P., and Reynolds, J. R. (Unpublished data, 1954)
494a. Saito, N., Kohman, T. P., and Stieff, L. R. (Unpublished data, 1954)
495. Sanderman, L. A., and Utterback, C. L., *Trans. Am. Geophys. Union*, **34**, 915–20 (1953)
496. Santomauro, L., and Cigna, A., *Ann. geofis. Rome*, **6**, 381–87 (1953)
497. Saunders, D. F., in *Annual Progress Report to U. S. Atomic Energy Commission, Contract AT(11-1)-178, Univ. Wisconsin* (1953)

498. Sawyer, G. A., and Wiedenbeck, M. L., *Phys. Rev.*, **76,** 1535–37 (1949); **79,** 490–94 (1950)
499. Saxon, D., *Phys. Rev.*, **76,** 986 (1949)
500. Sayag, G.-J., *Compt. rend.*, **232,** 2091–93 (1951)
501. Scharff-Goldhaber, G., (Reported by Goldhaber, M., and Hill, R. D.) *Revs. Modern Phys.*, **24,** 179–239 (1952)
502. Scheminzky, F., and Grabherr, W., *Tschermaks mineralog. petrog. Mitt.*, **2,** 257–82 (1951)
503. Selig, H., and Kohman, T. P. (Unpublished data, 1953). Reported briefly in Kohman, T. P., *Proceedings of Conference on Nuclear Processes in Geologic Settings*, 14–16 (Williams Bay, Wisconsin, September, 1953) (1954)
504. Shavrova, N. N., *Byull. Vulkanicheskoĭ Stantsii Kamehatke, No. 2*, 37–40 (1938)
505. Sheline, R. (Personal communication, 1953)
506. Shillibeer, H. A., Russell, R. D., Farquhar, R. M., and Jones, E. A. W., *Phys. Rev.*, **94,** 1793–94 (1954)
507. Shimokata, K., *J. Chem. Soc. Japan, Pure Chem. Sect.*, **73,** 580–83 (1952)
508. Shimokata, K., *Bull. Nagoya Inst. Technol.*, **4,** 367–73 (1952)
509. Shimokata, K., *J. Chem. Soc. Japan, Pure Chem. Sect.*, **75,** 67–70 (1954)
510. Sherk, P. M., *Phys. Rev.*, **75,** 789–91 (1949)
511. Singer, S. F., *Nature*, **170,** 728–29 (1952)
512. Singer, S. F., *Phys. Rev.*, **90,** 168 (1953)
513. Singer, S. F., *Mém. soc. roy. sci. Liège*, **13,** 339–49 (1953)
514. Singer, S. F., *Astrophys. J.*, **119,** 291–93 (1954)
515. Smith, P. V., Jr., *Science*, **116,** 437–39 (1952)
516. Smith, P. V., Jr., *Bull. Am. Assn. Pet. Geol.*, **38,** 377–404 (1954)
517. Smits, F., and Gentner, W., *Geochim. et Cosmochim. Acta.*, **1,** 22–27 (1950)
518. Starik, I. E., *Izvest. Akad. Nauk S.S.S.R., Ser. Geol.* (6), 11–19 (1952)
519. Stella, A., and Tamburino, S., *Rend. soc. mineralog. ital.*, **8,** 185–88 (1952)
520. Stewart, D. C., and Bentley, W. C., *Science*, **120,** 50–51 (1954)
521. Stieff, L. R., and Stern, T. W., *Science*, **115,** 706–8 (1952)
522. Stieff, L. R., Stern, T. W., and Milkey, R. G., *U. S. Geol. Surv. Circ.*, **271,** 19 pp. (1953)
523. Stieff, L. R., and Stern, T. W., *U. S. Geol. Surv. Report, TEI-322*, 15 pp. (1953)
524. Strome, F. C., Jr., *Univ. Microfilms* (Ann Arbor, Mich.), *Publ. No. 7739*, 99 pp. (1954); *Dissertation Abstracts*, **14,** 699 (1954)
525. Struve, O., *Sky and Telescope*, **12,** 203–5, 238–40 (1953)
526. Suess, H. E., *Phys. Rev.*, **73,** 1209 (1948)
527. Suess, H. E., *Experientia*, **5,** 278–79 (1949)
528. Suess, H. E., Hayden, R., J., and Inghram, M. G., *Nature*, **168,** 432–33 (1951)
529. Suess, H. E., *Geochim. et Cosmochim. Acta*, **2,** 76–79 (1951)
530. Suess, H. E., and Brown, H., *Phys. Rev.*, **83,** 1254–55 (1951)
531. Suess, H. E. (Personal communication, 1952)
531a. Suess, H. E., *Trans. Am. Geophys. Union*, **34,** 343A (1953).
532. Suess, H. E., *Proceedings of Conference on Nuclear Processes in Geologic Settings*, 52–56 (Williams Bay, Wisconsin, September, 1953) (1954)
533. Suess, H. E., *Science*, **120,** 5–7 (1954)
534. Sugarman, N., and Richter, H., *Phys. Rev.*, **73,** 1411–12 (1948)
535. Szteinsznaider, D., *J. phys. rad.* (8)**14,** 465–72 (1953)
536. Takubo, J., and Tatekawa, M., *J. Geol. Soc. Japan*, **57,** 1–5 (1951)
537. Takubo, J., Ueda, T., and Nishimura, S., *J. Geol. Soc. Japan*, **57,** 171–75 (1951)

538. Tamburino, S. M., and Stella, A., *Notiz. mineral. siciliana e calabrese*, **4,** 38–51 (1952)
539. Tatel, H. E., *J. Geophys. Research*, **55,** 329–36 (1950)
540. Taylor, G. L., *Am. J. Sci.*, **229,** 278–91 (1935)
540a. Te Punga, M. T., *New Zealand J. Sci. Technol.*, [B]**35,** 45–48 (1953)
541. ter Haar, D., *Sci. Monthly*, **77,** 173–81 (1953)
542. Thomas, H. A., Jr., Kleinschmidt, R. S., Parker, F. L., and Bell, C. G., Jr., *J. Am. Water Works Assoc.*, **45,** 562–68 (1953)
543. Thomson, S. J., and Wardle, G., *Geochim. et Cosmochim. Acta*, **5,** 169–84 (1954)
544. Thompson, M. E., *U. S. Geol. Survey Bull, 988-D*, 45–67 (1953)
545. Tilton, G. R., *U. S. Atomic Energy Commission Document, AECD-3182*, 50 pp. (1951)
546. Tilton, G. R., Patterson, C., and Inghram, M. G., *Bull. Geol. Soc. Amer.*, **63,** 1305A (1952)
547. Tilton, G. R., Aldrich, L. T., and Inghram, M. G., *Anal. Chem.*, **26,** 894–98 (1954)
547a. Tilton, G. R., Patterson, C., Brown, H., Inghram, M., Hayden, R., Hess, D., and Larsen, E., Jr., *U. S. Atomic Energy Commission Document, AECU-2840*, 52 pp. (1954)
548. Tomlinson, R. H., and Das Gupta, A. K., *Can. J. Chem.*, **31,** 909–14 (1953)
549. Trembaczowski, E., *Ann. Univ. Mariae Sklodowska Curie (Lublin), Sect. AA*, **6,** 15–24 (1952)
550. Trembaczowski, E., *Acta. Geophys. Polon.*, **1,** 126–42 (1953)
551. Tsivoglou, E. C., Ayer, H. E., and Holaday, D. A., *Nucleonics*, **11,** (9) 40–45 (1953)
552. Ubisch, H. v., *Geol. Fören. Stockholm Förh.*, **75,** 469–89 (1953)
553. Umemoto, S., *Japan Analyst*, **2,** 201–5 (1953)
554. Umemoto, S., *Bull. Chem. Soc. Japan*, **26,** 160–61 (1953)
555. Urey, H. C., *Geochim. et Cosmochim. Acta*, **1,** 209–77 (1951)
556. Urey, H. C., *Phys. Rev.*, **88,** 248–52 (1952); **90,** 1131 (1953)
557. Urey, H. C., *The Planets*, Appendix 3 (Yale Univ. Press, New Haven, Conn., 245 pp., 1952)
558. Urey, H. C., *The Planets*, Chapt. 5 (Yale University Press, New Haven, Conn., 245 pp., 1952)
559. Urry, W. D., *Am. J. Sci.*, **246,** 689–700 (1948)
560. Urry, W. D., *Am. J. Sci.*, **247,** 257–75 (1949)
561. Urry, W. D., *Trans. Am. Geophys. Union*, **30,** 171–80 (1949)
562. Venkatasubramanian, V. S., *J. Sci. Ind. Research (India)*, **12B,** 267–70 (1953)
563. Venkatasubramanian, V. S., *Proc. Indian Acad. Sci.*, **38A,** 376–80 (1953)
564. Vinogradov, A. P., Zadorozhnyi, I. K., and Zykov, S. I., *Doklady Akad. Nauk S.S.S.R.*, **85,** 1107–10 (1952)
565. Voitkevich, G. V., *Dok. Akad. Nauk S.S.S.R.*, **77,** 461–64 (1951)
566. Volchok, H. L., and Kulp, J. L., *Bull. Geol. Soc. Amer.*, **62,** 1487A (1951)
567. Volchok, H. L., and Kulp, J. L., *Bull. Geol. Soc. Amer.*, **63,** 1386A (1952)
568. Volchok, H. L., and Kulp, J. L. (Paper presented at Am. Assoc. Adv. Sci. Meeting, Boston, Mass., December, 1953)
569. Wagner, F., Jr., *U. S. Atomic Commission Document, ANL-4490*, p. 5 (1950)
570. Waldron, E. C., Schultz, V. A., and Kohman, T. P., *Phys. Rev.*, **93,** 254–55 (1954)
571. Walling, E., *Z. Naturforsch.*, **4a,** 153 (1949)

572. Wasserburg, G. J., and Hayden, R. J., *Phys. Rev.*, **93,** 645 (1954)
573. Wasserburg, G. J., and Hayden, R. J., *Trans. Am. Geophys. Union*, **35,** 381A (1954)
574. Wasserstein, B., *Nature*, **168,** 380 (1951)
575. Waters, A. C., and Granger, H. C., *U. S. Geol. Survey Circ.*, **224,** 1–26 (1953)
576. White, M. G., *U. S. Geol. Survey, Circ.*, **195,** 1–12 (1952)
577. Wickman, F. E., *Geol. Fören. Stockholm Förh.*, **64,** 465–76 (1942)
578. Wickman, F. E., *Arkiv Kemi Mineral. Geol.*, **16**(A23), 9 pp. (1943)
579. Wickman, F. E., *J. Geol.*, **56,** 61–66 (1948)
580. Wickman, F. E., *Geochim. et Cosmochim. Acta*, **5,** 97–110 (1954)
581. Wilkening, M. H., *Phys. Rev.*, **92,** 1080A (1953)
582. Wilkening, M. H., *Nucleonics*, **10**(6), 36–39 (1952)
583. Wilson, J. T., *Trans. Am. Geophys. Union*, **31,** 101–14 (1950)
584. Wilson, J. T., *Trans. Am. Geophys. Union*, **33,** 195–203 (1952)
585. Wilson, J. T., *Trans. Am. Geophys. Union*, **33,** 444–49 (1952)
586. Winter, R. G., *Phys. Rev.*, **85,** 687 (1952)
587. Young, R. W., and Muench, O. B., *Am. J. Sci.*, **251,** 784–88 (1953)
588. Yokoyama, Y., *J. Chem. Soc. Japan, Pure Chem. Sec.*, **70,** 399–402 (1949)
589. Zeller, E. J., *Bull. Geol. Soc. Amer.*, **62,** 1493A (1951)
590. Zeller, E. J., and Zeller, D. E. N, in *Annual Progress Report to U. S. Atomic Energy Commission. Contract AT(11-1)-178, Univ. Wisconsin* (1953)
591. Zeuner, F. E., *Nature*, **166,** 756–57 (1950)
592. Zeuner, F. E., *Dating the Past* (Methuen and Co., Ltd., London, 3rd. ed., 495 pp., 1952)

AUTHOR INDEX

A

Aamodt, L., 222, 248
Abribat, M., 412
Ackerman, I. B., 368
Adams, J. B., 6
Adams, N. I., Jr., 403
Adamson, D. M., 361
Addario, M. M. I., see Indovina Addario, M. M.
Ahrens, L. H., 410, 424, 425, 426, 435, 436
Aitken, A. L., 259, 260
Aitken, K. L., 416
Aizu, K., 241
Ajzenberg, F., 18
Albert, R. D., 55
Alburger, D. E., 55, 434
Alder, F., 34
Alderman, I. M., 368, 386
Aldrich, L. T., 89, 407, 408, 417, 425, 426
Alei, E., 233
Alexander, P., 390
Alford, K. L., 287
Alinder, E., 306
Allan, D. W., 420, 439
Allen, A. J., 380
Allen, B. M., 385
Allen, J. G., 383
Allen, J. R., 338
Allison, I. S., 432
Allison, S. K., 316, 328, 331, 340, 344
Almy, G. M., 28
Alpen, E. L., 383
Alper, C., 368, 370
Alpher, R. A., 420, 440, 441, 445
Alt, H. L., 391
Alter, A., 381
Altland, P. D., 377
Altman, K. I., 368
Amaldi, E., 277
Amarasingham, C., 388
Ambrosino, G., 182
Ames, D. P., 60, 406
Amstutz, G. C., 407
Anderson, C. D., 191, 277
Anderson, E. C., 56, 382, 383, 412, 413, 429, 430, 431, 432
Anderson, H., 222, 228, 232, 233
Anderson, K., 147, 150
Anderson, R. S., 388
Andrew, E. R., 45, 46
Andrews, G. A., 382
Andrews, H. L., 390
Angell, C. E., 228, 232
Anger, H. O., 379
Annis, M., 288
Antevs, E., 431, 432
Armenteros, R., 285, 286, 287, 288, 294, 295
Arndt, R. H., 411
Arnold, J. R., 405, 406, 412, 413, 414, 429, 430, 431
Arnold, W. H., 294, 304
Aron, W. A., 316, 329
Arrhenius, G., 429
Arrol, W. J., 410, 422
Arvy, L., 364
Asaro, F., 157-90; 159, 172, 174, 175, 176, 177, 178, 183
Asayama, T., 407
Ascoli, R., 151
Ascoli Balzanelli, A., 151
Ashizawa, T., 411
Ashkin, J., 222, 227, 228, 230, 231, 232, 315, 316, 324, 328, 329, 340
Ashler, F. M., 364
Ashwell, G., 362, 365, 366
Asling, C. W., 381
Astbury, J. P., 282, 288
Aswathanarayana, U., 415
Atkin, D., 408
Audric, D. N., 430
Auerbach, S. H., 382
Augustinsson, K., 369
Aurand, K., 378, 389
Auskaps, A. A., 386
Austern, N., 15, 16, 17, 25
Austin, M. K., 379
Austing, M. E., 361
Avery, E., 106
Ayer, H. E., 411
Azcona, J. M. L., de, see López de Azcona, J. M.

B

Bacher, R. F., 168, 235, 238, 239, 244
Backus, M. M., 428
Bacq, Z. M., 368, 386, 387, 388
Baddiley, J., 386
Baglioni, T., 369
Bähnisch, I., 404
Baillouw, J., 294, 304
Baker, J. M., 34
Bakker, C. J., 58, 328, 331
Baldinger, E., 104, 108, 343
Baldwin, G. C., 23
Ball, A. F., 406
Ballentine, R., 57
Ballin, J. C., 357, 368
Balzanelli, A. A., see Ascoli Balzanelli, A.
Bane, H. N., 378
Baranovskaya, N. V., 402, 423
Barbera, L., 407
Barendsen, G. W., 429, 430
Barkas, W. H., 346
Barker, H., 429, 430
Barker, K. H., 285, 286, 287, 288
Barnard, R. D., 369
Barnes, R. G., 34, 35
Barnes, S., 228, 232
Barnothy, J., 52, 54
Barnum, C. P., 391
Baroni, G., 277
Barron, E. S. G., 354, 355, 356, 359, 361, 363, 364
Bartholomew, R. M., 52, 58, 72
Bartlett, H. H., 431
Barton, G. W., 168
Basinger, C., 383
Baskin, R., 339, 342
Bassett, H. G., 96
Bassi, P., 155
Bassin, M., 378
Bassompierre, A., 45
Bate, G. L., 416, 417, 439
Bates, D. R., 344
Batt, O. D., 361, 385
Battey, J., 174
Battell, W. J., 99
Bauminger, R., 406
Bay, Z., 54, 104, 107, 108, 145, 152
Bayly, J. G., 52, 54, 59
Beamer, W. H., 406
Beer, K. E., 407, 408
Begemann, F., 60, 406, 418
Beiser, A., 274
Beling, J. K., 174
Bell, C. G., Jr., 412
Bell, G. I., 346
Bell, P. R., 54, 58, 63
Bell, R. E., 93-110; 54, 58, 98, 100, 101, 102, 104, 105, 208
Bellamy, E. H., 34
Benfield, A. E., 434
Benjamin, B. M., 34
Bennett, L. R., 388
Benoist, P., 405
Bentley, W. C , 409
Berestetski, V. B., 211, 212
Berger, M., 272, 273, 385
Bergquist, L., 368, 384
Beringer, R., 106, 192
Bernardini, G., 235, 236, 237, 238, 239, 240, 244, 248, 262, 266
Bernas, R., 159
Bernert, T., 427

Bernstein, W., 57, 134
Beroni, E. P., 408
Berthelot, A., 168, 180, 405
Bertolini, G., 343
Bethe, H., 233, 315, 316, 324, 328, 329, 340
Bethe, H. A., 14, 16, 25, 26, 29, 168, 179, 233, 266, 317
Bethell, F. H., 366, 385
Bettoni, M., 343
Betz, H., 361, 384, 386
Bew, E., Jr., 391
Bhabha, H. J., 317, 318, 319
Bhattacharya, K. L., 381
Bianchi, A. M., 155
Bier, M., 356
Billen, D., 361
Bingemann, M. E., 368, 384
Binggeli, E., 411
Binhammer, R. T., 388
Bink, N., 380
Birch, F., 403, 434, 435, 436, 437, 438, 442, 443
Birge, R. W., 152
Birks, J. B., 111, 114, 115, 120, 122, 124, 126
Bishop, G. R., 63
Bishop, M. E., 121
Bisi, A , 343
Biswas, S., 179, 180
Bitterli, P., 430
Bittman, L., 117, 123, 127
Bizard, C., 408
Bjørnerud, E. K., 294
Black, L. D., 129
Blackett, P. M. S., 191, 277
Blair, H. A., 360, 381
Blair, J. S., 261, 262, 263
Blandin-Vial, J., 159
Blaser, J., 222, 227, 288, 232
Blatt, J. M., 14, 18
Blau, H., 412, 420, 429
Bleaney, B., 34
Bleuler, E., 52, 54, 194
Blewett, J. P., 1-12; 5
Blewett, M. H., 1
Blifford, I. H., 411
Bloch, F., 42, 320
Bloch-Frankenthal, L., 385
Block, M. M., 254, 255
Bloembergen, N., 42, 43, 44, 45, 328, 331
Blomgren, R. A., 379
Bloom, W., 351
Blount, H. C., Jr., 367
Blum, J. M., 405
Blunck, O., 341
Boag, J. W., 381
Boato, G., 424, 443
Boche, R. D., 377
Bodansky, D., 222, 228, 232
Boecker, W. S., 416, 417, 418
Boever, A., 411
Bogaardt, M., 328
Boganik, N. S., 415
Bohlander, A., 360
Bohlin, N. J. G., 379
Bohr, A., 28, 172, 175, 178, 183, 185, 332
Bohr, N., 168, 344
Boiffard, J. A., 364
Boley, F. I., 55
Bonanomi, J., 119, 133
Bond, V. P., 379, 384, 387, 388
Bonet-Maury, P., 378, 379, 388
Bonetti, A., 306
Borkowski, C. J., 53
Bortner, T E., 343
Bose, A., 381
Bose, R., 415
Bothe, W., 105
Bothwell, J., 358
Botkin, A. L., 361, 385
Bouissieres, G., 60
Bowden, B. V., 166
Bowen, E. J., 124
Bowen, I. S., 445
Bowen, T., 339
Bowers, J. Z., 392
Bowers, K. D., 34
Bowie, S. H. U., 409
Boyd, C. A., 426
Boyd, G. E., 73
Boyd, M. J., 368, 370
Brabant, J. M., 407
Brace, K. C., 390, 391
Bradt, H. L., 194
Branyan, C. E., 58
Braun, H. A., 383
Bray, P. J., 34, 45
Brecher, G., 368
Breit, G., 224
Brennan, J. T., 380
Bridge, H., 287, 288, 289, 304
Bridgforth, E. B., 367, 377, 392
Briggs, G. H., 157, 166
Brin, M., 369
Brinkman, H. C., 344
Brix, P., 36
Brobeck, W. M., 4
Broda, E., 56
Broecker, W. S., 413, 414
Brolley, J. E., Jr., 77
Broniewski, A., 169
Brooks, R. E., 355
Brosi, A. R., 58, 62
Brower, D., 63
Brown, F., 52, 58, 68, 72, 73
Brown, H., 90, 403, 407, 408, 410, 419, 420, 424, 426, 435, 436, 441, 442, 443, 446
Brown, J. H., Jr., 408
Brown, K. L., 13
Brown, M. B., 387
Brown, R., 55, 58
Brown, R. H., 277
Brown, R. M., 45
Brown, S., 216
Brown, S. C., 56, 57, 202, 216
Brown, W. M. C., see Court Brown, W. M.
Brownell, G. L., 58, 63
Broyles, C. D., 62
Brucer, M., 382
Brueckner, K., 222, 224, 225, 227, 229, 231, 241, 248, 264, 266
Brues, A M., 368, 389
Brummit, H., 382
Bruner, H. D., 382
Bube, R. H., 136
Buchanam, J. S., 294, 302, 310
Buchanan, D. J., 367, 377, 388, 392
Bucher, W. H., 440, 443
Buck, W. L., 129, 131
Buckaloo, G. W., 390
Buddington, W. G., 360
Budini, P., 332, 337
Budy, A. M., 378
Buffa, P., 358
Bullard, E. C., 420, 436, 437, 439, 443
Bunting, C. H., 367
Burch, P. R., 383, 403
Burg, C., 367, 368
Burke, A. W., Jr., 388
Burke, B. F., 34
Burke, W. H., Jr., 429, 430
Burkhardt, J. L., 20, 21, 27
Burling, R. L., 415, 419, 440, 445
Burn, J. H., 369, 370
Burnett, W. T., Jr., 388
Burr, J. G., Jr., 56
Burtt, B. P., 60
Burwell, J. R., 285, 286, 287, 293
Busch, H., 358
Bush, S. G., 383
Butler, C. C., 285, 286, 287, 288, 308
Butler, C. L., 370
Butler, W. A., 28
Buttlar, H. v., 406, 418, 428
Byers, S. O., 355

C

Caceres, E., 389
Cachon, A., 285, 288
Cahen, L., 415
Calvery, H. O., 383
Camerini, U., 277
Camilla, A., 63
Canter, H. Y., 386
Careri, G., 424, 443
Carlson, B. C., 207, 319
Carothers, E. L., 382
Carr, D. R., 421
Carter, C. E., 366
Carter, R. E., 380

Carter, R. S., 340
Carttar, M. S., 362, 366, 378, 379, 391
Cartwright, W. F., 250, 254, 255
Carver, J. H., 17
Carver, T. R., 38
Casarett, G W., 382
Cassen, B., 383
Cassidy, J., 58
Cassidy, J. M., 54, 58, 63
Castagnoli, C., 277
Castanera, T. J., 384
Caswell, R. S., 53, 58, 61, 407
Catcheside, D. G., 351
Cavallo, L., 53, 58, 59, 60
Cavanaugh, P. E., 54, 58, 62, 63
Cebul, F. A., 383
Cerenkov, P. A., 141
Chackett, K. F., 410, 422, 442
Chadwick, J., 191
Chakreborty, K. P., 381
Chambers, F. W., 377
Chanutin, A., 363, 364, 368, 370
Chapman, W. H., 368
Charlesby, A., 390
Charpak, G., 404
Chase, H. B., 362
Chastain, S. M., 388
Chastel, R., 13
Cheever, F. S., 386
Cheng, A. L. S., 368, 384
Chetham-Strode, A., 159
Chevallier, A., 367, 368
Chew, G., 244, 261, 262, 263, 264, 266
Childs, R., 391
Childs, W. J., 58
Chilton, A. B., 331
Chin, P. H., 386
Choppin, G. R., 159, 169
Christaldi, P. S., 96
Christenberry, K. W., 380
Christensen, N., 392
Christensen, W. R., 390
Christian, E. J. B., 368, 389
Chu, T. L., 46
Church, E. L., 174, 175
Cigna, A., 412
Clark, D. D., 342
Clark, D. L., 250
Clark, F. L., 402, 403
Clark, J. W., 378, 379, 380
Clark, L. B., Sr., 52
Clark, R. K., 53, 54
Clarke, G., 361
Cleland, M. R., 108, 145, 152
Clement, J., 129
Coates, 286, 287
Cochran, K. W., 357, 358, 359, 362, 363, 364, 365, 366
Cogan, D. G., 380
Cohen, B. L., 77
Cohen, S. G., 406
Cohen, V. W., 34, 36
Cohn, O. H., 285, 286, 287, 293
Cohn, R. A., 61
Cohn, S. H., 364, 383
Cole, L. J., 387, 388
Colgate, S. A., 55
Collier, D., 431
Collins, C. B., 70, 75, 416, 417, 420, 421, 426, 439, 440, 441, 445
Collins, E. R., 166
Collins, G. B., 142
Colmery, B. H., Jr., 382
Comar, C. L., 378
Comsa, J., 387
Conard, R. A., 369
Condon, E. U., 157, 179
Congdon, C., 377
Coniglio, G., 367
Coniglio, J. C., 392
Conway, B. E., 388, 390
Cook, C. J., 347
Cook, G. B., 73
Cooke, H. B. S., 415
Cool, R., 227, 228, 229, 232
Cooley, R. S., 415
Coon, J. M., 377
Cooper, B. M., 382
Cooper, J. A. D., 391
Cooper, J. N., 331
Cooper, M., 409
Cooper, W. A., 294, 302, 310
Copp, D. H., 383
Corba, J. P. Y., 61
Corben, H. C., 191-218; 317
Cork, J. M., 58
Cormack, A. M., 434
Cornatzer, W. E., 368
Corson, D. R., 316
Cortini, G., 277
Coryell, C. D., 69, 72, 73, 74, 75
Costello, M. J., 362, 366
Cotter, G. J., 365, 388
Cotton, W. k., 383
Coulter, E. P., 362, 366
Coulter, M. P., 386
Courant, E. D., 5, 28
Courant, H., 288, 289, 304
Court Brown, W. M., 379, 384, 390
Cowan, C. E., 207
Cowan, C. L., Jr., 383
Cowan, F. P., 3
Cowan, W. E., 288
Cox, J. T., 34
Cox, R. S., Jr., 378, 379
Craig, D. H., 54
Craig, H., 431
Crane, H. R., 429, 430, 434
Cranna, N. G., 44
Crathorn, A. R., 429, 430
Craven, J. H., 53
Crawford, F. S., 249, 250
Critchfield, C. L., 18, 179
Crussard, J., 227
Culpepper, N., 58
Cumming, G. L., 420, 439
Cummings, O. K., 370
Cunningham, B. B., 402
Curatolo, M., 407
Curie, M., 406
Curran, S. C., 111, 343, 404, 405, 406, 415
Curtis, M. L., 406
Curtiss, L. F., 55, 56, 57, 407

D

Daggs, V. M., 383
Dahanayake, C., 306, 310
Dale, W. M., 354
Dalgarno, A., 344
Dalitz, R. H., 282, 283
Dalton, J. C., 409, 410, 422, 423, 435
Damon, P. E., 411, 412, 420, 421, 440
Dancoff, S , 263
Dandl, R. A., 58
Daniels, F., 426
Daniels, M., 390
Darby, W. J., 367, 377, 388, 392
Das Gupta, A. K., 425, 426
Das Gupta, N. N., 381
Daudel, R., 405
Dauer, M., 377
Dauvillier, A., 439
Davenport, V., 392
David, G. L., 89
Davidson, C. F., 407, 408
Davis, C. W., 426
Davis, G. L., 408, 410, 417, 425, 426, 435
Davis, R. C., 58
Davison, J. P., 368
Davisson, C M., 55
Dawson, K. B., 411
Day, A. E., 75
Day, P. L., 357
Dayhoff, E. S., 46
Dayton, B., 289, 304
de Azcona, J. M. L., see López de Azcona, J. M.,
DeBenedetti, S., 191-218; 104, 174, 191, 201, 202, 206, 207, 208, 209
Debierne, A., 406
Debley, V., 388
Dechamps, G., 386
Decker, A. B., 368
Deevey, E. S., Jr., 412, 420, 429, 430, 431, 432
DeGeer, E. H., 431
Dehmelt, H. G., 34, 36, 45
de Hoffmann, F., see Hoffmann, F. de
Deighton, M. O., 96, 97, 98,

101
de Jager, C., see Jager C. de
de Laboulaye,H., see Laboulaye, H. de
Delaney, C. F. G., 408, 422
de la Ripelle, M.F., see Fabre de la Ripelle, M.
Del Buono, G., 368
Dellaporta, N., 306
del Rio, C.S., see Rio,C.S. del
Demay, A., 407, 417
Demos, P. T., 77
Denson, J. R., 360, 391, 392
De Pasquali, G., 134
der Mateosian, E., see Mateosian, E. der
Deroin, J., 359, 365
DeShalit, A., 54, 172
DeStaebler, H. C., Jr., 289, 304, 308
Detrick, L. E., 388
Deuel, H. J., Jr., 368, 384
Deutsch, M., 54, 93, 192, 199, 202, 206, 207, 214, 216
Deutschmann, M., 287
Devaney, J. J., 179
de Vries, H., see Vries, H. de
Diamond, H., 159
Dicke, R. H., 143, 152
Dickinson, W. C., 77
Dickman, S., 354, 355, 356, 363, 364
Dieckman, C., 379
Diethorn, W. S., 429, 430
Dietrich, C. F., 54
Dilworth, C., 271-314; 220, 305
Dinning, J. S., 357
Dirac, P. A. M., 195
Dismuke, N., 70
Dixon, D., 404, 405, 406
Dixon, F. J., 386
Doak, J. B., 425
Dobson, R. L., 351
Doernbach, C., 366
Donaldson, D. M., 386
Douglas, D. L., 412, 429, 430
Doull, J., 357, 358, 359, 362, 363, 364, 366, 370, 377, 391
Dowdy, A. H., 390
Doyle, W. L., 365
Dreisler, K. K., 380
Drisko, R. M., 196, 197
Drost-Hansen, W., 72
DuBois, D. P., 351-76; 357, 358, 359, 362, 363, 364, 365, 366, 367, 377, 391, 392
Dudley, A., 69
Duerden, T., 146
Dulit, E., 214
DuLong, W. A., 59
DuMond, J. W. M., 55, 58, 62, 192, 207
Dunbar, D. N. F., 331
Dunjic, A., 387
Dunlavey, D. C., 159, 170, 405, 414
Dunworth, J. V., 52
Duplan, J. F., 384
Dupouy, G., 166
Durbin, R., 222, 250
Dyson, F. J., 265, 266

E

Eades, R. G., 45
Easton, W. C., 406
Eby, F. S., 126, 127, 134
Eckelmann, W. R., 412, 416, 417, 418, 429, 432, 439
Edwards, R. R., 69, 73, 74, 75, 411, 412, 414
Efner, J. A., 367, 377, 392
Ehrenberg, H. F., 416, 439
Eichel, H. J., 368, 370
Eisberg, R. M., 342
Eisenbud, M., 412
Eisinger, J. T., 36
Eklund, E., 404
Eklund, S., 404
Eldjarn, L., 386
Eldred, B., 377
Eldred, E., 377
Ellinger, F., 367
Ellinwood, L. E., 380
Elliot, J. C., 121, 122, 123, 124
Elliott, L. G., 175
Elliott, W. B., 358
Ellis, M. E., 387, 388
Elsasser, W., 168
Elsken, R. H., 46
Elson, L. A., 390
Ely, J. O., 359, 365, 367
Emmons, R. C., 407
Endt, P. M., 403, 434
Enerson, D. M., 383
Engelkemeir, A. G., 56, 64
Engelkemeir, D. W., 71, 72
Engelstad, O., 368
Entenman, C., 368, 391
Epstein, H. T., 390
Erichsen, L. von, 421
Ericson, D. B., 428
Ermolin, G. M., 402, 423
Esplin, D. W., 386
Evans, R. D., 51, 55, 57, 60, 407
Evans, T. C., 361
Eve, A. S., 406
Everett, J. W., 369
Exner, C., 407

F

Fabre, de la Ripelle, M., 405
Fabri, E., 282, 283
Fafarman, A., 412
Fairbairn, H. W., 427, 435
Fairhall, A. W., 77
Fairstein, E., 62
Faltings, V., 413, 414, 429, 430
Fan, C.-Y., 58, 59, 62
Fano, L., 52, 61, 62
Fano, U., 55
Faraggi, H., 405
Farquhar, R. M., 416, 417 420, 421, 423, 426, 439, 440, 441, 445
Faul, H., 401, 407, 412, 415
Fechter, H. R., 20
Feely, H. W., 412, 429
Feenberg, E., 25, 224
Feiner, F., 222, 227, 228, 232
Feinstein, R. N., 368, 370, 388
Feister, I., 55
Feld, B. T., 29, 174, 235
Feldman, C., 415
Ferentz, M., 23, 24
Ferguson, J. H., 387
Fergusson, G. J., 429
Ferkel, R. L., 364
Fermi, E., 210, 222, 228, 232, 233, 241, 242, 266, 332, 347, 434
Ferradini, C., 60
Ferrell, B. L., 77
Ferrell, R. A., 211, 212
Festa, C., 441
Feynman, R. P., 261, 264
Fields, P. R., 159
Fields, T. H., 250
Fillmore, P. G., 380
Finerty, J. C., 388
Finkel, M. P., 381
Finnegan, C., 386
Fireman, E. L., 406, 414, 433
Fischer, J., 99, 105, 106
Fischer, M. A., 362, 366
Fischer, P., 386
Fishler, M. C., 383, 387
Fishman, M., 386
Fiskell, J. G. A., 59
Fitch, V. L., 20
Fleischer, M., 401, 407, 429
Fleming, E. H., Jr., 402
Fleming, J. R., 338
Fleming, W. H., 76
Flint, J. S., 388
Flint, R. F., 430, 431, 432
Flinta, J., 404
Flood, V., 361
Florencio, W., 407, 415
Florsheim, W. H., 366
Flowers, B. H., 172
Flynn, K. F., 73, 75
Foldvari, A., 407
Foldy, L. L., 15, 265
Fonda, G. R., 131
Fong, P., 78
Foote, R. S., 14
Ford, G. P., 69, 70, 74, 76
Ford, K. W , 172, 185
Forro, M., 52, 54
Forssberg, A., 355, 361

Forstat, H., 342
Förster, T., 124
Fournier, G., 168
Fowler, P. H., 272, 277, 310
Fowler, W. B., 232, 287, 308
Fox, B. W., 383
Fox, J. G., 250
Fox, M., 390
Franchi, M., 388
Francis, J. E., 58
Franck, J., 132
Francois, P. E., 306, 310
Frank, I., 141
Franke, H. W., 431
Franseen, C. C., 364
Frauenfelder, H., 183
Frazer, J. S., 174
Fred, M., 34, 186
Freedman, A. J., 429, 430
Freedman, M. S., 69, 72
Freeman, J. R., 416
Fremlin, J. H., 406
Frenkel, J., 124, 132
Fretter, W. B., 277
Frey, H. B., 126
Fricke, H., 354
Friedell, H. L., 382, 387, 390
Friedlander, M. W., 308
Friedman, A. M., 159
Friedman, L., 57
Friesen, S. von, 306
Fritze, K., 423
Frohlich, H., 347
Fromm, E., 432
Frondel, C., 409
Frost, R. H., 343
Fry, D. W., 9
Fry, W. F., 274
Fryer, G., 405
Fujii, S., 264
Fujimoto, Y., 306, 310
Fulbright, H. W., 406
Fuller, E. G., 13, 28
Fulton, J. D., 386
Fulton, T., 212
Funi, F. G., 193, 197, 213
Funt, B. L., 129
Furberg, S. E., 64
Furchner, J., 382
Furst, M., 114, 117, 123, 127, 128
Furth, F. W., 386
Furth, J., 351, 377, 380, 385

G

Gabe, M., 364
Gabrielli, E. R., 386
Galbraith, W., 76, 151
Gammel, J., 263
Gamow, G., 157, 179, 439
Garlick, G. F. J., 111, 121, 131
Garrigue, H., 411, 412
Garrison, W. M., 381
Garstang, R. H., 344
Garwin, R. L., 101, 104, 207, 209
Gasvoda, B., 361
Gatti, E., 54
Gauthé, B., 405
Gayther, D. B., 287
Geiger, H., 406
Geiss, J., 420, 439, 440, 441
Gell-Mann, M., 219-70; 18, 23, 24, 266, 267
Genaud, P. E., 386
Gentner, W., 422, 423
Gérardin, L., 96
Gergel, M. V., 414
Gerhart, J. B., 207
Gerling, E. K., 402, 423, 424
Germanogli, E., 54
Geslin, M., 407
Getting, I. A., 144, 152
Ghiorso, A., 159, 167, 168, 169, 170, 179, 180, 186, 187, 402, 405, 406
Ghormley, J. A., 63, 64, 406
Giletti, B. J., 416
Gillespie, J., 415
Gillette, R. H., 137
Gilmore, J. S., 73
Ginnings, D. C., 406
Ginzton, E. L., 94
Gjessing, E. C., 368
Glass, J. J., 415, 417
Glass, R. A., 159, 167, 169, 170
Gleiser, C. A., 377
Glendenin, L. E., 69-80; 69, 71, 73, 74, 75, 76, 89
Glenn, W. E., 168
Glick, C., 391
Glicksman, M., 233
Glueckauf, E., 168
Godbole, R. D., 29
Godwin, H., 431
Goebel, K., 422, 423
Goeckerman, R. A., 74
Goertzel, G. H., 54
Gofman, J. W., 368
Goldberg, E. D., 420
Goldberger, M., 172, 175, 266, 267
Goldblatt, M., 406
Goldemberg, J., 13, 22, 23, 26, 28
Golden, J., 409, 410, 422, 435
Goldhaber, M., 23
Goldschmidt-Clermont, Y., 222, 235, 240, 272
Goldsmith, G. J., 52, 54
Goldstein, A., 69
Goldstein, M. J., 368
Goldwasser, E., 235, 236 237, 238, 239, 240, 248, 262, 335
Gomori, G., 364
Gong, J. K., 364, 383
Gonshery, L., 386
Goodman, C., 407
Goodman, R. D., 359, 392
Goodner, C. J., 392
Gordon, L. E., 386
Gordy, W., 34
Gorfinkle, L. G., 424, 425
Gorman, J., 222, 227, 228, 232
Gosh, S. K., 340
Gott, G. B., 408, 409, 411, 412
Gottfried, D., 419
Gottstein, K., 272, 273
Gould, B. S., 364
Grabherr, W., 409
Graham, R. L., 54, 58, 70, 75, 101, 102, 104, 105, 175, 208
Grahn, D., 377
Grande, P., 429, 430
Granger, H. C., 408
Gray, E. J., 360, 391, 392
Gray, E. P., 16
Gray, G. W., 445
Gray, I., 386
Gray, J. L., 360, 391, 392
Gray, L. H., 53, 63, 381, 385
Gray, P. R., 414
Gray, T. S., 126
Greenberg, J. S., 99
Greenman, V., 386
Greer, B. A., 75
Gregory, B., 293, 294, 295
Gregory, B. P., 286
Grenan, M. M., 360, 386
Griffin, J. B., 429
Griffiths, M., 64
Griffiths, G. M., 207
Grim, W. M., 126
Griswold, T. W., 38
Gros, C. M., 368, 387, 391
Gross, M. S., 412, 420, 429, 431
Grosse, A. V., 413, 414, 430
Grosse, H., 430
Grover, J. R., 174
Grummitt, W. E., 69
Gugelot, P. C., 136
Guillot, M., 174, 177
Guimaraes, D., 415
Gunst, S. B., 191
Guntz, A. A., 408
Gupta, A. K. D., see Das Gupta, A. K.
Gupta, N. N. D., see Das Gupta, N. N.
Gupta, R. L. S., see Sen Gupta, R. L.
Gurney, R. W., 157, 179
Gustafson, G. E., 368, 383, 386
Gustafson, P. F., 383
Gutenberg, B., 434, 435, 436, 437, 438
Guth, E., 17

Gutowsky, H. S., 34, 35, 45, 46

H

Haar, D. ter, 445
Hackett, P. L., 383
Haeberli, W., 343
Haenny, C., 411
Hadley, J., 222, 248
Hahn, B., 136
Hahn, O., 69, 406
Hahn, P. F., 51, 60, 382
Hahne, H. J., 386
Halbach, K., 34
Halban, H., 63
Hale, W. M., 386
Haley, T. J., 378, 388
Halicki, B., 430
Hall, H., 332, 333
Hall, J. J., 355
Halliday, D., 206, 214, 215
Halloway, A. F., 58, 59, 62
Halpern, I., 77, 174
Halpern, J., 13, 17, 18, 22, 23, 26
Halpern, O., 332, 333
Hamill, W. H., 56, 69
Hamilton, J. G., 381, 383
Hammermesh, B., 18
Hammond, C. W., 386
Handloser, J. S., 3
Hanna, G. C., 76
Hanna, R. C., 194
Hannan, R. S., 388
Hansen, R. A., 388
Hanson, A. O., 17, 319, 335
Harbottle, G., 61
Hardeman, G. E. G., 45
Hardwick, W. H., 72
Hardy, W. A., 34
Harel, J., 382
Harley, J. H., 411, 412
Harrick, N. J., 34, 35
Harrington, H., 367
Harris, D. R., 294, 304
Harris, G. G., 308
Harris, J. C., 331
Harris, P. S., 380
Harrison, F. B., 112, 114, 117, 123, 128, 129, 383
Harrison, H. C., 419
Harriss, E. B., 390
Harshaw, J. A., 133, 134
Hart, E. J., 354
Hart, H., 383
Harteck, P., 413, 414
Harvey, B. G., 76, 159, 169
Hase, H., 379
Hasegawa, A., 361
Haskins, J. R., 58
Hasted, J. B., 344
Hastings, J. M., 414, 446
Hataye, I., 412
Havens, W. W., Jr., 254, 255
Hawkings, R. C., 53, 56, 57, 58, 72
Haxel, O., 404, 406, 412
Hay, J. O., 133
Hayase, K., 408
Hayden, R., 71, 73, 75, 89, 90, 403, 404, 406, 414, 419, 423
Hayes, F. N., 129, 383, 412, 429, 430
Hayes, T. L., 368
Haynes, S. K., 62
Hayward, E., 13, 28
Hazen, W. E., 343
Hecht, F., 408
Hecht, H., 385
Hedgran, A., 62, 63, 192, 207
Hée, A., 410, 411
Heglin, J., 378, 388
Heintze, J., 406
Heinz, O., 274
Heisler, C., 390
Heitler, W., 191, 196, 224
Henderson, J. E., 142
Hendley, D. D , 370
Henkel, D. T., 388
Henkel, R. L., 77
Henley, E. M., 228, 259, 260
Herbert, F. J., 391, 392
Hereford, F. L., 194
Herman, R. C., 420, 440, 441, 445
Herve, A., 386, 387, 388
Herzog, L. F., 425, 442
Hess, D. C., 71, 75, 90, 403, 408, 410, 419, 424
Hess, D. N., 56
Heuse, O., 378, 389
Heusghem, J., 368
Hevesy, G., 361
Hewett, D. F., 415, 417
Hewitt, J. E., 368
Hewlett, W. R., 94
Hey, M. H., 410, 422
Heyningen, R. van, 381
Hibbard, L. U., 3
Hiby, J., 423
Hickman, J., 362, 365, 366
Hieke-Merlin, O., 407, 408
Higgins, G. H., 159, 169
Highman, B., 367, 377
Hildebrand, R. H., 145, 243, 251, 254, 255
Hilfinger, M. F., Jr., 387
Hill, D. H., 28
Hill, D. L., 78, 185
Hill, J. W., 409, 411
Hill, R. D., 62
Hincks, E. P., 405
Hine, M. G. N., 6
Hinman, G., 58, 63
Hirsch, G. M., 381
Hirschberg, D., 305
Hirschberg, L., 305
Hochman, A., 385
Hodson, A. L., 294, 304
Hoffman, B. G., 316, 329
Hoffman, D., 379
Hoffmann, F. de, 233, 266
Hofstadter, R., 20, 133, 134, 136, 150, 339, 342
Holaday, D. A., 411
Hollaender, A., 361
Holland, H. D., 411, 426, 428
Hollander, J. M., 159
Holm, C. H., 46
Holmes, A., 402, 414, 416, 417, 420, 426, 439, 440, 445
Holmes, B. E., 367
Holyk, W. K., 410, 425, 435, 436
Hopkins, J. I., 125
Horie, H., 172
Hornbostel, J., 194
Horne, E. T., 409
Horsley, R., 75
Horton, W. H., 96
Hough, J. L., 428
Houtermans, F. G., 53, 60, 404, 405, 406, 418, 420, 428, 434, 439, 440, 441, 446
Howell, W. D., 52, 58, 68, 99
Howland, B., 102
Howland, J. J., 168
Howland, J. W., 386
Hoyt, H. C., 62, 192
Hubbard, E. L., 328
Hubenet, H., 406
Huber, O., 54
Huber, P., 62, 104, 108, 343
Hudson, A., 339, 342
Hudson, G. W., 367, 377, 388, 392
Hugget, R. W., 285, 286, 287
Hughes, D. E., 387
Hughes, J. H., 408
Hughes, V., 209, 214
Huizenga, J. R., 70, 159, 169
Hulet, E. K., 159
Humbel, F., 54
Hummel, J. P., 159
Hunter, R. F., 56, 57
Hurley, P. M., 421, 426, 427, 428, 435
Hursh, F. B., 361
Hursh, J. B., 383
Hurst, G. S., 343
Huseby, R. A., 391
Huster, E., 404
Hutchinson, G. E., 412, 431
Hutton, C. O., 409
Huybrechts, M., 332
Hyams, B. D., 146
Hyde, E. K., 159, 168, 406
Hyde, H. I., 411
Hylleraas, E., 192
Hyndman, D., 46

I

Ibamoto, H., 46
Igo, G. J., 342
Iloff, E., 254, 255
Indovina Addario, M. M., 470
Ingerson, E., 403, 407, 408

Ingham, W. N., 407
Inghram, M. G., 81-92; 56, 69, 71, 73, 75, 85, 89, 90, 403, 406, 407, 408, 410, 414, 417, 419, 424, 435, 441
Ingle, D. J., 385
Ingols, R. S., 382
Iredale, P., 306, 310
Isaac, N., 406, 418, 427
Ishimori, I., 411, 412
Ishimori, T., 412
Israel, H., 411
Itoh, J., 46
Ivanenko, D. D., 405
Iverson, J., 431, 432
Ivy, A. C., 383
Iwadare, J., 264
Iwasaki, I., 411, 412
Iwatsuru, R., 363

J

Jackson, E., 360
Jackson, H. G., 159
Jackson, J. A., 117, 123
Jackson, J. D., 344
Jacobi, R. B., 410, 422
Jacobs, T., 415
Jacoe, P. W., 411
Jacques, R., 405
Jacquez, J. A., 377
Jaffe, G., 408
Jager, C. de, 406
Jain, P. L., 46
Jankus, V. Z., 318
Jarovoy, M., 410
Jarrett, H. S., 46
Jasberg, J. H., 94, 96
Jastrow, R., 264
Jauch, J. M., 54, 63
Jean, M., 405
Jeffries, C. D., 34
Jeffreys, H., 434, 435, 436, 438, 439
Jelley, J. V., 144, 151, 152, 156
Jenks, G. H., 54, 63, 64, 406
Jennings, F. L., 368
Jensen, E. N., 59
Jensen, F., 423
Jensen, H., 360, 361, 391
Jensen, J. H. D., 23
Jentschke, W., 183
Jentschke, W. K., 126, 127, 134
Jesse, W. P., 342, 343
Johansson, S., 55, 63
Johns, M. W., 175
Johnson, F., 430, 431
Johnson, F. B., 381
Johnson, V., 166
Johnston, W. M., 413
Joliot, F., 192
Jolliffe, A. W., 415
Jones, D. C., 384
Jones, E., Jr., 347
Jones, E. A. W., 403, 423
Jones, G. A., 18
Jones, G. M. D. B., 340
Jones, H. B., 367, 368, 387
Jones, J. W., 406
Jones, L. W., 13, 26
Jones, W. H., 77
Jones, W. M., 56, 63, 406
Jonker, J. L. H., 96
Jordan, D. L., 378, 379
Jordan, P., 405
Jordan, W. H., 58, 111
Jorgensen, T., Jr., 347
Jugenburg, A., 360
Jung, K., 438

K

Kahn, D., 331
Kaiser, E. P., 408
Kalkstein, M. I., 404, 406
Kallmann, H., 93, 114, 117, 118, 123, 124, 125, 127, 128, 136
Kallmann, H. E., 96
Kalnitsky, G., 358
Kamada, M., 412
Kanada, T., 46
Kane, J. A., 250
Kantz, A., 150
Kaplan, H. S., 387
Kaplan, J., 179, 180
Kaplan, W. D., 386
Karlik, B., 168
Karnofsky, D. A., 377
Karplus, R., 211, 212
Karraker, D. G., 168
Karzmark, C. J., 285, 286, 287, 293
Kastner, J., 58
Katcoff, S., 73, 74, 414, 446
Katz, L., 13, 22, 23, 26, 28
Katzman, J., 412
Kaufman, S., 413, 414, 432, 433
Kaufmann, B. N., 391
Kawin, B., 383
Kaykin, P. N., 65
Kearns, M. M., 410, 435, 436
Keck, J., 17, 235, 238, 239, 244
Keene, J. P., 344, 345, 346
Keevil, N. B., 407, 408, 419
Keinberger, C. A., 402
Keith, G. K., 357
Keller, R. N., 71
Keller, W. D., 408
Kelley, G. G., 58
Kelly, L. C., 96
Kelly, L. S., 367, 387, 391
Kemmer, N., 224, 260
Kemmerich, M., 404
Kent, D. C., 27
Kepp, R. K., 379
Kerman, H. D., 382
Kerr, P. F., 417
Kersten, H., 355
Ketelle, B. H., 58, 62
Kikuchi, C., 34, 36
Kim, Y. B., 285, 286, 287, 293
Kimball, A. W., Jr., 378
Kimball, C., 18
Kimball, R. F., 351
Kimeldorf, D. J., 384
Kimura, K., 408, 411, 415
Kip, A. F., 38, 46
Kirby, H. W., 406
Kiriyama, R., 46
Kirkaldy, J. S., 99
Kirschner, L. B., 360
Kirshenbaum, A. D., 413, 414, 430
Kisieleski, W. E., 364, 381
Kistler, K., 383
Kittel, C., 38, 46
Kjellberg, G., 429
Kleiber, G. S., 23
Klein, A., 211, 212
Klein, D. J., 62, 192
Kleinschmidt, R. S., 412
Klemperer, O., 192
Klinkenberg, F. A., 405
Kluyver, J. C., 403, 434
Knight, W. D., 39
Kniseley, R. M., 382
Koch, H. W., 14
Koch, J., 72
Koch, R., 360
Koczy, F. F., 429, 441
Koechlin, Y., 129
Koenigh, V. L., 390
Kofoed-Hansen, O., 72
Kohman, T. P., 401-62; 60 158, 168, 170, 401, 404, 405, 406, 414, 418, 426, 429, 430, 433, 439, 446
Kohn, H. I., 367
Kohn, W., 344
Kojima, S., 45, 46
Koletsky, S., 368, 386
Koltzman, R. B., 59
Konneker, W. R., 207
Kordik, P., 369, 370
Korson, R., 361, 385
Kory, R. C., 382
Koski, W. S., 123, 129
Koudijs, B., 328
Kovarik, A. F., 403
Kowitz, G., 385
Kramer, B., 114
Kramers, H. A., 344
Kraushaar, J. J., 175
Kraybill, H. L., 412, 431
Krebs, A., 388, 391
Kremers, H. C., 133, 134
Kretchmar, A. L., 385
Kristensen, P., 72
Kristiansson, K., 306
Kröger, F., 131, 137
Kroll, N., 265
Kröll, V. S., 427
Kruger, P. G., 126, 127

Kryder, G. D., 368, 384
Kulp, J. L., 411, 412, 413, 414, 416, 417, 418, 421, 426, 428, 429, 430, 432, 439, 442
Kunkel, H. O., 357, 370
Kupperian, J. E., Jr., 340, 342
Kurbatov, J. D., 58
Kuroda, P. K., 408, 411, 412, 414
Kusaka, R., 46
Kwiatkowski, H., 369

L

Laboulaye, H. de, 73
Lacassagne, A., 386
Lagarrigue, A., 293, 294, 295
Lal, D., 306
Lamarche, G., 44
Lamb, W. E., 46
Lambert, G., 387
Lamerton, L. F., 390
Lancker, J. van, 387, 388
Landahl, H. D., 361
Landau, L., 321, 341
Landau, L. D., 193, 211, 212
Landau, P., 385
Landy, J. J., 383
Lang, A. H., 416, 421
Lang, G., 63
Lang, L. G., 58
Langendorff, H., 384
Langer, L. M., 63
Langham, W. H., 380
Larsen, E., 90
Larsen, E. S., 408
Larsen, E. S., Jr., 419
Larson, Q. V., 73
Lartigue, O., 359, 360
Laszlo, D., 383
Laughlin, J. S., 379
Lauritsen, T., 18
Lavik, E. S., 367
Lavik, P. S., 390
Lawley, P. D., 124
Lawrence, J. H., 351, 379
Lawrence, J. S., 390
Lawson, J. D., 6
Lawson, J. L., 23
Lawson, J. S., Jr., 183
Lea, D. E., 353, 354
Lea, R., 232
Leamer, R., 63
Lebedev, V., 405
LeBihan, H., 386
Leblond, C. P., 367
Lecoin, M., 405
Lecolazet, R., 411
LeComte, J., 386
Le Couteur, K. J., 422
Leighton, R. B., 287, 288, 294
Leinfelder, P. J., 381
Leipuner, L., 202, 210
Leisegang, S., 341
Leite Lopes, J., 261, 264
Leland, W. T., 402, 417
LeMay, M., 362
Leonard, S., 222
Leonards, J. R., 390
Lepape, A., 407
Leprince-Ringuet, L., 277, 293, 294, 295
Lerner, S. R., 368
Leschi, J., 385
Leverenz, H. W., 131
Levi, H., 429, 430, 431, 432
Levine, C. A., 406, 414
Levinger, J. S., 13-32; 25, 26, 27, 29
Levinthal, C., 21
Levy, B., 360, 377, 385, 392
Levy, R. A., 46
Lew, H., 34, 35, 36
Lewis, A. E , 359, 388
Lewis, G. M., 404
Lewis, W. B., 166
Libby, W. F., 56, 69, 401, 405, 406, 412, 413, 414, 429, 430, 431, 432, 433
Lidofsky, L., 61
Liebecq, C., 358
Liebson, S. H., 121, 122, 123, 124
Lind, D. A., 55, 58, 62, 63, 207
Lind, S. C., 406
Lindeman, H., 411
Lindenbaum, S. J., 147, 227, 228, 232
Lindhard, J., 327, 330
Linn, J. G., Jr., 380
Lipmann, F., 386
Littauer, R. M., 17
Little, W. A., 115, 120, 122
Littman, A., 383
Livingston, M. S., 5, 10
Livingston, R., 34, 45
Loar, H., 222, 250
Lockett, E. E., 58, 59, 60, 61, 62, 63, 406
Lockhart, L. B., Jr., 411
Loefer, J. B., 388
Lofgren, E. J., 4
Logan, M. A., 355
London, F., 124
Long, J. V. P., 430
Longmire, C., 16
Lopes, J. L., see Leite Lopes, J.
López de Azcona, J. M., 415
Lord, J., 232
Lord, J. J., 338
Lorenz, E., 377
Lorenz, W., 384
Lotz, V., 382
Lourau, M., 359, 360, 391
Lovberg, R. H., 134, 135
Love, J. D., 408
Love, S. K., 411
Low-Beer, A., 367
Lowell, W. R., 408
Ludewig, S., 363, 364, 370
Lundby, A., 122, 142
Lusky, L. M., 383
Lutwak-Mann, C., 367
Lynen, F., 386
Lyon, M. F., 386
Lyon, W. S., 64

M

Mabumoto, S., 46
McCall, D. W., 34, 45
McCarthy, J. A., 406
McClure, R. E., 35
McCormick, G. H., 77
McCormick, W. G., 388
McCrady, E., 420, 440, 441
McCulloch, E., 388
McDaniel, B. D., 29
McDaniel, E. W., 429
McDonald, M. R., 388
McGarvey, B. R., 45
McGrath, J., 391
Macgregor, A. M., 424, 425
MacGregor, M. H., 404
McIntyre, J. A., 20, 134
MacIntyre, W. J., 138
McKee, R. W., 360
McKenzie, C. D., 166
MacKenzie, K. R., 328
Macklin, P., 61
McLaughlin, D. B., 437
McLean, F. C., 378
McLean, R., 364
McLellan, W. M., 382
McLernon, F., 108, 145, 152
MacLusky, G. J. R., 96, 97, 98, 101
McNair, A., 405, 406
McNally, J. R., Jr., 185
Macnamara, J., 70, 75, 76
Madansky, E., 107
Madansky, L., 174, 227, 228, 229, 232
Madsen, C. B., 331
Maeder, D., 63
Magnusson, L. B., 159, 169
Mahler, R. F., 379, 390
Mahmoud, H. M., 259, 260
Maisin, H., 387
Maisin, J., 387
Major, J. K., 64
Maletskos, C. J., 58, 63
Malling, L., 35
Mandart, M., 387
Mandel, P., 368, 391
Manduchi, C., 155
Manfredini, A., 277
Manger, G. E., 412
Mann, K. C., 65
Mann, W. B., 52, 53, 56, 57, 58
Manning, W. M., 70
Manov, G. G., 51-68: 56, 57, 407
Manring, E., 45
Marble, J. P., 409, 415

Marcus, S., 386
Marder, S., 209, 214
Marinelli, L. D., 53, 383
Marshak, A. J., 367
Marshak, R. E., 251
Marshall, J., 141-56; 99, 105, 106, 145, 152, 153, 252, 256
Marshall, J. F., 17
Marshall, L., 145, 252, 256
Marston, R. Q., 386
Martin, A. V., 415
Martin, D. G. E., 175
Martin, G. R., 406, 409, 410, 413, 422, 423, 435
Martin, P. C., 212
Martin, R., 222, 228, 232, 233
Martinelli, E. A., 155, 256
Mason, G. W., 414
Massey, H.J., 317
Massey, H.S.W., 344
Masuda, Y., 46
Mateosian, E. der, 61
Mather, J. W., 155, 256
Mather, R., 328, 331
Matsuda, F., 411
Matthews, C.M.E., 408
Maurer, P. H., 386
Maxwell, A. E., 437
Maxwell, E., 366
Mayer-Leibnitz, H., 207
Mayne, K. I., 410, 422, 423, 435
Mazur, M., 362, 364
Mazzanti, L., 388
Mead, J.F., 368
Mech, J. F., 414
Mech, J.R., 159
Mefferd, R. B., Jr., 388
Mehnert, K. R., 423
Meijer, H. R., 108
Meinke, W. W., 412
Meinschein, W. G., 429, 430
Melander, L., 63
Menard, H. W., 428
Mendelsohn, M. L., 389
Meneely, G. R., 382
Menon, M. G. K., 272, 273, 301, 303, 308
Meot, R., 386
Mercer, E. R., 409, 410, 422, 435
Meredith, W. J., 354
Merrill, P. W., 406
Merritt, W. F., 53, 58, 72
Meschan, I., 357
Messel, H., 332
Messiah, A. M. L., 251
Metcalf, R. P., 73
Metnieks, A., 410, 411
Metropolis, N., 233
Metzger, F. R., 63
Meyer, K. P., 104, 108
Meyer, L.H., 35, 46
Meyers, R. D., 122
Meyers, S., 406
Meyers, W. G., 382
Meyer-Schutzmeister, L., 53
Michel, L., 193
Mihelich, J. W., 62
Mikiewicz, E., 124
Mikuta, E. T., 370, 384, 387
Milholić, S., 419, 424
Milkey, R. G., 416, 417, 439
Millar, C. H., 405
Millar, D. D., 294, 302, 310
Miller, C. P., 386
Miller, D., 228, 232
Miller, R. W., 383, 386
Miller, W. W., 56, 57
Millet, W. E., 209
Mills, F. E., 335
Milne, W. L., 387
Milton, J. C. D., 174
Minami, E., 411, 412
Minkkinen, C. O., 73
Mins, W., 63
Minton, G. E., 208
Minton, G. H., 174
Mitchell, A. C. G., 52, 120
Mitchell, J. R., 367
Mitchell, R. B., 386
Moffatt, R. J. D., 63
Mohney, J. B., 361
Mohorovičić, S., 192
Mole, R. H., 360, 361, 369, 370, 380, 385, 386, 389, 390, 391
Møller, C., 319
Momyer, F. F., 168
Monroe, R. A., 385
Montalbetti, R., 13, 22, 23, 26
Montgomery, C. G., 192
Moody, N.F., 96, 97, 98, 99, 101
Moon, M. L., 54
Moon, R. J., 137, 138
Moore, C. E., 406
Moore, R. C., 415
Moreau, J., 61
Moret, R., 385
Morgan, J. E., 377
Morrison, P., 21, 22, 403
Morton, G. A., 108
Morton, M. E., 366
Mościcki, W., 429, 430
Moses, C., 380
Moses, H. A., 46
Moss, N., 76
Mott, N. F., 344
Mottelson, B. R., 28, 172, 175, 178, 183, 185
Mousuf, A. K., 403, 423
Muench, O. B., 415
Muirhead, H., 277
Mulholland, G. I., 405, 406
Muller, D. E., 62, 192
Muller, F., 293, 294, 295
Müller, K., 379
Mullin, C. J., 17
Mulvey, J. H., 272, 273
Munsun, R. J., 380
Muntz, J. A., 354, 355, 356, 359, 363, 364
Mytton, J. W., 412

N

Nagashima, K., 415
Nagle, D., 222, 228, 232, 233
Nakanishi, M., 408, 409, 411
Naldrett, S. N., 405
Nanjo, K., 363
Nathans, R., 13, 18, 22, 23, 26, 28
Neary, G. J., 380
Nedzel, V. A., 145
Neiler, J.H., 136
Nelson, D., 228, 232
Nencini, G., 424, 443
Neuerburg, G. J., 419
Neumann, H.M., 168
Neumayr, A., 385
Neve, R.A., 368
Neworaschkin, J. P., 368
Newth, J. A., 294, 302, 310
Nichols, R. T., 59
Nickson, J. J., 378
Nicola, M., 367
Nicolaysen, L. O., 408, 417, 425, 426
Niday, J. B., 71, 74
Nielsen, C. E., 343
Nier, A. O., 57, 402, 403, 404, 416, 417, 419, 420, 439, 441
Nier, D. T., 406
Nijgh, G. J., 58
Nims, L. F., 359, 391, 392
Nishimura, S., 415
Nishio, J., 411
Nizza, P., 377
Noe, J. D., 94, 96
Nord, F. F., 356
Norin, R., 408
Norinder, H., 410, 411
Norris, W. P., 364, 381, 382
North, N., 359
Novey, T., 61
Novick, A., 406
Noyes, P., 386

O

Oakley, D., 235, 240
Occhialini, G. P. S., 271-314; 191, 220
O'Ceallaigh, C., 272, 273, 295
Odian, A., 29
Ogawa, S., 45, 46
Okabe, I. S., 411
O'Kelley, G. D., 55, 62
Olbert, S., 288
Oliver, W. F., 59
Olkowsky, J., 73
Olmstead, C. A., 368
Olsen, J. L., 55, 62
O'Neill, G. K., 17

O'Neill, T., 383, 388
Oppenheimer, J. R., 317
Ord, M. G., 351, 359, 377, 390, 392
Ore, A., 192, 196, 206
Orear, J., 232
Osborn, G. K., 384
Osborne, L. S., 222, 235, 240
Oshima, Y., 411
Oster, H. L., 385
Otsuki, S., 264
Overbeek, A. J. W. M. v., 96
Overhauser, A. W., 38, 41
Owen, H. R., 416, 439
Owen, J., 46

P

Pabst, A., 409, 427
Page, D. I., 287
Page, L. A., 191
Pahl, M., 423
Paigen, K., 391
Pais, A., 282
Pake, G. E., 33-50; 45, 46
Pal, Y., 306
Palazzi, D., 384
Palmatier, E. D., 340, 342
Palmer, G. H., 416
Palumbo, D., 407
Paneth, F. A., 51, 60, 406, 410, 422, 423, 428, 435
Panofsky, W., 222, 248
Papp, G., 104, 108
Pappas, A.C., 73, 75
Paris, R., 384
Parker, F. L., 412
Parker, G. W., 34
Parks, J. M., Jr., 426
Parr, W. H., 383, 388, 391
Passeau, L., 387
Passman, S., 254, 255
Pasternack, S., 194
Patro, A. P., 179
Patt, H. M., 351, 360, 377, 380, 386, 387, 391
Patterson, C., 89, 90, 403, 407, 408, 410, 417, 419, 420, 424, 435, 436, 441
Patti, F., 378, 379, 388
Paul, D. E., 46
Pauli, W., 261
Paulissen, L. J., 386
Paull, J., 387
Pavlova, T. G., 424
Payne, A. H., 367, 391
Pearson, W. N., 388
Peaslee, D., 193
Peixoto, F., 415
Pellas, P., 421
Peppard, D. F., 414
Percival, W. S., 94
Perey, M., 177
Perkins, D. H., 310
Perkinson, J.D., Jr., 382
Perlman, I., 157-90; 74, 159, 167, 168, 172, 174, 175, 176, 177, 178, 179, 180, 183, 186, 187
Perlman, M. L., 23
Permutt, S., 381
Perrings, J. D., 390
Perry, A. M., 17
Perry, C. L., 54
Perry, J., 228, 232
Pesteil, P., 129
Petch, H. E., 44, 54, 98, 100, 101, 102, 104, 105, 175
Peters, B., 277, 306
Peters, R. A., 358
Peterschmitt, E., 407
Petersen, D. F., 351-76; 365, 366, 367
Peterson, V., 235, 238, 239, 244, 254, 255
Petrakis, N. L., 364
Pettersson, H., 427, 437
Pevsner, A., 147
Peyrou, C., 293, 294, 295
Pfotzer, G., 413
Phillips, H. B., 121
Phillips, P. H., 357, 370
Piatier, H., 162
Piccioni, O., 227, 228, 229, 232
Picciotto, E., 406, 408, 418, 427
Picciotto, E. E., 407, 408, 415
Piccirillo, R. T., 385
Pichat, L., 129
Piemonte, A., 369
Piénkowski, S., 408
Pierce, A. P., 412
Pierce, F. T., 368
Pierpoint, W. S., 387
Piggot, C. S., 408
Piguory, L., 377
Pines, D., 23, 24
Pinoir, R., 412
Pinson, E. A., 382
Pinson, W. H., 410, 435, 436, 442
Pirenne, J., 211, 212
Pirie, A., 381
Pirotte, M., 386
Platzman, R. L., 347
Pohl, E., 407
Pohle, E., 367
Pomeranchuk, I., 193
Pond, T. A., 201, 202, 210
Poole, J. H. J., 408, 442
Porschen, W., 170, 405
Portis, A. M., 46
Post, R. F., 102, 121
Potter, R. L., 366
Potter, V. R., 358, 359, 365
Potzger, J. E., 431, 432
Poulis, N. J., 45
Pound, R. V., 43, 44
Pouradier, J., 412
Powell, C. F., 277
Powell, J. L., 196
Powers, R. I., 61
Präg, R., 422, 423
Praytor, E. H., 361
Preiswerk, P., 63, 169, 172
Present, R. D., 23, 73
Preston, M. A., 179, 180, 184
Preston, W. M., 126
Prestwood, R. J., 60
Prevot-Bernas, A., 390
Priest, S. G., 392
Primakoff, H., 207
Pringle, R. W., 129, 405
Pringsheim, P., 123, 131
Prosser, C. L., 360, 363
Pryce, M. H. L., 168, 194
Puckett, N., 391
Purcell, E. M., 43, 45
Putnam, J. L., 53, 58, 63
Pyle, G., 159

Q

Quastler, H., 360, 379
Quimby, G. I., 432
Quinn, W. E., 45

R

Rabbitt, J. C., 401, 429
Radcliffe, J. M., 196
Radicatti, L. A., 18
Rafter, T. A., 429, 431
Rainey, F., 431
Rainwater, J., 20
Rajewsky, B., 378, 389
Rambach, W. A., 391
Ramm, C. A., 166
Ramsey, N. F., 34, 35
Randall, J. T., 121
Rankama, K., 443
Rankin, D., 65
Ransom, R., 391
Rasetti, F., 174, 207
Rasmussen, J. O., 177, 182, 185, 187
Rasmussen, J. O., Jr., 170, 179, 405
Ratier, J., 405
Rau, R. R., 294, 304
Rauch, R. F., 369
Ravenhall, D. G., 193
Ravilious, C. F., 122, 123, 124
Rayet, P., 386
Reasbeck, P., 410, 422, 423, 435
Reding, R., 360
Reed, G. W., 72, 75
Rehbock, D. J., 382
Reid, A. F., 430
Reif, F., 45
Reifman, A., 20, 24, 28
Reiling, V. G., 142
Reines, F., 383
Reinhart, F. E., 363

Remi, B., 305
Remley, M. E., 126, 127
Reuterswärd, C., 403
Révy, K., 365
Révy, L., 365
Revelle, R., 437
Reynolds, C. D., 407
Reynolds, F. L., 177
Reynolds, G. T., 128, 129, 286, 287, 294, 304
Reynolds, H. K., 331
Reynolds, J. H., 89, 406, 414
Reynolds, J. R., 418
Reynolds, S. A., 61, 63, 64
Rhodes, B., 388
Ribe, F., 346
Rich, J. A., 209
Richardson, H. O. W., 175
Richardson, J. R., 328, 331
Richings, H. J., 104, 208
Richman, C., 250, 251
Richmond, J. E., 368
Richter, H., 405
Riemenschneider, P. A., 387
Riezler, W., 170, 405
Riggs, H. E., 391
Ring, J., 228, 232
Ring, P. J., 45
Rio, C. S. del, 13, 28
Ripelle, M. F. de la, see Fabre de la Ripelle, M.
Ritson, D. M., 277, 332
Rittenberg, D., 81
Roberts, A., 54, 228, 232, 250
Roberts, F. H. H., Jr., 430
Robinson, C. V., 63, 64
Robinson, E. S., 406
Robinson, K. W., 108
Robinson, S. C., 416, 421
Rochat, O., 272, 273
Rochester, G. D., 277, 285, 288
Rodesch, J., 391
Rodgers, J., 415, 426
Rogers, B., 412, 429, 430
Rohinger, G,, 56
Rohrlich, F., 319
Rona, E., 409, 411
Rond, T. A., 210
Root, S. W., 382
Rose, D., 58, 63
Rose, D. C., 412
Rose, M. E., 54
Rose, R. G., 382
Rosenberg, S. A., 382
Rosenblatt, D. B., 411, 414, 439
Rosenblum, S., 159, 166, 172, 174, 177
Rosenfeld, A. H., 245, 254, 255, 266
Rosenstock, H. B., 411
Rosenthal, R. L., 367
Roser, F. X., 339
Ross, M., 266, 390
Ross, M. H., 359, 365, 367
Rossel, J., 119, 133
Rossi, B., 102, 277, 287, 288, 289, 304, 341
Rossi, G. B., 159
Rostagni, A., 443
Rotblatt, J., 329
Roth, J. S., 368, 370
Rothé, J. P., 407
Rowland, T. J., 44, 45
Ruark, A. E., 192
Rubadeau, D. O., 384
Rubinson, W., 73
Ruderman, M., 228, 259, 260, 265
Rugget, R. W., 293
Rugh, R., 360, 377, 382, 385, 386, 388, 392
Rüling, J., 411
Runnels, R. T., 408
Russell, R. D., 403, 416, 417, 420, 421, 423, 426, 439, 440, 441, 445
Rust, J. H., 378, 385
Ruth, H. J., 386
Rutherford, E., 406
Rutledge, W. C., 58

S

Sachs, A., 222, 228, 232
Sachs, D. C., 328, 331
Sachs, R. G., 14, 15, 16, 25, 239, 266
Sadauskis, J., 342, 343
Safford, R., 289, 304
Saika, A., 46
Saito, N., 401-62; 406, 408, 411, 412, 418
Sakakura, A. Y., 412
Salerno, P. R., 382, 387
Salomon, K., 368
Salpeter, E. E., 46
Salvani, G., 128
Salzman, F., 263
Sanderman, L. A., 408, 411, 429
Sanders, P., 380, 386
Sanderson, M. H., 383
Sands, M., 236, 248
Sands, R. H., 45
Sangster, R. C., 114, 123
Santangelo, M., 407, 424, 441, 443
Santomauro, L., 412
Sapadin, L., 377, 385
Saunders, D. F., 407, 426, 427
Sawyer, C. H., 369
Sawyer, G. A., 403, 434
Saxon, D., 434
Sayag, G.-J., 402
Sayeg, J. A., 379
Scarsi, L., 271-314; 220
Schaeffer, O. A., 414, 446
Schardt, A. W., 134
Scharff, M., 327, 330
Scharff-Goldhaber, G., 172, 405
Schechmeister, I. L., 386
Scheminzky, F., 409, 411
Schenck, J., 134, 136
Scherb, F., 29
Schiff, H., 344
Schiff, L. I., 17, 102
Schintlmeister, J., 168
Schjeide, O. A., 385
Schleicher, J. A., 408
Schlesinger, M. J., Jr., 368, 384
Schluter, R. A., 251, 257, 258
Schneider, E. E., 46
Schneider, H., 54
Schneider, M., 388
Schneiderman, H., 355
Schoenberg, M., 332
Schoenberg, M. D., 355
Schoenwetter, H. K., 99
Scholes, G., 390
Schoolman, H. M., 383
Schorr, M., 129
Schrader, E. F., 108
Schriever, B. D., 17
Schroeder, C. A., 102
Schuck, E. A., 359
Schuck, R. L., 383
Schultz, H. L., 106
Schultz, V. A., 170, 405
Schulz, A. G., 250
Schulz, R. J., 378
Schuman, R. P., 63
Schumann, G., 412
Schwachman, H., 364
Schwartz, M. C., 386
Schwarz, H. P., 391
Schwarzer, D., 406, 414, 433
Schweber, S. S., 266
Schwebel, A., 53, 59, 60, 407
Schweidler, E., 406
Schwinger, J., 212
Scott, K. G., 381, 383
Scott, M. B., 222, 235, 240
Scott, M. R., 52, 61, 62
Scott, W. E., 73
Scudder, J., 388
Seaborg, G. T., 70, 159, 167, 168, 169, 170, 174, 180, 186, 187, 405, 406, 414
Sedlet, J., 60, 406
Segal, G., 367
Segrè, E., 28, 328, 331
Seiler, J. A., 69, 71, 73
Seitz, F., 131, 133
Seki, L., 361
Selden, G. L., 392
Selig, H., 405, 406
Seliger, H. H., 53, 58, 59, 60
Sellers, P. A., 159
Sen Gupta, R. L., 343
Sengupta, S., 169
Serber, R., 222, 248, 317
Seymour, E. F. W., 45
Shaknov, I., 194

Shamos, M. H., 412
Shapiro, M. M., 338
Sharpe, J., 343
Shavrova, N. N., 412
Shaw, P. F. D., 34
Shaw, T. M., 46
Shearer, J. W., 199, 207
Sheline, G. E., 383
Sheline, R., 406
Sheline, R. K., 59
Shepard, W. D., 232
Shepherd, H. J., 388
Shepherd, L. R., 61
Sherk, P. M., 405
Sherman, D., 254, 255
Sherman, F. G., 362
Sherr, R., 207
Shillibeer, H. A., 403, 423
Shimauchi, A., 45
Shimokata, K., 411
Shipman, J. D., Jr., 102
Shiren, N. S., 121
Shoolery, J. N., 46
Shorey, W. R. J., 52, 58, 68
Shuey, R. L., 76
Shutt, R. P., 232, 287, 308
Siegbahn, K., 55, 63, 175
Siegel, R., 201, 202, 206, 209
Siegert, A. J. F., 15, 25
Siksna, R., 410, 411
Silver, L. M., 52, 62
Silverman, A., 21, 235, 236
Silverman, M. S., 386
Silvey, G., 34
Simanton, J. R., 429, 430
Simmons, D. H., 328
Simon, D. M., 73
Simons, C. S., 378
Simons, L., 191
Simpson, O. C., 179
Sinclair, W. K., 58, 59, 62
Singer, S F., 422, 423
Singer, T. P., 354, 355, 356, 363, 364
Sirvetz, M. H., 34, 36
Skarsvåg, K., 142
Skraba, W. J., 56
Slater, L. M., 159, 174
Slätis, H., 175
Slichter, C. P., 38, 45
Sluis, K. L. V., see Vander Sluis, K. L.,
Smales, A. A., 402
Smaller, B., 106
Smith, A., 61
Smith, B. W., 75
Smith, C. L., 390
Smith, D. B., 53
Smith, D. E., 360, 384, 390
Smith, F., 360, 361, 386
Smith, F. W., 124
Smith, H. P., 354
Smith, K. F., 34
Smith, P. V., Jr., 432
Smith, W. C., 410, 422
Smith, W. W., 361, 367, 368, 386
Smits, F., 423
Snell, W. A., 412, 429, 432
Snitzer, E., 344
Snyder, H., 317
Snyder, H. S., 5, 194
Snyder, J., 263
Sobel, E., 361
Sobering, S., 129
Sogo, P. B., 34
Sommers, S. C., 385
Sowerby, 286, 287
Sparrow, A. H., 351
Spear, F. G., 377, 378
Speckman, T. W., 383
Spees, A. H., 191
Spehler, H., 367
Spence, R. D., 46
Spence, R. W., 69, 70, 76, 406
Spencer-Palmer, H. J., 402, 403
Spiers, F. W., 383
Spradling, S., 391
Sprague, G., 386
Sreb, J. H., 58, 63
Stähelin, P., 169, 172
Stallwood, R. A., 250
Standil, S., 405
Stanley, C. W., 74
Stanley, J. P., 420, 439
Stapleton, G. E., 361
Starik, I. E., 415
Stearner, S. P., 368, 377, 379, 389
Stearns, M., 235, 236
Stearns, M. B., 13, 28
Stegun, I. A., 55
Stehle, P., 191
Stein, P. C., 29
Steinberg, E. P., 69-80; 69, 71, 72, 73, 74, 75, 76, 89
Steinberger, J., 222, 228, 232, 250
Steinwedel, H., 23
Stella, A., 407, 408
Stenstrom, K. W., 369, 391
Stephens, F., 159, 174, 175, 176, 177
Stephens, S. V., 377
Stern, M., 222, 227, 228, 232
Stern, T. W., 416, 417, 439
Sternheimer, R. M., 321, 332, 333, 335, 337, 340
Stets, J. F., 392
Stetson, H. C., 428
Stevens, C. M., 159
Stevens, K. M., 386
Stevens, K. W. H., 46
Stevens, W. H., 56
Stevenson, M. L., 249, 250
Stewart, A. L., 344
Stewart, A. T., 210
Stewart, D. C., 409
Stewart, E. C., 133, 134
Stewart, R., 367, 392
Stieff, L. R., 416, 417, 418, 439
Stiller, B., 338
Stockell, A., 367, 392
Stocken, L. A , 351, 359, 377, 390, 392
Stoddard, A. E., 58
Stokinger, H. E., 381
Stone, F., 391
Stoner, A., 159
Stoner, R. D., 386
Storer, J., 382
Storer, J. B., 380, 386, 391
Stork, D., 222
Story, V. M., 380
Strandberg, M. W. P., 34
Strassmann, F., 69, 423
Straube, R. L., 386, 387
Strauch, K., 13, 108
Strome, F. C., Jr., 406
Struve, O., 445
Studier, M. H., 159, 414
Stump, R., 209
Sturm, W. J., 166
Suess, H. E., 89, 406, 412, 413, 414, 424, 429, 430, 431, 445, 446
Suess, J., 388
Sugarman, N., 72, 73, 74, 75, 405
Sugihara, T., 405
Sullivan, J. C., 414
Sullivan, M. F., 357, 363
Sunyar, A. W., 64, 172
Suryan, G., 35
Sutton, E., 391, 392
Sutton, R. B., 250
Suzor, F., 404
Swank, R. K., 111-40; 121, 129, 131
Sweeton, F. H., 54, 63, 64, 406
Swift, M. N., 379, 384, 388
Swisher, S., 386
Symon, K. R., 341
Szendrei, M. E., 114
Szteinsznaider, D., 405

T

Tahmisian, T. N., 361
Taketa, S. T., 379, 384, 388
Taketani, M., 264
Takubo, J., 415
Talley, H., 209
Talmage, D. W., 386
Tamburino, S., 407, 408
Tamm, I., 141, 263
Tani, S., 264
Taplin, G. V., 386
Taplin, R. H., 99
Tatekawa, M., 415
Tatel, H. E., 442, 443
Tauber, H., 429, 431, 432
Taubman, J., 361
Taylor, A E., 315
Taylor, C. J., 126, 127
Taylor, G. L., 419
Taylor, H. W., 405
Teasdale, J., 235, 236, 238,

239, 244, 248
Telegdi, V. L., 13, 18, 28
Teller, E., 23, 132, 347
Temmer, G. M., 42, 174
Templeton, D. H., 168
Tepperman, H. M., 383
Te Punga, M. T., 429
ter Haar, D., see Haar, D. ter
Terrell, J., 73
Terwilliger, K. M., 13, 26
Tew, J. T., 360, 391, 392
Thew, K., 52, 61, 62
Thibaud, J., 191
Thirring, W., 434
Thoai, N. van, 367
Thode, H. G., 70, 75, 76
Thomas, C. O., 123
Thomas, D. A., 62
Thomas, H. A., Jr., 412
Thomas, R. H., 58, 59, 60, 61, 62, 63, 406
Thompson, B. J., 97
Thompson, B. W., 277
Thompson, M. E., 408
Thompson, R. W., 285, 286, 287, 293
Thompson, S. G., 159, 169, 170, 174, 175, 177, 178, 179, 405
Thompson, T., 328, 331
Thomson, J. F., 377-400; 362, 366, 370, 378, 379, 384, 387, 391
Thomson, S. J., 409, 410, 422, 423, 435
Thorndike, A. M., 232, 287, 308
Thurnher, B., 385
Tillotson, F. W., 382
Tilton, G. R., 82, 89, 90, 407, 408, 410, 417, 419, 420, 425, 426, 435, 441
Ting, Y., 45
Tinlot, J., 228, 232
Titov, N. E., 402, 423
Titterton, E. W., 13
Tobaliem, J., 63, 64
Tobias, C. A., 379, 384
Tollestrup, A., 151, 235, 238, 239, 244
Tomasini, G., 306
Tomita, K., 46
Tomkins, F. S., 34, 186
Tomlinson, R. H., 425, 426
Tompkins, M., 386
Tonhazy, N. E., 369
Torney, F., 129
Torrey, H. C., 43
Tourtellotte, W. W., 362, 366, 378, 379, 391
Touschek, B. F., 283
Townes, C. M., 34
Townsend, J., 46
Treiman, S. B., 204, 304
Trembaczowski, E., 411
Trenam, R. S., 34
Triebwasser, S., 46
Trowbridge, W. V., 377
Trum, B. F., 378, 385
Tryon, L. E., 412, 429, 432
Tsivoglou, E. C., 411
Tsukada, K., 45
Tubailem, J., 52, 58, 63
Tubiana, M , 385
Tuchman-Duplessis, H., 386
Tullis, J. L., 377
Tunnicliffe, P. R., 76
Turkevich, A., 71, 72, 74, 75
Turner, J. F., 63
Tusques, J., 385
Tweedie, M. C. K., 354
Tyree, E. B., 360, 378, 390
Tytell, A. A., 355
Tzara, C., 73

U

Ubisch, H. v., 415
Ueda, T., 415
Uehling, E. A., 315-50
Umbreit, W. W., 369
Umemoto, S., 411
Umezawa, M., 172
Uphoff, D., 377
Upton, A. C., 351, 377, 380, 385, 388
Urey, H. C., 407, 434, 437, 438, 443
Urry, W. D., 409, 411, 428, 438
Utterback, C. L., 408, 411, 429
Uyeki, E., 367

V

Valadares, M., 159, 172, 174, 177
Valentine, J. M., 343
Valentine, W. N., 390
Valladas, G., 159
Vander Sluis, K. L., 185
Van Heerden, P. J., 328, 331
van Heyningen, R., see Heyningen, R. van
van Lancker, J., see Lancker, J. van
Van Lershout, R., 58
Van Nortwick, H. S., 408
Van Rennes, A. B., 101
Van Sciver, W., 136
van Thoai, N., see Thoai, N. van
Van Valkenburg, P. A., 361
Venet, A. M., 412
Venkatasubramanian, V. S., 407, 424
Vermund, H., 391
Verster, N. F., 58
Vette, J., 235, 238
Vevasseur, J., 384
Vigneron, L., 274
Vincent, D. H., 53
Vinogradov, A. P., 420, 439, 441
Visscher, W. M., 266
Vogel, H. H., Jr., 378, 379, 380
Vogel, M., 392
Voight, A. F., 61
Voitkevich, G. V., 441
Volchok, H. L., 413, 426, 428, 430
Volkoff, G. M., 44
Von Dardel, G., 16
von Erichsen, L., see Erichsen, L. von
von Friesen, S., see Friesen, S. von
Vorteresz, V., 365
Voyvodic, L., 272
Vries, H. de, 429, 430

W

Waddington, C. Y., 306, 310
Waggoner, M. A., 54
Wagner, F., Jr., 406
Walcher, W., 404
Waldron, E. C., 170, 405
Walker, J., 175
Walker, R., 235, 236, 238, 239, 240, 244, 248
Walling, E., 425
Walske, M. C., 323, 327
Walters, M. C., 406
Waltner, A. W., 16
Wang, S. C., 386
Wangsness, R. K., 42
Wank, F. J., 408
Wapstra, A. H., 168
Warburton, E. K., 133, 134
Ward, J. C., 194, 261
Wardle, G., 422
Warner, W. L., 368
Warren, J. B., 207
Warren, S., 351, 382
Warshaw, S. D., 57, 145, 316, 328, 331, 340, 344, 347
Wase, A., 368, 370
Wasserburg, G. J., 89, 403, 404, 423
Wasserstein, B., 415
Watari, W., 264
Waters, A. C., 408
Watkins, G. D., 44
Watson, B. B., 207
Watson, K., 219-70; 222, 224, 225, 235, 236, 237, 241, 242, 243, 245, 248, 254
Wattenberg, A., 29
Waxler, S. H., 368
Way, K., 52, 61, 62, 70
Weaver, A., 232
Weaver, H. E., 34, 35
Weil, J. W., 29
Weinhouse, S., 430
Weinman, E. O., 368
Weinstein, R., 216
Weinstock, E. V., 17

Weiss, J., 390
Weisskopf, V. F., 14, 18
Weissman, S. I., 46
Weizsäcker, C. F., 168
Welch, G. P., 379, 384
Wells, F. H., 96, 97, 99, 101
Wentzel, G., 266
Wentzel, W. A., 151
Wenzel, W. A., 331
Wessel, G., 34, 35, 36
West, H. I., 134
Westcott, C. H., 99
Westman, A., 385
Westphal, U., 392
Wetherill, G. W., 76, 89
Weymouth, P. P., 387
Whalin, E. A., 17
Whaling, W., 331
Wheatley, J., 206, 214, 215
Wheeler, J. A., 28, 78, 168, 185, 192, 194
White, G. R., 274
White, M. G., 407, 408
White, N. G., 369
White, R. L., 34
Whitehead, M. N., 250
Whitehouse, W. J., 70, 76
Whiting, F. B., 425
Whittemore, W. L., 232, 287, 308, 340
Whittier, A. C., 346
Whyte, G. N., 58
Wick, G. C., 332
Wickman, F. E., 402, 419, 420, 425, 443
Wiedenbeck, M. L., 403, 404, 434
Wiegand, C., 96, 106
Wilcox, H. A., 250
Wilding, J. L., 378
Wiles, D. R., 75
Wilgain, S., 408
Wilkening, M. H., 411
Wilkerson, M. C., 367, 392
Wilkins, M. H. F., 121
Wilkinson, D. H., 17, 18
Wilkinson, G., 69
Willard, D., 289, 304
Williams, D., 45
Williams, D. L., 412, 429, 430
Williams, E. J., 321
Williams, F. C , 316, 329
Williams, G. A., 34
Wilson, E. J., 410, 422
Wilson, H. W., 404, 406
Wilson, J. E., 378, 379
Wilson, J. G., 275, 340
Wilson, J. T., 415, 416, 420, 439, 440, 443
Wilson, R., 13, 63, 250
Wilson, R. R., 29
Winckler, J. R., 147, 150, 339, 342
Winhold, E. J., 77
Winsberg, L., 71, 73
Winslow, A., 21, 22
Winslow, G. H., 179
Winter, R. G., 406
Wolfenstein, L., 193, 197, 213
Wolfgang, R. L., 413
Wolfson, J. L., 175
Wolkowitz, W., 359
Wood, B., 377
Wood, M., 52, 61, 62
Woodcock, C. C., 382
Woodward, R. N., 402, 403
Woodward, W. M., 17
Worlock, R., 235, 238, 239, 244
Wouthuysen, S. A., 265
Wright, C., 257, 258
Wright, G. T., 127
Wu, C. S., 55, 61, 194, 209, 214
Wu, S. S., 19
Wyant, D. G., 408
Wyard, S. S., 55
Wybourn, R. C., 388
Wyckoff, H. O., 142
Wyckoff, J. M., 174

Y

Yadov, H. N., 344
Yaffe, L., 52, 58, 72, 73, 75
Yamagata, N., 411
Yamagata, Y., 46
Yamaguchi, Y., 172
Yang, C., 193
Yasin, M., 306, 310
Yodh, G. B., 257, 258
Yokoyama, Y., 411, 412
York, C. M., 288, 294
Yoshida, S., 29, 172
Young, J. C., 386
Young, R. W., 415
Ypsilantis, T. J., 179, 180
Yu, T. P., 96
Yuan, L. C., 227, 228, 232
Yuan, L. C. L., 150

Z

Zadorozhnyi, I. K., 420, 439, 441
Zaffarano, D. J., 55
Zahn, C. T., 191
Zeldes, H., 45, 58, 62
Zeller, D. E. N., 426
Zeller, E. A., 381
Zeller, E. J., 426
Zeller, J. H., 377
Zemansky, M. W., 120
Zerwic, M. M., 359, 365
Zeuner, F. E., 415, 428, 431
Zimmerman, J. R., 46
Zuber, K., 191
Zwaan, C., 406
Zykov, S. I., 420, 439, 441

SUBJECT INDEX

A

Abundances, isotope, 402-10, 435-37
Accelerators, 1-11
Adaptation syndrome, 384
Air, Cerenkov radiation in, 151
Alkali halides
  as scintillators, 131-37
Alkali metals
  positron life in, 208-9
Alpha decay
  energy systematics for, 166-69
  theory of, 178-87
  see also Radioactivity, alpha
Alpha particles
  Cerenkov counting of, 147
  existence in nuclei of, 186-87
  radiation effects of, 364
  scintillation by, 126, 135-37
Alternating-gradient focusing, 5-7
Amplifiers
  distributed type, 94-96
  linear, 94-96
  "lock-in", 36
  in nuclear counting, 94-98
  photomultipliers and, 98
  secondary emission pentodes in, 96-97
Analysis, chemical
  with stable isotopes, 81-91
Animals, radiation effects on, 377
Annihilation
  of positronium, 207-10
  three quantum process of, 196-98
  two quantum process of, 195-96
Anthracene, as scintillator, 114, 126
Anthropology, 430-32
Antibiotics
  and postirradiation infection, 386
Archaeology, 430-32
Argon^{40}, 403, 423, 442
Astatine^{211}
  radiation toxicity of, 387
Atmosphere
  radioactivity in, 442-43
Atomic beams
  detector for, 35-37
Atomic collisions, 315-17

B

Bactericides
  and radiation therapy, 386
Barium isotopes
  fission yield of, 72-73
Beryllium^{7}, 414
Beryllium^{9}, 17
Beta decay
  energy balance and, 169-70
Beta emitters
  backscattering in, 404
Beta rays
  anthracene scintillation by, 114
  biological effects of, 381-83
  Cerenkov counting of, 145, 155
  lethal effects of, 377-81
  as scintillation exciter, 118, 126
  spectrometry of, 54-55
  standard radionuclides spectra, 56-64
Bevatron, 4
Bimolecular decay, 121, 136
Biochemistry
  carbohydrate metabolism and, 356-63
  fat, protein metabolism and, 367-69
  phosphorous metabolism and, 363-67
  radiation effects and, 351-71
    basic mechanisms of, 352-54
    direct cell damage in, 353
    studies in vitro of, 354-56
    toxic intermediates in, 352-53
  see also Radiobiology
Birmingham proton synchrotron, 3-4
Bismuth^{209}, 405
Bismuth^{210}, standards of, 60
Branching ratio
  measurement of, 81
Bremsstrahlung
  nuclear absorption of, 13

C

Calcium^{40}, 424, 435, 441
Calorimetry, radioactive, 52-54
Carbohydrates
  metabolism of, 356-63
Carbon^{14}
  half life of, 56-57, 406-7, 429-32
  natural distribution of, 412-13
  standard of, 56-57
Carbon dioxide
  radiation effects on output of, 360-61
Catalase, metabolism of, 370
Cataracts, 380-81
Cells, radiosensitivity of, 353
Cerenkov counters
  see Counters, Cerenkov
Cerenkov radiation
  and stopping power measurement, 329, 332, 337, 340
Cesium^{137}
  fission yield of, 72
  as scintillation exciter, 118
Charge, nuclear
  distribution in fission of, 73-74
Charge independence
  and nature of τ-meson, 282
  in pion-nucleon reactions, 219, 224-27, 245, 260
Chemical analysis
  see Analysis, chemical
Chemistry
  of positronium, 206
  see also Biochemistry
Cholinesterase, metabolism of, 369-70
Chopper, in atomic beam detector, 36
Chromium^{51}, 64
Citric acid, synthesis of, 358-59
Cloud chambers
  continuous type, 433
  errors in use of, 276
  as meson detector, 275-77
Cobalt^{60}
  biological effects from, 378
  standards of, 57-58
Coincidence circuits
  in Cerenkov counting, 154
  differential types, 108
  Rossi type, 102
Collisions, nucleon-nucleon, 245-60
Conduction electrons
  and nuclear spin polarization, 36-42
Cosmic history
  radioactivity and, 439-46
Cosmic rays
  and Cerenkov counters, 147, 151
  and meteoritic helium, 422-23
  and radiocarbon dating, 413, 423

Cosmology
radioactivity and, 401-46
Cosmotron, 1-3
heavy meson production with, 287, 308
Counters, Cerenkov, 141-56
in cosmic ray studies, 147, 151
focusing type, 152-55
gas type, 150-51
intensity in, 148-50
nonfocusing, 144-47
with pulse discrimination, 146-47
transmission type, 147
in velocity threshold detection, 145
Counters, gas, 56
Counters, scintillation
see Scintillators
Counters, 4π type, 53
Counters, and window, 53
Counting
absolute beta, 53
coincidence, 52-55, 102, 108, 154
fast electronics and, 93-109
Cross sections
for photonuclear reactions, 13-30
for pion-nucleon reactions, 222, 229-60
Crystals, scintillation of, 131-36
Curie, definition of, 51
Curium, spontaneous fission of, 76
Cysteamine, 386, 391
Cysteine, 363, 380, 386

D

Decay schemes, 54-55
Depolymerization
radiation, 390
Detection
nuclear, 93-109
Deuterons
fission of U with, 75
quadruple moment of, 35
photodisintegration of, 16-17
production of pions from, 234-45
radiation hazard from, 379
scintillator response to, 126
Diet
radiation toxicity and, 384
Disintegration rate
determination of, 52-54

E

Earth, history of, 439-46
Elastic waves, 119, 123
Electric fields
and positronium formation, 202, 206
Electrodynamics, quantum
meson theory and, 260
and positronium, 191-217
Electron shells
and heavy particle penetration, 322-27
Electronics, fast, 93-105
amplifiers in, 94-98
Electrons
binding energies of, 322-27
capture by charged particles of, 344-47
Cerenkov counting of, 145, 155
energy loss by, 319-20
in positronium, 191-217
Electroscope, recording, 52
Elements, age of, 445-46
Endocrines, and radiation toxicity, 384-86
Energy loss
in charged particle penetration, 317-22
average of, 321
Cerenkov radiation and, 336-38
electron binding and, 322-27
electron capture and, 344-47
of emulsions, 338-39
of gases, 340
ionization and, 342-43
for low energy particles, 347
polarization effects in, 321-22, 331-40
of scintillators, 339-40
statistical theory of, 330-31
Enzyme reactions
radiation effects on, 351-71
purity and, 355
in vitro, in vivo compared, 356, 363-64
Enzymes
assays in irradiated tissues, 362
in radiation damage, 381
Exchange
in nuclear interaction, 15, 28
Excitation potentials, atomic, 334-35
Explosions, nuclear, 412
Extinct natural radionuclides, 402, 414, 433
Eyes, neutron effects on, 380-81

F

Fatigue, and radiation toxicity, 384
Fats, metabolism of, 367-69
Fission
angular distribution of fragments in, 77
charge distribution in, 73
closed shell effects in, 74-76
collective nuclear model and, 78
high-energy, 74, 77
neutron induced, 70-76
by photons, 75, 77
products of, 69-78, 89
radiochemistry and, 69-78
spontaneous, 76-77, 89
ternary, 73
Fission fragments
electron capture by, 346
scintillator response to, 136
Fission isotopes
analysis with, 90
Fission yield
measurement of, 89
Fluorescence
scintillation and, 112, 120
Foods, radiation toxicity and, 384
Fossils, uranium in, 408
Free radicals
and hyperfine resonance, 46
in radiobiology, 389
Freon-12
ortho-para-positronium and, 200

G

Galena, geochronometry and, 420-21
Gallium^{72}, radiation toxicity of, 382
Gamma rays
absorption by nuclei of, 13-30
in alpha decay, 172-78
detection of, 150, 155
lethal effects of, 377-81
mass absorption coefficients for, 55
scattering of, 28-29
scintillation by, 118, 137
spectrometry of, 54-55
Gases
Cerenkov radiation in, 150-51
energy loss of muons in, 340
and tracer techniques, 88-90

Geochronometry, 405, 415-39
argon method, 403-4, 423-24
calcium^{40} method, 424
chemical method, 415
"extinct" natural radionuclides and, 433
isotope dilution analysis and, 89
lead isotope methods, 402, 406, 415-21
potassium^{40} method, 423-24
radiation damage method, 415, 426-27
Ra-Io method, 427-29
strontium method, 424-26
Geologic time
see Geochronometry
Geology
age of earth and, 415-39
"extinct" natural radionuclides in, 414-15
induced natural radionuclides in, 412-14
natural radionuclides in, 407-12
radioactivity in, 401-46
Geophysics, 401-46
Germanium diodes
in coincidence circuits, 106
in pulse analyzer, 101
Glaciation, dating of, 431, 433
Glands, radiation effects and, 357, 384-86
Glucose, absorption of, 359
Glycogen synthesis, 359
Gold, alpha emitting isotope of, 170
Gold^{198}
nuclear data on, 62
radiation toxicity of, 382
Granite
helium in, 421
natural radioactivity of, 419

H

Half life
of alpha emitters, 178
determination of, 52
of standard nuclei, 56-64
Heavy charged particles
passage through matter of, 315-47
Heavy elements, alpha decay of, 157-87
Heavy mesons
see Mesons, heavy
Helium ions
capture of electrons by, 346
Helium isotopes
in geology, 413, 421-28
Hibernation
radiation injury and, 391
Hormones, radiation treatment and, 386
Hydrogen
Lamb shift in, 46
molecular beam studies of, 35
see also Protons, Deutrons, Tritium
Hydrosphere
Carbon^{12}, tritium in, 412-14, 432-33
uranium, radium in, 409-12
Hyperfine spectra, 33-47
Hyperons
in S- and V- events, 288-89

I

Ice age, dating of, 431
Igneous rocks, composition of, 407-10, 419-23, 435
Impurities, effect on scintillators of, 124-25, 129
Independent particle model
see Nuclear Models
Insulators, positron life in, 209
Internal conversion, 54
Iodine
radiation effects on intake of, 361
Iodine^{131}
fission yield of, 72
radiation toxicity of, 382
standards of, 58-59
Ion optics, 5-7
Ionium
in geochronometry, 427-29
and ocean sedimentation, 427-29
Ionization
and charged particle penetration, 342-43
in liquid systems, 352, 354-56
in photographic tracks, 273-74
in radiobiology, 389
in scintillation process, 111-12
in atomic beam detector, 36
Iron isotopes, nuclear data on, 63
Isotope enrichment, 430
Isotopes, stable
analysis by dilution of, 81-91
evaluation of, 83-86
method of, 81-83
tracer preparation for, 86-90
supply of, 91
Isotopic spin, 18, 225-27, 260

K

K-capture
in Cr^{51}, Zn^{65} decay, 64
K-particles
interaction at rest of, 306-8
sign ratio in decay of, 305-6
see also K-mesons
Krypton isotopes, fission yield of, 72

L

Lanthanum^{138}, 405-6
Lead^{210}, standards of, 60
Lead isotopes
abundances of, 402, 415-21
in Th minerals, 417-18
in U minerals, 415-17
Lethal dose
LD_{50} tabulation of, 377
mechanisms in, 389-93
time factor in, 378-379
Light nuclei, electron capture by, 346-47
Liquids, as scintillators, 128-30
Lithium ions
Cerenkov counting of, 147
Lithium isotopes, nuclear resonance, 41-44
Liver, radiation effects on, 391
Lucite, in Cerenkov counters, 145, 148, 153
Luminescence
Cerenkov, 141-56
decay of, 120, 121
Lutecium^{176}, 405-6

M

Magic numbers
see Nuclear models
Magnetic moment
of positronium, 210-17
Magnets
design of, 5-7
of proton synchrotrons, 1-4
Mars, radiogenic heat of, 437
Mass, of heavy mesons, 281, 287, 290, 300, 309
Mass spectrometer
as analytical tool, 81-91
in fission yield measurements, 70, 74-75
and isotope dilution analysis, 81-91
Mercury, alpha emitting isotope of, 170
Mesons
cosmotron production of, 2
interaction of photons with, 17, 26, 29
theory of, 260-66
Mesons, heavy, 271-311
cloud chamber detection of, 275-77, 288-95
nomenclature for, 276-77
photographic detection of, 271-75
see also π-mesons, etc.

K- Mesons
definition of, 276
table of data on, 296-99
V-Mesons
decay of neutral, 286
definition of, 277
neutral type, 285-88
θ-Mesons
definition of, 277
neutral, mean life and decay of, 286-88
K-Mesons, 295, 301-2
μ-Mesons
Cerenkov counters and, 146-150
energy loss in gases of, 340
energy loss in scintillators of, 339-40
in K-meson decay, 301, 304-6
in S-particle decay, 293
π-Mesons
Cerenkov counters and, 150, 153
and charged V secondaries, 294
inelastic scattering of, 227, 230
in K-particle decay, 302-5
in neutral V-meson decay, 286
in n, p exchange, 15
from nucleon-nucleon reactions, 245-60
photoproduction of, 222, 234-45
angular distribution in, 239
resonance model and, 236-45
reactions with nucleons of, 219-69
angular momenta and, 220-24
charge independence and, 224-26
energy dependence of, 221-24
general principles of, 220-27
isotopic spin and, 225-27
scattering of, 220-24, 227-34
angular distributions, 232
in S-particle decay, 289, 292-93
τ-Mesons
decay of, 277, 282-83
definition of, 276
mass of, 279-81
mean life of, 281
in π-meson decay, 277
nature of, 282-85
Q of, 278, 281
spin, parity of, 283, 285
χ-Mesons, 303
Metabolism, radiation effects on, 356-70, 391
Metals
nuclear spin polarization in, 36-42
positron life in, 208-9
Meteorites
analysis of, 82, 90
composition of, 84, 90, 409-10, 413, 420-23, 435-37, 441-42
Meteorology
tritium distribution and, 433
Microanalysis
with stable isotopes, 81-91
Microwave spectroscopy, 33-47
Minerals
radioactivity in, 409
scintillations in, 137-38
Molecular beams, 35
Molecules
and nuclear resonance, 45-46
Moments, nuclear
tabulation of, 34

N

Neodymium, alpha emitting isotope of, 170
Neodymium^{144}, 405
Neptunium^{237}, natural, 414
Nervous system
and radiation exposure, 389-90
Neutrinos
and terrestrial heat, 434
Neutrons
binding energy of, 168
cosmotron production of, 2
"effective charge" of, 14, 17
fission induced by, 70-76
fluid model of, 23
nuclear binding of, 74-76
photoproduction of pions from, 234-45
radiation hazard from, 364, 379-81
radiative capture of, 16, 18
scintillation detection of, 134, 136
Nitric oxide
and ortho-para-positronium, 199
Nitrogen mustards, 359
Nuclear emulsions
see Photographic emulsions
Nuclear forces
meson theory and, 260-66
and pion-nucleon reaction, 219-69
see also Nuclear models
Nuclear geology, 401-46
Nuclear models, 19-28
and alpha decay, 175, 178, 186
collective, 23, 78
quasi-deuteron and, 22, 29
shell model, 19-21, 74, 76
subunit model, 22
Nuclear radius, 181
Nuclear shells, 74-76, 168-69, 172-78, 181
Nuclear size, 20
Nuclear spins
see Spins, nuclear
Nucleons, pion interaction of, 216-69

O

Oceanography
Ra, Io in sediments, 427
radiogenic heat and, 437
Optical systems
in Cerenkov counters, 152-55
Organic compounds
labelled, 56
radiation effects on, 354-56
Orogenics, radioactivity and, 416
Orthopositronium
annihilation radiation from, 201-5
Oxygen, radiation effects on consumption of, 360

P

Pair production, 55, 191
Parabiosis, 388
Parapositronium, 192, 199
Penetration, of heavy charged particles, 315-47
Petroleum, radiocarbon in, 432
Phenomenology
in pion reaction theory, 219
Phosphorescent decay, 121
Phosphorus, metabolism of, 363-67
Phosphorus^{32}
in radiation toxicity studies, 381
standards of, 59-60
Photodisintegration
of light nuclei, 16-19
see also Reactions, photonuclear
Photoeffect, nuclear, 14-30
Photofission, 75, 77
Photographic emulsions
angle measurements in, 274-75
errors in track measurements in, 272-73
grain count in, 338-39
K-particles in, 259-310
as meson detector, 271-75
range measurements in, 274
scattering measurements in, 272-73

use in georadiochemistry, 407-8
Photomultipliers, 98
in Cerenkov counting, 145, 148-50
spectral response of, 112-14
time constants of, 120
use with scintillators of, 114, 116
Photons
in Cerenkov radiation, 141-44, 148-50
meson interaction of, 17, 26, 29
nuclear interaction of, 13-30
in positronium annihilation, 193-98
and production of pions, 222, 234-45
in scintillation process, 111-12, 115, 119
see also Gamma rays, X-rays
Photonuclear reactions
see Reactions, photonuclear
Pions, see π-Mesons
Plasma oscillations
in n, p fluid model, 24
Plastics, as scintillators, 129-31
Plutonium
fission of, 69-78
natural, 414
poisoning by, 383
radiation toxicity of, 381
Polarization
effects in charged particle penetration, 331-40
of nuclear spins, 36-42
of positronium annihilation quanta, 194, 197
Polonium, radiation toxicity of, 381
Positronium, 191-217
annihilation in condensation of, 207-10
detection of, 200-1
discovery of, 198-200
fine structure of, 210-12
formation in condensed media of, 207-10
formation in gases of, 198-206
momentum prior to annihilation, 207
optical radiation from, 196
ortho state of, 192, 199
para state of, 192, 199
polarization of annihilation quanta, 194, 197
theory of annihilation of, 193-98
Zeeman effect in, 212-17
Positrons
energy loss of, 391-20
lifetime in solids of, 207-10
production of, 191
Potassium^{40}
in geological studies, 403, 410, 422-24, 435-36, 442
Potential barrier, 179, 184
Prophylaxis, radiation, 386-89
Protein metabolism, 367-69
Protons
counting of, 145-46
from deuteron disintegration, 16, 17
electron capture by, 345-47
fluid model of, 23
meson production and, 245-60
neutron capture of, 16
photoproduction of, 28
photoproduction of pions from, 234-45
scattering of pions by, 227-34
scintillator response to, 126, 135
in stopping power measurement, 328
thorium fission by, 77
see also Synchrotrons, proton
Pulse height analysis, 100-1, 146-47

R

Radiation
annihilation, 191-98
Cerenkov, 141-44, 148-50
in charged particle penetration, 318
Radiation damage
in geology, 421, 426-27
Radiation injury
treatment of, 352-53
Radiation protection
with cysteamine, 386
with cysteine, 380, 386
with detoxifying agents, 383
with endocrines, 385
with hormones, 386
Radioactivity
in geology, cosmology, 401-46
standards of, 51-65
and terrestrial heat, 434-35
units of, 51-52
Radioactivity, alpha, 157-87
absolute energies in, 166
complex spectra in, 171-72
decay energies in, 158-71
tabulation of, 160-65
energy balance cycles in, 169-70
energy profile for, 159
of even-even nuclides, 172-76, 182-85
of odd-odd nuclides, 177-78, 185-87
of rare earths, 170-71
spin effects in, 185-87
standards in, 166
theory of, 178-87
Radiobiology, vertebrate, 377-93
factors in radiosensitivity, 383-89
mechanisms of lethal action, 389-93
radiation toxicity in, 377-83
time factor in, 378-79
Radiocarbon, see Carbon^{14}
Radiochemistry, of low energy fission, 69-78
Radiofrequency spectroscopy of nuclei, 33-47
Radiogenic heat, 434-39, 446
Radiolead
half life of, 406
in nature, 411-12, 418-21
Radiomimetic chemical, 359
Radionuclides
and isotope dilution analysis, 90
polarization of, 42
spins, moments of, 34, 42
Radium
in nature, 410-12
standards of, 60
toxicity of, 364
Radium D-E, standards of, 60-61
Radon, in nature, 402, 411, 416
Ranges
in photographic emulsions, 274
of protons, alphas, 347
Rare earths
alpha emitters in, 170-71
fission yield of, 72
Reactions, photonuclear, 13-30
of deuteron, 16-17
experimental data on, 13
integrated cross sections for, 25-28
of light nuclei, 17-19
and nuclear models, 19-28
products of, 28-29
and radioactive capture, 18
theories of, 14-30
Resolution
of coincidence circuits, 101, 105, 108
of scintillators, 93
Resonance, nuclear, 34-47
Resonance theory
of photoproduction of pions, 237-45
Rhenium^{187}, 405-6
Rubidium^{87}, 404, 410, 426

S

S-particles, 288-93
  detection of, 288-89
  frequency of, 294-95
  mass, lifetime, decay data on, 290
Samarium^{147}, 405
Scalers, fast, 99
Scattering, in photographic emulsions, 272-73
Scintillators, 111-38
  alkali halides as, 131-37
  amplifiers for, 94-98
  basic process in, 111-12
  in beta, gamma spectrometry, 55, 118
  in C^{14} measurements, 430
  decay times of, 117, 119-23
  efficiencies of, 113-19
  electronics and, 93-109
  energy loss distributions in, 339-40
  in health monitoring, 383
  impurities, effects in, 119, 124-25, 129
  inorganic, 131-38
    tabulation of, 138
  organic, 123-31
    tabulation of, 128, 130
  quenching of, 127
  resolution of, 93-94
  self absorption in, 115, 120
  spectra of, 114, 119
  standardization of, 114
  temperature effects in, 118-19, 123
  use in positronium research, 199, 214
Sedimentary rocks
  composition of, 408, 411-13, 417-19, 423, 427-29
Selection rules
  for alpha decay, 172-78
  for positronium decay, 192-94
Shielding
  of part of body, 379, 388
  of proton synchrotrons, 1-3, 4
Showers
  in S-events, 292-93
Silver bromide
  charged particle energy loss in, 337-38
Sodium^{24}
  nuclear data on, 63
Sodium iodide
  as scintillator, 133-35
Solid state
  and nuclear resonance, 44-46
  positrons and, 207-10
  see also Scintillators
Solvents, organic
  use in scintillators of, 123-31
Spectra
  of scintillator photons, 114, 119
Spectrometry, beta, 54-55
Spectrometry, crystal, 55
Spectrometry, gamma, 54-55
Spectrometry, pair, 55
Spins, nuclear, 34-47
  polarization of, 36-42
  tabulation of, 34
Spontaneous fission, 76-77
Stable isotopes
  see Isotopes, stable
Standards, radioactive, 51-65
Stars, nuclear
  and origin of τ-mesons, 281
  sigma type, 277, 302, 305-8
Stilbene, as scintillator, 123, 128
Stopping number, 322-26
Stopping power, 328
Straggling, 340-42
Strong coupling
  nuclear model, 23
Strong focusing, 5-7
Strontium^{87}, 425
Strontium^{89}, radiation toxicity of, 383
Strontium^{90}
  in pitchblende, 414
  standards of, 61
Sulfhydryl enzymes, 355, 357
Supernucleons, electron, 9-11
  bremsstrahlung from, 151
Synchrotrons, proton, 1-11
  alternating gradient focusing in, 5-7
  beam extraction in, 2
  design studies of, 9-11
  magnet design of, 5-7
  orbit control in, 8
  proton injection in, 1, 3-4, 8
  radiofrequency units in, 2, 4
  shielding of, 2, 4
  targets in, 2
Systematics, alpha decay, 166-69

T

Tellurium^{100}, natural, 406
Terrestrial heat, 434-39
  temporal variations of, 437-39
Thallium, phosphor activation by, 133-35
Thallium^{204}, standards of, 61-62
Therapy, radiation, 386-89
Thermoluminescence, 426
Thorium
  fission of, 71
  in geology, 403, 407-10
  in meteorites, 409
  microanalysis for, 90
Thyroid radiosensitivity of, 361, 385-86
Tissues, animal
  radiosensitivity of, 353
  therapy with extracts of, 387
Toxicity, radiation, 377-89
Tracers, preparation of, 86-90
Trauma, and radiation toxicity, 383-84
Tritium
  gas counters and, 63-64
  half life of, 406
  natural distribution of, 413-14
  nuclear data on, 63-64
Tritium oxide, radiation toxicity of, 382
Tungstates, scintillations of, 137-38
Tungsten
  alpha emitting isotope of, 170

U

Ultraviolet, scintillator response to, 113, 119, 121
Unicellular systems, 361-62
Units, radioactive, 51
Uranium
  in geological studies, 402, 407-10, 415-18
  microanalysis for, 84, 90
Uranium^{236}
  as terrestrial heat source, 439
Uranium isotopes
  fission of, 69-78
  radiation toxicity of, 381

V

V-events, 288-95
V-particles, 293-94
  charge symmetry of, 294
  data on charged type, 290
  frequency of, 294-95
Vacuum tubes
  photomultipliers, 98
  secondary emission pentodes, 96-98
Volcanism
  radiogenic heat and, 439

W

Water
  in Cerenkov counters, 144
Wolfram^{178}, 405

X

X-rays
effects on
enzyme reactions of, 355-70
lethal effects of 377-81
for scintillator excitation, 117, 121

Y

Yields, fission, 69-78

Z

Zinc^{65}, nuclear data on, 64-65
Zinc sulfide
scintillation of, 136-37
Zircon
Pb, U, Th, He in, 90, 419, 421